FINAL REPORT

Improved Filed Evaluation of NAPL Dissolution and Source Longevity

ESTCP Project ER-200833

OCTOBER 2011

Michael C. Kavanaugh
Rula Deeb
Jennifer Nyman
Malcolm Pirnie, Inc.

Lloyd "Bo" Stewart
Praxis Environmental Technologies, Inc.

Mark Widdowson
Virginia Tech

ESTCP

REPORT DOCUMENTATION PAGE

1. REPORT DATE *(DD-MM-YYYY)*	2. REPORT TYPE	3. DATES COVERED *(From - To)*
1-11-2011	Final Report	Jan-2011-Nov-2011

4. TITLE AND SUBTITLE	5a. CONTRACT NUMBER
Improved Field Evaluation of NAPL Dissolution and Source Longevity	W912HQ-08-C-0006
	5b. GRANT NUMBER
	5c. PROGRAM ELEMENT NUMBER

6. AUTHOR(S)	5d. PROJECT NUMBER
Kavanaugh, Michael C.	ER-200833
Deeb, Rula A.	5e. TASK NUMBER
Nyman, Jennifer L.	
Stewart, Lloyd "Bo," D.	5f. WORK UNIT NUMBER
Widdowson, Mark A.	

7. PERFORMING ORGANIZATION NAME(S) AND ADDRESS(ES)	8. PERFORMING ORGANIZATION REPORT NUMBER
ARCADIS/Malcolm Pirnie 2000 Powell Street, 7th Floor Emeryville, CA 94619	4659009

9. SPONSORING/MONITORING AGENCY NAME(S) AND ADDRESS(ES)	10. SPONSOR/MONITOR'S ACRONYM(S)
SERDP/ESTCP 901 North Stuart Street, Suite 303 Arlington, VA 22203	SERDP/ESTCP
	11. SPONSOR/MONITOR'S REPORT NUMBER(S)

12. DISTRIBUTION/AVAILABILITY STATEMENT

Approved for public release; distribution is unlimited

13. SUPPLEMENTARY NOTES

14. ABSTRACT

At former Williams Air Force Base, the Air Force conducted a pilot test of thermally enhanced extraction (TEE) to reduce the mass and longevity of a multi-component NAPL fuel source in the saturated zone. Before and after the pilot test, novel tools were applied in the source zone to measure and analyze mass discharge. The tools included integral pumping tests combined with deployment of Passive Flux MetersTM and mutli-component modeling using the source zone depletion function of the model SEAM3D. Resulting data were synthesized into a model of NAPL architecture and mass dissolution. The change in the mass discharge rate pre- and post-TEE was compared to the mass removed from the subsurface during the TEE pilot test as a criterion for the success of the demonstration. Generalized results from the mass transfer testing at ST012 can be used at other sites to improve characterization approaches for NAPL source areas.

15. SUBJECT TERMS

NAPL, mass transfer, mass flux, PFM, source longevity, SEAM3D, LNAPL, DNAPL

16. SECURITY CLASSIFICATION OF:			17. LIMITATION OF ABSTRACT	18. NUMBER OF PAGES	19a. NAME OF RESPONSIBLE PERSON
a. REPORT	b. ABSTRACT	c. THIS PAGE	U	330	Rula Deeb
					19b. TELEPHONE NUMBER *(Include area code)* 510-596-8855

Reset

Standard Form 298 (Rev. 8/98)
Prescribed by ANSI Std. Z39.18

TABLE OF CONTENTS

TABLES

FIGURES

APPENDICES

Appendix A   Points of Contact
Appendix B   Technology Background
Appendix C   Site ST012 Investigation Results
Appendix D   Test Design

ACRONYMS

AFCEE	United States Air Force Center for Engineering and the Environment
AFRPA	Air Force Real Property Agency
AQWS	Aquifer Water Quality Standards
ARAR	Applicable or relevant and appropriate requirements
bgs	below ground surface
BTEX	benzene, toluene, ethylbenzene and xylenes
CERCLA	Comprehensive Environmental Response, Compensation and Liability Act
COC	chemical of concern
CSM	conceptual site model
DNAPL	dense non-aqueous phase liquid
DoD	Department of Defense
EPA	Environmental Protection Agency
ESTCP	Environmental Security Technology Certification Program
GC	gas chromatograph
gpm	gallons per minute
IPT	integrated pumping test
LNAPL	light non-aqueous phase liquid
LPZ	Low Permeability Zone
LSZ	Lower Saturated Zone
MCL	Maximum contaminant level
MNA	monitored natural attenuation
MTT	mass transfer test
NAPL	non-aqueous phase liquid
NPL	National Priorities List
PHC	petroleum hydrocarbon
ppb	parts per billion
psig	pounds per square inch gauge
PFM	passive flux meter
RAO	remedial action objective
ROD	Record of Decision
RODA	Record of Decision Amendment
SEAM3D	Sequential Electron Acceptor Model, 3D transport model
SERDP	Strategic Environmental Research and Development Program
SVE	soil vapor extraction
SZD	source zone depletion
TCM	Trichloromethane
TEE	thermally enhanced extraction
TOC	total organic carbon
TOR	time of remediation
TPH	total petroleum hydrocarbons
UST	underground storage tank
UWBZ	Upper Water Bearing Zone
VOC	volatile organic compound
WAFB	Williams Air Force Base

ACKNOWLEDGEMENTS

EXECUTIVE SUMMARY

The Department of Defense (DoD) needs improved methods for estimating the mass of non-aqueous phase liquids (NAPLs) in subsurface environments contaminated from past releases of these compounds. In addition, predicting their persistence into the future, and the impact of NAPL source reduction on the time to achieve remedial action objectives (RAOs) at compliance locations remains a significant challenge at these sites. Data are required to support scientifically defensible decisions regarding when and to what intensity active remediation efforts should be pursued at NAPL-contaminated sites before transition to passive remedies such as natural attenuation. The primary objective of this project was to evaluate a methodology to improve decision-making on the extent of source remediation required to meet RAOs at both light NAPL (LNAPL) and dense NAPL (DNAPL) impacted sites.

Current techniques to estimate the persistence of NAPL sources are very uncertain without better specification of the mass of NAPL, the constituents of the NAPL, the NAPL "architecture" (i.e., the geometry of the NAPL distribution in the subsurface), and the dissolution rate of NAPL components in groundwater (referred to collectively in this report as the source zone depletion [SZD] function). The traditional approach to characterizing the SZD function involves estimation of NAPL dissolution rates from concentration measurements in discrete locations in the downgradient plume multiplied by an estimated groundwater velocity calculated from site specific data.

However, this approach yields only a snapshot estimate and is subject to large errors in estimating the groundwater velocity due to large spatial variation in aquifer properties. In addition, the measurements of downgradient groundwater concentrations and velocities are generally insufficient to differentiate source mass discharge from changes due to biological or chemical degradation occurring in the plume downgradient from the source zone. Further, current interpretations of standard field data typically employ numerical models with the simple input of a contaminant mass discharge rate from the NAPL source zone without an estimate of the total source mass and with mass transfer rates estimated from empirical correlation functions.

To address deficiencies in field measurements for assessing SZD functions, new approaches were field-tested at Site ST012 on the former Williams Air Force Base, Arizona (WAFB, now known as Williams Gateway Airport). In 2001, the Air Force initiated a study to evaluate remedial strategies for NAPL contamination at Site ST012 including field tests and modeling. From 2008 through 2010, the Air Force conducted and evaluated a pilot test of thermally enhanced extraction (TEE) as a suitable technology for reducing the mass and longevity of a multi-component fuel source (jet fuel) residing in the saturated zone. A rising water table (approximately four feet per year) over the last two decades created a submerged smear zone of fuel NAPL (chemicals present in the NAPL include benzene, toluene, ethylbenzene, xylenes [BTEX] and naphthalene) spanning a depth of about 75 feet and resulting in a long-term source to groundwater of a number of chemicals of concern (COCs) including benzene, naphthalene and other constituents of fuel NAPL.

The Air Force independently pursued an innovative combination of newly developed diagnostic techniques to conduct an evaluation of the benefits of partial NAPL source reduction. These included Passive Flux Meters™ (PFMs), integral pumping tests (IPTs), and modeling using the

solute transport code SEAM3D (Sequential Electron Acceptor Model, 3D transport model) with an enhanced input SZD function. SEAM3D is an advective-dispersive numerical solute transport model that simulates the full range of natural attenuation processes (biodegradation, sorption, dilution and dispersion, volatilization, and diminishing source mass discharge) in groundwater systems. SEAM3D also explicitly simulates the dissolution of a NAPL source zone based on fundamental mass transfer analyses and a calibrated SZD function for purposes of scaling the results from the TEE test scale to the entire NAPL zone at the site. Additionally, tracer tests were performed during the IPTs to characterize preferential and asymmetric groundwater flow paths.

The field measurements (IPT and PFMs) were performed both before and after the TEE pilot test within a portion of the NAPL source zone at ST012. The testing provided data related to NAPL architecture and rates of mass transfer from the NAPL to the aqueous phase. The tests measured mass transfer characteristics on length scales varying from a few feet (PFM data) to the 70-foot distance between injection and extraction wells (IPT data) within the TEE cell. Groundwater samples from multiple extraction and monitoring wells provided data on intermediate length scales. The data collected on the various scales before and after the TEE pilot test were synthesized into a working quantitative model of the NAPL architecture and mass dissolution rate for the SEAM3D enhanced SZD function.

Multi-scale field measurements during the IPT are collectively referred to as the "Mass Transfer Test" (MTT). The IPT was performed by injecting clean water in the center of the test cell and extracting groundwater from six extraction wells located on a circular periphery; although other injection-extraction configurations were possible (e.g., a single dipole with intermediate monitoring wells). The concentration of a dissolved compound increased as the water traveled through the NAPL-bearing soils to the extraction wells, controlled by the component's equilibrium solubility in water and the local mass transfer. The combined mass removal rate at the extraction wells defined a bulk mass transfer coefficient for the soil volume flushed with clean water.

Groundwater flow was assessed by injecting a bromide tracer pulse in the center well and by observing breakthrough curves at each of the monitoring wells. Tracer arrival times in monitoring wells corresponded to flow velocities at specific depths, and, when compared to the known mean groundwater velocity, provided indications of preferential and asymmetric flow. PFMs were deployed in the monitoring wells to further assess the rates of mass transfer. The PFMs provided data on the vertical distribution of contaminant and groundwater fluxes within the monitoring wells. Flux is defined as the mass of groundwater or contaminant passing through a given cross-sectional area per unit time. The mass discharge (in units of mass per time) can be calculated from flux measurements by integration of the mass flux values over the cross-sectional area of interest. Data collected during the pre- and post-TEE MTTs were interpreted using SEAM3D.

The flow chart shown in Figure ES-1 outlines the general procedure for the methodology in which results of a MTT are integrated into a numerical modeling framework to calculate the time of remediation (TOR) under various remedial scenarios. This approach seeks to circumvent the reliance (or at least reduce emphasis) on long-term source depletion data to calibrate the SZD function associated with a site solute transport model. The aim is to reduce the uncertainty associated with estimates of source and plume longevity through the direct measurement of a

bulk mass transfer coefficient, which is then used to produce more accurate modeling results of the TOR.

To our knowledge, the IPT and PFMs have not been combined previously to provide data for a mass transfer analysis with an appropriate model (see below), with the intent of leveraging the advantage of each technique. Because of the unique smear zone at Site ST012, the results are applicable to a broader class of sites than just those impacted with LNAPL, including those contaminated with DNAPLs.

<div style="border:2px solid purple; padding:10px;">

Calibrated Site Model
- Groundwater flow (*MODFLOW*)
- Solute transport & attenuation (*SEAM3D)*
- Source zone depletion (*SEAM3D)*

</div>

⬇

<div style="border:2px solid purple; padding:10px;">

Validate Source Zone Model
- Mass Transfer Tests
  - IPT with tracer
  - PFMs

</div>

⬇

<div style="border:2px solid purple; padding:10px;">

Estimate source and plume longevity under various remedial scenarios

</div>
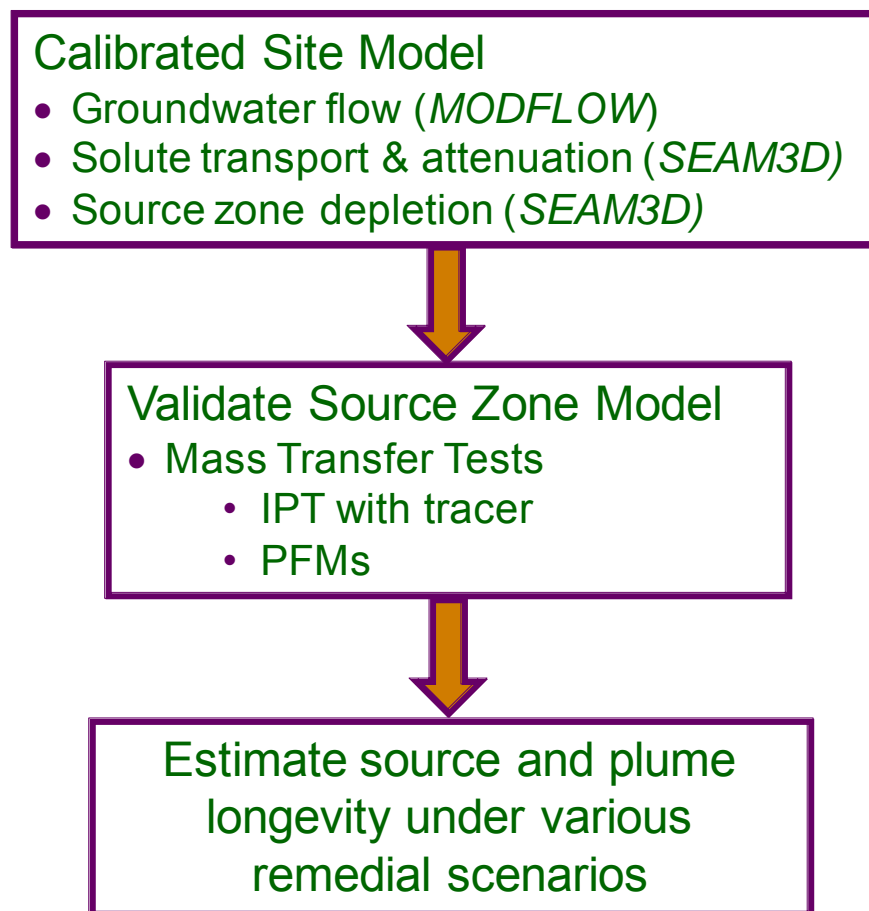
Figure ES-1. Flow chart outlining the methodology of combining mass transfer testing and source zone remediation with the SEAM3D site model to reduce uncertainty associated with the SZD function and its use in long-term simulations to estimate time of remediation.

Specific quantitative performance objectives for the methodology evaluated during this project were related to three topics:

1. Groundwater flow field through a heterogeneous source zone.

2. NAPL architecture and contaminant mass discharge in the source zone.

3. Reduction in contaminant mass discharge resulting from a reduction in NAPL mass or a change in NAPL composition.

These quantitative objectives were assessed primarily by comparing the SEAM3D numerical model results to the observed field data. Two qualitative performance objectives were evaluated, including the ease of implementing the field test procedures and the cost to perform the test.

The performance objectives, their data requirements and success criteria, and the overall evaluation of the results are summarized in Table ES-2.

Table ES-2. Performance Objectives.

Performance Objective	Data Requirements	Success Criteria	Results
Quantitative Performance Objectives			
Estimate of Source Zone Hydrogeologic Parameters	Pre- and post-TEE data: Monitoring well data in the TEE cell: ▪ Bromide tracer histories ▪ PFM alcohol depletion results ▪ Water levels Injection rate of water and extraction rate of groundwater in the TEE cell.	Average PFM velocity within a factor of two of average velocity based on injection rate. Arrival times of tracer peaks at monitoring wells within a factor of two of estimates based on PFM velocity measurements.	The success criteria were achieved for both tracer and PFM data at all monitored locations. With increasing distance from the injection well, the match with tracer data eroded as a result of bromide sensor limitations, the influence of unsteady pumping from perimeter extraction wells, and, possibly, heterogeneity not captured in the geologic model.
Estimate of Source Zone Contaminant Parameters	Pre- and post-TEE data: Mass transfer test data in the TEE cell: ▪ Hydrocarbon concentrations at monitoring wells ▪ PFM mass flux results Dissolved phase concentration data from monitoring wells in the TEE cell and near source.	Pre-TEE test: Range of results for NAPL mass within range of pre-TEE estimates derived from independent measures. Post-TEE test: Mean error between observed equilibrium source zone concentrations and simulated concentrations using SEAM3D within one order of magnitude.	The pre-TEE criterion was successfully achieved. The model also accurately captured transient and steady-state concentration responses of both benzene and toluene, ethylbenzene, and xylenes (TEX) following injection of clean water during the pre-TEE MTT. The post-TEE success criterion was met, even with variable treatment and variable NAPL composition across the test cell.

Estimate of Reduction in Contaminant Mass Discharge as a Result of Partial Source Reduction	Pre- and post-TEE data: MTT data in the TEE cell: - Hydrocarbon concentrations at extraction and monitoring wells - PFM mass flux and water velocity results - Injection and extraction rates in the TEE cell - Mass of contaminants extracted TEE Pilot Test Data - Mass of contaminants extracted during pilot test	Correlation of change in mass discharge rate between pre- and post-TEE MTTs to the measured mass removed. Mean error between observed equilibrium source zone mass discharge at extraction wells and that simulated with SEAM3D within one order of magnitude.	The post-TEE modeling of benzene concentrations and mass discharges matched nearly exactly the observed mass removed from the test cell during the TEE pilot test. The mean error between the observed equilibrium source zone mass discharge and that simulated with SEAM3D was well within one order of magnitude in the two wells closest to the injection well. The objective was achieved in the deep interval of other wells but the error exceeded one order of magnitude in the shallow screens of the three monitoring wells closest to extraction wells. The exceedances resulted from variable thermal treatment across the cell, which was not captured by the modeling assumption of uniform NAPL composition across the cell.
Qualitative Performance Objectives			
Ease of Simultaneous Implementation of an IPT and PFMs	Pre- and post-TEE data: Monitoring well data in the TEE cell: - Bromide tracer histories - Hydrocarbon concentrations in monitoring wells Injection rate of water and extraction rate of groundwater in the TEE cell.	Ease in determination of the optimal timing and duration of PFM deployment within the IPT.	This performance objective was successfully met as PFMs were not deployed until equilibrium concentrations were observed in the TEE cell. Possible skewing of PFM results by NAPL floating in the wells was mitigated by well purging and a PFM "swipe" test.

			PFM and IPT costs were readily segregated from other costs with an existing pump and treat system in place. Costs to install a temporary pump and treat system are contingent on site-specific conditions such as depth to water, contaminant, concentrations, discharge requirements, and required pumping rates.
Incremental Costs of IPT and PFM Deployment	Operational cost data.	Segregation of PFM and IPT incremental costs above those of ongoing operations.	

The success criteria for both the quantitative and qualitative performance objectives were achieved, except at three monitoring locations for the third performance objective. This variance was the result of uneven thermal treatment across the cell, which was not captured by the modeling assumption of uniform NAPL composition across the cell. Although the solute transport model (SEAM3D) can account for variability in NAPL residual saturation in space, this level of sophistication was not specified in the Demonstration Plan for this project.

To support the numerical modeling results, in particular the assumed mass transfer coefficients, a more simplistic analytical model was derived for determining bulk NAPL mass transfer coefficients from the pseudo steady-state concentration data, and these values were compared to values calculated from correlations in the literature based on flow through a uniformly distributed NAPL. This large difference was expected as the heterogeneities in a real subsurface tend to discourage contact between flowing water and residual NAPL, whereas the flow is forced through the residual NAPL in laboratory column studies. These data suggest that literature correlations based on a uniformly distributed NAPL in a homogeneous soil would overpredict mass transfer in heterogeneous field settings by two to three orders of magnitude.

The average bulk mass transfer coefficients estimated from the analytical model range from 0.0076 to 0.104 d^{-1}. The values employed in the numerical modeling ranged from 0.05 to 0.5 d^{-1}, and therefore may have modestly overpredicted the mass dissolution rate in the source zone, but they were of the same order of magnitude. Overall, the MTTs and associated modeling were successfully able to directly measure a bulk mass transfer coefficient and relate the source mass to the mass discharge, which resulted in a more accurate SZD function for estimating source persistence and the benefits of partial source reduction for reduction of the TOR.

Using the steady-state site solute transport model as a starting point, simulations were conducted to determine which model input parameters associated with the source zone exerted the greatest impact on time of remediation estimates for Site ST012. Results of the sensitivity analysis are summarized in Figure ES-2 using sensitivity coefficients for three parameters: 1) NAPL mass, 2) percent benzene in the multi-component source, and 3) NAPL mass transfer coefficient (K^{NAPL}). The results show the relative importance of each input parameter in terms of controlling TOR for this specific site model. Results of this analysis for this site show the least sensitivity to K^{NAPL}. However, historically K^{NAPL} has been the most challenging parameter to measure in field settings, and attempts at estimating field-scale K^{NAPL} have relied upon very long-term

groundwater monitoring data (e.g., 20 to 40 years of data), which is costly to obtain. The methodology evaluated in this demonstration thus improves the accuracy of the model parameter that has historically been the most difficult and costly to estimate.
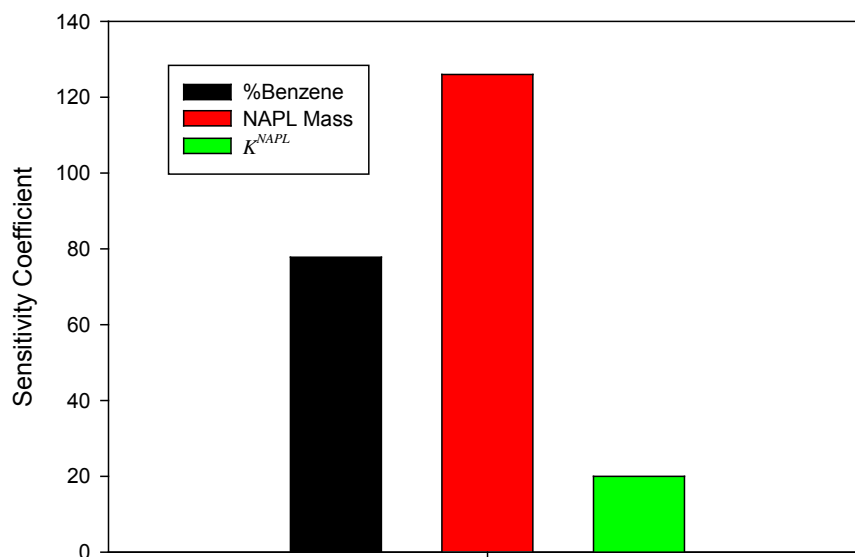
Figure ES-2. Sensitivity analysis for time to reach 5 µg/L of benzene at a specific point of compliance at Site ST012 based on MNA only and natural source depletion.

The MTTs and associated modeling were successfully able to measure directly a bulk mass transfer coefficient and relate the absolute source mass to the mass discharge, which resulted in a more accurate SZD function for estimating of source persistence and the result of partial source reduction.

Costs for implementing the methodology at Site ST012 were analyzed, and a cost model was developed that incorporated the elements needed to implement the methodology at other sites. A primary determinant for the total cost to perform the testing is the existence of operating infrastructure to pump and treat relatively large quantities of contaminated groundwater for days or weeks. If pump-and-treat is active at a facility and monitoring wells exist within the source area, or if the installation of such a system is anticipated as part of the site remediation, the cost of performing the mass transfer testing is almost solely for the analytical data. Sites requiring such infrastructure usually involve a NAPL source and involve pump-and-treat as part of more intensive technologies such as electrical resistance heating, steam injection, surfactant floods, recirculating chemical oxidation, etc. The costs for data analyses in the form of modeling to determine the source strength and mass transfer characteristics are less variable than the field implementation; however, the modeling costs do vary with the complexity of the site, the intensity of data collection, and the experience of the modeler.

If pump-and-treat is active at a facility and monitoring wells exist within the source area, or if the installation of such a system is anticipated as part of the site remediation, the costs of the methodology are almost solely for the analytical data and associated analyses and are a small increment of site operating costs in comparison to the scientifically defensible data collected.

This methodology can be applied at sites with LNAPL or DNAPL and can improve the scientific defensibility of decisions regarding when and to what extent active source remediation efforts should be pursued.

1.0   INTRODUCTION

1.1   BACKGROUND

1.1.1   *Motivation*

The Department of Defense (DoD) needs improved methods for estimating the mass of non-aqueous phase liquids (NAPLs) in subsurface environments contaminated from past releases of these compounds. In addition, predicting their persistence into the future, and the impact of NAPL source reduction on the time to achieve remedial action objectives (RAOs) at compliance locations remains a significant challenge at these sites. Data are required to support scientifically defensible decisions regarding when and to what intensity active remediation efforts should be pursued at NAPL-contaminated sites before transition to passive remedies such as natural attenuation. The lack of accurate and technically defensible estimates of NAPL source mass and persistence is a major obstacle for determining the optimal path to site closure at most DoD facilities impacted by NAPLs. For fuel NAPLs (i.e., petroleum hydrocarbons), relying on monitored natural attenuation (MNA) or natural attenuation (NA) may not be acceptable to regulators because of the long duration (>100 years) of attenuation processes (e.g., dissolution, dilution and degradation) to achieve RAOs. The primary objective of this project was to evaluate a methodology to improve decision-making on the extent of source remediation required to meet RAOs at both light NAPL (LNAPL) and dense NAPL (DNAPL) impacted sites.

Current techniques to estimate the persistence of NAPL sources are very uncertain without better specification of the mass of NAPL, the constituents of the NAPL, the NAPL "architecture" (i.e., the geometry of the NAPL distribution in the subsurface), and the dissolution rate of NAPL components in groundwater (referred to collectively in this report as the source zone depletion [SZD] function). The traditional approach to characterizing the SZD function involves estimation of NAPL dissolution rates from concentration measurements in discrete locations in the downgradient plume multiplied by an estimated groundwater velocity calculated from site specific data.

However, this approach yields only a snapshot estimate and is subject to large errors in estimating the groundwater velocity due to large spatial variation in aquifer properties. In addition, the measurements of downgradient groundwater concentrations and velocities are generally insufficient to differentiate source mass discharge from changes due to biological or chemical degradation occurring in the plume downgradient from the source zone. Further, current interpretations of standard field data typically employ numerical models with the simple input of a contaminant mass discharge rate from the NAPL source zone without an estimate of the total source mass and with mass transfer rates estimated from empirical correlation functions.

The relationship between the mass of NAPL in the source zone and the mass dissolution rate is the subject of current academic research. The motivation for this project was to demonstrate a methodology based on the unique combination of novel field measurement techniques with associated modeling based on field scale data. This methodology is then used to establish a site specific relationship between source mass and mass discharge from the source zone. A measurable relationship between these two parameters yields more accurate SZD functions for

estimating source persistence and the impacts of partial source reduction on the time of remediation (TOR) to achieve the site RAOs.

1.1.2   *Site ST012*

To address deficiencies in field measurements for assessing SZD functions, new approaches were field-tested at Site ST012 on the former Williams Air Force Base, Arizona (WAFB, now known as Williams Gateway Airport). In 2001, the Air Force initiated a study to evaluate remedial strategies for NAPL contamination at Site ST012 including field tests and modeling. From 2008 through 2010, the Air Force conducted and evaluated a pilot test of thermally enhanced extraction (TEE) as a suitable technology for reducing the mass and longevity of a multi-component fuel source (jet fuel) residing in the saturated zone. A rising water table (approximately four feet per year) over the last two decades created a submerged smear zone of fuel NAPL (chemicals present in the NAPL include benzene, toluene, ethylbenzene, xylenes [BTEX] and naphthalene) spanning a depth of about 75 feet and resulting in a long-term source of a number of chemicals of concern (COCs) including benzene, naphthalene and other constituents of fuel NAPL to groundwater at a mass discharge rate resulting in groundwater concentrations exceeding federal Maximum Contaminant Levels (MCLs) and State of Arizona Aquifer Water Quality Standards (AWQSs) for the relevant COCs.

 Previous studies indicated that these RAOs would not be achieved within several hundred years if the final remedial action was MNA. Because this long time frame was unacceptable to the lead regulators, the Air Force agreed to evaluate additional source removal options. At ST012, the previous Record of Decision (ROD) will be amended through implementation of the Comprehensive Environmental Response, Compensation, and Liability Act (CERCLA) ROD Amendment (RODA) procedures. The previous ROD included pump-and-treat via horizontal wells as a component of the remedy, but this technology was abandoned with the failure of the horizontal wells to produce groundwater at appreciable rates (BEM Systems, 2010).

The RODA will address the Remedial Action Objectives (RAOs) for the ST012 saturated zone remedy, and will specify the COCs, the remedial action levels to be achieved by the remedy, and the points of RAO compliance for assessing the performance of any remedy.

1.1.3   *Technology Overview*

In 2001, when the Air Force initiated the evaluation of remedial strategies for depletion of the NAPL contamination at Site ST012, diagnostic tools to assess source longevity were inadequate for making scientifically defensible decisions on whether or not full-scale remediation of the NAPL source zones was needed. Because of the uncertainty of existing tools for characterizing SZD functions, the Air Force independently pursued an innovative combination of newly developed diagnostic techniques to conduct an evaluation of the benefits of partial NAPL source reduction. This combination of field measurements was applied before and after the pilot test of TEE to support decisions on whether or not future site-wide implementation of partial source reduction using the TEE technology would be required to reduce the timeframe for MNA to attain RAOs.

TEE is a technology that combines soil vapor extraction (SVE), groundwater and NAPL extraction via pumping, and injection of steam, air and/or a mixture of air and steam over

specified time intervals. Initially, groundwater pumping, NAPL extraction, and SVE are applied. Steam and/or air are then injected to heat the saturated subsurface zone and enhance the recovery of mobile NAPL and dissolved contaminants. With the heating, vapor concentrations of the COCs increase, providing an increase in mass removal of the COCs via SVE. After steam injection, a mixture of air and steam are injected to continue contaminant recovery at elevated temperatures and to continue the heating of lower permeability saturated soils not subject to advective mass transfer.

The objective of TEE is to maximize recovery of NAPL residing in permeable intervals and preferentially remove the more volatile, soluble components (e.g., benzene) from residual NAPL and to remove NAPL constituents present in less permeable zones within the source zone based on the impacts of soil heating. The performance of the TEE pilot test at Site ST012 yielded a measurable reduction in NAPL volume and a substantial depletion of the most soluble components (BEM Systems, 2010). The result was a decrease in the mass transfer rate of COCs to groundwater in most of the target aquifer zone and a significant reduction in the groundwater concentrations of NAPL components within the TEE target volume.

The impact of partial source reduction by TEE at ST012 on the NAPL dissolution rate was evaluated by a unique combination of field measurements including Passive Flux Meters™ (PFMs), integral pumping tests (IPTs), and modeling using the solute transport code SEAM3D (Sequential Electron Acceptor Model, 3D transport model) with an enhanced input SZD function. SEAM3D is an advective-dispersive numerical solute transport model that simulates the full range of natural attenuation processes (biodegradation, sorption, dilution and dispersion, volatilization, and diminishing source mass discharge) in groundwater systems (Waddill and Widdowson, 1998; Waddill and Widdowson, 2000). SEAM3D also explicitly simulates the dissolution of a NAPL source zone based on fundamental mass transfer analyses, and under the Strategic Environmental Research and Development Program (SERDP) Project ER-1349, the SEAM3D NAPL Package (version 2) was recently updated to include a subroutine that incorporates a calibrated SZD function for purposes of scaling the results from the TEE test scale to the entire NAPL zone at the site. Additionally, tracer tests were performed during the IPTs.

A brief overview of these technologies is provided here; detailed background and description is provided in Section 3.1. The field measurements (IPT and PFMs) were performed both before and after the TEE pilot test within a portion of the NAPL source zone at ST012. The testing provided data related to NAPL architecture and rates of mass transfer from the NAPL to the aqueous phase. "NAPL architecture" is a term applied to characterizing the relative amounts of NAPL present in pools versus distributed vertical ganglia and present in coarse (permeable) versus fine (less permeable) aquifer material. The mass dissolution rates of NAPL components are dependent upon the NAPL contact area with mobile groundwater; hence ganglia generally yield a higher dissolution rate than the same volume of NAPL existing as a pool. The tests measured mass transfer characteristics on length scales varying from a few feet (PFM data) to the 70-foot distance between injection and extraction wells (IPT data) within the TEE cell. As described in Section 3.1, groundwater samples from multiple extraction and monitoring wells provided data on intermediate length scales. The data collected on the various scales before and after the TEE pilot test were synthesized into a working quantitative model of the NAPL architecture and mass dissolution rate for the SEAM3D enhanced SZD function.

Multi-scale field measurements during the IPT are collectively referred to as the "Mass Transfer Test" (MTT). The IPT was performed by injecting clean water in the center of the test cell and extracting groundwater from six extraction wells located on a circular periphery; although other injection-extraction configurations were possible (e.g., a single dipole with intermediate monitoring wells). The concentration of a dissolved compound increased as the water traveled through the NAPL-bearing soils to the extraction wells, controlled by the component's equilibrium solubility in water and the local mass transfer. The combined mass removal rate at the extraction wells defined a bulk mass transfer coefficient for the soil volume flushed with clean water. Concentrations of fuel components were also measured at 12 monitoring wells located within the TEE cell at varying distances from the center injection well. The 12 wells were screened over two vertical soil horizons at six locations.

Groundwater flow was assessed by injecting a bromide tracer pulse in the center well and by observing breakthrough curves at each of the monitoring wells. Tracer arrival times in monitoring wells corresponded to flow velocities at specific depths, and, when compared to the known mean groundwater velocity, provided indications of preferential and asymmetric flow. PFMs were deployed in the monitoring wells to further assess the rates of mass transfer. The PFMs provided data on the vertical distribution of contaminant and groundwater fluxes within the monitoring wells. Flux is defined as the mass of groundwater or contaminant passing through a given cross-sectional area per unit time. The mass discharge (in units of mass per time) can be calculated from flux measurements by integration of the mass flux values over the cross-sectional area of interest. Data collected during the pre- and post-TEE MTTs were interpreted using SEAM3D.

The flow chart shown in Figure 1-1 outlines the general procedure for the methodology in which results of a MTT are integrated into a numerical modeling framework to calculate the time of remediation (TOR) under various remedial scenarios. This approach seeks to circumvent the reliance (or at least reduce emphasis) on long-term source depletion data to calibrate the SZD function associated with a site solute transport model. The aim is to reduce the uncertainty associated with estimates of source and plume longevity through the direct measurement of a bulk mass transfer coefficient, which is then used to produce more accurate modeling results of the TOR. Because of the unique smear zone at Site ST012, the results are applicable to a broader class of sites than just those impacted with LNAPL, including those contaminated with DNAPLs.

```
┌─────────────────────────────────────────┐
│  Calibrated Site Model                   │
│   • Groundwater flow (MODFLOW)           │
│   • Solute transport & attenuation (SEAM3D) │
│   • Source zone depletion (SEAM3D)       │
└─────────────────────────────────────────┘
                    │
                    ▼
┌─────────────────────────────────────────┐
│  Validate Source Zone Model              │
│   • Mass Transfer Tests                  │
│        • IPT with tracer                 │
│        • PFMs                            │
└─────────────────────────────────────────┘
                    │
                    ▼
┌─────────────────────────────────────────┐
│  Estimate source and plume               │
│  longevity under various                 │
│  remedial scenarios                      │
└─────────────────────────────────────────┘
```
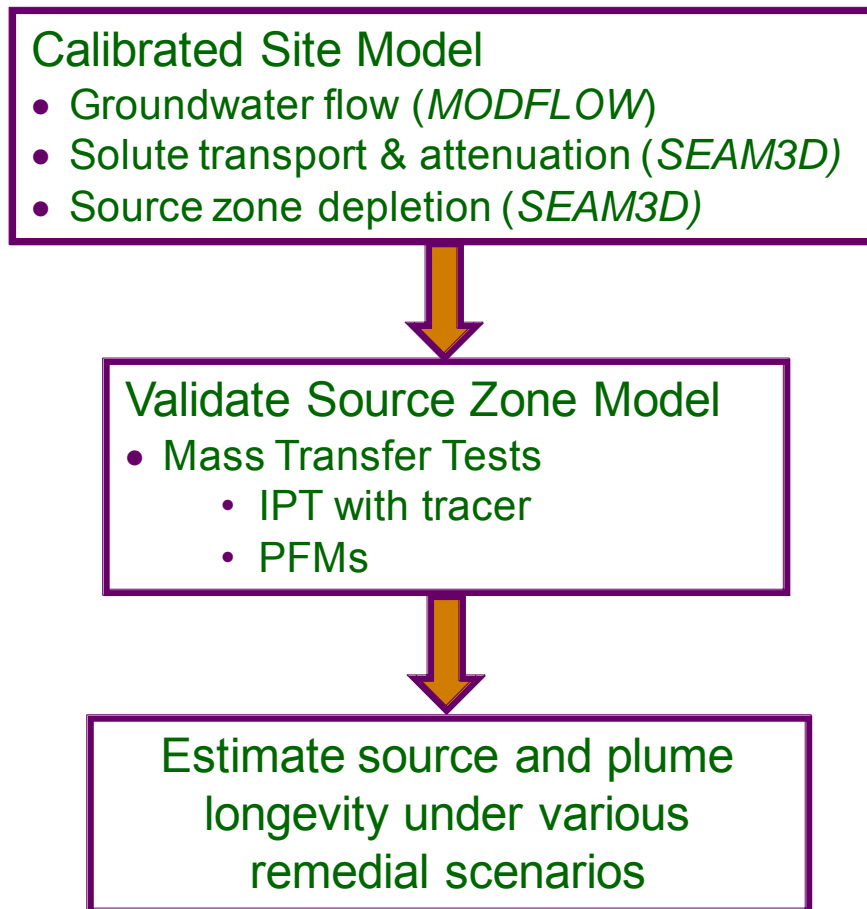
Figure 1-1. Flow chart outlining the methodology of combining mass transfer testing and source zone remediation with the SEAM3D site model to reduce uncertainty associated with the SZD function and its use in long-term simulations to estimate time of remediation.

1.2 OBJECTIVE OF THE DEMONSTRATION

The Air Force intended to generate data that could be used for decision making based on improved characterization of the NAPL contamination at ST012 through the analysis of the pre- and post-TEE MTTs. The MTTs and TEE pilot test were performed by the Air Force's contractor, BEM Systems, Inc. The primary ESTCP activities were in support of the post-TEE mass transfer test and development and evaluation of the proposed methodology for application to other NAPL impacted sites.

The uncertainty of estimating the impact of NAPL depletion on duration of cleanup has often resulted in early reliance on containment remedies (USEPA, 2003). Hence, ESTCP funds were used to perform the following tasks:

1. Evaluate a generalized methodology for assessing the benefits of NAPL source depletion with a solid scientific basis using the innovative tools employed at ST012;

2. Validate key elements of the methodology via peer review;

3. Document costs and estimate the costs of application at other sites; and

4. Disseminate the results of the study throughout the Air Force and other DoD entities (i.e., technology transfer).

1.3 REGULATORY DRIVERS

Aqueous solubilities of common NAPL constituents found at DoD facilities often greatly exceed drinking water standards including federal MCLs. Table 1-1 lists federal MCLs for selected common COCs found in the petroleum-based NAPL (primarily jet fuel) at Site ST012. Mass dissolution of fuel components from NAPL can result in concentrations at locations near the source zone persistently above the MCLs for hundreds of years if left untreated.

Table 1-1. Federal Maximum Contaminant Levels (MCLs) for Selected NAPL Constituents.

Constituent	Federal MCL (µg/L)
Benzene	5
Toluene	1,000
Ethylbenzene	700
Total Xylenes	10,000
Naphthalene	0.14[1]
Trimethylbenzenes	12-15[1]

Source for MCLs: http://www.epa.gov/safewater/contaminants/index.html#organic.
[1] EPA Region IX Screening Levels for residential tap water.

2.0   SITE DESCRIPTION

2.1   SITE LOCATION AND HISTORY

Originally occupying 4,042 acres, WAFB was constructed in Mesa, Arizona in 1941 as a flight training school. See Figure 2-1 for the location of WAFB and ST012. Throughout its history, pilot training was the primary mission of WAFB. A wide variety and large number of aircraft were based at WAFB, including prop-driven and jet aircraft. Surrounding land uses include the General Motors Desert Proving Ground, irrigated agricultural land, and commercial and residential developments.

WAFB was placed on the National Priorities List (NPL) in 1989 and officially closed in September 1993. The WAFB Disposal and Reuse Final Environmental Impact Statement was filed with the Environmental Protection Agency (EPA) in June 1994. The Air Force Base Conversion Agency (now known as the Air Force Real Property Agency [AFRPA]) identified and assigned the priority of the disposal and reuse of each parcel based on market demand and the reuse goals of the local community. Within WAFB, Site ST012 is the location of the former liquid fuels storage area, which encompasses approximately 13 acres within WAFB (Figure 2-1). Fueling operations were conducted at the base from 1941 until 1991.

A substantial portion of the remaining cleanup at WAFB addresses fuel releases at ST012. Soil and groundwater at ST012 have been affected by releases of JP-4 and AVGAS. These releases are attributable to multiple documented fuel releases between 1977 and 1989 and other undocumented releases during base operations over a 50-year period. All underground storage tanks (USTs) and the associated fuel distribution lines were removed from ST012 in early 1991.

Figure 2-1. Location of the Former Williams AFB and Site ST012.

The TEE pilot test configuration was a circular treatment cell with injection of steam and air in central injection wells and extraction of contaminants at perimeter extraction wells. The location of the circular TEE test cell within Site ST012 is illustrated in Figure 2-2. The test cell was located within the boundaries of historical detections of NAPL in monitoring wells. The site map shows 56 groundwater monitoring wells, 33 SVE wells, 12 groundwater extraction wells, two injection wells, and four soil vapor monitoring points. The two abandoned horizontal wells are also indicated on Figure 2-2.

TEE Cell
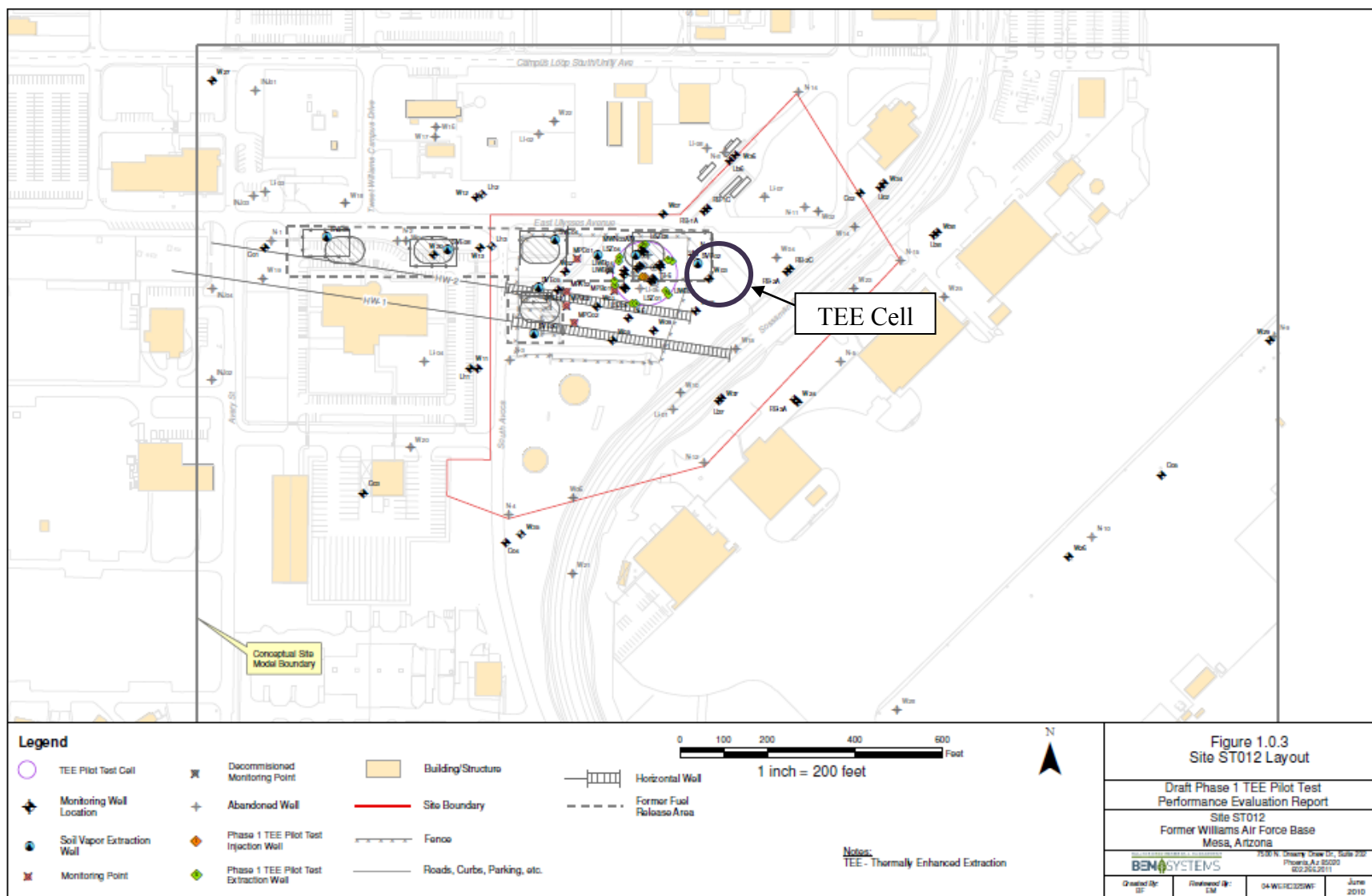
Figure 2-2. Location of the TEE Test Cell within Site ST012.

2.2   SITE GEOLOGY/HYDROGEOLOGY

An extensive conceptual site model (CSM) describing the site physical conditions of ST012 was developed by the Air Force and is available as Appendix A to the ST012 TEE Pilot Test Performance Evaluation Report (BEM Systems, 2010). This CSM provides a compilation of data from previous site investigations and confirms the rise in groundwater that created the extensive smear zone of NAPL contamination. The following discussion briefly summarizes relevant information presented in the CSM.

The CSM vertical profile (0 – 245 feet below ground surface [ft bgs]) is a heterogeneous mix of alternating fine-grained and coarse-grained units (Figure 2-3). Coarse-grained units range in thickness from less than one foot to more than 20 feet, and a few of the larger units appear to be continuous across the site. The geologic materials in the saturated zone have been subdivided into four main hydrostratigraphic units:

- The Upper Water Bearing Zone (UWBZ), extending vertically from the water table (currently at approximately 160 ft bgs) to 195 ft bgs;

- The Low Permeability Zone (LPZ), extending from approximately 195 ft to 210 ft bgs;

- The Lower Saturated Zone (LSZ) extending from approximately 210 ft to 240 ft bgs; and

- The Aquitard, occurring at approximately 240 ft bgs.

The LPZ effectively separates the deeper LSZ from the shallower UWBZ with respect to remediation. Pumping tests have shown the two zones act independently on the timescale of remediation. As a result of this independence, the MTT described previously was applied in each zone.

The water table beneath ST012 has been rising at an average rate of about 3.4 feet per year for the last two decades and is expected to continue to do so for some period of time, with the potential for further degradation of groundwater from fuel constituents currently in the vadose zone. In the 1960s and early 1970s, regional groundwater levels declined due to extensive withdrawal and to diversion and/or retention of major sources of groundwater recharge for flood control (Appendix A, BEM Systems, 2010). During the fuel releases at Site ST012, the estimated low level for the water table was 232 ft bgs. Water level data for wells located on and near the former WAFB show groundwater levels have been rising steadily since about 1978. Groundwater within the LSZ, once apparently unconfined, now appears to be under semiconfined conditions.
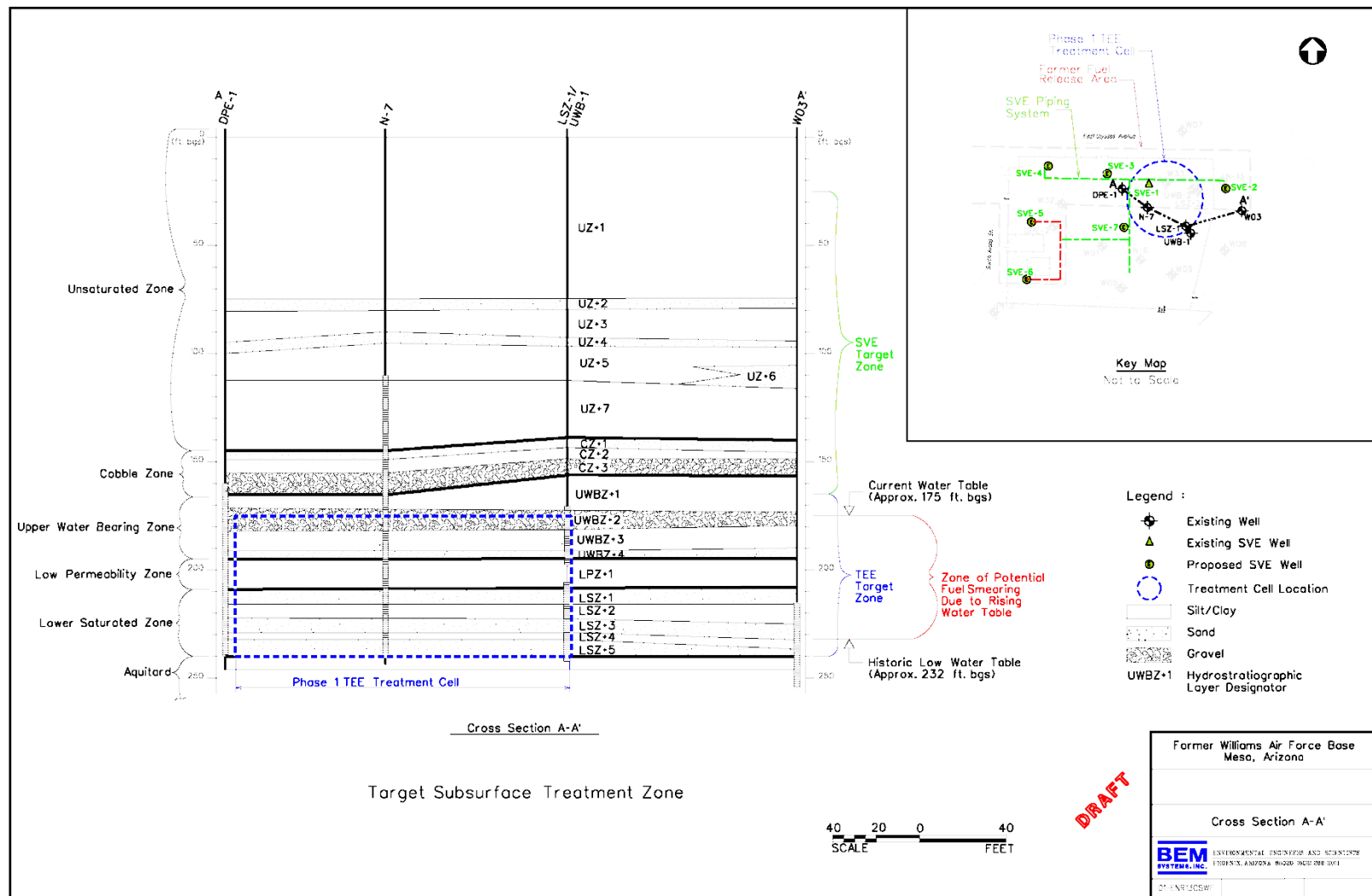
Figure 2-3. Representative Geologic Cross-Section at Site ST012.

Before the start of the TEE pilot test (August 2008), the rising water table entered the silt/clay soil interval labeled UWBZ+1 and potentially reached the bottom of the Cobble Zone, which overlies the UWBZ at a depth of about 159 ft bgs (see Figure 2-3 and Figure 2-4). The fine-grained unit UWBZ+1 likely created semiconfined conditions in the UWBZ similar to the LSZ. Steam injection into the UWBZ was observed during the pilot test to travel predominantly in a horizontal direction, further substantiating the semiconfined condition of the UWBZ.

Conditions in the UWBZ and LSZ differed in that soils in the UWBZ were generally of a lower permeability than the LSZ, and the UWBZ lacked a dominant permeable zone like LSZ+5 (Figure 2-3).

2.3   CONTAMINANT DISTRIBUTION

Details of previous site investigations can be found in Appendix A of the TEE Pilot Test Work Plan (BEM Systems, 2007). Select results of previous site investigations are attached as Appendix C to this report, Site ST012 Investigation Results.

Fuel contamination, including mobile and immobile NAPL present in the saturated zone, serves as a continuing source for dissolved-phase groundwater contamination. The total mass and distribution of NAPL in the saturated zone is not known; however, field evidence suggests NAPL is smeared across all but the lower 10 to 15 feet of the LSZ (as a result of initial fuel infiltration and the subsequent rising water table from an estimated low of 232 ft bgs). NAPL may be preferentially present in the following subsurface settings:

- Trapped in the upper portions of coarse-grained layers underlying fine-grained layers;

- Within fine-grained layers, particularly near interfaces with coarse-grained layers.

The TEE pilot test was designed to address groundwater impacted by smeared fuel contamination in the saturated zone, comprised of the UWBZ, LPZ, and LSZ (Figure 2-4). The TEE test cell was located within the lateral footprint known to be contaminated with smeared NAPL. The results of the TEE pilot test can be found in the TEE Performance Evaluation Report (BEM Systems, 2010).

As indicated in Figure 2-4, the UWBZ was spanned by a single screen in each of the monitoring wells from about 170 to 195 ft bgs. These wells are referred to as the "A-horizon" wells. The LSZ was divided into two subunits with separate monitoring well screens for each. The fine-grained soils are found in the upper two thirds of the LSZ (referred to as the "B-horizon" on Figure 2-4) and were monitored with screens that extended from about 205 to 220 ft bgs. The dominant coarse interval found at bottom of the LSZ was referred to as the "C-horizon" and is shown on Figure 4-5 ("LSZ+5" on Figure 2-3). C-horizon screens were located from about 230 feet to 245 ft bgs, extending into the underlying Aquitard. The C-horizon was found to contain very little residual NAPL as compared to the A- and B-horizons; however, this interval is the most transmissive. Figures in Appendix C illustrate the placement of the TEE test cell within the historic boundaries of detected NAPL and the interpreted plume of dissolved benzene in the C-, B- and A-horizons, respectively.
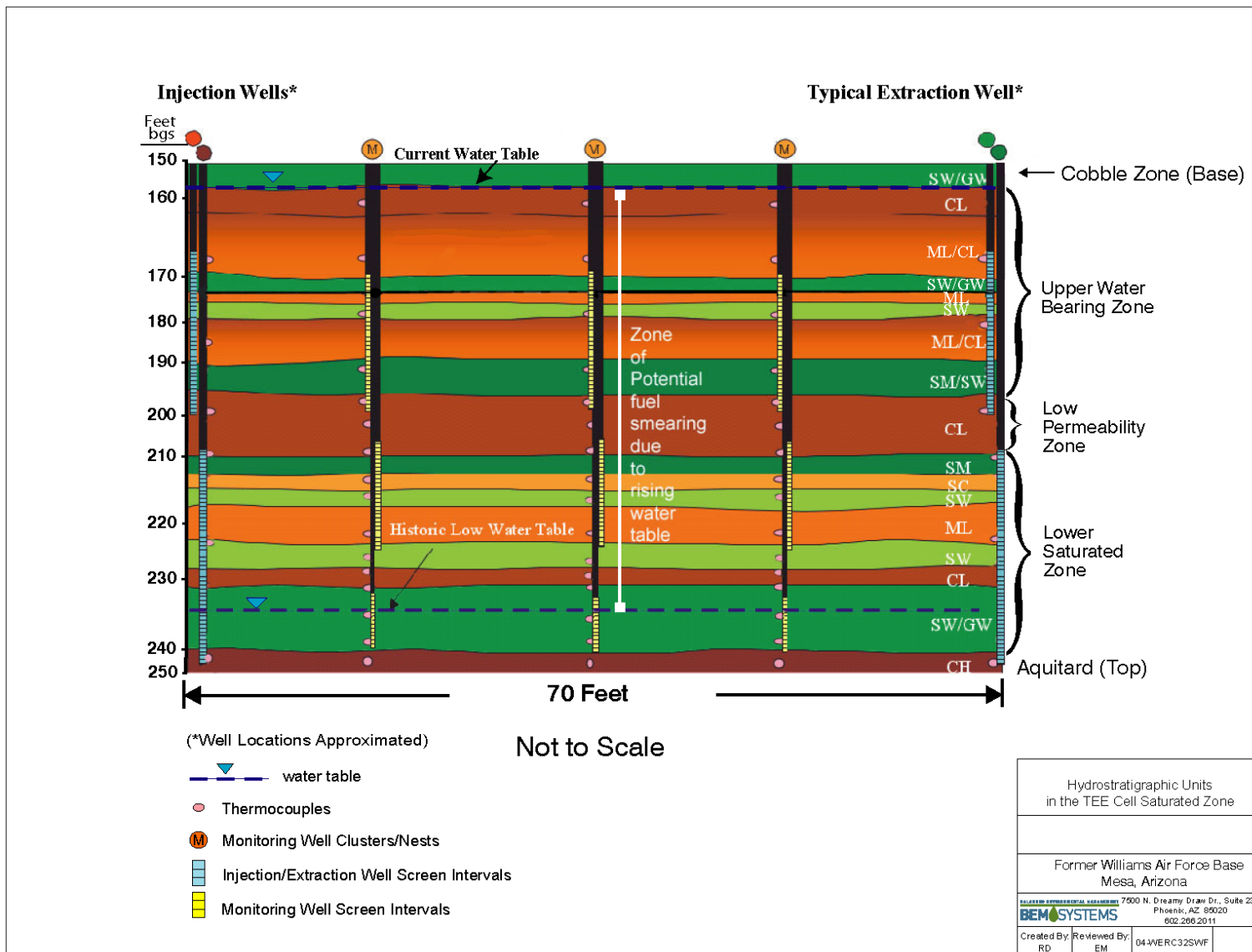
Figure 2-4. Cross-Section with Zone of Smeared NAPL.

3.0   TECHNOLOGY

As described in Section 1.0, the Air Force has independently pursued development of a MTT to provide parameters that define the SZD function quantitatively at Site ST012 in sufficient detail to reduce the uncertainty in site-specific estimates of the TOR and subsequent remedial decisions on the extent of NAPL source depletion required. The measurements were performed both before and after a pilot test of TEE within a portion of the source area at ST012, providing a measured mass removed and the resulting change in the mass discharge rate. Typically, IPTs and PFMs are applied downgradient from a NAPL zone, but this novel application within the source zone was intended to define the SZD term in greater detail. To our knowledge, the IPT and PFMs have not been combined previously to provide data for a mass transfer analysis with an appropriate model (see below), with the intent of leveraging the advantage of each technique.

3.1   TECHNOLOGY DESCRIPTION

The MTT within the source zone sought to generate data suitable for estimating NAPL mass and describing the source zone function for alternative NAPL architectures (e.g., ganglia versus pooled distribution of NAPL) in the source zone. For such estimates, mass transfer coefficients specific to the NAPL architecture must be determined. Appendix B describes the individual elements of the MTT, the unique characterization of NAPL obtained from the approach, and the calibration of the SZD function using the model SEAM3D. The MTT is briefly summarized in this section.

The Mass Transfer Test: Integral Pumping Test with Passive Flux Meters Deployed in the Source Zone

At Site ST012, IPTs were implemented in the portion of the source zone where the TEE pilot test was performed and included tracer testing and PFM deployment. The IPT was performed by injecting clean water in the center of the test cell and extracting on the periphery through six extraction wells. A pulse of bromide tracer was introduced to assess the flow velocities. PFMs were installed in 12 monitoring wells within the test cell after the flows and concentrations had stabilized in response to the steady central water injection. The tests were performed both before and after the TEE pilot test, although conditions were not identical between the two tests.

**Figure 3-1. Conceptual Application of IPT and PFMs.
Circles represent concentration measurements in groundwater samples from monitoring wells along the groundwater flow path.**

The conceptual cross-section of the MTT illustrated in Figure 3-1 shows clean water traveling through soil containing residual NAPL with extraction at the periphery of the NAPL contamination. As the water travels through the NAPL zone, contaminants are dissolved into the flowing water according to groundwater flow paths, the architecture of the residual NAPL and the rate of mass transfer. Measurements of the groundwater flow rate and concentrations at extraction after a complete pore volume sweep yield a pseudo-steady state mass dissolution rate for this imposed flow condition. If the imposed flow rate is low, the water may become saturated

with dissolved contaminant yielding no information on the rates of mass transfer beyond such saturation. This condition is labeled "Low Flow" in Figure 3-1. A higher flow which does not become saturated is also illustrated in Figure 3-1 and labeled "Desired Flow." Concentrations measured in intermediate monitoring well screens provide mass dissolution rates for horizontal subsets of the soil volume. Arrays of PFMs deployed in the monitoring wells can further segregate and refine the concentration and flow data vertically. An advantage of the PFMs for this application over other vertically discrete sampling devices is the additional capability to measure groundwater fluxes allowing contaminant mass fluxes, not just concentrations, to be measured as a function of depth.

The MTT provides dynamic data more suitable to transient SZD function evaluation than the traditional approach of monitoring relatively static groundwater concentrations downgradient of a source coupled with water level-derived estimates of groundwater velocity. The combined application of the IPT and PFMs in the source zone during the MTT has significant potential to improve the accuracy of estimates of vertical and horizontal NAPL distribution and mass discharge. Data analysis is discussed in Sections 5.0 and 6.0.

SEAM3D with Enhanced Source Zone Depletion (SZD) Function

A major task within this ESTCP effort was to validate the use of field-scale bulk mass transfer coefficients in SZD functions for estimating source persistence and the impacts of partial source reduction on plume longevity and evaluate the methodology's application to other sites contaminated with both light and dense NAPL. The data analysis involved varying the bulk mass transfer coefficient in the SZD function described previously and comparing groundwater concentrations calculated with the solute transport model SEAM3D to measured groundwater concentrations. A detailed description of the application of SEAM3D for this purpose is provided in Appendix B.

3.2   TECHNOLOGY DEVELOPMENT

Technology development was not conducted prior to the field demonstration as part of this ESTCP project, but, as described above, elements of the technology were developed during previous SERDP and ESTCP projects. Results of these projects are documented in the corresponding SERDP and ESTCP reports.

Laboratory-based studies to develop field-scale mass transfer coefficients applicable to the modeling of NAPL sources were funded by SERDP (Illangasekare et al., 2006). The ESTCP Project at Site ST012 is roughly an extension of this laboratory work to the field scale. PFMs were the subject of a previous ESTCP effort (Project CU-0114) and were demonstrated and validated at a number of field sites (Hatfield et al., 2004). The first version of the SEAM3D NAPL Package was developed through SERDP project CU-1062. The code has been enhanced over time, including improvements to the NAPL Package and the inclusion of physically-based attenuation mechanisms under SERDP project ER-1349.

3.3 ADVANTAGES AND LIMITATIONS OF THE TECHNOLOGY

Detailed listings of the advantages and limitations of IPTs, PFMs, and SEAM3D are provided in Appendix B.

Table 3-1 lists the SEAM3D input parameters required for simulating the MTTs and a brief description of how the values were determined during this ESTCP project. These parameters are described in detail in Appendix B.

Table 3-1. SEAM3D Mass Transport and NAPL Mass Transfer Parameters.

Parameter	Method for Determining	Source of Data
$q(x,y,z)$ = Darcy velocity distribution	Matching flow conditions observed during MTTs using MODFLOW2000.	Injection and extraction rates in the TEE cell; Hydraulic head at wells; Hydraulic conductivity and θ.
α_L/α_T = Dispersivities	Matching observed tracer response.	Tracer concentrations at wells.
C_i^{eq} = aqueous solubility ρ_i = mass density ω_i = molecular weight	Known properties	Chemistry handbooks.
$M(x,y,z)$ = NAPL concentrations m_i = mass fractions	Direct input of observed spatial distributions of NAPL mass; Matching pre-MTT volatile organic compound (VOC) concentration time series using SEAM3D	Pre-MTT source zone characterization; Historical VOC concentration data and NAPL composition at monitoring wells.
k^{NAPL} = field-scale mass transfer coefficient	Verify initial condition by simulating pre-MTT VOC concentration time series using SEAM3D; Matching pre-TEE MTT VOC data at wells using SEAM3D.	Initial estimate from Park and Parker (2005); Historical VOC concentration data at monitoring wells; MTT test data.

The overall methodology developed herein is an innovative combination of field measurements on various scale lengths including PFMs and IPTs with a bromide tracer (the MTT), and modeling using SEAM3D with an enhanced input SZD function.

Primary advantages of the overall methodology are as follows:

- It provides a robust and defensible testing and model for evaluating multiple scenarios of various magnitudes of source zone reduction (i.e. partial source depletion) and the impact on plume longevity in support of decision making with respect to meeting site-specific RAOs.

- This methodology represents a novel approach for estimating and constraining model input parameters that result in more accurate predictions of source depletion and plume longevity. Typically, the source term for site models is calibrated to historical data sets without any direct measurement of source parameters (e.g., field-scale mass transfer coefficient). Through application of the source zone model to data generated through the MTTs, uncertainty in estimating the time of remediation (i.e., time to reach compliance) can be significantly reduced.

- Another advantage of the overall technology is cost savings through leveraging site assets and completed modeling studies. Specifically, existing site infrastructure (pumping/injection and monitoring wells) may be adapted and utilized for MTTs. Well-documented site models for groundwater flow and solute transport may serve as a starting point for implementing SEAM3D and updating the site model for estimates of the TOR for a range of points of compliance.

4.0 PERFORMANCE OBJECTIVES

Specific quantitative performance objectives for the methodology evaluated during this project were related to following three topics:

1. Groundwater flow field through a heterogeneous source zone.

2. NAPL architecture and contaminant mass discharge in the source zone.

3. Reduction in contaminant mass discharge resulting from a reduction in NAPL mass or a change in NAPL composition.

These quantitative objectives were assessed primarily by comparing the SEAM3D numerical model results to the observed field data. Two qualitative performance objectives were evaluated, including the ease of implementing the field test procedures and the cost to perform the test.

Performance objectives for evaluating the MTT are summarized in Table 4-1 and include the three quantitative objectives and two qualitative objectives described above. A synopsis of their evaluation is provided in this section, and further details are provided in Section 6.0.

The success criteria for both the quantitative and qualitative performance objectives were achieved, except at three monitoring locations for the third performance objective. This variance was the result of uneven thermal treatment across the cell, which was not captured by the modeling assumption of uniform NAPL composition across the cell. Although the solute transport model (SEAM3D) can account for variability in NAPL residual saturation in space, this level of sophistication was not specified in the Demonstration Plan and associated field measurements for this project. Overall, the MTTs and associated modeling were successfully able to directly measure a bulk mass transfer coefficient and relate the source mass to the mass discharge, which resulted in a more accurate SZD function for estimating of source persistence and the result of partial source reduction.

Table 4-1. Performance Objectives.

Performance Objective	Data Requirements	Success Criteria	Results
Quantitative Performance Objectives			
Estimate of Source Zone Hydrogeologic Parameters	Pre- and post-TEE data: Monitoring well data in the TEE cell: ▪ Bromide tracer histories ▪ PFM alcohol depletion results ▪ Water levels Injection rate of water and extraction rate of groundwater in the TEE cell.	Average PFM velocity within a factor of two of average velocity based on injection rate. Arrival times of tracer peaks at monitoring wells within a factor of two of estimates based on PFM velocity measurements.	The success criteria were achieved for both tracer and PFM data at all monitored locations. With increasing distance from the injection well, the match with tracer data eroded as a result of bromide sensor limitations, the influence of unsteady pumping from perimeter extraction wells, and, possibly, heterogeneity not captured in the geologic model.
Estimate of Source Zone Contaminant Parameters (listed in Table 3-1)	Pre- and post-TEE data: Mass transfer test data in the TEE cell: ▪ Hydrocarbon concentrations at monitoring wells ▪ PFM mass flux results Dissolved phase concentration data from monitoring wells in the TEE cell and near source.	Pre-TEE test: Observed benzene concentrations are captured by SEAM3D simulations using initial NAPL mass estimate in SEAM3D. Post-TEE test: Mean error between observed equilibrium source zone concentrations and simulated concentrations using SEAM3D within one order of magnitude.	The pre-TEE criterion was successfully achieved. The model accurately captured transient and steady-state concentration responses of both benzene and toluene, ethylbenzene, and xylenes (TEX) following injection of clean water during the pre-TEE MTT. The post-TEE success criterion was met, even with variable treatment and variable NAPL composition across the test cell.

Estimate of Reduction in Contaminant Mass Discharge as a Result of Partial Source Reduction	Pre- and post-TEE data: MTT data in the TEE cell: • Hydrocarbon concentrations at extraction and monitoring wells • PFM mass flux and water velocity results • Injection and extraction rates in the TEE cell • Mass of contaminants extracted <u>TEE Pilot Test Data</u> • Mass of contaminants extracted during pilot test	Correlation of change in mass flux between pre- and post-TEE MTTs to the measured mass removed. Mean error between observed equilibrium source zone mass discharge at extraction wells and that simulated with SEAM3D within one order of magnitude.	The post-TEE modeling of benzene concentrations and mass fluxes matched nearly exactly the observed concentrations, thus validating the estimated mass removed from the test cell during the TEE pilot test. The mean error between the observed equilibrium source zone mass discharge and that simulated with SEAM3D was well within one order of magnitude in the two wells closest to the injection well. The objective was achieved in the deep interval of other wells but the error exceeded one order of magnitude in the shallow screens of the three monitoring wells closest to extraction wells. The exceedances resulted from variable thermal treatment across the cell, which was not captured by the modeling assumption of uniform NAPL composition across the cell.
Qualitative Performance Objectives			
Ease of Simultaneous Implementation of an IPT and PFMs	Pre- and post-TEE data: Monitoring well data in the TEE cell: • Bromide tracer histories • Hydrocarbon concentrations in monitoring wells Injection rate of water and extraction rate of groundwater in the TEE cell.	Ease in determination of the optimal timing and duration of PFM deployment within the IPT.	This performance objective was successfully met as PFMs were not deployed until equilibrium concentrations were observed in the TEE cell. Possible skewing of PFM results by NAPL floating in the wells was mitigated by well purging and a PFM "swipe" test.

Incremental Costs of IPT and PFM Deployment	Operational cost data.	Segregation of PFM and IPT incremental costs above those of ongoing operations.	PFM and IPT costs were readily segregated from other costs with an existing pump and treat system in place. Costs to install a temporary pump and treat system are contingent on site-specific conditions such as depth to water, contaminant, concentrations, discharge requirements, and required pumping rates.

4.1 PERFORMANCE OBJECTIVE: ESTIMATE OF SOURCE ZONE HYDROGEOLOGIC PARAMETERS

This quantitative performance objective was to validate a method of measuring groundwater velocities through the source zone and interpreting these data to produce hydraulic conductivity estimates. Specifically, the PFM data included measurements of groundwater flux, which were to be used to generate vertical profiles of velocity variation. Assuming a uniform applied head, the velocity profiles were to be used to calculate soil hydraulic conductivity profiles. Analysis of the pre- and post-TEE MTTs, including tracer test results, was accomplished using local models implemented in the GMS (Groundwater Modeling System) platform using MODFLOW. Starting with a calibrated site model for ambient groundwater flow at ST012, the approach involved refining the existing model to simulate flow and transport only within the TEE cell and simulating the groundwater pumping and water injection during the MTTs, both pre-TEE and post-TEE.

4.1.1 *Data Requirements*

Data requirements for this objective included stratigraphic data within the TEE cell such as boring logs of soil type, water levels in monitoring and extraction wells, transient concentration response of tracer at monitoring wells within the TEE cell, PFM results, and pre-TEE and post-TEE monitoring well data collected at source zone monitoring wells and wells located downgradient and adjacent to the TEE cell. Additional hydrogeologic input parameters were derived from readily available site reports and data collected in association with the TEE pilot test. MTT data included pumping and injection rates, water level data, injection tracer concentrations, and monitoring well tracer data. Results from the PFMs were to provide a secondary means of model calibration of NAPL parameters (NAPL mass, composition and mass transfer coefficient) and a more detailed delineation of vertical hydraulic conductivity variations.

4.1.2 *Success Criteria*

A primary determinant of success for this objective was that the range of vertically discrete water velocities from PFM data was consistent with measured injection and extraction rates. Specifically, the average of the PFM groundwater velocity measurements should have been within a factor of two (i.e., +100% / -50%) of the average velocity based on a mass balance of

the measured injection rate. A second independent measure was provided by the slug injection of a tracer mixed into the injected water. The arrival times of tracer peaks at monitoring wells should have been within a factor of two of time estimates based on PFM velocity measurements.

4.1.3 *Evaluation of Success*

The success criterion was achieved at all monitored locations. For both the pre- and post-TEE tracer tests, the local SEAM3D model of the TEE cell captured breakthrough characteristics related to travel time and the rise to peak concentrations at monitoring wells closest to the injection well (wells 18 and 28 feet away). At both wells, the model matched the time of travel with a differential between the observed and simulated breakthrough time varying by no more than a factor of two. Differences in the time of travel may be a result of temporal variability in the withdrawal rates at the peripheral pumping wells in the TEE cell. At more distal monitoring wells, the tracer concentration decayed to levels close to the detection limit of the bromide sensor. As such, modeling results achieved a better match with the observed data at wells closer to the injection well relative to the more distant monitoring wells.

Vertical distributions of Darcy velocity derived from the PFMs in individual monitoring wells and simulated flow rates with depth calculated with the groundwater flow model compared favorably for all monitored wells. An excellent match was achieved in the wells closest to the injection well (18 and 28 feet from the injection well). However, the vertical location of the PFMs in some wells may have missed a thin layer of high permeability sand. Overall, the results provide a good match, particularly in the fine sand layers, and met the success criterion.

4.2 PERFORMANCE OBJECTIVE: ESTIMATE OF SOURCE ZONE CONTAMINANT PARAMETERS

This quantitative performance objective was to validate a method to determine source zone parameters applicable to prediction of NAPL mass discharge and source longevity under different remedial strategies related to the extent of source removal required. Starting with a calibrated local model of the TEE cell from the first objective, source zone parameters (i.e., input to the SEAM3D NAPL Package) were determined through calibration to the hydrocarbon concentrations at monitoring wells within the TEE cell and mass flux measurements based on PFM results. After simulating the pre-TEE MTT results, the process was repeated for the post-TEE test to evaluate mass removal, compositional changes, and post-remediation mass transfer rates following completion of the TEE pilot test.

4.2.1 *Data Requirements*

Data requirements for this objective included hydrostratigraphic and compound-specific data within the TEE cell such as boring logs of soil type, transient responses of hydrocarbon concentrations at monitoring wells within the TEE cell, PFM results, and pre-TEE and post-TEE monitoring well data collected at source zone monitoring wells and wells located downgradient and adjacent to the TEE cell. Additional hydrogeologic input parameters were derived from readily available site reports and data collected in association with the TEE pilot test. MTT data included pumping and injection rates, water level data, injection concentrations, and monitoring well data (hydrocarbon concentrations). Results from the PFMs were to provide a secondary means of model calibration. Historical pre-TEE monitoring well data collected at source zone

monitoring wells and wells located downgradient and adjacent to the TEE cell (i.e., within the hydrocarbon plume) were also used. Post-TEE data were collected after concentrations stabilized and the site cooled to near ambient temperatures.

4.2.2 *Success Criteria*

Previous estimates of the NAPL mass in the TEE cell were based on groundwater and soil hydrocarbon concentration data and NAPL thicknesses measured in wells. These values were updated during the TEE pilot test based on literature values and the observed mass removed during the TEE pilot test, and the initial mass estimate used in the SEAM3D modeling was based on these updated values. The pre-TEE model simulations were expected to accurately match the breakthrough and short-term equilibrium concentrations of benzene data at TEE cell monitoring wells.

The objective associated with the post-TEE test was considered successful if the equilibrium source zone concentrations and simulated concentrations using SEAM3D were within one order of magnitude. Similar to the pre-TEE success criteria, the analysis was deemed successful if the SEAM3D simulations matched the post-TEE benzene concentrations measured at TEE cell monitoring wells.

4.2.3 *Evaluation of Success*

During the pre-TEE MTT, the local SEAM3D transport model accurately captured transient concentration responses of both benzene and TEX following injection of clean water and also the equilibrium concentrations during extended flushing. The model input variables that most directly controlled the equilibrium concentrations were the NAPL mass transfer coefficient, NAPL saturation (i.e., NAPL mass) and the NAPL composition, specifically the benzene mass fraction. Estimates of typical residual NAPL saturations for specific soil types (Adamski and Charbeneau, 2010) were employed in the model initial condition, and NAPL mass transfer coefficients were varied to match the concentration data measured in the monitoring wells. The success criterion for the pre-TEE MTT was met since simulated benzene concentrations nearly exactly matched the observed concentrations.

For the post-TEE test, the observed concentrations in the TEE cell showed much greater variability among the monitoring wells compared to the pre-TEE case. This variability was primarily the result of variable treatment within the cell that likely yielded a non-uniform NAPL composition in the cell. The soils around the monitoring wells closest to injection received much more thermal treatment than those near the periphery. Despite the variable treatment, the success criterion to match the post-TEE concentrations with modeling within an order-of-magnitude was met.

4.3 PERFORMANCE OBJECTIVE: ESTIMATE OF REDUCTION IN CONTAMINANT MASS DISCHARGE AS A RESULT OF PARTIAL SOURCE REDUCTION

This quantitative performance objective was to validate a method for estimating the reduction of mass discharge resulting from partial removal of NAPL mass from a source area. The goal was to evaluate the potential benefit of a remediation approach for partial mass removal required to

meet a specified cleanup metric. This important performance objective was to be met by synthesizing the field measurements of groundwater velocity and mass transfer described in Performance Objectives described in 4.1and 4.2.

4.3.1   *Data Requirements*

Data requirements for this objective included hydrostratigraphic data within the TEE cell, transient concentration responses of hydrocarbon concentrations at monitoring wells within the TEE cell, PFM results, and pre-TEE and post-TEE monitoring well data collected at source zone monitoring wells and wells located downgradient and adjacent to the TEE cell. In addition, the total mass of contaminant removed from the test cell during the TEE pilot test was used. Other data required for the objective were described in the prior two objectives (in Sections 4.1 and 3.2).

4.3.2   *Success Criteria*

A primary criterion of success for this objective was correlating the change in mass flux between pre- and post-TEE MTTs to the mass removed from the test cell during the TEE pilot test. This criterion is complex and was determined from multiple applications of SEAM3D to match mass transfer data as described in Objective 4.2. The model was first calibrated to the pre-TEE mass transfer data and then to the post-TEE mass transfer data. Within a reasonable number of iterations, the mass subtracted from the pre-TEE model of the test cell to achieve a calibration to the post-TEE data was to have been within ± 50% of the observed mass removed from the test cell during the TEE pilot test. In addition, the mean error between the observed equilibrium source zone mass discharge and that simulated with SEAM3D was not expected to exceed one order of magnitude.

4.3.3   *Evaluation of Success*

The local solute transport model described for the first two objectives was used to calculate the mass flux of benzene at monitoring wells. In the field, this was directly determined using PFMs installed in the B interval monitoring wells during the latter phase of both the pre- and post-TEE MTTs. For the pre-TEE MTT, a reasonable match between the observed and calculated benzene mass flux in each model layer was obtained, meeting this performance objective. Results for the post-TEE MTT were favorable at the monitoring wells nearest to the injection well. At the more distant wells, the observed benzene mass flux from the PFMs was over an order of magnitude greater than the model-simulated results. As described previously, the benzene concentrations in the TEE cell showed much greater variability among the monitoring wells after treatment as compared to the pre-TEE values. This variability was likely the result of variable treatment within the cell that yielded a non-uniform NAPL composition in the cell. The mean error between the observed equilibrium source zone mass discharge and that simulated with SEAM3D for the post-TEE MTT was well within one order of magnitude in the two wells closest to the injection well but exceeded one order of magnitude in the three monitoring wells closest to the extraction wells.

Estimates of initial NAPL mass for both the pre- and post-TEE model simulations were based on field measurements and analyses associated with the TEE pilot test, including the observed mass removed from the cell during the TEE pilot test. The reasonable match between observed and

simulated benzene mass flux at most monitoring locations during the MTTs validates these estimates.

4.4 PERFORMANCE OBJECTIVE: EASE OF SIMULTANEOUS IMPLEMENTATION OF AN IPT AND PFMS

This qualitative performance objective was to assess the ease of deploying PFMs during an IPT. A primary concern was the timing and duration of PFM placement. Because of soil heterogeneities, different soil volumes are swept for different duration times by the injected water. Hence, equilibrium between aquifer material with flowing water, lesser permeable soils, and contaminated soil volumes was difficult to assess. Optimally, PFMs would not be deployed until nearing this equilibrium to avoid sample collection over a period of changing NAPL constituent concentrations. This objective evaluates the method of determining the timing and duration of PFM deployment. An additional potential complication was that a thin layer of floating NAPL could skew results by contaminating the outside of a PFM during placement.

4.4.1 *Data Requirements*

Data requirements for this objective included hydrostratigraphic data within the TEE cell, injection and extraction rates, and transient concentration responses of tracer at monitoring wells. In addition, each well with PFMs was monitored for the existence of a NAPL layer in the well casing prior to deployment and again before retrieval.

4.4.2 *Success Criteria*

Criteria for success in determining the optimal timing and duration of PFM deployment within the IPT were qualitatively evaluated from the consistency and utility of PFM data. For example, NAPL smearing on a PFM during deployment could yield locally high concentrations of benzene or other petroleum hydrocarbons. If the adsorbent in the PFM was saturated with contaminants, the duration of deployment may have been too long. The length of the deployment period was determined from concentrations measured in the monitoring well and estimates of local groundwater velocity based on head gradients.

4.4.3 *Evaluation of Success*

This performance objective was successfully met as PFMs were not deployed until equilibrium concentrations were observed in the TEE cell. The Pre-TEE MTT included a tracer test that verified a volume-based calculation for the timing of the PFM deployment. The total pore volume of the target soil volume was calculated and the PFMs were not deployed until this volume of clean water had been injected. The tracer concentration histories identified soil heterogeneities and preferential flowpaths where the injected water flowed. The tracer results indicated more than two pore volumes of water passed through flowpaths prior to the PFM deployment. The contaminant concentrations in the monitoring wells were measured during the water injection and were observed to stabilize, as described in Section 4.2, before PFM deployment.

An additional concern was the possibility of a thin layer of floating NAPL skewing results by contaminating the outside of a PFM during placement. All wells were bailed of any visible

NAPL and purged of three well volumes just prior to the deployment of the PFMs. In addition, a "swipe" test was performed whereby a dummy PFM was installed and immediately withdrawn and sampled for any NAPL contact. A small fraction of the PFM results were slightly adjusted based on the results of the swipe test.

4.5   PERFORMANCE OBJECTIVE: INCREMENTAL COSTS OF IPT AND PFM DEPLOYMENT

This performance objective was to estimate the incremental costs of performing an integral pumping test in a source zone and the deployment of PFMs for vertical delineation of flow and contaminants.

4.5.1   *Data Requirements*

Data requirements included operational costs of an existing pump and treat system or the costs for a temporary extraction and treatment system, costs for field technicians to implement the IPT, and costs for deployment and analysis of PFMs.

4.5.2   *Success Criteria*

Success of this criterion was achieved if PFM and IPT incremental costs could be segregated and compared to baseline operating costs.

4.5.3   *Evaluation of Success*

PFM and IPT costs were successfully segregated, and are presented in Section 7.0.

A primary determinant for the total cost to perform the testing is the existence of operating infrastructure to pump and treat relatively large quantities of contaminated groundwater for days or weeks. If pump-and-treat is active at a facility and monitoring wells exist within the source area, or if the installation of such a system is anticipated as part of the site remediation, the cost of performing the mass transfer testing is almost solely for the analytical data and is a small increment of site operating costs in comparison to the scientifically defensible data collected. Costing of a pump-and-treat facility is not unique to the mass transfer test and standard practice can be followed.

5.0   TEST DESIGN

At ST012, the innovative MTT and data analyses described in Section 2.0 was applied before and after the application of the TEE technology in the pilot test cell. In addition, as described in this section, the MTT was performed in two intervals of the saturated zone, UWBZ and the LSZ, within the test cell.

The primary purpose of the pre-TEE mass transfer test in the saturated zone was to determine the rate of dissolution (i.e., mass loading) of hydrocarbon constituents from residual NAPL to water flowing through the pilot test area under known conditions. These measurements were interpreted to assess the individual NAPL constituent mass loading to groundwater under natural flow conditions and used as input for solute transport modeling. The mass transfer test was repeated after the TEE pilot test to provide data for the fate and transport modeling to calculate the reduced mass loading of chemicals of concern COCs to groundwater in the source area of ST012 after a measured mass of contaminants was extracted (i.e., partial source reduction). These data, along with other TEE pilot test performance data, allowed forecasts of the mass loading of COCs to groundwater in the source area of ST012 resulting from various scenarios of TEE implementation.

With the data from these applications of the MTT at ST012, the procedure was evaluated for application to other NAPL sites. This section provides the details of the field measurements and data analyses. An overview of the TEE pilot test is also provided. More details on the design and construction of the TEE treatment system can be found in the TEE Pilot Test Work Plan (BEM Systems, 2007).

5.1   CONCEPTUAL EXPERIMENTAL DESIGN

The layouts of injection wells, extraction wells, and monitoring wells to perform the mass transfer tests and the TEE pilot test at ST012 in the LSZ and UWBZ are depicted in Figure 5-1 and 5-2, respectively. The test cell was located within a portion of ST012 where substantial accumulation of NAPLs was known to exist. This location provided a suitable setting for evaluation of the effectiveness of TEE to treat source areas, and the configuration of wells afforded the opportunity to test the technology for assessing the NAPL architecture and mass transfer characteristics. TEE was expected to have varying degrees of effectiveness in removing individual components of the NAPL as a result of their varying chemical properties. BTEX compounds were expected to be highly amenable to treatment via TEE because of their relatively high vapor pressures and high aqueous solubility. Naphthalene is less volatile and was expected to undergo a lesser degree of removal from the NAPL in response to TEE. However, naphthalene has a very high aqueous solubility compared to other semi-volatile fuel components, and its solubility increases markedly with temperature. Also, during the TEE pilot test, more soil treatment and higher temperatures occurred near the steam injection wells and less treatment and lower temperatures were observed with increasing distance from the central steam injection wells (LSZ-07 and UWBZ-07 in Figure 5-1 and Figure 5-2, respectively).

The testing was conducted within a single treatment cell having a diameter of about 140 feet and across the two vertical zones represented by the LSZ and UWBZ. Each zone contained a central injection well surrounded by six perimeter extraction wells screened across the full depth of the

zone in the treatment cell. The test cell also contained six monitoring well nests (3 screens) within the cell interior.
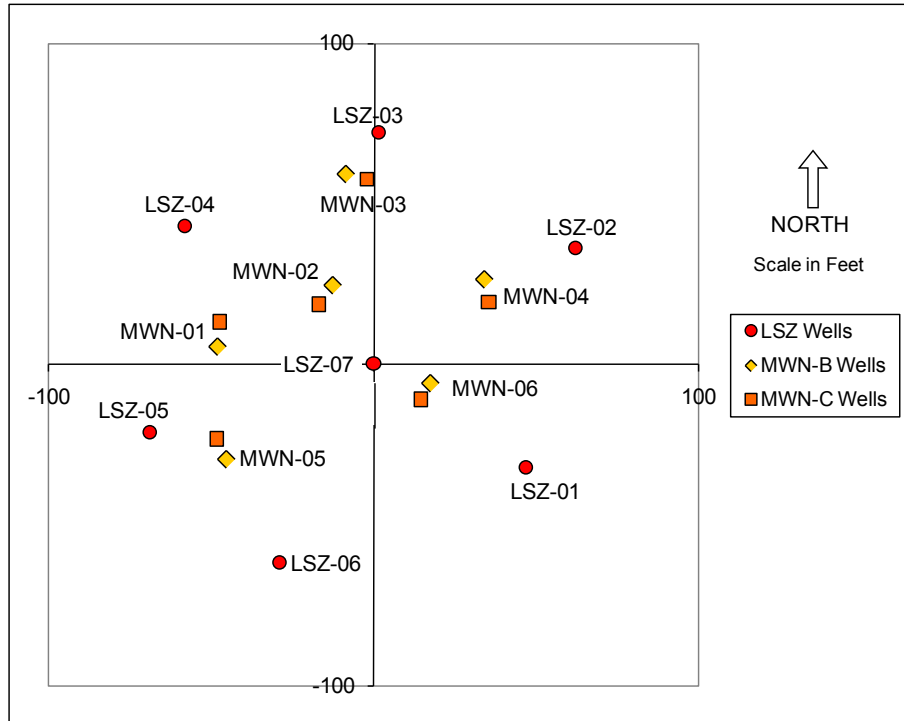
Figure 5-1. Layout of Central Injection ("LSZ-07"), Peripheral Extraction ("LSZ" wells) and Monitoring Wells ("MWN" wells) in the LSZ.
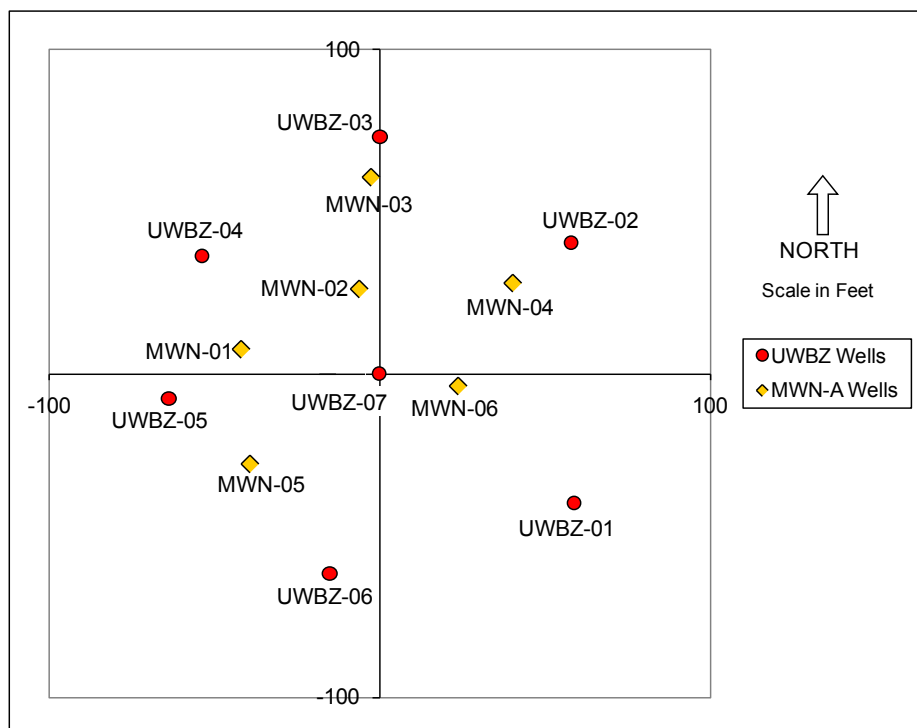
Figure 5-2. Layout of Central Injection ("UWBZ-07"), Peripheral Extraction ("UWBZ" wells) and Monitoring Wells ("MWN" wells) in the UWBZ.

The interior monitoring wells provided groundwater and vapor samples for assessing the performance of the pilot test, tracer and contaminant concentration data for the IPT, and locations for deployment of the PFMs. The monitoring wells in the LSZ included six screens in the C-horizon and six screens in the B-horizon as shown in Figure 5-1. The UWBZ had six monitoring wells with single screens spanning the full depth of the A-horizon (i.e., UWBZ) as indicated on Figure 5-2. Thermocouples were installed with each C-horizon monitoring well to monitor subsurface temperature changes from with depth as the TEE pilot test proceeded. The approximate vertical interval for the testing spanned about 80 feet. For this depth interval, the target volume for the test cell was about 46,000 cubic yards.

The testing at ST012 was initiated with the collection of pre-test soil, groundwater, and NAPL samples in both the LSZ and UWBZ to establish baseline conditions prior to operation of the TEE pilot test. The soil samples were collected during installation of monitoring wells in 2004 to assess the distribution of contaminants in the subsurface. Groundwater samples from monitoring wells located within and surrounding the treatment cell were collected prior to the first mass transfer test and the operation of the pilot test. NAPL samples were collected from a few wells to characterize pre-treatment NAPL composition. Further details of this pre-test sampling are provided in Section 5.2.

The first step in the operation of the TEE pilot test was groundwater pumping to establish hydraulic isolation, recover mobile NAPL, and lower the water table as much as practical. The vertical placement of the pump intakes in the wells was designed to satisfy, to the degree possible, the competing objectives of drawing down the potentiometric surface sufficiently to attain hydraulic isolation of the cell and capturing as much mobile NAPL drawn to the wells as possible. Placement of the pump intakes was based on estimated well drawdown predicted from hydraulic analysis of pumping test results and the results of groundwater flow modeling. Data from this phase of the test allows an assessment of pump-and-treat as a remedial alternative for the site.

After equilibration of the flows and drawdown from groundwater extraction, the pre-treatment mass transfer test was initiated and completed in Fall 2008 in each zone (LSZ and UWBZ). In both zones, the IPT consisted of water injection in the central well to create a known total flow through the target soil volume. Early in the IPT a pulse of bromide tracer was introduced in the central injection well and its appearance and concentration at monitoring wells was measured to provide hydrogeologic data on permeable pathways, groundwater velocities, and residence time distributions to characterize the subsurface flow regime. After sweeping at least one theoretical pore volume of water through the permeable soils, the concentrations of contaminants were measured in monitoring wells to determine the pseudo-steady rate of dissolution of fuel components out of residual NAPL and into flowing groundwater. Samples from monitoring wells closest to the injection well yielded groundwater concentrations significantly less than the baseline concentrations for all NAPL constituents. After collecting samples for measurement of contaminant concentrations, the PFMs were installed in the B- and A-horizon monitoring wells to provide vertically discrete measurements of water and contaminant fluxes in these horizons during steady continuous injection and extraction of groundwater. Retrieval of the PFMs signaled the end of the pre-TEE Mass Transfer Test. Bromide tracer histories were expected to be consistent with PFM water flux measurements, and contaminant concentrations were expected to be related to a depth-averaged PFM contaminant flux.

The TEE pilot test was initiated October 28, 2008 with the start of steam injection in the LSZ, followed by steam injection in the UWBZ two weeks later. In both zones, after steam breakthrough in the extraction wells, steam injection continued at a reduced rate to provide additional heating of the low permeability soils. After low permeability soils within each zone were heated to at least 120ºF, co-injection of air was initiated to improve vapor contact with the residual NAPL and encourage volatilization of NAPL components residing in low permeability soils. After operating in this quasi-steady mode for about four weeks, the injection of steam was discontinued while the injection of ambient air and water continued to cool the soils by vaporizing and recovering pore liquids. Water injection was continued through November 2009.

Following the TEE pilot test and after six months of subsurface cooling (to below 120ºF), post-treatment mass transfer measurements were conducted in the LSZ and UWBZ in a manner similar to that conducted during the pre-treatment tests. Steady water injection occurred at the site for about six months after steam injection ceased to cool the site to near ambient conditions. The water injection and groundwater extraction rates coincided with the desired values for the mass transfer testing; hence, flow conditions were established for an extended period yielding multiple measures of the contaminant concentrations in monitoring wells during the imposed flow configuration and the total mass removal rate. A bromide tracer pulse was injected into the LSZ in September 2009 and PFMs were deployed in November 2009 to evaluate the post-TEE mass transfer conditions. These applications of the mass transfer tests were the focus of this work and are described in detail in the following sections.

5.2   BASELINE CHARACTERIZATION

Soil, groundwater, and NAPL samples along with groundwater elevations were collected by the Air Force to establish baseline conditions prior to the pre-TEE mass transfer test and the operation of the TEE pilot test in the LSZ and UWBZ (BEM, 2010). The same suite of samples to provide post-TEE data was collected after the pilot test to provide baseline measures of new site conditions. Data from these sampling events were provided by the Air Force for this ESTCP-funded effort and are described in Appendix D.

In general, soil concentrations of benzene and other light hydrocarbons decreased by one to two orders of magnitude in the more permeable LSZ and about one order of magnitude in the more heterogeneous UWBZ. Lesser reductions were observed in the silty clays of the LPZ and UWBZ+1. As described below the BTEX makeup in the UWBZ NAPL was also less than that of the LSZ because of previous soil vapor extraction; hence concentrations in the UWBZ had been reduced before the TEE pilot test such that TEE results between the two intervals were roughly equivalent.

Groundwater concentrations of petroleum hydrocarbons after the test, including benzene, were lower than before the test in most TEE cell sampling locations. Concentration reductions were greater in samples from monitoring wells closest to the injection wells. Major reductions occurred throughout the LSZ and in all locations of the UWBZ except MWN03A located next to an extraction well and MWN01A where little treatment occurred.

Characterization of NAPL composition at the site was critical for accurate modeling of multi-component mass transfer as the components have varying physical chemical properties and thus

their molecular interactions will affect their fate in applying any modeling. The objective of NAPL sampling and analysis was to provide an estimate of average baseline composition of the NAPL source term for predictive modeling and to evaluate the change in NAPL composition resulting from thermal treatment. The fuel released at the site was suspected to consist of Jet Propulsion fuel No. 4 (JP-4) and some fraction of aviation gasoline. NAPL samples were collected from three wells in November 2006 before the TEE pilot test. NAPL samples were collected from six wells and analyzed to characterize post-TEE pilot test NAPL composition in December 2009. Additional details of the sampling and the analytical results can be found in the TEE Pilot Test Evaluation Report (BEM, 2010).

Different NAPL compositions were developed for the UWBZ and the LSZ to be used in the model, as the UWBZ was unsaturated at the time of NAPL release and was subjected to soil vapor extraction from 1997 to 2003. Variability in the composition of the NAPL in the two zones was thus anticipated. The rising water table entered the bottom of the UWBZ (~195 ft bgs) during 1998 and reached the fine-grained unit separating the top of the UWBZ from the overlying Cobble Zone (~172 ft bgs) in 2004. Hence, the residual NAPL in the UWBZ was initially weathered by natural volatilization and further weathered by soil vapor extraction before becoming submerged. The result is a lower initial mass fraction of volatile compounds than found in the deeper LSZ NAPL that was weathered primarily by dissolution as was expected.

The mass fractions of fuel constituents in the NAPL were estimated using the maximum reported groundwater concentrations. It was assumed that this maximum value approximates the effective solubility of the compound, thus allowing estimates of the NAPL composition based on Raoult's law. These estimates were used to calculate mass fractions in the local residual NAPL both before and after the TEE Pilot Test to supplement the NAPL analyses.

The composition of the original released NAPL was selected from detailed analyses of JP-4 published by the USAF (Smith et al., 1981) and from the analyses of NAPL samples collected from wells at ST012. Classes of hydrocarbons were combined to reduce the number of components in the model NAPL, as JP-4 is a mixture of over 100 hydrocarbon compounds. The estimated composition included 31 components, some of which were surrogate compounds representing a broader class of fuel compounds. For numerical modeling, the 31-component composition was further reduced to ten components through mass-weighted averaging by combining classes of hydrocarbons while maintaining BTEX and naphthalene as separate components. The resulting NAPL compositions for the LSZ and UWBZ to be used in the model are presented in Table 5-1 and Table 5-2, respectively.

Table 5-1. Model NAPL Compositions in the LSZ.

C#	Compound or Group	Pre-TEE LSZ (% mass)	Pre-TEE LSZ Effective Solubility (mg/L)	Post-TEE LSZ (% mass)	Post-TEE LSZ Effective Solubility (mg/L)
6	Benzene	0.830	26.8	0.101	3.3
7	Toluene	2.900	22.7	0.535	4.2
8	Ethylbenzene	1.400	2.8	0.510	1.0
8	Total Xylenes	3.030	6.1	0.740	1.5
10	Naphthalene	0.500	0.44	0.184	0.17
9	1,2,4-Trimethylbenzene	1.100	0.56	1.147	0.59
9	1,3,5-Trimethylbenzene	0.370	0.34	0.378	0.35
	Other Aromatics	7.37	1.5	7.878	1.6
	Isoalkanes and Paraffins	54.41	8.4	58.23	9.0
	n-Alkanes	28.09	0.97	30.29	1.1
	Total	100.00	70.60	100.00	22.8

Table 5-2. Model NAPL Compositions in the UWBZ.

C#	Compound or Group	Pre-TEE UWBZ (% mass)	Pre-TEE UWBZ Effective Solubility (mg/L)	Post-TEE UWBZ (% mass)	Post-TEE UWBZ Effective Solubility (mg/L)
6	Benzene	0.222	8.0	0.076	2.7
7	Toluene	0.730	6.3	0.540	4.7
8	Ethylbenzene	0.970	2.1	0.640	1.4
8	Total Xylenes	2.350	5.3	1.330	3.0
10	Naphthalene	0.570	0.56	0.140	0.14
9	1,2,4-Trimethylbenzene	2.000	1.1	2.007	1.13
9	1,3,5-Trimethylbenzene	0.450	0.46	0.445	0.45
	Other Aromatics	12.02	2.6	12.24	2.6
	Isoalkanes and Paraffins	46.85	3.2	47.93	3.3
	n-Alkanes	33.84	0.16	34.66	0.16
	Total	100.00	29.8	100.00	19.6

5.3   TREATABILITY OR LABORATORY STUDY RESULTS

One-dimensional column studies were performed to assess mass dissolution rates from prepared three-component, residual NAPL subjected to a waterflood, a non-condensable vapor flow (i.e., soil vapor extraction), a steamflood, and the co-injection of air and steam. The purpose of the testing was to measure mass transfer from a residual NAPL of uniform geometry during the flow

of various fluids and at various temperatures as experienced during the TEE pilot test. Published literature has little data on mass transfer into a multi-phase carrier fluid. These experiments provided mass transfer data under differing remedial scenarios. The experimental setup was designed to provide nearly ideal contact between the residual NAPL and carrier fluid is assumed; i.e., the resulting mass transfer coefficients are likely maximum values for a residual NAPL. In addition, the data provided insight to potential variability in the residual NAPL composition as a result of variable TEE treatment. The results of the laboratory columns tests are provided in Appendix E.

5.4   DESIGN AND LAYOUT OF TECHNOLOGY COMPONENTS

The mass transfer tests were performed using the system constructed by the Air Force for the TEE pilot test. The TEE pilot test system incorporated shallow (UWBZ) and deep (LSZ) well pairs as part of the process well design. A total of 32 groundwater injection, extraction and monitoring wells were installed to support the TEE Pilot Test; these wells were also used for the mass transfer tests. Figures 5-1 and 5-2 illustrate the groundwater extraction, injection and monitoring well network locations. The aboveground TEE system and the wells of the TEE cell are pictured in Figure 5-3. During the mass transfer testing, the TEE treatment system provided conditioned water for injection to the subsurface through two process wells, pumping from 12 extraction wells, and treatment of extracted liquids before discharge to a sanitary sewer or disposal.

Additional descriptions of system process wells, monitoring wells, extraction pumps, water injection, and extracted groundwater treatment system are provided in Appendix D.
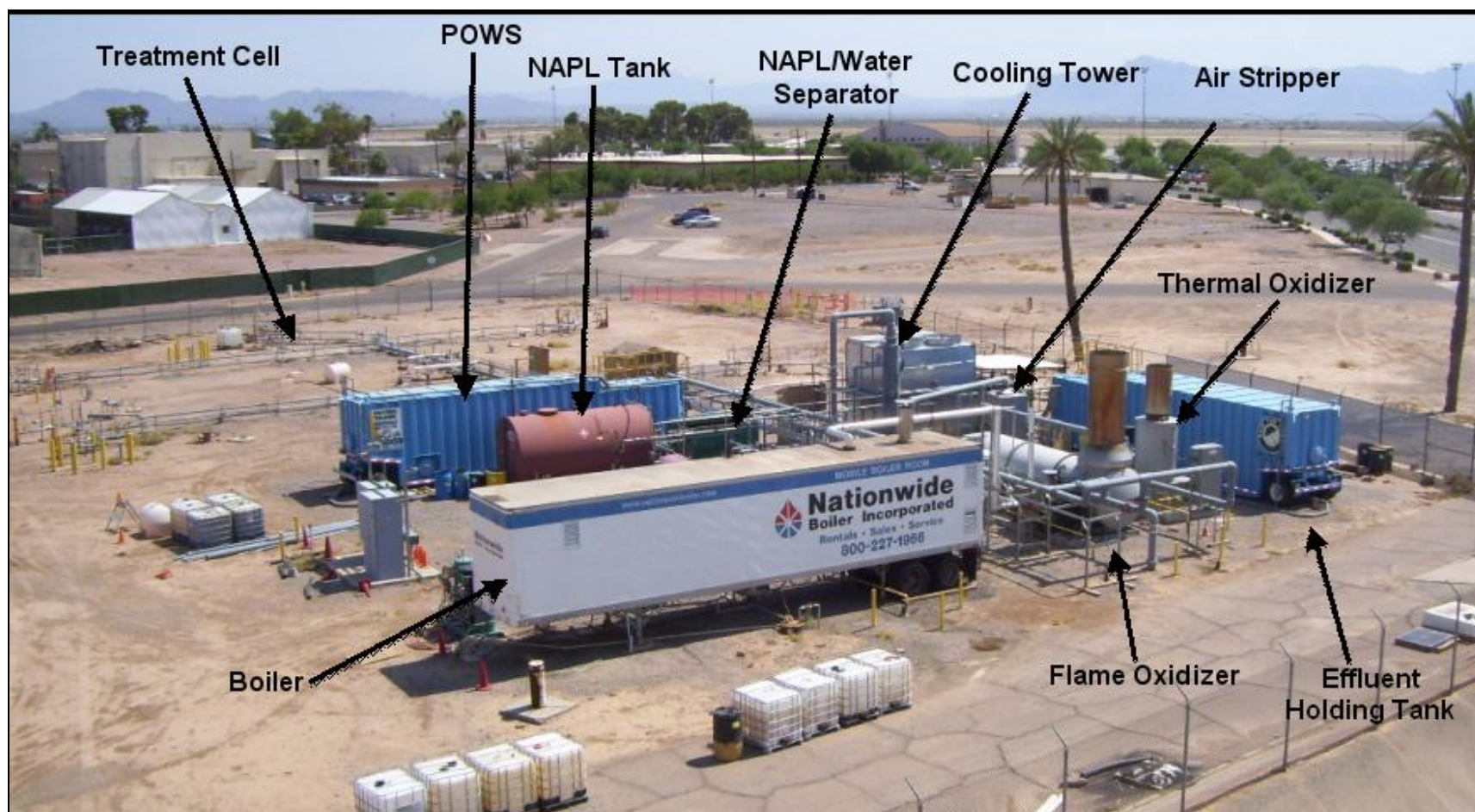
Figure 5-3. View of TEE System at ST012 (facing northeast, July 2, 2008).

5.5   FIELD TESTING

The field testing to characterize mass transfer from residual NAPL across a smear zone was performed with the system described in previous sections. The testing within each zone (LSZ and UWBZ) occurred in the following sequence both before and after the TEE pilot test:

1. Establish steady groundwater extraction in the six perimeter wells,
2. Establish steady central water injection,
3. Measure groundwater concentrations in monitoring wells and extraction wells throughout the mass transfer test,
4. Introduce bromide tracer pulse in the water injection,
5. Measure bromide breakthrough curves at select monitoring well screens,
6. Deploy passive flux meters at select depths and in select monitoring well screens,
7. Retrieve passive flux meters, and
8. Terminate mass transfer test and proceed with other Air Force tasks.

The above procedure was repeated four times during this project. A timeline summarizing the field activities in each zone is provided in Figure 5-4.

Task	2008					2009												2010	
	A	S	O	N	D	J	F	M	A	M	J	J	A	S	O	N	D	J	F
Baseline Sampling																			
- Soil Sampling (2004)																			
- Groundwater Sampling (2006)																			
LSZ PreTEE Mass Transfer Test	█	█	█																
- Tracer Test		█																	
- PFM Deployment (B-horizon)			█																
UWBZ PreTEE Mass Transfer Test	█	█																	
- Tracer Test		█																	
- PFM Deployment (A-horizon)		█																	
TEE Pilot Test						▓	▓	▓	▓	▓									
PostTEE Cooling & Monitoring											▓	▓	▓	▓					
LSZ PostTEE Mass Transfer Test														█	█				
- Tracer Test															█				
- PFM Deployment (B-horizon)																█			
UWBZ PostTEE Mass Transfer Test														█	█				
- PFM Deployment (A-horizon)																█			
Soil and Groundwater Sampling																	█	█	

Figure 5-4. Field Testing Timeline.

The baseline soil and groundwater sampling events were summarized in Section 5.2. The specific mass transfer test procedures and sampling for each event are described for both the LSZ and UWBZ before and after the TEE pilot test in C.

5.6   SAMPLING METHODS

An extensive sampling and analysis plan was prepared by the U.S. Air Force and can be found in the TEE Pilot Test Work Plan (BEM, 2007). This plan includes a detailed field sampling plan and associated quality assurance project plan that define sampling intervals and strategies for all activities associated with the TEE pilot test at ST012. The sampling associated with the mass transfer tests occurred at various phases as indicated in Figure 5-4. The analytical methods performed on the samples are summarized in Table 5-3. The sampling included baseline and post-treatment soil, groundwater and NAPL sampling and analyses to provide starting and ending measurements. Groundwater sampling and analyses was performed during each mass transfer test. The pre-TEE groundwater analyses were performed solely with the field GC while the post-TEE analyses included state-certified laboratory analyses. During the tracer tests, bromide concentrations in monitoring wells were measured and logged with calibrated AquiStar Temphion submersible Smart pH/ISE/Redox Sensors™. A post-TEE tracer test was not performed in the UWBZ. Passive flux meters were deployed, retrieved and analyzed by University of Florida personnel during each mass transfer test although PFMs were not deployed in the C-horizon of the LSZ.

Detailed descriptions of sampling methods are provided in Appendix D. Analyses performed on the data from the MTTs are summarized in Appendix B, and details of groundwater and solute transport modeling are provided in Appendix F.

Table 5-3. Total Number and Types of Samples Collected.

Component	Matrix	Number of Samples	Analyte(s)	Location
Baseline sampling	Soil	75	BTEXN, TPH	Five monitoring wells (15 per boring)
	Groundwater: Laboratory measurement	18	BTEXN, TPH	Six, triple-nested TEE monitoring wells
	NAPL	6	BTEXN, TPH	Monitoring wells with floating NAPL
Technology performance sampling: LSZ Pre-TEE Mass Transfer Test	Groundwater: Field measurement	Weekly grab samples for one month	BTEXN, TPH	Twelve B- and C-horizon monitoring wells
	Bromide in groundwater	Logged at 5 minute interval	Bromide ion by Smart Sensor	Six, double-nested TEE monitoring wells
	Passive Flux Meter	18	Benzene, TPH, alcohol depletion	Six B-horizon monitoring wells
Technology performance sampling: UWBZ Pre-TEE Mass Transfer Test	Groundwater: Field measurement	Weekly grab samples for one month	BTEXN and TPH	Six A-horizon monitoring wells
	Bromide in groundwater	Logged at 5 minute interval	Bromide ion by Smart Sensor	Four A-horizon monitoring wells
	Passive Flux Meter	18	Benzene, TPH, alcohol depletion	Six A-horizon monitoring wells
Technology performance sampling: LSZ Post-TEE Mass Transfer Test	Groundwater: Laboratory measurement	12	BTEXN and TPH	Twelve B- and C-horizon monitoring wells
	Groundwater: Field measurement	Weekly grab samples for 5 months	BTEXN and TPH	Twelve B- and C-horizon monitoring wells
	Bromide in groundwater	Logged at 5 minute interval	Bromide by submerged	Six TEE monitoring wells
	Passive Flux Meter	15	Benzene, TPH, alcohol depletion	Five B-horizon monitoring wells
Technology performance sampling: UWBZ Post-TEE Mass Transfer Test	Groundwater: Laboratory measurement	6	BTEXN and TPH	Six TEE monitoring wells in the A-horizon
	Groundwater: Field measurement	Weekly grab samples for 5 months	BTEXN and TPH	Six A-horizon monitoring wells
	Passive Flux Meter	18	Benzene, TPH, alcohol depletion	Six A-horizon monitoring wells
Post-treatment sampling	Soil	75	BTEXN, TPH	Adjacent to monitoring wells (15 per boring)
	Groundwater: Laboratory measurement	36	BTEXN, TPH	Six TEE monitoring wells in the A-horizon
	NAPL	7	BTEXN, TPH	Monitoring wells with floating NAPL

Table 5-4. Analytical Methods for Sample Analysis.

Matrix	Analyte	Method	Container	Preservative	Holding Time
Soil	TPH	8015M	4-oz glass jar	Cooled/Frozen	14 days
	BTEXN	8260C	40-mL VOA vials	Methanol	14 days
Groundwater	TPH	8015M	1-L amber glass bottles	HCl	14 days
	BTEXN	8260C	40-mL VOA vials	HCl	14 days
NAPL	TPH	8015M	40-mL VOA vials	Cooled	7 days
	BTEXN	8260C	40-mL VOA vials	Cooled	7 days

5.7   SAMPLING RESULTS

This section summarizes the primary sampling data from the MTTs performed in the LSZ and UWBZ of the TEE cell both before and after the TEE Pilot Study. Detailed results and discussion are provided in Appendix D. Results from the tracer tests are first discussed, followed by the concentration data, and then the PFM data. The discussion of sampling results includes simple analyses and comparison of data for consistency and to provide context for the modeling presented in Section 6.0.

5.7.1   *Tracer Test Data*

Tracer tests were performed in the UWBZ and LSZ during water injection for the IPT before the performance of the TEE pilot test at ST012 to identify preferential flow paths and quantify soil heterogeneities in the NAPL source zone. The well configurations in the LSZ and UWBZ are provided in Figures 5-1 and 5-2, respectively. The tracer test was repeated in the LSZ after the TEE pilot test.

The tracer test in each zone was initiated after approximately two weeks of groundwater extraction in the ring of extraction wells. Potassium bromide was mixed with water and metered into water injected through the central injection wells. One day of clean water injection preceded the steady introduction of the bromide tracer (~2,000 mg/L) over a four-hour period in the pre-TEE testing. Bromide sensors were placed in monitoring well screens in each zone during the tracer test and recorded the bromide concentration at discrete depths within the screen interval every 5 to 10 minutes for approximately two weeks.

Details of the conditions of the three tracer tests are provided in Appendix D, along with the bromide tracer responses and full interpretations of the tracer tests using a finite difference model.

A summary of the bromide responses from the LSZ testing is illustrated in Figure 5-5 where the bromide peak arrival time is plotted as a function of radius from the injection well. The arrival time is relative to the start of the bromide injection pulse. This figure also includes two theoretical bounding plots. The first is the arrival time assuming uniform radial, isotropic flow through the entire aquifer depth interval. The second curve assumes flow is uniformly radial but through only 25% of the aquifer depth interval. These bounds illustrate the layered heterogeneity in the LSZ as most points fall closer to the 25% plot indicating flow through a small fraction of the aquifer. Also, the data for MWN02-C (25 feet) are above the isotropic curve suggesting asymmetric flow away from this location while MWN02-B (28 feet) is below the 25% flow assumption indicating a strong preference for flow to the northwest in the B-horizon. The opposite trend is evident in the data from MWN06 (18 feet) located to the southeast of the injection well. The only location with a significant change between the pre- and post-testing is MWN06-B. The response in the post-TEE tracer test was much slower than in the pre-TEE test suggesting the B-horizon in this direction became less permeable during the TEE pilot test.

Figure 5-5. Tracer Peak Arrival Time as a Function of Radius from the Injection Well.

Results of the parameter fitting for the LSZ tracer test are summarized in Table 5-5. Analogous results for the UWBZ are provided in Appendix D.

Table 5-5. Summary of LSZ Tracer Test Parameter Fitting.

	Q/H (gpm/ft)	Dispersion (ft)	Q (gpm)	H (ft)	Q/H (gpm/ft)	Dispersion (ft)	Q (gpm)	H (ft)	Q/H (gpm/ft)	Dispersion (ft)	Q (gpm)	H (ft)
		MWN06	(Pre-TEE)			MWN02	(Pre-TEE)			MWN04	(Pre-TEE)	
B-horizon		Radius = 18.2 feet				Radius = 27.7 feet				Radius = 42.9 feet		
Layer 1	2.14	0.6	6	2.8	20.00	0.2	1	0.05	2.60	1.2	19.5	7.5
Layer 2					15.15	0.1	5	0.33	7.14	0.2	0.5	0.07
Layer 3					1.40	1	16	11.43				
C-horizon		Radius = 18.2 ft				Radius = 25.1 ft				Radius = 40.2 ft		
Layer 1	3.00	2	13	4.33	1	0.2	13	13	3.75	0.9	15	4
Layer 2	24.6	0.2	16	0.65								
Total	4.50		35	7.78	1.41		35	24.81	3.03		35	11.57
Flow Layers				20%				65%				30%
		MWN06	(PostTEE)			MWN02	(PostTEE)			MWN04	(PostTEE)	
B-horizon		Radius = 18.2 feet				Radius = 27.7 feet						
Layer 1	0.39	2	5.8	15	5.0	4.5	24	4.8		Not measured		
C-horizon		Radius = 18.2 ft				Radius = 25.1 ft				Radius = 40.2 ft		
Layer 1	0.80	2	4.9	6.13	1	0.9	13	13	4.21	0.9	24	5.7
Layer 2	3.2	1	28.3	8.84								
Total	1.30		39	30.0	2.08		37	17.8	4.21		24	5.7
Flow Layers				79%				47%				15%

NOTE:

For uniform, symmetric flow in the LSZ, Q/H would equal 35 gpm / (243 – 205 ft) = 0.92 gpm/ft.

5.7.2 *Concentration and Flow Data*

Appendix D presents the concentration data collected at monitoring wells and measured flow rates during the mass transfer testing. These data were used to calculate mass fluxes through the TEE cell and allow an evaluation of the change in flux resulting from the application of TEE. The complete set of groundwater concentrations measured in the TEE monitoring wells is attached in Appendix D. The data include BTEX, TPH and hydrocarbon concentrations for ranges of carbon numbers. This report and the analyses in Section 6.0 focus on benzene concentrations in groundwater as the chemical of concern. Other laboratory analytical reports, quality assurance reports, calibration procedures, etc. can be found in the TEE Pilot Test Performance Evaluation Report (BEM, 2010) and the TEE Pilot Test Work Plan (BEM, 2007).

The RESSQ program (Javandel et al., 1984) used to determine the uniform flow configurations during the mass transfer tests also calculates theoretical velocities at specified locations in the aquifer (i.e., the monitoring wells). Multiplying the velocity by the well concentration yields the mass flux. The calculated uniform benzene mass fluxes for the C- and B-horizons in the LSZ are provided in Table 5-6. The B-horizon had an average of 83% reduction in benzene flux while the deeper, more permeable C-horizon had a reduction in benzene flux of 99%. One location, MWN01-B increased in benzene flux after the TEE pilot test.

Table 5-6. Calculated Benzene Mass Fluxes in the LSZ during the Mass Transfer Testing.

Well	Radius (feet)	Pre-TEE Benzene Nov 06 (mg/L)	Pre-TEE RESSQ Velocity (cm/day)	Pre-TEE Average Flux (g/m²/day)	Post-TEE Benzene Nov 09 (mg/L)	Post-TEE RESSQ Velocity (cm/day)	Post-TEE Average Flux (g/m²/day)	Flux Reduction
MWN01B	48.33	18	54.5	9.81	23	73.7	16.95	-73%
MWN02B	27.69	24	114.3	27.44	0.012	135.5	0.02	100%
MWN03B	59.80	17	69.7	11.85	0.81	73.0	0.59	95%
MWN04B	42.86	26	76.7	19.94	0.92	100.2	0.92	95%
MWN05B	54.05	20	48.6	9.73	2	79.6	1.59	84%
MWN06B	18.20	24	174.8	41.95	0.0028	190.6	0.01	100%
Average B				**20.12**			**3.35**	**83%**
MWN01C	49.02	2.8	56.9	1.59	0.011	75.9	0.01	99%
MWN02C	25.14	5.5	125.4	6.90	0.017	150.9	0.03	100%
MWN03C	57.40	5	84.5	4.22	0.58	91.5	0.53	87%
MWN04C	40.22	8.3	81.2	6.74	0.0092	105.3	0.01	100%
MWN05C	53.62	3.9	59.3	2.31	0.01	99.1	0.01	100%
MWN06C	18.18	10	174.2	17.42	0.0014	185.1	0.00	100%
Average C				**6.54**			**0.10**	**99%**

The flux reduction at each monitoring well location is plotted in Figure 5-6 as a function of radius from the injection well. The locations closest to the injection well were expected to receive more treatment and a greater reduction than those further away. This trend is generally followed in both horizons except for the increase in flux calculated for MWN01-B. Sample analyses in this well were indicative of a local residual NAPL that received little treatment.
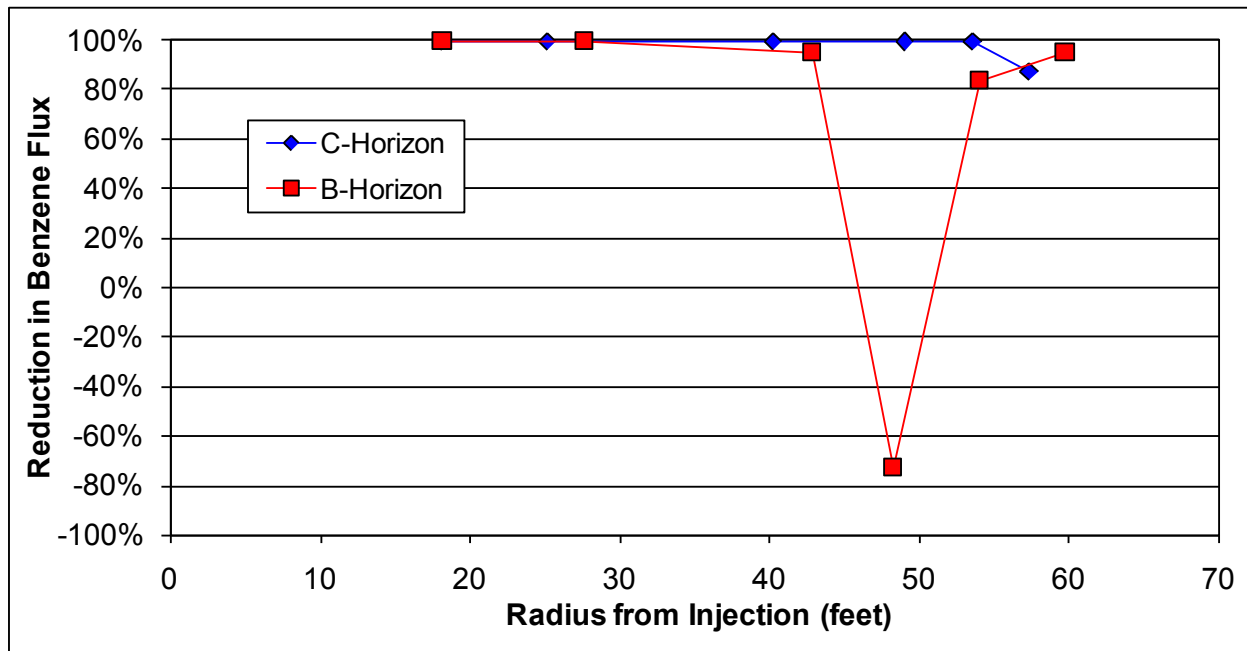
Figure 5-6. Benzene Mass Flux Reduction from Concentrations in the LSZ Monitoring Wells.

The calculated uniform benzene mass fluxes for the A-horizon in the UWBZ are provided in Table 5-7. The A-horizon had an average 48% reduction that is significantly less than the results in the LSZ. The UWBZ was observed to be more heterogeneous and the thermal treatment was less intense as less energy per cubic volume was injected in the UWBZ. Two locations, MWN01-A and MWN03-A had calculated increases in benzene flux after the TEE pilot test. However, both these locations had relatively low initial benzene concentrations in November 2006. With the rising water table, the grab samples in 2008 suggest the benzene concentration was higher in MWN01-A during the pre-TEE mass transfer test and that the TEE pilot test left the concentration unchanged at this location.

Table 5-7. Calculated Benzene Mass Fluxes in the UWBZ during the Mass Transfer Testing.

Well	Radius (feet)	Pre-TEE Benzene Nov 06 (mg/L)	Pre-TEE RESSQ Velocity (cm/day)	Pre-TEE Average Flux (g/m²/day)	Post-TEE Benzene Nov 06 (mg/L)	Post-TEE RESSQ Velocity (cm/day)	Post-TEE Average Flux (g/m²/day)	Flux Reduction
MWN01A	42.48	0.76	76.2	0.58	2.9	62.2	1.80	-211%
MWN02A	26.93	2.1	116.8	2.45	0.0067	90.5	0.01	100%
MWN03A	60.73	0.26	165.4	0.43	1.6	52.2	0.84	-94%
MWN04A	48.95	2.9	40.0	1.16	1.2	58.2	0.70	40%
MWN05A	48.40	7.8	45.2	3.52	3.3	40.2	1.32	62%
MWN06A	24.06	1.2	71.9	0.86	0.019	102.9	0.02	98%
Average A				1.50			0.78	48%

The flux reduction at each monitoring well location is plotted in Table 5-7 as a function of radius from the injection well. The locations closest to the injection well were expected to receive more treatment and a greater reduction than those further away. This trend is generally followed except for the increases in flux calculated for MWN01-A and MWN03-A as discussed above.
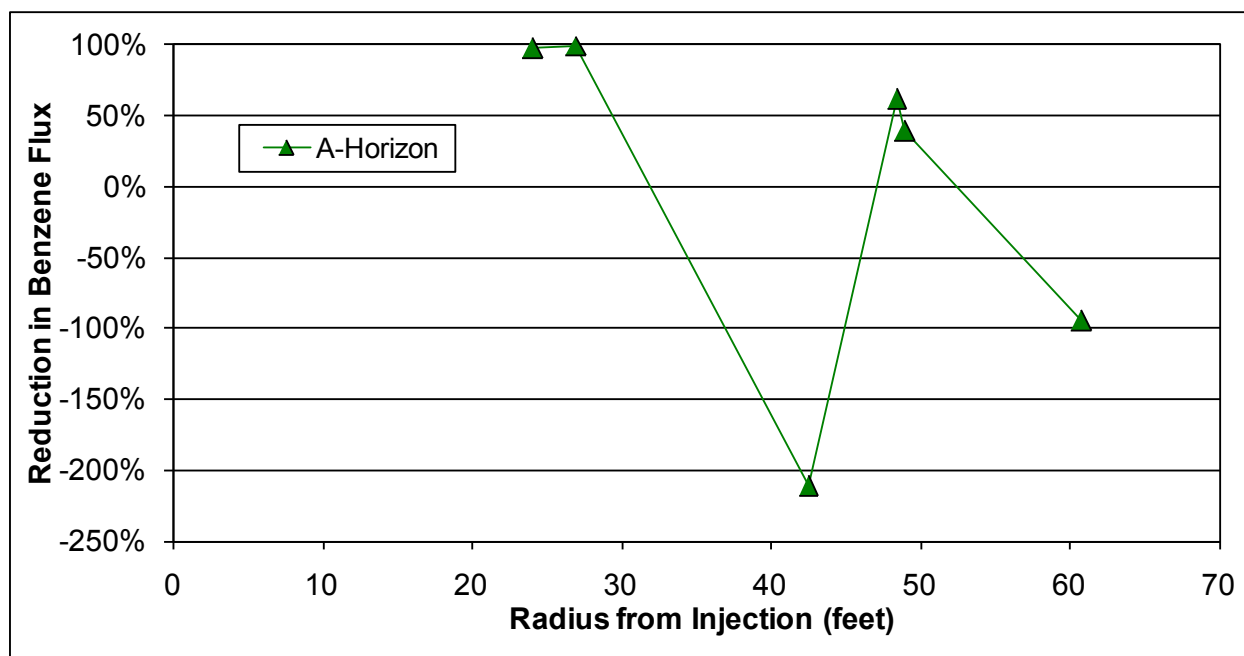
Figure 5-7. Benzene Mass Flux Reduction from Concentrations in UWBZ Monitoring Wells.

5.7.3 *Passive Flux Meter Results*

PFMs were used to measure the groundwater flux and contaminant mass flux during the forced flow conditions (injection and extraction wells were active) both before and after the TEE pilot

test. For the PFMs, flux refers to the mass of water and /or contaminants flowing per unit area at a measured depth in a well screen averaged over a given period of time. Detailed results of the PFM analysis before and after the TEE Pilot Test are provided in Appendix D, and the Final Report on the PFM deployment and results is provided as Appendix G. This section summarizes the results.

The average benzene flux per well is shown in Figure 5-8 and provides a comparison of average flux on a well-by-well basis, not taking into account the vertical variability of the fluxes within each well.
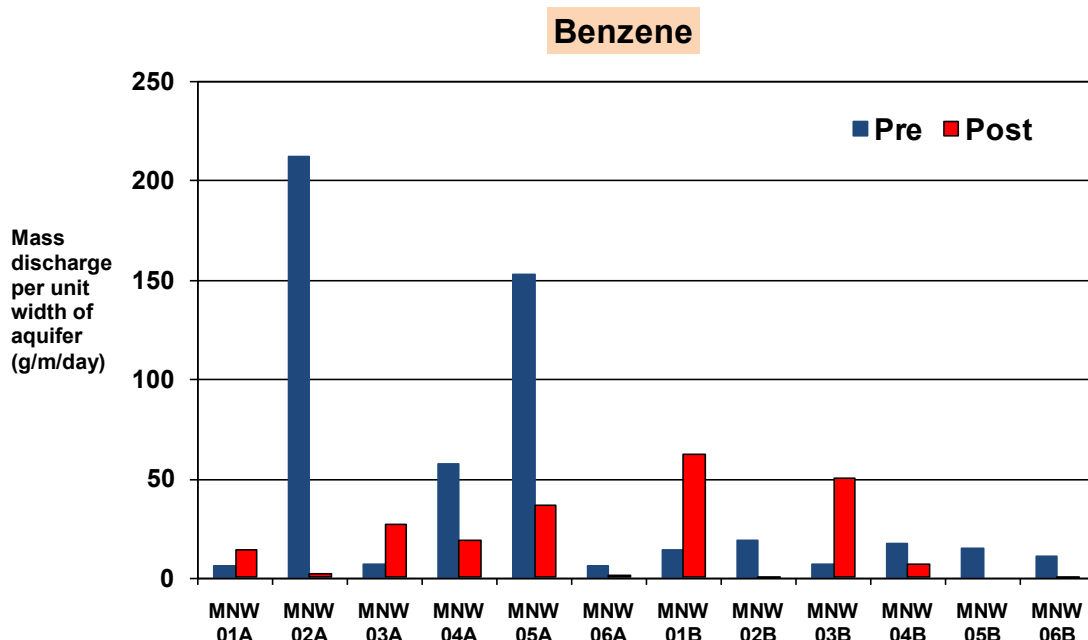
Figure 5-8. Average Benzene Mass Discharge per Well for Pre- and Post- TEE Tests.

The average benzene flux during the pre-TEE deployment was highest in wells MWN-02A and -05A in the UWBZ, with the highest observed benzene flux measured as 68 g/m^2/day in well MWN-05A. The next highest flux was observed in well MWN-04A with one sample at 50 g/m^2/day. Benzene mass flux was lower in all other wells during the pre-TEE deployment. The highest measured benzene flux in the LSZ was 8.14 g/m^2/day in well MWN-04B.

Theoretical streamlines for groundwater extraction, water injection and regional groundwater flow during the pre- and post-TEE deployments of PFMs in the A- and B-horizons were presented in Section 5.5. The RESSQ program (Javandel et al., 1984) used to determine the streamlines assuming uniform flow during the PFM deployments also calculates theoretical velocities at specified locations in the aquifer (i.e., the monitoring wells). The calculated velocities from the pre-TEE flow conditions are presented in Table 5-8 along with the PFM-measured values for the well-average Darcy velocity. The PFM-measured velocities were generally one order of magnitude lower than the theoretical value. The trend in the PFM data is

consistent with the B-horizon being less transmissive than the deeper C-horizon. The only
location with a PFM-value exceeding the theoretical uniform value was in MWN02-A.

Table 5-8. Calculated and PFM Measured Darcy Velocities during the Pre-TEE Testing.

Well	Radius (ft)	RESSQ Velocity (cm/day)	Average PFM Velocity (cm/day)	(RESSQ –PFM) /RESSQ (%)
MWN01A	42.48	76.2	10.9	86%
MWN02A	26.93	116.8	144	-23%
MWN03A	60.73	165.4	19.3	88%
MWN04A	48.95	40.0	23.8	41%
MWN05A	48.40	45.2	29.7	34%
MWN06A	24.06	71.9	31.3	56%
MWN01B	48.33	54.5	9.4	83%
MWN02B	27.69	114.3	11.9	90%
MWN03B	59.80	69.7	10.2	85%
MWN04B	42.86	76.7	9.8	87%
MWN05B	54.05	48.6	12.9	73%
MWN06B	18.20	174.8	23.8	86%
MWN01C	49.02	56.9	nm	-
MWN02C	25.14	125.4	nm	-
MWN03C	57.40	84.5	nm	-
MWN04C	40.22	81.2	nm	-
MWN05C	53.62	59.3	nm	-
MWN06C	18.18	174.2	nm	-

The RESSQ-calculated uniform velocities for the post-TEE flow conditions are presented in
Table 5-9 along with the PFM-measured values for the well-average Darcy velocity. The PFM-
measured velocities were again roughly one order of magnitude less than the theoretical uniform
values with the exception of MWN03-A which nearly matched the theoretical value. The major
changes in the PFM measures between the pre- and post-TEE measures was in well MWN02-A
where the velocity was more than one order of magnitude less after the TEE pilot test. If the
PFMs were optimally deployed in the subsurface and the absolute values were accurate, the PFM
measured fluxes should vary both above and below the theoretical values. Having all values in a
horizon either higher or lower than the theoretical uniform flow value suggests the absolute
values are biased.

Table 5-9. Calculated and PFM Measured Darcy Velocities during the Post-TEE Testing.

Well	Radius (ft)	RESSQ Velocity (cm/day)	Average PFM Velocity (cm/day)	(RESSQ –PFM) /RESSQ (%)
MWN01A	42.48	62.2	26.0	58%
MWN02A	26.93	90.5	8.70	90%
MWN03A	60.73	52.2	50.5	3%
MWN04A	48.95	58.2	28.1	52%
MWN05A	48.40	40.2	26.5	34%
MWN06A	24.06	102.9	13.9	86%
MWN01B	48.33	73.7	17.6	76%
MWN02B	27.69	135.5	72.8	46%
MWN03B	59.80	73.0	3.90	95%
MWN04B	42.86	100.2	12.9	87%
MWN05B	54.05	79.6	-	-
MWN06B	18.20	190.6	17.4	91%
MWN01C	49.02	75.9	nm	-
MWN02C	25.14	150.9	nm	-
MWN03C	57.40	91.5	nm	-
MWN04C	40.22	105.3	nm	-
MWN05C	53.62	99.1	nm	-
MWN06C	18.18	185.1	nm	-

Multiplying the uniform, RESSQ-calculated velocity by the measured well concentration of benzene yields the benzene mass flux at that location. The calculated uniform benzene mass fluxes are provided in Table 5-10 along with the well-averaged values measured with the PFMs. All pre-TEE PFM measures of benzene mass flux exceeded the theoretical values in the A-horizon of the UWBZ. Conversely, in the B-horizon of the LSZ, the PFM measures of benzene flux were all less than the theoretical values although the values are generally within one order of magnitude.

Table 5-10. Calculated and PFM Measured Benzene Fluxes during the Pre-TEE Testing.

Well	Radius (ft)	RESSQ Benzene Flux (g/m²/day)	Average PFM Benzene Flux (g/m²/day)	(RESSQ –PFM) /RESSQ (%)
MWN01A	42.48	0.58	1.20	-107%
MWN02A	26.93	2.45	37.9	-1447%
MWN03A	60.73	0.43	1.10	-156%
MWN04A	48.95	1.16	3.70	-219%
MWN05A	48.40	3.52	31.3	-789%
MWN06A	24.06	0.86	1.50	-74%
MWN01B	48.33	9.81	3.5	64%
MWN02B	27.69	27.44	4.6	83%
MWN03B	59.80	11.85	1.9	84%
MWN04B	42.86	19.94	4.0	80%
MWN05B	54.05	9.73	3.8	61%
MWN06B	18.20	41.95	2.7	94%
MWN01C	49.02	1.59	nm	-
MWN02C	25.14	6.90	nm	-
MWN03C	57.40	4.22	nm	-
MWN04C	40.22	6.74	nm	-
MWN05C	53.62	2.31	nm	-
MWN06C	18.18	17.42	nm	-

The RESSQ-calculated benzene mass fluxes for the post-TEE flow conditions are presented in Table 5-11 along with the PFM-measured values for the well-averaged benzene flux. The PFM-measured values were again all higher than the theoretical values in the A-horizon. In contrast to the pre-TEE findings, the post-TEE PFM-measured fluxes were all higher than the theoretical values except in well MWN01B where the values nearly matched.

The major changes in the PFM measures between the pre- and post-TEE measures were in wells MWN01-B and MWN03-B where the benzene flux increased. The increase at MWN01-B is consistent with the prediction from the theoretical value; however, the increase at MWN03-B was not consistent with the concentration-based prediction of a decrease of more than one order of magnitude. The PFM data are explored more fully in Section 6.0.

Table 5-11. Calculated and PFM Measured Benzene Fluxes during the Post-TEE Testing.

Well	Radius (ft)	RESSQ Benzene Flux (g/m²/day)	Average PFM Benzene Flux (g/m²/day)	(RESSQ –PFM) /RESSQ (%)
MWN01A	42.48	1.80	2.5	-39%
MWN02A	26.93	0.01	0.2	-1900%
MWN03A	60.73	0.84	4.7	-460%
MWN04A	48.95	0.70	3.1	-343%
MWN05A	48.40	1.32	6.3	-377%
MWN06A	24.06	0.02	0.1	-400%
MWN01B	48.33	16.95	14.4	15%
MWN02B	27.69	0.02	0.10	-400%
MWN03B	59.80	0.59	11.4	-1832%
MWN04B	42.86	0.92	1.60	-74%
MWN05B	54.05	1.59	-	-
MWN06B	18.20	0.01	0.10	-900%
MWN01C	49.02	0.01	nm	-
MWN02C	25.14	0.03	nm	-
MWN03C	57.40	0.53	nm	-
MWN04C	40.22	0.01	nm	-
MWN05C	53.62	0.01	nm	-
MWN06C	18.18	0.00	nm	-

5.7.4 *Source Mass Estimates*

Estimates for the mass of NAPL in the TEE cell were developed by the U.S. Air Force and the methodology is described in detail in the TEE Pilot Test Performance Evaluation Report (BEM, 2010). The NAPL mass estimation procedures and results are summarized in Appendix D. These mass estimates, the concentrations and fluxes from Section 5.7.2, and the PFM data of Section 5.7.3 are used in Section 6.0 to evaluate the mass transfer tests and the utility of the approach for predicting the longevity of a multi-component NAPL source zone. The total mass, and therefore the NAPL saturation, was reduced by less than 10 percent in each zone by TEE during the pilot test. Hence, the flow conditions in the subsurface with respect to mass transfer between the residual NAPL and injected water were very similar between the pre-TEE and the post-TEE testing. The major change in test conditions was in the benzene content of the residual NAPL which was reduced by 88% and 65% in the LSZ and UWBZ, respectively, as a result of the TEE pilot test.

6.0 PERFORMANCE ASSESSMENT

The methodology of the MTT was evaluated before and after the TEE pilot test at WAFB according to five quantitative and qualitative criteria. Section 4.0 presented a description of each objective, data requirements, success criteria, and a brief summary of the evaluation of success for each objective. This section provides the details and analyses to support the evaluation of each performance objective. Though data was collected in both the UWBZ and LSZ during the MTTs, the quantitative performance objectives were evaluated using data only from the LSZ due to the intensity of the modeling efforts.

A numerical groundwater flow and solute transport model (see Appendix F) and an analytical model were used for assessing the quantitative performance objectives, beginning with estimates of source zone hydrogeologic and contaminant NAPL dissolution parameters. Although the complexity of ST012 required a comprehensive numerical model, at sites that are relatively homogeneous, an analytical model may be sufficient.

A comprehensive, three-dimensional numerical site model for groundwater flow at ST012 served as the foundation for a smaller-scale (local) model for simulating the pre-TEE and post-TEE tracer tests and MTTs performed in the LSZ. Figure 6-1 and Figure 6-2 depicts the ST012 site model for the LSZ . Nested within the larger model is the local model. As shown in the figure, the model captures the stratigraphy at ST012 and lithologic variations associated with the LSZ. Boring logs taken from locations in the vicinity of the TEE cell were interpolated, and, where necessary, extrapolated to generate a three-dimensional representation of the LSZ.

The local model for simulating the MTT was constructed using the Groundwater Modeling Software (GMS), which serves as a pre- and post-processing utility for MODFLOW2000, MT3DMS, SEAM3D and several other modeling codes. The active area of the local flow model incorporates the TEE cell and adjacent areas (see Figure 6-1 and Figure 6-2). Bromide transport during the pre- and post-TEE tracer tests was simulated using a conservative (non-reactive) species with the model code MT3DMS. Additional information and details of the modeling are provided in Appendix F.

Figure 6-1. Areal Extent of the Local Model for MTT Simulations.
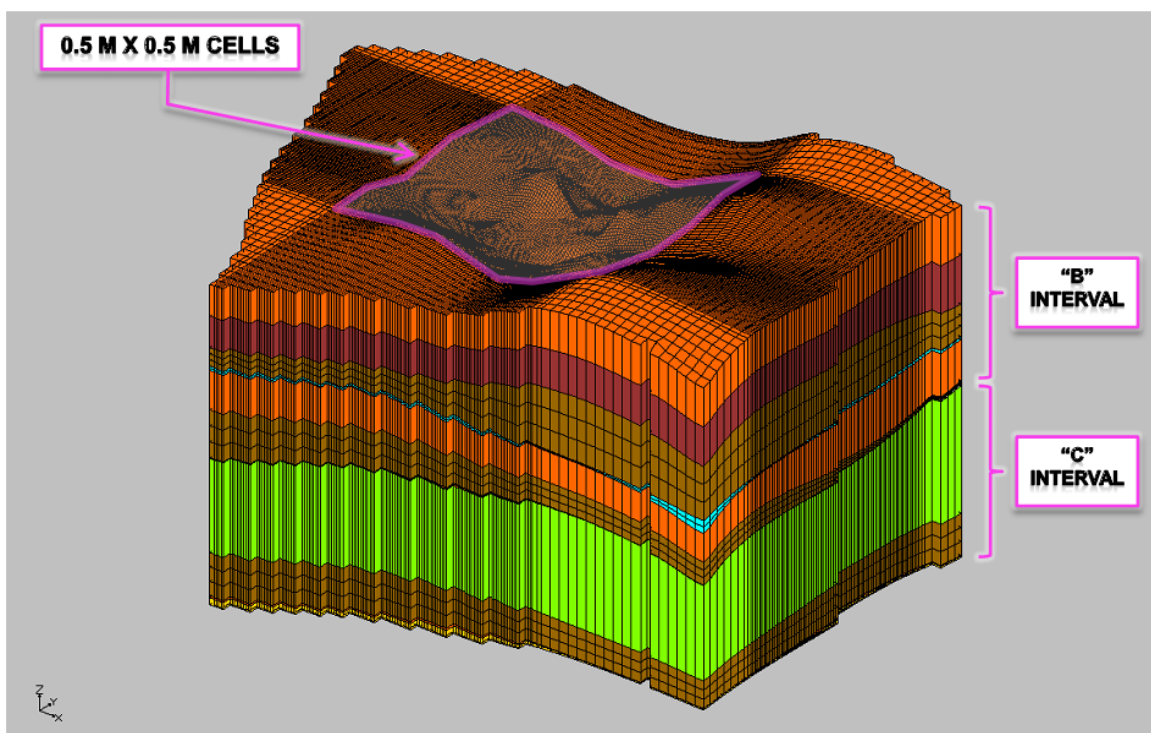
Figure 6-2. Three-Dimensional Representation of the Site and Local Models of the Lower Saturated Zone (LSZ).

6.1 PERFORMANCE OBJECTIVE: ESTIMATE OF SOURCE ZONE HYDROGEOLOGIC PARAMETERS

This quantitative performance objective was to validate a method of measuring groundwater velocities through the source zone and interpreting these data to produce hydraulic conductivity estimates. Estimates of hydrogeologic parameters were derived from simulations of the pre-TEE and post-TEE tracer tests using the local model of the LSZ depicted in Figure 6-2.

Figure 6-3 shows a comparison of the observed and simulated breakthrough concentration of the bromide tracer in the B-horizon at monitoring well MWN-06B for the pre-TEE (upper plot) and post-TEE (lower plot) tracer tests. These data were selected for comparison because MWN-06B was the observation point closest to the injection well (18 feet away), and provided a higher degree of confidence relative to data collected at other monitoring wells.

For both the pre- and post-TEE tracer tests, the model captures breakthrough characteristics related to travel time and the rise to peak concentrations at MWN-06B. Figure 6-4 is a comparison of model results with observed tracer concentration data at MWN-02B for the post-TEE tracer test. Again, the model captures the key characteristics of the tracer breakthrough at the monitoring well next-closest to the injection well (28 feet away). At both wells, the model does a credible job of matching the time of travel with a differential between the observed and simulated breakthrough time varying by no more than a factor of two.
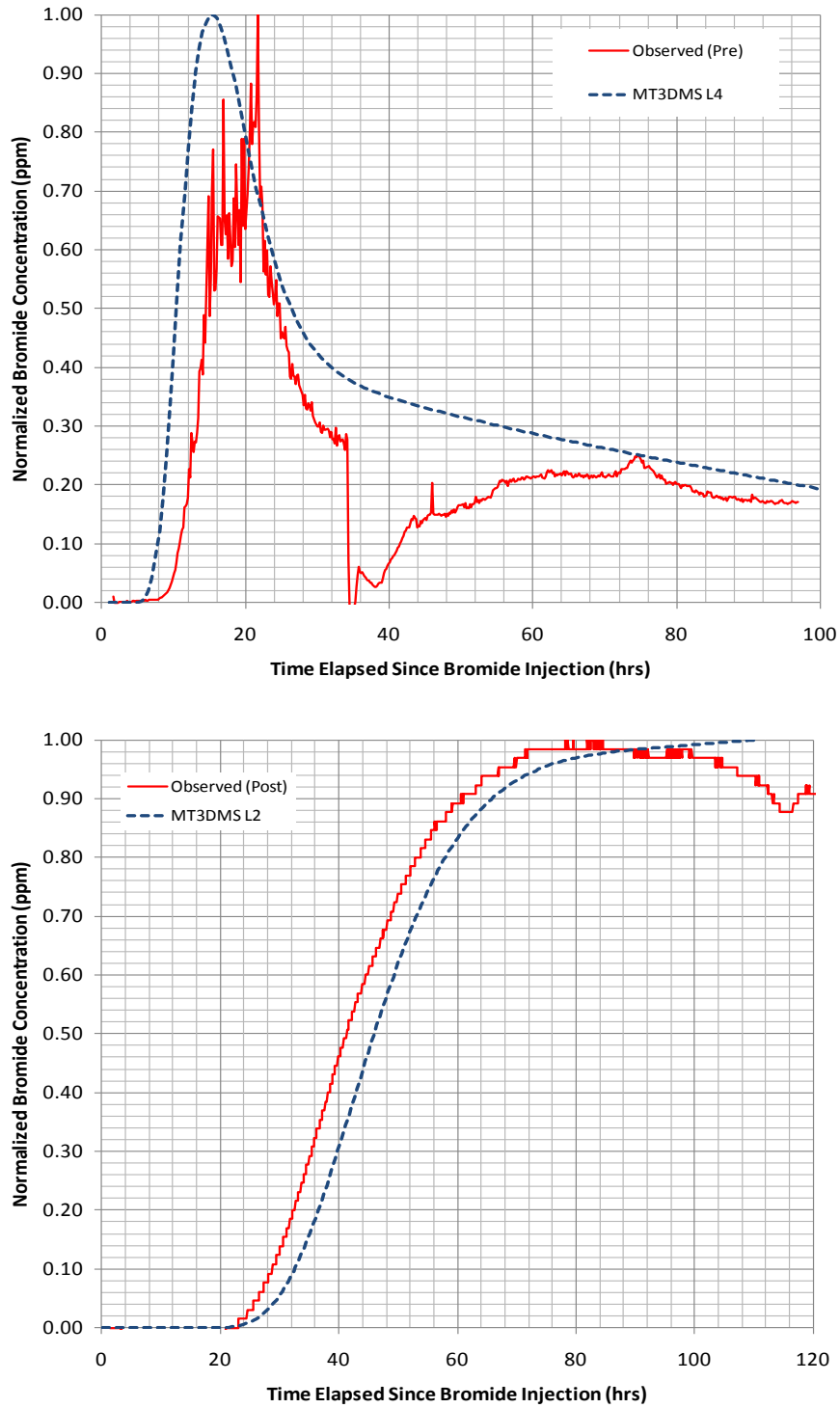
Figure 6-3. Comparison of Observed and Simulated Bromide Concentrations for the Pre-TEE (upper) and Post-TEE (lower) Tracer Tests at MWN-06B.
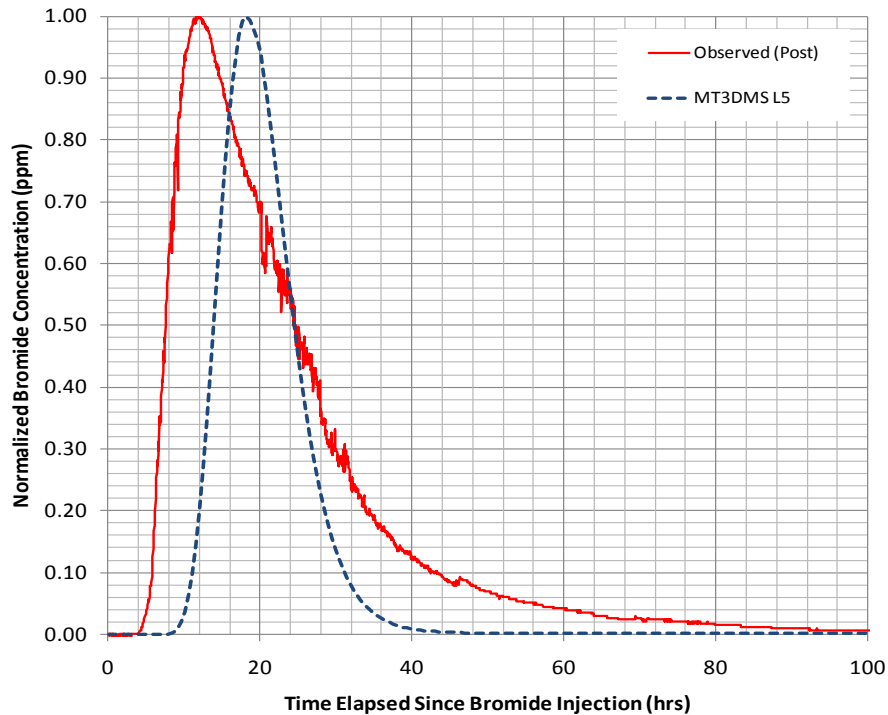
Figure 6-4. Simulated and Observed Post-TEE Tracer Test Bromide Concentrations at MWN-02B.

A primary determinant of success for this objective was that the range of vertically discrete water velocities from PFM data was consistent with measured injection and extraction rates. Specifically, the average of the PFM groundwater velocity measurements should have been within a factor of two (i.e., +100% / -50%) of the average velocity based on a mass balance of the measured injection rate. Plots of post-TEE PFM Darcy velocity data derived from the PFMs and simulated flow rates with depth in the B-horizon derived from the groundwater flow model provide a comparison at both MWN-06 and -02 (Figure 6-5, upper and lower plots, respectively). Vertical location of the PFMs in MWN-06 may have missed the thin layer of high permeability sand, but, overall, the results provide a reasonable match, particularly in the fine sand layers. At MWN-02, the under- prediction of Darcy velocity using the model is consistent with under predicted time of travel and may explain the differential in the observed and simulated breakthrough concentrations. These results are consistent with the conclusions of simplified tracer test modeling in which a thin, permeable lens was identified in MWN06-C and a higher than expected permeability was suggested in MWN02-B (see Table 5-5).

The success criterion was achieved at all monitored locations. For both the pre- and post-TEE tracer tests, the local numerical SEAM3D model of the TEE cell captured breakthrough characteristics related to travel time and the rise to peak concentrations at monitoring wells closest to the injection well (wells 18 and 28 feet away). At both wells, the model matched the time of travel with a differential between the observed and simulated breakthrough time varying by no more than a factor of two. Differences in the time of travel may be a result of temporal variability in the withdrawal rates at the peripheral pumping wells in the TEE cell. At more distal monitoring wells, the tracer concentration decayed to levels close to the detection limit of the

bromide sensor. As such, modeling results achieved a better match with the observed data at wells closer to the injection well relative to the more distant monitoring wells.

Figure 6-5. Comparison of Post-TEE PFM Darcy Velocity with Depth in the B Interval with Values of the Darcy Velocity in Model Layers Simulated Using MODFLOW2000 at MWN-06B (upper) and MWN-02B (lower).

6.2 PERFORMANCE OBJECTIVE: ESTIMATE OF SOURCE ZONE CONTAMINANT PARAMETERS

This quantitative performance objective was to validate a method to determine source zone parameters applicable to prediction of NAPL mass discharge and source longevity under different remedial strategies. Starting with a calibrated local model of the TEE cell from the first objective, source zone parameters (i.e., input to the SEAM3D NAPL Package) were determined through calibration to the hydrocarbon concentrations at monitoring wells within the TEE cell and mass flux measurements based on PFM results. After simulating the pre-TEE MTT results, the process was repeated for the post-TEE test to evaluate mass removal, compositional changes, and post-remediation mass transfer rates following completion of the TEE pilot test.

For the purpose of simulating the two MTTs in the LSZ, the aforementioned local model was simplified by limiting the active area to the model layers corresponding to the upper region of the LSZ with focus on data collected from wells screened in the B-horizon (Figure 6-6).Before and after the TEE pilot test, PFMs were deployed in the B-horizon and not in the deeper C-horizon. SEAM3D was used for all of these simulations, which provided the ability to simulate the rate of mass transfer from a NAPL source.
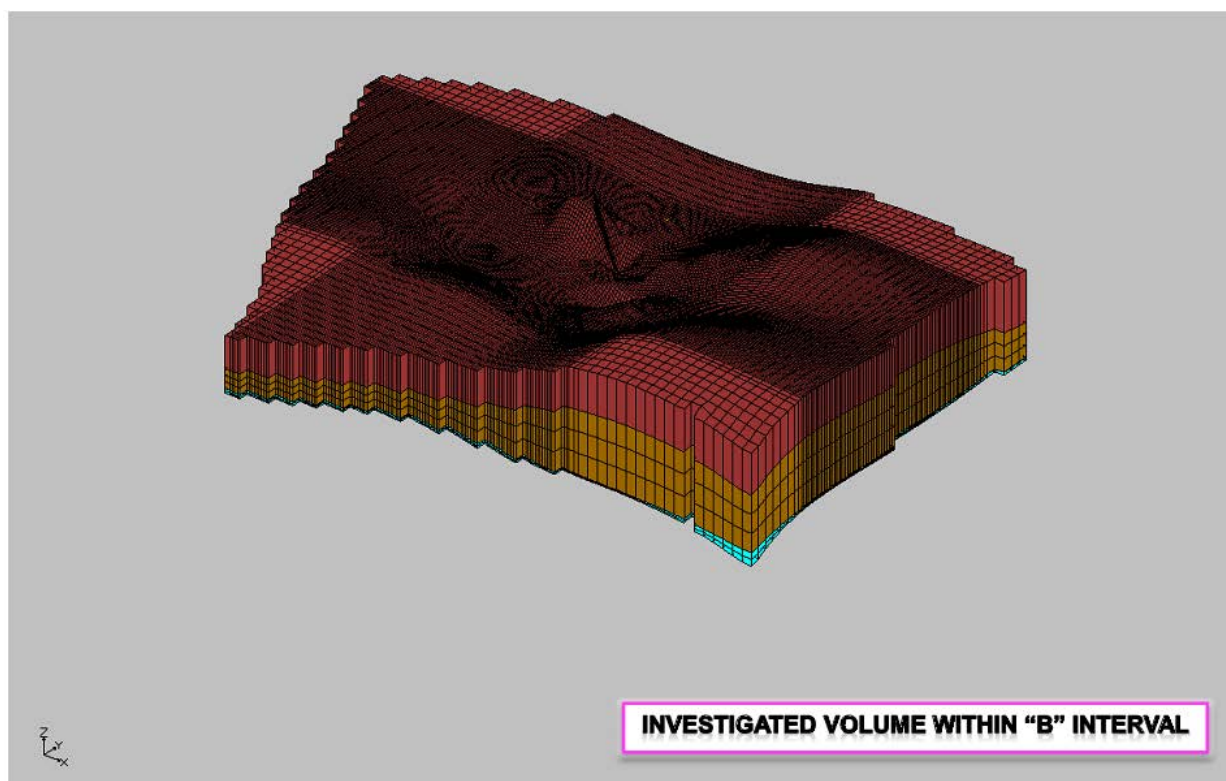
Figure 6-6. Revised Local Model for Simulating the Pre- and Post-TEE Mass Transfer Tests in the B Horizon of LSZ.

Table 6-1 shows the NAPL properties (mass fraction, solubility and molecular weight) specified in the local models for the pre-TEE and post-TEE LSZ MTTs. The model NAPL consisted of

four components that included two volatile components (benzene and TEX), one semi-volatile group comprised of naphthalene and trimethylbenzene, and an inert fraction comprised of low-solubility aromatics and aliphatics. NAPL compositions were based on historical analysis of NAPL samples and recent analysis of NAPL samples performed in support of the TEE pilot test, as described in Section 5.2. For more detail, see Appendix F. For the post-TEE LSZ MTT, changes in composition were based on results of the TEE pilot test including monitoring well data collected to assess post-TEE conditions.

NAPL mass estimates for the pre-TEE MTT were determined using residual saturation values based on soil type developed by Adamski and Charbeneau (personal communication, 2010). These mass estimates are described in detail in Appendix D. Residual saturation values varied with depth, ranging from 2.8-7.7% depending on the soil type at the depth of interest. For the post-TEE MTT, NAPL concentrations (NAPL mass per mass of aquifer solids) were modified for mass removal resulting from thermal treatment, and the NAPL composition was modified in the treated areas to reflect preferential extraction of the more volatile and soluble compounds from the NAPL. The percentage of NAPL removed from the pilot TEE cell was based on the results of the TEE pilot test. Sensitivity of this estimate was evaluated in terms of the initial equilibrium benzene and TEX (toluene, ethylbenzene and total xylenes) concentrations under natural gradient flow and the equilibrium concentrations reached during the MTT.

Table 6-1. NAPL Composition- Pre-TEE and Post-TEE MTT Models.

NAPL Constituent	% Mass		Solubility (mg/L)	Molecular Weight (g/mol)
	Pre-TEE	Post-TEE		
Benzene	0.83	0.10	1780.0	78.11
TEX	7.33	1.79	299.75	100.62
Semi-Volatile Compounds	1.97	1.71	58.3	122.22
Inert Fraction	89.87	96.40	--	114.80

Figure 6-7 shows the benzene (upper plot) and TEX (lower plot) concentrations observed at monitoring well MWN-06B during the pre-TEE LSZ MTT and simulated using the local transport model. With the introduction of clean groundwater at the central injection well (LSZ07), concentrations declined as the cleaner water reached various monitoring wells. Steady-state benzene and TEX concentrations (i.e., steady-state concentrations) were reached within days. Evaluation of the transient behavior of concentrations was limited by the availability of data. Breakthrough of cleaner water mimicked the tracer breakthrough, and, as a result, steady-state concentration was the primary target for comparison.

The gradual increase in the observed equilibrium concentrations reflected a decrease in the groundwater velocity when the pumping well LSZ01 was turned off on 9/2/2008 (Figure 6-7). This variation in pumping was not included in the groundwater flow model, and as such, the rise in the equilibrium concentrations would not be simulated by the transport model. For both the

benzene and TEX, the model accurately captured responses following injection including the equilibrium concentrations of the pre-TEE MTT. The model input variables that most directly controlled the equilibrium concentrations were the NAPL mass transfer coefficient and the NAPL composition, specifically the benzene mass fraction.

For the post-TEE test, concentrations in the TEE cell showed much greater variability among the monitoring wells compared to the pre-TEE case. This variability was primarily the result of variable treatment within the cell that yielded non-uniform NAPL composition and distribution in the cell. The initial rise and drop in the simulated benzene concentrations (Figure 6-8, upper plot) reflected an inconsistency between the initial condition and the initial equilibrium concentration determined using the NAPL Package. A similar response was observed in the simulated TEX concentrations (Figure 6-8, lower plot). However, the local solute transport model provided a reasonable representation of the decrease in the concentration over time at MWN-06B. The simulated equilibrium benzene concentration (340 µg/L) was within an order of magnitude of the observed value (79 µg/L), whereas the match between the observed and simulated TEX equilibrium concentrations (750 µg/L and 690 µg/L, respectively) was much improved.

The sensitivity of the post-TEE equilibrium benzene and TEX concentrations at MWN-06B to the NAPL mass transfer coefficient and the NAPL mass fraction of benzene are also shown in Figure 6-8. By reducing the NAPL mass transfer coefficient an order of magnitude relative to the pre-TEE test, an improved match with the benzene concentration was realized, but a poorer match with the TEX concentration was apparent (Figure 6-8, upper and lower plots, respectively). The mass fraction of benzene in the post-TEE NAPL likely varied by an order-of-magnitude across the cell whereas the TEX content was likely more consistent. To assess sensitivity of the benzene mass fraction, simulations were performed in which the percent benzene in the NAPL was reduced and increased by a factor of two relative to the assumed value shown in Table 6-1 (0.10%). Using the lower NAPL mass transfer coefficient (0.05 d^{-1}), equilibrium benzene concentration varied from 130 to 6 µg/L and bracketed the baseline simulated and observed concentrations (80 µg/L and 79 µg/L, respectively).
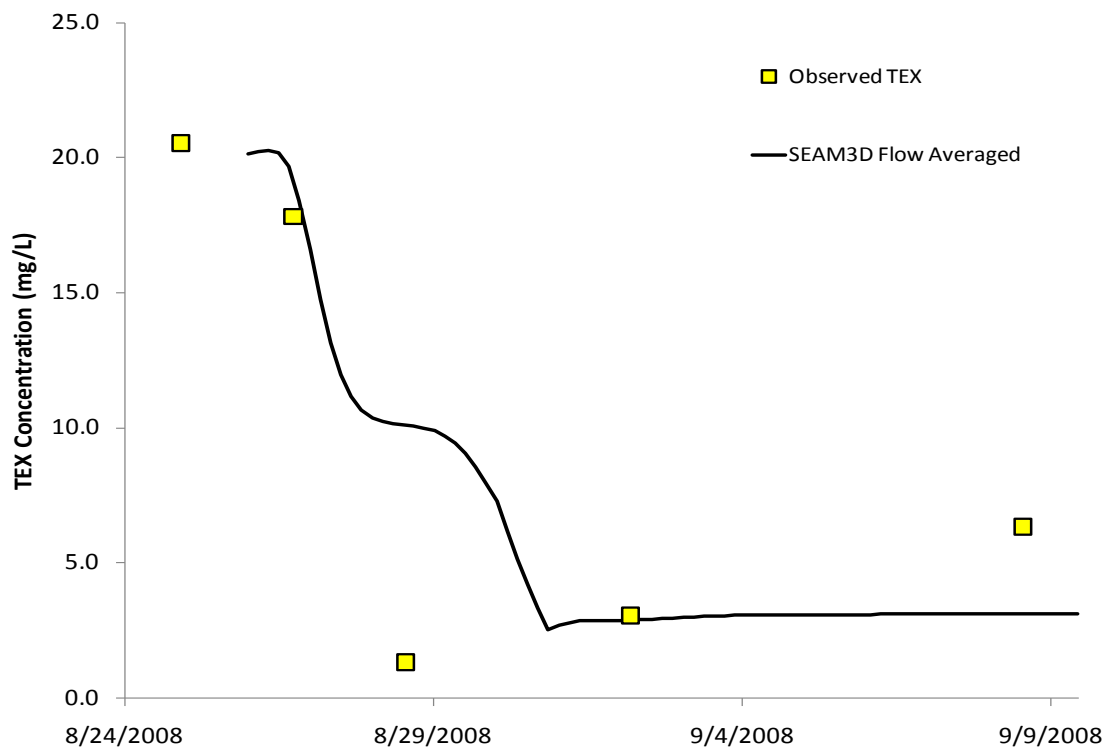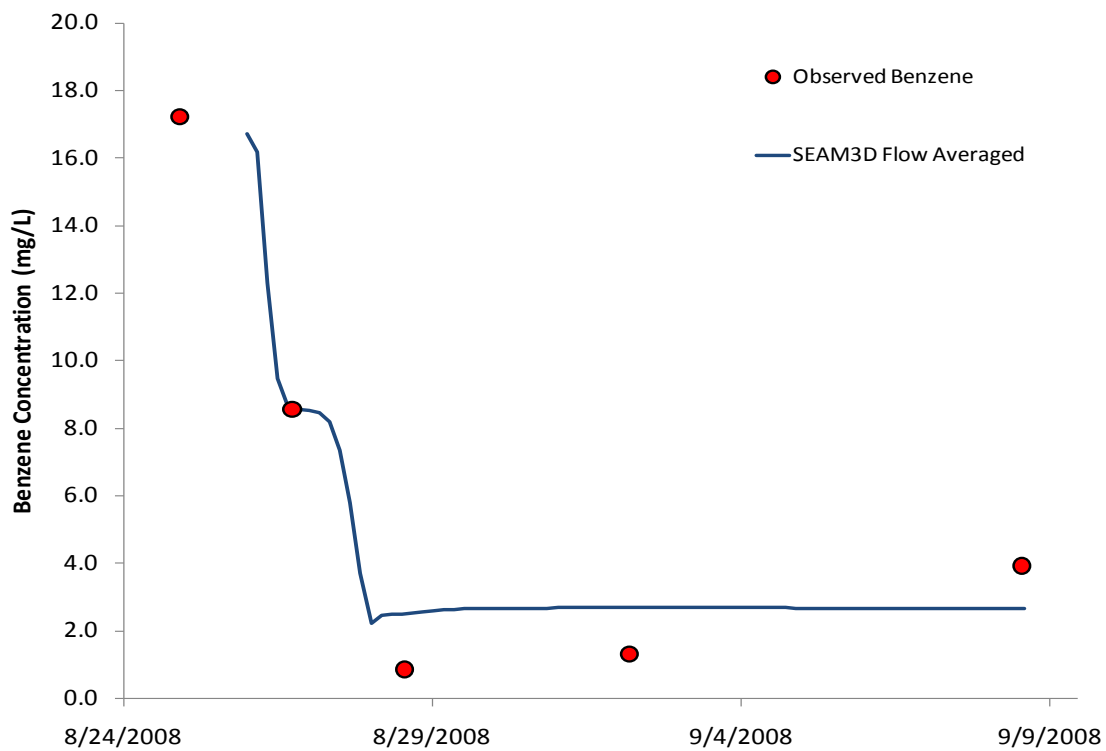
Figure 6-7. Pre-TEE Mass Transfer Test Results Showing Observed and Simulated Flow-Weighted Benzene (upper) and TEX (lower) Concentrations at MWN-06B.
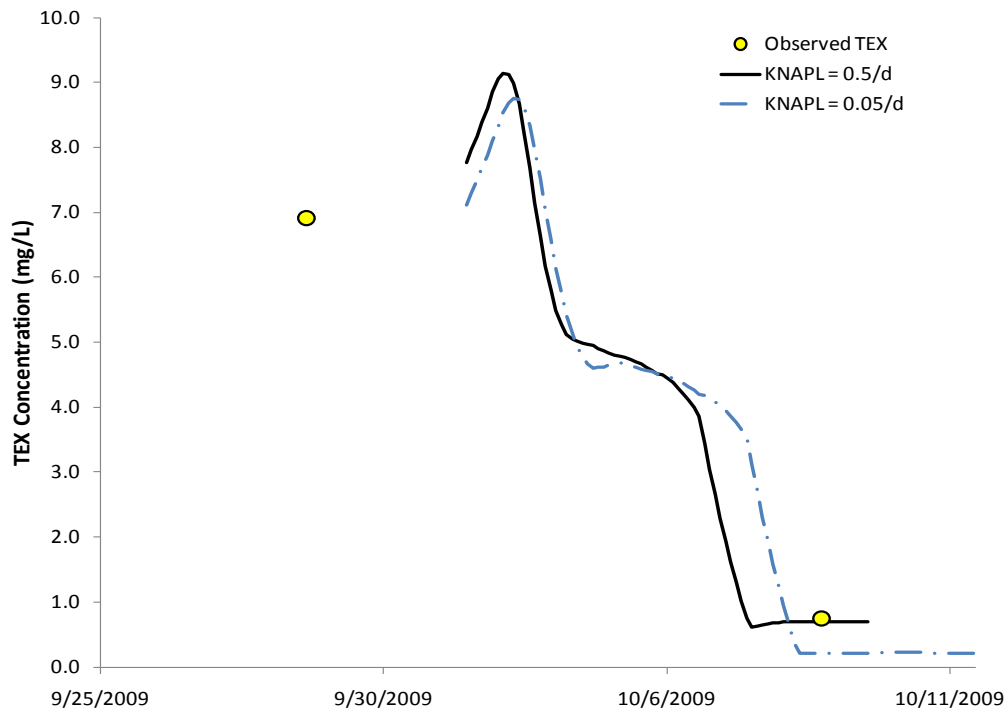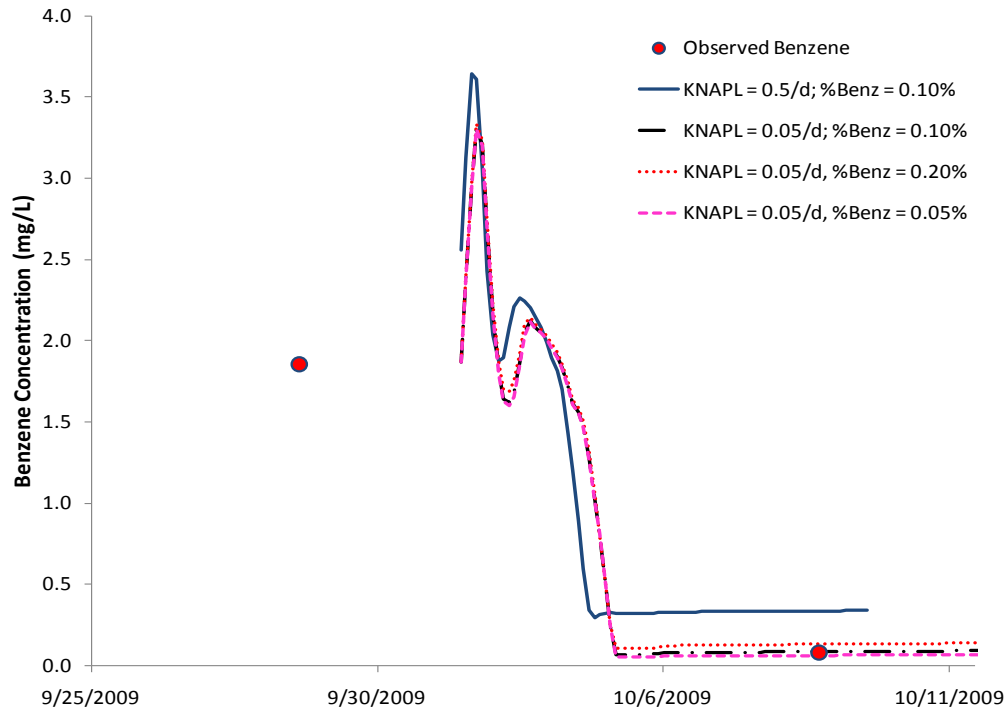
Figure 6-8. Post-TEE Mass Transfer Test Results Showing Observed and Simulated Flow-Weighted Benzene (upper) and TEX (lower) Concentrations at MWN-06B. KNAPL refers to the NAPL mass transfer coefficient.

A summary of results provides an overall representation of the success of the local solute transport model to simulate the equilibrium benzene concentration associated with the pre-TEE and the post-TEE LSZ MTTs (Figure 6-9, upper and lower plots, respectively) for the five monitoring wells nearest to injection well LSZ07. The plot order is based on proximity to the injection well. In both the pre-TEE and post-TEE tests, the accuracy of the model to match concentration data did not appear to decrease with radial distance. For the post-TEE test, the simulated equilibrium benzene concentrations were uniformly greater than the observed concentrations. The larger concentration at MWN-05B reflected a relatively stagnant zone in the flow field during the MTT, which was captured in the simulation results. Results for the variation in the NAPL mass transfer coefficient from 0.50 d^{-1} to 0.05 d^{-1} are shown for the post-TEE MTT (Figure 6-9 lower plot). Model sensitivity to the NAPL mass transfer coefficient generally decreased with increased radial distance from the injection well. In conclusion, Figure 6-9 provides a finding that the success criterion for Performance Objective 4.2 to match the post-TEE concentrations with modeling within an order-of-magnitude was adequately met.
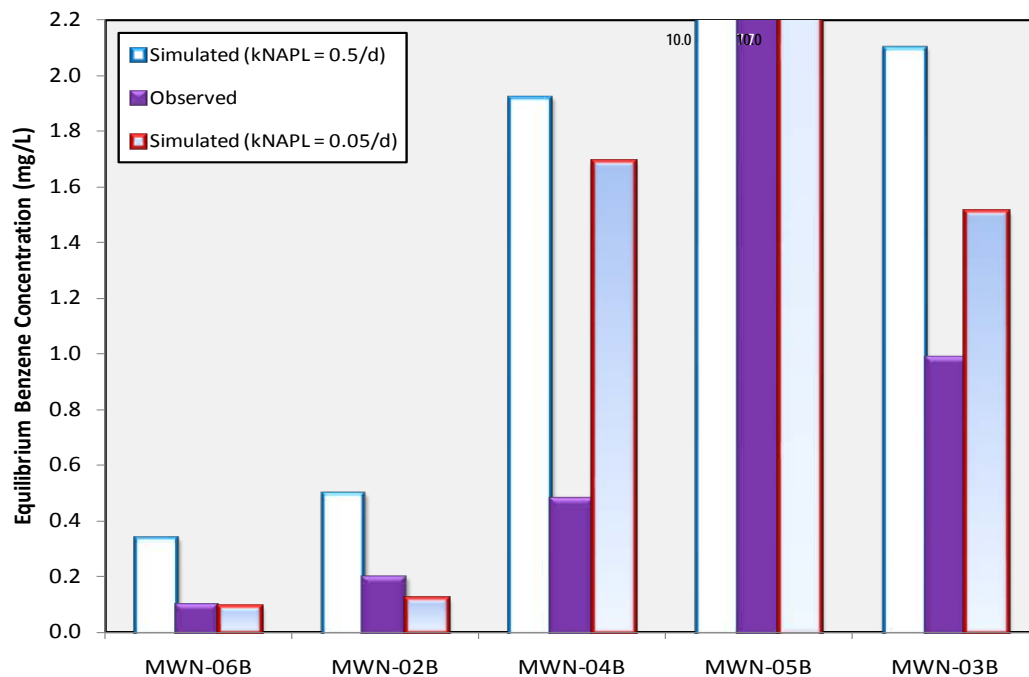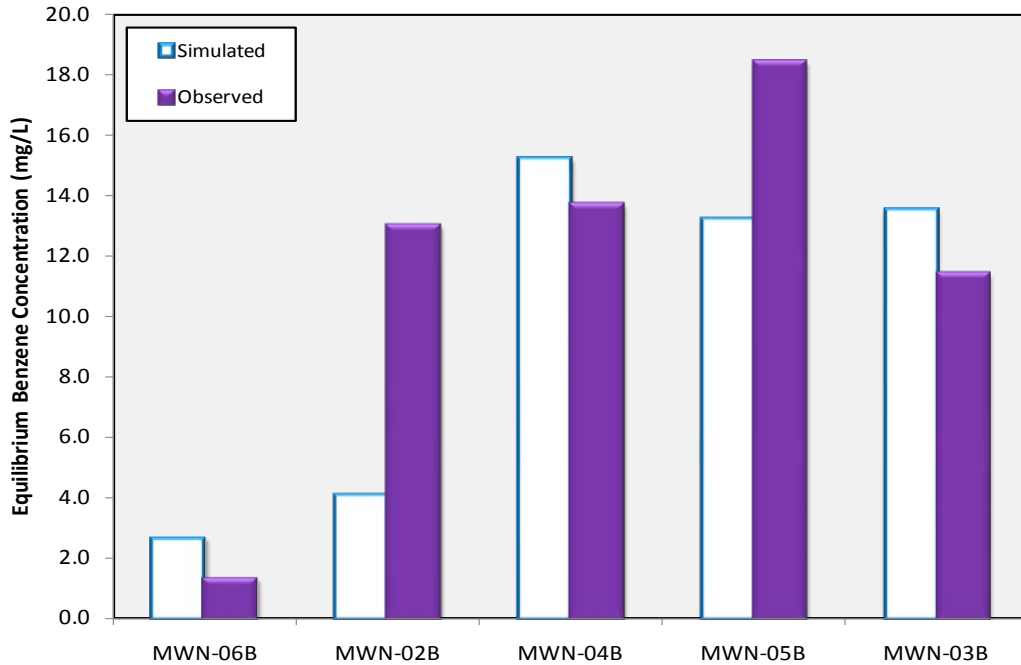
Figure 6-9. Comparison of Observed and Simulated Pre-TEE (upper) and Post-TEE (lower) Mass Transfer Test Equilibrium (pseudo steady-state) Benzene Concentrations at B Interval Monitoring Wells.
Wells ordered left to right by proximity to the center injection well LSZ07. Sensitivity to the mass transfer coefficient (kNAPL) is shown for the post-TEE results.

To support the numerical modeling results, in particular the assumed mass transfer coefficients, a more simplistic analytical model was derived for determining bulk NAPL mass transfer coefficients from the pseudo steady-state concentration data. The model derivation is found in Appendix H, and includes a dimensionless mass transfer parameter, σ. This dimensionless parameter can be fit to the concentration data and, as derived in Appendix H, is related linearly to the bulk mass transfer coefficient. With σ determined from a fit to the field data, the relationship yields a measure of the bulk mass transfer coefficient that is applicable to other flow regimes as described below. It allows the bulk mass transfer coefficient to be calculated for any flow regime at the site by introducing the local velocity. Correlations for the mass transfer coefficient developed from column studies of flow through residual NAPL (Mayer and Miller, 1996) were used for comparison.

To provide a more intuitive comparison between the data fit parameter, σ, mass transfer correlations in the literature, and field bulk mass transfer coefficients, the mass transfer correlations were averaged over the radius of testing. The volume-averaged bulk mass transfer coefficients provided in Appendix H are shown in Table 6-2. The fits to field data are roughly three orders of magnitude less than the values calculated from correlations based on flow through a uniformly distributed residual NAPL. This large difference was expected as the heterogeneities in a real subsurface tend to discourage contact between flowing water and residual NAPL, whereas the flow is forced through the residual NAPL in laboratory column studies. These data suggest that literature correlations based on a uniformly distributed NAPL in a homogeneous soil would overpredict mass transfer in heterogeneous field settings by two to three orders of magnitude.

The average bulk mass transfer coefficients determined from the field data provide a defensible measure of this parameter for use in modeling. The average bulk mass transfer coefficients estimated from the analytical model range from 0.0076 to 0.104 d^{-1}. The values employed in the numerical modeling reported above in this report ranged from 0.05 to 0.5 d^{-1}, and therefore may have modestly overpredicted the mass dissolution rate in the source zone, but they were of the same order of magnitude.

Table 6-2. Comparison of Average Bulk Mass Transfer Coefficients.

Test	σ	$\left(\overline{K}_i\right)_{\text{data fit}}$ (d^{-1})	$\left(\overline{K}_i\right)_{\text{correlation}}$ (d^{-1})
PreTEE B-Horizon	0.0073	0.104	31.9
PostTEE B-Horizon	0.0025	0.036	31.9
PreTEE C-Horizon	0.0030	0.044	11.8
PostTEE C-Horizon	0.00052	0.0076	11.8

In conclusion, the mass transfer parameter values presented in Table 6-2 allow the bulk mass transfer coefficient under ambient conditions to be estimated. The redefined dimensionless mass transfer parameter, σ, is independent of velocity. Hence, the ambient groundwater velocity at the site can be inserted to calculate estimates of the bulk mass transfer coefficients in the two

horizons under ambient conditions, and a defensible mass dissolution rate from the source area over time can be determined, and remedial timeframes can be more accurately estimated.

6.3   PERFORMANCE OBJECTIVE: ESTIMATE OF REDUCTION IN CONTAMINANT MASS DISCHARGE AS A RESULT OF PARTIAL SOURCE REDUCTION

This quantitative performance objective was to validate a method for estimating the reduction of mass discharge resulting from partial removal of NAPL mass from a source area. The goal was to evaluate the potential benefit of a remediation approach for partial mass removal required to meet a specified cleanup metric. Using the local solute transport model described for the first two objectives, this performance objective was assessed by comparing methods for calculating the change in mass flux of benzene at monitoring wells. In the field, this was directly determined using PFMs in the B interval monitoring wells during the latter phase of both the pre- and post-TEE MTTs.

The estimated masses extracted from within the TEE test cell are discussed in Appendix D. Approximately 90% of the benzene within the LSZ test volume was extracted. In the field, the change in mass flux was directly determined for the LSZ using PFMs installed in the B interval monitoring wells during the latter phase of the MTTs and also from measured monitoring well concentrations and modeled water fluxes. Simulated benzene mass flux was based on the MODFLOW-calculated Darcy flux at the model layer and grid cell associated with each PFM monitoring point and the simulated benzene concentration from SEAM3D results. Estimates for the change in benzene flux were also calculated from the uniform LSZ flow model and the measured benzene concentrations as presented in Section 5.7 and summarized in Table 5-6. This simple modeling indicates the benzene mass flux was reduced by 83% in the B-horizon and 99% in the C-horizon of the LSZ. Hence, the post-TEE modeling was easily within ± 50% of the observed mass removed from the test cell during the TEE pilot test successfully meeting this performance objective.

Figure 6-10 and Figure 6-11 are a summary of results from the numerical modeling with SEAM3D for the most permeable strata within the B interval showing both the pre-TEE and post-TEE benzene mass flux results at each monitoring well. These results correspond to the uppermost permeable sand (Figure 6-10, model layer 2) and the most permeable and thickest sand layer in the lower depth of the B interval (Figure 6-11, model layer 7). At wells where no PFM was aligned with a model layer, PFM benzene mass flux values from neighboring locations were averaged.

Because the location of model layers did not precisely match the frequency of the deployed PFMs, differences between the simulated and observed results likely reflect the lack of vertical detail in the model. However, for the pre-TEE MTT, a reasonable match between the observed and calculated benzene mass flux in each model layer was obtained (upper plots of Figure 6-10 and Figure 6-11). At wells closest to the injection (MWN-06B and MWN-02B), the observed flux was generally greater than the simulated values. At the more distant wells, no consistent trend in the error was apparent.

Results for the post-TEE MTT (lower plots of Figure 6-10 and Figure 6-11) were favorable at the two monitoring wells nearest to the injection well (MWN-06B and MWN-02B). At the more distant wells (MWN-04B, -01B and -02B), the observed benzene mass flux from the PFMs was over an order of magnitude greater than the model-simulated results. This was likely an outcome of assuming uniform benzene removal within the TEE cell for model input, specifically the benzene mass fraction. In particular, the monitoring wells closest to the extraction wells had contaminants driven and drawn to these locations and a much shorter duration of thermal treatment than locations close to the injection well.
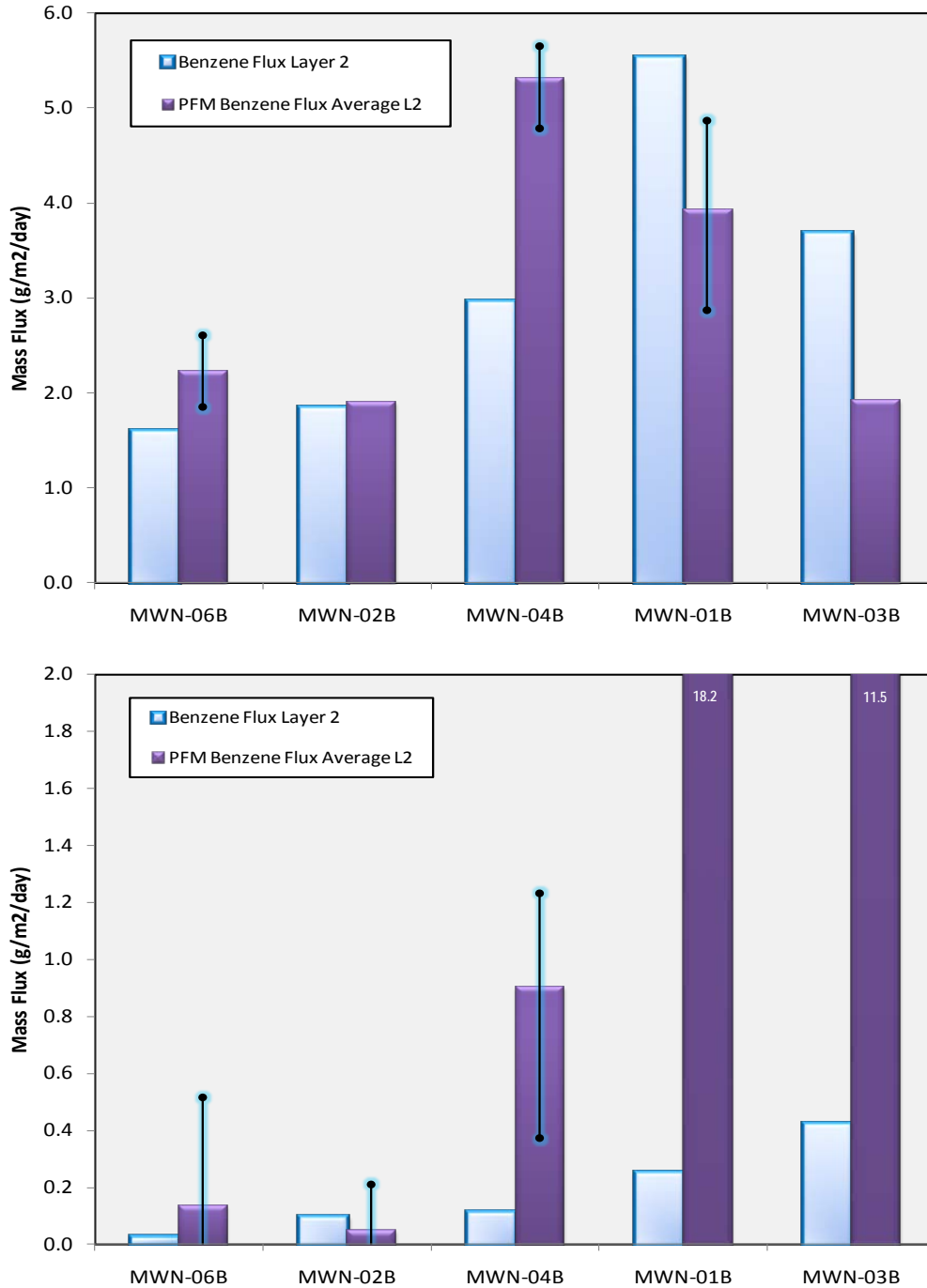
Figure 6-10. Comparison of Pre-TEE (upper) and Post-TEE (lower) MTT Observed Benzene Mass Flux Derived from PFMs to Simulated Values. Calculated Using the Local Solute Transport Model at the Uppermost Permeable Strata in the B interval (model layer 2).
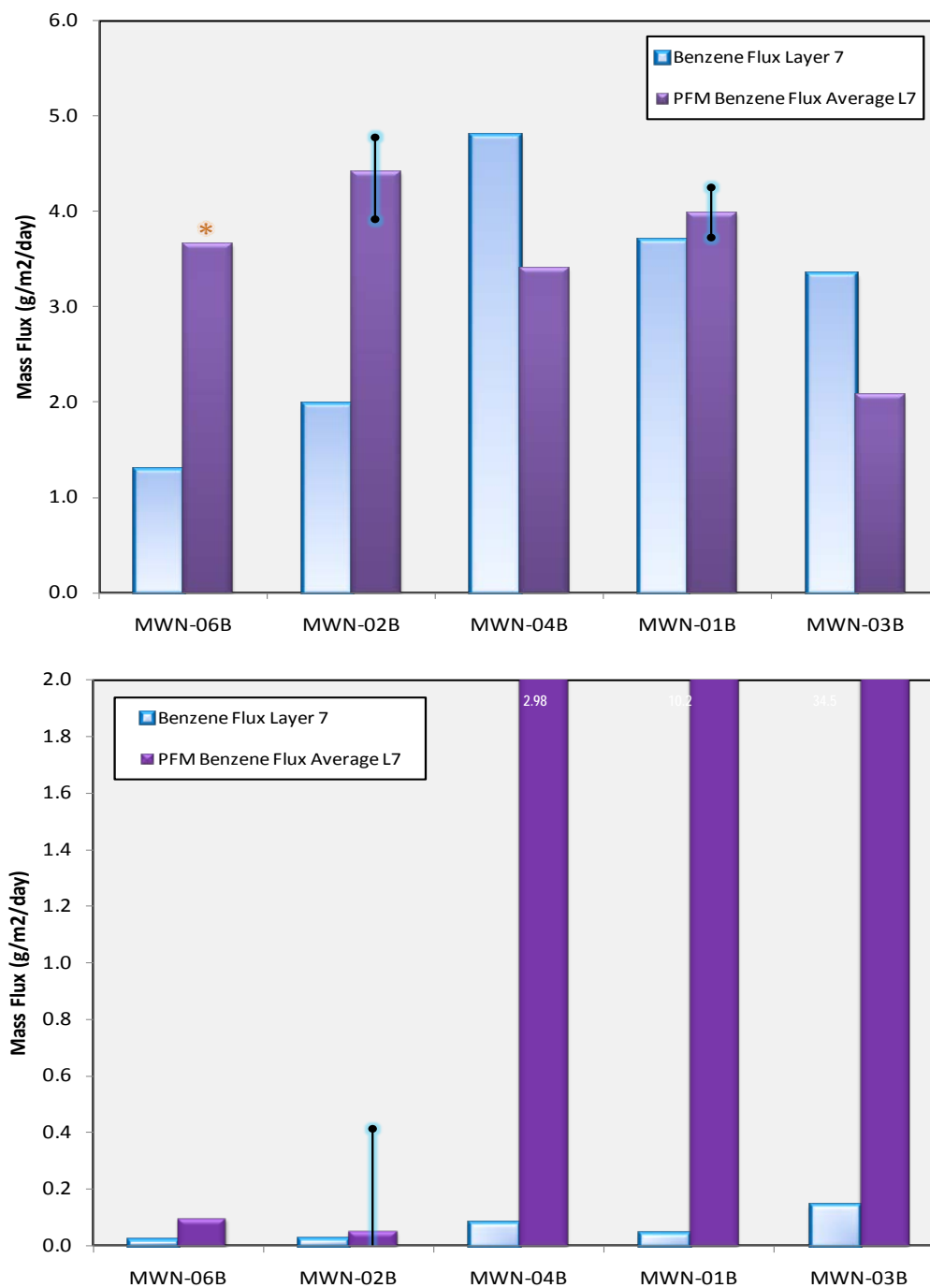
Figure 6-11. Comparison of Pre-TEE (upper) and Post-TEE (lower) MTT Observed Benzene Mass Flux.
PFMs are compared to model-simulated values calculated using the local solute transport model at one of two permeable strata of the lower regions in the B interval (model layer 7). Asterisks indicate vertically-averaged observed PFM data.

For the pre-TEE MTT, a reasonable match between the observed and calculated benzene mass flux in each model layer was obtained, meeting this performance objective. Results for the post-TEE MTT were favorable at monitoring wells nearest to the injection well. At the more distant wells, the observed mass flux from the PFMs was over an order of magnitude greater than the model-simulated results.

As described previously, the benzene concentrations in the TEE cell showed much greater variability among the monitoring wells after treatment as compared to the pre-TEE values. This variability was likely the result of variable treatment within the cell that yielded a non-uniform NAPL composition in the cell. In particular, the monitoring wells closest to the extraction wells had contaminants driven and drawn to these locations and a much shorter duration of thermal treatment than locations close to the injection well. Although the transport model can account for variability in NAPL residual saturation in space, this level of sophistication was not specified in the Demonstration Plan. The mean error between the observed equilibrium source zone mass discharge and that simulated with SEAM3D was well within one order of magnitude in the two wells closest to the injection well but exceeded one order of magnitude in the three monitoring wells closest to the extraction wells.

6.4 PERFORMANCE OBJECTIVE: EASE OF SIMULTANEOUS IMPLEMENTATION OF AN IPT AND PFMS

This performance objective was successfully met as PFMs were not deployed until equilibrium concentrations were observed in the TEE cell monitoring wells. The pre-TEE MTT included a tracer test that verified a volume-based calculation for the timing of the PFM deployment. The total pore volume of the target soil volume was calculated, and the PFMs were not deployed until this volume of clean water had been injected. The tracer concentration histories identified soil heterogeneities and preferential flowpaths where the injected water flowed. The tracer results indicated more than two pore volumes of water passed through flowpaths prior to the PFM deployment. The contaminant concentrations in the monitoring wells were measured during the water injection and were observed to stabilize as described in Section 6.2.

The implementation of PFMs during an IPT has benefits to both technologies. For the PFMs, a better defined flow field is developed during an IPT than provided by natural flow conditions and an increased pore water velocity increases the resolution of the PFM measured velocity. For the IPT, vertical discretization of water and contaminant fluxes obtained from the PFMs provides a greater level of detail than monitoring data alone and enhances the utility of the test.

An additional concern with PFM use was the possibility of a thin layer of floating NAPL skewing results by contaminating the outside of a PFM during placement. All wells were bailed of any visible NAPL and purged of three well volumes just prior to the deployment of the PFMs. In addition, a "swipe" test was performed whereby a dummy PFM was installed and immediately withdrawn and sampled for any NAPL contact. A small fraction of the PFM results were slightly adjusted based on the results of the swipe test.

6.5 PERFORMANCE OBJECTIVE: INCREMENTAL COSTS OF IPT AND PFM DEPLOYMENT

This performance objective was to estimate the incremental costs of performing an integral pumping test in a source zone and the deployment of PFMs for vertical delineation of flow and contaminants. IPT and PFM costs were successfully segregated, and are detailed in Sections 7.1.1 and 7.1.2, respectively. Major cost drivers for the MTT are analyzed in Section 7.2.

If pump-and-treat is active at a facility and monitoring wells exist within the source area, or if the installation of such a system is anticipated as part of the site remediation, the IPT and PFM costs are almost solely for the analytical data and are a small increment of site operating costs in comparison to the scientifically defensible data collected.

7.0 COST ASSESSMENT

The objective of this project was to develop tools providing state-of-the-art approaches to characterizing the mass, distribution, and projected longevity of NAPL source areas, as well as the potential costs and benefits of partial source reduction. To achieve this objective, two innovative field measurements were combined and applied in a new configuration (referred to as mass transfer testing), and modeling was developed to facilitate interpretation of these field measurements to meet the objective. This section provides information to reasonably estimate costs at other sites for implementing the mass transfer test procedures and interpreting the data.

A primary determinant for the total cost to perform the testing is the existence of operating infrastructure to pump and treat relatively large quantities of contaminated groundwater for days or weeks. If pump-and-treat is active at a facility and monitoring wells exist within the source area, or if the installation of such a system is anticipated as part of the site remediation, the cost of performing the mass transfer testing is almost solely for the analytical data. Sites requiring such infrastructure usually involve a NAPL source and involve pump-and-treat as part of more intensive technologies such as electrical resistance heating, steam injection, surfactant floods, recirculating chemical oxidation, etc. The costs for data analyses in the form of modeling to determine the source strength and mass transfer characteristics are less variable than the field implementation; however, the modeling costs do vary with the complexity of the site, the intensity of data collection, and the experience of the modeler.

7.1 COST MODEL

The cost elements considered in the cost model for implementing the mass transfer testing at a site are summarized in Table 7-1. The model considers the following ten elements:

- Surface Infrastructure
- Subsurface Infrastructure
- Baseline Hydrogeologic Characterization
- Baseline Contaminant Characterization
- Mass Transfer Test Plan
- Integral Pumping Test
- Tracer Test
- PFM Deployment
- Data Analyses
- Waste disposal

Surface infrastructure typically involves a permanent or temporary facility for the treatment of contaminated groundwater and permitted discharge into a sanitary sewer. Groundwater pumping tests to characterize aquifer permeability are common; however, durations are typically 72 hours or less. This short duration allows pumped water to be treated off-site but is generally too short for the mass transfer test described in this report. The quantities of water pumped in the mass transfer test would typically require a permitted treatment and discharge facility. Costing of such a facility is not unique to the mass transfer test and standard practice can be followed. Contaminated groundwater is expected to be the primary waste from the mass transfer testing

and is therefore waste disposal is not considered further in the cost model.

Table 7-1. Cost Model for the Mass Transfer Test Field Effort.

Cost Element	Data Tracked During the Demonstration	Costs	
Surface Infrastructure	• Operational groundwater treatment and discharge system • No unique requirements	Standard practice	
Subsurface Infrastructure	• Extraction / injection well installation • Monitoring well installation • Groundwater extraction pumps • No unique requirements	Standard practice	
Baseline Hydrogeolgic Characterization	• Hydrogeologic assessment of boring logs, pumping tests, etc. • Review of available site investigation data and reports	Standard practice	
Baseline Contaminant Characterization	• Collect groundwater samples from extraction and monitoring wells before injection and extraction • Analysis of groundwater samples for contaminants of concern • Review of available site investigation data and reports	Standard practice	
Mass Transfer Test Plan	• Conceptual design of mass transfer test (e.g., flowrates, duration, sampling frequencies, sampling equipment) • Preparation of a test plan	Project Engineer, 40 hr	$5,000
Integral Pumping Test	• Establish pseudo-steady-state flow field in the source zone and maintain flows for desired period of flushing (minimum one equivalent pore volume within the source zone) • Sample and analyze groundwater from extraction and monitoring wells at frequencies specified in the test plan • Measure water levels across the test area as specified in the test plan	Standard practice – assume 8 sampling/monitoring events during the integral pumping test. For example, during a 4-week test, two samples per week are collected from each sampling location and analyzed for COCs by the appropriate method. The current project utilized a calibrated, on-site GC with off-site QA/QC.	
Tracer Test	• Purchase and meter tracer (e.g., potassium bromide) into injected water • Calibrate, deploy and monitor submersible bromide sensors in monitoring wells	Field Technician, 16 hr Project Engineer, 8 hr Unit: $/lb for tracer Unit: $/sensor per rental week or purchase	$1,200 $1,000 $50/lb $1,700 sensor purchase
PFM Deployment	• PFM deployment, retrieval and analyses	Vendor: Lump Sum	$50,000
Data Analyses	See Table 7-2		
Waste disposal	Standard disposal, no cost tracking	NA	

The existence or need for the installation of subsurface infrastructure is also non-unique for costing, and standard practice can be employed. However, the location and density of injection, extraction, and monitoring wells for the mass transfer testing may be different from existing infrastructure. Often, extraction and monitoring wells are placed downgradient from sources rather than within the source area. This practice is driven by the expectation that (1) monitoring wells within a NAPL source will yield little data other than measures of equilibrium solubility between the NAPL and groundwater, and (2) extraction wells should be placed downgradient for containment of the dissolved plume. For sites with an appreciable groundwater velocity and an aged NAPL source, monitoring wells within the source area are not likely to be in equilibrium with the NAPL and can provide valuable information on the mass dissolution rate. Similarly, extraction from within the source area can also provide containment as well as mass removal, though the rate of extracted groundwater must be higher and the water generally requires a greater degree of treatment than the downgradient water. Hence, extraction and monitoring wells installed in a NAPL source area to support a mass transfer test would have significant value beyond the testing period.

Baseline characterizations are assumed to be part of the standard site investigation, and a good conceptual site model is assumed to accompany any remedial effort. Hence, the baseline hydrogeologic and contaminant characterizations are not included in assessing the cost of the mass transfer test and standard practice can be followed. However, the mass transfer testing is intended to add an order-of-magnitude improvement to the characterization of the site and conceptual site model for evaluating cleanup options. Hence, the cost model for this technology demonstration only addresses the incremental costs of performing the field measurements and the additional data analyses including computer modeling.

Three cost elements were considered in more detail: integral pumping test (IPT) in the source zone with water and tracer injection, passive flux meter (PFM) deployment, and computer modeling for data interpretation. The preparation of the mass transfer test plan is also included in Table 7-1. The actual cost during the field demonstration was monitored. As shown in Table 7-1, the preparation of the test plan required approximately 40 hours of time from a project engineer or geologist.

7.1.1 *Cost Element: Integral Pumping Test including Tracer Test*

Procedures followed in performing the integral pumping test are detailed in Section 5.5. For sites operating an existing pump-and-treat system, additional field tasks to perform the IPT include: connecting a water supply to a single central well, adding a concentrated tracer solution to injected water (duration on the order of hours), and monitoring the movement of tracer and water through the subsurface over an extended period (on the order of weeks). Tracer and water movement measurements can be achieved with dedicated, downhole sensors for the tracer and water levels. These data can be recorded automatically at specified intervals and downloaded as required to monitor progress. Costs for the IPT and tracer test include the water connection, water, a mixing tank, metering pump, a tracer salt, rental of downhole sensors, labor to mix and inject the tracer, and labor to collect and compile data. Detailed costs tracked during the field demonstration are provided in Table 7-1. For this demonstration, the tracer was bromide, for which downhole sensors were modified by the vendor (Instrumentation Northwest Inc.) to withstand high levels of dissolved fuel components.

Other costs for the IPT beyond the baseline pump-and-treat system include frequent sampling and laboratory analysis of water samples from monitoring and extraction wells. The number of samples required to lower model uncertainty and the contaminant of concern may justify the use of field instruments or a field laboratory compared to a fixed laboratory. For costing purposes, 8 sampling/monitoring events during the integral pumping test were assumed. For example, during a 4-week test, two samples per week are collected from each sampling location and analyzed for compounds of concern by an appropriate method. The current demonstration utilized a calibrated, on-site GC to analyze for fuel aromatic compounds in water and 1 out of 20 samples were shipped to an off-site laboratory for QA/QC analyses. Labor to collect groundwater samples from monitoring wells can vary widely depending upon the depth to water, as the depth determines the most effective purging and sampling technique.

7.1.2 *Cost Element: Passive Flux Meter Deployment*

Tracking costs for the deployment of the passive flux meters is straightforward, as a vendor provides services for placement, retrieval and analysis of the data. Costs for implementation at specific sites can be obtained from the vendor and are available in the ESTCP technology demonstration report on PFMs (ESTCP, 2006). Other costs include support to the vendor via staging of shipped equipment and site access. The effort to incorporate the PFM data into modeling for the NAPL source strength and longevity are described in the next subsection.

For this field demonstration, the total cost for the PFM vendor was approximately $50,000 and included two mobilizations to the site (before and after the TEE pilot test), deployment of PFMs in 12 wells for each mobilization, and analysis of 12 depth-discrete samples within each well. Hence, 144 samples were collected and analyzed before and after the TEE pilot study. The effort yielded 276 measures of groundwater and contaminant fluxes within the TEE pilot test cell. In the post-TEE deployment, one set of PFMs (12 samples) could not be retrieved from the monitoring well, and the PFMs were destroyed in the effort to extract them from the well.

The total cost of the PFM deployment also included a vendor evaluation of the changes in the flux data resulting from the TEE pilot test.

7.1.3 *Cost Element: Data Analyses*

The five primary tasks for data analyses and reporting associated with implementation of a comprehensive numerical model of mass transfer testing are listed in Table 7-2 along with the estimated labor effort required to complete them. As described previously, the costs for computer modeling depend on the size and complexity of the site. Prior to developing the TEE cell model, data were reviewed, and an assessment of the NAPL source was performed. Development of a modeling plan included a description of the conceptual model, detailed plans for construction of the numerical model, and assembly of input parameters. Implementation of the TEE cell model involved model calibration of groundwater flow in parallel with calibration of the tracer transport model. Following this step, the model was applied to simulate the observed pre-TEE mass transfer test observed data. The procedure for model implementation was repeated for simulating the post-TEE mass transfer test. Detailed descriptions of the primary modeling tasks from this demonstration, listed in Table 7-2, are provided below to illustrate the modeling effort.

Table 7-2. Cost Model for the Mass Transfer Test Data Analysis.

Cost Element	Data Tracked During the Demonstration	Costs	
Initial Model Setup	• Determine appropriate model domain and develop numerical grid	Project Engineer, 16 hr	$2,000
	• Translate boundary conditions: Site model to local model	Project Engineer, 4 hr	$500
	• Combine regional and local boring information to develop three-dimensional depiction of hydrostratigraphy in area of interest and translate to model layering and property assignment	Project Engineer, 56 hr	$7,000
Source Zone Hydrogeologic Parameters	• Simulate transient behavior of hydraulic heads under induced gradient conditions and compare to observed system response at monitoring wells - develop acceptable state of calibration with respect to head conditions	Project Engineer, 40 hr	$5,000
	• Simulate transport of conservative (non-reactive) tracer compound; Evaluate appropriateness of model specifications using tracer breakthroughs at the monitoring well locations as calibration data	Project Engineer, 112 hr	$14,000
	• Compare model-predicted resultant flows (resultant vector through cell) to PFM-derived Darcy velocity results - achieve acceptable match between simulated and observed conditions	Project Engineer, 40 hr	$5,000
Source Zone Contaminant Parameters	• Evaluate appropriate time period over which MTT is to be simulated; Determine what simplification steps may be required to provide reasonable simulation times (e.g., steady state vs. transient flow)	Project Engineer, 16 hr	$2,000
	• Initialize SEAM3D NPL package using observed NAPL composition and residual saturation data; Simulate Phase I of MTT at outset of forced gradient conditions (injection /extraction); Compare to sampling performed within monitoring well network.	Project Engineer, 56 hr	$7,000
	• Extend transport simulation through period corresponding to PFM deployment; Compare model results (resultant flow versus simulated concentration) to PFM-derived mass flux measurements at monitored locations.	Project Engineer, 56 hr	$7,000
Reduction in Contaminant Mass Discharge as a Result of Partial Source Reduction	• Repeat SEAM3D simulations for post-treatment case; Initialize model using observed post-treatment NAPL composition and residual saturation.	Project Engineer, 32 hr	$4,000
	• Revise mass transfer coefficient (model input), as necessary, within area of influence to minimize error; Evaluate sensitivity to input parameters (i.e., NAPL composition, residual saturation).	Project Engineer, 56 hr	$7,000
Reporting	• Summarize results	Project Engineer, 56 hr	$7,000
	• Finalize report and develop appendices describing modeling steps	Project Engineer, 112 hr	$14,000

Initial Model Setup
- Determining the appropriate model domain and developing the numerical grid is likely to be an iterative process with a finer grid resolution in the vicinity of pumping/injection wells and a variable grid spacing and/or distance to lateral and/or vertical boundaries.
- Boundary conditions for the site-wide model must be translated to a local model for the NAPL source area. This translation is achieved by stressing the site-wide model and evaluating the influence of chosen boundaries, i.e., determining if boundaries are placed at sufficient distances from active wells.
- Regional and local boring information must be combined to develop a three-dimensional depiction of the hydrostratigraphy in the area of interest and translated to model layering and property assignment. The hydraulic properties may be controlled by specifications at the site model scale, but a more finely-spaced grid may require additional parameter refinement during the calibration phase.

Source Zone Hydrogeologic Parameters
- The model must be calibrated to simulate transient behavior of hydraulic heads observed under induced gradient conditions. An acceptable state of calibration must be attained with respect to head conditions before proceeding with the modeling. The validity of these data may be questionable depending on several site-specific factors, including the diameter of the test cell. Optimization software may also be implemented at this stage, such as Parameter ESTimation (PEST).
- Next, the model must simulate transport of a conservative (non-reactive) tracer compound. Calibration to tracer breakthrough curves at the monitoring well locations support the use of the model. Multi-level sampling is of particular importance in highly stratified systems.
- Model-predicted resultant flows (resultant vector through cell) are compared to PFM-derived Darcy velocity results to achieve an acceptable match between simulated and observed conditions. The extent and severity of NAPL contamination within the source zone may prevent the collection of valid data, particularly with respect to pre-treatment (pre-steam injection in the case of WAFB) conditions.

Source Zone Contaminant Parameters
- The appropriate time period over which MTT is to be simulated is evaluated, and simplification steps are determined to provide reasonable simulation times (e.g., steady state vs. transient flow). This step may require running multiple models for different periods to refine parameter determination (calibration).
- The SEAM3D NPL package is initialized using observed NAPL composition and residual saturation data. The MTT is simulated at the outset of forced gradient conditions (injection /extraction) and compared to the sampling results within monitoring well network. The period of the simulation will likely depend on characteristics of the source zone, including the nature of NAPL contamination, as well as the relative magnitude of the gradient being induced. These factors will translate to the rate at which observed concentrations drop: a more rapid response may yield a shorter period of simulation.
- The transport simulation is extended through the pseudo-steady period of PFM deployment, and model results (resultant flow versus simulated concentration) are compared to PFM-derived mass flux measurements at monitored locations. The PFM

deployment period will dictate the construction of the model with respect to time. PFM comparisons may require significant interpretation if intervals span multiple model layers.

Reduction in Contaminant Mass Discharge as a Result of Partial Source Reduction

- SEAM3D simulations are repeated for the post-treatment case. The model is initialized using observed post-treatment NAPL composition and residual saturation. Post-treatment conditions should be based on a reliable analysis of the characteristics of the NAPL within the treated zone. The area of influence may also be an important factor to consider at this stage.
- The mass transfer coefficient (model input) is revised, as necessary, within area of influence to minimize the error. An evaluation of sensitivity to input parameters (i.e., NAPL composition, residual saturation) should be undertaken with specific consideration of model sensitivity to NPL package input parameters. Optimization software may expedite the completion of this process.

Reporting

- Results should be summarized in an executive summary.
- The report is finalized, and appendices are developed describing modeling steps. A complete description of the modeling effort and results should be provided, including liberal use of graphics.

For this demonstration, MODFLOW and SEAM3D were utilized to complete the numerical modeling. SEAM3D is available at no cost to DoD employees and DoD's on-site contractors. The current cost to purchase SEAM3D via the GMS platform is $3,850 for a single license, which includes MODFLOW.

7.2   COST DRIVERS

Section 7.1 provided information to reasonably estimate costs for implementing the mass transfer test procedures described in this report at other sites. A primary driver for the total cost to perform the testing is the existence, or lack, of operating infrastructure to pump and treat relatively large quantities of contaminated groundwater for days or weeks as well as a the existence of a suitable array of monitoring wells. If pump-and-treat is active at a facility and monitoring wells exist within the source area, the cost of performing the mass transfer testing is almost solely for the analytical data and is a small increment of site operating costs in comparison to the scientifically defensible data collected.

As described in Section 7.1, the location and density of injection, extraction, and monitoring wells for the mass transfer testing is likely to be different from existing infrastructure. Generally, extraction and monitoring wells are placed downgradient from sources rather than within the source area as those locations provide evidence for natural attenuation and limit the groundwater extraction rate for containment. However, for sites with an appreciable groundwater velocity and an aged NAPL source, monitoring wells within the source area are likely to provide valuable information on the mass dissolution rate, and extraction from within the source area can provide a direct measure of mass dissolution rate while simultaneously providing plume containment.

Hence, the installation of additional extraction and monitoring wells within a NAPL source zone may be necessary to complete a mass transfer test, but these installations would have significant value beyond the testing period.

The costs for data analyses in the form of modeling to determine the source strength and mass transfer characteristics vary with the complexity of the site, the intensity of data collection, and the experience of the modeler. If sufficient data do not exist to justify the use of a numerical model such as SEAM3D, this report includes order-of-magnitude models for assessing mass transfer as described in Section 6.2 and Appendix H.

8.0   IMPLEMENTATION ISSUES

8.1   IMPLEMENTATION ISSUES DURING THE PILOT TEST

Implementation issues encountered during field testing are discussed in this section, including those specific to the IPT, PFMs, and data interpretation.

8.1.1   *IPT*

The injection of water is relatively simple; however, a forced flow IPT requires an extended period of injection and extraction, along with tracer tests, to demonstrate attainment of a pseudo-steady-state condition for flow and NAPL mass dissolution. Water injection may require a separate injection permit in some areas. At sites without an existing pump-and-treat system, the mass transfer testing described in this report may be cost-prohibitive.

For the IPT with tracer testing, all materials and equipment are standard commercial off-the-shelf items. ST012 monitoring wells were much deeper than standard, and longer cables had to be fitted to the tracer detectors, adding cost and time to the schedule. The tracer detectors used in the pre-TEE testing were not compatible with fuel aromatics and degraded over time. The detectors were modified by the manufacturer and proved to be reliable and durable during the post-TEE tracer test.

Measuring tracer concentrations in a long-screened monitoring well can be problematic. If the measure is made passively, i.e., via an in situ detector, the concentration measurement is depth-specific and may not be representative of a well-averaged value attained from purging. If heterogeneities are known to exist along the well screen, multiple tracer detectors deployed in the well could provide valuable, depth-discrete data on breakthrough curves in various intervals.

Collecting monitoring well samples for analysis at frequencies sufficient to capture trends in concentration changes can be time consuming and expensive. For deep monitoring wells with relatively long screens, purging of wells to collect a representative groundwater sample is time consuming and produces a large quantity of water requiring treatment. Grab samples, particularly if floating LNAPL is suspected and/or the well screen is completely submerged, may not be representative of water in the formation surrounding the well screen.

An on-site laboratory is recommended to analyze water samples to reduce costs and to allow near real-time concentration data. Shipping samples off-site with standard turn-around times is generally not practical or cost effective. Certified laboratory data are not required for the IPT, as the data are used for engineering purposes.

8.1.2   *PFMs*

The PFMs are supplied, deployed and interpreted by a single vendor, which could result in a long lead time for deployment (e.g., on the order of months). PFMs are not a direct measurement of flux; professional judgment and interpretation are required to obtain usable results. The vendor analysis of data generated by the PFMs is not transparent; calibration procedures and data were not supplied, nor was the method of translating measured data into flux data.

An additional concern was the possibility of a thin layer of floating NAPL skewing results by contaminating the outside of a PFM during placement. In this demonstration, all wells were

bailed of any visible NAPL and purged of three well volumes just prior to the deployment of the PFMs. In addition, a "swipe" test was performed whereby a dummy PFM was installed and immediately withdrawn and sampled for any NAPL contact. A small fraction of the PFM results were slightly adjusted based on the results of this swipe test. The accuracy of this correction is somewhat uncertain, however, and care should be taken to avoid using PFMs in wells that contain NAPL.

8.1.3 *Data Interpretation*

The complexity of data interpretation is proportional to the heterogeneity of a site. Heterogeneity requires higher-resolution data to justify the use of numerical modeling, but such modeling can provide a more reliable prediction of future outcomes than other approaches, as discussed in the next section. Simple analytical models can be used to interpret data at sites that are somewhat homogeneous. A high degree of heterogeneity results in a data set with a high degree of variability that is not suited for interpretation with analytical models. Such forecasts from analytical models have too much uncertainty to be useful for remedial decision-making, whereas the numerical modeling performed with SEAM3D can reduce that uncertainty to an acceptable level if sufficient data are available.ing

8.2 IMPLEMENTATION OF THE TECHNOLOGY AT OTHER SITES

Remediation timeframes for reaching site-specific RAOs at compliance locations are largely dependent on the persistence of a contaminant source zone flux combined with the natural attenuation capacity of the groundwater system (Chapelle et al., 2004). At present, studies demonstrating the use of computational tools to predict time of remediation (TOR) have been limited by a lack of well-documented sites where source zone remediation has resulted in a reduction in groundwater contaminant concentrations that satisfy regulatory mandates within a reasonable timeframe. However, numerical and analytical models serve an ever increasing role as a tool for decision-makers at sites where source zone remediation combined with MNA may be a viable long-term remedial option.

Figure 8-1 depicts a commonly-used strategy for the application of a comprehensive numerical model at sites to determine TOR relative a site-specific RAO. The site groundwater flow and solute transport model is calibrated to historical data sets that may or may not reflect the application of engineered remediation technologies to either a) reduce source zone mass flux, b) control or manage the aqueous phase plume, or c) both a and b. As demonstrated from source zone concentration data from a chloroethene-contaminated site (Figure 8-1), the availability of monitoring data spanning decades does not guarantee that well-defined trends in contaminant concentration needed for the calibration of a SZD function will materialize (Parker et al., 2010).
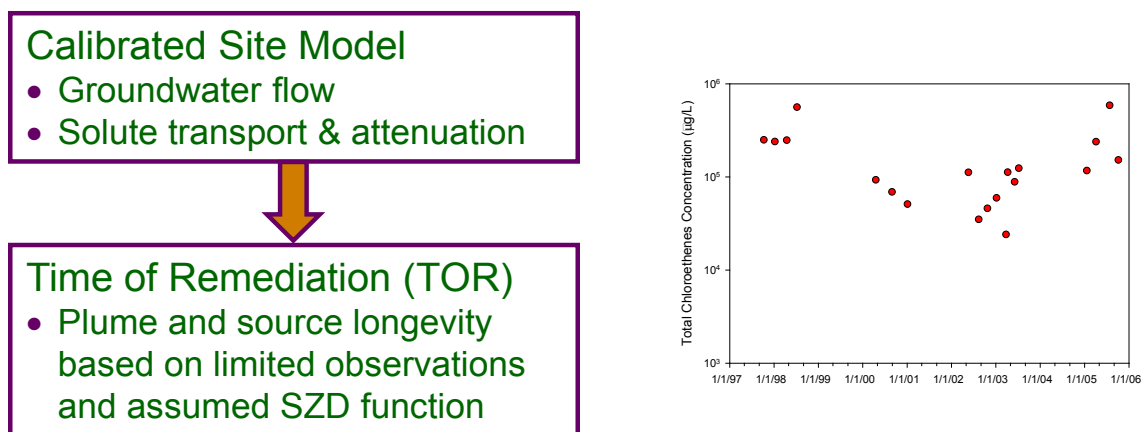
Figure 8-1. Flow Chart (left) Describing Two Basic Steps for Modeling Time of Remediation at Contaminated Sites using Historical Concentration Data Collected at Monitoring Wells Near the Source (right) to Calibrate the SZD Function.

As a means of illustrating the application of the proposed technology at other sites, a model representing the multi-component NAPL source and stable benzene plume at Site ST012 will be used to demonstrate this approach. Figure 8-2 depicts the distribution of benzene concentrations in the LSZ prior to application of the thermal remediation technology in the TEE cell to remove NAPL mass. Although the model is based on site conditions at ST012, the results shown are designed for the purpose of illustration only. Plume stability is a function of natural attenuation processes associated with aerobic and anaerobic biodegradation that have been documented at ST012.
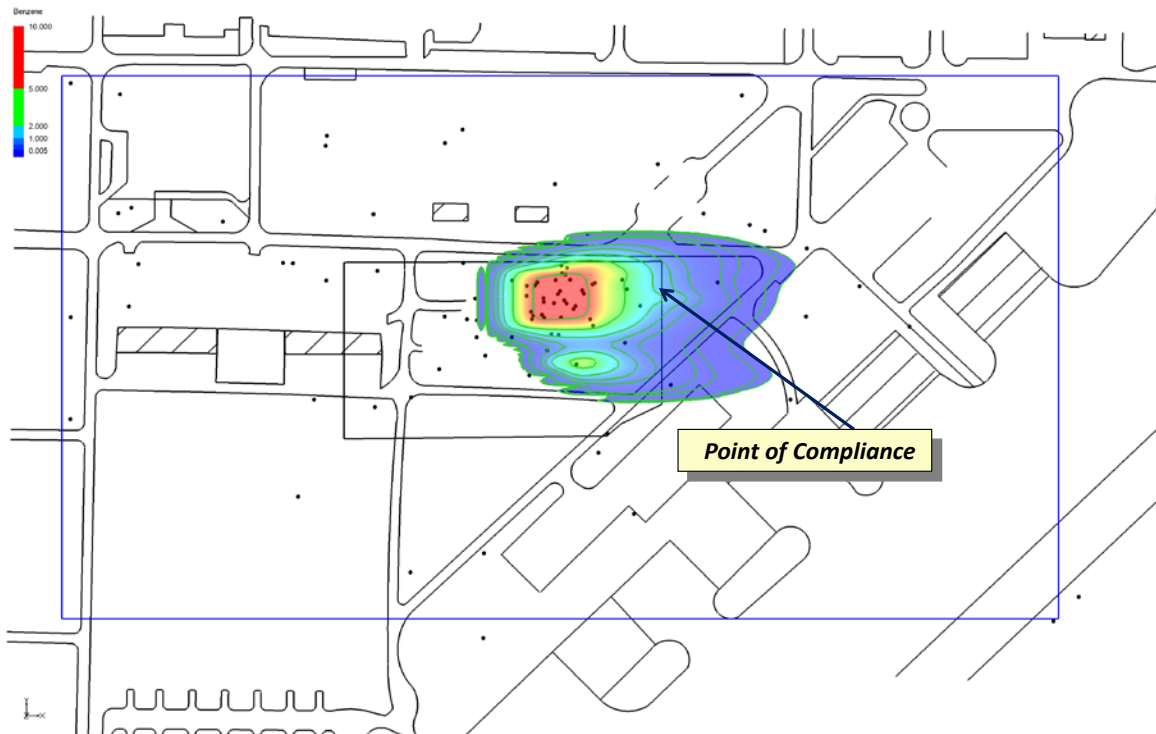
Figure 8-2. Simulated Steady-State Benzene Plume Representative of Pre-TEE Site Conditions at Site ST012 Showing a Hypothetical Point or Boundary of Regulatory Compliance.

Using the steady-state site model as a starting point, simulations were conducted to determine what model input parameters associated with the source zone exerted the greatest impact on TOR at the point or boundary of compliance shown in Figure 8-2. A comparison of long-term simulations (100 years) with and without additional source remediation with TEE shows the expected acceleration in TOR with reduction of source mass relative to MNA only Figure 8-3).
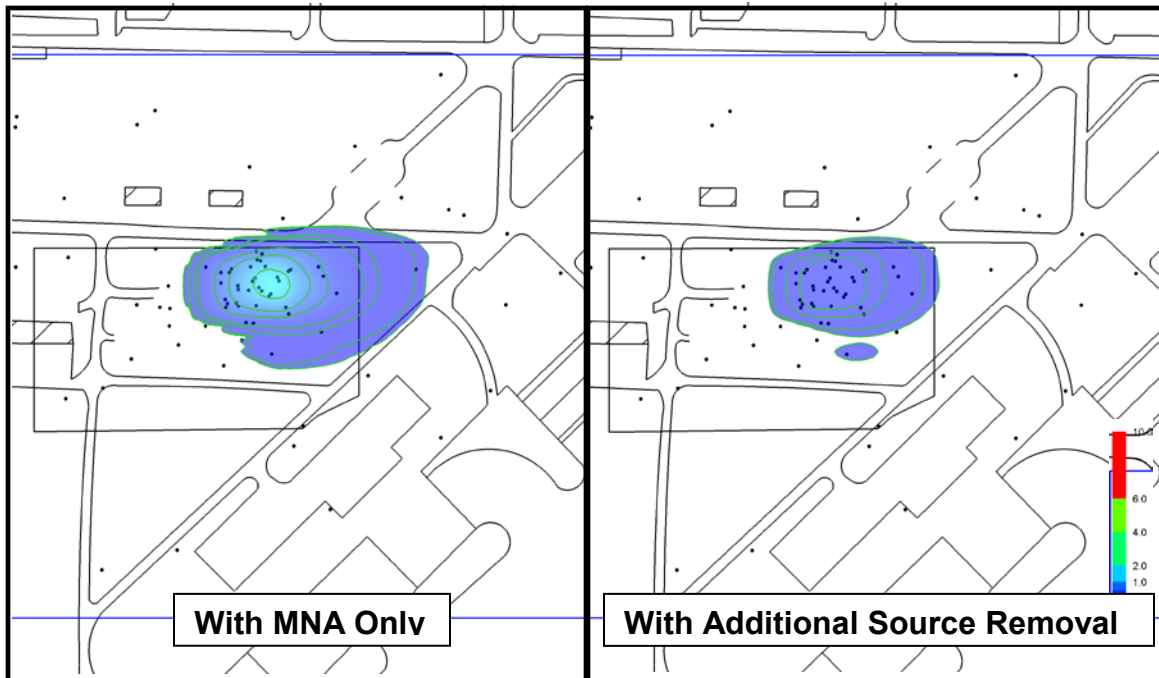
Figure 8-3. Simulated Benzene Plumes Representative of Post-TEE Site Conditions at 100 Years with Additional Source Removal (right) versus MNA Only (left).

A relative sensitivity analysis was conducted for three model parameters: 1) NAPL mass, 2) percent benzene in the multi-component source, and 3) NAPL mass transfer coefficient (K^{NAPL}). Results of the sensitivity analysis are summarized in Figure 8-4 using relative sensitivity coefficients. The sensitivity coefficients in the bar chart were quantified by systematically increasing and decreasing each input parameter and noting the change to the time to reach the benzene MCL at the point of compliance. The results show the relative importance of each input parameter in terms of controlling TOR for this specific site model. Results of this analysis for this site show the least sensitivity to K^{NAPL}. However, historically K^{NAPL} has been the most challenging parameter to measure in field settings, and attempts at estimating field-scale K^{NAPL} have relied upon very long-term groundwater monitoring data (e.g., 20 to 40 years of data), which is costly to obtain. The methodology evaluated in this demonstration thus improves the accuracy of the model parameter that has historically been the most difficult and costly to estimate.
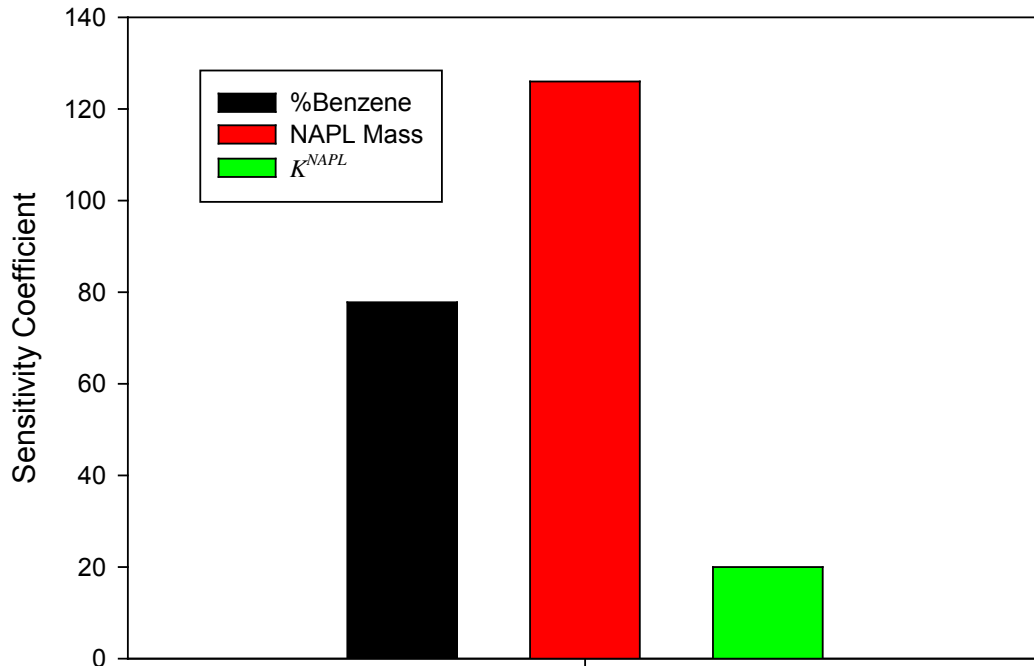
Figure 8-4. Sensitivity analysis for time to reach 5 μg/L of benzene at the point of compliance shown in Figure 8-2 based on MNA only and natural source depletion.

The flow chart shown in Figure 8-6 outlines the general procedure for the methodology in which results of a MTT are integrated into the overall estimation of TOR using a comprehensive numerical model. This approach seeks to circumvent the reliance (or at least reduce emphasis) on long-term source depletion data to calibrate the SZD function associated with a site solute transport model. The aim is to reduce the uncertainty associated with post-remediation TOR estimates through the direct measurement of K^{NAPL}.

At Site ST012, the other source input parameters were either directly measureable or were estimated using routine field measurements. The percentages of benzene and other hydrocarbon components present in the jet fuel were quantified by collecting floating free product and analyzing the components in the laboratory. The distribution of NAPL was estimated based on historical observations of the presence and concentration of jet fuel in soil samples and the areal extent of free product. NAPL mass was estimated based on lithologic description of each strata within the LSZ and an assumed residual saturation. The latter was based on empirical data collected at a wide range of fuel-contaminated sites.
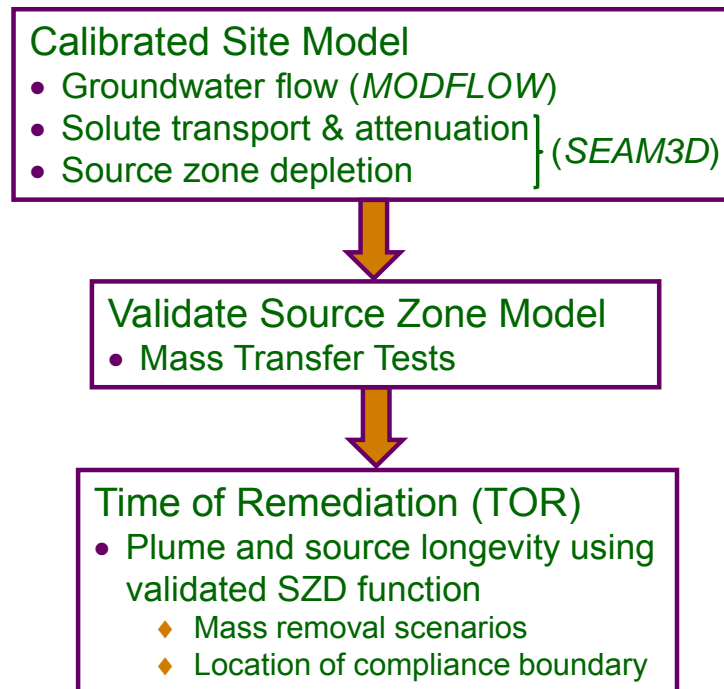
Figure 8-5. Flow chart outlining the proposed approach of combining mass transfer testing and source zone remediation with the SEAM3D site model to reduce uncertainty associated with the SZD function and its use in long-term TOR simulations.

The methodology may be employed to quantify K^{NAPL} prior to the application of source reduction and under post-remediation conditions (i.e., pre-TEE and post-TEE, respectively). The flow chart in Figure 8-6 depicts the approach for improving the parameterization of the pre-remediation model. For example, a site groundwater flow and solute transport model may exist and previously calibrated using historical monitoring data collected through the site. In this case, the pre-remediation MTT provides an improved estimate of K^{NAPL} for the source zone model. Figure 8-7 illustrates how estimates of K^{NAPL} based on a post-remediation MTT serves as a precursor to simulation of TOR following source reduction.
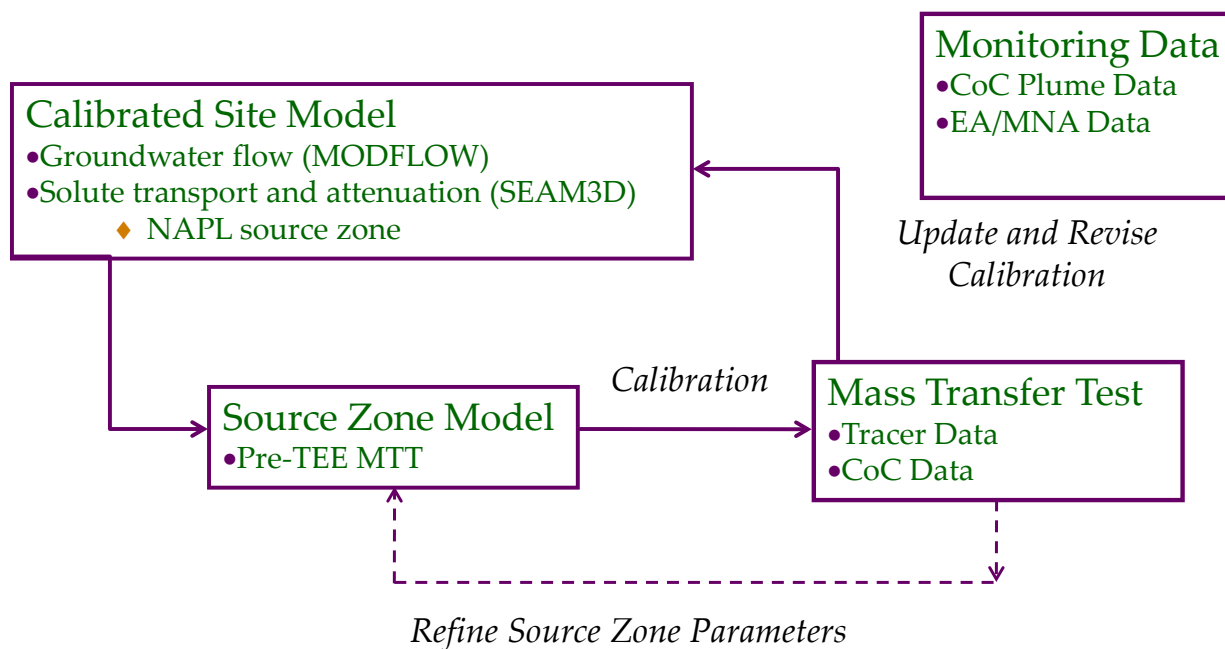
Figure 8-6. Approach for updating an existing site solute transport model with the results of a mass transfer test (pre-remediation MTT) to improve model performance for simulating long-term contaminant source mass flux without source reduction (i.e., MNA only).
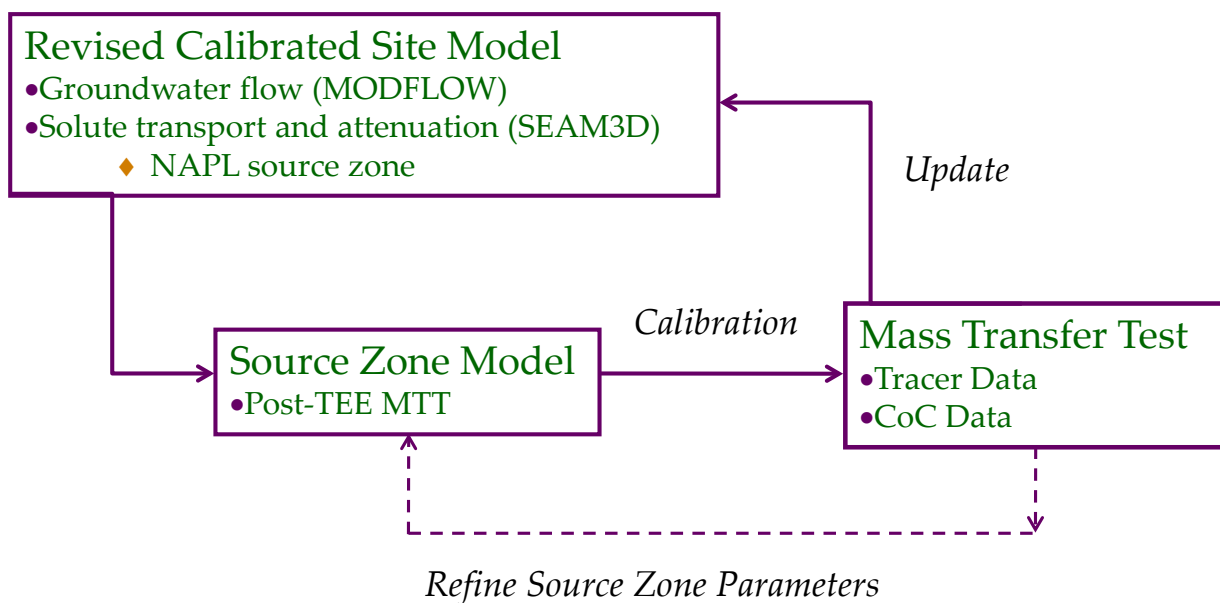
Figure 8-7. Flow chart illustrating the integration of post-remediation MTT results as a precursor to executing simulation of remediation scenarios.

This demonstration evaluated a methodology in which results of a MTT (IPT with a tracer and PFMs) are integrated into the overall estimation of time of remediation under various remedial scenarios using a comprehensive numerical model. Overall, the MTTs and associated modeling were successfully able to measure directly a bulk mass transfer coefficient and relate the absolute source mass to the mass discharge, which resulted in a more accurate SZD function for estimating of source persistence and the result of partial source reduction. If pump-and-treat is active at a facility and monitoring wells exist within the source area, or if the installation of such a system is anticipated as part of the site remediation, the costs of the methodology are almost solely for the analytical data and associated analyses and are a small increment of site operating costs in comparison to the scientifically defensible data collected. This methodology can be applied at sites with LNAPL or DNAPL and can improve the scientific defensibility of decisions regarding when and to what extent active source remediation efforts should be pursued.

9.0 REFERENCES

Annable, M.D., Hatfield, K., Cho, J., Klammler, H., Parker, B.L., Cherry, J.A., Rao, P.S. 2005. Field-scale evaluation of the passive flux meter for simultaneous measurement of groundwater and contaminant fluxes. Environmental Science & Technology, 39(18): 7194-7201.

Bauer, S., Bayer-Raich, M., Holder, T., Kolesar, C., Muller, D., Ptak, T. 2004. Quantification of groundwater contamination in an urban area using integral pumping tests. Journal of Contaminant Hydrology, 75(3-4): 183-213.

Bayer-Raich, M., Jarsjö, J., Liedl, R., Ptak, T., Teutsch, G. 2006. Integral pumping test analyses of linearly sorbed groundwater contaminants using multiple wells: Inferring mass flows and natural attenuation rates. Water Resources Research, 42: W08411, doi:10.1029/2005WR004244.

BEM Systems, Inc. 2007. Final ST012 Phase 1 Thermally Enhanced Extraction (TEE) Pilot Test Work Plan. Former Williams Air Force Base, Mesa, Arizona. United States Air Force. November 2007.

BEM Systems, Inc. 2010. Draft Final Phase I Thermal Enhanced Extraction (TEE) Pilot Test Performance Evaluation Report. Former Williams Air Force Base, Mesa, Arizona. November.

Broholm, K., Feenstra, S., Cherry, J.A. 1999. Solvent release into a sandy aquifer. 1. Overview of source distribution and dissolution behavior. Environmental Science & Technology, 33(5): 681-690.

Broholm, K., Feenstra, S., Cherry, J.A. 2005. Solvent release into a sandy aquifer. 2. Estimation of DNAPL mass based on a multi-component dissolution model. Environmental Science & Technology, 39(1): 317-324.

Chapelle, F.H., M.A. Widdowson, J.S. Brauner, E. Mendez, and C.C. Casey. 2004. Methodology for estimating times of remediation associated with monitored natural attenuation, USGS Water Resources Investigation Report 03-4057, 51 pp.

Charbeneau, R.J. 2000. Groundwater Hydraulics and Pollutant Transport. Long Grove, IL: Waveland Press, Inc.

Christ, J.A., Ramsburg, C.A., Pennell, K.D., Abriola, L.M. 2006. Estimating mass discharge from DNAPL source zones using upscaled mass transfer coefficients: An evaluation using multiphase numerical simulations. Water Resources Research, 42: W11420, doi:10.1029/2006WR004886.

Doherty, J. 2004. PEST: Model independent parameter estimation. 5th edition. Watermark Numerical Computing.

ESTCP. 2006. "Field Demonstration and Validation of a New Device for Measuring Water and Solute Fluxes NASA LC-34 SITE," February 2006.

Falta, R.W., Rao, P.S., Basu, N. 2005. Assessing the impacts of partial mass depletion of in DNAPL source zones. 1. Analytical modeling of source strength functions and plume response. Journal of Contaminant Hydrology, 78(4): 259-280.

Farhat, S.K., Newell, C.J., Nichols, E.M.. 2006. *User's Guide: Mass Flux Tool Kit*. Available at http://www.estcp.org/Technology/upload/ER-0430-MassFluxToolkit.pdf.

Hatfield, K., Annable, M., Cho, J., Rao, P.S.C., Klammler, H. 2004. A direct passive method for measuring water and contaminant fluxes in porous media. Journal of Contaminant Hydrology, 75(3-4): 155-181.

Illangasekare, T., Munakata Marr, J., Siegrist, R., Kenichi Soga, K. 2006. Mass Transfer from Entrapped DNAPL Sources Undergoing Remediation: Characterization Methods and Prediction Tools. SERDP Project No. CU-1294.

Jarsjö, J., Bayer-Raich, M., Ptak, T. 2005. Monitoring groundwater contamination and delineating source zones at industrial sites: Uncertainty analyses using integral pumping tests. Journal of Contaminant Hydrology, 79(3-4): 107-134.

Javandel, I., Doughty, C., and Tsang, C.F. 1984. Ground Water Transport: Handbook of Mathematical Models. American Geophysical Union, Washington, DC.

Mayer, A.S., Miller, C.T. 1996. The influence of mass transfer characteristics and porous media heterogeneity on nonaqueous phase dissolution. Water Resources Research, 32(6): 1551-1567.

Mercado, A. 1967. The spreading pattern of injected waters in a permeability stratified aquifer. In: Artificial Recharge of Aquifers and Management of Aquifers, Symposium of Haifa, March 1967. IAHS Publication Number 72: 23-36.

Miller, C.T., Poirier-McNeill, M.M., Mayer, A.S. 1990. Dissolution of trapped nonaqueous phase liquids: Mass transfer characteristics. Water Resources Research, 26(11); 2783-2796.

Nambi, I.M., Powers, S.E. 2003. Mass transfer correlations for nonaqueous phase liquid dissolution from regions with high initial saturations. Water Resources Research, 39(2), 1030, doi:10.1029/2001WR000667.

Park, E., Parker, J.C. 2005. Evaluation of an upscaled model for DNAPL dissolution kinetics in heterogeneous aquifers. Advances in Water Resources, 28(12): 1280-1291.

Parker, J. C., Park, E. 2004. Modeling field-scale dense nonaqueous phase liquid dissolution kinetics in heterogeneous aquifers. Water Resources Research, 40: W05109, doi:10.1029/2003WR002807.

Parker, J.C., Park, E., Tang, G. 2008. Dissolved plume attenuation with DNAPL source remediation, aqueous decay and volatilization – Analytical solution, model calibration and prediction uncertainty. Journal of Contaminant Hydrology, 102(1-2): 61-71.

Parker, J. C., U. Kim, M. Widdowson, P. Kitanidis, R. Gentry. Effects of model formulation and calibration data on uncertainty in dense nonaqueous phase liquids source dissolution predictions. Water Resources Research, 46, W12517, doi:10.1029/2010WR009361, 2010.

Powers, S.E., Loureiro, C.O., Abriola, L.M., Weber Jr., W.J. 1991. Theoretical study of the significance of nonequilibrium dissolution of nonaqueous phase liquids in subsurface systems. Water Resources Research, 27(4): 463–477.

Powers, S.E., Abriola, L.M., Weber, Jr., W.J. 1992. An experimental investigation of nonaqueous phase liquid dissolution in saturated subsurface systems: Steady state mass transfer rates. 1992. Water Resources Research, 28(10): 2691-2705.

Powers, S.E., Abriola, L.M., Weber, Jr., W.J. 1994. An experimental investigation of nonaqueous phase liquid dissolution in saturated subsurface systems: Transient mass transfer rates. Water Resources Research, 30(2): 321-332.

Ptak, T., Schwarz, R., Holder, T., Teutsch, G. 2000. Teil II: Numerische Lösung und Anwendung in Eppelheim. Grundwasser, 5(4): 176-183.

Rao, P.S.C., Jawitz, J.W., Enfield, C.G., Falta Jr., R.W., Annable, M.D., Wood, A.L. 2001. Technology integration for contaminated site remediation: Cleanup goals and performance metrics. Sheffield, UK. Groundwater Quality: Natural and Enhanced Restoration of Groundwater Pollution, no. 274, p. 571-578.

Saenton, S., Illangasekare, T.H. 2007. Upscaling of mass transfer rate coefficient for the numerical simulation of dense nonaqueous phase liquid dissolution in heterogeneous aquifers. Water Resources Research, 43: W02428, doi: 10.1029/2005/WR004274.

Schwarz, R., Ptak, T., Holder, T., Teutsch, G. 1998. Groundwater risk assessment at contaminated sites: a new approach for the inversion of contaminant concentration data measured at pumping wells. In: Herbert, M., Kovar, K. (Eds.), Groundwater Quality: Remediation and Protection, IAHS Publication, Vol. 250. IAHS Press, Oxfordshire, OX10 8BB, United Kingdom, 68–71.

Smith, J.H., Harper, J.C., Jaber, H. 1981. Analysis and environmental fate of air force distillate and high density fuels. Engineering and Services Laboratory, Air Force Engineering and Services Center, Tyndall Air Force Base, FL. ESL-TR-81-54.

Teutsch, G., Ptak, T., Schwarz, R., Holder, T. 2000. Teil I: Beschreibung der Grundlagen. Grundwasser, 4, 170– 175.

USEPA. United States Environmental Protection Agency. Kavanaugh, M. and P.S.C. Rao. 2003. *The DNAPL remediation challenge: is there a case for source depletion?* EPA/600/R-03/143.

Waddill, D.W., Widdowson, M.A. 1998. Three-dimensional model for subsurface transport and biodegradation. ASCE Journal of Environmental Engineering, 124: 336-344.

Waddill, D.W., Widdowson, M.A. 2000. SEAM3D: A Numerical Model for Three-Dimensional Solute Transport and Sequential Electron Acceptor-Based Biodegradation in Groundwater. U.S. Army Engineer Research and Development Center Technical Report ERDC/EL TR-00-18, Vicksburg, MS.

Zheng, C., Bennett, G.D. 2002. Applied Contaminant Transport Modeling. 2nd edition. New York: John Wiley and Sons, Inc.

Zhu, J., Sykes, J.F. 2004. Simple screening models for NAPL dissolution in the subsurface. Journal of Contaminant Hydrology, 72: 245-258.

APPENDIX A: POINTS OF CONTACT

POINT OF CONTACT Name	ORGANIZATION Name Address	Phone Fax E-mail	Role in Project
Michael Kavanaugh	Geosyntec Consultants 475 14th St Suite 400 Oakland, CA 94612	P: 510-836-3034 F: 510-836-3036 mkavanaugh@geosyntec.com	Principal Investigator
Rula Deeb	ARCADIS/Malcolm Pirnie 2000 Powell Street, 7th Floor Emeryville, CA 94608	P: 510-507-9596 F: 510-507-9596 Rula.Deeb@arcadis-us.com	Project Manager
Jennifer Nyman	ARCADIS/Malcolm Pirnie 2000 Powell Street, 7th Floor Emeryville, CA 94608	P: 510-596-9602 F: 510-596-9602 Jennifer.Nyman@arcadis-us.com	Deputy Project Manager
Lloyd "Bo" Stewart	PRAXIS Environmental Technologies, Inc. 1440 Rollins Road Burlingame, CA 94010	P: 650-548-9288 F: 650-548-9287 Bo@Praxis-Environ.com	Field implementation, data evaluation and reporting
Mark Widdowson	Virginia Polytechnic Institute & State University 200 Patton Hall Blacksburg, VA 24061	P: 540-231-7153 F: 540-231-7532 mwiddows@vt.edu	Modeling
Jim Mercer	GeoTrans, Inc. 21335 Signal Hill Plaza Suite 100 Sterling, VA 20164	P: 703-444-7000 F: 703-444-1685 jmercer@geotransinc.com	Technical Advisor

APPENDIX B

TECHNOLOGY BACKGROUND

The methodology tested in this study is an innovative combination of field measurements on various scale lengths that include Passive Flux Meters™ (PFMs), integral pumping tests (IPTs) with a bromide tracer, and modeling using the computer model SEAM3D with an enhanced input SZD function. The measurements were performed both before and after a pilot test of TEE within a portion of the source area at ST012, providing a measured mass removed and the resulting reduction in the mass dissolution rate. This appendix provides a detailed description of these measurements and model, as well as the background of their development and their advantages and limitations.

B.1   TECHNOLOGY DESCRIPTION

The MTT within the source zone sought to generate data suitable for estimating NAPL mass and describing the source zone function for alternative NAPL architectures (e.g., ganglia versus pooled distribution of NAPL) in the source zone. For such estimates, mass transfer coefficients specific to the NAPL architecture must be determined. Many mass transfer studies in porous media are available from the chemical engineering literature and many laboratory studies of single-component NAPL dissolution are available in the environmental literature (e.g., Miller et al., 1990; Powers et al., 1991, 1992, and 1994; Mayer and Miller, 1996). The development of field-scale mass transfer coefficients applicable to the modeling of NAPL sources is an area of active research (Nambi and Powers, 2003; Parker and Park, 2004; Christ et al., 2006). Recently, SERDP funded an extensive laboratory-based research effort into the rates of mass transfer from entrapped NAPL sources undergoing remediation (Illangasekare et al., 2006). The following sections describe the individual elements of the MTT, the unique characterization of NAPL obtained from the approach, and the methodology used to scale up the test results using the model SEAM3D.

Integral Pumping Test

The IPT was primarily developed in the late 1990s by Teutsch et al. (2000), Ptak et al. (2000) and Schwarz et al. (1998). Only a few field applications are reported in the literature (examples include Bauer et al., 2004 and Jarsjö et al., 2005). In its simplest form, an IPT is pump-and-treat utilized to form a complete capture zone of dissolved contaminants while minimizing disturbance to natural flow conditions. The concept is illustrated in the top depiction of Figure B-1, labeled "Traditional Integral Pumping Test." Contaminants dissolve into groundwater passing through a NAPL-containing soil volume and are captured in downgradient extraction wells. The rate of mass capture represents the total, quasi-steady mass discharge rate for the source assuming that the capture zone of the IPT encompasses the entire mass dissolved from the source area. As suggested in Figure B-1, the IPT provides little information regarding the architecture of the NAPL. In more complex but more rapid applications, the IPT test is performed in established downgradient plumes and the concentration in the pumping well is measured as a function of time. Inversion algorithms are employed to determine concentration variation within the dissolved plume (Bayer-Raich et al., 2006; Farhat et al., 2006). However, the

data analyses in these tests are focused on reconstructing the distribution of dissolved contaminants in the plume prior to active pumping, rather than on determining the SZD function, as is the focus of this work. Compared to monitoring well data, a traditional IPT test increases the volume of the aquifer that is sampled and is capable of interrogating the entire aquifer volume located between monitoring wells, avoiding the risk of missing narrow contaminant plumes. However, longer term pumping can interfere with the natural flow of groundwater through the source zone and distort the results. In addition, this method can be costly due to large volumes of water requiring treatment and disposal.

Traditional Integral Pumping Test

Impermeable Top

W

H

$C_0=0$

$U=\dfrac{Q}{WH}$

NAPL Zone

Pumping Well
$C_{ext}=\int_e C(x,y,z')Q(x,y,z')dz'/Q_{ext}$
$M_{ext}=Q_{ext}\,C_{ext}$

Impermeable Bottom

Traditional PFM Evaluation

Impermeable Top

W

H

$C_0=0$

$U=\dfrac{Q}{WH}$

NAPL Zone

Monitoring Wells
$C_{mon}=\int_m C(x,y,z')dz'$

Impermeable Bottom

$J_{PFM}=UC(x,y,z)$

W = width of flow cross-section through NAPL zone	C_{ext} = concentration in extracted groundwater
H = height of flow cross-section through NAPL zone	Q_{ext} = volumetric extraction rate
Q = volumetric flow rate through cross-section	M_{ext} = mass extraction rate of contaminant
U = velocity of groundwater	C_{mon} = concentration in monitoring well
C_0 = ambient concentration entering NAPL zone	J_{PFM} = contaminant flux measured by PFM at x,y,z
C(x,y,z) = concentration at position x,y,z	

Figure B-1. Conceptual Models of Field Mass Transfer Testing.

Passive Flux Meters

PFMs have been developed over the past decade by the University of Florida as a tool to assess the mass discharge from source zones without the need for groundwater pumping (Hatfield et al., 2004; Annable et al., 2005). PFMs indirectly measure groundwater flux and directly measure contaminant flux at discrete locations as illustrated in the middle pane of

Figure B-1, labeled "Traditional PFM Evaluation." A vertical array of PFMs deployed in multiple monitoring wells traversing the cross-section of a contaminant plume can be used to define the flow and mass flux distribution across the monitored plane. Interpolation and integration of the data yields the mass discharge of contaminants from the source area. With sufficient data, the measurements could be inverted to suggest the volume and shape of the source NAPL zone.

A PFM is a nylon mesh tube filled with a sorbent/tracer mixture (Hatfield et al., 2004; Annable et al., 2005). Various applications of the PFM can be found at www.enviroflux.com. PFMs are typically inserted into groundwater monitoring wells where they passively intercept ambient groundwater flow. Inside the PFM is a permeable sorbent that retains NAPL components dissolved in the groundwater. The sorbent mixture is also preloaded with specified amounts of resident tracers. The tracers are leached from the sorbent as groundwater flows through the PFM. The loss of resident tracer is proportional to the flow of water through the well. For most organic contaminants, activated carbon is used as the sorbent, and a suite of different alcohols are used for the resident tracers. With a known exposure period, measured loss of resident tracer, and measured gain of contaminant, the flux of contaminants through the well is calculated (Hatfield et al., 2004). In addition, the sorbent/tracer mixture can be separated into discrete segments with rubber spacers to yield mass flux measurements that vary with depth along a single well screen. A schematic of a typical PFM is provided in Figure B-2.

When deployed in a network of downgradient monitoring wells, PFMs acquire data similar to the IPT test; however, whereas the IPT interrogates a very large volume of the aquifer, each PFM measures only a small volume of the aquifer (i.e., more like point measurements). Hence, the primary drawback of the method is the possibility of not intersecting a high flow, high contaminant flux preferential conduit within the aquifer. PFMs are capable of providing some insight into NAPL architecture, particularly in the vertical direction, since they can be stacked in monitoring wells to provide a detailed vertical distribution of contaminant and groundwater fluxes. A relatively dense network of monitoring wells with PFMs is recommended to ensure that narrow, highly concentrated contaminant flow paths are not mischaracterized. At a minimum, monitoring wells should be spaced as necessary to define the width of a plume, and within each monitoring well a PFM should be placed adjacent to each major soil stratum identified during characterization.
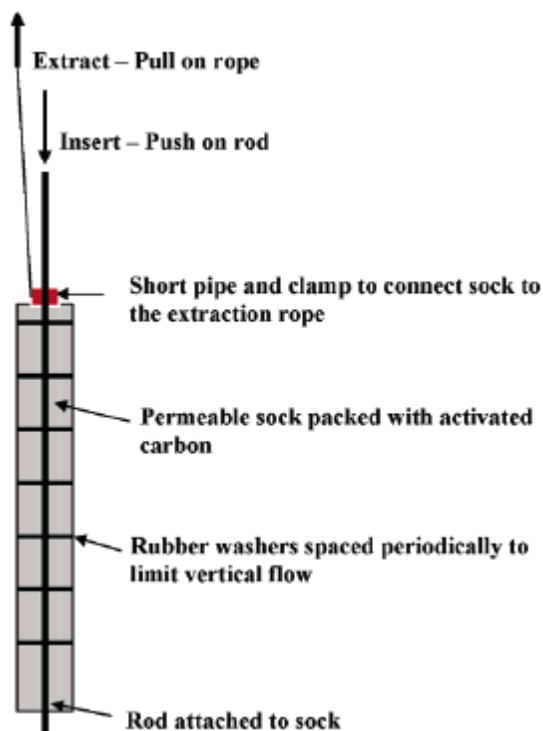
Figure B-2. Passive Flux Meter Schematic.

Source: Annable et al., 2005

PFMs were the subject of a previous ESTCP effort (Project CU-0114) and were demonstrated and validated at a number of field sites (Hatfield et al., 2004). PFMs have been deployed at over 20 contaminated sites (Annable et al., 2005), but PFMs have not been deployed previously at sites contaminated with a multi-component NAPL. In addition, PFMs are generally deployed at sites under natural groundwater flow conditions—not under an imposed flow (Farhat et al., 2006). The Air Force's application at WAFB was the first deployment of PFMs in a multi-component source zone and also the first field application with an imposed flow.

The Mass Transfer Test: Integral Pumping Test with Passive Flux Meters Deployed in the Source Zone

At Site ST012, IPTs were implemented in the portion of the source zone where the TEE pilot test was performed and included tracer testing and PFM deployment. The IPT was performed by injecting clean water in the center of the test cell and extracting on the periphery through six extraction wells. A pulse of bromide tracer was introduced to assess the flow velocities. PFMs were installed in 12 monitoring wells within the test cell after the flows and concentrations had stabilized in response to the steady central water injection. The tests were performed both before and after the TEE pilot test, although conditions were not identical between the two tests.

The layout of the wells in the deeper of two flow horizons [i.e., the lower saturated zone (LSZ)] at the site is illustrated in Figure B-3. The figure also includes idealized streamlines for the flow

conditions in the pre-TEE testing assuming a uniform aquifer. The LSZ extends from about 210 to 240 feet below ground surface (bgs) and is semi-confined between two aquitards. The regional groundwater Darcian velocity was modeled flowing from west to east at 60 feet per year. Each streamline represents a flow of one gallon per minute (gpm). The steady injection rate was 35 gpm and the total extraction rate was 59 gpm. Theoretical stagnation zones between the extraction wells are apparent. The well layout also shows the monitoring well pairs in the LSZ denoted as MWN-B (screened ~ 205 to 220 feet bgs) and MWN-C (screened ~ 230 to 245 feet bgs). The injection and extraction wells spanned the full depth of the LSZ.
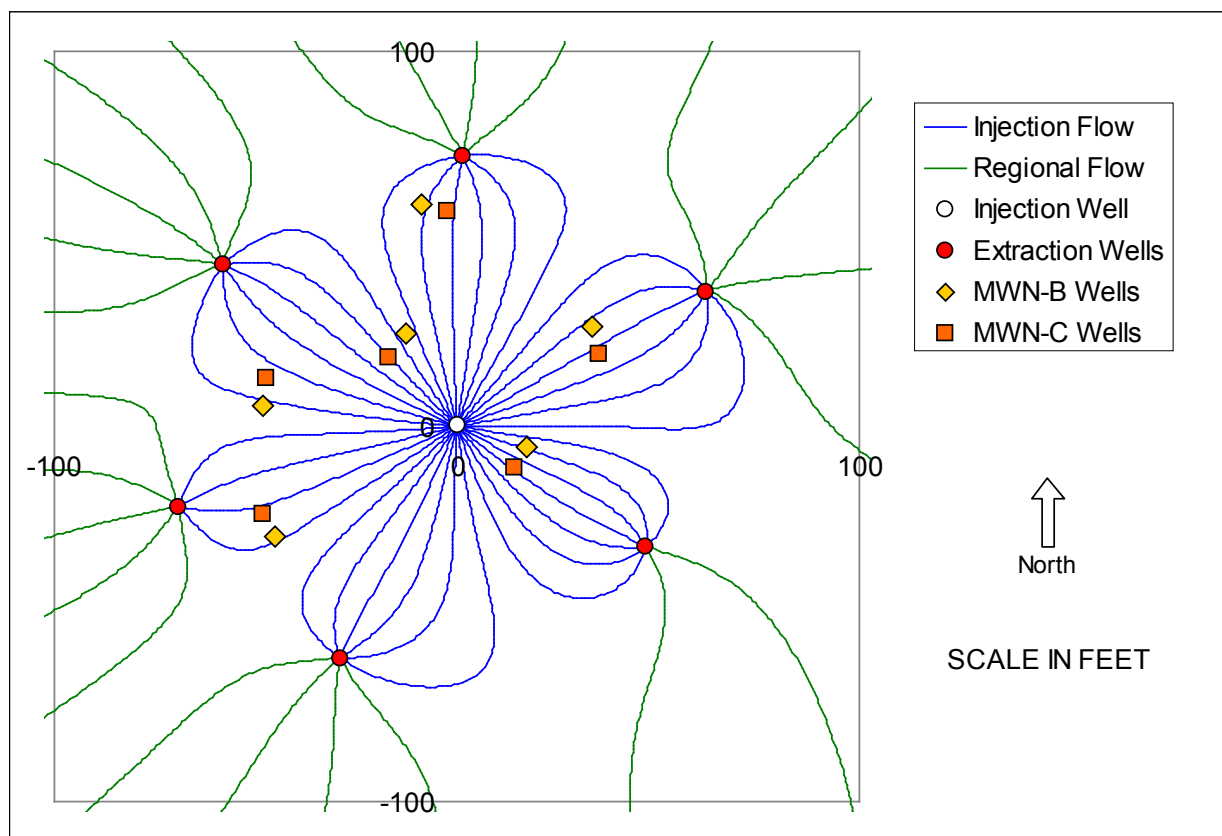
Figure B-3. Layout of Test Wells at ST012 and Idealized Mass Transfer Test Streamlines.

The IPT provided overall mass discharge data on the scale of the pilot test, a circular area with a 70-foot radius as indicated in Figure B-3. The extraction wells completely capture contaminant mass dissolved into the injected water in the modeling of the idealized scenario. The concentration of dissolved compounds increases as the water travels through the NAPL-bearing soils to the extraction wells, limited by the compound's solubility in water. For a multi-component NAPL, the equilibrium solubility of component i is proportional to its mole fraction in the NAPL (f_i) and its pure component aqueous solubility (C_i^{sol}). After achieving transport equilibrium throughout the cell, the combined mass removal rate ($\dot{M}_i$) at the extraction wells

defines a bulk mass transfer coefficient ($K_{i,IPT}$) for the entire soil volume (V_{IPT}) flushed with clean water:

$$\dot{M}_i = K_{i,IPT}\left(f_i\, C_i^{sol} - C_{i,ext}\right)V_{IPT} = QC_{i,ext} \qquad \text{Equation (1)}$$

$$K_{i,IPT} = \frac{QC_{i,ext}}{\left(f_i\, C_i^{sol} - C_{i,ext}\right)V_{IPT}} \qquad \text{Equation (2)}$$

Q is the total water injection rate and balanced extraction rate and $C_{i,ext}$ is the concentration in the extracted water. This bulk mass transfer coefficient is easily measured but does not provide insight to the NAPL architecture and mass release rate under different flow conditions. As an example, for the specific flow conditions shown in Figure B-3, the calculated bulk mass transfer coefficient for the pilot test volume in the LSZ was:

$$K_{i,IPT} = \frac{(35\,\text{gpm})(5.3\,\text{mg/L})}{[(0.0116)(1{,}780\,\text{mg/L}) - 5.3\,\text{mg/L}]\pi(70\,\text{ft})^2(30\,\text{ft})} \times \frac{(1{,}440\,\text{min/day})}{(7.48\,\text{gal/ft}^3)}$$

$$K_{i,IPT} = 0.005\,\text{day}^{-1}$$

Results of the source zone IPT supplemented with intermediate monitoring wells and depth-discrete flux measurements within the flushed source area provided an areal and vertical refinement of SZD function characterization. Details of this approach are provided in Section **Error! Reference source not found.** of the main report, Test Design. In addition, this approach yielded data on the varying distribution and dissolution of different NAPL components in the vicinity of the NAPL. The measurements are illustrated conceptually in Figure B-4.
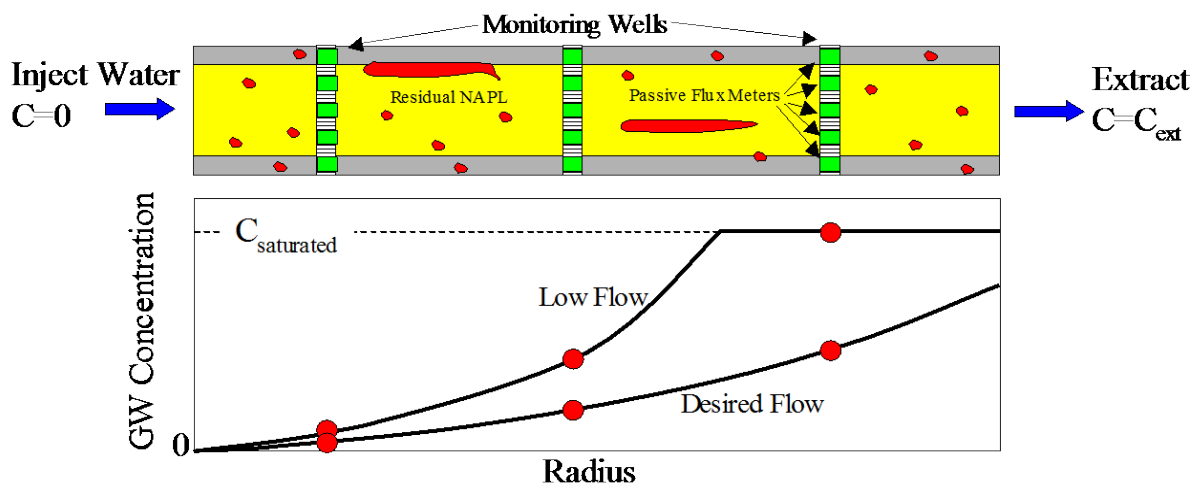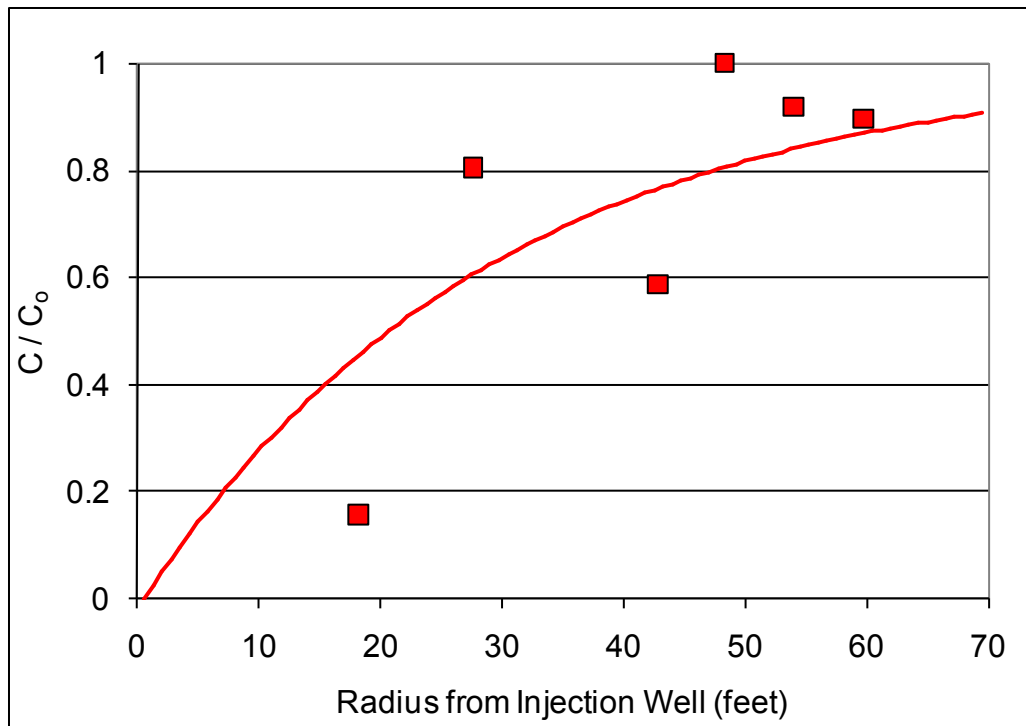
Figure B-4. Conceptual Application of IPT and PFMs.
Circles represent concentration measurements in groundwater samples from monitoring wells along the groundwater flow path.

The conceptual cross-section of the MTT illustrated in Figure B-4 shows clean water traveling through soil containing residual NAPL with extraction at the periphery of the NAPL contamination. As the water travels through the NAPL zone, contaminants are dissolved into the flowing water according to groundwater flow paths, the architecture of the residual NAPL and the rate of mass transfer. Measurements of the groundwater flow rate and concentrations at extraction after a complete pore volume sweep yield a pseudo-steady mass dissolution rate for this imposed flow condition. If the imposed flow rate is low, the water may become saturated

with dissolved contaminant yielding no information on the rates of mass transfer beyond such saturation. This condition is labeled "Low Flow" in Figure B-4. A higher flow which does not become saturated is also illustrated in Figure B-4 and labeled "Desired Flow." Concentrations measured in intermediate monitoring well screens provide mass dissolution rates for horizontal subsets of the soil volume. Arrays of PFMs deployed in the monitoring wells can further segregate and refine the concentration and flow data vertically. An advantage of the PFMs for this application over other vertically discrete sampling devices is the additional capability to measure groundwater fluxes allowing contaminant mass fluxes, not just concentrations, to be measured as a function of depth.

The MTT provides dynamic data more suitable to transient SZD function evaluation than the traditional approach of monitoring relatively static groundwater concentrations downgradient of a source coupled with water level-derived estimates of groundwater velocity. The combined application of the IPT and PFMs in the source zone during the MTT has significant potential to enhance estimates of vertical and horizontal NAPL distribution and mass discharge. Interpretation of the data is discussed below and in Section **Error! Reference source not found.**.

SEAM3D with Enhanced Source Zone Depletion (SZD) Function

A major task within this ESTCP effort is to provide a method for scale up of the field data beyond its site-specific use by the Air Force by validating the use of field-scale bulk mass transfer coefficients and generalizing the results for application to both light and dense NAPL-contaminated sites. The data analysis involved varying the bulk mass transfer coefficient in the SZD function described previously and comparing groundwater concentrations calculated with the solute transport model SEAM3D to measured groundwater concentrations.

SEAM3D is an advective-dispersive solute transport model that simulates the full range of natural attenuation processes (biodegradation, sorption, dilution and dispersion, volatilization, and diminishing source mass flux) in groundwater systems (Waddill and Widdowson, 1998; Waddill and Widdowson, 2000). The SEAM3D Biodegradation Package simulates mass loss of electron donors (e.g., hydrocarbon compounds derived from light NAPL sources) that serve as growth substrates for heterotrophic bacteria in the subsurface, and the consumption of electron acceptors associated with aerobic and anaerobic respiration. Mass loss terms due to biodegradation are functions of the specific process (e.g., sulfate reduction) and electron donor/acceptor concentrations. SEAM3D is innovative in that it allows for the evolution of redox conditions within a plume with time and space as solid-phase electron acceptors are depleted. SEAM3D also accounts for the contribution of aerobic biodegradation to concentration changes around the edges of a plume due to the mixing of dissolved oxygen.

Another distinguishing feature of SEAM3D is the manner in which it explicitly simulates dissolution of a NAPL source zone. The SEAM3D NAPL Package calculates the mass balance of each NAPL component using a mass transfer function that models mass flux at the grid-block size based on field-scale measurements. The first version of the SEAM3D NAPL Package (developed through SERDP project CU-1062) is intended primarily for field-scale applications where high-resolution descriptions of the source zone (i.e., NAPL architecture) are difficult, if not impossible, to obtain. SERDP project ER-1349 led to the development of a practical field-

scale model for estimating chlorinated ethene fluxes versus time from source zones considering effects of mass depletion that were shown to be applicable to DNAPL pool sources, and residual DNAPL sources, as well as intermediate and combined source types (Parker and Park, 2004; Park and Parker, 2005; Parker et al., 2007). The SZD function may be written in the form

$$\dot{M}_i = \kappa \left(\frac{M}{M_o} \right)^{\Gamma} Q \left(C_{eq,i} - C_i \right)$$
Equation (3)

where $\dot{M}_i$ is mass per unit time of species i leaving the source zone, κ is a dimensionless mass transfer coefficient, $C_{eq,i}$ is the effective solubility of species i, C_i is the average dissolved phase concentration exiting the source, Q is the volumetric flow rate through the source, M is the current total source mass, M_o is the mass at a specified time, and Γ is an empirical depletion exponent based on field observations. For a pure solvent source, $C_{eq,i}$ is a constant, while for a multi-component mixture, it is equal to the pure solubility of each species times its respective mole fraction in the NAPL mixture (i.e., via Raoult's Law). Version 2 of SEAM3D includes a new NAPL Dissolution Package (implemented in ER-1349) that calculates grid-block dissolution rates for each NAPL component using the field-scale mass transfer function (Equation 3). By design, the function does not involve any parameters that would require small-scale characterization of the distribution or geometry of NAPL, groundwater velocities, etc., which are generally impractical to obtain in the real world. However, this function is related to real world measures of mass transfer incorporated in the bulk mass transfer coefficient. The relation given by comparing with Equation 1 is:

$$\kappa \left(\frac{M}{M_o} \right)^{\Gamma} = \frac{K_i V}{Q} = \frac{K_i L}{U}$$
Equation (4)

with Q=UWH and V=WHL where W, H and L are the source volume dimensions. The bulk mass transfer coefficient is generally related to flow velocity (U), average soil grain size, soil porosity, NAPL saturation, and characteristic source length in the direction of flow (L) through a Sherwood number correlation (e.g., Miller et al., 1990):

$$K_i = \left(\frac{D_{w,i}}{d_p^2} \right) \beta_0 \left(Re \right)^{\beta_1} \left(\theta S_N \right)^{\beta_2}$$
Equation (5)

where:

$$Re = \frac{U d_p}{\nu_w} = \text{Reynolds Number}$$

K_i = bulk mass transfer coefficient between NAPL ganglion and soil

S_N = residual saturation of NAPL in the aquifer

$D_{w,i}$ =   molecular diffusion coefficient of compound i in water

d_p =   mean soil particle diameter

θ = soil porosity

U =   groundwater velocity

ν_w =   kinematic viscosity of water

β =   mass transfer correlation parameters

The right-hand side of Equation 4 shows the dimensionless source function to be equivalent to the product of the residence time of groundwater in the source zone and the bulk mass transfer coefficient. Equations 3 and 4 were used to relate field measures of mass transfer with modeling in SEAM3D as described below.

Recent work has developed SZD models to account for the reduction in the contaminant mass flux leaving the source zone with the reduction in contaminant mass over time while incorporating fluid flux, spatial variation in NAPL saturation, and flow bypass through the use of an upscaled SZD function (Parker and Park 2004; Zhu and Sykes 2004; Falta et al. 2005; Park and Parker 2005; Christ et al. 2006). The solution can be simplified to the general form of the following equation:

$$\frac{C_{out}}{C_{out}^{t=0}} = \left(\frac{M(t)}{M_o} \right)^{\Gamma}$$

Equation (6)

where $C_{out}^{t=0}$ = initial flux-weighted concentration.

The SZD function (Equation 6) combined with an equation for the NAPL mass loss over time has been proposed for use in: 1) estimating time of remediation for the long-term depletion of a NAPL source zone (i.e., the timeframe for concentrations of COCs to reach acceptable levels), and 2) predicting the decrease in the contaminant mass discharge resulting from a reduction in the source zone mass following application of a remediation technology. Recent SERDP projects (ER-1292, -1293, -1294, and -1295) have addressed the latter question for the case of DNAPL source zones. For example, ER-1294 investigated the effect of surfactant- and biologically-enhanced dissolution, chemical oxidation, and thermal treatment on contaminant mass flux applied to pure-phase PCE and TCE sources. However, the experiments and analysis did not consider the case of a multi-component NAPL source.

An inherent assumption associated with Equation 6 is that the source zone is comprised of a single-component NAPL, and thus, the solution does not account for the NAPL compositional changes over time. Potential problems with this assumption are illustrated by comparing the results of Equation 6 to data collected at a controlled-release, multi-component NAPL field experiment (Broholm et al. 1999; Broholm et al. 2005). Previous literature has suggested that the values of the correlation coefficient range from $0.5 \leq \Gamma \leq 2.0$, where the upper and lower values

are applicable to ganglia- and pool-dominated sources, respectively (Falta et al. 2005). Equation 6 was used to calibrate the solution to the observed data presented in Broholm et al. (2005). The calibrated results show Γ = 7.5 for the most soluble component (Figure B-5), a much greater value that previously determined. This preliminary analysis suggests that compositional changes in a NAPL are important and depletion of a multi-component NAPL is not adequately addressed by the single-component upscaled SZD function.

The SEAM3D NAPL Package considers multi-component NAPL sources. For this problem, Raoult's Law is used to calculate the effective solubility and equilibrium concentration of each NAPL component in groundwater. With each time step, SEAM3D solves an equation of mass balance for each NAPL component and calculates the effective solubilities and equilibrium concentrations as the composition of the NAPL changes with time. Furthermore, version 2 of the SEAM3D NAPL Package includes a form of Equation 3 to simulate mass transfer from the NAPL phase to the aqueous phase.
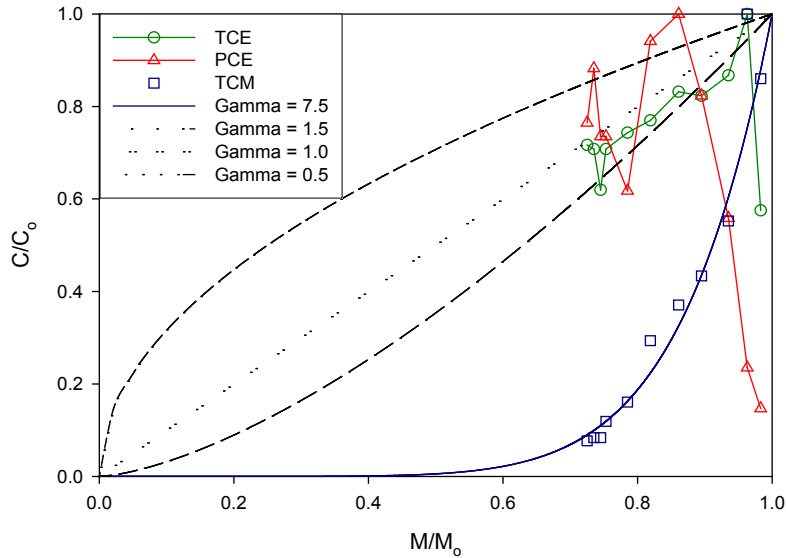
Figure B-5. Comparison of Data to the Source Zone Depletion Function for a Multi-Component Field Experiment.

Source: Broholm et al., 2005

SEAM3D solves the equation of mass balance for multiple species and categories of solutes including volatile organic compounds (VOCs) in the mobile aqueous phase

$$\theta R \frac{\partial C_i}{\partial t} = -\frac{\partial}{\partial x}(q_s C_i) + \frac{\partial}{\partial x}\left(\theta D \frac{\partial C_i}{\partial x}\right) + Q_s C_i^* + M_{source,i}^{NAPL} - M_{sin ks,i} \qquad \text{Equation (7)}$$

where C_i is aqueous phase concentration for a VOC, x is distance, t is time, θ is aquifer porosity, q_s is Darcy's velocity, D is hydrodynamic dispersion coefficient, Q_s is volumetric flow rate per

unit aquifer volume representing fluid source/sink, C_i^* is VOC concentration associated with the point source/sink, $M_{source,i}^{NAPL}$ is the VOC mass source term, and $M_{sink,i}$ accounts for VOC loss due to biodegradation and physical removal mechanisms (e.g., volatilization).

The mass transfer rate between NAPL and groundwater is modeled in SEAM3D using a first order mass transfer function

$$M_{source,i}^{NAPL} = K(C_i^{eq} - C_i)$$
Equation (8)

where K is a time-dependent mass transfer coefficient (units of 1/time), which is based on the upscaled mass transfer function (Equation 3) as

$$K(t) = k^{NAPL}\left(\frac{V}{V_o}\right)^{\Gamma}$$
Equation (9)

where V is the volume of NAPL present at time t per unit aquifer volume (i.e., within a given model cell in the numerical model), V_o is the NAPL volume per aquifer volume at time t_o, and k^{NAPL} is a field-scale mass transfer coefficient corresponding to V_o.

The NAPL volume is updated after each time-step assuming

$$\frac{dV}{dt} = \sum_{i=1}^{N}\frac{M_i^{NAPL}}{\rho_i}$$
Equation (10)

where ρ_i is the mass density of pure species i and N is the number of soluble NAPL phase constituents.

Multiple NAPL functions may be applied to individual model cells to enable complex source "architectures" to be simulated. For example, mixtures of residual NAPL and NAPL pools or lenses may require specification of sources with values of the exponent Γ less than 1 (pools/lenses) and greater than 1 (residual). For the special case where $\Gamma = 0$, the mass transfer rate coefficient is independent of the NAPL mass present.

The equilibrium aqueous concentration of species i in contact with NAPL is computed based on Raoult's Law as

$$C_i^{eq} = f_i C_i^{Sol}$$
Equation (11)

where C_i^{eq} is the aqueous solubility of pure species i, and f_i is the mole fraction of species i in the NAPL. The latter is computed as

$$f_i = \frac{C_i^{NAPL}/\omega_i}{I^{NAPL}/\omega_I + \sum_{j=1}^{N}C_j^{NAPL}/\omega_j}$$
Equation (12)

where C_i^{NAPL} is the NAPL phase mass of VOC species i (or j) per unit dry soil mass; I^{NAPL} is the NAPL phase concentration of "inert" (i.e., assumed insoluble) constituents; ω_I is the molecular weight of the "inert" species; and ω_i is the molecular weight of soluble constituent i (or j). Note that this model does not account for any co-solvency effects.

The use of the multi-component SZD function to simulate contaminant mass flux for the pre- and post-pilot test conditions was a critical demonstration/validation issue. Validation of the SZD function to the multi-component NAPL dissolution problem was beyond the scope of SERDP project ER-1349. The pilot test at ST012 provided an excellent case for validation of a multi-component SZD function because of the variation in the NAPL architecture in the source zone. Site data indicated both ganglia in the smear zone and pooled NAPL were present. The multi-component NAPL source zone data provided a level of analysis not available from a single component NAPL site because of the different partitioning characteristics for each component of the NAPL. This validation is particularly relevant to the application of remediation technologies impacted by differences in the volatility of individual components, such as thermal treatment.

B.2   ADVANTAGES AND LIMITATIONS OF THE TECHNOLOGY

The measurement and interpretation of contaminant flux from a NAPL source zone is an active area of research. The mass release rate over time and persistence of the source depend upon the groundwater flow paths and the "architecture" of the NAPL within a source zone. In the traditional approach, groundwater concentrations and ambient water levels are measured in monitoring wells to estimate the groundwater flow velocity using Darcy's equation and the resulting contaminant mass discharge from a source. This approach relies upon sampling of an extremely small volume of the overall plume and yields little information about the long-term behavior of the source or the impact of aquifer heterogeneities on local flux. IPTs were introduced to sample much larger volumes of aquifers; however, data interpretation based on extraction rates and concentration histories are limited because of aquifer heterogeneities and uncertain source zone architecture of the NAPLs. Several new approaches have been developed over the past decade and are being field tested to provide more accurate data. These include multi-level samplers installed across transects and PFMs installed across monitoring wells screens. These technologies have been deployed full-scale at field sites and were utilized at Site ST012. Vertically segmented PFMs were deployed in two-level monitoring wells during an IPT. In addition, these technologies were applied within the source zone to produce a very discrete data set for the vertical and horizontal assessment of NAPL architecture.

The primary advantages for field measurements with an IPT are:

- Field implementation is relatively simple and is similar to pump and treat.

- An IPT interrogates the entire contaminated aquifer, thereby reducing the effect of small scale variability that may bias point measurements and minimizing the risk of missing narrow contaminant plumes.

- Measured mass removal rates during an IPT provide a bounding value for the mass dissolution rate under natural flow conditions.

- The addition of a tracer to injected water during an IPT is straightforward and the tracer data provide information on aquifer heterogeneities and anisotropies.

- Little, if any, capital expenditures at sites with an operating groundwater extraction and treatment system are incurred.

The primary limitations for field measurements with an IPT are:

- Wastewater disposal and pumping well installation are needed (if not already present).

- Heterogeneous aquifers and asymmetrical well capture zones require a large number of pumping wells with consequent difficulty in data interpretation.

- A large NAPL plume requires a large number of pumping wells.

- A lengthy test duration is required.

- The action of pumping groundwater changes the flow through the source zone and the resulting mass dissolution may not be representative of natural flow conditions.

- Without additional measurements, the mass removal rate during an IPT provides little insight on the NAPL architecture or the behavior of the mass dissolution rate over the long term.

- In downgradient applications, natural attenuation (e.g., via biological degradation) can interfere with source assessment.

As indicated above, the IPT determines a total, quasi-steady mass release rate for the source and provides little information regarding NAPL architecture. The addition of PFMs and multi-level monitoring wells yields more discrete data, however.

The primary advantages for field measurements of mass flux using PFMs are:

- Point measurements of contaminant flux and water flux are provided.

- PFMs can be stacked in monitoring wells to yield a vertical discretization of mass fluxes.

- When deployed within a source area, PFMs supply data to assess source architecture and strength.

- PFMs avoid the uncertainty associated with estimating the hydraulic conductivity and gradients relevant to the location where mass flux is being measured.

The primary limitations for field measurements with PFMs are:

- Each PFM measures only a small volume of the aquifer.

- PFMs deployed in monitoring wells located in the well mixed plume downgradient from the source zone do not provide detailed data on the architecture of the NAPL zone or the distribution of mass dissolution.

- Deployment of PFMs requires multiple field mobilizations to place the meters and then to retrieve the meters.

- Results are interpreted by the PFM vendor, without transparency to the end-user.

- Interpretation of raw data from the PFM relies upon several assumptions, including that the fluid streamlines within the PFM are parallel, groundwater flow is horizontal through the PFM, PFM tracers are not degraded in situ, and sorption to the PFM sorbent is not competitive or rate-limited. These assumptions are not validated in each field deployment of the PFMs.

- PFMs should not be used in wells that contain NAPL, as shown in this field demonstration.

SEAM3D is a comprehensive solute transport model that was a product of a SERDP-funded project (CU-1062). The code has been enhanced over time, including improvements to the NAPL Package and the inclusion of physically-based attenuation mechanisms (under SERDP project ER-1349). SEAM3D is implemented using the DoD Groundwater Modeling System (GMS), which is maintained by the U.S. Army Corps Engineering Research and Development Center (ERDC) and Brigham Young University and has been rigorously tested, verified, and documented (Waddill and Widdowson, 1998). However, the upscaled SZD function has not been tested and validated for a multi-component NAPL.

SEAM3D offers several advantages to assess and interpret pilot testing of partial source reduction:

- SEAM3D is a fully-comprehensive three-dimensional solute transport model linked to MODFLOW (a groundwater flow model) and is not constrained to a particular flow field or hydrostratigraphic model. This is critical for evaluating MTTs with injection and recovery wells.

- The SEAM3D NAPL Package incorporates multi-component dissolution kinetics where each NAPL component's mass is conservative over time. The rate of mass transfer from the NAPL phase to the aqueous phase may be rendered in terms of the volume of NAPL present and is variable with time.

- SEAM3D is ideally suited for simulating long-term MNA in aqueous plumes (of both petroleum hydrocarbons and chlorinated solvents) because model inputs to SEAM3D are consistent with variables known to control NAPL persistence (i.e., NAPL mass and component-based mass fractions and dissolution rates), and both aerobic and anaerobic biodegradation are simulated using the SEAM3D Biodegradation Package.

The major disadvantage of using SEAM3D is the requirement for input parameters and data for calibration associated with any comprehensive 3D solute transport model. However, these data

requirements can be addressed through evaluation of source zone characterization data and pilot test results augmented with literature values for certain parameters. The specific requirements of solute transport modeling should be considered early in the planning for source zone characterization activities and pilot testing of source zone treatment.

Table B-1 lists the SEAM3D input parameters required for simulating the MTTs and a brief description of how the values were determined during this ESTCP project.

Table B-1. SEAM3D Mass Transport and NAPL Mass Transfer Parameters.

Parameter	Method for Determining	Source of Data
$q(x,y,z)$ = Darcy velocity distribution	Matching flow conditions observed during MTTs using MODFLOW2000.	Injection and extraction rates in the TEE cell; Hydraulic head at wells; Hydraulic conductivity and θ.
α_L/α_T = Dispersivities	Matching observed tracer response.	Tracer concentrations at wells.
C_i^{eq} = aqueous solubility ρ_i = mass density ω_i = molecular weight	Known properties	Chemistry handbooks.
$M(x,y,z)$ = NAPL concentrations m_i = mass fractions	Direct input of observed spatial distributions of NAPL mass; Matching pre-MTT VOC concentration time series using SEAM3D	Pre-MTT source zone characterization; Historical VOC concentration data and NAPL composition at monitoring wells.
k^{NAPL} = field-scale mass transfer coefficient	Verify initial condition by simulating pre-MTT VOC concentration time series using SEAM3D; Matching pre-TEE MTT VOC data at wells using SEAM3D.	Initial estimate from Parker and Park (2005); Historical VOC concentration data at monitoring wells; MTT test data.
Γ = depletion exponent	Matching post-TEE MTT VOC data at wells using SEAM3D.	Initial estimate from Parker and Park (2005); MTT test data.

The overall methodology developed herein is an innovative combination of field measurements on various scale lengths that include the three technologies described above, namely, PFMs, IPTs with a bromide tracer, and modeling using SEAM3D with an enhanced input SZD function.

Primary advantages of the overall methodology are as follows:

- The MTT provides a robust and defensible testing and computational tool for evaluating multiple scenarios for source zone reduction and the impact on plume longevity in support of decision making with respect to meeting site-specific RAOs.

- This approach represents a novel methodology for estimating and constraining model input parameters that result in predictions of source depletion and plume longevity. Typically, the source term for site models are calibrated to historical data sets without any direct measurement of source parameters (e.g., field-scale mass transfer coefficient). Through application of the source zone model to data generated through the MTTs, uncertainty in estimating the time of remediation (i.e., time to reach compliance) can be significantly reduced.

- Another advantage of the overall technology is cost savings through leveraging site assets and completed modeling studies. Specifically, existing site infrastructure (pumping/injection and monitoring wells) may be adapted and utilized for MTTs. Well-documented site models for groundwater flow and solute transport may serve as a starting point for implementing SEAM3D and updating the site model for time of remediation estimate.

APPENDIX C: SITE ST012 INVESTIGATION RESULTS

Sources:

BEM Systems, Inc. 2007. Final ST012 Phase 1 Thermally Enhanced Extraction (TEE) Pilot Test Work Plan, Appendix A. Former Williams Air Force Base, Mesa, Arizona. United States Air Force. November 2007.

Consensus Statement No. 2008-03, Former Williams Air Force Base Site ST012 Reference Boundary Well Installation, and Mass Transfer Test in the Upper Water Bearing Zone in Support of the, Thermal Enhanced Extraction (TEE) Pilot Test. Former Williams AFB, Mesa, Arizona. November 2008.

N

Estimated Extent of
Dissolved Phase
Benzene Plume (>5 µg/L)

Former Fuel Release Area

CSM Boundary

Phase 1 TEE Pilot Test Cell

Wells:

Existing Wells

Decommissioned Wells

Existing SVE Wells

Phase 1 TEE Pilot
Test Injection Wells

Phase 1 TEE Pilot
Test Extraction Wells

Phase 1 TEE Pilot Test
Monitoring Well Clusters

Existing Vapor
Monitoring Points

Decommissioned
Monitoring Point

200   0   200
Feet

Former Williams Air Force Base
Mesa, Arizona

ST012 Conceptual Site Model

Dissolved Benzene Plume
in Groundwater, 2004

BEM
SYSTEMS, INC.

Environmental Engineers and Scientists
Phoenix, AZ 85020 (602) 266-2011

04-WERC25SWF   May 2007   Figure A4-2

Former Fuel
Release Area

Estimated Extent of
Dissolved Benzene Plume

\\Phoenix\active\GIS\GIS_Projects\WilliamsAFB\ST012\Maps\04WERC25_03\TEE_PilotTest_WP\Draft\FigA4-2_BenzenePlume.mxd

WEST

Feet (BGS)

FENCE A

SB-13 SB-01
SB-15
SB-12 SB-03
SB-05 SB-14
SB-11
SB-07
EAST
Feet (BGS)
SB-09b

0
-50
-100
-150
-200

0
-50
-100
-150
-200

FENCE B

WEST   EAST
SB-04
SB-10

Feet (BGS)
SB-06
SB-08

Feet (BGS)

0
-50
-100
-150
-200

0
-50
-100
-150
-200

LEGEND

Data Collected 1993

Benzene Concentration (mg/kg)

Less than 1 Below Detection Level	50-100
1-10	100+
10-50	

Key Soil Units

Predominantly coarse - grain soils: sand, gravel, clayey/silty sand, clayey/silty gravel

Cobble Zone

KEY MAP

FENCE A
SB-14
SB-13 SB-01 SB-03
SB-05
SB-07
SB-15 SB-12
SB-11
SB-10
SB-09b
SB-04
SB-08
FENCE B
SB-06

NORTH

0   100   200
Horizontal Scale (Feet)

0
50
100
Vertical Scale (Feet)

Former Williams Air Force Base
Mesa, Arizona

ST012 Conceptual Site Model

Estimated Benzene Distribution in Soil

BEM SYSTEMS, INC. ENVIRONMENTAL ENGINEERS and SCIENTISTS
PHOENIX, ARIZONA 85020 (602) 266-2011

| 04-WERC25SWF | May 2007 | Figure A4-3 |

Inset Area (enlarged):

UWB03, MWN03AB, MWN03C, SVE01, W33, LSZ03, LSZ02, UWB02, N13, SVE02, SVE03, DPE01, LSZ04, UWB04, MWN02AB, MWN02C, MWN04AB, MWN04C, MPA01, MWN01C, UWB07, LSZ07, MWN06AB, MWN01AB, N07, MWN06C, LSZ05, UWB05, MWN05C, LI06, LSZ01, SVE07, MWN05AB, UWB01, W01, LSZ06, UWB06, N06

50 0 50 Feet

Legend:

- Estimated Extent of Dissolved Phase Benzene Plume (>5 µg/L)
- Former Fuel Release Area
- CSM Boundary
- Phase 1 TEE Pilot Test Cell

Wells:

- Existing Wells
- Decommissioned Wells
- Existing SVE Wells
- Phase 1 TEE Pilot Test Injection Wells
- Phase 1 TEE Pilot Test Extraction Wells
- Phase 1 TEE Pilot Test Monitoring Well Clusters
- Existing Vapor Monitoring Points
- Decommissioned Monitoring Point
- Wells with Historic Measurable NAPL Thickness (>0.01 feet) Various Types

200 0 200 Feet

Former Williams Air Force Base
Mesa, Arizona

ST012 Conceptual Site Model

Monitoring Wells with Measurable NAPL

Site ST012
Potentiometric Surface Map
(January 2008)

Former Williams Air Force Base
Mesa, Arizona

ST012_GSL.dwg | Figure 3-1

Legend

- — · — · — ST012 Site Boundary
- ▨ Existing Building
- ✛ Monitoring Well Location
- ✵ Abandoned Monitoring Well Location
- 1180.59 Groundwater Elevation Relative to Mean Sea Level (ft MSL)
- NA Not Available. Top of Casing Elevation not Included in Survey Dated May 2005.
- — — — Potentiometric Contour Line (Dashed Where Inferred)

ST012-W27 NA
ST012-N14 1176.27
ST012-N08 1176.18
ST012-N11 1175.98
ST012-W12 1177.69
ST012-N02 NA
ST012-N01 NA
ST012-N13 1177.74
ST012-N07
ST012-N15 1175.21
ST012-N06 NA
ST012-N03 1179.72
ST012-W05 NA
ST012-N05 1176.33
ST012-N09 NA
ST012-N12 1177.38
ST012-N04 1178.88
ST012-N10 NA

E Utah Ave.
E Unity Ave.
E Ulysses Ave.
E Upton Ave.
E Unger Ave.
S Avery St.
S Tweet St.
S Avoca St.
S Kent
S Sossaman Rd

REGISTERED GEOLOGIST
CERTIFICATION
45328
JAY B. HARBIN
ARIZONA U.S.A.
Date Signed
Expires 12/31/2009

100   0   200
Feet

File: G:\Williams_AFB\Drawings\CADD\ST012\GW_Monitoring_Report\2008_June\ST012_GSL.dwg   Layout: Fig 3-1   Plotted: May 31, 2008 - 2:15pm

Legend

—·—·—	ST012 Site Boundary
▮	Existing Building
✦	Monitoring Well Location
✷	Abandoned Monitoring Well Location
140	Benzene Concentration (μg/L)

✳	Submerged Well Screen
ND	Not Detected
NS	Not Sampled
F	The result is positively identified but the associated numeric value is below the reporting limit.
———	Benzene Concentration Contour Line

Well labels shown on map:

- ST012-W27 ND
- ST012-N14 0.18 F
- ST012-N08 ND
- ST012-W12 4.7
- ST012-N11 1,200
- ST012-N01 ND
- ST012-N02 ND
- ST012-N13 1,400
- ST012-N07
- ST012-N15 1.9
- ST012-N06 1,700
- ST012-N03 140
- ST012-W05 16,000
- ST012-N09 ND
- ST012-N05 1.7
- ST012-N12 ND
- ST012-N04 0.79
- ST012-N10 NS

Streets: E Utah Ave., E Unity Ave., E Ulysses Ave., E Upton Ave., E Unger Ave., S Avery St., S Tweet St., S Avoca St., S Kent, S Sossaman Rd.

Contour values: 5, 50, 500, 5000

REGISTERED GEOLOGIST
CERTIFICATION
45328
JAY B. HARBIN
Date Signed
ARIZONA U.S.A.
Expires 12/31/2009

Site ST012
Benzene Concentration
Distribution Map
(January 2008)
Former Williams Air Force Base
Mesa, Arizona

ST012_GSL.dwg | Figure 3-4

100 0 200
Feet

File: G:\Williams_AFB\Drawings\CADD\ST012\GW_Monitoring_Report\2008_June\ST012_GSL.dwg   Layout: Fig 3-4   Plotted: May 31, 2008 – 2:16pm

APPENDIX D

TEST DESIGN

This effort developed a general procedure combining field measurements and modeling to calculate accurate and technically defensible estimates of source mass and persistence at NAPL-contaminated sites. The effort leveraged a pilot test of TEE at ST012 where an identical site-specific goal exists. At ST012, the innovative mass transfer test and data analyses described in Section 3 of the main report were applied before and after the application of the TEE technology the pilot test cell. In addition, as described in this appendix, the mass transfer test was performed in two practically independent intervals of the saturated zone, the Upper Water Bearing Zone (UWBZ) and the Lower Saturated Zone (LSZ), within the test cell. The mass removed during the TEE pilot test and the replication of the testing in two intervals produced two sets of input data for modeling to assess the impact of mass reduction achieved by TEE on source longevity. With the data from these applications of the mass transfer test at ST012, the procedure was evaluated and generalized for applicability to other NAPL sites. This appendix provides the details of the field measurements. An overview of the TEE pilot test is also provided. Section 6 of the main report describes the data analyses. More details on the design, construction, operation and evaluation of the TEE treatment system can be found in the TEE Pilot Test Work Plan (BEM, 2007) and the TEE Pilot Test Performance Evaluation Report (BEM, 2010).

1.1   CONCEPTUAL EXPERIMENTAL DESIGN

The layouts of injection wells, extraction wells, and monitoring wells to perform the mass transfer tests and the TEE pilot test at ST012 in the LSZ and UWBZ are depicted in Figure D-1 and Figure D-2, respectively. The test cell was located within a portion of ST012 where substantial accumulations of NAPL were known to exist as shown in Figures in Appendix C. This location provided a suitable setting for evaluation of the effectiveness of TEE to treat heavily contaminated source areas, and the configuration of wells afforded the opportunity to test a practical approach to assessing the NAPL architecture and mass transfer characteristics. TEE was expected to have varying degrees of effectiveness in removing individual components of the NAPL as a result of their varying chemical properties. BTEX compounds were expected to be highly amenable to treatment via TEE because of their relatively high vapor pressures and high solubilities. Naphthalene is less volatile and was expected to undergo a lesser degree of removal in response to TEE. However, naphthalene has a very high aqueous solubility compared to other semi-volatile fuel components that increases with temperature. Also, the TEE pilot test yielded more soil treatment and higher temperatures near the injection wells and less treatment and lower temperatures with increasing distance from the central steam injection wells (LSZ-07 and UWBZ-07 in Figure D-1 and Figure D-2).

The testing was conducted within a single treatment cell having a diameter of about 140 feet and across the two vertical zones represented by the LSZ and UWBZ. Each zone contained a central injection well surrounded by six perimeter extraction wells screened across the full depth of the zone. The test cell also contained six monitoring well nests (3 screens) within the cell interior.
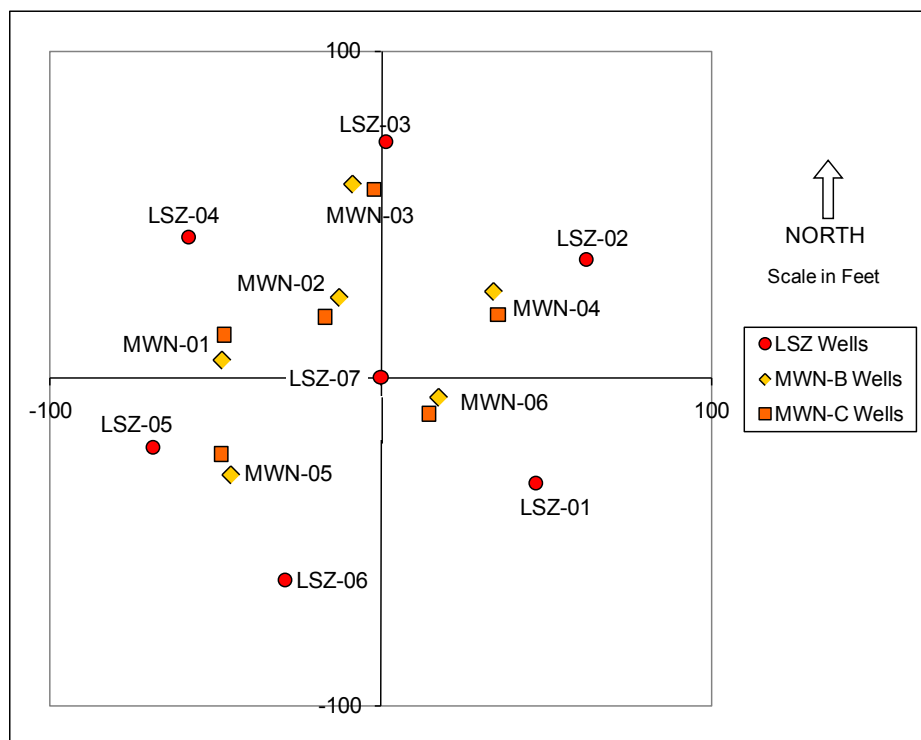
Figure D-1. Layout of Injection, Extraction and Monitoring Wells in the LSZ.
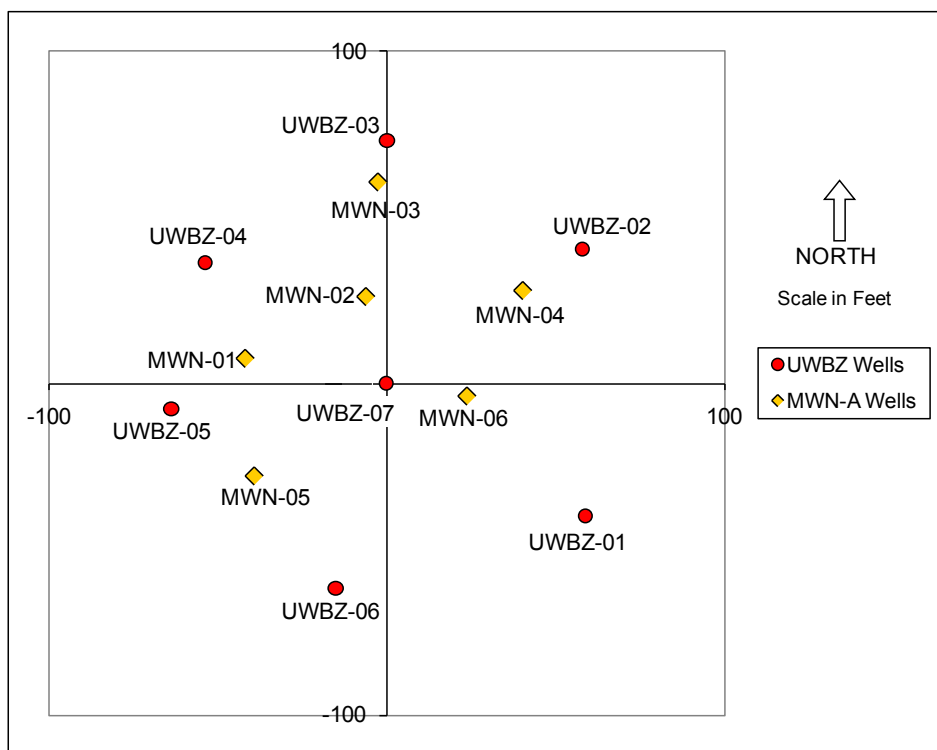
Figure D-2. Layout of Injection, Extraction and Monitoring Wells in the UWBZ.

The interior monitoring wells provided groundwater and vapor samples for assessing the performance of the pilot test, data for the IPT, and locations for deployment of the PFMs. The monitoring wells in the LSZ included six screens in the C-horizon and six screens in the B-horizon as shown in Figure D 1. The UWBZ had six monitoring wells with single screens spanning the full depth of the A-horizon (i.e., UWBZ) as indicated in Figure D 2. Thermocouples were installed with each C-horizon monitoring well to monitor subsurface temperature changes from the vadose zone down to the Aquitard as the TEE pilot test proceeded. The approximate vertical interval for the testing spanned about 80 feet. For this depth interval, the target volume for the test cell was about 46,000 cubic yards. The testing at ST012 was initiated with the collection of pre-test soil, groundwater, and NAPL samples in both the LSZ and UWBZ to establish baseline conditions prior to operation of the TEE pilot test. The soil samples were collected during installation of monitoring wells in 2004 to assess the distribution of contaminants in the subsurface. Groundwater samples from monitoring wells located within and surrounding the treatment cell were collected prior to the first mass transfer test and the operation of the pilot test. NAPL samples were collected from a few wells to characterize pre-treatment NAPL composition. Further details of this pre-test sampling are provided in the following section.

The first step in the operation of the TEE pilot test was groundwater pumping to establish hydraulic isolation, recover free NAPL, and lower the water table as much as practical. The placement of the pump intakes in the wells was designed to satisfy, to the degree possible, the competing objectives of drawing down the potentiometric surface sufficiently to attain hydraulic isolation of the cell and capturing as much mobile NAPL drawn to the wells as possible. Placement of the pump intakes was based on estimated well drawdown predicted from hydraulic analysis of pumping test results and the results of groundwater modeling. Data from this phase of the test allows an assessment of pump-and-treat as a remedial alternative for the site.

After equilibration of the flows and drawdown from groundwater extraction, the pre-treatment mass transfer test was initiated and completed in Fall 2008 in each zone (LSZ and UWBZ). In both zones, the IPT consisted of water injection in the central well to create a known total flow through the target soil volume. Early in the IPT a pulse of bromide tracer was introduced in the central injection well and its appearance and concentration at monitoring wells was measured to provide hydrogeologic data on permeable pathways, groundwater velocities, etc. After sweeping at least one theoretical pore volume of water through the permeable soils, the concentrations of contaminants were measured in monitoring wells for evaluating the pseudo-steady rate of dissolution of fuel components out of residual NAPL and into flowing the groundwater. Monitoring wells closest to the injection well yielded concentrations significantly less than the baseline concentrations. After measuring contaminant concentrations, the PFMs were installed in the B- and A-horizon monitoring wells to provide vertically discrete measures of water and contaminant fluxes along the screen intervals during steady injection and extraction of groundwater. Retrieval of the PFMs signaled the end of the Pre-TEE Mass Transfer Test. Bromide tracer histories were expected to coincide with PFM water flux measurements and monitoring well contaminant concentrations were expected to be related to a depth-averaged PFM contaminant flux.

The TEE pilot test was initiated October 28, 2008 with the start of steam injection in the LSZ, followed by steam injection in the UWBZ two weeks later. In both zones, after steam breakthrough in the extraction wells, steam injection continued at a reduced rate to provide additional heating of the low permeability soils. After low permeability soils within each zone were heated to at least 120ºF, co-injection of air was initiated to improve vapor contact with the residual NAPL and encourage volatilization of NAPL components residing in low permeability soils. After operating in this quasi-steady mode for about four weeks, the co-injection of steam was discontinued while the injection of ambient air and water continued to cool the soils by vaporizing and recovering pore liquids. Water injection was continued through November 2009.

Following the TEE pilot test and after subsurface conditions cooled sufficiently, post-treatment mass transfer measurements were conducted in the LSZ and UWBZ in a manner similar to that conducted during the pre-treatment tests. Steady water injection occurred at the site for about six months after steam injection ceased to cool the site to near ambient conditions. The water injection and groundwater extraction rates coincided with the desired values for the mass transfer testing; hence, flow conditions were established for an extended period yielding multiple measures of the contaminant concentrations in monitoring wells during the imposed flow configuration and the total mass removal rate. A bromide tracer pulse was injected into the LSZ in September 2009 and PFMs were deployed in November 2009 to evaluate the post-TEE mass transfer conditions. These applications of the mass transfer tests were the focus of this work and are described in detail in the following sections.

Evaluation of the pilot test involved assessment of contaminant reduction through multiple lines of evidence (see Section 6 of the main report). The mass transfer tests performed before and after the application of TEE were compared and the calculated change in dissolution rates were evaluated with the estimated mass removed. In addition, once the system cooled to near ambient temperatures (i.e., below 100ºF), boreholes were drilled within the cell to allow collection of soil samples from similar intervals as were sampled during the pre-test soil sampling. The results of analyses of the post-test soil samples were compared to the pre-test samples to provide an additional measure of the degree of treatment. Post-test groundwater samples were also collected after the water injection and extraction were terminated to assess possible rebound.

1.2   BASELINE CHARACTERIZATION

Soil, groundwater, and NAPL samples along with groundwater elevations were collected by the Air Force to establish baseline conditions prior to the Pre-TEE mass transfer test and the operation of the Phase 1 TEE Pilot Test in the LSZ and UWBZ (BEM, 2010). Equivalent post-TEE data were collected after the pilot test to provide baseline measures of new site conditions. Data from these sampling events were provided by the Air Force for this ESTCP-funded effort.

The pre-test soil sampling provided information on the nature and distribution of soil contamination within the saturated zone inside the treatment cell. Pre-test soil samples were collected in 2004 during the drilling of five of the six deep monitoring wells (MWN02C through MWN06C) shown in Figure D-1. Fifteen soil samples were collected from various lithologic layers from 249 to 160 feet bgs at each boring representing the LSZ, LPZ, and UWBZ for a total of 75 soil samples. Table D-1 lists the benzene concentration detected in each soil sample. Data

for toluene, ethylbenzene, m,p-xylenes, naphthalene and total hydrocarbons are provided in the TEE Pilot Test Evaluation Report (BEM, 2010).

Table D-1. Pre- and Post-Test Soil Sample Analytical Results for Benzene.

Depth (ft)	Concentration of Benzene (mg/kg)									
	MWN-02	TB-02	MWN-03	TB-03	MWN-04	TB-04	MWN-05	TB-05	MWN-06	TB-06
160.5	11 DF	0.27 U	NS	NS	NS	0.0022 U	NS	NS	NS	NS
161	NS	NS	NS	NS	NS	NS	NS	NS	0.38	NS
161.5	NS	NS	6.6 J	23	NS	NS	NS	NS	NS	NS
165	NS	NS	NS	NS	NS	NS	5.1 DMJ	2.7 U	NS	0.61 U
165.5	NS	NS	NS	NS	5.4	0.0023 U	NS	NS	NS	NS
167	NS	NS	47 DJ	8.6	NS	NS	NS	NS	NS	NS
170	120 D	0.0023	NS	NS	NS	NS	NS	NS	16 MQ	0.31 U
172	59 D	0.27 U	NS	NS	NS	NS	NS	NS	NS	NS
173	NS	NS	8.6 J	5.9	NS	NS	NS	NS	NS	NS
174	NS	NS	NS	NS	NS	NS	NS	NS	4.8 MQ	1.4 U
175	NS	NS	0.51 J	0.018	0.42 U	0.0023 U	29 DMJ	2.7 U	NS	NS
175.5	15 D	0.0021	NS	NS	NS	NS	NS	NS	NS	NS
177.5	NS	NS	0.026 F	0.00069	NS	NS	NS	NS	NS	NS
181	NS	NS	0.11 F	0.0026	0.43 F	0.0023 U	NS	NS	NS	NS
182.5	NS	NS	NS	NS	NS	NS	NS	NS	4.3 MQJ	0.32 F
185	0.57 F	0.02 M	NS	NS	NS	NS	25 MJ	2.9 U J	NS	NS
187	NS	NS	NS	NS	74 D	0.35	NS	NS	NS	NS
189	NS	NS	NS	NS	NS	NS	NS	NS	50 MQJ	6.8
192	NS	NS	0.098 F	6.2	NS	NS	NS	NS	NS	NS
192.5	6.7	NS	NS	NS	NS	NS	NS	NS	NS	NS
193	NS	NS	NS	NS	NS	NS	NS	NS	36 MQ	5.2
195	NS	NS	NS	NS	4.6	0.0017 F	NS	NS	NS	NS
195.5	NS	NS	4.7 J	4.9	NS	NS	0.52 U	2.4 F	34 MQJ	38
198	0.36 F	0.28 U	NS	NS	14 D	0.29 U	NS	NS	NS	NS
200	NS	NS	80 DJ	66	NS	NS	240 MJ	2.6 U	NS	NS
201	NS	NS	NS	NS	8.8	0.0023 U	NS	NS	25 MQJ	72
204	130 D	0.0024	NS	NS	NS	NS	NS	NS	NS	NS
206.5	NS	NS	NS	NS	2.8	0.0026 U	NS	NS	NS	NS
207	140 D	0.29 U	9	11 M	NS	NS	NS	NS	70 MQ	19
208	NS	NS	NS	NS	NS	NS	86 M	0.24 U	NS	NS
211.5	NS	NS	1.5	0.087	4.7	0.0022 U	NS	NS	NS	NS
213	33 D	0.0022	NS	NS	NS	NS	NS	NS	NS	NS
214	NS	NS	NS	NS	NS	NS	NS	NS	46 MQ	1
216	NS	NS	NS	NS	14 D	0.0023 U	NS	NS	NS	NS
217	NS	NS	NS	NS	NS	NS	NS	NS	2 MQ	0.28 U
218.5	NS	NS	NS	NS	NS	NS	35 M	0.0023 U	NS	NS
219	15 D	NS	NS	NS	NS	NS	NS	NS	NS	NS
222	NS	NS	NS	NS	NS	NS	0.78 M	0.04	NS	NS
223	NS	NS	NS	NS	NS	NS	NS	NS	52 MQ	1.3 U
225	NS	0.0025	2.1	0.02	NS	NS	NS	NS	NS	NS
226	NS	NS	NS	NS	2.2	0.0021 U	0.6 M	0.0006 F	NS	NS
228.5	NS	NS	NS	NS	NS	NS	0.45 FM	0.0023 U	NS	NS
229	NS	NS	NS	NS	NS	NS	NS	NS	0.26	0.0031
230	NS	NS	1.2	0.011	NS	NS	NS	NS	NS	NS
231	NS	NS	NS	NS	0.64 U	0.0021 U	NS	NS	NS	NS
232	1.1	0.0022	NS	NS	NS	NS	NS	NS	NS	NS
233.5	NS	NS	NS	NS	NS	NS	0.56 U	0.0022 U	NS	NS
235	NS	NS	NS	NS	0.62 U	0.0024 U	0.43 U	0.0024 U	NS	NS
235.5	NS	NS	NS	NS	NS	NS	NS	NS	0.47	0.00094 F
236.5	0.53 U	0.0022	NS	NS	NS	NS	NS	NS	NS	NS
238	11 DF	0.27 U	NS	NS	NS	0.0022 U	NS	NS	NS	NS
240	NS	NS	NS	NS	NS	NS	NS	NS	0.38	NS
243	NS	NS	6.6 J	23	NS	NS	NS	NS	NS	NS
244	NS	NS	NS	NS	NS	NS	5.1 DMJ	2.7 U	NS	0.61 U
245	NS	NS	NS	NS	5.4	0.0023 U	NS	NS	NS	NS
246.5	NS	NS	47 DJ	8.6	NS	NS	NS	NS	NS	NS
249	120 D	0.0023	NS	NS	NS	NS	NS	NS	16 MQ	0.31 U

Notes: B - Analyte is also detected in the laboratory blank.
             D - Analyte identified at a secondary dilution.
             F - Analyte is positively identified but associated numerical value is below the practical quantitation
             limit.
             J - Result is detected below the reporting limit and/or is an estimated concentration.
             M - Spiked sample recovery not within control limits.
             NS - Not Sampled.
             Q - Data rejected.
             U - Analyte analyzed for but undetected at the corresponding quantitation limit.

Table D-1 also includes the accompanying soil benzene data collected in November and
December 2009 after the TEE pilot test. Those borings are labeled Table D-2 through Table D-6
and were located within eight feet of wells MWN-02C to MWN-06C, respectively, to provide a
comparable data set. The post-test data are listed adjacent to the pre-test data in Table D-1 to
provide a snapshot of the change in mass resulting from the TEE pilot test. The green shaded
data represents reductions in concentration, the orange-shaded data indicates an increase, and the
blue-shaded data do not have directly comparable data. These results suggest benzene in soil was
reduced across the cell except within the LPZ near MWN-06 and in a few additional depths at
MWN-03. MWN-06 was located closest to the injection wells while MWN-03 was the furthest
and was also located proximate to an extraction well such that contaminants were drawn and
driven through its location. The soil sampling results for BTEX and naphthalene are summarized
in Table D-2 where reductions in average soil concentrations at equivalent soil horizons between
pre- and post-TEE are listed. In general, soil concentrations of benzene and other light
hydrocarbons decreased by one to two orders of magnitude in the more permeable LSZ and
about one order of magnitude in the more heterogeneous UWBZ. Lesser reductions were
observed in the silty clays of the LPZ and UWBZ+1. As described below the BTEX makeup in
the UWBZ NAPL was also less than that of the LSZ because of previous soil vapor extraction;
hence concentrations in the UWBZ had been reduced before the TEE pilot test such that TEE
results between the two intervals were roughly equivalent.

Table D-2. Reduction in Average Soil Concentrations between Pre- and Post-TEE.

Soil Horizon	Depth Interval (ft bgs)	Benzene (%)	Toluene (%)	Ethyl-benzene (%)	m&p-Xylenes (%)	Naphthalene (%)
UWBZ+1	160-170	68%	50%	47%	62%	24%
UWBZ	170-195	88%	89%	84%	83%	58%
LPZ	195-205	61%	53%	65%	54%	56%
LSZ-B	205-230	94%	94%	96%	95%	95%
LSZ-C	230-242	99%	100%	100%	100%	96%

Pre-test groundwater samples were collected and analyzed in November and December 2006.
The objective of pre-test groundwater sampling was to provide a baseline of COC concentrations
in groundwater prior to active TEE treatment of the saturated zone. Post-test groundwater
samples were collected and analyzed from November 2009 to January 2010. Similar to soil data,
post-test groundwater data were compared with pre-test data to assess the effect of thermal
treatment and to provide baseline data for the mass transfer tests. Table D-3 lists the benzene
concentration detected in each interior monitoring well. Data for toluene, ethylbenzene, m,p-

xylenes, naphthalene and total hydrocarbons are provided in the TEE Pilot Test Evaluation Report (BEM, 2010).

Table D-3. Pre- and Post-Test Groundwater Sample Analytical Results for Benzene.

Soil Horizon	Pre-TEE Benzene (mg/L)	Post-TEE Benzene (mg/L)	Reduction (%)
MWN-01 A	0.76	0.97	-28%
MWN-02 A	2.1	0.029	99%
MWN-03 A	0.26	2.4	-823%
MWN-04 A	2.9	0.42	86%
MWN-05 A	7.8	2.7	65%
MWN-06 A	1.2	0.05	96%
MWN-01 B	18	1.1	94%
MWN-02 B	24	0.024	100%
MWN-03 B	17	2.2	87%
MWN-04 B	26	2.4	91%
MWN-05 B	20	-	-
MWN-06 B	24	0.011	100%
MWN-01 C	2.8	0.057	98%
MWN-02 C	5.5	2	64%
MWN-03 C	5	3.2	36%
MWN-04 C	8.3	0.057	99%
MWN-05 C	3.9	2	49%
MWN-06 C	10	0.34	97%

Groundwater concentrations of petroleum hydrocarbons after the test, including benzene, were lower than before the test in most TEE cell sampling locations. Concentration reductions were greater in samples from monitoring wells closest to the injection wells. Major reductions occurred throughout the LSZ and in all locations of the UWBZ except MWN03A located next to an extraction well and MWN01A where little treatment occurred.

Characterization of NAPL composition at the site is critical for accurate modeling of multi-component mass transfer as the components do not act independently. The objective of NAPL sampling and analysis was to provide a baseline composition of the NAPL source term for predictive modeling and to evaluate the change in NAPL composition resulting from thermal treatment. The fuel released at the site was suspected to consist of Jet Propulsion fuel No. 4 (JP-4) and some fraction of aviation gasoline. Three NAPL samples were collected from select wells in November 2006 before the TEE pilot test. Six NAPL samples were collected from select wells and analyzed to characterize post-TEE Pilot Test NAPL composition in December 2009. Details of the sampling and the analytical results can be found in the TEE Pilot Test Evaluation Report (BEM, 2010).

Different model NAPL compositions were developed for the UWBZ and the LSZ, as the UWBZ was unsaturated at the time of NAPL release and was subjected to soil vapor extraction from 1997 to 2003. The rising water table entered the bottom of the UWBZ (~195 ft bgs) during 1998 and reached the fine-grained unit separating the top of the UWBZ from the overlying Cobble Zone (~172 ft bgs) in 2004. Hence, the residual NAPL in the UWBZ was initially weathered by

natural volatilization and further weathered by soil vapor extraction before becoming submerged. The result is a lower initial mass fraction of volatile compounds than found in the deeper LSZ NAPL that was weathered primarily by dissolution.

Maximum concentrations of BTEX and naphthalene in groundwater at the site were assumed to be measures of the effective solubility of each compound in the local NAPL. The effective solubility is proportional to the compound's mass fraction according to Raoult's Law. Hence, groundwater concentrations were used to calculate mass fractions in the local residual NAPL both before and after the TEE pilot test to supplement the NAPL analyses. The maximum benzene concentrations are found in Table D-3. Maximum detected concentrations of other fuel components, assumed to represent each compound's effective solubility, from the pre- and post-TEE groundwater sampling are listed in Table D-4 and Table D-5 for the LSZ and UWBZ, respectively. The last column in these tables shows the percentage reduction in the concentration resulting from TEE. These reductions are expected to be nearly equivalent to the reductions in mass fraction of these compounds in the post-TEE residual NAPL.

Table D-4. Effective Solubilities from Maximum Concentrations in the LSZ.

NAPL Component	Pre-TEE Nov 2006 milligram per liter (mg/L)	Post-TEE Jan 2010 (mg/L)	%Reduction
Benzene	26	3.2	88%
Toluene	22	4.1	81%
Ethylbenzene	2.7	1	63%
mp-Xylenes	4.3	0.79	82%
o-Xylene	1.9	0.78	59%
Isopropylbenzene	0.14	NA	-
n-Propylbenzene	0.13	NA	-
135-Trimethylbenzene	ND	NA	-
124-Trimethylbenzene	0.54	NA	-
Naphthalene	0.43	0.16	63%
TOTAL PHC	130	22	83%

Table D-5. Effective Solubilities from Maximum Concentrations in the UWBZ.

NAPL Component	Pre-TEE Nov 2006 (mg/L)	Post-TEE Jan 2010 (mg/L)	%Reduction
Benzene	7.8	2.7	65%
Toluene	6.2	4.6	26%
Ethylbenzene	2.1	1.4	33%
mp-Xylenes	3.8	2.1	45%
o-Xylene	1.6	0.98	39%
Isopropylbenzene	0.16	NA	-
n-Propylbenzene	0.15	NA	-
135-Trimethylbenzene	0.45	NA	-
124-Trimethylbenzene	1.1	NA	-
Naphthalene	0.55	0.14	75%
TOTAL PHC	66	42	36%

The impact of soil vapor extraction in the UWBZ, before the rising water table submerged the residual NAPL, is evident in the relatively low benzene and toluene concentrations measured before the TEE Pilot Test. The maximum pre-TEE concentrations of benzene and toluene in the LSZ were more than three times higher than in the UWBZ where SVE was applied.

Model compositions were developed for NAPL present in the subsurface TEE cell before and after the Pilot Test based the NAPL analyses, effective solubilitites, and literature data. The model components for the NAPL were selected from detailed analyses of JP-4 published by the USAF (Smith et al., 1981) and from the analyses of NAPL samples collected from wells at ST012. Classes of hydrocarbons were combined to reduce the number of components in the model NAPL, as JP-4 is a mixture of over 100 hydrocarbon compounds. The model included 31 components, some of which were surrogate compounds representing a broader class of fuel compounds. For numerical modeling, the 31-component models were further reduced to ten components through mass-weighted averaging by combining classes of hydrocarbons while maintaining BTEX and naphthalene as separate components. The resulting model NAPL compositions are presented in Table D-6 and Table D-7 for the LSZ and UWBZ, respectively.

Table D-6. Model NAPL Compositions in the LSZ.

C#	Compound or Group	Pre-TEE LSZ (% mass)	Pre-TEE LSZ Effective Solubility (mg/L)	Post-TEE LSZ (% mass)	Post-TEE LSZ Effective Solubility (mg/L)
6	Benzene	0.830	26.8	0.101	3.3
7	Toluene	2.900	22.7	0.535	4.2
8	Ethylbenzene	1.400	2.8	0.510	1.0
8	Total Xylenes	3.030	6.1	0.740	1.5
10	Naphthalene	0.500	0.44	0.184	0.17
9	1,2,4-Trimethylbenzene	1.100	0.56	1.147	0.59
9	1,3,5-Trimethylbenzene	0.370	0.34	0.378	0.35
	Other Aromatics	7.37	1.5	7.878	1.6
	Isoalkanes and Paraffins	54.41	8.4	58.23	9.0
	n-Alkanes	28.09	0.97	30.29	1.1
	Total	100.00	70.60	100.00	22.8

Table D-7. Model NAPL Compositions in the UWBZ.

C#	Compound or Group	Pre-TEE UWBZ (% mass)	Pre-TEE UWBZ Effective Solubility (mg/L)	Post-TEE UWBZ (% mass)	Post-TEE UWBZ Effective Solubility (mg/L)
6	Benzene	0.222	8.0	0.076	2.7
7	Toluene	0.730	6.3	0.540	4.7
8	Ethylbenzene	0.970	2.1	0.640	1.4
8	Total Xylenes	2.350	5.3	1.330	3.0
10	Naphthalene	0.570	0.56	0.140	0.14
9	1,2,4-Trimethylbenzene	2.000	1.1	2.007	1.13
9	1,3,5-Trimethylbenzene	0.450	0.46	0.445	0.45
	Other Aromatics	12.02	2.6	12.24	2.6
	Isoalkanes and Paraffins	46.85	3.2	47.93	3.3
	n-Alkanes	33.84	0.16	34.66	0.16
	Total	100.00	29.8	100.00	19.6

1.3   TREATABILITY OR LABORATORY STUDY RESULTS

One-dimensional column studies were performed to assess mass dissolution rates from a residual, multi-component NAPL subjected to a waterflood, a non-condensable vapor flow (i.e., soil vapor extraction), a steamflood, and the co-injection of air and steam. The purpose of the testing was to allow a direct comparison of mass transfer from residual NAPL during the flow of various fluids and at various temperatures. Published literature has little data on mass transfer into a multi-phase carrier fluid. The data provided insight to potential changes in the residual NAPL as a result of TEE and implications for interpreting the post-TEE mass transfer test. The results of the laboratory columns tests are provided in Appendix E.

1.4   DESIGN AND LAYOUT OF TECHNOLOGY COMPONENTS

The TEE Pilot Test system at Site ST012 was constructed from 2003 through 2008 and a layout of the TEE pilot test is provided in Figure D-3. The primary components of the system include the network of wells installed for extraction, injection and monitoring; the systems for treatment of extracted fluids and vapors; and the piping for distribution of water, air, steam, extracted fluids and vapors and electrical power. The TEE pilot test system incorporated shallow (UWBZ) and deep (LSZ) well pairs as part of the process well design. Injection wells were used for steam, air, and water injection. Perimeter extraction wells were used for groundwater, NAPL, and vapor extraction. A total of 32 groundwater injection, extraction and monitoring wells were installed to support the Phase 1 TEE Pilot Test. Figure D-3 illustrates the groundwater extraction, injection and monitoring well network locations supporting the TEE Pilot Test. The constructed TEE system was also used to perform the mass transfer tests. The system is pictured in Figure D-4. During the mass transfer testing, the TEE treatment system provided conditioned water for injection to the subsurface through two process wells, pumping from 12 extraction wells, and treatment of extracted liquids before discharge to a sanitary sewer or disposal.
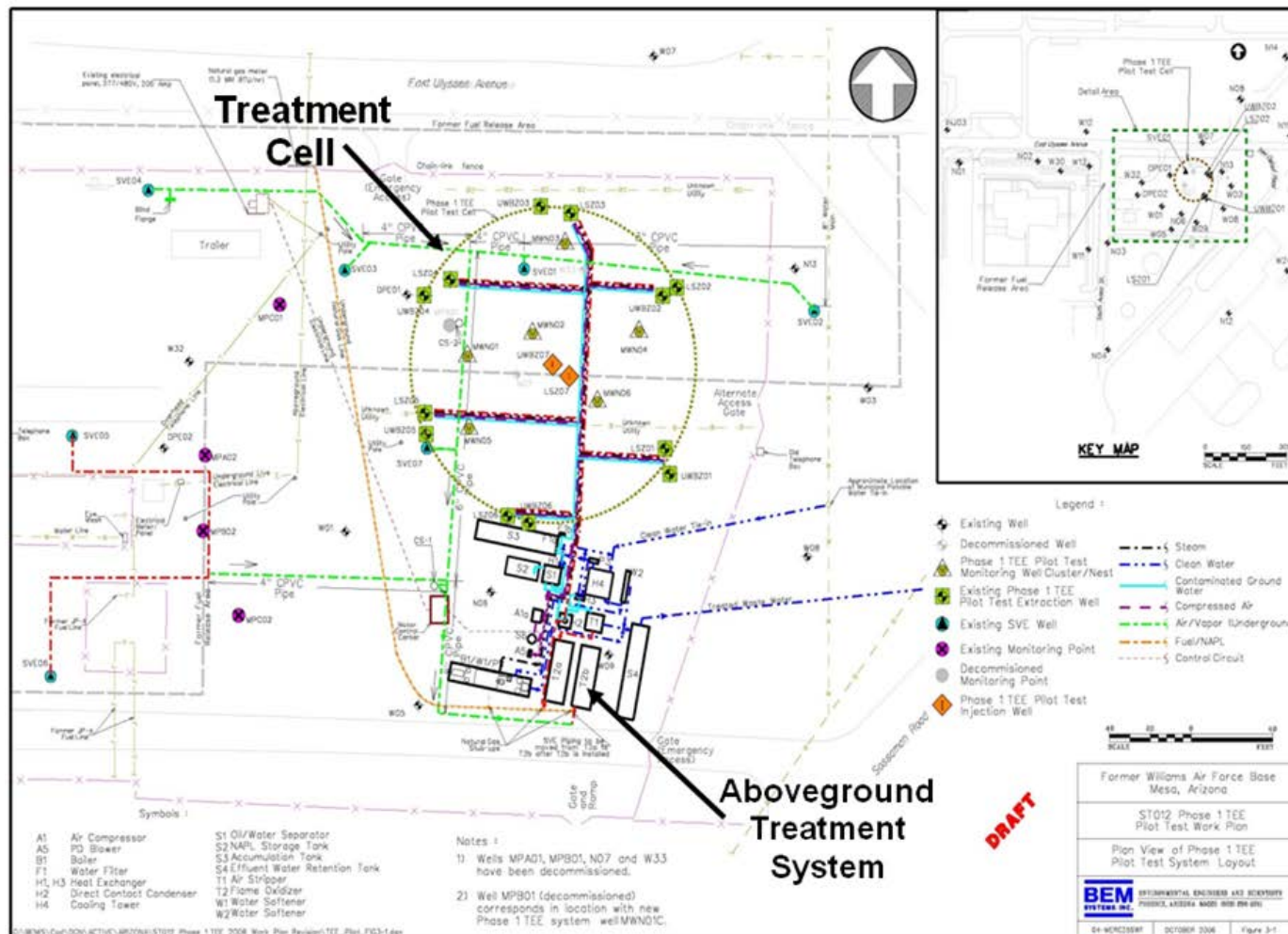
Figure D-3. Detailed Layout of Injection, Extraction, and Monitoring Well Locations.
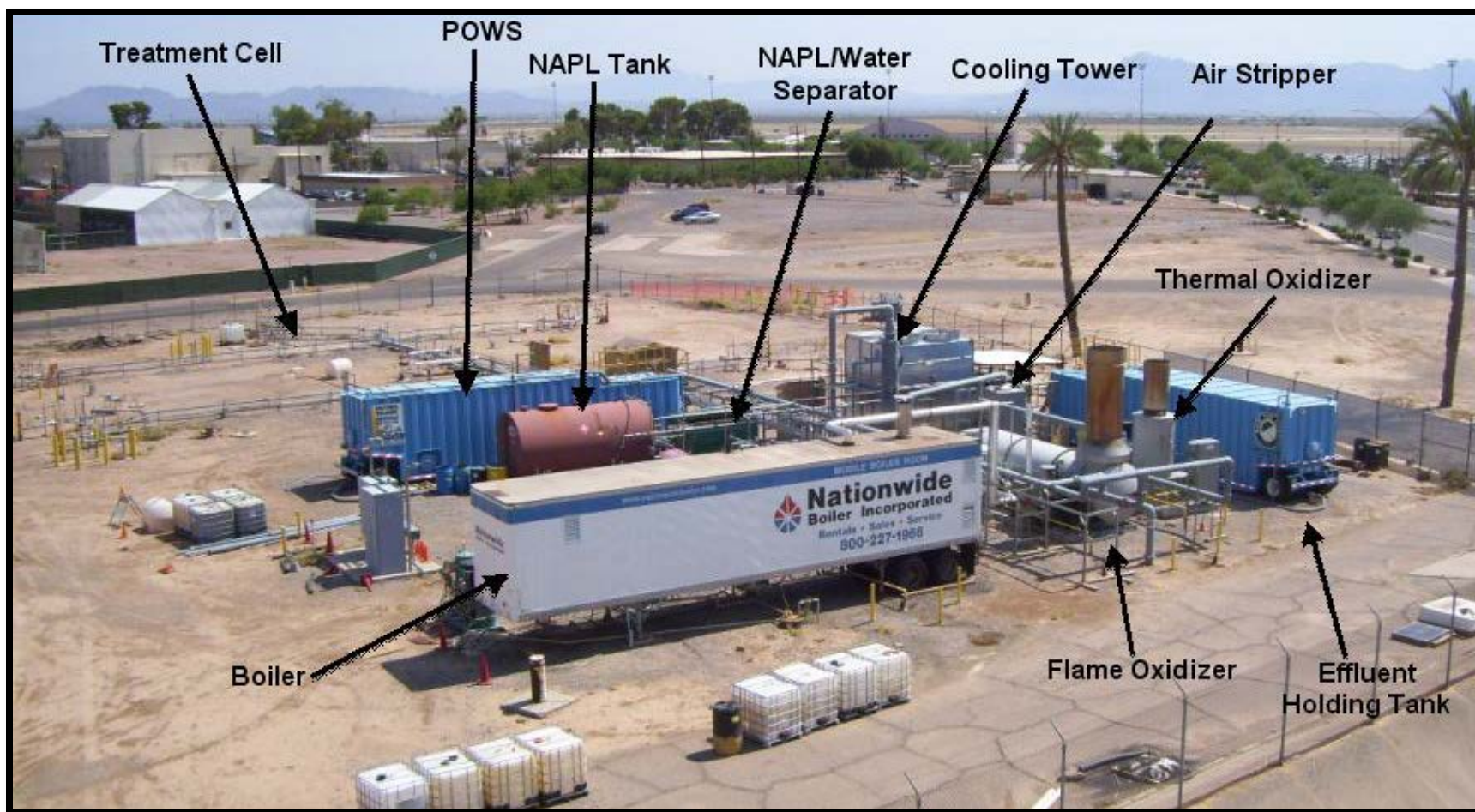
Figure D-4. View of TEE System at ST012 (facing northeast, July 2, 2008).

1.1.1. Process Wells

The pilot test injection/extraction system was comprised of two central injection wells and 12 extraction wells as illustrated in Figure D-3. The process wells were designed for maximum temperature of 300 °F and pressures up to 50 pounds per square inch gauge (psig) regardless of planned operational use of injection or extraction. Two injection-wells (LSZ07, UWBZ07), installed in July and August 2004, were used for steam, air, water, and chemical tracer injection. The twelve, dual-phase extraction wells (LSZ01 through LSZ06 and UWBZ01 through UWBZ06) were installed between May 2003 and August 2004 and were used for groundwater, NAPL, and vapor extraction. Each extraction well was designed to yield up to 15 gallons per minute (gpm) per well to allow changes to the individual well flow rates to be made during the operation of the system.

The LSZ wells were drilled to a total depth of approximately 245 ft bgs and were designated as LSZ01 through LSZ07. The UWBZ wells were drilled to a total depth of about 200 ft bgs and were designated as UWBZ01 through UWBZ07. Each process well was constructed of five-inch diameter Schedule 40 mild steel threaded blank casing and five-inch diameter Type 304 stainless steel threaded continuous wire wrap well screen equipped with a threaded or factory installed stainless steel end cap. A five-foot length of casing was added at the bottom of the UWBZ wells to create a sump. This sump allowed placement of the pump below the screened interval, if desired, maximizing the available screen length for groundwater capture. A one-inch diameter mild steel drop tube was attached to the outside of each well casing. Construction details for the LSZ and UWBZ process wells are illustrated in Figure D-5 and Figure D-6, respectively.
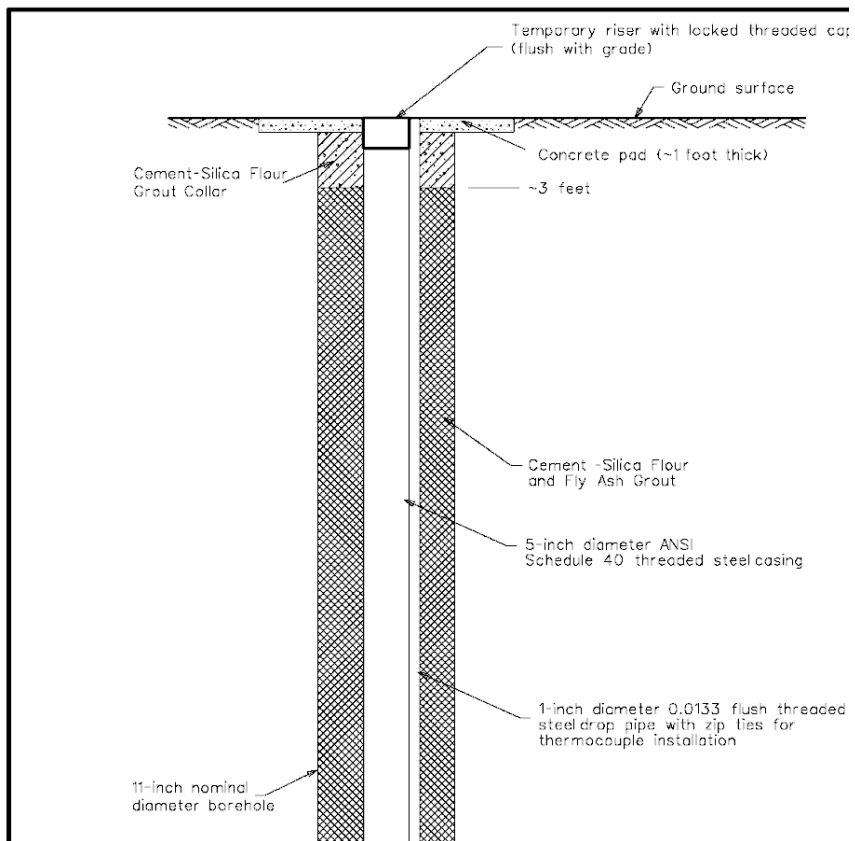
Figure D-5. Injection/Extraction Well Design in the LSZ.

Temporary riser with locked threaded cap
(flush with grade)

Ground surface

Concrete pad (~1 foot thick)

Cement-Silica Flour
Grout Collar

~3 feet

Cement -Silica Flour
and Fly Ash Grout

5-inch diameter ANSI
Schedule 40 threaded steel casing

1-inch diameter 0.0133 flush threaded
steel drop pipe for thermocouple install

11-inch nominal
diameter borehole
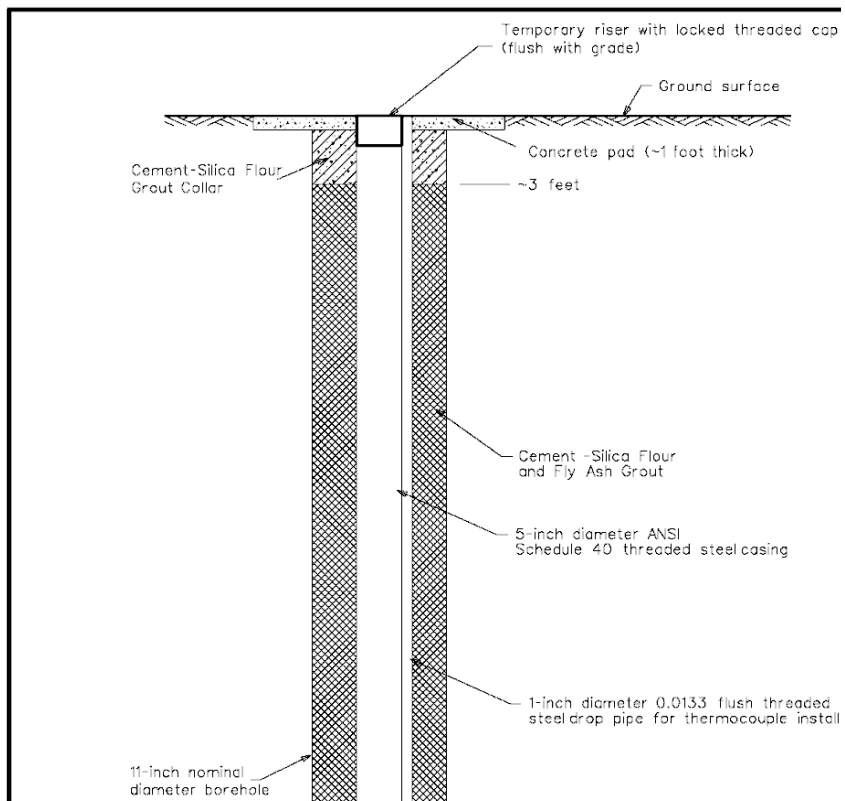
Figure D-6. Injection/Extraction Well Design in the UWBZ.

1.1.2. Monitoring Wells

Six monitoring well clusters (designated as MWN01 though MWN06) were installed within the pilot test cell at varying distances from the injection well pair. The monitoring wells were used to monitor conditions within the cell prior to, during, and following pilot test operations. The number of monitoring wells in the TEE pilot test cell was intended to allow a greater density of data collection in that cell for evaluation of the mass transfer tests, to evaluate the effectiveness of TEE implementation at this site, and to support refinement of the full-scale TEE design.

Each monitoring cluster consisted of three wells screened at successively deeper intervals within the saturated zone: the shallowest screened in the UWBZ and the intermediate and deepest screened at two intervals in the LSZ. Two of the wells (the shallow and intermediate screen intervals) were installed as a nest in a single borehole. The intermediate well was screened in the upper portion of the LSZ (approximately 210-220 ft bgs), and the shallow well was screened in the UWBZ (approximately 170-190 ft bgs). The deep well (screened approximately 232-242 ft bgs) was installed in a separate borehole drilled adjacent to the corresponding well nest and contained a one-inch diameter mild steel drop tube in which digital temperature monitoring devices (DigiTCs) were installed. The monitoring wells were designated MWN01 through MWN06 as indicated in Figure D-1 through Figure D-3, with the shallow, intermediate, and deep wells at each location being designated A, B, and C, respectively (e.g., MWN01A, MWN01B, and MWN01C).
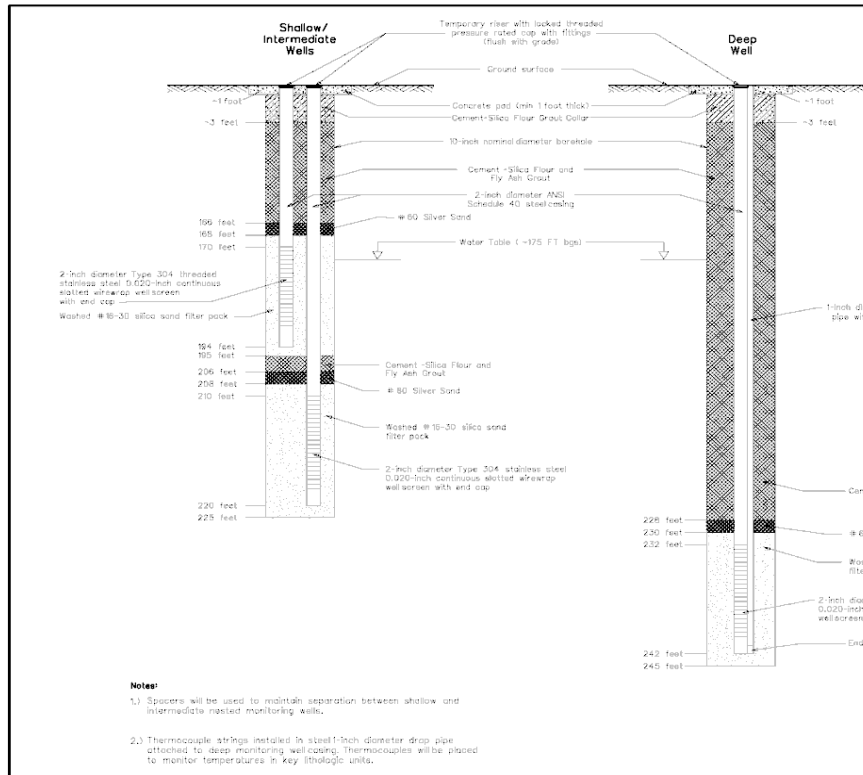
Figure D-7. Monitoring Well Design.

The monitoring wells included dedicated water level indicators for measuring the water table elevation during various phases of the testing. Water level indicators were also installed within the UWBZ and LSZ extraction well casings to monitor water levels within the wells. The water level indicator leads extended aboveground and connected to instrumentation for automated recording of readings at specified time intervals that could be varied depending upon test requirements.

1.1.3. Extraction Pumps

The extraction systems consisted of two sets of total fluids pumps: one for the UWBZ and one for the LSZ. The liquid effluent from these pumps was directed through a heat exchanger and then into a NAPL/water separator. Separated NAPL was collected in a tank for disposal. Water from the separator was pumped to an air stripper for treatment prior to discharge into the City of Mesa sewer system. Details of the treatment system can be found in the TEE Pilot Test Work Plan (BEM, 2007). Clean Environment Model AP-4 pumps were installed in the extraction wells screened in the UWBZ. These pneumatically driven pumps were intended to maintain the water table at the pump intake and remove any floating NAPL that collected in the well. A modified Grundfos high temperature electric pump provided extraction the LSZ. The extraction rate was specified for these pumps and the intake remained submerged allowing a small volume of NAPL to collect in the well above the intake.

1.1.4. Water Injection

Water was injected into the UWBZ and the LSZ to perform the mass transfer tests and also following thermal treatment to maintain hydraulic isolation of the cell during groundwater sampling. The injection rate was 35-36 gpm in the LSZ and about 18 gpm in the UWBZ. The wellhead fitting for steam injection was utilized as the connection point for the water injection. The water supply for all the process activities had a minimum line pressure of 40 psig although the water entered the subsurface at the specified rates via gravity feed. Water was conveyed to the injection well through flexible hose connected between the supply point and the wellhead assembly. The injection wellhead assembly included a flow control valve and a check valve. A water flow totalizer was temporarily added to the wellhead assembly to measure the water injection. The flow was adjusted with the flow control valve to the desired injection rate.

1.1.5. Groundwater Extraction Treatment System

The TEE treatment system was designed to provide treatment for the fuel related contaminants that include free floating NAPL, dissolved petroleum hydrocarbons, and vapor phase petroleum hydrocarbons. The system was comprised of a number of unit processes to treat liquid phase media extracted from the subsurface during the mass transfer tests.

The liquid treatment system started with extracted groundwater being pumped into a 21,000 gallon holding tank where the residence time allowed separation of oil and water to occur. This tank was fitted with a floating skimmer to transfer accumulated NAPL to a NAPL storage tank for disposal. The water then flowed through an oil/water separator (OWS) for further separation with recovered NAPL directed to the NAPL storage tank. From the OWS, the groundwater was pumped into a holding tank to regulate process flow. From the holding tank, the water was processed through an air stripper, where volatile chemicals were separated and sent to a flame oxidizer for destruction. The stripped water was pumped into the Final Effluent Tank (FET). The groundwater was then passed through a granular activated carbon system before final discharge to the City of Mesa POTW and after meeting all applicable discharge requirements. Figure D-3 and Figure D-4 illustrate the primary components of the treatment system. The liquid treatment system was constructed to process up to 120 gallons of extracted groundwater per minute. The vapor extraction system had a capacity to withdraw up to 1,500 standard cubic feet per minute (scfm) of air from the subsurface (BEM, 2007).

1.5 FIELD TESTING

The Air Force intended to improve the characterization of the NAPL contamination at ST012 through the analysis of the pre- and post-TEE mass transfer tests performed in each of the UWBZ and LSZ soil intervals. The mass transfer tests and TEE pilot test were performed by the Air Force's contractor. The primary ESTCP activities were in support of the post-TEE mass transfer test and generalization of the results to other sites. The primary purpose of the pre-TEE mass transfer test in the saturated zone was to determine the rate of dissolution (i.e., mass loading) of hydrocarbon constituents from residual NAPL to water flowing through the pilot test area under known conditions. These measurements were interpreted to assess the individual NAPL constituent mass loading to groundwater under natural flow conditions and used as input

to fate and transport modeling. The mass transfer test was repeated after the TEE pilot test to provide data for the fate and transport modeling to calculate the reduced mass loading of chemicals of concern (COCs) to groundwater in the source area of ST012 after a measured mass of contaminants was extracted (i.e., partial source reduction). These data, along with other TEE pilot test performance data, allowed scientifically defensible forecasts of the mass loading of COCs to groundwater in the source area of ST012 resulting from various scenarios of TEE implementation. An additional purpose for the mass transfer test was to characterize flow conditions within the pilot test area. The site was known to be layered and was thought to be anisotropic with respect to flow direction (e.g., water may flow in preferential directions). The mass transfer tests yielded indications of preferential layers and directions for flow.

The field testing to characterize mass transfer from residual NAPL across a smear zone was performed with the system described in previous sections. The testing within each zone (LSZ and UWBZ) occurred in the following sequence both before and after the TEE pilot test:

1. Establish steady groundwater extraction in the six perimeter wells,
2. Establish steady central water injection,
3. Measure groundwater concentrations in monitoring wells and extraction wells throughout the mass transfer test,
4. Introduce bromide tracer pulse in the water injection,
5. Measure bromide breakthrough curves at select monitoring well screens,
6. Deploy passive flux meters at select depths and in select monitoring well screens,
7. Retrieve passive flux meters, and
8. Terminate mass transfer test and proceed with other Air Force tasks.

The above procedure was repeated four times during this project. A timeline summarizing the field activities in each zone is provided in Figure D-8.

	2008					2009												2010	
Task	A	S	O	N	D	J	F	M	A	M	J	J	A	S	O	N	D	J	F
Baseline Sampling																			
- Soil Sampling (2004)																			
- Groundwater Sampling (2006)																			
LSZ Pre-TEE Mass Transfer Test																			
- Tracer Test																			
- PFM Deployment (B-horizon)																			
UWBZ Pre-TEE Mass Transfer Test																			
- Tracer Test																			
- PFM Deployment (A-horizon)																			
TEE Pilot Test																			
Post-TEE Cooling & Monitoring																			
LSZ **Post-TEE** Mass Transfer Test																			
- Tracer Test																			
- PFM Deployment (B-horizon)																			
UWBZ **Post-TEE** Mass Transfer Test																			
- PFM Deployment (A-horizon)																			
Soil and Groundwater Sampling																			

Figure D-8. Field Testing Timeline.

The baseline soil and groundwater sampling events were summarized in previous sections. The specific mass transfer test procedures and sampling for each event are now described for both the LSZ and UWBZ before and after the TEE pilot test. Throughout the testing in both zones groundwater samples were collected from monitoring and extraction wells and analyzed with an on-site gas chromatograh (GC). Each sample was screened for BTEX and TPH using a field SRI Instruments 8610C [TM] Gas Chromatograph (GC).

1.1.6. *Pre-TEE Mass Transfer Testing in the LSZ*

Before the initial mass transfer test and TEE pilot test, groundwater extraction was started 11 August 2008 and continued for approximately two weeks to provide baseline mass extraction rates from individual extraction wells. During this period, the extraction rates from individual LSZ wells were typically maintained between 5 and 9 gpm. Flow fluctuations were attributed to the deficiencies in pneumatic-drive displacement piston pumps (Blackhawk Technology Company). These pumps were unable to extract groundwater at rates high enough to meet the increased specific capacity of each well resulting from the rise in the water table and the desired total extraction rate of 60 gpm. The Blackhawk pumps were subsequently replaced in mid-October 2008 with electric-submersible pumps (Grundfos Model 16S15-14 Teflon) to compensate for increased specific capacity at each of the six LSZ-extraction wells and increased operational reliability.

On August 26, 2008, clean water injection was initiated at approximately 35 gpm in the central well LSZ07 with the original pneumatic-drive pumps operating in extraction wells. Water injection represented the start of the integral pumping test as the clean water swept through the target soil volumes. Groundwater samples were collected and analyzed with an on-site GC before and during the water injection from LSZ monitoring and extraction wells. Pumping was intermittent from some of the wells and the pump in LSZ05 failed completely during the IPT and the tracer test. The average extraction rate from each well during the tracer test is provided in Table D-8 under the heading, "IPT / Tracer." Average extraction rates after the subsequent installation of the electric submersible pumps is provided in Table D-8 under the heading, "PFM."

Table D-8. LSZ Extraction Rates during the Pre-TEE IPT and PFM Deployment.

Well	IPT / Tracer (gpm)	PFM (gpm)
Extraction		
LSZ01	15.2	9.6
LSZ02	10.4	9.3
LSZ03	4.9	10.1
LSZ04	13.5	10.8
LSZ05	0.0	8.5
LSZ06	11.5	9.9
TOTAL	55.5	58.2
Injection		
LSZ07	35	35

Water levels in the LSZ treatment cell were allowed to equilibrate for approximately 24 hours after the start of water injection and then a slug of potassium bromide tracer was introduced into the injected water. The tracer was 98% pure potassium bromide, manufactured by Spectrum Chemicals and Laboratory Products Company. On 27 August 2008, 208 pounds of potassium bromide was mixed into the injected water over a four hour period to yield a constant bromide concentration pulse of 1,931 mg/L. Seven AquiStar Temphion submersible Smart pH/ISE/Redox Sensors™ were used to gather bromide ion concentration and temperature data during and after tracer injection. Six sensors were used to measure the potassium bromide tracer concentrations in 12 LSZ monitoring wells. The seventh sensor was used to monitor samples collected from the LSZ extraction wells.

Idealized flow streamlines during the tracer test are depicted in Figure D-9 where results from the analytical model RESSQ (Doughty, Tsang and Javandel, 1985) are plotted. The extraction and injection rates provided in Table D-8 and the wells are identified in Figure D-1. The calculations were based on the following assumptions:
- LSZ is a uniform, isotropic aquifer;
- LSZ thickness is 35 feet;
- LSZ porosity is 30%;
- Regional groundwater velocity is 58.2 feet per year; and
- Regional groundwater flow is west to east (left to right on Figure D-9).
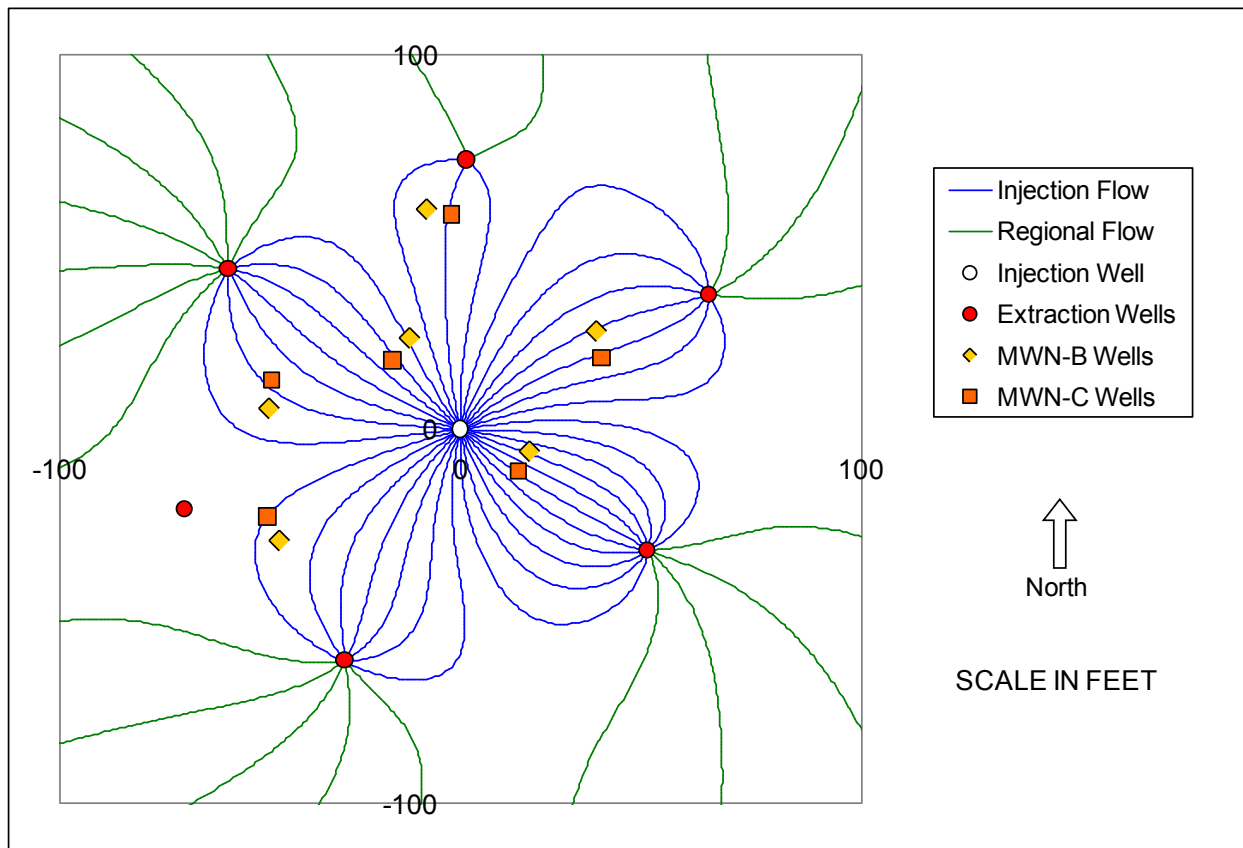
Figure D-9. Idealized Streamlines in the LSZ during the pre-TEE IPT with Tracer Test.

Figure D-1 displays the configuration of a central injection well (LSZ07) surrounded by six extraction wells (LSZ01 to LSZ06) with twelve interior monitoring wells ("B" and "C" screens of MWN01 through MWN06). The loss of extraction from LSZ05 is evident; however, theoretically, all of the monitoring well screens were swept by the injected water. The pathlines illustrated in Figure D-9 originating from the central injection well are equal to streamlines separated by a one gallon per minute flow. The pathlines originating from the upgradient regional groundwater flow approximate streamlines also separated by one gpm.

The times for potassium bromide tracer to travel to each LSZ well within the TEE cell are discussed later. Preferential flow is evident in the tracer arrival times. In particular, travel through the B-horizon was much slower than in the deeper, more permeable C-horizon with one exception. Tracer appearance in MWN02-B was rapid indicating a preferential pathway to the northwest of injection well LSZ07. The nature of the flow and the layering in the LSZ are examined in detail in Section 6 of the main report. Once the tracer had appeared in all of the extraction wells on day 21 (approximately three weeks from initial injection), the system reflected near equilibrium conditions with respect to flow and hydrocarbon dissolution. Groundwater samples were collected from LSZ monitoring wells and LSZ extraction wells. The samples were analyzed for BTEX and TPH using field GCs. The pneumatic-driven extraction pumps were then replaced with the electric submersible pumps.

After the replacement of the LSZ groundwater extraction pumps in October 2008, site flow conditions were re-established with the average extraction rates provided in the "PFM" column of Table D-8. Idealized streamlines calculated with RESSQ are illustrated in Figure D-10. Theoretically, the flow was significantly more uniform than during the IPT. Passive Flux Meters™ (PFMs) were then installed in LSZ monitoring wells MWN01B through MWN06B on 23 October 2008 by University of Florida personnel. Three connected PFMs were installed in each of the six MWNB wells, for a total of 18 PFMs. Free-phase NAPL was observed and removed from MWNB wells using disposable bailers and twine prior to the installation of the PFMs. After four days of exposure to treatment cell flow, the PFMs were removed and analyzed by University of Florida personnel. The PFM is a nylon mesh tube filled with a sorbent/tracer mixture. Inside the PFM is a permeable sorbent that retains NAPL components dissolved into the groundwater. The sorbent mixture is also preloaded with specified amounts of resident tracers. The tracers are leached from the sorbent as groundwater flows through the PFM. The loss of resident tracer is proportional to the flow of water through the well. Because of budget constraints, PFMs were not installed in the deeper, less-contaminated C-series monitoring wells. Retrieval of the PFMs on 27 October 2008 marked the end of the pre-TEE mass transfer testing in the LSZ and the TEE pilot test proceeded with the initiation of steam injection in the LSZ on 28 October 2008.
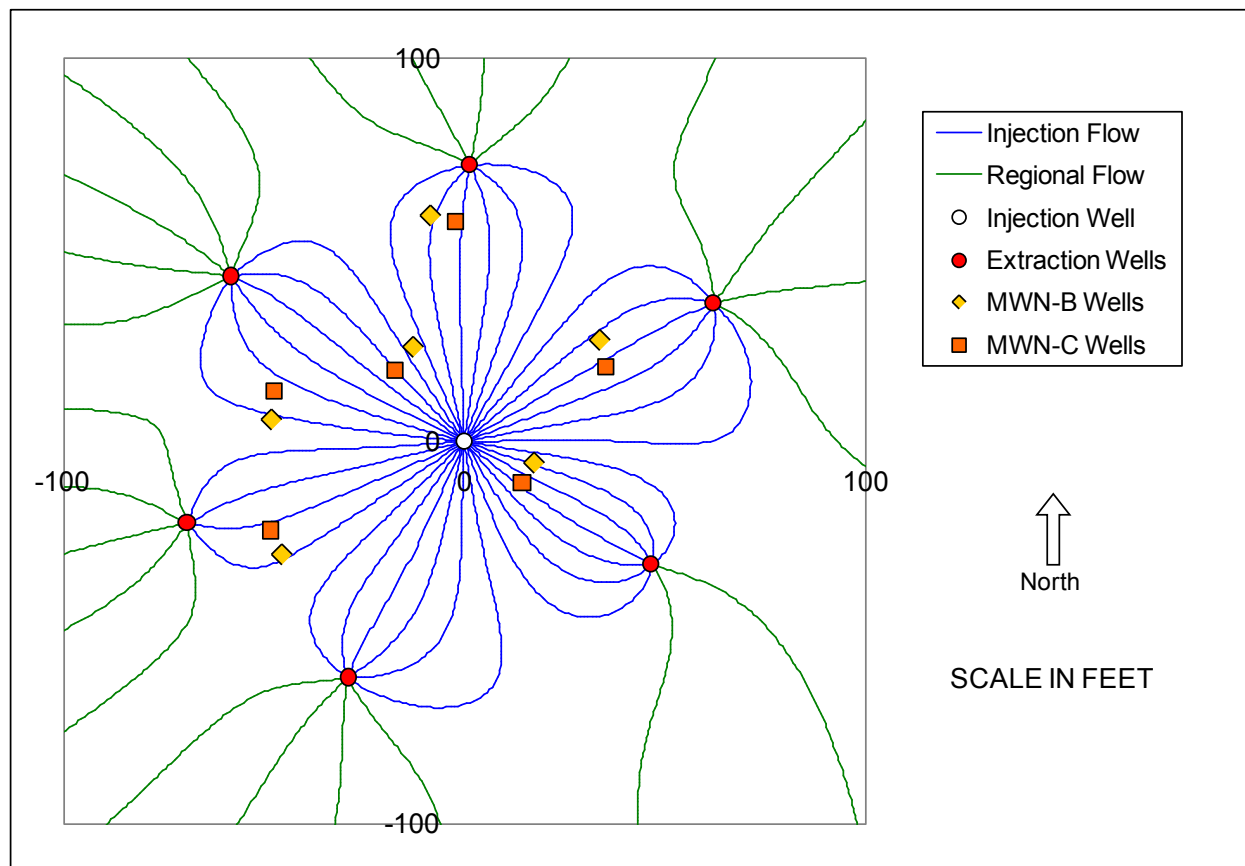
Figure D-10. Idealized Streamlines in the LSZ during the pre-TEE PFM Deployment.

1.1.7. Post-TEE Mass Transfer Testing in the LSZ

After the TEE pilot test was completed in May 2009, substantial residual heat remained in the subsurface and a cooling period was provided before collecting the post-TEE mass transfer data. Groundwater extraction with central injection was started 20 May 2009 and continued through 17 November 2009. Water injection at 39 gpm allowed for continued flushing of contaminants while promoting the complete cooling of the TEE cell to below 120°F. Temperatures at LSZ monitoring wells were monitored using a manually placed thermocouple wire. Liquid discharge temperatures of the groundwater at LSZ extraction wells were monitored at the wellheads. Groundwater and NAPL grab samples were collected by field staff and analyzed with a field GC for BTEX and TPH during the cooling period. LSZ extraction and monitoring well liquid samples were collected and analyzed approximately weekly. After the site had cooled sufficiently, a post-TEE tracer test was performed.

The average extraction rate from each well during the post-TEE tracer test is provided in Table D-9 under the heading, "IPT / Tracer." Average extraction rates during the 4-day PFM deployment are provided in Table D-9 under the heading, "PFM." Note that the pump in extraction well LSZ05 was inoperable throughout the tracer test but was repaired and brought back on line for the PFM deployment. Idealized flow streamlines during the tracer test are depicted in Figure D-11 where results from the analytical model RESSQ (Doughty, Tsang and Javandel, 1985) are plotted. Each streamline represents one gallon per minute. Under ideal conditions, the injected water is shown to travel outside the treatment cell where the extraction rates were zero and low in wells LSZ05 and LSZ06, respectively. A slug of potassium bromide tracer was introduced into the injected water for 24 minutes on 20 October, 2009. The tracer was mixed into the injected water to yield an average bromide concentration of 2,113 mg/L. Six AquiStar® Temphion™ submersible Smart pH/ISE/Redox Sensors were used to gather bromide ion concentration and temperature data during and after tracer injection. The sensors were used to measure the potassium bromide tracer ion concentrations in six LSZ monitoring wells. Arrival of the bromide tracer slug was monitored at LSZ monitoring wells MWN01C, MWN02B, MWN02C, MWN04C, MWN06B and MWN06C.

Table D-9. LSZ Extraction Rates during the Post-TEE IPT and PFM Deployment.

Well	IPT / Tracer (gpm)	PFM (gpm)
Extraction		
LSZ01	12.1	11.1
LSZ02	13.2	17.7
LSZ03	13.0	12.0
LSZ04	11.8	17.5
LSZ05	0.0	17.4
LSZ06	3.5	5.4
TOTAL	53.6	81.1
Injection		
LSZ07	39	39
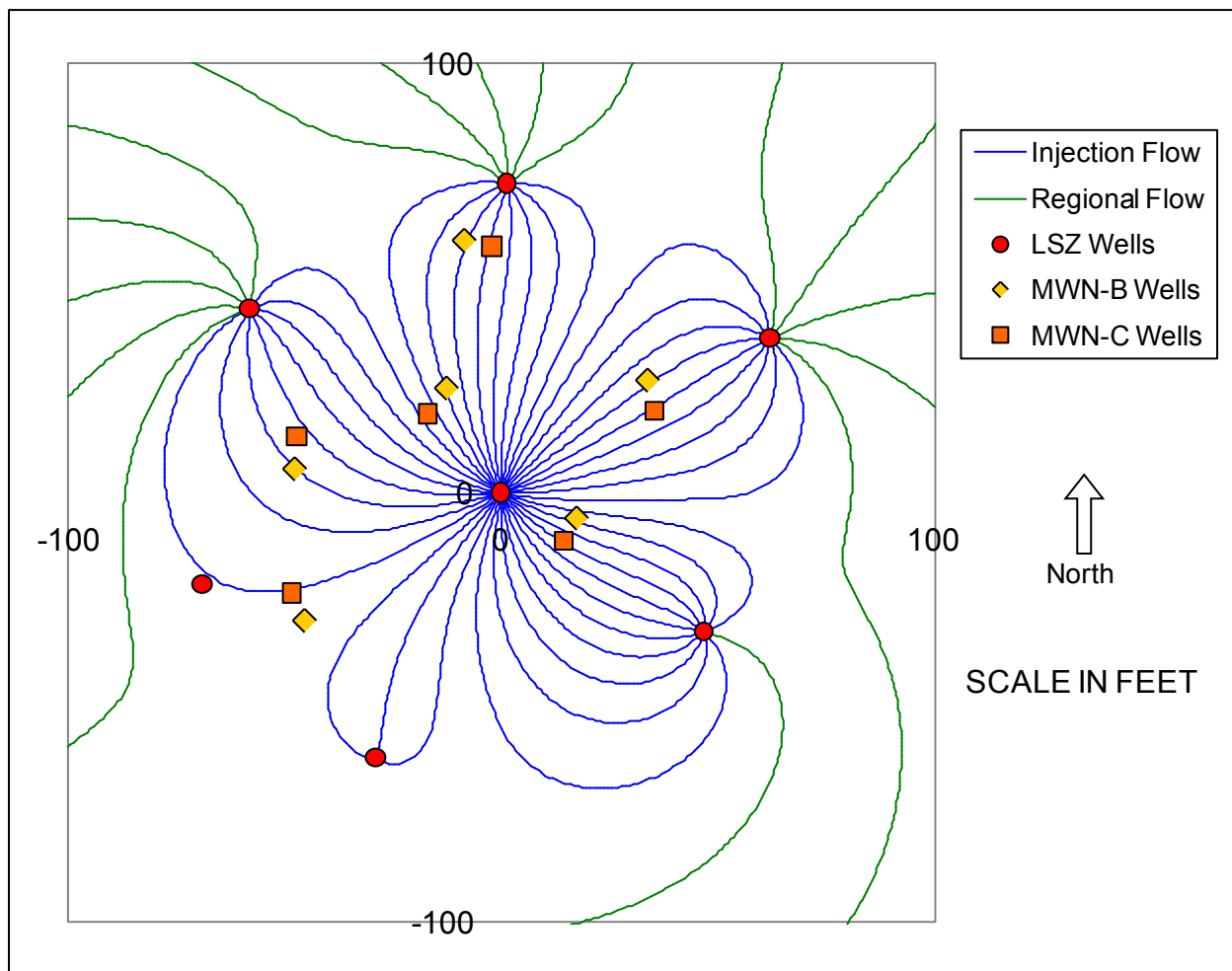
Figure D-11. Idealized Streamlines in the LSZ during the post-TEE IPT with Tracer Test.

The University of Florida personnel installed PFMs in monitoring wells MWN01B through
MWN06B on 12 November 2009 and 13 November 2009. Idealized streamlines calculated with
RESSQ using the "PFM" rates in Table D-9 are illustrated in Figure D-12. Theoretically, the
flow was significantly more uniform with an operable pump in LSZ05 than during the tracer test
with no extraction in LSZ05. Three connected PFMs were installed in each of the six MWNB
wells, for a total of 18 PFMs. Free phase NAPL, if present, was removed from MWN01B
through MWN06B using disposable bailers and twine prior to the installation of the PFMs. After
four days of exposure to groundwater flow, the PFMs were removed from five MWNB wells and
analyzed for benzene and TPH by University of Florida personnel. Three PFMs, located in well
MWN05B, were lodged in the well and could not be removed. These three PFMs were
abandoned in the well after unsuccessful retrieval attempts were made using heavy equipment.
Because of budget constraints, PFMs were not installed in the deeper, less-contaminated C-series
monitoring wells. Retrieval of the PFMs on 17 November 2009 marked the end of the post-TEE
mass transfer testing in the LSZ.
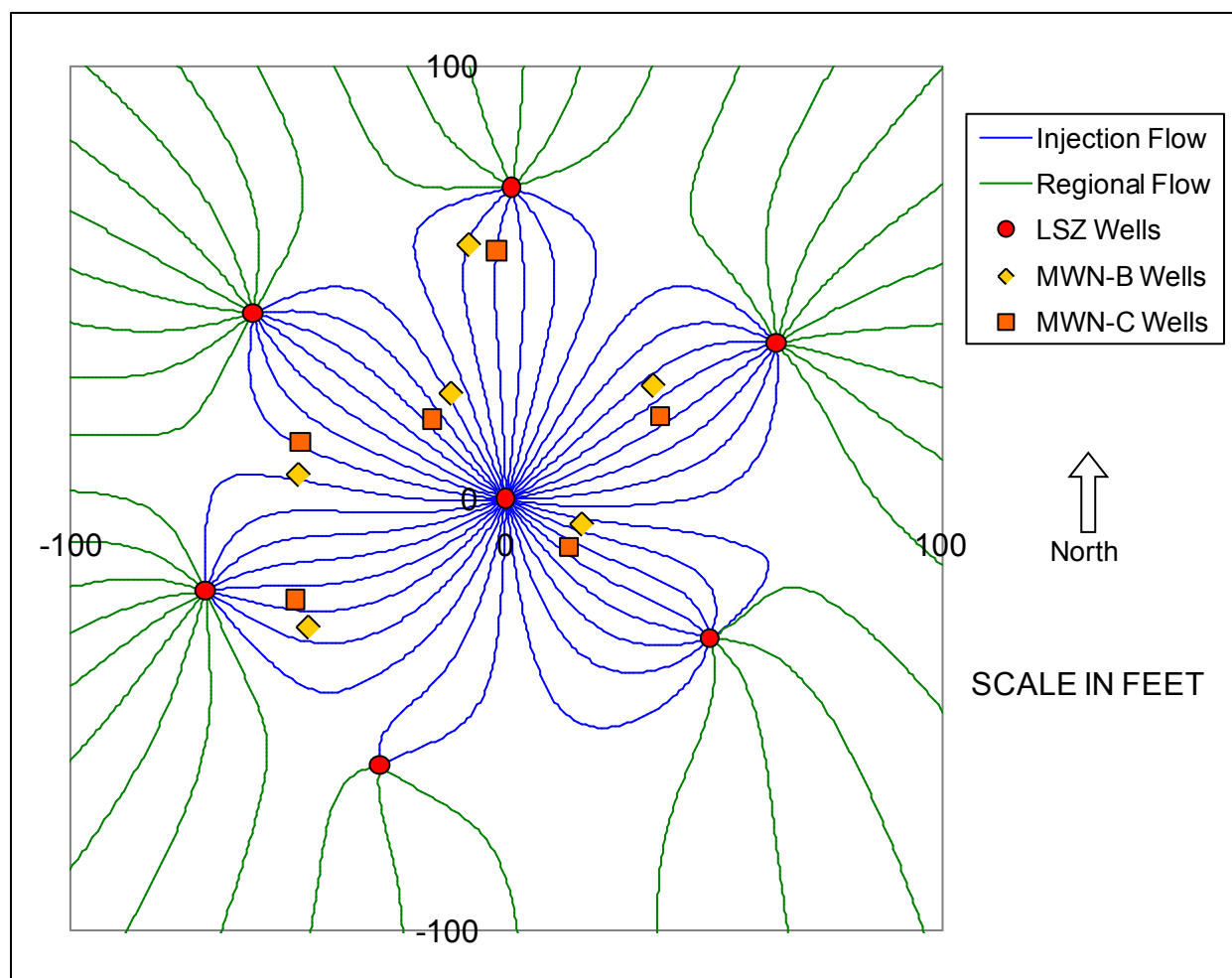
Figure D-12. Idealized Streamlines in the LSZ during the post-TEE PFM Deployment.

1.1.8. Pre-TEE Mass Transfer Test in the UWBZ

Before the initial mass transfer test in the UWBZ and TEE pilot test, groundwater extraction was started in six UWBZ wells (UWBZ01 through UWBZ06) on the perimeter of the treatment cell. The pumping commenced 11 August 2008 using Clean Environment model AP-4 top-loading, pneumatic displacement pumps and continued through the initiation of the IPT on 26 August 2008. Depth to groundwater data was collected from extraction wells UWBZ01 through UWBZ06 and monitoring wells MWN01A through MWN06 A. Groundwater flow rates were collected both manually and utilizing Seametrics Type IP81B ^{TM} flow meters at the UWBZ extraction wells.

On 26 August 2008, clean water injection was initiated at approximately 18 gpm in the central well UWBZ07. Water injection represented the start of the integral pumping test as the clean water swept through the target soil volumes. Groundwater samples were collected and analyzed with an on-site GC before and during the water injection from UWBZ monitoring and extraction wells. Pumping was intermittent from some of the wells and the pump in UWBZ02 failed completely during the IPT and the tracer test. The average extraction rate from each well during the tracer test is provided in Table D-10 under the heading, "IPT / Tracer." Average extraction rates during the four-day deployment of PFMs are provided In Table D-10 under the heading, "PFM."

Table D-10. UWBZ Extraction Rates during the Pre-TEE IPT and PFM Deployment.

Well	IPT / Tracer (gpm)	PFM (gpm)
Extraction		
UWBZ01	0.4	0.4
UWBZ02	0.0	0.0
UWBZ03	7.0	13.6
UWBZ04	3.6	3.6
UWBZ05	5.2	7.7
UWBZ06	5.4	8.3
TOTAL UWBZ	21.6	33.6
Injection		
UWBZ07	18	18

Water levels in the UWBZ treatment cell were allowed to equilibrate for approximately 48 hours after the start of water injection and then a slug of potassium bromide tracer was introduced into the injected water. The tracer was 98% pure potassium bromide, manufactured by Spectrum Chemicals and Laboratory Products Company. On 28 August 2008, 208 pounds of potassium bromide was mixed into the injected water over a four hour period to yield a constant bromide concentration pulse of 1,851 mg/L. Seven AquiStar Temphion submersible Smart pH/ISE/Redox Sensors™ were used to gather bromide ion concentration and temperature data during and after tracer injection. Six sensors were used to measure the potassium bromide tracer concentrations in six UWBZ monitoring wells. The seventh sensor was used to monitor samples collected from the UWBZ extraction wells.

Idealized flow streamlines during the tracer test are depicted in Figure D-13 where results from the analytical model RESSQ (Doughty, Tsang and Javandel, 1985) are plotted. The extraction and injection rates provided in Table D-10 and the wells are identified in Figure D-2. The calculations were based on the following assumptions:

- UWBZ is a uniform, isotropic aquifer;
- UWBZ thickness is 30 feet;
- UWBZ porosity is 30%;
- Regional groundwater velocity is 23.2 feet per year; and
- Regional groundwater flow is west to east (left to right on Figure D-13).
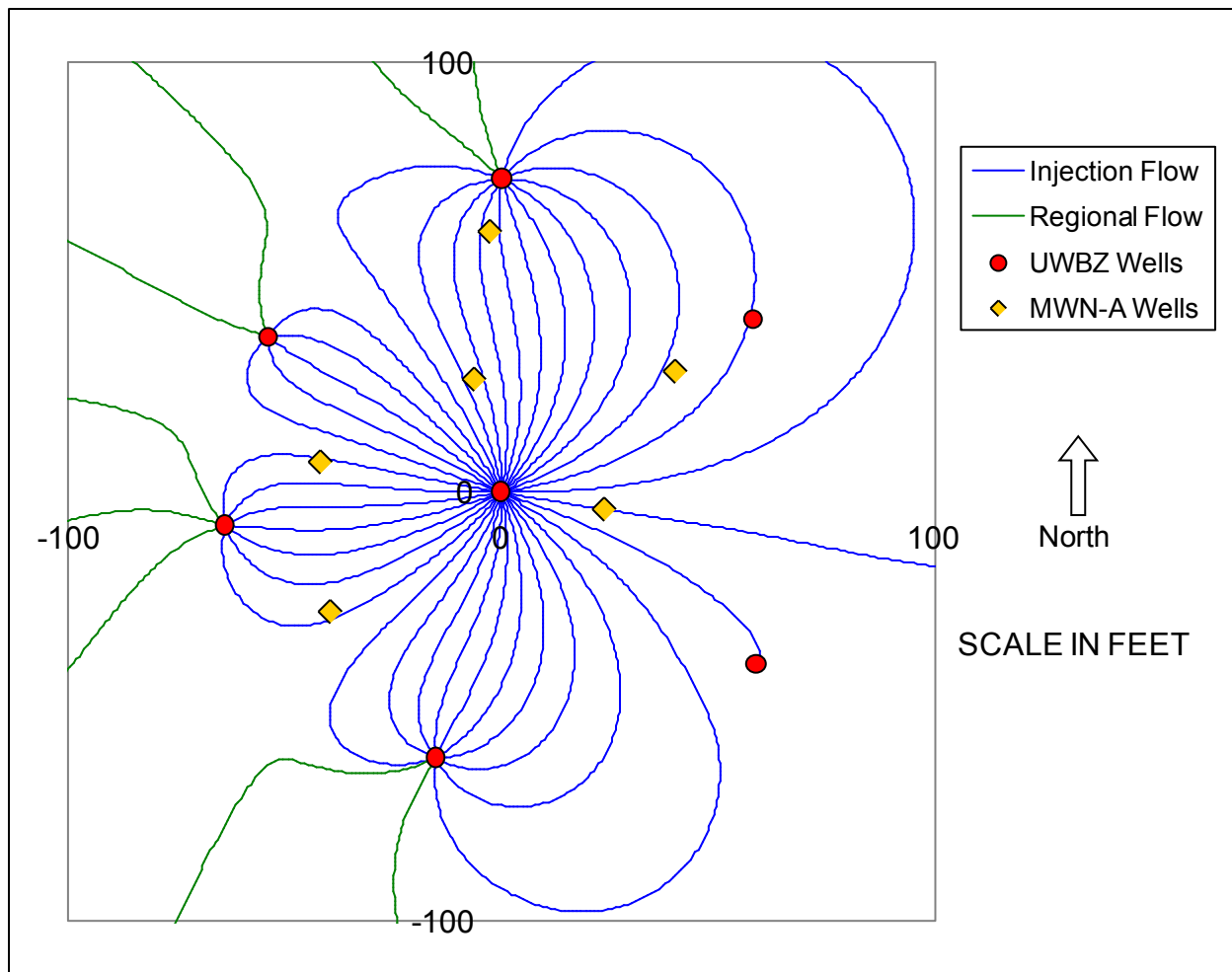
Figure D-13. Idealized Streamlines in the UWBZ during the pre-TEE IPT with Tracer Test.

Each streamtube represents one half gpm of flow from the central injection well (UWBZ07) to the surrounding extraction wells (UWBZ01 to UWBZ06) passing through six interior monitoring wells ("A" screens of MWN01 through MWN06). The pathlines originating from the upgradient

regional groundwater flow approximate streamlines also separated by one half gpm. The loss of extraction from UWBZ02 and the low flow from UWBZ01 are evident with the loss of containment on the east side of the cell.

The times for the bromide tracer to travel to each UWBZ well within the TEE cell are discussed later and preferential flow is evident in the tracer arrival times. Tracer appearance in MWN02-A and MWN04-A were relatively rapid indicating a preferential pathway to the north of injection well UWBZ07. The tracer was slow to reach MWN06-A, closest to the injection well, however, extraction in that direction was low. Once the tracer had appeared in all of the extraction wells by day 20 (approximately three weeks from initial injection), the system reflected near equilibrium conditions with respect to flow and hydrocarbon dissolution. Groundwater samples were collected from UWBZ monitoring wells and UWBZ extraction wells. The samples were analyzed for BTEX and TPH using field GCs.

Immediately after the tracer test and under pseudo-steady mass transfer conditions, PFMs were installed in UWBZ monitoring wells MWN01A through MWN06A on 18 September 2008 by University of Florida personnel. Three connected PFMs were installed in each of the six MWNA wells, for a total of 18 PFMs. Free phase NAPL was observed and removed from MWNA wells using disposable bailers and twine prior to the installation of the PFMs. After four days of exposure to groundwater flow, the PFMs were removed and sampled for benzene and TPH by University of Florida personnel. During the deployment, flow in the UWBZ was relatively steady and the average flow rates are provided in the "PFM" column of Table D-10. Idealized streamlines calculated with RESSQ are illustrated in Figure D-14. Again, extraction from the east side of the cell was very low; however, the total extraction rate was 50% higher than during the tracer test such that containment within the cell was approximated theoretically. Retrieval of the PFMs on 22 September 2008 marked the end of the pre-TEE mass transfer testing in the UWBZ.
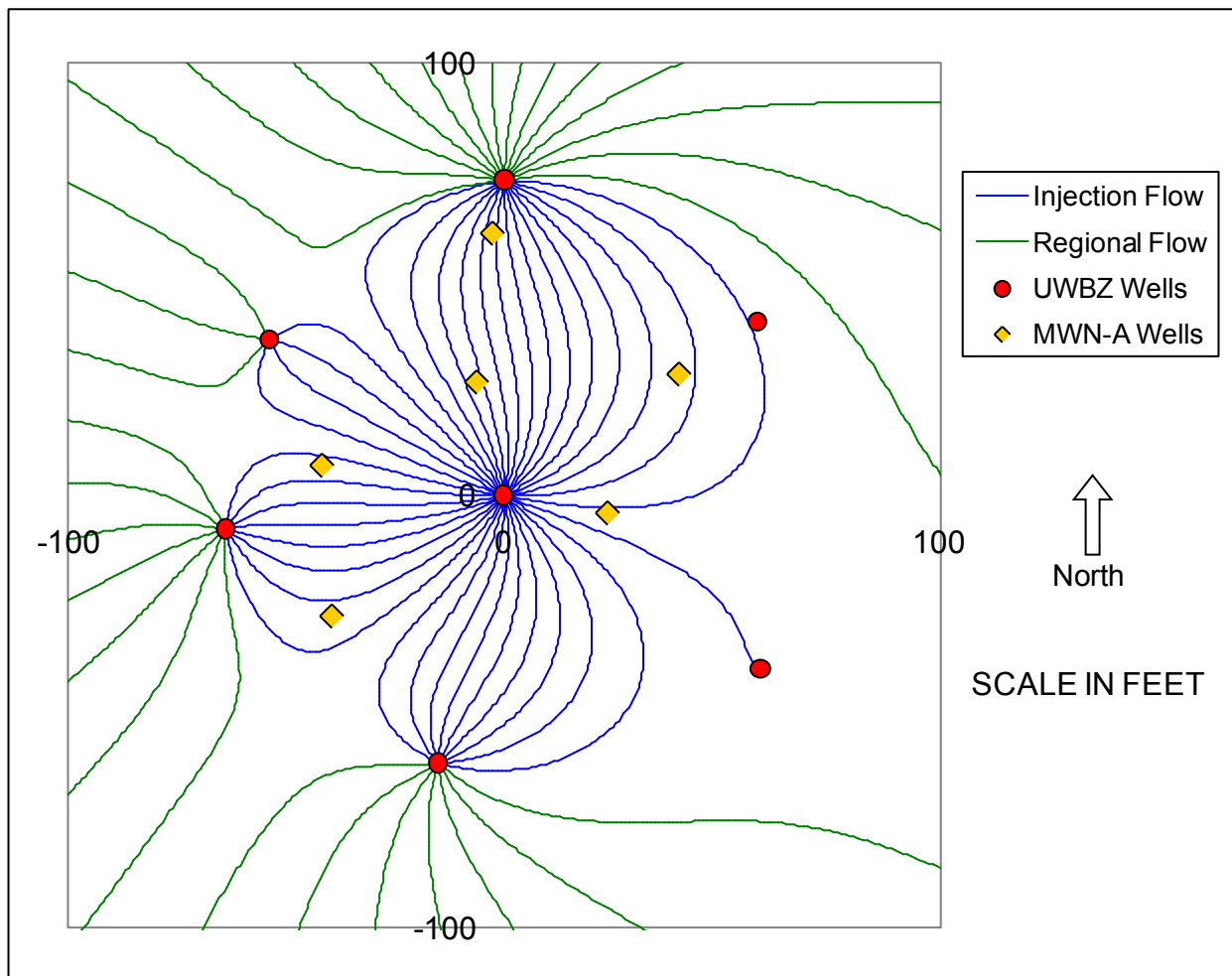
Figure D-14. Idealized Streamlines in the UWBZ during the pre-TEE PFM Deployment.

1.1.9. Post-TEE Mass Transfer Test in the UWBZ

After the TEE pilot test was completed in May 2009, substantial residual heat remained in the subsurface and a cooling period was provided before collecting the post-TEE mass transfer data. Groundwater extraction continued with the start of central water injection on 18 May 2009 and continued through 17 November 2009. Water injection at 18 gpm allowed for continued flushing of contaminants while promoting the complete cooling of the TEE cell to below 120°F. Temperatures at UWBZ monitoring wells were monitored using a manually placed thermocouple wire. Liquid discharge temperatures of the groundwater at UWBZ extraction wells were monitored at the wellheads. Groundwater and NAPL grab samples were collected by field staff and analyzed with a field GC for BTEX and TPH during the cooling period. UWBZ extraction and monitoring well liquid samples were collected and analyzed approximately weekly. A post-TEE tracer test was not performed in the UWBZ.

The University of Florida personnel installed PFMs in monitoring wells MWN01A through MWN06A on 12 November 2009 and 13 November 2009. Three connected PFMs were installed in each of the six MWNA wells, for a total of 18 PFMs. Free phase NAPL, if encountered, was removed from MWN01A through MWN06A using disposable bailers and twine prior to the installation of the PFMs. After four days of exposure to groundwater flow, the PFMs were removed from the six MWNA wells and analyzed for benzene and TPH by University of Florida personnel. Following retrieval of the UWBZ PFMs on 17 November 2009, a PFM was inserted and immediately retrieved and sampled in each of the UWBZ wells. This test was performed to provide a background comparison to consider the effect of passing the PFM through free product at the water table. Retrieval of the PFMs on 17 November 2009 marked the end of the post-TEE mass transfer testing in the UWBZ.

Average extraction rates during the 4-day PFM deployment are provided in Table D-11 under the heading, "PFM." Note the extraction was much more uniform than during the pre-TEE deployment as the pump in UWBZ02 was repaired before the TEE pilot test started and well UWBZ01 was redeveloped. Idealized flow streamlines during the PFM deployment are depicted in Figure D-15 where results from the analytical model RESSQ (Doughty, Tsang and Javandel, 1985) are plotted. Each streamline represents one half gallon per minute. Theoretically, a portion of the injected water traveled outside the target cell volume before being extracted. As presented in Table D-11, the total extraction rate only slightly exceeded the total injection rate such that containment was tenuous with the presence of a background local groundwater flow velocity.

Table D-11. UWBZ Extraction Rates during the Post-TEE PFM Deployment.

Well	PFM (gpm)
Extraction	
UWBZ01	3.9
UWBZ02	3.3
UWBZ03	2.7
UWBZ04	3.3
UWBZ05	3.2
UWBZ06	3.9
TOTAL UWBZ	20.3
Injection	
UWBZ07	18
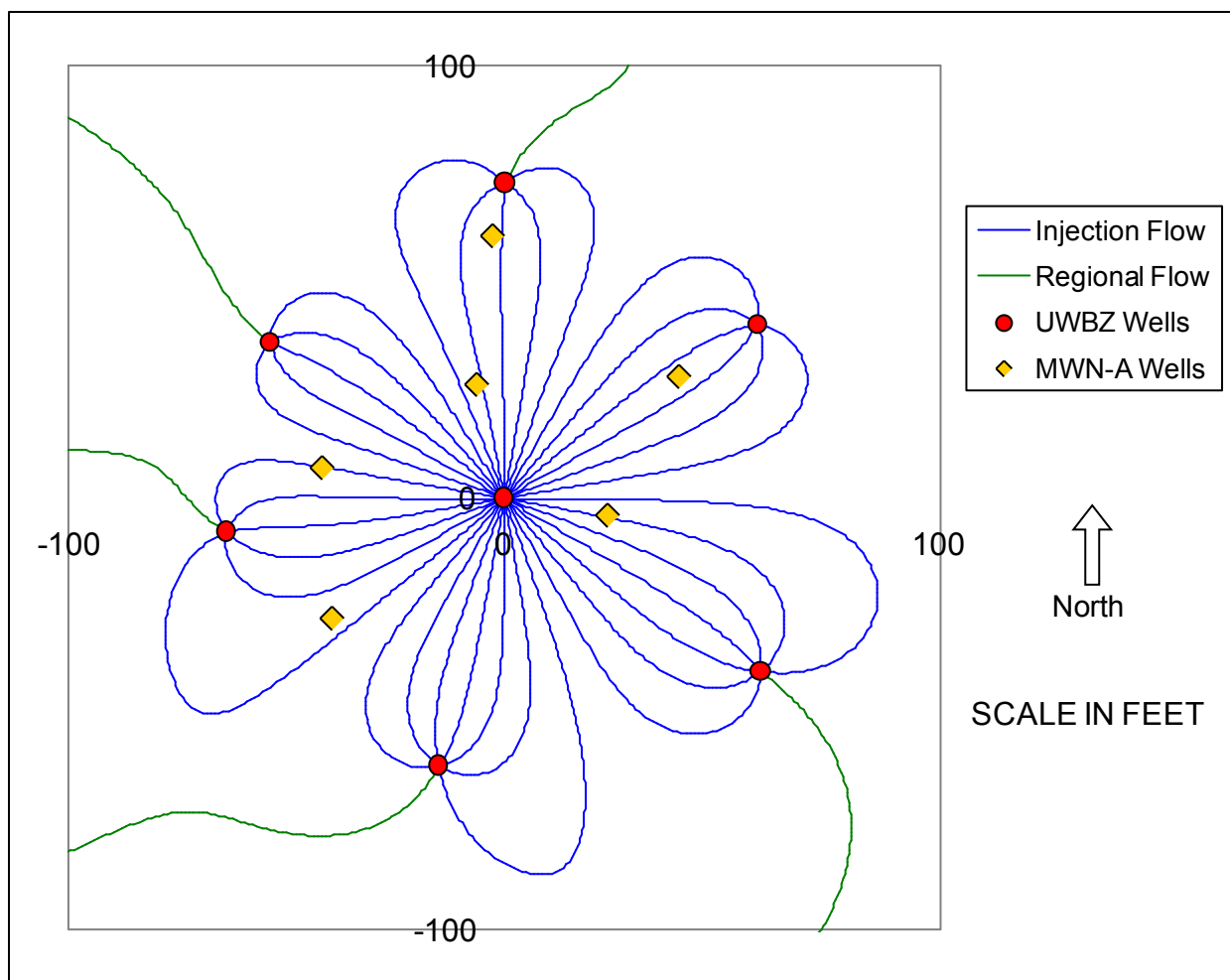
Figure D-15. Idealized Streamlines in the UWBZ during the post-TEE PFM Deployment.

1.1.10.   *Post-Treatment Sampling, System Shutdown and Demobilization*

On 17 November 2009, the water injection was terminated in both the LSZ and UWBZ. Groundwater extraction continued until 20 November 2009 when all operations were terminated by the site contractor (BEM Systems, Inc.). Subsequently, soil, groundwater, and NAPL samples were collected to establish post-treatment conditions within the treatment cell and in the areas downgradient of the cell for evaluation of the Pilot Test performance.

The post-test soil sampling provided information on the nature and distribution of soil contamination within the saturated zone inside the treatment cell following thermal treatment. Post-test soil samples were collected from November to December 2009, during the advancement of five soil borings (TB-2 through TB-6) within the TEE Pilot Test treatment cell. The benzene concentrations measured in these samples are presented in Table D-1 alongside the baseline concentrations measured before the pilot test. The purpose of post-test groundwater sampling was to assess changes in COC concentration and MNA parameters in groundwater both within and downgradient of the treatment cell as a result of treatment. The purpose of post-test NAPL sampling was to assess the composition of NAPL within the source area and the treatment

cell. Seven NAPL samples from LSZ and UWBZ monitoring wells located within and surrounding the treatment cell were collected and analyzed.

The responsibility for the disposition of all equipment, wells, piping, supplies and waste at ST012 remained with the Air Force and its contractors at the end of the field work associated with this ESTCP project.

1.6   SAMPLING METHODS

An extensive sampling and analysis plan was prepared by the U.S. Air Force and can be found in the TEE Pilot Test Work Plan (BEM, 2007). This plan includes a detailed field sampling plan and associated quality assurance project plan that define sampling intervals and strategies for all activities associated with the TEE pilot test at ST012. The sampling associated with the mass transfer tests occurred at various phases as indicated in Table D-12. The analytical methods performed on the samples are summarized in Table D-13. The sampling included baseline and post-treatment soil, groundwater and NAPL sampling and analyses to provide starting and ending measurements. Groundwater sampling and analyses was performed during each mass transfer test. The pre-TEE groundwater analyses were performed solely with the field GC while the post-TEE analyses included state-certified laboratory analyses. During the tracer tests, bromide concentrations in monitoring wells were measured and logged with calibrated AquiStar Temphion submersible Smart pH/ISE/Redox Sensors™. A post-TEE tracer test was not performed in the UWBZ. Passive flux meters were deployed, retrieved and analyzed by University of Florida personnel during each mass transfer test although PFMs were not deployed in the C-horizon of the LSZ.

1.6.1   Soil Sampling and Analyses

As described previously, 15 soil samples were collected from each of five borings during the installation of monitoring wells (MWN02C through MWN06C) before the TEE pilot test to support baseline contaminant mass and distribution estimation (completed in 2004). Upon completion of drilling each day, 5 grams of soil from each of the samples were inserted into a laboratory prepared 40 milliliter (mL) methanol preserved Volatile Organic Analysis (VOA) vial and an unpreserved 4-ounce (oz) glass jar was filled with soil remaining from the sample. Soil samples were labeled, manifested, packed on ice for preservation, custody sealed, and shipped to Chemtech Laboratory in Mountainside, New Jersey for analysis. Volatile Organic Compounds (VOCs) including benzene, toluene, ethyl benzene, xylenes, and naphthalene (BTEXN) by Method 8260B and PHC (Method 8015) (BEM, 2004).

Post-TEE in November and December 2009, BEM collected comparable soil samples in boreholes adjacent to the monitoring wells. Fifteen soil samples were collected from the various lithologic layers at each boring that represent the Aquitard, LSZ, LPZ and UWBZ for a total of 75 soil samples. The samples were collected with two and five-inch diameter split spoons and split spoons were placed in an ice bath for 30 to 45 minutes. After cooling in the ice bath, 30 grams of soil from each of the 75 samples were collected using six, 5-gram En Core disposable volumetric sampling devices and one unpreserved 4 oz glass jar was filled with soil remaining from the sample. Soil samples were labeled, manifested, packed on ice for preservation, custody

sealed, and shipped to Test America laboratory in Denver, Colorado for analysis of % soil moisture, VOCs (Method 8260B) including BTEXN and PHC (Method 8015) (BEM, 2007). Both the pre-TEE and post-TEE soil sampling laboratory reports and BEM Quality Assurance/Quality Control (QA/QC) Compliance Reports are provided in appendices to the TEE Pilot Test Performance Evaluation Report (BEM, 2010).

1.6.2   Groundwater Sampling and Analyses

Baseline groundwater samples were collected from 9 November 2006 through 27 November 2006. After removing NAPL from the surface of the water table in each well (to less than 1/8th of an inch thick) with disposable Teflon bailers, BEM purged the well by three well casing volumes and collected a groundwater sample using a submersible pneumatic pump. Groundwater samples were collected from 18 monitoring well screens completed at six locations (MWN01A, B, C through MWN06 A, B, C). The samples (plus QA/QC samples) were analyzed for volatile organic compounds (VOCs, EPA Method 8260B), petroleum hydrocarbons (PHCs, Modified EPA Method 8015), total organic carbon (TOC, EPA Method 9020), dissolved oxygen (field analysis), nitrate (EPA Method 353.2), ferrous iron (field analysis), sulfate (EPA Method 300.0), methane (Method RSK-175), sulfide (field analysis), and alkalinity (field analysis). These analyses and tests supported baseline contaminant mass and distribution estimation, and baseline natural attenuation parameter conditions.

Groundwater samples were collected during pre- and post-TEE mass transfer testing to assess mass transfer conditions. The samples were collected from injection wells, extraction wells, and treatment cell monitoring wells. The samples were analyzed for PHCs and speciation for BTEX with a calibrated on-site GC. A small number of samples were sent to an off-site laboratory for analysis by EPA Method 8015 modified for TPH and BTEX. Groundwater grab samples were collected weekly from each of the 18 TEE pilot test system monitoring wells (MWN01A, B, C through MWN06A, B, C) and analyzed on-site using the field GC for PHCs and BTEXN for a period of approximately five months.

Post-test groundwater samples were collected monthly for a three-month period from November 2009 through January 2010. After removing NAPL from the surface of the water table in each well (to less than 1/8th of an inch thick) with disposable Teflon bailers, BEM collected samples using a submersible pneumatic pump. BEM purged wells to be sampled at a discharge rate between 0.25 and 1.5 gpm until water chemistry parameters stabilized to within 10 % or three well casing volumes of groundwater were removed, whichever occurred first, before collecting samples for laboratory analysis. BEM performed field analyses for ferrous iron, sulfide and alkalinity. Groundwater samples were labeled, manifested, packed on ice for preservation, custody sealed, shipped to Test America laboratory in Denver, Colorado and analyzed for VOC (Method 8260B), PHC (Method 8015B), methane (Method RSK-175), TOC (Method 9020), Nitrate (Method 353.2), and Sulfate (Method 300.0) (BEM, 2007).

Table D-12. Total Number and Types of Samples Collected.

Component	Matrix	Number of Samples	Analyte(s)	Location
Baseline sampling	Soil	75	BTEXN, TPH	Five monitoring wells (15 per boring)
	Groundwater: Laboratory measurement	18	BTEXN, TPH	Six, triple-nested TEE monitoring wells
	NAPL	6	BTEXN, TPH	Monitoring wells with floating NAPL
Technology performance sampling: LSZ Pre-TEE Mass Transfer Test	Groundwater: Field measurement	Weekly grab samples for one month	BTEXN, TPH	Twelve B- and C-horizon monitoring wells
	Bromide in groundwater	Logged at 5 minute interval	Bromide ion by Smart Sensor	Six, double-nested TEE monitoring wells
	Passive Flux Meter	18	Benzene, TPH, alcohol depletion	Six B-horizon monitoring wells
Technology performance sampling: UWBZ Pre-TEE Mass Transfer Test	Groundwater: Field measurement	Weekly grab samples for one month	BTEXN and TPH	Six A-horizon monitoring wells
	Bromide in groundwater	Logged at 5 minute interval	Bromide ion by Smart Sensor	Four A-horizon monitoring wells
	Passive Flux Meter	18	Benzene, TPH, alcohol depletion	Six A-horizon monitoring wells
Technology performance sampling: LSZ **Post-TEE** Mass Transfer Test	Groundwater: Laboratory measurement	12	BTEXN and TPH	Twelve B- and C-horizon monitoring wells
	Groundwater: Field measurement	Weekly grab samples for 5 months	BTEXN and TPH	Twelve B- and C-horizon monitoring wells
	Bromide in groundwater	Logged at 5 minute interval	Bromide by submerged	Six TEE monitoring wells
	Passive Flux Meter	15	Benzene, TPH, alcohol depletion	Five B-horizon monitoring wells
Technology performance sampling: UWBZ **Post-TEE** Mass Transfer Test	Groundwater: Laboratory measurement	6	BTEXN and TPH	Six TEE monitoring wells in the A-horizon
	Groundwater: Field measurement	Weekly grab samples for 5 months	BTEXN and TPH	Six A-horizon monitoring wells
	Passive Flux Meter	18	Benzene, TPH, alcohol depletion	Six A-horizon monitoring wells
Post-treatment sampling	Soil	75	BTEXN, TPH	Adjacent to monitoring wells (15 per boring)
	Groundwater: Laboratory measurement	36	BTEXN, TPH	Six TEE monitoring wells in the A-horizon
	NAPL	7	BTEXN, TPH	Monitoring wells with floating NAPL

Table D-13. Analytical Methods for Sample Analysis.

Matrix	Analyte	Method	Container	Preservative	Holding Time
Soil	TPH	8015M	4-oz glass jar	Cooled/Frozen	14 days
	BTEXN	8260C	40-mL VOA vials	Methanol	14 days
Groundwater	TPH	8015M	1-L amber glass bottles	HCl	14 days
	BTEXN	8260C	40-mL VOA vials	HCl	14 days
NAPL	TPH	8015M	40-mL VOA vials	Cooled	7 days
	BTEXN	8260C	40-mL VOA vials	Cooled	7 days

1.6.3 NAPL Sampling and Analyses

A disposable Teflon bailer was used to collect the NAPL samples. The NAPL samples were analyzed for VOCs including benzene, ethylbenzene, toluene, xylenes and naphthalene (BTEXN) (Method 8260B) and Petroleum Hydrocarbons (PHC) (Method 8015). Collection of pre-TEE NAPL samples from two wells within the treatment cell (LSZ05 and UWBZ02). Post-TEE, seven NAPL samples were collected from LSZ and UWBZ monitoring wells located within and surrounding the treatment cell and analyzed. The NAPL samples were collected on 22 December 2009 with disposable Teflon bailers. NAPL samples were labeled, manifested, packed on ice for preservation, custody sealed, shipped to Friedman & Bruya Laboratory in Seattle, Washington and six samples were analyzed for VOCs using EPA Method 8260C.

1.6.4 Bromide Tracer Sampling and Analyses

During the tracer tests, bromide concentrations in monitoring wells were measured and logged with calibrated AquiStar Temphion submersible Smart pH/ISE/Redox Sensors™. The sensors contain hard memory and recorded the bromide concentration and water temperature every five minutes in stand-alone mode. The data were downloaded onto a portable computer.

1.6.5 Passive Flux Meter Sampling and Analyses

On September 18, 2008 eighteen (18) passive flux meters (PFMs) were deployed in six UWBZ wells. Three PFMs were deployed in each well and all PFMs were constructed in 5-foot lengths. In three wells (MWN-01A, MWN-03A, MWN-06A) the PFMs were deployed with 5-foot spacing between (i.e. there was one 5-foot PFM at the base of the well screen, 5-feet of open screen, another 5-foot PFM, 5-feet of open screen, and a final 5-foot PFM at the top of screen). In the three remaining wells (MWN-02A, MWN-04A, MWN-05A) three connected PFMs were deployed (for 15 feet of continuous PFM) at the base of the well screen. On September 22, 2008 all 18 PFMs were successfully retrieved and sampled (corresponding to a deployment length of 4 days). On September 23, 2008, a PFM was inserted and immediately retrieved and sampled in each of the UWBZ wells. These "swipe tests" were taken in order to provide a background comparison to consider the effect of passing the PFM through free product at the water table. The sorbent material in each PFM was composited and subsampled by placing a known weight

of the sorbent in a measured volume of methanol. The methanol extracts were shipped to a laboratory at the University of Florida and analyzed for benzene, TPH, and resident alcohols. On October 23, 2008 eighteen (18) PFMs were deployed in the six LSZ B-horizon monitoring wells. In all six wells, three connected PFMs were deployed (for 15 feet of continuous PFMs) covering the entire 15-foot length of well screen. These wells were screened from about 205 ft bgs to 220 ft bgs. PFMs were not deployed in deeper C wells, generally screened from 230 to 245 ft bgs that intersect more permeable strata of the LSZ. On October 27, 2008 all 18 PFMs were successfully retrieved and then sampled and analyzed as described above.

The post-TEE deployment was initiated on November 12, 2009 when twenty one (21) PFMs were deployed in seven of the wells at the TEE Treatment Cell. An additional 15 PFMs were deployed the next day for a total of 36 PFMs in the UWBZ and LSZ wells. The locations of the PFMs in the wells were identical to those in the pre-TEE deployment conducted in 2008. On November 16, 2009 PFMs from six of the seven wells deployed four days earlier were successfully retrieved and sampled. The methanol extracts were shipped to a laboratory at the University of Florida and analyzed for benzene, TPH, and resident alcohols. Three PFMs, located in well 5B, were lodged in the well and could not be removed following application of several removal techniques. These PFMs were abandoned in the well after unsuccessful attempts to retrieve using heavier equipment. Also on this day, 4 of the 6 swipe tests were conducted in the UWBZ wells. These tests were conducted shortly after PFM retrieval (approximately 3 hours). On November 17, 2009 the PFMs from the remaining 5 wells were successfully retrieved and sampled. The remaining swipe tests were conducted following removal of the PFMs.

1.6.6   Calibration of Analytical Equipment

Analytical instruments were calibrated in accordance with the analytical methods. Field equipment such as the bromide sensors were calibrated according to the manufacturer's specifications. All analytes reported were present in the initial and continuing calibrations, and these calibrations met the acceptance criteria specified in the TEE Pilot Test Work Plan (BEM, 2007). All results reported were within the calibration range. Results outside the calibration range were deemed unsuitable for quantitative work and only gave an estimate of the true concentration. Records of standard preparation and instrument calibration were maintained. Records unambiguously traced the preparation of standards and their use in calibration and quantitation of sample results. Calibration standards were traceable to standard materials.

Instrument calibration was checked using all of the analytes listed in the QC acceptance criteria table in Appendix G7 of the TEE Pilot Test Work Plan for the method. All calibration criteria satisfied SW-846 requirements at a minimum. The initial calibration was checked at the frequency specified in the method using materials prepared independently of the calibration standards. Multipoint calibrations contained the minimum number of calibration points specified in the method with all points used for the calibration being contiguous. If more than the minimum number of standards were analyzed for the initial calibration, all of the standards analyzed were included in the initial calibration. The only exception to this rule was a standard that has been statistically determined as being an outlier can be dropped from the calibration, providing the requirement for the minimum number of standards is met. Acceptance criteria for the calibration check are presented in Appendix G7 of the TEE Pilot Test Work Plan. Analyte

concentrations were determined with either calibration curves or response factors (RFs). For GC and gas chromatography/mass spectroscopy (GC/MS) methods, when using RFs to determine analyte concentrations, the average RF from the initial five-point calibration was used. The continuing calibration was not used to update the RFs from the initial five-point calibration. In addition, the concentration used for the calibration verification sample was at or below the middle of the calibration curve. Finally, the lowest standard used was at or below the reporting limit (RL) for each analyte in the method.

1.6.7   *Quality Assurance Sampling*

Quality assurance samples for laboratory analyses included one duplicate, one equipment blank, and one matrix spike / MSD per twenty primary samples submitted to the commercial laboratory. QA samples for analyses with the field GC included one duplicate and one equipment blank per twenty primary samples analyzed with the field GC. All laboratory reports and accompanying BEM Quality Assurance/Quality Control (QA/QC) Compliance Reports are provided in appendices to the TEE Pilot Test Performance Evaluation Report (BEM, 2010).

1.6.8   *Decontamination Procedures*

Decontamination procedures are described in detail in the Standard Operating Procedure for Personnel and Equipment Decontamination, Attachment G1-1 to Appendix G of the TEE Pilot Test Work Plan (BEM, 2007).

1.6.9   *Sample Documentation*

Documentation procedures are described in detail in Appendix G of the TEE Pilot Test Work Plan (BEM, 2007) and include sample labels, chain of custody forms, field logbooks, and laboratory records.

1.7   SAMPLING RESULTS

This section provides the primary sampling data from the forced flow mass transfer tests performed in the LSZ and UWBZ of the TEE cell both before and after the TEE Pilot Study. Results from the tracer tests are first discussed, followed by the concentration data, and then the PFM data. The discussion of sampling results includes simple analyses and comparison of data for consistency and to provide context for the modeling presented in Section 6 of the main report.

1.7.1   *Tracer Test Data*

Tracer tests were performed in the UWBZ and LSZ during water injection for the IPT before the performance of the TEE pilot test at ST012 to identify preferential flow paths and quantify soil heterogeneities in the NAPL source zone. The well configurations in the LSZ and UWBZ are provided in Figure D-1 and Figure D-2, respectively. The tracer test was repeated in the LSZ after the TEE pilot test.

The tracer test in each zone was initiated after approximately two weeks of groundwater extraction in the ring of extraction wells. Potassium bromide was mixed with water and metered into water injected through the central injection wells. One day of clean water injection preceded the steady introduction of the bromide tracer (~2,000 mg/L) over a four-hour period in the Pre-TEE testing. Bromide sensors were placed in monitoring well screens in each zone during the tracer test and recorded the bromide concentration at discrete depths within the screen interval every 5 to 10 minutes for approximately two weeks.

A significant issue during the Pre-TEE tracer test was oxidation of the protective film on the windows of the downhole bromide sensors. Over time, the protective film was compromised and resulted in erroneous bromide readings. Complete failure resulted in abrupt spikes to unrealistically high bromide readings. The error increased over time until complete failure was evident as observed in the data described later. A second potential source of error was the placement of bromide sensors at discrete depths along the well screens and the possibility of incomplete mixing of the bromide within the well screen volume such that the bromide readings may not have been representative of the full screen interval. In the UWBZ, readings from all but one screen were deemed unusable or not representative of the screen. The manufacturer of the bromide sensors was contacted and the result was modifications to the sensors to make them compatible with elevated concentrations of aromatic compounds. The modified sensors were used without degradation of the readings in a post-TEE tracer test in the LSZ.

1.7.1.1   *LSZ Tracer Tests*

Tracer tests were performed in the UWBZ and LSZ during water injection for the IPT before the performance of the TEE pilot test at ST012 to identify preferential flow paths and quantify soil heterogeneities in the NAPL source zone. The well configurations in the LSZ and UWBZ are provided in Figure D-1 and Figure D-2, respectively. The tracer test was repeated in the LSZ after the TEE pilot test. The tracer test in each zone was initiated after approximately two weeks of groundwater extraction in the ring of extraction wells. Potassium bromide was mixed with water and metered into water injected through the central injection wells. One day of clean water injection preceded the steady introduction of the bromide tracer (~2,000 mg/L) over a four-hour period in the Pre-TEE testing. Bromide sensors were placed in monitoring well screens in each zone during the tracer test and recorded the bromide concentration at discrete depths within the screen interval every 5 to 10 minutes for approximately two weeks.

Table D-14. Well Locations in the LSZ.

Well	X-location (feet)	Y-location (feet)	Radius from Injection (feet)
LSZ-01	46.7	-32.2	56.7
LSZ-02	62.1	36.0	71.7
LSZ-03	1.4	72.1	72.1
LSZ-04	-58.2	43.0	72.3
LSZ-05	-69.0	-21.4	72.3
LSZ-06	-28.9	-61.8	68.2
LSZ-07	0.00	0.00	0.50
MWN-01B	-48.0	5.5	48.3
MWN-02B	-12.7	24.6	27.7
MWN-03B	-8.6	59.2	59.8
MWN-04B	33.7	26.5	42.9
MWN-05B	-45.3	-29.4	54.0
MWN-06B	17.3	-5.7	18.2
MWN-01C	-47.3	13.0	49.0
MWN-02C	-17.0	18.5	25.1
MWN-03C	-2.2	57.4	57.4
MWN-04C	35.3	19.2	40.2
MWN-05C	-48.3	-23.4	53.6
MWN-06C	14.5	-11.0	18.2

Note: X- and Y- coordinates are relative to the injection well location

The LSZ test conditions both before and after the TEE Pilot Test are summarized in Table D-15. Flow conditions were similar in the two tests; however, the post-TEE total extraction rate was about 40% higher than the pre-TEE rate. Also, the duration of the tracer pulse was only 23.5 minutes in the post-TEE test versus the four-hour pulse in the pre-TEE test.

Table D-15. Tracer Test Bromide Injections in the LSZ.

Parameter	Pre-TEE	Post-TEE
Water Injection Start	8/26/2008 9:46	-
Water Injection Rate	35 gpm	39 gpm
Bromide Injection Start	8/27/2008 10:57	10/20/2009 15:19:00
Bromide Injection Stop	8/27/2008 14:56	10/20/2009 15:42:30
Bromide Concentration	1951 ppm	2113 ppm
Total Extraction Rate	58.2 gpm	81.1 gpm

Note: gpm = gallons per minute

The measured bromide concentration histories in the C-horizon and the B-horizon of the LSZ during the pre-TEE tracer testing are plotted in Figure D-16 and Figure D-17, respectively. A nearly undispersed peak appeared after three hours at MWN06-C located at a radius of 18 feet southeast of the injection well and persisted for about 4 hours, equal to the time of bromide injection. A second peak was detected in this well after 12 hours of bromide injection. The tracer next appeared in the C-horizon at MWN04-C located 40 feet from the injection well and then MWN02-C located at 25 feet. In the B-horizon, the first tracer detection was in MWN02-B after only eight hours of injection and a second peak appeared after 61 hours. The bromide arrived at

MWN06-B after 19 hours. The sensor failed completely in MWN04-B. The bromide reading from the sensor in MWN01-B was indeterminate between an actual response and oxidation of the protective film. The bromide arrival in the overlying B-horizon at MWN06 was slow indicating this interval was less permeable than the deeper C-horizon. However, the opposite trend was observed in MWN02 located to the northwest of the injection well.

The measured bromide concentration histories in the C-horizon and the B-horizon of the LSZ during the post-TEE tracer testing are plotted in Figure D-18 and Figure D-19, respectively. The first peak appeared in the C-horizon after 4.6 hours at MWN06-C located closest to the injection well. A second peak appeared after 10 hours similar to the Pre-TEE tracer test. As in the Pre-TEE test, the tracer next appeared in the C-horizon at MWN04-C located 40 feet from the injection well and then MWN02-C located at 25 feet. In the B-horizon, the first tracer detection was in MWN02-B after twelve hours of injection; a second peak was not detected but this was likely the result of the short pulse. The bromide arrived at MWN06-B much later than in the Pre-TEE test.

The approximate arrival times of the peaks through each LSZ well location are summarized in Table D-16.

Table D-16. Tracer Peak Arrival Times in the LSZ Monitoring Wells.

Well	Radius from Injection (feet)	Pre-TEE Detection of Peaks (elapsed hours)	Post-TEE Detection of Peaks (elapsed hours)
MWN-01B	48.3	nm	nm
MWN-02B	27.7	8.2, 61.0	12.1
MWN-03B	59.8	nm	nm
MWN-04B	42.9	sensor failure	nm
MWN-05B	54.0	nm	nm
MWN-06B	18.2	19.0	~85
MWN-01C	49.0	nm	95.5
MWN-02C	25.1	72.7	81.8
MWN-03C	57.4	nm	nm
MWN-04C	40.2	50.6	43.3
MWN-05C	53.6	nm	nm
MWN-06C	18.2	3.16, 12.2	4.6, 9.7

Notes:

gpm = gallons per minute
nm = not measured
X- and Y- coordinates are relative to the injection well location
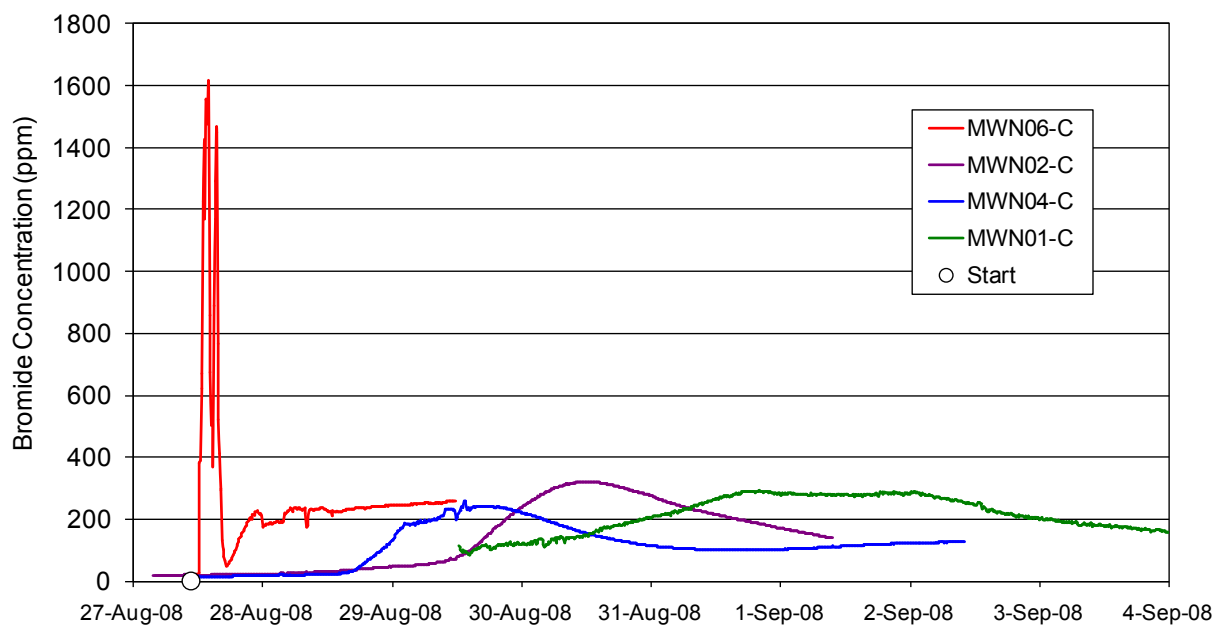
Figure D-16. Pre-TEE Bromide Tracer Response in the C-Horizon of the LSZ.
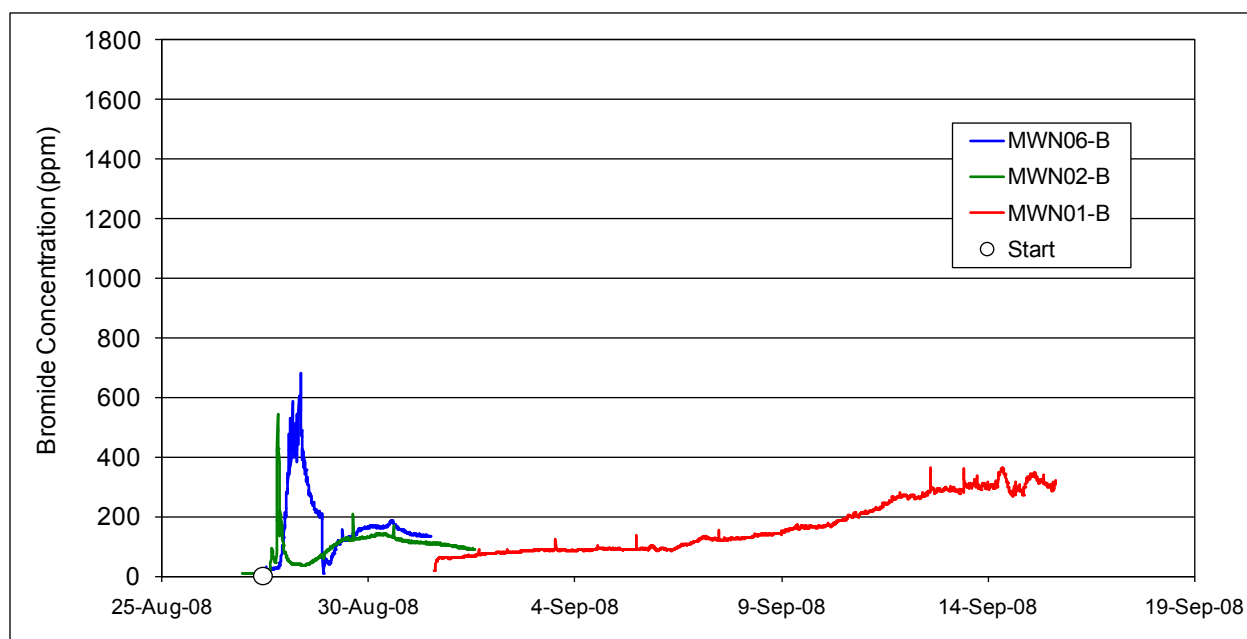
Figure D-17. Pre-TEE Bromide Tracer Response in the B-Horizon of the LSZ.
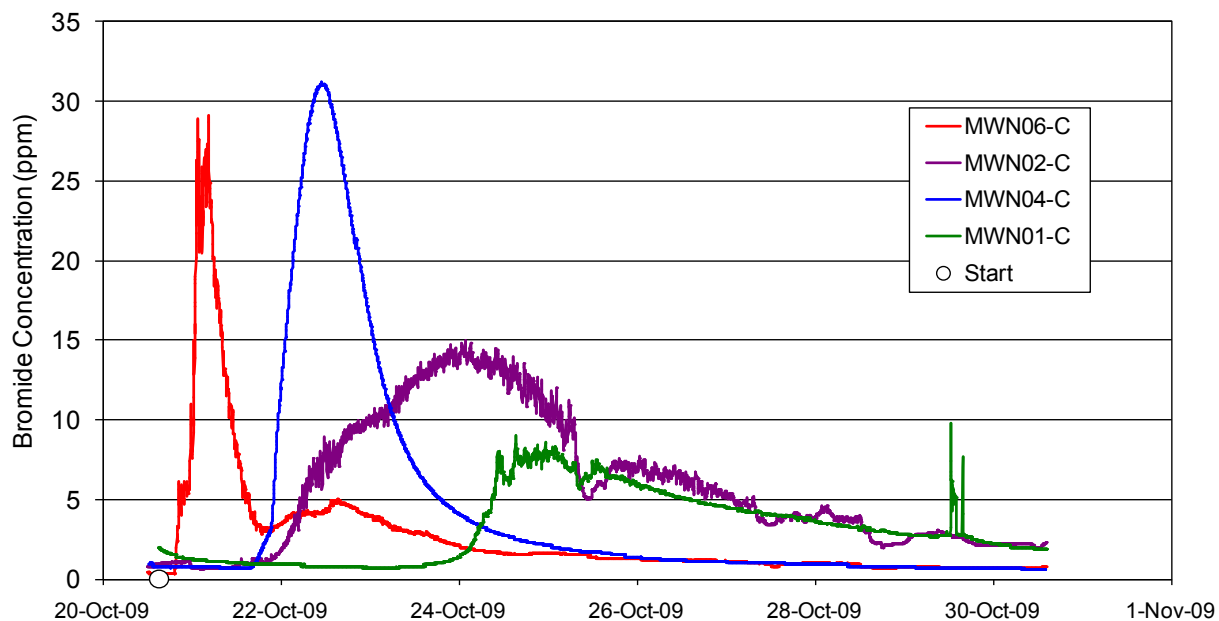
Figure D-18. Post-TEE Bromide Tracer Response in the C-Horizon of the LSZ.
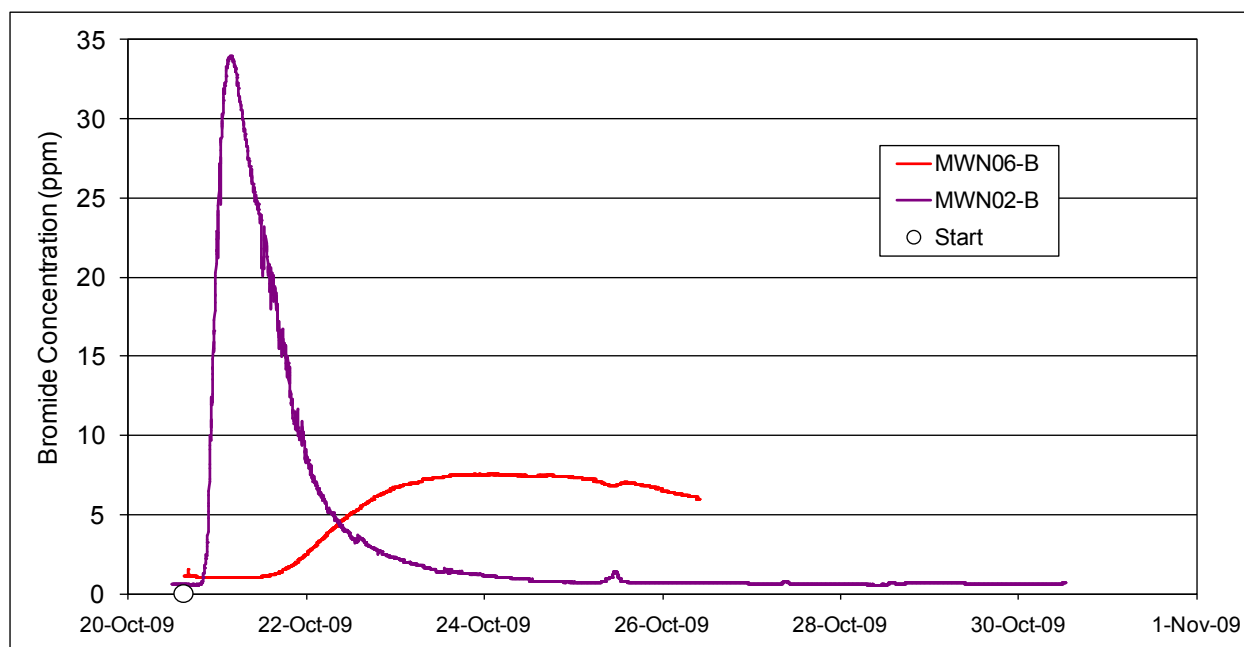
Figure D-19. Post-TEE Bromide Tracer Response in the B-Horizon of the LSZ.

A summary of the bromide responses from the LSZ testing is illustrated in Figure D-20 where the bromide peak arrival time is plotted as a function of radius from the injection well. The arrival time is relative to the start of the bromide injection pulse. This figure also includes two theoretical bounding plots. The first is the arrival time assuming uniform radial, isotropic flow through the entire aquifer depth interval. The second curve assumes flow is uniformly radial but through only 25% of the aquifer depth interval. These bounds illustrate the layered heterogeneity in the LSZ as most points fall closer to the 25% plot indicating flow through a small fraction of the aquifer. Also, the data for MWN02-C (25 feet) are above the isotropic curve suggesting asymmetric flow away from this location while MWN02-B (28 feet) is below the 25% flow assumption indicating a strong preference for flow to the northwest in the B-horizon. The opposite trend is evident in the data from MWN06 (18 feet) located to the southeast of the injection well. The only location with a significant change between the pre- and post-testing is MWN06-B. The response in the post-Tee tracer test was much slower than in the pre-TEE test suggesting the B-horizon in this direction became less permeable during the TEE pilot test.

Figure D-20. Tracer Peak Arrival Time as a Function of Radius from the Injection Well.

1.7.1.2   *Tracer Test Interpretation in the LSZ*

Simple data interpretation was achieved by fitting a finite difference solution of equations describing tracer movement to measured bromide concentration histories in the monitoring wells. The flow model assumed symmetric radial flow through a confined soil stratum of uniform thickness and uniform permeability. The mathematical problem describing the tracer model under these assumptions is (Tang & Peaceman, 1987):

$$\frac{Q}{2\pi Hr}\left[\alpha_r\frac{\partial^2 C}{\partial r^2}-\frac{\partial C}{\partial r}\right]=\frac{\partial C}{\partial t}$$

subject to boundary and initial conditions:

$$C-\alpha_r\frac{\partial C}{\partial r}=C_{inj}(t)\qquad \text{at } r=r_w$$

$$C=0\qquad\qquad\text{for r approaching infinity}$$

$$C=0\qquad\qquad\text{for t=0}$$

The injection concentration, C_{inj}, is zero for times when bromide is not injected and a steady value during the pulsed injection period. The governing equation has only four parameters: the known radius of the injection well r_w, the measured injection concentration, the measured injection rate Q divided by the aquifer thickness H, and the radial dispersion coefficient α_r. The thickness and number of soil layers in the aquifer transmitting the tracer are not generally known and flow is not generally isotropic (i.e., perfectly radial). Hence, the two parameters varied to match the field data in subsequent data interpretation are Q/H and the radial dispersion coefficient. Q/H is equivalent to a local velocity at radius r when divided by $2\pi r$ and the aquifer porosity. The above mathematical problem was solved and validated using the technique of Tang and Peaceman (1987). The A-, B-, and C-horizons were allowed to have multiple soil strata along the screen interval by assuming each stratum acted independently and by assuming the measured concentration was equal to a well-mixed concentration in the monitoring well screen. The modeling was initiated by identifying one or more peaks (representing one or more soil intervals) in the concentration history at a monitoring well. For each peak, the arrival time of the maximum concentration at the known radius defined the volumetric flux, i.e., the volumetric flow rate divided by the soil stratum thickness, Q/H. The shape of the peak was governed by the radial dispersion coefficient as described above. Mass balances on the injected water and injected bromide provided constraints for the resulting strata concentrations. For example, consider the appearance of N peaks in a monitoring well spanning the full injection interval for steady injection rate Q_{inj}:

$$C_{well}(t)=\frac{\sum_{i=1}^{N}Q_iC_i(t)}{\sum_{i=1}^{N}Q_i}=\frac{1}{Q_{inj}}\sum_{i=1}^{N}Q_iC_i(t)$$

In addition, for a known injection rate and known values of the volumetric fluxes for each stratum, a best-fit solution is found by iterating among flow rates for each soil stratum assuming the total flow among the strata equals the injection rate. The iteration is a two-parameter fit as the dispersion within each stratum is a function of its flow rate and dispersion coefficient such that the dispersion coefficient must also be varied to match the shape of the concentration histories. Finally, for steady flow and a constant tracer injection concentration, the finite difference solution for each soil interval must satisfy:

$$C_{inj}\Delta t_{inj}=\int_{t=0}^{\infty}C_i(t)dt$$

In this approach to interpretation, possible asymmetry in radial flow was ignored and the calculated interval thickness was a maximum because the total injected flow was assumed to move through the screen intervals. Hence, the thickness of each flow interval determined from the modeling is likely an overestimate and the degree of heterogeneity underestimated.

The mathematical model described above was used to fit parameters to match the bromide responses at the monitoring wells. The two parameters were Q/H (i.e., the velocity) and the radial dispersion coefficient. For MWN06-C at a radius of 18 feet, the results for the pre- and post-TEE tracer tests are plotted in Figure D-21 and Figure D-22. The fits for MWN06-B are provided in Figure D-23 and Figure D-24. The plots for MWN02-C at 25 feet are provided in Figure D-25 and Figure D-26, and the results for MWN02-B at 28 feet are provided in Figure D-27 and Figure D-28. The plots for MWN04-C at a radius of 40 feet are provided in Figure D-29 and Figure D-30. The pre-TEE bromide response in MWN04-B is shown in Figure D-31 and the post-TEE response in MWN01-C is plotted in Figure D-32.

The results of the parameter fitting are listed in Table D-17. The parameters Q/H and the dispersivity were varies under a best fit was achieved with the field data. Q/H is bounded by the injection rate and the thickness of the LSZ. For the B and C horizon profiles together, the total flow was assumed to be symmetric and equal to the injection rate, i.e., the total flow through all the layers equaled the injection rate. With this constraint and the fit for Q/H, the thickness of each flow layer could be estimated. Assuming uniform symmetric flow with an injection rate of 35 gpm and an LSZ thickness of 38 feet, the uniform flow Q/H is 0.92 gpm/ft.

The estimated thickness of each flow layer is given Table D-17 under the heading "H". The total thickness of these flow layers at each monitoring well divided by the total thickness of the LSZ yields the estimated percentage of the LSZ in which significant flow occurs. For MWN06, flow occurred through about 20% of the LSZ before the TEE pilot test and increased to 79% after the test. However, conditions before the pilot test included a very narrow interval (0.65 feet) in the C-horizon that transmitted two-thirds of the injected water. This interval was not evident in the post-TEE results. In addition, flow through the B-horizon slowed as the estimated thickness of the flow interval increased by a factor of five. Opposite effects were observed in MWN02 where the percentage of the LSZ transmitting significant flow decreased from 65% to 47%. Post-TEE bromide response was not measured in MWN04-B; however, the bromide response in MWN04-C was little changed by the TEE pilot test. In the pre-TEE tracer test, location MWN04 yielded flow in only 30% of the LSZ profile. The estimated dispersion coefficients ranged from 0.1 to 4.5 feet but generally fell between 0.2 and 2.0 feet.
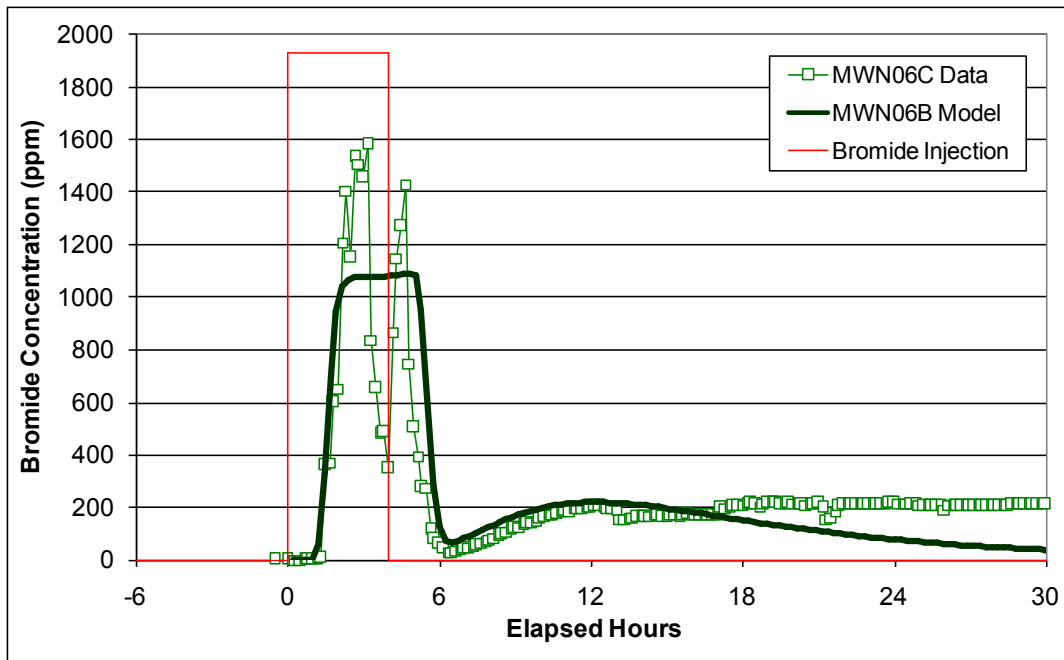
Figure D-21. Pre-TEE Bromide Tracer Response in the LSZ at MWN06C (Radius = 18.2 feet).
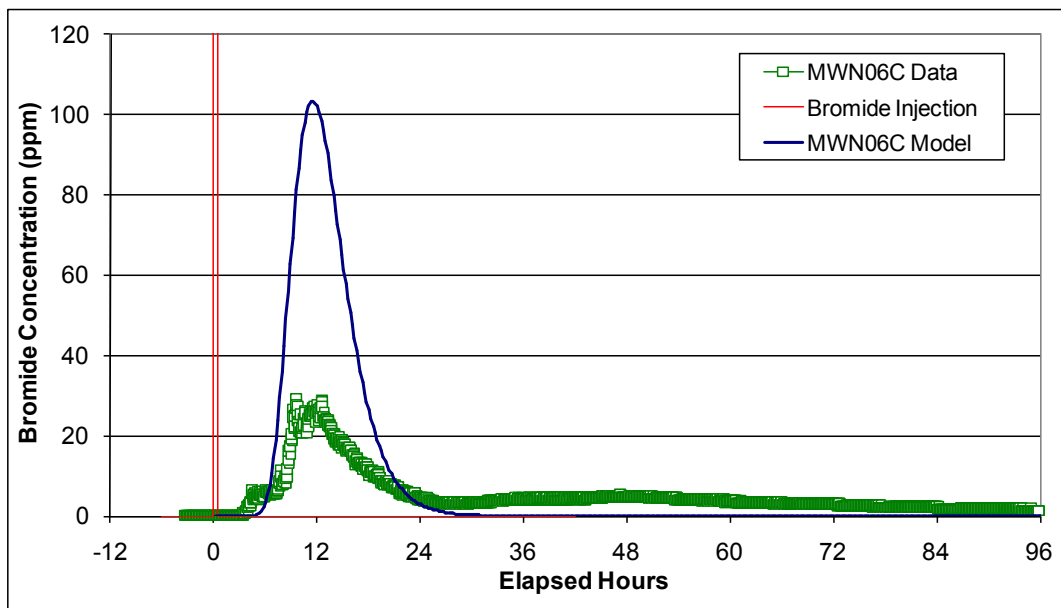
Figure D-22. Post-TEE Bromide Tracer Response in the LSZ at MWN06C (Radius = 18.2 feet).
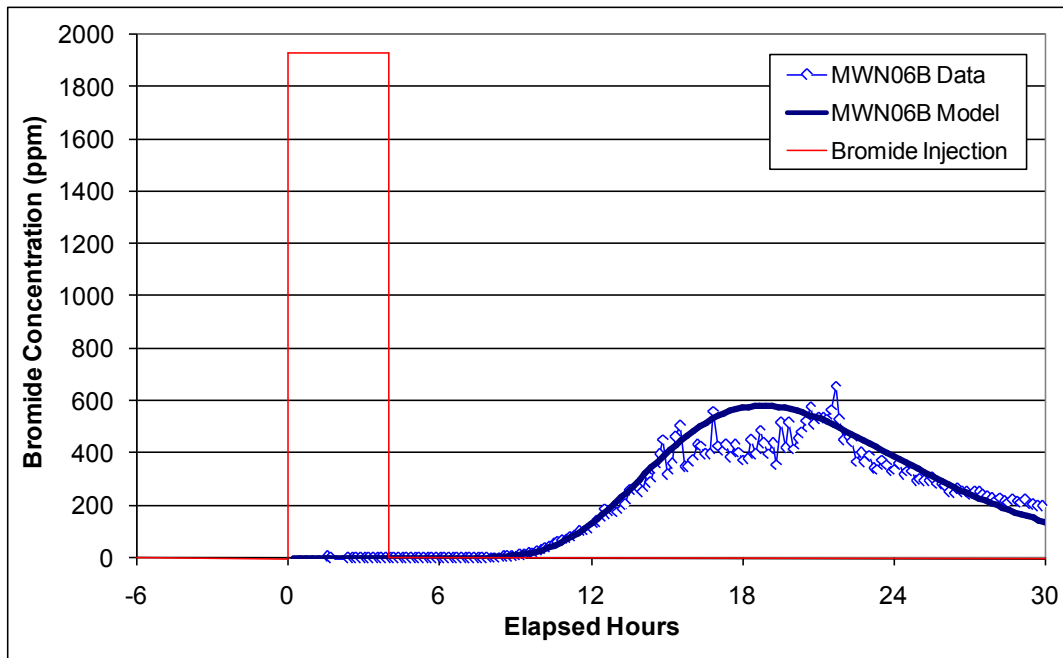
Figure D-23. Pre-TEE Bromide Tracer Response in the LSZ at MWN06B (Radius = 18.2 feet).
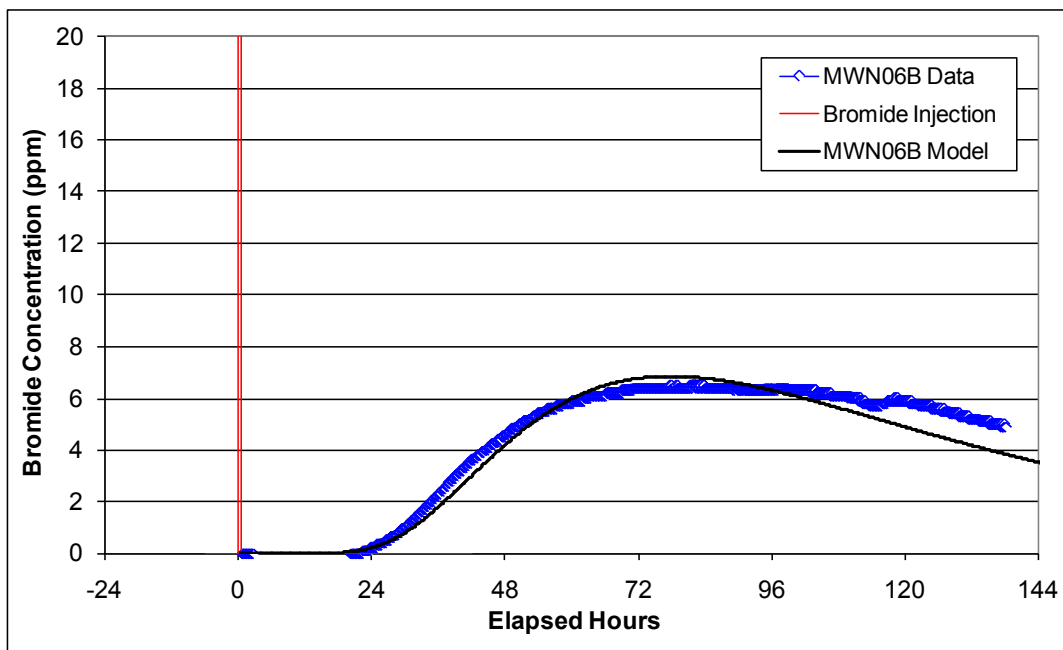
Figure D-24. Post-TEE Bromide Tracer Response in the LSZ at MWN06B (Radius = 18.2 feet).
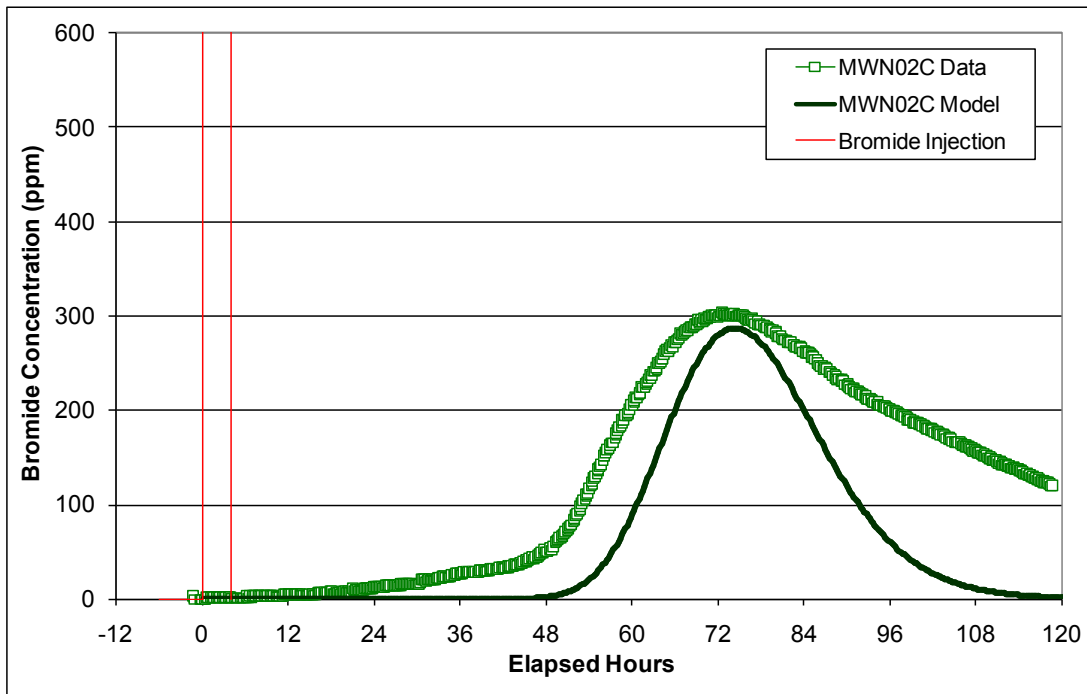
Figure D-25. Pre-TEE Bromide Tracer Response in the LSZ at MWN02C. (Radius = 25.1 feet).
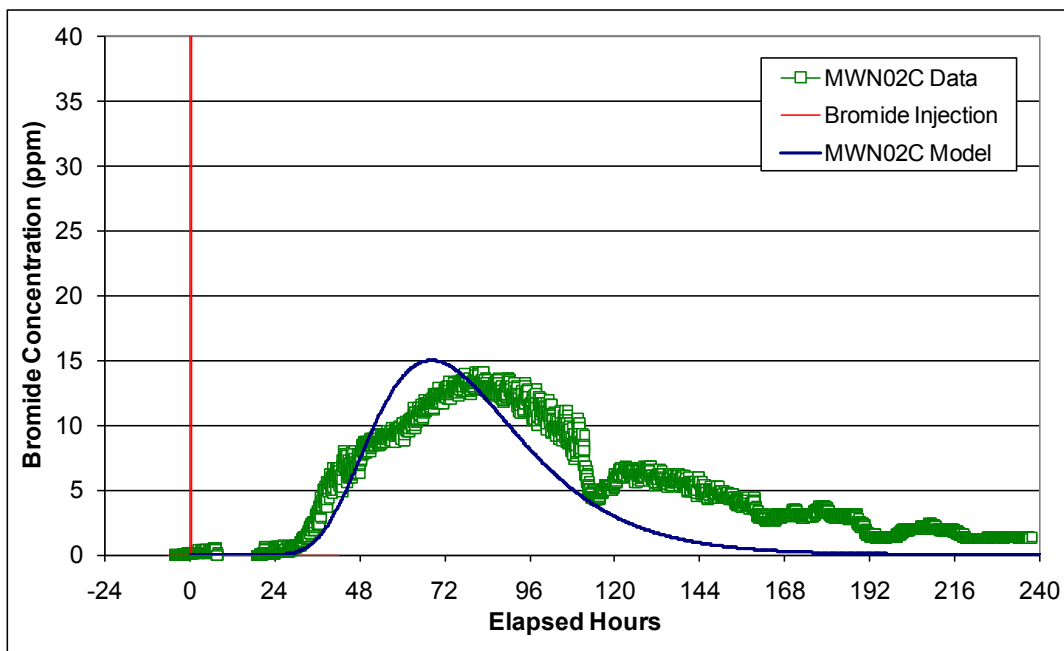
Figure D-26. Post-TEE Bromide Tracer Response in the LSZ at MWN02C (Radius = 25.1 feet).
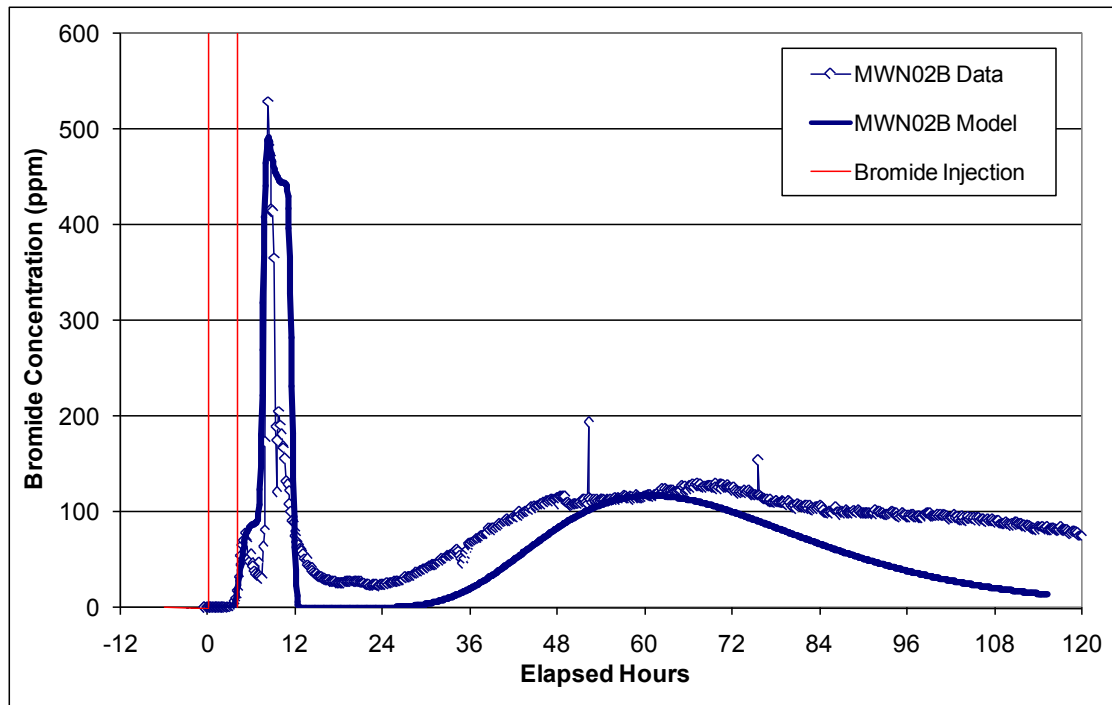
Figure D-27. Pre-TEE Bromide Tracer Response in the LSZ at MWN02B (Radius = 27.7 feet).
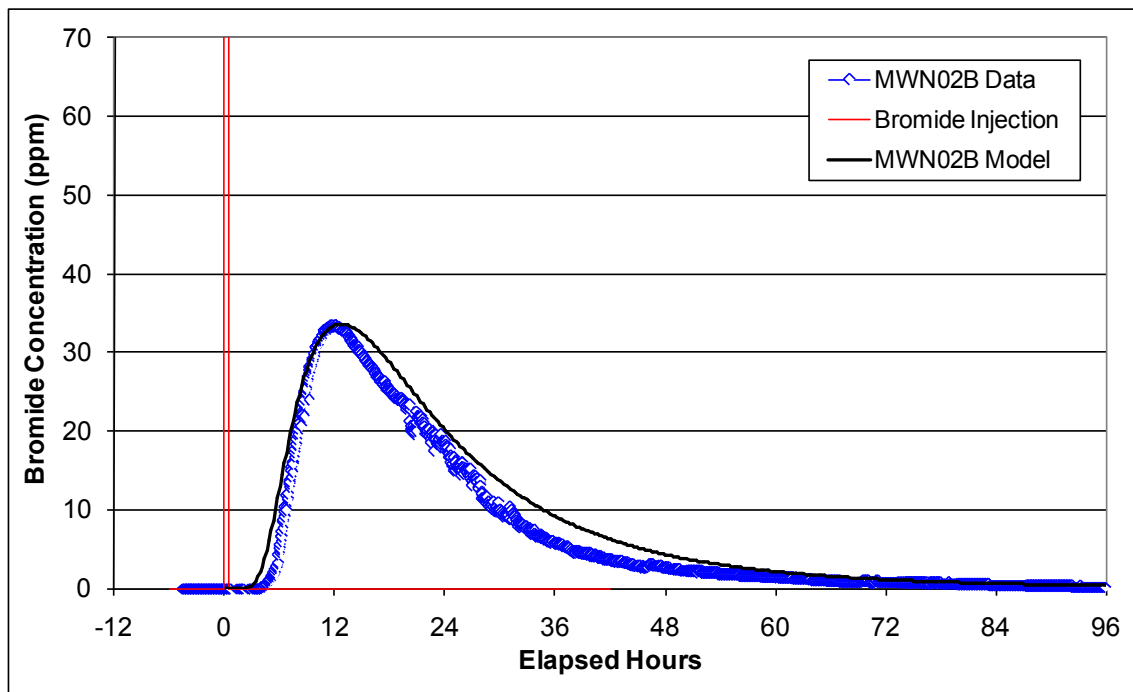
Figure D-28. Post-TEE Bromide Tracer Response in the LSZ at MWN02B (Radius = 27.7 feet).
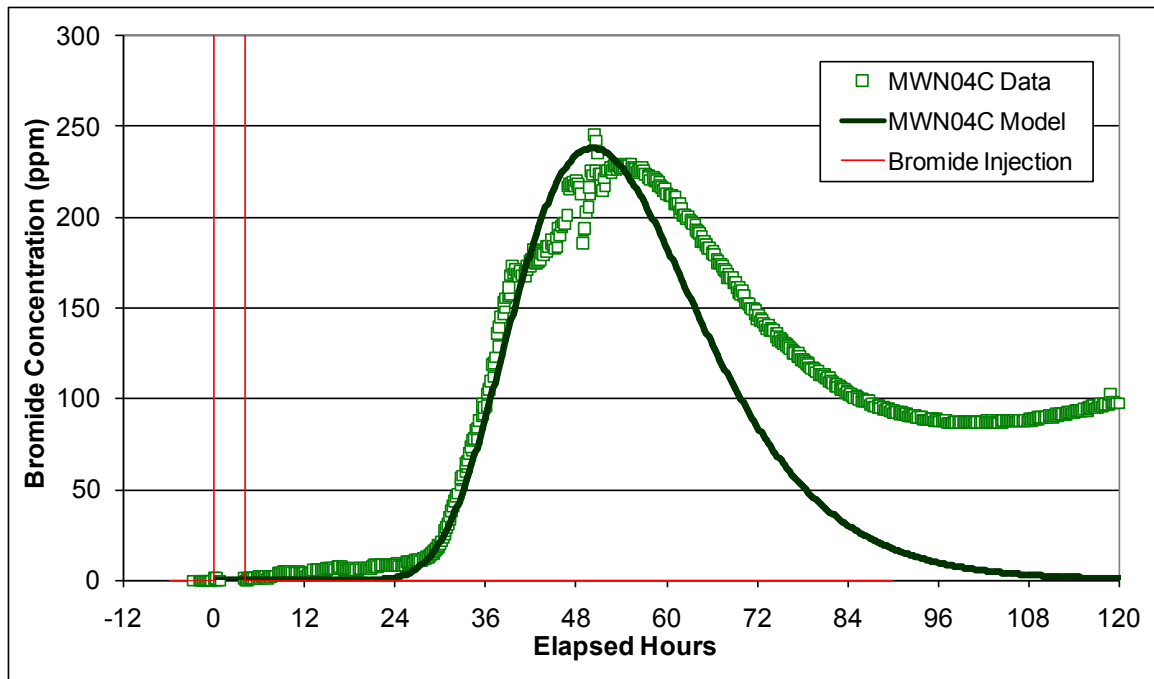
Figure D-29. Pre-TEE Tracer Tracer Response in the LSZ at MWN04C (Radius = 40.2 feet).
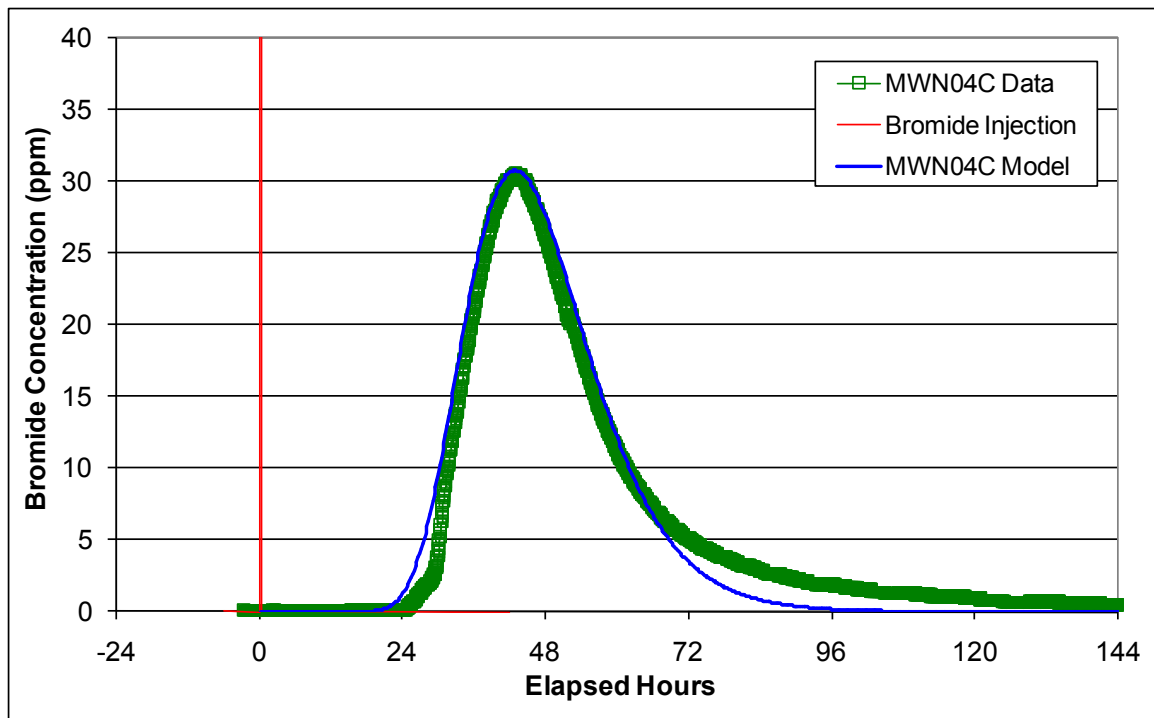
Figure D-30. Post-TEE Tracer Response in the LSZ at MWN04C (Radius = 40.2 feet).
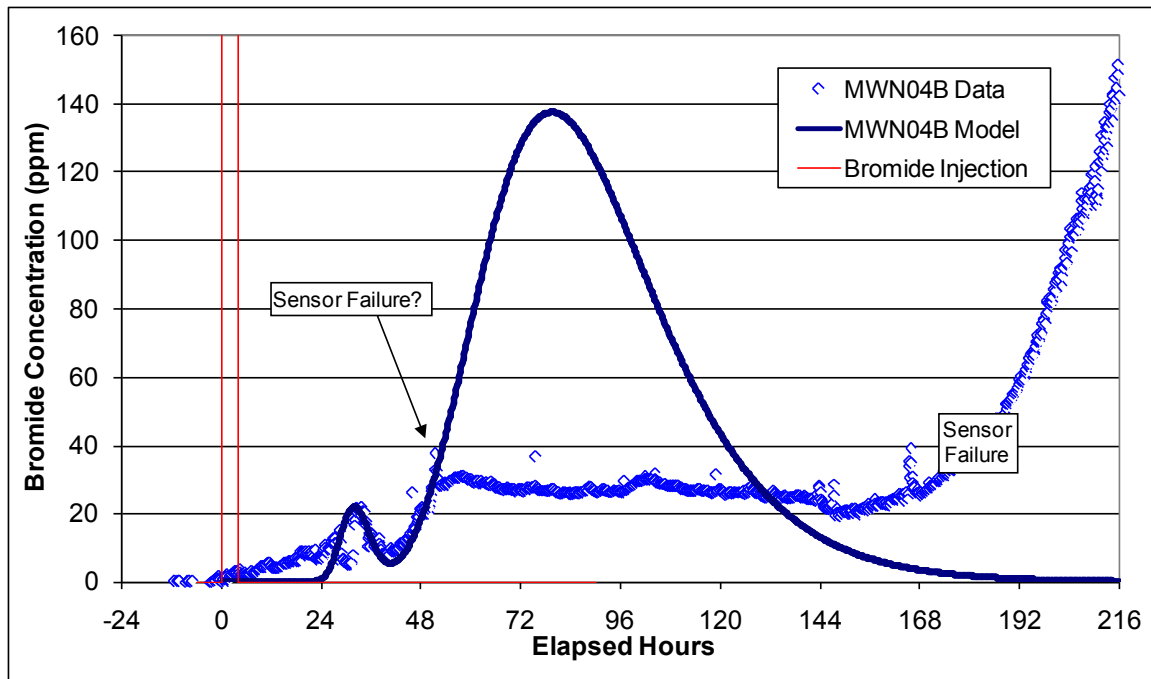
Figure D-31. Pre-TEE Tracer Response in the LSZ at MWN04B (Radius = 42.9 feet).
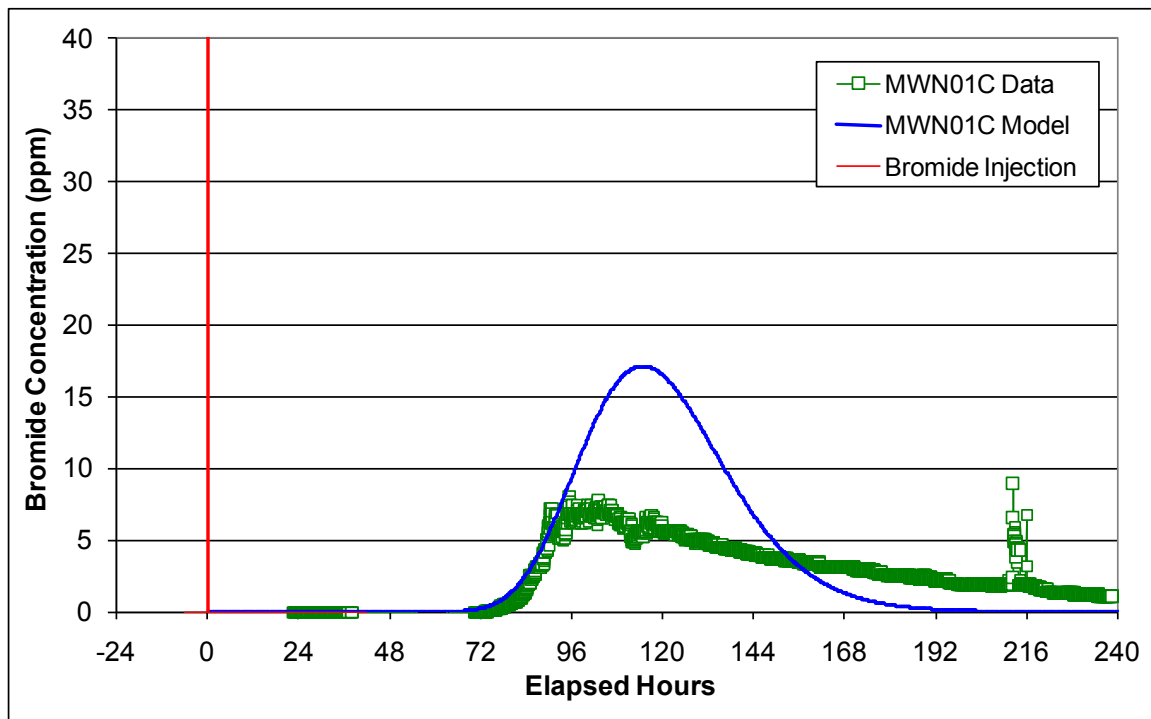
Figure D-32. Post-TEE Tracer Response in the LSZ at MWN01C (Radius = 49.0 feet).

Table D-17. Summary of LSZ Tracer Test Parameter Fitting.

	Q/H (gpm/ft)	Dispersion (ft)	Q (gpm)	H (ft)	Q/H (gpm/ft)	Dispersion (ft)	Q (gpm)	H (ft)	Q/H (gpm/ft)	Dispersion (ft)	Q (gpm)	H (ft)
	MWN06 (Pre-TEE)				**MWN02 (Pre-TEE)**				**MWN04 (Pre-TEE)**			
B-horizon	Radius = 18.2 feet				Radius = 27.7 feet				Radius = 42.9 feet			
Layer 1	2.14	0.6	6	2.8	20.00	0.2	1	0.05	2.60	1.2	19.5	7.5
Layer 2					15.15	0.1	5	0.33	7.14	0.2	0.5	0.07
Layer 3					1.40	1	16	11.43				
C-horizon	Radius = 18.2 ft				Radius = 25.1 ft				Radius = 40.2 ft			
Layer 1	3.00	2	13	4.33	1	0.2	13	13	3.75	0.9	15	4
Layer 2	24.6	0.2	16	0.65								
Total	4.50		35	7.78	1.41		35	24.81	3.03		35	11.57
Flow Layers				20%				65%				30%
	MWN06 (Post-TEE)				**MWN02 (Post-TEE)**				**MWN04 (Post-TEE)**			
B-horizon	Radius = 18.2 feet				Radius = 27.7 feet							
Layer 1	0.39	2	5.8	15	5.0	4.5	24	4.8		Not measured		
C-horizon	Radius = 18.2 ft				Radius = 25.1 ft				Radius = 40.2 ft			
Layer 1	0.80	2	4.9	6.13	1	0.9	13	13	4.21	0.9	24	5.7
Layer 2	3.2	1	28.3	8.84								
Total	1.30		39	30.0	2.08		37	17.8	4.21		24	5.7
Flow Layers				79%				47%				15%

NOTE:

For uniform, symmetric flow in the LSZ, Q/H would equal 35 gpm / (243 – 205 ft) = 0.92 gpm/ft.

1.7.1.3   UWBZ Tracer Test

The well configuration in the UWBZ is illustrated in Figure D-2. The flow configuration during the UWBZ tracer test is provided in Figure D-13 with the average flow rates listed in Table D-10. The well layout consisted of a central injection well (UWBZ07) surrounded by six extraction wells screened across the UWBZ (screened ~170-195 ft bgs) although no extraction was occurring in UWBZ02 and only a low rate was extracted from UWBZ01. The locations of the injection, extraction and monitoring wells in the UWBZ are listed in Table D-18, with all distances in feet relative to the location of the injection well, UWBZ07.

Table D-18. Well Locations in the UWBZ.

Well	X-location (feet)	Y-location (feet)	Radius from Injection (feet)
UWBZ-01	58.9	-40.0	71.2
UWBZ-02	58.1	40.2	70.6
UWBZ-03	0.1	72.9	72.9
UWBZ-04	-53.9	36.2	64.9
UWBZ-05	-63.9	-7.7	64.3
UWBZ-06	-15.0	-61.8	63.6
UWBZ-07	0.00	0.00	0.50
MWN-01A	-41.8	7.3	42.5
MWN-02A	-6.3	26.2	26.9
MWN-03A	-2.8	60.7	60.7
MWN-04A	40.1	28.1	49.0
MWN-05A	-39.5	-27.9	48.4
MWN-06A	23.7	-4.1	24.1

This section presents the tracer test results for the UWBZ during the pre-TEE testing. A tracer test was not performed during the post-TEE mass transfer test. The UWBZ tracer test conditions are summarized in Table D-19. The bromide pulse lasted four hours.

Table D-19. Pre-TEE Tracer Test Injection in the UWBZ.

Parameter	UWBZ
Water Injection Start	8/26/2008 9:46
Water Injection Rate	35 gpm
Bromide Injection Start	8/27/2008 10:57
Bromide Injection Stop	8/27/2008 14:56
Bromide Concentration	1951 ppm
Total Extraction Rate	33.5 gpm

At the start of the UWBZ tracer test, bromide sensors were placed in monitoring wells MWN06-A (24 feet) and MWN02-A (27 feet). The sensor in MWN06-A failed rapidly in the presence of high concentrations of dissolved aromatics. The measured bromide concentration in monitoring well MWN02A during the pre-TEE tracer test is plotted in Figure D-33. A moderately dispersed peak appeared after only six hours at MWN02-A northwest of the injection well and persisted for

about 3 hours, equal to the time of bromide injection. A second peak was detected in this well after 10 hours of bromide injection.
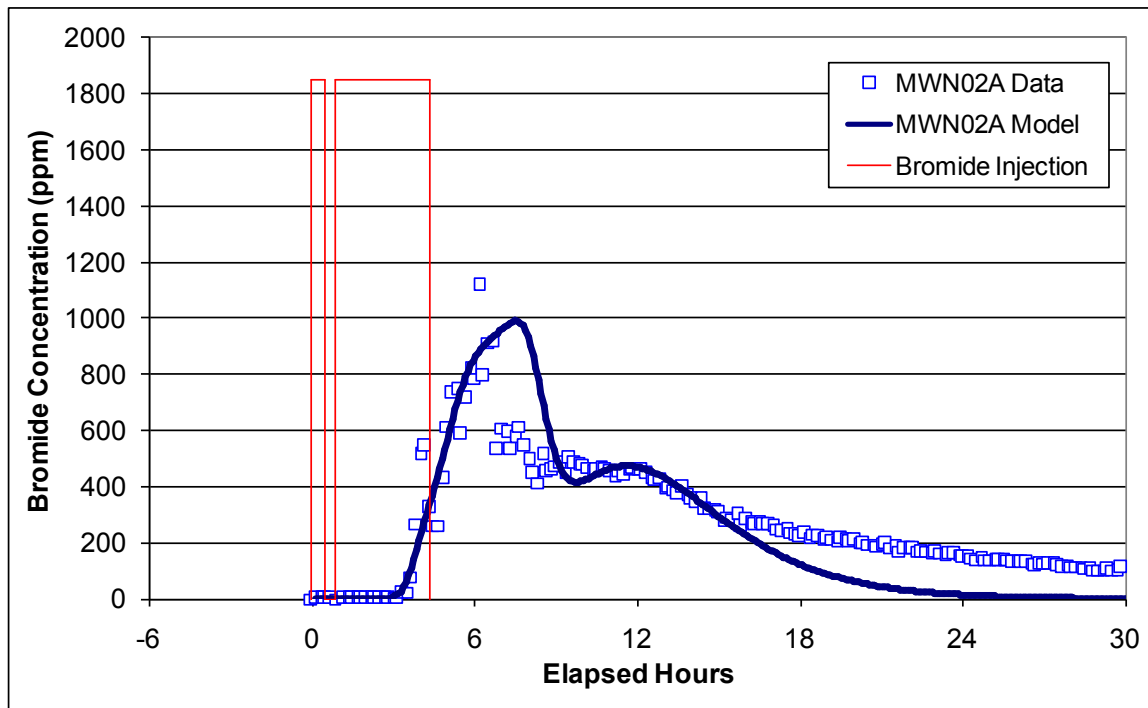
Figure D-33. Bromide Tracer Response in the UWBZ at MWN02A (Radius = 26.9 feet).

The UWBZ tracer data were analyzed using the methods described in the previous section. The model results matched to the data are plotted in Figure D-33. The parameter fits for MWN02-A are provided in Table D-20 and suggest water flows through a very small fraction of the aquifer. As noted below, Table D-20, values of Q/H in the UWBZ greater than 0.72 gpm/ft indicate preferential flow paths. MWN02A had a total Q/H of 11.8 gpm/ft and therefore flow was transmitted through only 6% of the UWBZ profile. This result is consistent with the LSZ results where higher percentages were calculated as the LSZ soils are known to be more permeable than the UWBZ soils. Dispersion coefficients fit to the data were 0.6 and 1.0 feet, consistent the values fit to the data in the LSZ.

Table D-20. Summary of UWBZ Tracer Test Parameter Fitting.

	MWN02		(Pre-TEE)	
	Q/H (gpm/ft)	Dispersion (ft)	Q (gpm)	H (ft)
A-horizon	Radius = 26.9 feet			
Layer 1	20.24	0.6	8.5	0.42
Layer 2	8.64	1.0	9.5	1.10
Total	11.84		18	1.52
Flow Layers				6%

NOTE: For uniform, symmetric flow in the UWBZ, Q/H equals 18 gpm /(195–170 ft) = 0.72 gpm/ft

1.7.2 Concentration and Flow Data

This section presents the concentration data collected at monitoring wells during the mass transfer testing and measured flow rates. These data are used to calculate mass fluxes through the TEE cell and allow an evaluation of the change in flux resulting from the application of TEE. The complete set of groundwater concentrations measured in the TEE monitoring wells is attached at the end of this appendix. The data include BTEX, TPH and hydrocarbon concentrations for ranges of carbon numbers. The gas chromatograph was calibrated with a range of alkanes and the retention times were used to separate the TPH concentration into various ranges such as hexane and lower, heptane-octane, nonane-decane, etc. This report and the analyses in Section 6 of the main report focus on benzene concentrations in groundwater as the chemical of concern. The measured concentrations of other compounds are included for future analyses. Other laboratory analytical reports, quality assurance reports, calibration procedures, etc. can be found in the TEE Pilot Test Performance Evaluation Report (BEM, 2010) and the TEE Pilot Test Work Plan (BEM, 2007).

The field GC data at the end of this appendix also include notations for the type of groundwater sample collected: bailer or purged. In most cases, a grab sample was collected using a bailer. As described previously, the groundwater sampling procedure started with a check for any NAPL floating in the monitoring well casing. If detected, a bailer was used to extract liquids until no more NAPL was visible in the bailer and no NAPL could be detected at the water table interface. After NAPL removal, a clean bailer was used to collect a grab sample of the groundwater in the casing. This procedure did not always provide a sample representative of groundwater conditions adjacent to the well screen as NAPL slowly accumulated in some of the monitoring well casings and impacted these grab samples. Samples to be shipped off-site were collected under the typical purging protocol and provided a more representative sample. The purging protocol was very labor intensive (3-5 samples per day) compared to the grab samples (12-18 samples per day); however, the grab samples provided valuable data.

Concentrations measured in purged groundwater samples before the pre-TEE mass transfer test and in purged groundwater samples after the post-TEE mass transfer test were presented previously with other baseline data. Those data are used in this section for comparison with the data collected during the mass transfer tests.

1.7.2.1   LSZ Results

The idealized flow configurations during the pre- and post-TEE mass transfer tests in the LSZ are illustrated in Figure D-9 and Figure D-11, respectively. The benzene concentrations measured in the C-horizon and B-horizon monitoring wells are plotted in Figure D-34 and Figure D-35, respectively. The plots are provided in order from closest to furthest distance from the injection well. The bailed samples in 2008 were collected during the pre-TEE mass transfer test and the samples from June 2009 to January 2010 were collected after the TEE pilot test. The primary data collection period during the post-TEE mass transfer test was in November 2009. The plots include purged samples collected and analyzed during the post-TEE mass transfer test that are considered representative of groundwater conditions adjacent to the sampled well. General observations for each C-horizon monitoring well are as follows:

- Monitoring well MWN06-C was located in the most permeable interval and closest to the injection well at a distance of 18 feet. The decrease in benzene concentration at this location was near the cleanup goal.
- A decrease was also observed in MWN02-C at a distance of 25 feet; however, a rebound in benzene concentration was observed after the water injection was terminated. The first purged sample was collected during the final week of water injection while the two subsequent samples were collected after water injection was terminated.
- MWN04-C was located 40 feet from the injection well and grab samples suggest an increase in benzene concentration; however, NAPL collected in its casing and purged samples yielded much lower and more representative concentrations.
- The grab samples collected during the pre-TEE mass transfer test from MWN01-C, located 49 feet from the injection well, showed a well defined decay. Post-TEE grab samples in MWN01-C suggested little change in benzene concentration before and after TEE; however, the purged samples were much lower. The post-TEE grab sample concentrations suggest NAPL resided in the well casing above the screen and compromised sampling until purging with a pump cleared the NAPL.
- Well screen MWN05-C was located 54 feet from the injection well in a poorly swept area of the TEE cell and benzene concentration were lower after TEE but a rebound was observed when the water injection was terminated.
- MWN03-C was located 57 feet from the injection well and very close to an extraction well such that contaminants were both pushed and pulled to this location. Hence, little if any change in benzene concentration was affected and NAPL was present in the well casing. This location also showed a rebound in benzene concentration when the water injection was terminated.
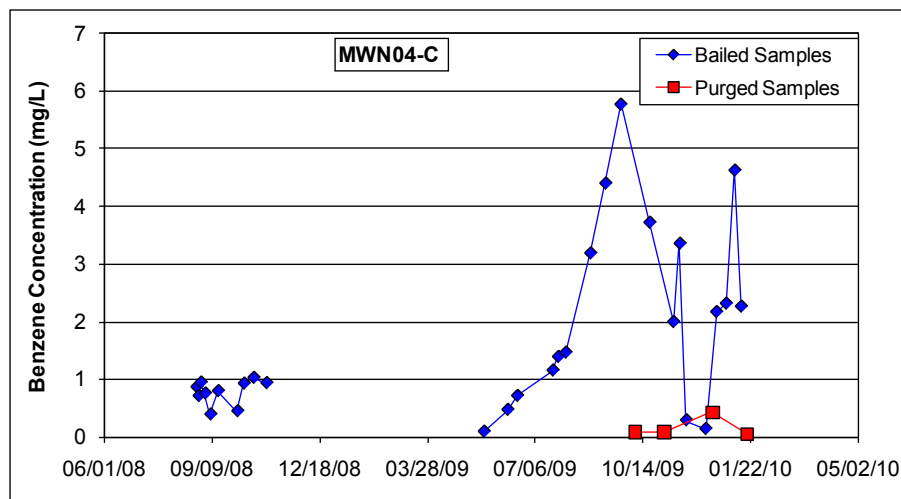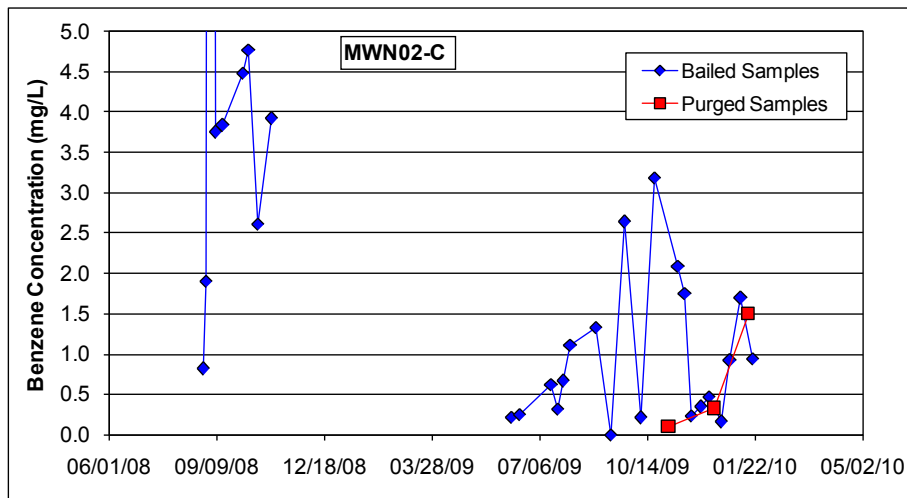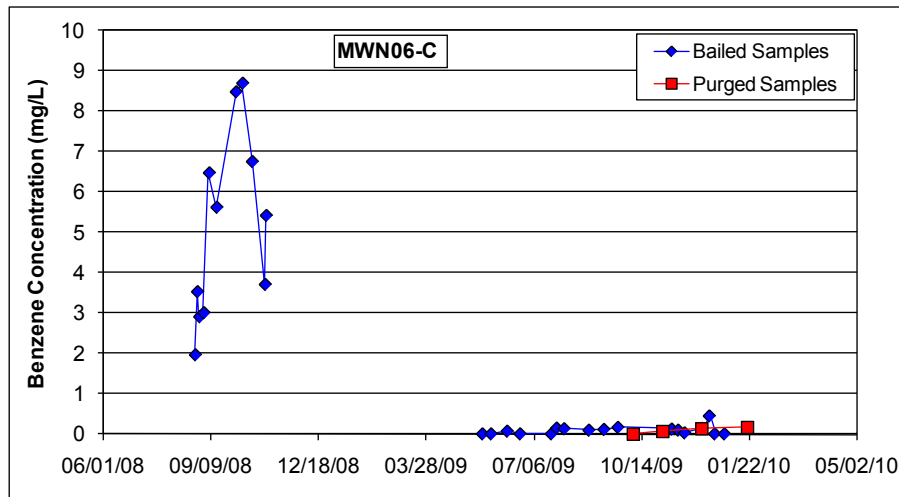
Figure D-34. Benzene Concentration Histories in C-Horizon Monitoring Wells.
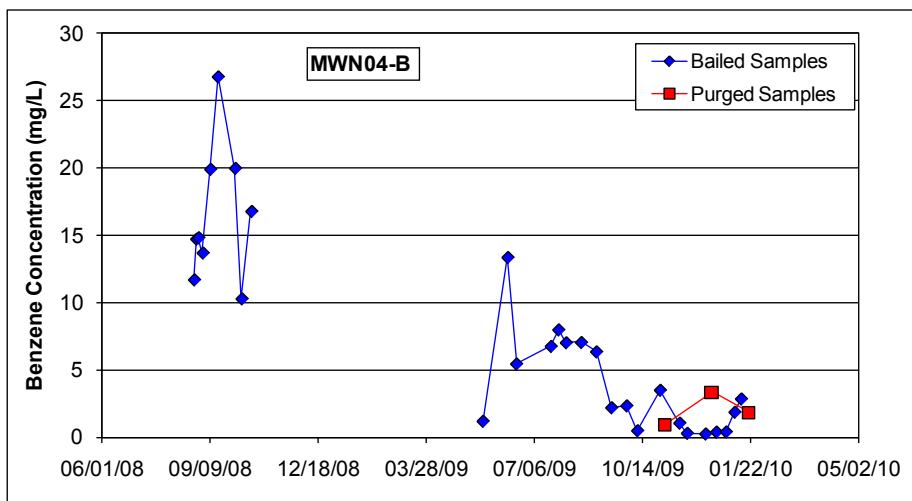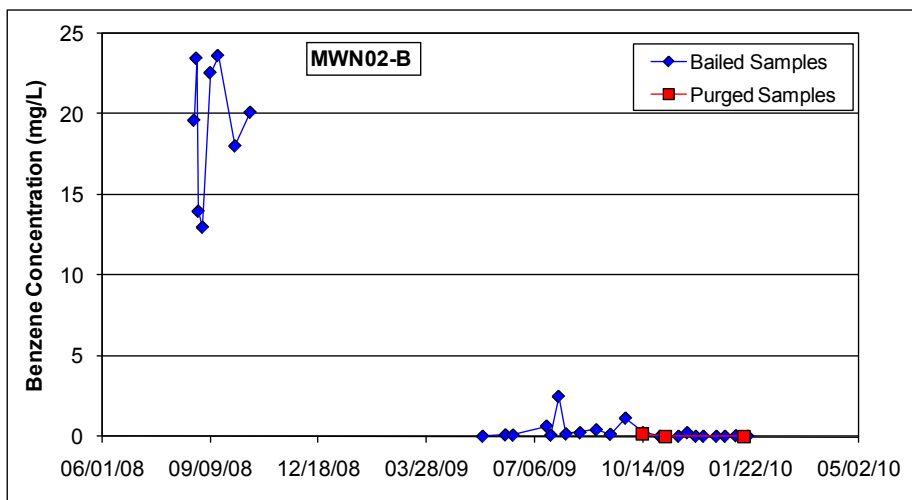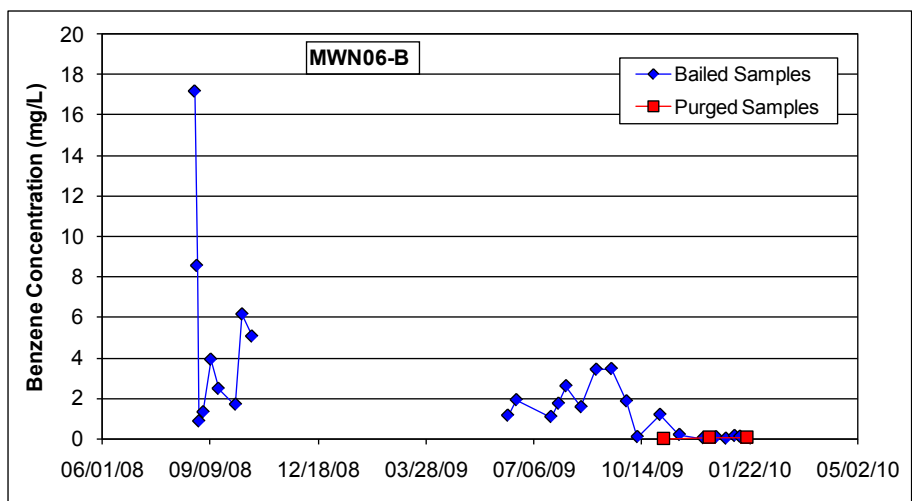
Figure D-34. Benzene Concentration Histories in C-Horizon Monitoring Wells (Continued).

Figure D-35. Benzene Concentration Histories in B-Horizon Monitoring Wells.
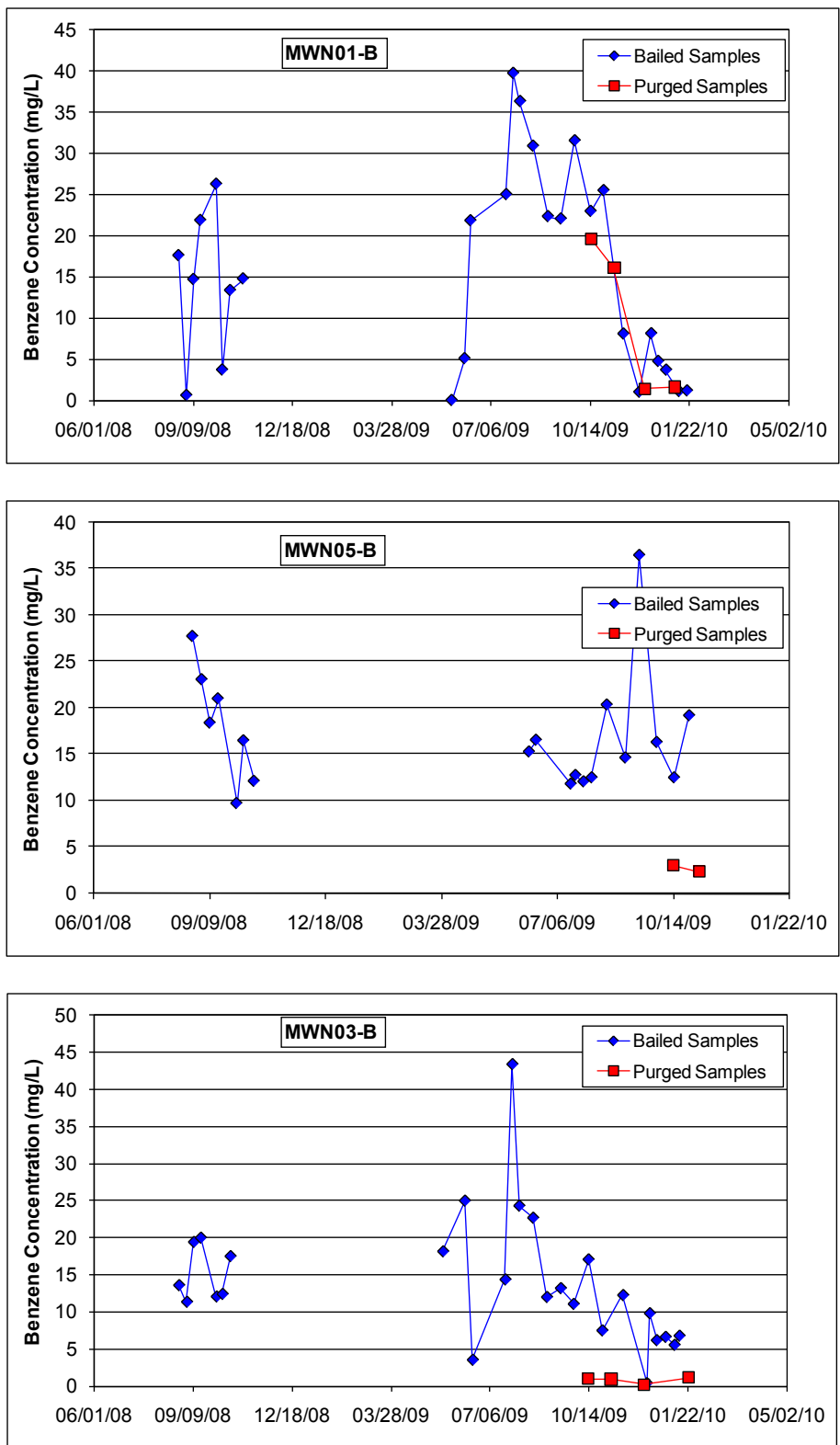
Figure D-35 Benzene Concentration Histories in B-Horizon Monitoring Wells (Continued).

In general, the initial benzene concentrations in the B-horizon monitoring wells were much higher than in the C-horizon suggesting the more permeable C-horizon was subjected to more weathering and the mass of NAPL in the B-horizon was greater than in the C-horizon. Observations for each B-horizon monitoring well plotted in Figure D-35 are as follows:

- Monitoring well MWN06-B was located closest to the injection well at a distance of 18 feet. The decrease in benzene concentration at this location was near the cleanup goal.
- A similar decrease was also observed in MWN02-B at a distance of 28 feet. Recall from the tracer test this location and depth appeared to have preferential pathways allowing more treatment than the deeper MWN02-C where a rebound in the benzene concentration was observed.
- MWN04-B was located 43 feet from the injection well and both grab and purged samples suggest a significant decrease in benzene concentration.
- The grab samples collected during the pre-TEE mass transfer test from MWN01-B, located 48 feet from the injection well were indicative of a local NAPL. Post-TEE grab samples in MWN01-B suggested little change in benzene concentration before and after TEE, if not an increase. The post-TEE grab sample concentrations suggest NAPL resided in the well casing above the screen; however, the initial purged samples further indicate NAPL resided in the vicinity of the well. When the water injection was terminated the concentration dropped by an order of magnitude indicating injected water was passing through a NAPL-contaminated zone before reaching MWN01-B.
- Well screen MWN05-B was located 54 feet from the injection well in a poorly swept area of the TEE cell. Based on bailed samples, the benzene concentration was unchanged; however, the purged samples were an order of magnitude lower suggesting NAPL in the casing compromised the grab samples.
- MWN03-B was located 60 feet from the injection well and very close to an extraction well such that contaminants were both pushed and pulled to this location. Hence, little if any change in benzene concentration was expected. The bailed grab sample results suggest no change or that NAPL was present in the well casing; however, the purged samples representative of the surrounding soils were an order of magnitude lower.

The RESSQ program (Doughty, Tsang and Javandel, 1985) used to determine the uniform flow configurations during the mass transfer tests also calculates theoretical velocities at specified locations in the aquifer (i.e., the monitoring wells). Multiplying the velocity by the well concentration yields the mass flux. The calculated uniform benzene mass fluxes for the C- and B-horizons in the LSZ are provided in Table D-21. The B-horizon had an average of 83% reduction in benzene flux while the deeper, more permeable C-horizon had a reduction in benzene flux of 99%. One location, MWN01-B increased in benzene flux after the TEE pilot test.

Table D-21. Calculated Benzene Mass Fluxes in the LSZ during the Mass Transfer Testing.

Well	Radius (feet)	Pre-TEE Benzene Nov 06 (mg/L)	Pre-TEE RESSQ Velocity (cm/day)	Pre-TEE Average Flux (g/m²/day)	Post-TEE Benzene Nov 09 (mg/L)	Post-TEE RESSQ Velocity (cm/day)	Post-TEE Average Flux (g/m²/day)	Flux Reduction
MWN01B	48.33	18	54.5	9.81	23	73.7	16.95	-73%
MWN02B	27.69	24	114.3	27.44	0.012	135.5	0.02	100%
MWN03B	59.80	17	69.7	11.85	0.81	73.0	0.59	95%
MWN04B	42.86	26	76.7	19.94	0.92	100.2	0.92	95%
MWN05B	54.05	20	48.6	9.73	2	79.6	1.59	84%
MWN06B	18.20	24	174.8	41.95	0.0028	190.6	0.01	100%
Average B				**20.12**			**3.35**	**83%**
MWN01C	49.02	2.8	56.9	1.59	0.011	75.9	0.01	99%
MWN02C	25.14	5.5	125.4	6.90	0.017	150.9	0.03	100%
MWN03C	57.40	5	84.5	4.22	0.58	91.5	0.53	87%
MWN04C	40.22	8.3	81.2	6.74	0.0092	105.3	0.01	100%
MWN05C	53.62	3.9	59.3	2.31	0.01	99.1	0.01	100%
MWN06C	18.18	10	174.2	17.42	0.0014	185.1	0.00	100%
Average C				**6.54**			**0.10**	**99%**

The flux reduction at each monitoring well location is plotted in Figure D-36 as a function of radius from the injection well. The locations closest to the injection well were expected to receive more treatment and a greater reduction than those further away. This trend is generally followed in both horizons except for the increase in flux calculated for MWN01-B. As noted above, sample analyses in this well were indicative of a local residual NAPL that received little treatment.
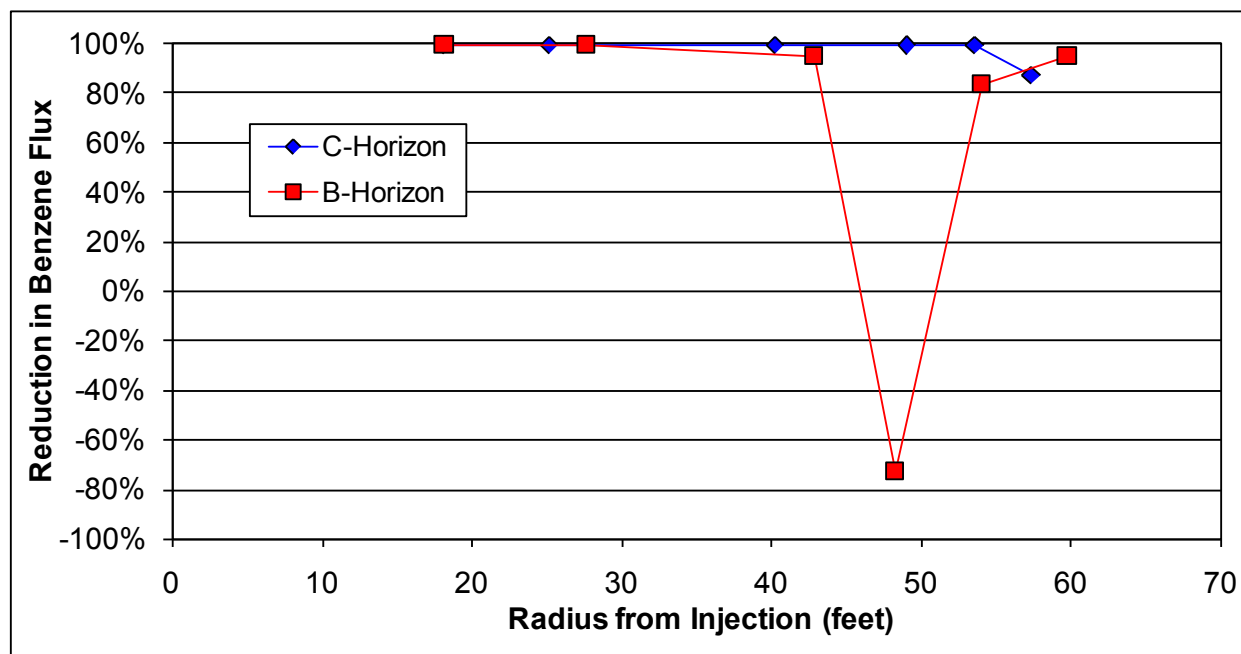
Figure D-36. Benzene Mass Flux Reduction from Concentrations in LSZ Monitoring Wells.

1.7.2.2   UWBZ Results

The idealized flow configurations during the pre- and post-TEE mass transfer tests in the UWBZ are illustrated in Figure D-13 and Figure D-15, respectively. The benzene concentrations measured in the A-horizon monitoring wells are plotted in Figure D-37. The plots are provided in order from closest to furthest distance from the injection well. The bailed samples in 2008 were collected during the pre-TEE mass transfer test and the samples from June 2009 to January 2010 were collected after the TEE pilot test. The primary data collection period during the post-TEE mass transfer test was in November 2009. The plots include purged samples collected and analyzed during the post-TEE mass transfer test that are considered representative of groundwater conditions adjacent to the sampled well.

General observations for each A-horizon monitoring well are as follows:

- Monitoring well MWN06-A was located closest to the injection well at a distance of 24 feet. The decrease in benzene concentration at this location was near the cleanup goal.
- A decrease was also observed in MWN02-A at a distance of 27 feet. Post-TEE grab samples were elevated because of NAPL in the well casing; however, the purged samples yielded benzene concentrations more than one order of magnitude less than the initial concentration.
- The grab samples collected during the pre-TEE mass transfer test from MWN01-A, located 43 feet from the injection well, showed a decay. Post-TEE grab samples in MWN01-A suggested little change in benzene concentration before and after TEE; however, the purged samples were lower. The benzene concentration decreased further after the cessation of water injection implying the injected water was passing through NAPL-contaminated soil before arriving at MWN01-A.
- Well screen MWN05-A was located 48 feet from the injection well in a poorly swept area of the TEE cell and benzene concentrations appeared higher after TEE. The benzene concentration decreased after the cessation of water injection implying the injected water was passing through NAPL-contaminated soil before arriving at MWN05-A. NAPL contamination appeared to reside in the vicinity o fMWN05-A both before and after the TEE pilot test.
- MWN04-A was located 49 feet from the injection well and grab samples suggest an increase in benzene concentration; however, NAPL collected in its casing and purged samples yielded much lower and more representative concentrations of the surrounding soil and a small reduction in benzene concentration.
- MWN03-A was located 61 feet from the injection well and very close to an extraction well such that contaminants were both pushed and pulled to this location. Hence, little if any change in benzene concentration was expected and NAPL was present in the well casing. This location showed an increase in benzene concentration from bailed samples but the purged samples were commensurate with initial concentrations.
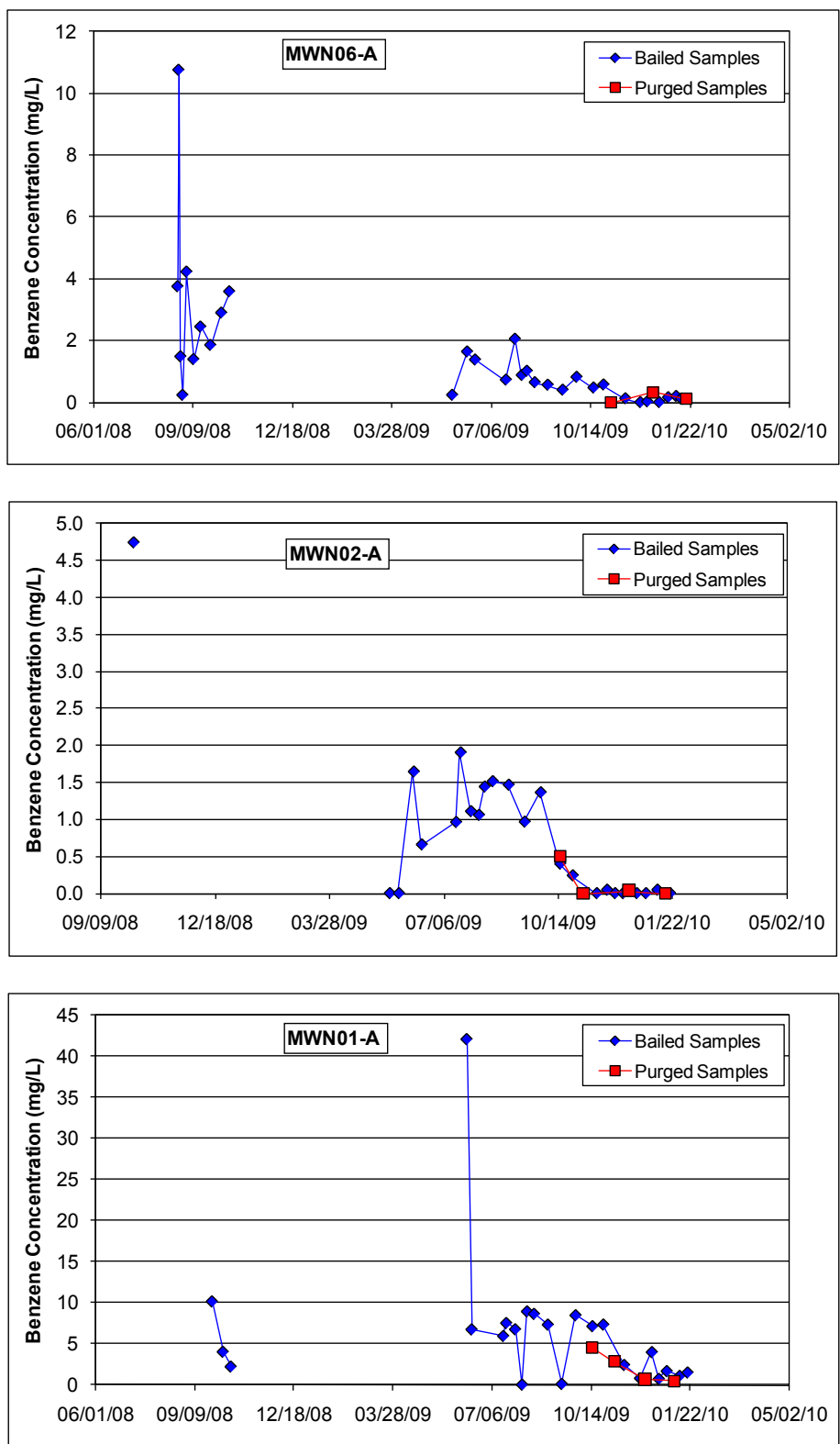
Figure D-35. Benzene Concentration Histories in A-Horizon Monitoring Wells.
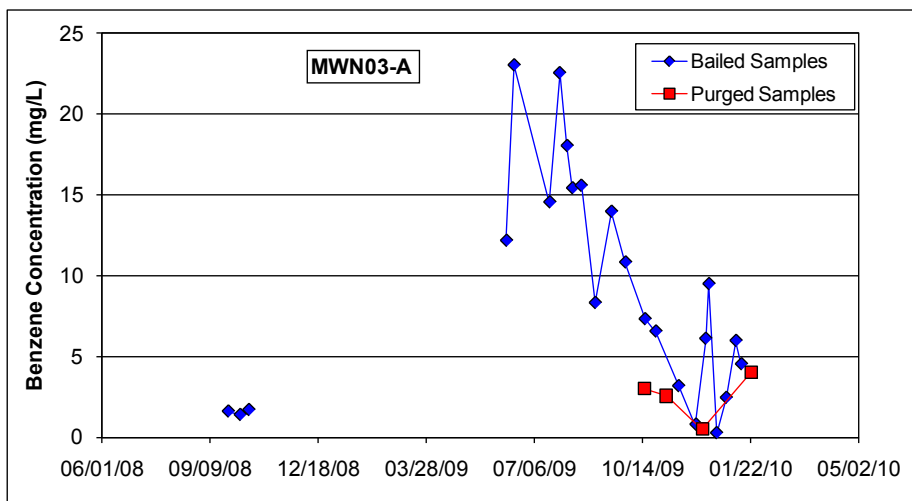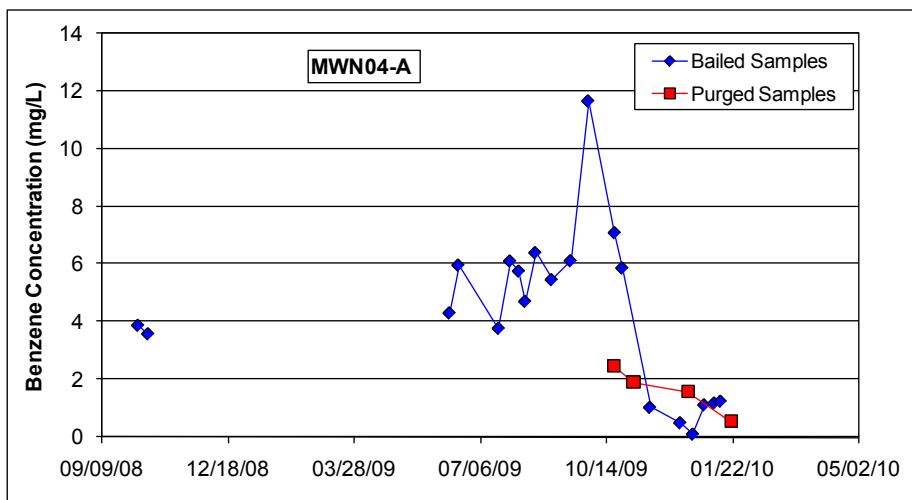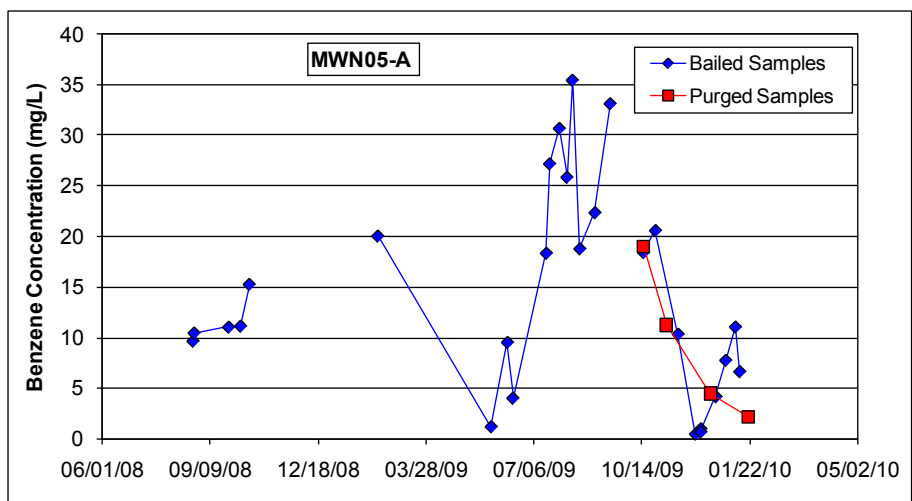
Figure D-35. Benzene Concentration Histories in A-Horizon Monitoring Wells (Cont.)

The RESSQ program (Doughty, Tsang and Javandel, 1985) used to determine the uniform flow configurations during the mass transfer tests also calculates theoretical velocities at specified locations in the aquifer (i.e., the monitoring wells). Multiplying the uniform velocity by the well concentration yields the mass flux. The calculated uniform benzene mass fluxes for the A-horizon in the UWBZ are provided in Table D-22. The A-horizon had an average 48% reduction that is significantly less than the results in the LSZ. The UWBZ was observed to be more heterogeneous and the thermal treatment was less intense as less energy per cubic volume was injected in the UWBZ. Two locations, MWN01-A and MWN03-A had calculated increases in benzene flux after the TEE pilot test. However, both these locations had relatively low initial benzene concentrations in November 2006. With the rising water table, the grab samples in 2008 suggest the benzene concentration was higher in MWN01-A during the pre-TEE mass transfer test and that the TEE pilot test left the concentration unchanged at this location. Concentration data from MWN03-A show a definite increase in benzene concentration after the pilot test but recall this monitoring well was located only 13 feet from an extraction well and received little treatment.

Table D-22. Calculated Benzene Mass Fluxes in the UWBZ during the Mass Transfer Testing.

Well	Radius (feet)	Pre-TEE Benzene Nov 06 (mg/L)	Pre-TEE RESSQ Velocity (cm/day)	Pre-TEE Average Flux (g/m^2/day)	Post-TEE Benzene Nov 06 (mg/L)	Post-TEE RESSQ Velocity (cm/day)	Post-TEE Average Flux (g/m^2/day)	Flux Reduction
MWN01A	42.48	0.76	76.2	0.58	2.9	62.2	1.80	-211%
MWN02A	26.93	2.1	116.8	2.45	0.0067	90.5	0.01	100%
MWN03A	60.73	0.26	165.4	0.43	1.6	52.2	0.84	-94%
MWN04A	48.95	2.9	40.0	1.16	1.2	58.2	0.70	40%
MWN05A	48.40	7.8	45.2	3.52	3.3	40.2	1.32	62%
MWN06A	24.06	1.2	71.9	0.86	0.019	102.9	0.02	98%
Average A				1.50			0.78	48%

The flux reduction at each monitoring well location is plotted in Figure D-36 as a function of radius from the injection well. The locations closest to the injection well were expected to receive more treatment and a greater reduction than those further away. This trend is generally followed except for the increases in flux calculated for MWN01-A and MWN03-A as discussed above.

Figure D-36. Benzene Mass Flux Reduction from Concentrations in UWBZ Monitoring Wells.

1.7.3 Passive Flux Meter Results

PFMs were used to measure the groundwater flux and contaminant mass flux during the forced flow conditions (injection and extraction wells were active) both before and after the TEE pilot test. For the PFMs, flux refers to the mass of water and /or contaminants flowing per unit area at a measured depth in a well screen averaged over a given period of time. Detailed results of the PFM analysis before and after the TEE Pilot Test are provided in Appendix G. This section summarizes the results.

1.7.3.1 PFM Data Collection

Both pre-TEE and post-TEE benzene mass flux profiles are displayed in Figure D-37 and the Darcy groundwater flux profiles are provided in Figure D-38. The figures include the results from both the A-horizon and B-horizon well deployments and are referenced to depth below ground surface. The average benzene flux per well is shown in Figure D-39 and provides only a comparison of average flux on a well-by-well basis, not taking into account the vertical variability of the fluxes within each well as provided in the profiles of Figure D-37.
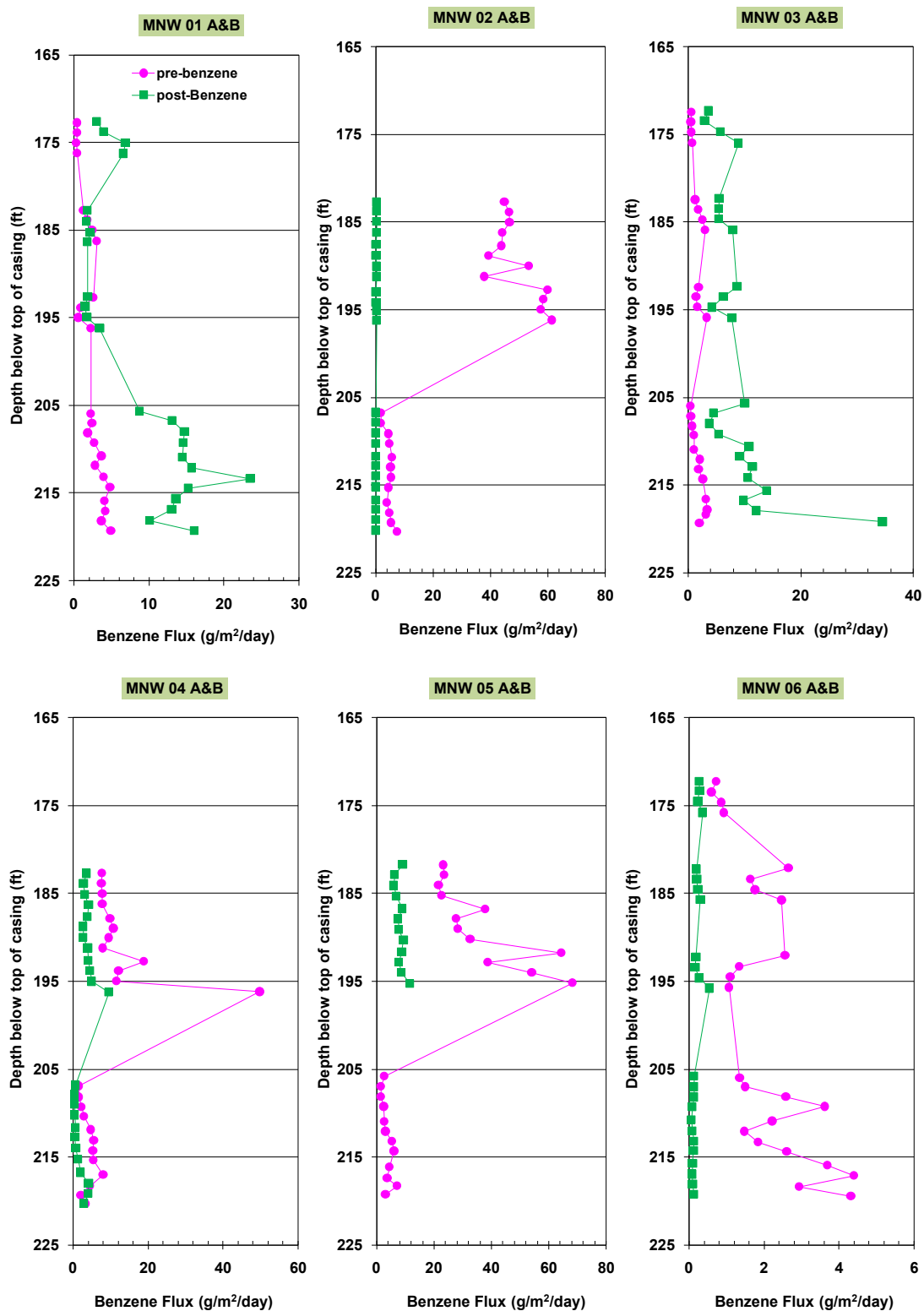
Figure D-37. Pre- and Post-TEE Benzene Mass Flux Profiles.
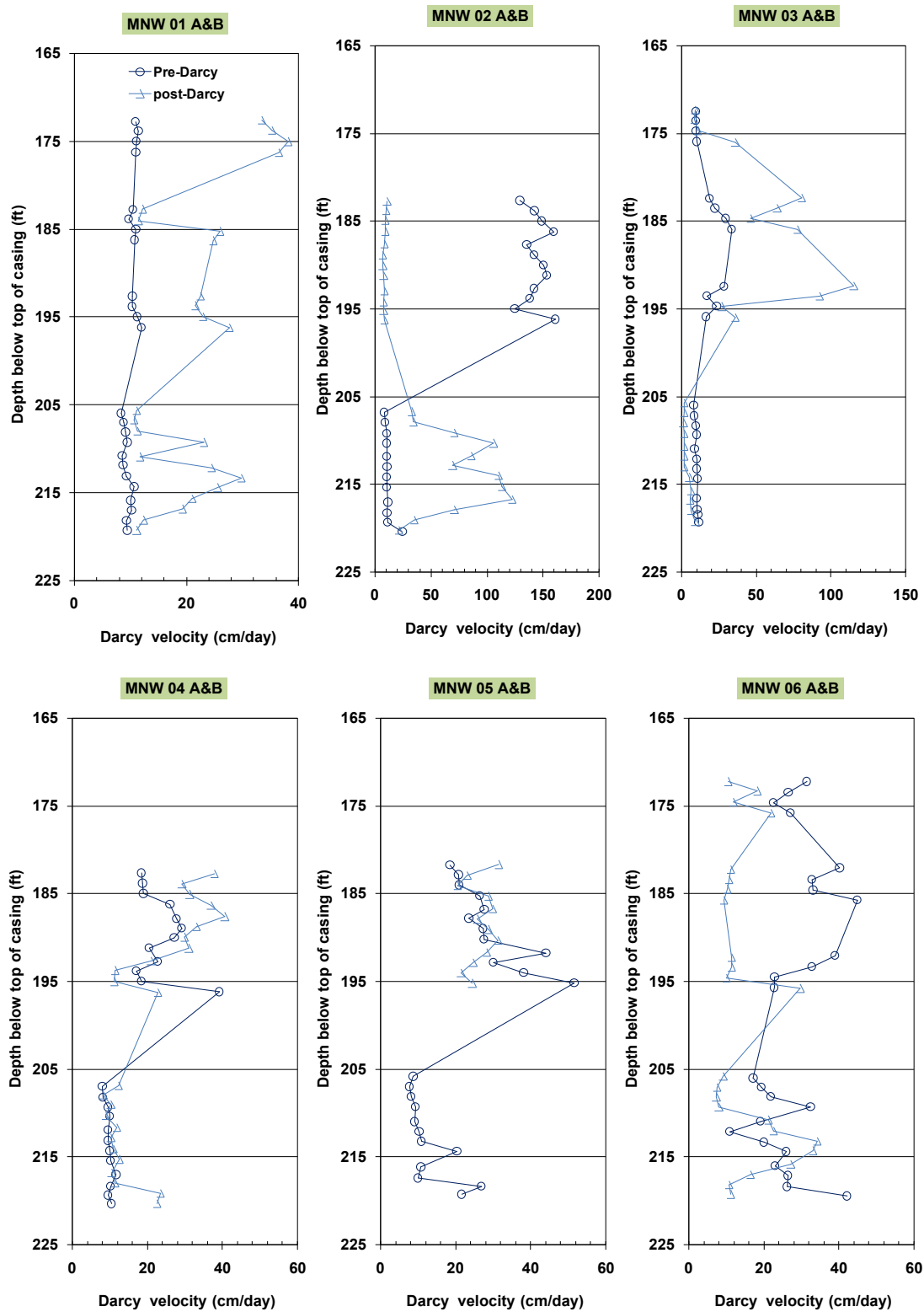
Figure D-38. Pre- and Post-TEE Darcy Groundwater Flux Profiles.
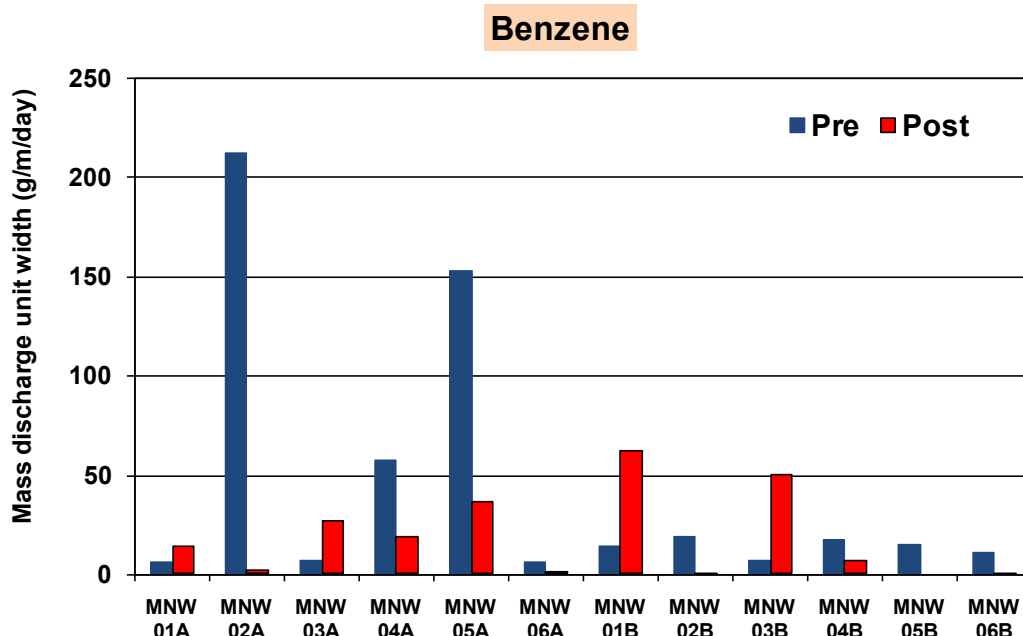
Figure D-39. Average Benzene Mass Fluxes for Pre- and Post-TEE Tests.

The pre-TEE Darcy velocities range from a high of 160 cm/day observed in the UWBZ well MWN-02A to a low of about 10 cm/day in several of the wells. The high value in MWN-02A is a result of its close proximity to the injection well (UWBZ07). Well MWN-06 also yielded high Darcy velocities (up to 40 cm/day) and is also located near the injection wells (UWBZ07 and LSZ07). During the pre-TEE testing the average Darcy flux in the UWBZ (43 cm/day) was higher than the B-horizon of the LSZ (13 cm/day). Based upon the relative permeability of the different horizons, it is probable the majority of the flow in the LSZ traveled through the deeper C-horizon of the LSZ from about 232 to 244 ft bgs where PFMs were not deployed.

The average benzene flux during the pre-TEE deployment was highest in wells MWN-02A and -05A in the UWBZ. With the highest observed benzene flux being 68 g/m^2/day in well MWN-05A. The next highest flux was observed in well MWN-04A with one sample at 50 g/m^2/day. All other wells exhibited much lower benzene mass flux during the pre-TEE deployment. The highest measured benzene flux in the LSZ was 8.14 g/m^2/day in well MWN-04B.

The post-remedial Darcy velocities range from a high of 122 cm/day in the LSZ well MWN-02B and 115 cm/day the UWBZ well MWN-03A to a low of about 3 cm/day in the LSZ well MWN-03B. The high value in MWN-02 is likely a result of its close proximity to the injection well. During the post-remedial measurements the average Darcy flux in the UWBZ (26 cm/day) was roughly equivalent to the B-horizon of the LSZ (25 cm/day).

The benzene mass flux during the post-TEE testing was highest in wells MWN-01B and 03B in the LSZ, with values of 23.5 g/m^2/day and 34.5 g/m^2/day, respectively. These two wells also had higher average mass flux when compared to the other wells (Figure D-39). The highest average benzene flux in the UWBZ was observed in well MWN-5A at 11.7 g/m^2/day.

1.7.3.2   Comparison of PFM Data with Conventional Data

Theoretical streamlines for groundwater extraction, water injection and regional groundwater flow during the pre- and post-TEE deployments of PFMs in the A- and B-horizons were presented above. The RESSQ program (Doughty, Tsang and Javandel, 1985) used to determine the streamlines assuming uniform flow during the PFM deployments also calculates theoretical velocities at specified locations in the aquifer (i.e., the monitoring wells). The calculated velocities from the pre-TEE flow conditions are presented in Table D-23 along with the PFM-measured values for the well-average Darcy velocity. The PFM-measured velocities were generally one order of magnitude lower than the theoretical value. The trend in the PFM data is consistent with the B-horizon being less transmissive than the deeper C-horizon. The only location with a PFM-value exceeding the theoretical uniform value was in MWN02-A.

Table D-23. Calculated and PFM Measured Darcy Velocities during the Pre-TEE Testing.

Well	Radius (ft)	RESSQ Velocity (cm/day)	Average PFM Velocity (cm/day)	(RESSQ –PFM) /RESSQ (%)
MWN01A	42.48	76.2	10.9	86%
MWN02A	26.93	116.8	144	-23%
MWN03A	60.73	165.4	19.3	88%
MWN04A	48.95	40.0	23.8	41%
MWN05A	48.40	45.2	29.7	34%
MWN06A	24.06	71.9	31.3	56%
MWN01B	48.33	54.5	9.4	83%
MWN02B	27.69	114.3	11.9	90%
MWN03B	59.80	69.7	10.2	85%
MWN04B	42.86	76.7	9.8	87%
MWN05B	54.05	48.6	12.9	73%
MWN06B	18.20	174.8	23.8	86%
MWN01C	49.02	56.9	nm	-
MWN02C	25.14	125.4	nm	-
MWN03C	57.40	84.5	nm	-
MWN04C	40.22	81.2	nm	-
MWN05C	53.62	59.3	nm	-
MWN06C	18.18	174.2	nm	-

The RESSQ-calculated uniform velocities for the post-TEE flow conditions are presented in Table D-42 along with the PFM-measured values for the well-average Darcy velocity. The PFM-measured velocities were again roughly one order of magnitude less than the theoretical uniform values with the exception of MWN03-A which nearly matched the theoretical value. The major changes in the PFM measures between the pre- and post-TEE measures was in well MWN02-A where the velocity was more than one order of magnitude less after the TEE pilot test.

Table D-24. Calculated and PFM Measured Darcy Velocities during the Post-TEE Testing.

Well	Radius (ft)	RESSQ Velocity (cm/day)	Average PFM Velocity (cm/day)	(RESSQ –PFM) /RESSQ (%)
MWN01A	42.48	62.2	26.0	58%
MWN02A	26.93	90.5	8.70	90%
MWN03A	60.73	52.2	50.5	3%
MWN04A	48.95	58.2	28.1	52%
MWN05A	48.40	40.2	26.5	34%
MWN06A	24.06	102.9	13.9	86%
MWN01B	48.33	73.7	17.6	76%
MWN02B	27.69	135.5	72.8	46%
MWN03B	59.80	73.0	3.90	95%
MWN04B	42.86	100.2	12.9	87%
MWN05B	54.05	79.6	-	-
MWN06B	18.20	190.6	17.4	91%
MWN01C	49.02	75.9	nm	-
MWN02C	25.14	150.9	nm	-
MWN03C	57.40	91.5	nm	-
MWN04C	40.22	105.3	nm	-
MWN05C	53.62	99.1	nm	-
MWN06C	18.18	185.1	nm	-

Multiplying the uniform, RESSQ-calculated velocity by the measured well concentration of benzene yields the benzene mass flux at that location. The calculated uniform benzene mass fluxes are provided in Table D-25 along with the well-averaged values measured with the PFMs. All pre-TEE PFM measures of benzene mass flux exceeded the theoretical values in the A-horizon of the UWBZ. Conversely, in the B-horizon of the LSZ, the PFM measures of benzene flux were all less than the theoretical values although the values are generally within one order of magnitude.

Table D-25. Calculated and PFM Measured Benzene Fluxes during the Pre-TEE Testing.

Well	Radius (ft)	RESSQ Benzene Flux (g/m²/day)	Average PFM Benzene Flux (g/m²/day)	(RESSQ –PFM) /RESSQ (%)
MWN01A	42.48	0.58	1.20	-107%
MWN02A	26.93	2.45	37.9	-1447%
MWN03A	60.73	0.43	1.10	-156%
MWN04A	48.95	1.16	3.70	-219%
MWN05A	48.40	3.52	31.3	-789%
MWN06A	24.06	0.86	1.50	-74%
MWN01B	48.33	9.81	3.5	64%
MWN02B	27.69	27.44	4.6	83%
MWN03B	59.80	11.85	1.9	84%
MWN04B	42.86	19.94	4.0	80%
MWN05B	54.05	9.73	3.8	61%
MWN06B	18.20	41.95	2.7	94%
MWN01C	49.02	1.59	nm	-
MWN02C	25.14	6.90	nm	-
MWN03C	57.40	4.22	nm	-
MWN04C	40.22	6.74	nm	-
MWN05C	53.62	2.31	nm	-
MWN06C	18.18	17.42	nm	-

The RESSQ-calculated benzene mass fluxes for the post-TEE flow conditions are presented in Table D-26 along with the PFM-measured values for the well-averaged benzene flux. The PFM-measured values were again all higher than the theoretical values in the A-horizon. In contrast to the pre-TEE findings, the post-TEE PFM-measured fluxes were all higher than the theoretical values except in well MWN01B where the values nearly matched.

The major changes in the PFM measures between the pre- and post-TEE measures were in wells MWN01-B and MWN03-B where the benzene flux was measured to increase. The increase at MWN01-B is consistent with the prediction from the theoretical value; however, the increase at MWN03-B was not consistent with the concentration-based prediction of a decrease of more than one order of magnitude. The PFM data are explored more fully in Section 6 of the main report.

Table D-26. Calculated and PFM Measured Benzene Fluxes during the Post-TEE Testing.

Well	Radius (ft)	RESSQ Benzene Flux (g/m²/day)	Average PFM Benzene Flux (g/m²/day)	(RESSQ –PFM) /RESSQ (%)
MWN01A	42.48	1.80	2.5	-39%
MWN02A	26.93	0.01	0.2	-1900%
MWN03A	60.73	0.84	4.7	-460%
MWN04A	48.95	0.70	3.1	-343%
MWN05A	48.40	1.32	6.3	-377%
MWN06A	24.06	0.02	0.1	-400%
MWN01B	48.33	16.95	14.4	15%
MWN02B	27.69	0.02	0.10	-400%
MWN03B	59.80	0.59	11.4	-1832%
MWN04B	42.86	0.92	1.60	-74%
MWN05B	54.05	1.59	-	-
MWN06B	18.20	0.01	0.10	-900%
MWN01C	49.02	0.01	nm	-
MWN02C	25.14	0.03	nm	-
MWN03C	57.40	0.53	nm	-
MWN04C	40.22	0.01	nm	-
MWN05C	53.62	0.01	nm	-
MWN06C	18.18	0.00	nm	-

1.7.4 Source Term Estimates for the Mass Transfer Tests

The estimated NAPL compositions during the pre-TEE and post-TEE mass transfer tests are provided in Table D-6 and Table D-7 for the LSZ and UWBZ, respectively. With a determination of the benzene content in the NAPL, the total mass of benzene can be calculated from estimates of the total NAPL in the source zone. Estimates for the NAPL in the TEE cell were developed by the U.S. Air Force and the methodology is described in detail in the TEE Pilot Test Performance Evaluation Report (BEM, 2010). The NAPL estimation procedures and results are summarized below.

Realistic assumptions for residual NAPL saturations in differing soil types were multiplied by the estimated volumes of each soil type within the TEE cell and the NAPL density to calculate an estimated initial mass of NAPL within the TEE cell. A literature review of field measures of initial and residual NAPL saturation at fuel-contaminated sites was performed. The recent works by Adamski et al. (2005) and Charbeneau (2007) and a presentation by Adamski and Charbeneau were used to select the representative average NAPL saturations for each hydrostratigraphic layer at ST012 and are listed in Table D-27. Also included in the table are values for the average layer thickness, as derived from GMS outputs, Unified Soil Classification System soil type, and total soil porosity of the particular soil types (Aquaveo, 2009; American Society for Testing And Materials [ASTM], 1985).

Table D-27. NAPL Saturation Assumptions from the Literature.

Hydrostratigraphic Unit	Layer Average Thickness (feet)	Soil Type	Total Soil Porosity	NAPL Saturation
UWBZ +1	13.06	Silt/Clay (CL)	0.35	0.028
UWBZ +2	7.0	Sand w/Fines (SM)	0.32	0.059
UWBZ +3	6.2	Silt/Clay (CL)	0.35	0.028
UWBZ +4	9.0	Sand w/Fines (SM)	0.32	0.059
LPZ	12.3	Silt/Clay (CL)	0.35	0.028
LSZ + 1	9.3	Sand w/Fines (SM)	0.32	0.059
LSZ + 2	4.3	Silt/Clay (CL)	0.35	0.028
LSZ + 3	5.3	Sand w/Fines (SM)	0.32	0.059
LSZ + 4	5.3	Silt/Clay (CL)	0.35	0.028
LSZ + 5	15.5	Sand (SW)	0.32	0.077

Source: (Aquaveo, 2009)

The initial volume of NAPL in each layer of the TEE cell was calculated by multiplying the literature NAPL saturation by the layer volume, total porosity, and a TEE cell area of 12,730 square feet. The calculated values for the NAPL volumes are listed in Table D-28. The total volume of NAPL in the UWBZ was 46,630 gallons and in the LSZ was 71,672 gallons. A volume of 11,522 gallons was calculated for the LPZ separating the UWBZ and LSZ.

Table D-28. Mass Estimates for the TEE Cell Based on Literature NAPL Saturation Values.

Hydrostratigraphic Unit	Soil Volume (cubic feet)	Total Soil Porosity	NAPL Saturation	NAPL (gallons)
UWBZ +1	166,259	0.35	0.028	12,188
UWBZ +2	88,842	0.32	0.059	12,547
UWBZ +3	78,617	0.35	0.028	5,763
UWBZ +4	114,219	0.32	0.059	16,131
UWBZ Cumulative	447,937	0.34	0.041	46,630
LSZ + 1	118,755	0.32	0.059	16,772
LSZ + 2	54,601	0.35	0.028	4,003
LSZ + 3	68,066	0.32	0.059	9,613
LSZ + 4	66,869	0.35	0.028	4,902
LSZ + 5	197,386	0.32	0.077	36,382
LSZ Cumulative	505,678	0.33	0.058	71,672

Calculations for the initial mass of benzene in the TEE cell are summarized in Table D-29 where a NAPL density of 6.57 pounds per gallon is assumed.

Table D-29. Estimated Masses of Benzene in the TEE Cell Interior.

Parameter	Pre-TEE LSZ	Pre-TEE UWBZ	Post-TEE LSZ	Post-TEE UWBZ
NAPL Volume (gal)	71,672	46,630	67,413	42,371
NAPL Benzene Content	0.83%	0.222%	0.101%	0.076%
Benzene Mass (lbs)	3,908	680	447	212

The calculated benzene masses are based on the estimated mass fractions of benzene in residual NAPL before and after the pilot test, assumed to be uniform across the cell. Based on these

estimates, a mass of 3,461 pounds of benzene was extracted from the LSZ during the pilot test and 468 pounds from the UWBZ. The measured masses of contaminants removed from the TEE cell interior during the TEE pilot test are presented in Table D-30 (BEM, 2010). The 2,060 pounds of benzene extracted from the LSZ compares well with the literature-based estimate of 3,461 pounds. The NAPL saturation for the deepest LSZ layer (LSZ+5), coinciding with the C-horizon, was likely an overestimate. Historically, the water table did not drop significantly into this interval and therefore a smear zone was not likely to exist. As shown in Table D-28, LSZ+5 held half of the estimated NAPL in the LSZ. Hence, the estimated benzene removal and measured removal are on the same order. In the UWBZ, the measured extraction of 787 pounds exceeds the literature-based estimate of 468 pounds suggesting NAPL saturations in the UWBZ may be higher.

Table D-30. Estimated Masses Extracted from the TEE Cell Interior.

Zone	Benzene (pounds)	Toluene (pounds)	Ethyl-benzene (pounds)	m&p-Xylenes (pounds)	o-Xylene (pounds)	TPH (pounds)
UWBZ	787	704	372	544	469	30,400
LSZ	2,060	1,110	453	624	526	27,000
NAPL	294	1,020	663	1,100	406	55,960
Total	3,140	2,830	1,490	2,270	1,400	113,000

These mass estimates, concentrations and fluxes, and the PFM data are used in Section 6 of the main report to evaluate the mass transfer tests and the utility of the approach for predicting the longevity of a multi-component NAPL source zone. As indicated in this section, the total mass, and therefore the NAPL saturation, was reduced by less than 10 percent in each zone. Hence, the flow configuration with respect mass transfer from a residual NAPL was very similar between the pre-TEE and the post-TEE testing. The major change in test conditions was in the benzene content of the residual NAPL which was reduced by 88% and 65% in the LSZ and UWBZ, respectively, as a result of the TEE pilot test.

Field GC Analyses

Date	Notes	Benzene	Toluene	Ethylbenzene	mpXylenes	oXylene	C6<=	C7C8	C9C10	C11C12	C13C14	C15>=	TPH
MWN01A													
9/26/2008	Bailed sample	10.16	1.83	1.33	2.67	0.85	3.36	6.35	4.02	2.48	0.19	0.00	33.22
10/7/2008	Bailed sample	4.01	1.25	1.40	2.11	0.99	2.58	3.68	2.51	1.21	0.08	0.00	19.82
10/15/2008	Bailed sample	2.20	1.11	0.84	1.11	0.26	2.49	1.91	2.48	1.16	0.00	0.00	13.56
6/10/2009	Bailed sample	42.17	43.73	8.42	11.20	6.93	11.99	53.18	10.18	0.78	0.16	0.00	188.76
6/15/2009	Bailed sample	6.74	15.90	4.64	6.30	3.82	9.22	14.38	4.33	1.02	0.23	0.12	66.70
7/17/2009	Bailed sample	5.93	9.13	2.86	3.36	1.65	5.46	5.50	4.23	0.19	0.03	0.00	38.34
7/20/2009	Bailed sample	7.52	14.40	4.32	6.18	2.67	6.41	9.65	1.51	0.41	0.34	0.00	53.41
7/29/2009	Bailed sample	6.76	9.20	2.95	3.88	1.88	5.17	14.17	3.42	0.45	0.19	0.22	48.28
8/5/2009	Bailed sample	0.00	10.65	2.69	3.62	1.59	1.91	5.14	2.99	0.41	0.15	0.11	29.26
8/10/2009	Bailed sample	8.94	8.37	0.77	5.26	2.18	6.35	4.68	3.31	0.27	0.17	0.09	40.37
8/17/2009	Bailed sample	8.64	14.96	4.48	6.07	3.27	6.22	11.23	7.22	0.97	0.09	0.04	63.19
8/31/2009	Bailed sample	7.33	12.30	2.45	3.22	1.62	4.83	4.47	4.00	0.53	0.15	0.00	40.90
9/14/2009	Bailed sample	0.08	13.18	3.26	4.42	1.94	2.99	6.05	3.42	0.30	0.11	0.04	35.80
9/28/2009	Bailed sample	8.47	13.94	3.98	5.41	4.12	6.99	10.20	7.13	2.42	0.09	0.00	62.75
10/15/2009	Sampled after purge	4.51	7.48	1.69	2.29	1.00	4.32	2.57	1.65	0.06	0.00	0.00	25.55
10/15/2009	Bailed sample	7.13	11.18	2.44	3.38	4.00	4.93	6.37	4.12	0.37	0.00	0.00	43.91
10/26/2009	Bailed sample	7.33	14.16	4.17	6.51	3.69	3.98	5.90	6.72	1.69	0.05	0.00	54.21
11/6/2009	Sampled after purge	2.89	5.53	1.48	1.92	0.89	2.30	1.93	1.34	0.08	0.00	0.00	18.35
11/16/2009	Bailed sample	2.40	3.10	0.49	0.74	0.36	3.13	1.37	0.49	0.04	0.00	0.02	12.12
12/2/2009	Bailed sample	0.78	1.15	0.17	0.30	0.10	0.66	0.70	0.15	0.00	0.00	0.00	4.01
12/7/2009	Sampled after purge	0.76	1.04	0.20	0.38	0.26	1.41	0.35	0.23	0.00	0.04	0.00	4.68
12/14/2009	Bailed sample	3.97	5.92	1.44	2.22	1.26	5.14	4.45	2.26	0.73	0.01	0.00	27.40
12/14/2009	Duplicate	3.90	5.74	1.47	2.28	1.48	4.95	4.31	2.57	1.85	0.49	0.00	29.02
12/21/2009	Bailed sample	0.70	0.12	0.00	0.00	0.00	7.30	2.65	1.15	0.83	0.14	0.00	12.89
12/29/2009	Bailed sample	1.65	2.05	0.68	0.95	0.44	3.78	1.57	0.75	0.10	0.00	0.00	11.96
1/5/2010	Sampled after purge	0.54	0.57	0.28	0.28	0.11	2.03	0.46	0.22	0.01	0.00	0.00	4.51
1/11/2010	Bailed sample	1.06	1.47	0.38	0.54	0.26	1.70	1.01	0.37	0.02	0.00	0.00	6.82
1/19/2010	Bailed sample	1.48	1.83	0.61	0.90	0.44	3.90	1.22	0.50	0.31	0.05	0.00	11.25
MWN02A													
10/7/2008	Bailed sample	4.75	1.33	5.58	0.36	4.43	5.82	8.29	11.87	2.46	0.00	0.00	44.89
5/19/2009	Bailed sample	0.00	0.00	0.00	0.00	0.00	0.32	0.00	0.03	0.21	0.82	0.00	1.38
5/27/2009	Bailed sample	0.00	0.00	0.00	0.00	0.00	0.14	0.00	0.00	0.26	0.90	0.07	1.37

6/9/2009	Bailed sample	1.65	6.00	2.80	4.14	1.55	0.23	3.91	3.31	0.00	0.09	0.04	23.72
6/16/2009	Bailed sample	0.66	2.06	0.77	1.13	0.61	0.59	1.32	0.52	0.13	0.00	0.05	7.84
7/16/2009	Bailed sample	0.96	1.56	0.25	0.85	0.39	1.29	0.78	0.74	0.03	0.12	0.63	7.61
7/20/2009	Bailed sample	1.91	2.14	0.44	1.68	0.68	1.29	1.75	0.18	0.06	0.11	0.29	10.52
7/20/2009	Duplicate	1.29	2.77	0.98	1.74	0.71	0.98	2.06	0.21	0.00	0.21	0.13	11.09
7/29/2009	Bailed sample	1.11	2.63	0.89	1.76	0.84	0.98	1.14	1.52	0.22	0.15	0.08	11.32
8/5/2009	Bailed sample	1.06	2.58	0.77	1.78	0.84	0.89	1.21	1.32	0.15	0.00	0.00	10.61
8/10/2009	Bailed sample	1.44	3.83	1.08	0.13	0.98	1.17	1.57	1.17	0.07	0.08	0.04	11.56
8/17/2009	Bailed sample	1.52	4.73	1.61	2.87	1.36	1.28	1.85	2.26	0.20	0.00	0.04	17.71
8/31/2009	Bailed sample	1.47	3.42	0.96	1.88	0.92	1.16	1.77	1.50	0.15	0.14	0.00	13.36
9/14/2009	Bailed sample	0.97	2.76	0.35	1.74	0.75	1.00	1.15	1.02	0.00	0.15	0.00	9.89
9/28/2009	Bailed sample	1.36	2.76	1.03	1.77	0.88	1.70	1.55	1.44	0.12	0.12	0.00	12.73
10/15/2009	Sampled after purge	0.49	1.37	0.66	1.00	0.52	0.70	0.55	0.73	0.00	0.03	0.00	6.06
10/15/2009	Bailed sample	0.40	1.18	0.42	0.73	0.37	0.48	0.40	0.41	0.00	0.00	0.00	4.40
10/26/2009	Bailed sample	0.24	1.33	0.67	0.98	0.00	0.41	0.52	0.56	0.00	0.00	0.00	4.70
11/4/2009	Sampled after purge	0.00	0.00	0.00	0.00	0.00	0.25	0.00	0.00	0.00	0.00	0.00	0.25
11/16/2009	Bailed sample	0.00	0.00	0.00	0.00	0.00	0.24	0.00	0.00	0.00	0.00	0.00	0.24
11/25/2009	Bailed sample	0.05	0.00	0.00	0.00	0.00	0.89	0.02	0.00	0.00	0.00	0.00	0.96
12/2/2009	Bailed sample	0.00	0.00	0.00	0.00	0.00	0.37	0.00	0.03	0.00	0.15	0.00	0.56
12/9/2009	Bailed sample	0.00	0.00	0.00	0.00	0.00	0.70	0.00	0.00	0.00	0.00	0.00	0.70
12/14/2009	Sampled after purge	0.04	0.00	0.00	0.00	0.00	1.18	0.23	0.00	0.00	0.00	0.00	1.44
12/21/2009	Bailed sample	0.00	0.00	0.00	0.00	0.00	1.32	0.00	0.00	0.00	0.00	0.01	1.33
12/29/2009	Bailed sample	0.00	0.00	0.00	0.00	0.00	0.96	0.00	0.00	0.00	0.00	0.00	0.96
1/8/2010	Bailed sample	0.05	0.20	0.10	0.18	0.10	1.19	0.08	0.10	0.00	0.00	0.00	2.01
1/15/2010	Sampled after purge	0.00	0.00	0.00	0.00	0.00	2.00	0.00	0.00	0.00	0.00	0.01	2.01
1/19/2010	Bailed sample	0.00	0.00	0.00	0.00	0.00	1.30	0.00	0.00	0.00	0.00	0.00	1.30
MWN03A													
9/26/2008	Bailed sample	1.58	0.33	0.24	2.78	1.10	8.09	1.63	2.56	0.58	0.00	0.00	18.89
9/26/2008	Duplicate	1.60	0.29	0.22	2.78	1.09	8.04	1.27	2.50	0.67	0.00	0.00	18.46
10/7/2008	Bailed sample	1.37	0.13	0.35	3.17	1.24	6.50	0.88	3.02	0.93	0.00	0.00	17.59
10/15/2008	Bailed sample	1.68	0.00	0.00	2.37	0.11	9.51	1.31	1.88	0.25	0.00	0.00	17.10
11/19/2008	Bailed sample	111.44	20.34	9.50	14.40	12.04	537.95	245.27	17.12	2.36	0.14	0.00	970.58
6/10/2009	Bailed sample	12.16	13.52	2.31	3.40	1.54	2.89	11.46	2.56	0.48	0.06	0.00	50.37
6/17/2009	Bailed sample	23.03	27.58	3.82	5.57	2.07	17.39	14.02	1.34	0.00	0.00	0.11	94.93
7/20/2009	Bailed sample	14.54	8.47	1.48	2.10	1.26	25.56	13.74	0.49	0.22	0.27	0.06	68.19

Date	Type												
7/29/2009	Bailed sample	22.55	28.90	3.48	4.94	1.77	14.69	12.62	3.30	0.15	0.00	0.00	92.40
8/5/2009	Bailed sample	18.03	23.74	3.50	5.20	2.09	12.31	9.92	3.83	0.64	0.18	0.17	79.62
8/10/2009	Bailed sample	15.41	30.76	5.27	7.73	3.09	10.82	12.17	4.06	0.82	0.21	0.11	90.44
8/18/2009	Bailed sample	15.57	41.77	24.35	11.74	4.53	11.94	16.26	12.44	0.61	0.00	0.04	139.26
8/31/2009	Bailed sample	8.30	22.99	4.03	5.94	2.26	6.88	9.43	4.23	0.47	0.11	0.00	64.64
9/15/2009	Bailed sample	13.96	21.82	3.91	5.01	0.00	8.67	7.71	5.65	0.56	0.11	0.00	67.40
9/28/2009	Bailed sample	10.82	18.52	4.21	3.15	2.92	8.18	10.45	4.61	1.63	0.19	0.00	64.68
10/16/2009	Sampled after purge	2.98	4.77	1.08	2.12	0.90	2.90	2.02	1.40	0.05	0.00	0.00	18.20
10/16/2009	Bailed sample	7.30	9.99	2.69	4.06	2.15	7.06	10.03	3.46	0.21	0.00	0.00	46.94
10/26/2009	Bailed sample	6.54	12.25	4.15	6.68	3.17	5.60	7.21	5.80	1.25	0.00	0.00	52.66
11/5/2009	Sampled after purge	2.55	2.33	0.47	0.94	0.43	2.65	1.35	0.50	0.00	0.00	0.00	11.21
11/16/09	Bailed sample	3.15	3.22	1.31	2.27	1.14	2.13	4.59	2.25	0.76	0.19	0.02	21.04
12/2/2009	Bailed sample	0.77	1.14	0.23	0.35	0.17	0.91	1.09	0.25	0.04	0.00	0.00	4.94
12/8/2009	Sampled after purge	0.49	0.47	0.10	0.13	0.06	1.17	0.22	0.10	0.00	0.00	0.00	2.74
12/11/2009	Bailed sample	6.09	11.09	2.56	3.48	1.19	2.44	7.37	2.32	0.04	0.02	0.00	36.59
12/14/2009	Bailed sample	9.48	17.93	3.76	4.99	1.88	3.28	11.63	3.53	0.11	0.00	0.00	56.58
12/21/2009	Bailed sample	0.24	0.00	0.00	0.00	0.00	12.89	0.50	0.03	0.52	0.22	0.00	14.39
12/30/2009	Bailed sample	2.43	5.95	1.91	2.72	1.26	1.23	3.18	2.48	1.15	0.46	0.04	22.83
1/8/2010	Bailed sample	5.96	15.33	4.46	6.21	2.79	2.49	10.16	5.02	0.91	0.04	0.01	53.38
1/13/2010	Bailed sample	4.51	10.55	4.06	5.63	4.25	2.31	9.92	7.72	1.04	0.00	0.00	49.99
1/22/2010	Sampled after purge	4.00	5.51	1.36	1.82	1.53	3.29	10.96	2.07	0.24	0.00	0.00	30.78
MWN04A													
8/17/2008	Bailed sample	0.00	0.00	0.00	0.00	0.00	22.18	0.00	0.00	0.00	10.83	0.00	33.00
10/7/2008	Bailed sample	3.87	4.27	3.04	9.93	2.84	7.11	6.56	7.05	0.71	0.00	0.00	45.39
10/7/2008	Duplicate	3.77	3.97	2.85	7.17	2.63	7.13	6.27	6.49	0.76	0.00	0.00	41.05
10/15/2008	Bailed sample	3.58	4.28	2.59	7.03	1.92	5.89	4.56	4.89	0.87	0.09	0.00	35.71
6/11/2009	Bailed sample	4.30	4.37	1.78	3.83	2.40	0.47	2.94	2.35	0.43	0.10	0.03	23.00
6/18/2009	Bailed sample	5.96	10.64	2.46	3.87	1.57	7.08	6.38	1.40	0.50	0.04	0.03	39.93
6/18/2009	Duplicate	6.20	10.63	2.23	3.54	1.37	6.64	6.14	1.08	0.18	0.04	0.00	38.05
7/20/2009	Bailed sample	3.77	8.05	2.33	3.85	1.47	4.31	5.69	0.56	0.07	0.18	0.36	30.62
7/29/2009	Bailed sample	6.11	13.06	3.08	4.91	2.01	4.77	5.61	4.02	0.79	0.25	0.00	44.61
8/5/2009	Bailed sample	5.76	12.56	2.58	3.95	1.63	4.12	5.58	2.76	0.22	0.23	0.00	39.39
8/10/2009	Bailed sample	4.70	7.21	2.34	3.63	1.57	4.46	4.50	2.72	0.27	0.12	0.15	31.68
8/18/2009	Bailed sample	6.39	11.81	1.86	2.80	1.15	5.22	5.23	1.86	0.05	0.00	0.00	36.38
8/31/2009	Bailed sample	5.46	14.43	3.31	5.37	2.41	5.23	5.70	4.64	1.79	0.39	0.00	48.72

Date	Type												
9/15/2009	Bailed sample	6.11	13.06	2.48	3.88	1.53	5.29	4.94	2.37	0.28	0.06	0.00	40.01
9/29/2009	Bailed sample	11.66	16.05	4.42	6.40	4.21	14.61	23.20	8.01	1.63	0.04	0.00	90.23
10/20/2009	Sampled after purge	2.47	6.72	1.00	1.58	0.66	2.43	2.71	0.98	0.00	0.00	0.00	18.55
10/20/2009	Bailed sample	7.09	11.98	2.54	3.87	2.40	8.19	10.84	4.01	0.53	0.00	0.00	51.45
10/26/2009	Bailed sample	5.86	11.56	3.92	6.43	3.80	8.34	10.24	6.82	2.00	0.09	0.00	59.06
11/4/2009	Sampled after purge	1.92	2.96	0.72	1.14	0.39	2.67	1.28	0.61	0.00	0.00	0.00	11.70
11/17/2009	Bailed sample	1.03	1.81	0.51	0.91	0.40	1.96	1.24	0.54	0.00	0.00	0.00	8.40
12/11/2009	Bailed sample	0.49	0.42	0.18	0.32	0.11	1.17	0.31	0.23	0.01	0.00	0.00	3.24
12/17/2009	Sampled after purge	1.60	0.81	0.52	0.98	0.29	2.04	1.47	0.63	0.02	0.00	0.00	8.38
12/21/2009	Bailed sample	0.10	0.00	0.00	0.00	0.00	1.71	0.00	0.00	0.00	0.08	0.00	1.88
12/30/2009	Bailed sample	1.11	1.14	0.57	0.91	0.34	2.13	2.19	0.77	0.09	0.00	0.00	9.25
1/7/2010	Bailed sample	1.18	1.51	0.48	0.92	0.36	1.41	1.80	0.91	0.11	0.00	0.00	8.69
1/12/2010	Bailed sample	1.24	1.59	0.54	0.94	0.35	1.55	1.80	0.79	0.05	0.00	0.00	8.83
1/20/2010	Sampled after purge	0.55	0.27	0.16	0.37	0.11	0.77	0.40	0.17	0.00	0.00	0.00	2.79
MWN05A													
8/17/2008	Bailed sample	0.00	0.00	0.00	0.00	0.00	0.29	0.03	0.00	0.00	0.04	0.00	0.36
8/20/2008	Bailed sample	0.00	0.17	0.00	0.17	0.00	0.42	0.05	0.04	0.00	0.00	0.00	0.86
8/24/2008	Bailed sample	9.63	17.65	2.79	4.04	1.53	4.93	10.65	2.73	0.23	0.06	0.00	54.24
8/24/2008	Duplicate	13.75	25.36	4.39	6.56	3.14	5.49	15.96	5.24	0.60	0.00	0.00	80.49
8/25/2008	Bailed sample	10.43	15.84	2.90	4.49	1.50	4.05	10.12	3.18	0.32	0.00	0.00	52.84
9/26/2008	Bailed sample	11.01	12.44	0.34	6.42	3.37	5.62	14.01	5.21	0.98	0.08	0.00	59.50
10/7/2008	Bailed sample	11.12	10.62	4.38	6.97	3.74	8.33	14.92	6.76	0.95	0.03	0.00	67.82
10/15/2008	Bailed sample	15.26	15.35	4.28	6.58	3.10	8.79	16.39	5.66	0.68	0.00	0.00	76.08
11/19/2008	Bailed sample	1.77	5.08	1.36	2.53	1.15	0.21	2.44	1.87	0.19	0.03	0.09	16.72
11/19/2008	Bailed sample	29.06	21.66	6.94	11.90	5.31	8.53	22.95	8.68	1.26	0.00	0.00	116.29
2/11/2009	Bailed sample	20.06	22.41	5.55	9.82	6.71	3.97	15.05	12.13	3.02	0.21	0.03	98.96
5/27/2009	Bailed sample	1.13	0.00	0.00	0.00	0.00	0.68	1.00	0.00	0.41	0.97	0.05	4.24
6/11/2009	Bailed sample	9.50	9.89	2.58	4.90	1.34	8.30	6.76	1.19	0.07	0.19	0.07	44.80
6/16/2009	Bailed sample	3.97	13.88	2.89	4.16	1.45	5.99	7.28	0.97	0.00	0.06	0.04	40.70
7/17/2009	Bailed sample	18.35	17.79	3.23	3.81	1.71	13.37	9.00	4.17	0.09	0.00	0.00	71.53
7/20/2009	Bailed sample	27.22	33.30	6.78	10.12	3.72	18.93	17.69	1.33	0.17	0.21	0.15	119.62
7/29/2009	Bailed sample	30.74	32.75	3.25	7.57	3.35	18.58	21.24	5.69	0.96	0.07	0.11	124.30
8/5/2009	Bailed sample	25.89	27.72	3.91	5.57	2.33	15.72	10.87	3.82	0.31	0.14	0.07	96.37
8/10/2009	Bailed sample	35.53	45.76	7.52	11.04	5.01	20.43	45.51	8.63	2.05	0.45	0.00	181.93
8/17/2009	Bailed sample	18.79	26.37	3.96	5.84	3.13	12.43	10.14	5.77	1.78	0.04	0.05	88.31

8/17/2009	Duplicate	22.62	33.52	5.15	7.44	4.37	15.03	15.59	7.95	1.44	0.03	0.11	113.24
8/31/2009	Bailed sample	22.37	39.61	6.08	8.80	3.54	14.22	14.95	6.26	0.48	0.18	0.00	116.50
9/14/2009	Bailed sample	33.19	33.65	4.41	6.06	2.25	19.32	12.84	4.18	0.15	0.11	0.00	116.18
9/29/2009	Bailed sample	0.10	28.08	0.00	4.06	2.76	4.25	10.72	2.63	0.17	0.00	0.00	52.76
10/15/2009	Sampled after purge	18.96	23.78	2.30	2.97	1.17	11.21	7.80	1.83	0.05	0.00	0.00	70.07
10/15/2009	Bailed sample	18.42	25.70	3.76	5.30	1.08	13.20	13.02	4.36	0.49	0.08	0.00	85.41
10/26/2009	Bailed sample	20.60	2.09	15.07	9.55	3.98	17.67	6.57	10.90	0.32	0.00	0.00	86.75
11/5/2009	Sampled after purge	11.20	20.14	2.56	3.60	1.30	8.02	6.63	2.26	0.00	0.00	0.00	55.70
11/6/2009	Duplicate	10.51	16.41	1.81	2.51	0.94	7.81	5.45	1.47	0.00	0.00	0.00	46.90
11/16/2009	Bailed sample	10.32	24.34	3.83	5.25	1.78	10.95	10.01	3.46	0.08	0.00	0.00	70.01
11/16/2009	Duplicate	10.20	22.24	3.13	4.41	1.60	11.05	9.15	2.89	0.07	0.00	0.00	64.74
12/2/2009	Bailed sample	0.41	5.31	0.75	0.81	0.35	1.14	1.74	0.52	0.00	0.00	0.00	11.02
12/7/2009	Bailed sample	0.93	2.29	0.30	0.39	0.14	1.12	0.78	0.22	0.00	0.00	0.00	6.17
12/7/2009	Bailed sample	0.61	1.27	0.18	0.19	0.11	1.21	0.43	0.13	0.10	0.00	0.00	4.24
12/16/2009	Sampled after purge	4.42	11.26	3.18	4.32	1.68	12.74	5.86	2.96	0.08	0.01	0.00	46.52
12/21/2009	Bailed sample	4.11	8.89	1.89	2.49	1.03	3.61	4.52	0.71	0.09	0.07	0.00	27.41
12/30/2009	Bailed sample	7.72	15.24	2.52	2.77	1.29	4.94	8.82	2.15	0.11	0.00	0.00	45.57
1/8/2010	Bailed sample	11.03	23.72	3.70	3.85	2.06	4.75	9.11	2.18	0.04	0.00	0.00	60.44
1/12/2010	Bailed sample	6.60	14.76	3.01	3.08	1.44	3.91	9.48	1.72	0.01	0.00	0.00	44.01
1/20/2010	Sampled after purge	2.14	4.10	0.76	0.93	0.44	6.22	2.28	0.63	0.00	0.00	0.00	17.50
MWN06A													
8/17/2008	Bailed sample	0.00	0.19	0.00	0.12	0.00	0.09	0.06	0.03	0.00	0.05	0.00	0.54
8/20/2008	Bailed sample	0.00	0.00	0.00	0.00	0.00	0.44	0.00	0.03	0.00	0.00	0.00	0.47
8/24/2008	Bailed sample	3.75	0.00	0.00	2.90	0.00	9.68	2.63	1.03	0.05	0.00	0.03	20.07
8/25/2008	Bailed sample	10.75	6.18	3.92	9.27	7.54	0.00	37.47	12.08	3.00	0.37	0.03	90.61
8/27/2008	Bailed sample	1.48	0.66	0.45	0.95	0.16	6.90	3.74	1.77	0.43	0.03	0.00	16.58
8/29/2008	Bailed sample	0.23	0.00	0.00	0.00	0.00	1.18	0.27	0.00	0.00	0.00	0.00	1.68
9/2/2008	Bailed sample	4.22	1.74	1.02	2.82	1.39	6.70	7.59	2.48	0.22	0.10	0.00	28.27
9/9/2008	Bailed sample	1.39	1.21	1.29	2.44	0.99	3.22	1.96	2.23	0.28	0.00	0.00	15.00
9/16/2008	Bailed sample	2.44	1.81	1.05	2.42	0.47	3.42	2.83	1.64	0.08	0.00	0.00	16.17
9/26/2008	Bailed sample	1.85	1.81	1.02	1.89	0.70	3.43	2.20	1.37	0.07	0.00	0.00	14.34
10/7/2008	Bailed sample	2.89	2.65	2.05	5.02	1.43	5.40	3.17	4.00	0.93	0.11	0.00	27.65
10/15/2008	Bailed sample	3.58	3.34	2.15	4.96	1.05	9.48	3.91	3.58	0.62	0.00	0.00	32.70
5/27/2009	Bailed sample	0.24	0.00	0.00	0.00	0.00	0.23	0.21	0.00	0.00	0.00	0.00	0.67
6/11/2009	Bailed sample	1.64	6.27	3.63	5.48	2.32	1.26	5.58	2.22	0.56	0.25	0.00	29.20

6/19/2009	Bailed sample	1.38	5.17	0.68	4.31	2.15	1.83	5.54	2.29	0.58	0.18	0.00	24.12
7/20/2009	Bailed sample	0.73	1.49	0.23	0.30	0.10	0.92	0.77	0.04	0.08	0.00	0.12	4.78
7/29/2009	Bailed sample	2.05	2.80	3.62	5.15	5.53	2.03	12.05	10.90	2.59	0.07	0.11	46.90
8/5/2009	Bailed sample	0.88	2.18	1.48	2.41	1.17	1.15	1.95	2.04	0.34	0.20	0.07	13.86
8/10/2009	Bailed sample	1.01	2.59	1.59	2.35	1.58	1.12	3.43	2.56	0.50	0.03	0.04	16.80
8/18/2009	Bailed sample	0.64	1.03	1.19	1.94	1.25	0.91	2.28	2.28	0.16	0.00	0.07	11.75
8/31/2009	Bailed sample	0.56	0.78	0.70	1.18	0.52	0.91	0.54	1.17	0.08	0.25	0.07	6.77
9/15/2009	Bailed sample	0.40	0.32	0.40	1.31	0.86	0.63	0.60	1.52	0.47	0.21	0.03	6.76
9/29/2009	Bailed sample	0.82	0.70	0.70	1.63	0.94	1.41	1.49	1.75	0.07	0.07	0.00	9.59
10/16/2009	Bailed sample	0.47	0.83	0.49	0.82	0.40	0.87	0.45	0.57	0.04	0.00	0.00	4.94
10/26/2009	Bailed sample	0.57	1.05	0.63	0.96	0.88	0.86	1.55	1.27	0.13	0.06	0.00	7.94
11/3/2009	Sampled after purge	0.00	0.00	0.00	0.00	0.00	0.25	0.00	0.00	0.00	0.00	0.00	0.25
11/17/2009	Bailed sample	0.12	0.06	0.06	0.05	0.07	0.52	0.12	0.05	0.00	0.02	0.02	1.09
12/2/2009	Bailed sample	0.00	0.00	0.00	0.00	0.00	0.44	0.00	0.00	0.00	0.00	0.00	0.44
12/9/2009	Bailed sample	0.02	0.00	0.00	0.00	0.00	1.22	0.01	0.00	0.00	0.00	0.00	1.25
12/15/2009	Sampled after purge	0.32	0.00	0.16	0.19	0.11	0.83	0.42	0.21	0.01	0.00	0.00	2.25
12/21/2009	Bailed sample	0.00	0.00	0.00	0.20	0.07	1.23	0.34	0.06	0.03	0.04	0.00	1.96
12/30/2009	Bailed sample	0.16	0.26	0.24	0.32	0.61	0.66	0.83	0.92	0.67	0.41	0.00	5.07
1/7/2010	Bailed sample	0.20	0.10	0.18	0.33	0.23	0.50	0.49	0.48	0.02	0.00	0.00	2.54
1/12/2010	Bailed sample	0.11	0.22	0.23	0.38	0.16	0.41	0.31	0.19	0.02	0.00	0.01	2.04
1/18/2010	Sampled after purge	0.12	0.00	0.14	0.12	0.09	0.63	0.11	0.12	0.00	0.02	0.00	1.35

Date	Notes	Benzene	Toluene	Ethylbenzene	mpXylenes	oXylene	C6<=	C7C8	C9C10	C11C12	C13C14	C15>=	TPH
MWN01B													
8/25/2008	Bailed sample	17.60	1.47	4.34	6.61	4.12	12.02	15.05	6.32	0.86	0.00	0.00	68.39
9/2/2008	Bailed sample	0.60	0.00	0.26	0.33	0.20	0.57	0.29	0.25	0.07	0.00	0.00	2.57
9/9/2008	Bailed sample	14.70	0.31	2.92	4.83	1.53	7.63	6.96	3.00	0.08	0.00	0.00	41.95
9/16/2008	Bailed sample	21.87	0.22	4.65	7.61	2.11	9.15	10.24	4.85	0.18	0.00	0.00	60.87
10/2/2008	Bailed sample	26.27	1.70	11.34	18.88	3.12	14.93	16.51	13.87	2.35	0.14	0.00	109.11
10/8/2008	Bailed sample	3.70	1.27	1.44	1.90	0.74	2.58	2.66	2.66	1.31	0.00	0.00	18.26
10/16/2008	Bailed sample	13.36	3.21	3.28	4.73	3.38	9.90	15.48	6.83	1.38	0.03	0.00	61.56
10/29/2008	Bailed sample	14.77	6.55	2.10	3.17	1.16	8.04	9.46	2.10	0.05	0.03	0.00	47.42
5/27/2009	Bailed sample	0.00	0.00	0.00	0.00	0.00	0.09	0.00	0.00	0.93	1.98	0.17	3.17
6/9/2009	Bailed sample	5.07	8.15	1.81	2.55	0.97	2.25	6.79	1.36	0.10	0.05	0.05	29.14
6/15/2009	Bailed sample	21.83	21.07	0.80	3.80	1.43	4.97	9.08	0.78	0.00	0.00	0.03	63.78
7/21/2009	Bailed sample	25.01	27.71	4.34	6.27	2.72	15.37	13.84	1.64	0.15	0.10	0.19	97.33
7/28/2009	Bailed sample	39.74	39.35	2.09	7.49	3.28	21.59	15.06	4.35	0.41	0.15	0.07	133.57
8/4/2009	Bailed sample	36.32	34.40	4.82	7.02	3.11	20.73	12.97	5.45	1.08	0.25	0.00	126.15
8/17/2009	Bailed sample	30.89	33.45	5.33	7.58	2.96	18.29	12.88	5.36	0.13	0.03	0.08	116.97
9/1/2009	Bailed sample	22.33	22.49	3.84	5.28	2.86	15.36	10.57	5.23	0.57	0.14	0.00	88.67
9/14/2009	Bailed sample	22.04	22.02	2.93	4.14	1.74	27.44	7.98	2.94	0.36	0.00	0.00	91.59
9/28/2009	Bailed sample	31.54	28.44	3.81	5.28	2.38	21.21	11.47	3.94	0.17	0.11	0.04	108.39
10/14/2009	Sampled after purge	19.62	16.43	1.68	2.31	0.82	9.92	5.37	1.30	0.00	0.00	0.00	57.45
10/14/2009	Bailed sample	22.97	17.86	2.02	2.66	1.06	14.89	7.97	1.79	0.16	0.00	0.00	71.38
10/27/2009	Bailed sample	25.49	24.65	2.86	5.50	2.21	16.25	9.11	5.13	0.09	0.00	0.00	91.29
11/6/2009	Sampled after purge	16.16	16.21	1.94	2.78	0.96	9.62	5.23	1.67	0.00	0.00	0.00	54.58
11/16/09	Bailed sample	8.07	10.23	2.60	3.86	1.41	3.61	10.32	2.11	1.26	0.13	0.00	43.60
12/2/2009	Bailed sample	1.00	1.22	0.31	0.43	0.15	1.18	1.01	0.28	0.00	0.00	0.00	5.58
12/7/2009	Sampled after purge	1.47	1.07	0.20	0.26	0.09	2.34	0.68	0.03	0.00	0.00	0.00	6.13
12/14/2009	Bailed sample	8.11	5.83	1.05	1.29	0.58	5.18	7.85	0.71	0.00	0.00	0.00	30.59
12/21/2009	Bailed sample	4.74	1.58	0.14	0.44	0.18	13.46	1.29	0.51	0.23	0.10	0.00	22.67
12/29/2009	Bailed sample	3.68	1.01	0.33	0.05	0.12	8.30	1.24	0.72	0.38	0.45	0.02	16.30
1/6/2010	Sampled after purge	1.68	1.75	1.07	1.21	0.52	2.15	1.92	0.67	0.07	0.00	0.00	11.04
1/11/2010	Bailed sample	1.08	0.88	0.45	0.48	0.21	2.24	1.44	0.34	0.05	0.00	0.00	7.16
1/19/2010	Bailed sample	1.16	0.96	0.54	0.64	0.27	2.86	1.41	0.36	0.00	0.00	0.00	8.18
MWN02B													
8/25/2008	Bailed sample	19.63	0.31	3.25	4.61	0.23	10.49	8.99	2.79	0.09	0.04	0.00	50.44

Date													
8/27/2008	Bailed sample	23.49	0.84	3.34	4.83	0.25	8.90	10.96	2.81	0.09	0.00	0.00	55.51
8/29/2008	Bailed sample	13.98	0.61	1.87	3.74	1.24	7.38	8.07	3.08	0.25	0.06	0.00	40.28
9/2/2008	Bailed sample	12.99	1.19	2.68	5.59	2.11	6.03	9.64	4.40	0.93	0.04	0.00	45.61
9/9/2008	Bailed sample	22.59	3.60	4.16	9.35	2.38	9.15	12.35	4.95	1.09	0.00	0.03	69.65
9/16/2008	Bailed sample	23.65	4.56	5.00	10.50	2.65	9.93	14.07	6.83	0.83	0.00	0.00	78.02
10/2/2008	Bailed sample	18.04	4.02	7.88	16.06	10.42	11.09	31.53	20.88	4.09	0.11	0.00	124.11
10/16/2008	Bailed sample	20.13	3.78	3.40	6.77	2.96	52.24	15.36	6.57	1.06	0.00	0.00	112.28
10/29/2008	Bailed sample	148.44	29.82	13.97	20.68	11.02	584.60	284.67	17.41	0.62	0.04	0.00	1111.26
5/19/2009	Bailed sample	0.00	0.00	0.00	0.00	0.00	0.30	0.00	0.00	0.48	0.82	0.04	1.64
6/9/2009	Bailed sample	0.09	0.19	0.16	0.29	0.10	0.03	0.14	0.15	0.03	0.09	0.00	1.27
6/16/2009	Bailed sample	0.07	0.00	0.00	0.00	0.00	0.03	0.00	0.00	0.00	0.04	0.00	0.14
7/17/2009	Bailed sample	0.63	1.94	0.58	0.77	0.41	1.12	0.87	0.80	0.00	0.00	0.00	7.12
7/21/2009	Bailed sample	0.07	0.33	0.20	0.28	0.12	0.44	0.27	0.00	0.06	0.09	0.14	2.00
7/28/2009	Bailed sample	2.47	3.50	0.55	0.84	0.45	1.49	1.16	0.53	0.14	0.03	0.04	11.21
8/4/2009	Bailed sample	0.14	0.78	0.26	0.48	0.29	0.11	0.24	0.28	0.00	0.00	0.00	2.58
8/17/2009	Bailed sample	0.22	1.36	0.54	0.90	0.50	0.52	0.42	0.63	0.04	0.00	0.04	5.17
9/1/2009	Bailed sample	0.40	1.51	0.80	1.23	0.25	0.62	0.61	0.92	0.03	0.03	0.00	6.41
9/14/2009	Bailed sample	0.12	0.82	0.35	0.71	0.33	0.64	0.29	0.52	0.03	0.13	0.00	3.94
9/28/2009	Bailed sample	1.13	2.24	0.77	1.36	0.65	1.56	0.93	1.02	0.18	0.15	0.00	9.98
10/14/2009	Sampled after purge	0.16	0.00	0.00	0.00	0.00	0.45	0.11	0.00	0.00	0.03	0.00	0.76
10/14/2009	Bailed sample	0.23	0.65	0.00	0.00	0.00	0.38	0.20	0.00	0.00	0.09	0.00	1.54
10/30/2009	Bailed sample	0.00	0.33	0.00	0.38	0.19	0.31	0.10	0.15	0.00	0.00	0.00	1.47
11/4/2009	Sampled after purge	0.00	0.27	0.11	0.22	0.10	0.25	0.08	0.09	0.00	0.00	0.00	1.12
11/16/09	Bailed sample	0.00	0.00	0.00	0.00	0.00	0.22	0.00	0.00	0.00	0.00	0.11	0.33
11/24/2009	Bailed sample	0.22	0.25	0.00	0.00	0.00	0.74	0.19	0.00	0.00	0.00	0.00	1.41
12/2/2009	Bailed sample	0.00	0.00	0.00	0.00	0.00	0.56	0.00	0.00	0.00	0.00	0.00	0.56
12/9/2009	Bailed sample	0.00	0.00	0.00	0.00	0.00	0.41	0.00	0.00	0.00	0.00	0.00	0.41
12/21/2009	Bailed sample	0.00	0.00	0.00	0.00	0.00	1.03	0.00	0.00	0.00	0.00	0.00	1.03
12/29/2009	Bailed sample	0.00	0.00	0.00	0.00	0.00	1.00	0.00	0.00	0.00	0.00	0.00	1.00
1/8/2010	Bailed sample	0.03	0.12	0.07	0.14	0.06	1.38	0.05	0.07	0.00	0.00	0.00	1.93
1/15/2010	Sampled after purge	0.00	0.00	0.00	0.00	0.00	1.35	0.00	0.00	0.00	0.00	0.00	1.35
1/19/2010	Bailed sample	0.00	0.00	0.00	0.00	0.00	1.14	0.00	0.00	0.00	0.00	0.00	1.14
MWN03B													
8/16/2008	Bailed sample	0.00	0.00	0.00	0.00	0.00	0.42	0.00	0.04	0.06	0.03	0.00	0.55
8/25/2008	Bailed sample	13.61	12.78	1.63	2.41	3.95	2.28	10.18	2.64	0.07	0.04	0.00	49.58

9/2/2008	Bailed sample	11.36	11.83	1.52	2.25	1.14	2.06	8.92	1.66	0.07	0.00	0.00	40.80
9/9/2008	Bailed sample	19.45	21.30	4.52	8.25	4.11	2.95	16.13	6.95	1.31	0.03	0.05	85.05
9/16/2008	Bailed sample	20.02	19.02	3.10	5.37	2.64	3.22	15.44	4.53	0.38	0.00	0.00	73.72
10/2/2008	Bailed sample	12.08	0.64	3.30	5.77	3.53	3.47	6.70	6.08	1.82	0.05	0.00	43.42
10/8/2008	Bailed sample	12.42	11.72	2.20	3.66	2.08	2.68	9.29	3.36	0.50	0.00	0.00	47.92
10/16/2008	Bailed sample	17.53	15.01	2.32	3.71	2.11	4.35	13.68	3.10	0.62	0.00	0.00	62.43
10/29/2008	Bailed sample	7.82	5.27	0.82	0.75	0.61	2.60	5.37	0.65	0.00	0.00	0.00	23.89
5/19/2009	Bailed sample	18.18	0.00	1.73	2.56	1.09	4.44	14.95	1.70	0.22	0.98	0.18	46.03
6/10/2009	Bailed sample	25.02	28.52	4.43	6.27	2.07	8.82	25.44	3.22	0.00	0.04	0.06	103.90
6/18/2009	Bailed sample	3.53	5.46	1.28	0.16	1.06	3.30	2.75	1.50	0.62	0.16	0.04	19.86
7/21/2009	Bailed sample	14.38	21.70	3.35	4.33	3.94	12.64	12.57	0.60	0.00	0.24	0.07	73.81
7/28/2009	Bailed sample	43.46	54.10	9.34	13.09	7.60	35.93	57.02	13.23	1.59	0.21	0.10	235.65
8/4/2009	Bailed sample	24.34	25.73	1.87	4.52	1.86	14.31	10.48	2.86	0.25	0.12	0.05	86.39
8/18/2009	Bailed sample	22.71	26.07	3.91	5.38	2.26	14.46	11.24	3.76	0.08	0.00	0.05	89.93
9/1/2009	Bailed sample	12.01	19.33	2.91	4.21	1.67	8.44	7.79	1.92	0.14	0.09	0.00	58.52
9/15/2009	Bailed sample	13.21	23.53	0.00	5.90	2.30	9.82	8.87	2.88	0.21	0.07	0.00	66.79
9/28/2009	Bailed sample	11.08	14.73	2.60	3.66	1.31	10.10	7.14	2.52	0.05	0.08	0.11	53.38
10/13/2009	Bailed sample	17.09	18.92	4.64	6.67	3.89	16.60	24.92	7.51	1.25	0.00	0.00	101.49
10/13/2009	Sampled after purge	0.99	1.13	0.54	0.91	0.46	1.22	0.59	0.69	0.00	0.05	0.00	6.58
10/27/2009	Bailed sample	7.50	12.30	3.71	5.86	3.19	6.64	9.38	5.62	0.92	0.06	0.06	55.25
11/5/2009	Sampled after purge	0.89	0.99	0.31	0.44	0.23	0.79	0.63	0.32	0.00	0.00	0.00	4.60
11/17/09	Bailed sample	12.27	13.05	3.02	4.31	1.98	7.39	19.07	3.61	0.20	0.05	0.13	65.08
12/8/2009	Sampled after purge	0.17	0.13	0.06	0.09	0.05	0.71	0.11	0.05	0.00	0.00	0.00	1.37
12/11/2009	Bailed sample	0.37	0.49	0.00	0.20	0.07	0.80	0.36	0.11	0.00	0.01	0.00	2.41
12/14/2009	Bailed sample	9.82	12.04	2.56	3.90	1.50	3.85	10.74	2.71	0.08	0.00	0.00	47.19
12/21/2009	Bailed sample	6.18	6.34	1.10	1.59	0.62	6.05	3.34	0.27	0.01	0.00	0.01	25.52
12/30/2009	Bailed sample	6.63	1.62	0.10	0.00	1.86	11.80	2.44	1.04	1.17	0.55	0.00	27.22
1/8/2010	Bailed sample	5.55	9.33	3.75	5.37	4.60	2.00	12.01	8.41	1.62	0.02	0.00	52.66
1/13/2010	Bailed sample	6.79	9.24	4.15	5.98	5.45	6.45	12.21	9.55	1.55	0.00	0.00	61.38
1/22/2010	Sampled after purge	1.13	1.13	0.29	0.36	0.23	0.58	0.94	0.16	0.00	0.00	0.00	4.82
MWN04B													
8/16/2008	Bailed sample	0.00	0.00	0.00	0.00	0.00	0.22	0.00	0.10	0.00	0.03	0.06	0.42
8/25/2008	Bailed sample	11.71	10.03	1.83	2.58	1.30	2.39	8.58	2.09	0.10	0.00	0.00	40.61
8/27/2008	Bailed sample	14.74	11.92	1.60	2.09	1.00	3.63	10.34	1.37	0.00	0.00	0.00	46.69
8/29/2008	Bailed sample	14.84	10.90	1.42	1.81	0.88	4.20	10.06	1.28	0.00	0.03	0.00	45.43

Date	Type												
9/2/2008	Bailed sample	13.70	12.86	1.22	2.35	1.16	2.66	10.40	1.58	0.06	0.00	0.00	45.99
9/9/2008	Bailed sample	19.93	20.46	4.26	6.30	3.27	4.26	16.12	5.75	0.60	0.00	0.00	80.96
9/16/2008	Bailed sample	26.81	18.49	2.72	3.59	1.96	3.58	18.02	2.86	0.09	0.00	0.00	78.11
10/2/2008	Bailed sample	20.00	19.60	4.02	12.39	2.86	6.33	16.81	7.96	1.67	0.07	0.00	91.71
10/8/2008	Bailed sample	10.29	9.78	2.04	2.88	1.50	2.60	8.02	2.66	0.39	0.00	0.00	40.16
10/17/2008	Bailed sample	16.80	15.64	2.69	3.54	1.76	0.82	12.86	2.92	0.12	0.00	0.00	57.16
10/29/2008	Bailed sample	1.14	1.12	0.13	0.45	0.24	1.50	1.09	0.28	0.03	0.00	0.04	6.02
5/19/2009	Bailed sample	1.18	0.09	0.67	1.23	0.53	1.76	3.21	0.66	0.42	0.96	0.00	10.72
6/11/2009	Bailed sample	13.37	28.34	7.22	11.63	5.00	4.83	15.30	4.16	0.68	0.38	0.00	90.90
6/19/2009	Bailed sample	5.45	0.29	3.25	6.04	6.24	3.76	4.68	7.29	0.60	0.06	0.00	37.66
7/21/2009	Bailed sample	6.75	6.25	2.68	5.24	4.12	5.22	6.65	6.58	1.61	0.43	0.11	45.64
7/28/2009	Bailed sample	7.98	6.61	1.62	3.48	1.91	4.14	2.05	2.53	0.20	0.10	0.12	30.76
8/4/2009	Bailed sample	7.02	16.04	1.68	3.45	2.06	3.73	5.23	2.95	0.51	0.21	0.04	42.92
8/18/2009	Bailed sample	7.04	6.83	1.83	3.76	2.01	4.23	2.22	2.84	0.22	0.00	0.00	30.99
9/1/2009	Bailed sample	6.35	7.99	2.78	5.21	4.64	4.36	3.74	8.43	2.78	0.39	0.05	46.70
9/15/2009	Bailed sample	2.19	3.44	1.41	2.89	2.82	1.90	1.81	4.87	1.87	0.08	0.00	23.29
9/29/2009	Bailed sample	2.33	4.18	1.96	3.49	2.10	2.64	3.28	3.23	0.12	0.00	0.00	23.34
10/9/2009	Bailed sample	0.48	1.33	0.27	0.40	0.22	0.53	0.52	0.29	0.00	0.04	0.00	4.07
10/30/2009	Bailed sample	3.49	8.66	1.71	3.13	2.08	2.57	3.00	3.86	2.17	0.20	0.00	30.87
11/4/2009	Sampled after purge	0.93	2.68	0.61	0.89	0.40	1.60	0.83	0.51	0.00	0.00	0.00	8.45
11/17/2009	Bailed sample	1.04	2.31	0.65	0.94	0.50	1.44		0.77	0.12	0.03	0.02	7.83
11/24/2009	Bailed sample	0.29	0.28	0.00	0.05	0.00	0.87	0.23	0.01	0.00	0.00	0.00	1.73
12/11/2009	Bailed sample	0.24	0.59	0.08	0.10	0.06	0.49	0.30	0.07	0.00	0.00	0.00	1.93
12/17/2009	Sampled after purge	3.33	11.96	2.38	2.91	1.34	1.93	5.62	1.48	0.05	0.00	0.00	31.00
12/21/2009	Bailed sample	0.38	1.29	0.00	0.16	0.90	1.49	3.24	0.62	0.01	0.00	0.00	8.09
12/30/2009	Bailed sample	0.39	2.67	0.59	0.88	0.35	1.11	1.57	0.63	0.00	0.00	0.04	8.23
1/7/2010	Bailed sample	1.86	5.33	1.20	1.79	0.86	1.49	4.03	1.27	0.04	0.00	0.00	17.87
1/13/2010	Bailed sample	2.84	6.29	1.99	2.65	2.20	2.49	10.79	3.68	0.43	0.00	0.00	33.37
1/20/2010	Sampled after purge	1.80	0.88	0.87	0.20	0.44	0.94	1.40	0.18	0.00	0.00	0.00	6.70
MWN05B													
8/16/2008	Bailed sample	0.00	0.00	0.00	0.00	0.00	0.00	0.00	0.00	0.00	0.00	0.00	0.00
8/25/2008	Bailed sample	27.73	8.42	1.83	2.28	0.91	9.59	15.01	1.64	0.00	0.00	0.00	67.40
9/2/2008	Bailed sample	23.06	9.78	3.29	3.93	1.66	19.51	18.02	3.70	0.07	0.00	0.00	83.02
9/9/2008	Bailed sample	18.38	6.76	2.46	4.31	1.94	7.21	10.68	5.53	0.12	0.00	0.04	57.43
9/16/2008	Bailed sample	20.99	7.85	2.63	3.68	0.25	7.23	12.15	2.23	0.00	0.00	0.00	57.00

Date	Type												
10/2/2008	Bailed sample	9.70	6.52	2.05	3.00	1.41	3.97	6.42	2.54	0.26	0.00	0.00	35.88
10/8/2008	Bailed sample	16.47	10.47	3.46	2.81	2.44	5.98	10.92	3.54	0.65	0.00	0.00	56.74
10/17/2008	Bailed sample	12.10	4.47	1.68	0.68	1.02	6.82	7.16	1.09	0.04	0.00	0.00	35.05
10/29/2008	Bailed sample	2.25	1.52	0.71	0.48	0.27	5.90	4.17	0.46	0.03	0.00	0.00	15.79
11/19/2008	Bailed sample	206.07	103.30	59.49	87.91	77.66	677.82	500.81	134.82	35.09	7.67	0.97	1891.61
12/12/2008	Bailed sample	141.89	68.57	8.93	11.70	7.35	581.16	272.32	13.39	0.48	0.00	0.09	1105.89
6/11/2009	Bailed sample	15.27	14.24	2.28	3.31	1.34	14.30	8.80	1.10	0.21	0.07	0.05	60.98
6/17/2009	Bailed sample	16.53	17.04	3.25	3.87	1.86	12.81	9.45	24.66	6.82	0.09	0.03	96.42
7/17/2009	Bailed sample	11.81	10.93	1.97	2.25	0.99	10.03	6.37	2.39	0.04	0.00	0.00	46.78
7/21/2009	Bailed sample	12.73	16.50	3.09	4.72	1.83	9.64	9.80	0.87	0.11	0.11	0.04	59.45
7/28/2009	Bailed sample	12.05	13.53	2.36	3.81	0.94	8.85	5.24	2.99	0.31	0.16	0.14	50.38
8/4/2009	Bailed sample	12.48	15.60	2.30	3.43	1.66	18.89	6.46	2.86	0.40	0.13	0.05	64.26
8/17/2009	Bailed sample	20.33	23.03	3.48	5.10	2.31	13.36	8.70	3.82	0.37	0.00	0.03	80.53
9/2/2009	Bailed sample	14.62	14.20	2.68	3.98	0.00	11.29	8.92	3.20	0.45	0.09	0.00	59.43
9/14/2009	Bailed sample	36.46	37.16	4.91	6.79	2.58	21.04	14.35	5.47	0.12	0.33	0.00	129.20
9/29/2009	Bailed sample	16.29	14.73	2.10	2.69	1.22	12.57	7.31	1.97	0.03	0.03	0.00	58.94
10/14/2009	Sampled after purge	2.99	4.66	1.18	1.67	0.67	2.58	2.46	1.12	0.00	0.00	0.00	17.34
10/14/2009	Bailed sample	12.48	11.25	2.23	3.11	1.84	11.51	11.62	2.73	0.23	0.00	0.00	57.01
10/27/2009	Bailed sample	19.17	24.19	6.80	10.27	5.50	15.08	16.27	10.01	1.96	0.03	0.00	109.29
11/5/2009	Sampled after purge	2.40	2.55	1.10	1.69	0.76	2.04	1.20	1.17	0.05	0.00	0.00	12.98
MWN06B													
8/16/2008	Bailed sample	0.00	0.00	0.00	0.00	0.00	0.40	0.00	0.04	0.00	0.00	0.00	0.44
8/25/2008	Bailed sample	17.22	13.10	2.45	3.32	1.67	10.07	14.37	2.32	0.04	0.00	0.00	64.55
8/27/2008	Bailed sample	8.57	9.16	2.72	4.13	1.80	4.91	7.60	3.18	0.16	0.00	0.00	42.24
8/29/2008	Bailed sample	0.86	0.25	0.34	0.57	0.15	3.29	0.69	0.39	0.00	0.00	0.00	6.54
9/2/2008	Bailed sample	1.31	0.73	0.67	1.13	0.53	3.05	2.01	0.88	0.13	0.12	0.00	10.55
9/9/2008	Bailed sample	3.92	0.00	0.00	5.11	1.22	3.45	3.06	0.00	0.27	0.07	0.00	17.11
9/16/2008	Bailed sample	2.47	1.38	0.82	1.43	0.51	5.09	2.76	0.94	0.04	0.00	0.00	15.45
10/2/2008	Bailed sample	1.69	1.34	0.78	1.33	0.45	3.52	1.87	0.93	0.05	0.00	0.00	11.96
10/8/2008	Bailed sample	6.16	7.15	1.98	3.15	1.18	4.90	6.36	2.21	0.09	0.00	0.00	33.17
10/17/2008	Bailed sample	5.07	6.66	2.23	3.57	1.86	3.98	7.57	3.33	0.38	0.04	0.00	34.70
10/29/2008	Bailed sample	6.14	11.04	3.37	5.86	3.10	4.84	8.37	5.09	0.68	0.00	0.00	48.49
6/11/2009	Bailed sample	1.14	2.30	0.45	0.19	0.36	0.09	0.99	0.44	0.00	0.04	0.03	6.04
6/19/2009	Bailed sample	1.91	3.13	0.81	1.20	0.70	1.19	1.86	0.51	0.11	0.07	0.03	11.50
7/21/2009	Bailed sample	1.07	1.99	0.59	0.92	0.24	0.80	1.37	0.16	0.15	0.17	0.08	7.54

7/28/2009	Bailed sample	1.73	3.32	0.84	1.33	0.42	1.17	1.21	0.98	0.21	0.17	0.05	11.44
8/4/2009	Bailed sample	2.60	3.75	0.73	1.09	0.54	1.78	1.35	0.60	0.08	0.19	0.12	12.83
8/18/2009	Bailed sample	1.56	2.41	0.81	1.25	0.85	1.35	0.00	1.15	0.03	0.00	0.08	9.49
9/1/2009	Bailed sample	3.42	6.22	1.83	3.02	1.65	2.53	2.70	2.89	0.29	0.06	0.00	24.60
9/15/2009	Bailed sample	3.45	6.04	1.57	2.74	1.20	2.61	2.21	2.58	0.51	0.17	0.00	23.08
9/29/2009	Bailed sample	1.85	3.17	1.03	1.82	0.89	2.02	1.54	1.43	0.14	0.25	0.00	14.14
10/9/2009	Bailed sample	0.08	0.22	0.11	0.25	0.18	0.16	0.10	0.15	0.00	0.04	0.00	1.28
10/30/2009	Bailed sample	1.18	1.72	0.50	0.92	0.15	1.04	0.75	0.61	0.00	0.00	0.00	6.89
11/3/2009	Sampled after purge	0.00	0.00	0.00	0.00	0.00	0.39	0.00	0.00	0.00	0.00	0.00	0.39
11/17/2009	Bailed sample	0.19	0.12	0.10	0.13	0.06	0.52	0.12	0.08	0.00	0.00	0.00	1.31
12/9/2009	Bailed sample	0.02	0.00	0.00	0.00	0.00	1.23	0.01	0.00	0.00	0.00	0.00	1.27
12/15/2009	Sampled after purge	0.05	0.00	0.00	0.00	0.00	0.94	0.05	0.00	0.00	0.00	0.00	1.04
12/21/2009	Bailed sample	0.07	0.07	0.07	0.15	0.00	0.85	0.08	0.02	0.00	0.00	0.00	1.32
12/30/2009	Bailed sample	0.00	0.00	0.00	0.00	0.00	0.98	0.00	0.00	0.00	0.02	0.00	1.01
1/7/2010	Bailed sample	0.13	0.05	0.05	0.08	0.06	0.54	0.14	0.05	0.00	0.00	0.00	1.10
1/12/2010	Bailed sample	0.10	0.09	0.13	0.19	0.09	0.43	0.08	0.11	0.00	0.00	0.00	1.23
1/18/2010	Sampled after purge	0.04	0.00	0.00	0.00	0.00	0.47	0.02	0.00	0.00	0.00	0.00	0.53

Date	Notes	Benzene	Toluene	Ethylbenzene	mpXylenes	oXylene	C6<=	C7C8	C9C10	C11C12	C13C14	C15>=	TPH
MWN01C													
8/25/2008	Bailed sample	2.29	0.53	0.47	0.50	0.17	1.76	1.25	0.31	0.03	0.00	0.10	7.40
9/2/2008	Bailed sample	2.23	0.21	0.37	0.25	0.00	3.01	1.27	0.17	0.00	0.00	0.00	7.53
9/7/2008	Bailed sample	1.88	0.09	0.40	0.13	0.00	3.92	1.27	0.19	0.00	0.00	0.00	7.88
9/14/2008	Bailed sample	1.53	0.00	0.00	0.00	0.00	2.28	1.11	0.48	0.00	0.00	0.00	5.41
10/8/2008	Bailed sample	1.25	0.00	0.25	0.12	0.00	2.45	1.09	0.17	0.00	0.00	0.00	5.33
10/16/2008	Bailed sample	1.20	0.10	0.53	0.49	0.46	1.93	1.12	1.43	0.42	0.00	0.00	7.68
10/29/2008	Bailed sample	0.77	0.20	0.30	0.36	0.15	0.93	0.52	0.22	0.00	0.00	0.00	3.45
5/19/2009	Bailed sample	1.62	0.00	0.00	0.00	0.00	0.20	1.14	0.00	0.00	0.56	0.00	3.53
5/27/2009	Bailed sample	0.27	0.00	0.00	0.00	0.00	0.00	0.19	0.00	0.45	1.86	0.15	2.92
6/9/2009	Bailed sample	1.83	2.23	0.56	0.75	0.33	0.73	2.03	0.46	0.00	0.09	0.04	9.04
6/15/2009	Bailed sample	1.13	1.47	0.32	0.38	0.19	0.15	0.64	0.06	0.04	0.00	0.04	4.42
7/16/2009	Bailed sample	1.69	1.66	0.33	0.36	0.22	1.40	0.67	0.39	0.11	2.82	1.49	11.13
7/22/2009	Bailed sample	1.40	1.78	1.54	0.00	0.37	1.99	1.43	0.27	0.25	0.45	0.42	9.90
7/27/2009	Bailed sample	0.25	0.29	0.00	0.12	0.00	0.65	0.20	0.03	0.04	0.14	0.11	1.84
8/3/2009	Bailed sample	3.01	3.46	0.64	0.91	0.45	1.82	1.17	0.62	0.16	0.07	0.15	12.46
8/26/2009	Bailed sample	1.91	2.55	0.71	1.30	0.53	1.54	0.85	0.96	0.17	0.07	0.00	10.58
9/9/2009	Bailed sample	1.17	1.58	0.47	0.72	0.39	1.00	0.49	0.46	0.00	0.07	0.00	6.35
9/22/2009	Bailed sample	1.42	1.44	0.37	0.52	0.25	1.41	0.45	0.31	0.04	0.00	0.00	6.20
10/7/2009	Bailed sample	0.00	0.00	0.00	0.00	0.00	0.06	0.00	0.00	0.00	0.00	0.03	0.09
10/20/2009	Bailed sample	1.36	2.12	0.76	1.29	0.61	0.89	0.69	0.85	0.00	0.00	0.00	8.57
11/2/2009	Sampled after purge	0.00	0.10	0.11	0.11	0.12	0.21	0.03	0.12	0.00	0.00	0.00	0.80
11/10/2009	Bailed sample	1.34	0.40	0.44	0.78	0.33	0.25	0.80	0.47	0.00	0.00	0.00	4.81
11/17/09	Bailed sample	0.78	0.99	0.29	0.48	0.20	0.66	0.69	0.35	0.01	0.00	0.00	4.46
11/23/2009	Bailed sample	0.19	0.15	0.00	0.00	0.00	0.57	0.05	0.00	0.00	0.00	0.00	0.96
12/7/2009	Bailed sample	0.11	0.11	0.00	0.00	0.00	1.09	0.03	0.00	0.00	0.00	0.00	1.34
12/16/2009	Sampled after purge	0.39	0.00	0.05	0.05	0.00	5.52	0.27	0.01	0.00	0.00	0.00	6.29
12/21/2009	Bailed sample	0.15	0.37	0.13	0.65	0.00	4.19	0.40	0.33	0.21	0.18	0.00	6.60
12/29/2009	Bailed sample	0.44	0.48	0.16	0.27	0.13	2.59	0.15	0.15	0.00	0.08	0.00	4.46
1/6/2010	Sampled after purge	0.04	0.04	0.15	0.11	0.00	6.00	0.15	0.00	0.00	0.00	0.00	6.48
1/11/2010	Bailed sample	0.29	0.29	0.11	0.15	0.06	1.59	0.23	0.09	0.00	0.00	0.00	2.83
1/19/2010	Bailed sample	0.31	0.25	0.10	0.14	0.05	2.49	0.11	0.05	0.00	0.00	0.00	3.50
1/19/2010	Duplicate	0.36	0.28	0.06	0.12	0.06	2.43	0.26	0.05	0.00	0.00	0.00	3.62
MWN02C													

8/27/2008	Bailed sample	0.81	0.34	0.14	0.25	0.00	1.13	0.46	0.10	0.00	0.00	0.00	3.25
8/29/2008	Bailed sample	1.90	0.67	0.27	0.45	0.19	1.78	1.08	0.25	0.00	0.03	0.00	6.62
8/29/2008	Duplicate	2.44	0.87	0.00	0.45	0.22	2.00	1.37	0.25	0.00	0.00	0.00	7.61
9/2/2008	Bailed sample	39.70	19.00	8.60	13.93	5.54	38.08	27.03	7.24	0.20	0.04	0.00	159.34
9/7/2008	Bailed sample	3.75	0.85	0.73	0.97	0.28	7.39	2.42	0.39	0.00	0.00	0.00	16.78
9/14/2008	Bailed sample	3.84	0.84	1.72	2.67	0.74	4.15	2.27	1.96	0.09	0.11	0.00	18.38
9/14/2008	Duplicate	3.48	0.71	1.30	2.03	0.60	3.94	2.04	1.37	0.05	0.00	0.00	15.53
10/2/2008	Bailed sample	4.49	0.82	1.33	2.10	0.60	6.02	2.86	1.53	0.06	0.00	0.00	19.80
10/8/2008	Bailed sample	4.78	1.01	1.42	2.13	0.00	3.67	2.69	1.42	0.06	0.00	0.00	17.18
10/16/2008	Bailed sample	2.61	0.67	0.00	1.74	0.76	2.05	1.35	1.49	0.22	0.00	0.00	10.88
10/29/2008	Bailed sample	3.92	0.88	1.97	3.18	1.59	3.92	4.39	2.36	0.05	0.00	0.00	22.26
6/9/2009	Bailed sample	0.22	6.13	5.63	8.06	5.01	0.13	8.19	8.20	0.67	0.23	0.00	42.46
6/16/2009	Bailed sample	0.25	4.61	3.46	5.09	2.13	0.22	4.05	1.97	0.23	0.17	0.00	22.20
7/16/2009	Bailed sample	0.61	9.17	6.68	7.84	3.63	1.09	4.01	9.17	0.45	0.00	0.38	43.05
7/22/2009	Bailed sample	0.32	6.63	5.99	9.42	3.96	1.05	4.26	6.03	0.82	0.69	0.00	39.16
7/27/2009	Bailed sample	0.66	8.28	0.00	8.31	3.37	0.29	2.95	4.28	0.00	0.14	0.09	28.37
8/3/2009	Bailed sample	1.11	12.94	6.99	10.10	4.62	0.79	4.98	7.65	1.12	0.13	0.12	50.55
8/26/2009	Bailed sample	1.33	7.37	4.07	6.07	2.58	0.81	2.45	4.65	0.68	0.17	0.03	30.19
9/9/2009	Bailed sample	0.00	13.32	7.01	10.89	4.95	0.76	4.63	8.25	0.92	0.10	0.00	50.85
9/22/2009	Bailed sample	2.64	7.97	3.04	4.69	1.93	2.27	2.76	3.22	0.09	0.07	0.00	28.68
10/7/2009	Bailed sample	0.21	0.51	0.25	0.42	0.14	0.44	0.22	0.22	0.00	0.06	0.00	2.46
10/20/2009	Bailed sample	3.19	7.89	2.78	4.67	1.98	2.09	2.96	3.58	0.35	0.00	0.00	29.50
11/2/2009	Sampled after purge	0.10	0.14	0.12	0.15	0.17	0.30	0.04	0.12	0.00	0.00	0.00	1.14
11/11/09	Bailed sample	2.09	4.45	1.21	2.11	0.80	0.97	2.81	1.39	0.25	0.00	0.09	16.17
11/17/2009	Bailed sample	1.75	3.52	1.12	2.02	0.85	1.45	1.58	1.58	0.24	0.07	0.00	14.19
11/23/2009	Bailed sample	0.23	0.30	0.00	0.12	0.00	0.53	0.09	0.03	0.00	0.00	0.00	1.30
12/2/2009	Bailed sample	0.34	0.21	0.18	0.32	0.13	0.56	0.07	0.20	0.00	0.03	0.00	2.03
12/9/2009	Bailed sample	0.47	1.14	0.38	0.75	0.27	1.02	0.41	0.39	0.05	0.00	0.00	4.89
12/14/2009	Sampled after purge	0.32	0.22	0.25	0.14	0.11	3.85	0.43	0.20	0.00	0.00	0.00	5.52
12/21/2009	Bailed sample	0.16	0.00	0.35	0.00	0.00	1.37	0.97	0.16	0.04	0.00	0.00	3.05
12/21/2009	Duplicate	0.00	0.00	0.00	0.05	0.00	2.64	0.54	0.01	0.00	0.00	0.00	3.25
12/29/2009	Bailed sample	0.91	1.78	0.52	1.01	0.37	0.61	1.19	0.67	0.02	0.00	0.00	7.08
1/8/2010	Bailed sample	1.69	4.40	1.60	3.20	1.62	0.88	3.30	2.92	0.66	0.00	0.00	20.27
1/15/2010	Sampled after purge	1.50	0.09	0.21	0.20	0.05	5.07	0.69	0.12	0.00	0.00	0.00	7.94
1/19/2010	Bailed sample	0.94	1.61	0.59	1.22	0.42	0.86	1.23	0.91	0.04	0.00	0.00	7.84

MWN03C												
8/25/2008	Bailed sample	1.57	0.86	0.20	0.30	0.14	0.07	0.99	0.17	0.00	0.00	0.00	4.31
9/2/2008	Bailed sample	2.21	0.99	0.37	0.51	0.15	2.92	1.35	0.32	0.00	0.00	0.00	8.82
9/7/2008	Bailed sample	0.00	0.34	0.19	0.21	0.10	2.04	0.19	0.11	0.00	0.00	0.00	3.19
9/14/2008	Bailed sample	1.27	0.47	0.31	0.44	0.11	1.73	0.75	0.23	0.00	0.00	0.00	5.31
10/2/2008	Bailed sample	0.78	0.33	0.27	0.40	0.12	1.49	0.44	0.28	0.00	0.00	0.00	4.11
10/8/2008	Bailed sample	1.74	0.68	0.43	0.61	0.00	2.08	1.01	0.38	0.00	0.00	0.00	6.93
10/16/2008	Bailed sample	1.31	0.60	0.30	0.61	0.30	2.31	0.85	0.51	0.08	0.00	0.00	6.89
10/29/2008	Bailed sample	1.77	0.80	0.46	0.72	0.29	2.17	1.12	0.56	0.04	0.00	0.00	7.94
10/29/2008	Bailed sample	1.69	0.64	0.37	0.46	0.00	2.34	1.02	0.26	0.00	0.00	0.00	6.77
5/19/2009	Bailed sample	0.36	0.00	0.00	0.00	0.31	0.29	0.39	0.17	0.43	1.07	0.08	3.10
5/29/2009	Bailed sample	0.32	0.00	0.00	0.00	0.00	0.15	0.28	0.00	0.10	1.05	0.08	1.98
6/9/2009	Bailed sample	2.22	3.84	0.75	1.17	0.57	0.26	2.43	0.61	0.09	0.22	0.04	12.20
6/23/2009	Bailed sample	3.27	6.04	1.12	1.89	0.71	1.95	2.80	0.44	0.00	0.00	0.00	18.21
7/22/2009	Bailed sample	7.74	14.66	5.09	8.49	3.48	5.32	6.50	4.99	0.76	0.70	0.28	58.01
7/27/2009	Bailed sample	7.93	13.69	3.25	5.19	1.97	5.36	5.75	3.55	0.35	0.18	0.03	47.26
7/27/2009	Duplicate	7.52	12.56	2.66	4.06	1.63	5.19	5.08	2.84	0.25	0.05	0.09	41.92
8/3/2009	Bailed sample	6.73	10.56	2.54	4.02	1.57	4.65	4.50	2.85	0.20	0.00	0.10	37.72
8/3/2009	Duplicate	12.52	12.11	3.26	5.30	2.30	7.39	5.29	4.08	0.73	0.11	0.05	53.13
8/26/2009	Bailed sample	3.82	6.07	2.02	3.14	1.26	3.19	2.45	2.30	0.13	0.18	0.00	24.55
9/9/2009	Bailed sample	3.53	7.06	2.73	4.49	1.97	1.02	2.50	3.21	0.18	0.07	0.00	26.75
9/22/2009	Bailed sample	3.66	4.92	1.44	2.16	0.93	3.49	2.23	1.38	0.00	0.10	0.00	20.31
10/7/2009	Sampled after purge	0.50	0.92	0.38	0.52	0.27	0.82	0.41	0.35	0.00	0.00	0.00	4.17
10/21/2009	Bailed sample	1.00	2.99	0.78	0.40	0.60	2.14	1.12	0.66	0.06	0.00	0.00	9.74
11/3/2009	Sampled after purge	0.45	0.57	0.12	0.21	0.00	0.66	0.18	0.09	0.00	0.00	0.00	2.29
11/11/2009	Bailed sample	2.42	2.78	0.63	0.95	0.43	1.83	1.04	0.55	0.00	0.00	0.00	10.62
11/17/09	Bailed sample	1.22	2.47	0.57	0.92	0.37	0.68	1.50	0.59	0.00	0.00	0.20	8.51
11/17/09	Duplicate	1.31	2.62	0.51	0.77	0.32	0.72	1.60	0.47	0.00	0.00	0.12	8.45
11/23/2009	Bailed sample	0.38	0.51	0.09	0.11	0.13	0.76	0.36	0.09	0.00	0.00	0.01	2.45
11/23/2009	Duplicate	0.35	0.57	0.13	0.19	0.08	0.89	0.33	0.11	0.00	0.00	0.00	2.67
12/11/2009	Bailed sample	2.42	4.18	1.10	1.72	0.60	1.39	3.32	1.08	0.02	0.00	0.00	15.84
12/16/2009	Sampled after purge	4.13	2.30	1.47	0.49	0.61	2.27	3.11	0.87	0.03	0.00	0.00	15.30
12/16/2009	Duplicate	4.56	2.79	2.00	0.67	0.94	2.29	3.53	1.25	0.04	0.00	0.00	18.07
12/21/2009	Bailed sample	0.00	0.00	0.00	0.00	0.00	3.19	0.04	0.00	0.00	0.00	0.00	3.23
12/30/2009	Bailed sample	2.15	1.32	0.00	0.00	0.00	3.75	0.82	0.16	0.14	0.02	0.00	8.35

1/8/2010	Bailed sample	5.22	10.13	2.70	4.27	1.63	1.96	6.58	2.34	0.21	0.00	0.00	35.05
1/13/2010	Bailed sample	2.16	3.08	0.83	1.25	0.54	1.27	2.57	0.84	0.03	0.00	0.00	12.56
1/21/2010	Sampled after purge	2.49	3.29	0.80	0.69	0.34	1.14	2.49	0.31	0.00	0.00	0.00	11.55
MWN04C													
8/25/2008	Bailed sample	0.87	0.37	0.19	0.82	0.12	1.19	0.53	0.40	0.00	0.03	0.00	4.51
8/27/2008	Bailed sample	0.71	0.78	0.26	0.41	0.13	1.58	0.59	0.22	0.00	0.03	0.00	4.70
8/29/2008	Bailed sample	0.95	0.53	0.14	0.27	0.00	1.92	0.62	0.11	0.00	0.00	0.00	4.53
9/2/2008	Bailed sample	0.76	0.39	0.18	0.29	0.14	1.71	0.45	0.20	0.00	0.00	0.00	4.12
9/7/2008	Bailed sample	0.39	0.14	0.11	0.17	0.10	0.29	0.21	0.10	0.00	0.00	0.00	1.50
9/14/2008	Bailed sample	0.80	0.27	0.12	0.28	0.10	1.45	0.47	0.14	0.00	0.00	0.04	3.67
10/2/2008	Bailed sample	0.45	0.15	0.00	0.26	0.11	1.20	0.24	0.10	0.00	0.00	0.07	2.58
10/8/2008	Bailed sample	0.93	0.34	0.24	0.41	0.14	0.12	0.51	0.27	0.05	0.00	0.00	3.01
10/17/2008	Bailed sample	1.03	0.41	0.35	0.45	0.15	2.36	0.66	0.31	0.00	0.00	0.03	5.75
10/29/2008	Bailed sample	0.94	0.34	0.18	0.33	0.10	1.80	0.51	0.20	0.00	0.00	0.04	4.43
5/19/2009	Bailed sample	0.09	0.00	0.00	0.00	0.00	0.34	0.04	0.00	0.08	0.91	0.14	1.60
6/10/2009	Bailed sample	0.47	1.23	0.52	0.84	0.32	0.04	0.80	0.49	0.03	0.13	0.07	4.96
6/19/2009	Bailed sample	0.71	4.49	0.53	0.00	0.64	0.73	1.62	0.55	0.15	0.00	0.00	9.42
7/22/2009	Bailed sample	1.16	44.48	2.06	3.52	1.63	0.80	13.91	3.07	0.50	0.34	0.46	71.95
7/27/2009	Bailed sample	1.39	4.22	1.57	2.52	1.06	1.21	1.56	2.01	0.27	0.24	0.11	16.15
8/3/2009	Bailed sample	1.47	3.79	1.09	4.17	0.85	1.25	1.45	2.01	0.20	0.21	0.08	16.57
8/26/2009	Bailed sample	3.19	8.46	2.81	4.62	1.72	2.89	3.82	3.56	0.32	0.16	0.00	31.56
9/9/2009	Bailed sample	4.41	12.03	3.07	4.81	1.99	0.82	4.40	3.43	0.11	0.08	0.00	35.15
9/23/2009	Bailed sample	5.78	13.72	3.04	4.52	1.05	4.34	5.72	2.96	0.09	0.05	0.00	41.28
10/6/2009	Sampled after purge	0.08	0.14	0.00	0.32	0.20	0.28	0.04	0.14	0.03	0.06	0.00	1.30
10/20/2009	Bailed sample	3.73	8.01	1.65	2.40	0.91	2.86	3.23	1.56	0.04	0.00	0.00	24.38
11/2/2009	Sampled after purge	0.08	0.16	0.12	0.14	0.12	0.29	0.20	0.11	0.00	0.00	0.00	1.22
11/11/09	Bailed sample	2.00	3.91	1.11	1.63	0.66	1.31	3.07	1.14	0.05	0.01	0.05	14.93
11/17/2009	Bailed sample	3.36	6.78	2.03	3.12	1.43	2.80	4.47	2.80	0.41	0.04	0.00	27.25
11/23/2009	Bailed sample	0.29	0.36	0.06	0.12	0.04	0.87	0.28	0.06	0.00	0.00	0.00	2.08
12/11/2009	Bailed sample	0.14	0.23	0.04	0.06	0.00	0.64	0.07	0.03	0.00	0.00	0.00	1.22
12/17/2009	Sampled after purge	0.43	0.47	0.26	0.35	0.12	1.15	0.67	0.13	0.00	0.00	0.00	3.57
12/21/2009	Bailed sample	2.17	0.93	0.00	0.00	0.00	4.64	0.77	0.23	0.09	0.28	0.06	9.18
12/30/2009	Bailed sample	2.32	4.10	1.19	1.71	0.70	1.41	3.06	1.19	0.03	0.00	0.00	15.71
12/30/2009	Duplicate	0.00	0.43	0.00	0.00	0.00	3.76	0.64	0.00	0.00	0.00	0.00	4.83
1/7/2010	Bailed sample	4.64	12.73	4.03	6.29	2.64	1.35	6.86	5.05	1.05	0.16	0.00	44.79

1/13/2010	Bailed sample	2.27	5.11	2.20	3.48	1.62	2.27	3.81	3.24	1.71	0.44	0.00	26.14
1/18/2010	Sampled after purge	0.05	0.00	0.00	0.00	0.00	0.22	0.02	0.00	0.00	0.00	0.00	0.29
MWN05C													
8/25/2008	Bailed sample	2.07	2.68	0.51	0.37	0.36	1.73	1.81	0.34	0.00	0.00	0.00	9.87
9/2/2008	Bailed sample	1.50	2.73	0.75	0.56	0.53	2.67	3.27	0.30	0.00	0.00	0.00	12.31
9/7/2008	Bailed sample	2.45	3.69	1.08	0.78	0.87	0.19	2.29	0.82	0.04	0.00	0.00	12.21
9/14/2008	Bailed sample	3.12	4.66	1.43	1.01	1.12	2.43	2.92	1.22	0.05	0.00	0.00	17.97
10/2/2008	Bailed sample	2.46	3.51	1.62	0.85	0.94	2.10	2.23	1.63	0.07	0.00	0.03	15.45
10/8/2008	Bailed sample	3.64	4.45	1.14	0.78	0.83	3.91	3.15	0.87	0.04	0.00	0.00	18.80
10/17/2008	Bailed sample	2.10	2.60	0.78	0.54	0.62	2.38	1.89	0.64	0.04	0.00	0.00	11.60
10/29/2008	Bailed sample	1.56	2.15	0.65	0.50	0.49	1.64	1.42	0.45	0.03	0.00	0.00	8.88
5/19/2009	Bailed sample	0.40	0.00	0.00	0.00	0.00	1.67	0.22	0.00	0.12	0.91	0.07	3.40
5/27/2009	Bailed sample	0.00	0.00	0.00	0.00	0.00	0.21	0.03	0.00	0.40	1.15	0.13	1.93
6/11/2009	Bailed sample	0.48	0.60	0.31	0.47	0.00	1.24	0.39	0.04	0.00	0.12	0.00	3.66
6/17/2009	Bailed sample	16.34	37.03	2.96	10.77	3.92	9.62	15.77	2.97	0.51	0.00	0.03	99.94
7/16/2009	Bailed sample	0.91	1.15	0.67	0.86	0.47	2.27	0.51	0.93	0.00	0.00	0.26	8.05
7/22/2009	Bailed sample	0.95	1.47	0.78	1.29	0.00	1.87	0.72	0.64	0.24	0.49	0.24	8.68
7/27/2009	Bailed sample	1.17	1.60	0.63	1.00	0.45	2.09	0.52	0.72	0.24	0.08	0.09	8.60
8/4/2009	Bailed sample	1.41	2.05	0.88	1.34	0.63	2.41	0.72	1.17	0.22	0.16	0.00	10.99
8/26/2009	Bailed sample	1.52	2.36	1.06	1.80	0.74	2.01	0.87	1.44	0.20	0.13	0.03	12.18
9/9/2009	Bailed sample	1.50	2.28	1.82	2.88	1.46	1.46	0.81	2.31	0.10	0.08	0.00	14.70
9/22/2009	Bailed sample	2.01	3.01	1.02	1.75	0.58	2.52	1.03	1.83	0.12	0.00	0.00	13.89
10/7/2009	Bailed sample	0.42	0.00	0.19	0.13	0.00	0.52	0.00	0.09	0.04	0.00	0.00	1.38
10/21/2009	Bailed sample	1.03	1.42	0.43	0.74	0.43	0.61	0.47	0.49	0.00	0.00	0.00	5.63
11/3/2009	Sampled after purge	0.00	0.11	0.12	0.24	0.18	0.37	0.04	0.15	0.00	0.00	0.00	1.21
11/11/2009	Bailed sample	1.29	1.53	0.40	0.67	0.32	0.78	1.07	0.38	0.00	0.00	0.00	6.45
11/17/09	Bailed sample	0.21	0.28	0.11	0.10	0.07	0.60	0.18	0.07	0.00	0.02	0.03	1.65
12/7/2009	Bailed sample	0.28	0.21	0.00	0.00	0.00	0.56	0.19	0.00	0.00	0.09	0.04	1.38
12/7/2009	Duplicate	0.28	0.25	0.07	0.09	0.05	1.70	0.11	0.04	0.00	0.00	0.00	2.60
12/16/2009	Sampled after purge	2.39	0.33	0.74	0.51	0.22	11.03	1.34	0.58	0.05	0.01	0.00	17.20
12/21/2009	Bailed sample	0.00	0.00	0.05	0.16	0.00	3.59	0.45	0.07	0.36	0.04	0.00	4.72
12/30/2009	Bailed sample	0.76	1.02	0.33	0.48	0.22	0.70	0.69	0.31	0.00	0.00	0.00	4.51
1/8/2010	Bailed sample	1.23	2.19	0.68	1.08	0.56	1.50	0.73	0.77	0.04	0.00	0.00	8.77
1/12/2010	Bailed sample	0.55	1.12	0.42	0.59	0.26	0.78	0.62	0.34	0.00	0.00	0.00	4.68
1/20/2010	Sampled after purge	1.16	0.00	0.19	0.08	0.04	8.06	0.56	0.03	0.00	0.00	0.00	10.12

MWN06C												
8/25/2008	Bailed sample	1.96	1.12	0.24	0.31	0.11	2.08	1.20	0.18	0.00	0.00	0.00	7.19
8/25/2008	Duplicate	2.02	1.04	0.21	0.29	0.11	2.32	1.21	0.17	0.00	0.03	0.00	7.40
8/27/2008	Bailed sample	3.52	1.99	0.53	0.69	0.24	3.26	3.36	0.97	0.03	0.03	0.00	14.62
8/29/2008	Bailed sample	2.90	1.40	0.31	0.27	0.10	2.69	1.73	0.18	0.00	0.03	0.00	9.62
9/2/2008	Bailed sample	3.00	1.54	0.32	0.44	0.17	3.69	1.83	0.40	0.00	0.04	0.00	11.44
9/7/2008	Bailed sample	6.47	4.18	0.99	1.14	0.49	4.49	4.24	0.80	0.03	0.00	0.00	22.84
9/14/2008	Bailed sample	5.62	3.40	0.90	1.00	0.49	4.47	3.59	0.78	0.03	0.00	0.00	20.28
10/2/2008	Bailed sample	8.48	5.10	1.53	1.52	0.69	4.91	5.51	1.23	0.06	0.00	0.00	29.03
10/8/2008	Bailed sample	8.69	4.90	2.87	1.41	0.66	14.46	7.82	2.11	0.19	0.00	0.00	43.12
10/17/2008	Bailed sample	6.75	4.20	1.50	1.50	0.63	5.25	4.62	1.25	0.04	0.00	0.00	25.74
10/29/2008	Bailed sample	3.70	1.61	0.63	0.71	0.40	2.92	3.13	0.59	0.07	0.00	0.00	13.75
10/30/2008	Bailed sample	5.41	1.60	3.63	3.47	5.53	0.03	7.12	9.84	3.85	0.21	0.00	40.68
5/19/2009	Bailed sample	0.00	0.00	0.00	0.00	0.00	0.12	0.00	0.00	0.36	1.05	0.00	1.53
5/27/2009	Bailed sample	0.00	0.00	0.00	0.00	0.00	0.15	0.00	0.00	0.32	0.88	0.00	1.34
6/11/2009	Bailed sample	0.07	0.26	0.20	0.44	0.30	0.29	0.25	0.23	0.43	0.10	0.00	2.55
6/23/2009	Bailed sample	0.00	0.22	0.10	0.22	0.12	0.22	0.15	0.04	0.03	0.07	0.00	1.17
7/22/2009	Bailed sample	0.00	0.16	0.13	0.29	0.15	0.45	0.12	0.12	0.17	0.69	0.04	2.33
7/27/2009	Bailed sample	0.14	0.57	0.15	0.46	0.23	0.67	0.21	0.34	0.71	0.12	0.06	3.65
8/3/2009	Bailed sample	0.13	0.00	0.30	0.68	0.30	0.40	0.09	0.57	1.19	0.06	0.04	3.76
8/26/2009	Bailed sample	0.09	0.41	0.24	0.58	0.25	0.34	0.16	0.33	0.00	0.06	0.00	2.46
9/9/2009	Bailed sample	0.11	1.23	0.87	1.56	0.83	0.40	0.38	1.43	0.18	0.04	0.00	7.03
9/22/2009	Bailed sample	0.16	1.98	0.47	0.00	0.52	0.18	0.61	0.68	0.49	0.09	0.00	5.18
10/6/2009	Sampled after purge	0.00	0.00	0.00	0.00	0.00	0.12	0.00	0.00	0.00	0.00	0.00	0.12
10/6/2009	Duplicate	0.00	0.00	0.00	0.00	0.00	0.11	0.00	0.00	0.00	0.00	0.00	0.11
11/2/2009	Sampled after purge	0.06	0.25	0.14	0.17	0.28	0.39	0.42	0.16	0.00	0.00	0.00	1.88
11/11/09	Bailed sample	0.12	1.55	0.20	0.54	0.22	0.60	0.53	0.27	0.00	0.00	0.07	4.11
11/17/2009	Bailed sample	0.09	1.98	0.15	0.54	0.22	0.34	0.61	0.24	0.00	0.00	0.04	4.22
11/23/2009	Bailed sample	0.03	0.13	0.00	0.06	0.00	0.76	0.05	0.02	0.00	0.00	0.00	1.05
12/9/2009	Bailed sample	0.14	0.06	0.00	0.00	0.00	0.83	0.08	0.00	0.00	0.00	0.00	1.11
12/9/2009	Sampled after purge	0.14	0.08	0.05	0.07	0.05	0.82	0.13	0.05	0.00	0.00	0.02	1.40
12/16/2009	Bailed sample	0.44	0.38	0.04	0.20	0.10	0.83	0.41	0.08	0.00	0.00	0.00	2.49
12/21/2009	Bailed sample	0.00	0.00	0.00	0.00	0.00	0.90	0.08	0.00	0.00	0.00	0.00	0.99
12/30/2009	Bailed sample	0.00	0.00	0.00	0.00	0.00	0.37	0.00	0.00	0.00	0.00	0.00	0.37
1/7/2010	Bailed sample	0.41	0.38	0.09	0.21	0.11	0.32	0.37	0.10	0.00	0.00	0.00	2.00

| 1/12/2010 | Bailed sample | 0.23 | 0.23 | 0.09 | 0.20 | 0.09 | 0.50 | 0.20 | 0.10 | 0.00 | 0.00 | 0.00 | 1.64 |
| 1/20/2010 | Sampled after purge | 0.17 | 0.00 | 0.00 | 0.00 | 0.00 | 0.71 | 0.07 | 0.00 | 0.00 | 0.00 | 0.00 | 0.96 |

Appendix E

Multi-Component NAPL Mass Transfer under Varied Flow Conditions

A sequence of one-dimensional column tests were performed to allow a direct comparison of mass transfer under different flow conditions from a multi-component nonaqueous phase liquid (NAPL).

Experimental Setup

The NAPL consisted of three primary components as follows:

Mineral Oil	85.1% by weight	80.2% by volume
o-Xylene	9.9% by weight	14.1% by volume
Trichloroethylene (TCE)	5.0% by weight	5.7% by volume

The mineral oil was effectively insoluble and non-volatile at the testing temperatures and was considered inert. TCE has a relatively high solubility compared to o-xylene (i.e., 1100 mg/L compared 175 mg/L) and is more volatile. The column dimensions and the sand pack properties were:

Column Length	45.7 cm
Column Diameter	7.0 cm
Column Volume	1,752 cm^3
Sand Pack Mesh	#2-/16
Average Sand Grain Size	1.0 mm
Sand Porosity	0.38
Dry Air Permeability	863 darcies
NAPL Volume	24 cm^3
NAPL Saturation	10.1%

The NAPL was emplaced in a 16.5-cm length of the column by mixing the NAPL, sand and residual water to attain a uniform 10.1% NAPL saturation in the pore space. The column was oriented vertically with injection at the top and extraction of effluent from the bottom. The column also featured five T-type thermocouples placed at the cross-sectional center of the column and equally spaced along the length of the column (separated by a distance of 7.6 cm). Two pressure ports were also located 15.2 and 30.4 cm from the injection point. The column setup with instrumentation is pictured in Figure E-1. The picture also shows the steam generator used to provide energy injection along with the water supply powered by a constant flow peristaltic pump. An air compressor (not shown) supplied air for injection. The air flow rate was controlled by a flowmeter to provide a constant injection rate. The steam and air was mixed, when desired, to provide energy injection to heat the column and provide temperature-dependent data on mass transfer from a NAPL in unsaturated soil. Samples of effluent were analyzed using an HP 6890 gas chromatograph (GC) with flame ionization detector. The GC was calibrated to detect TCE and o-xylene in both water and vapor samples over the range of concentrations observed in the bench-scale testing.
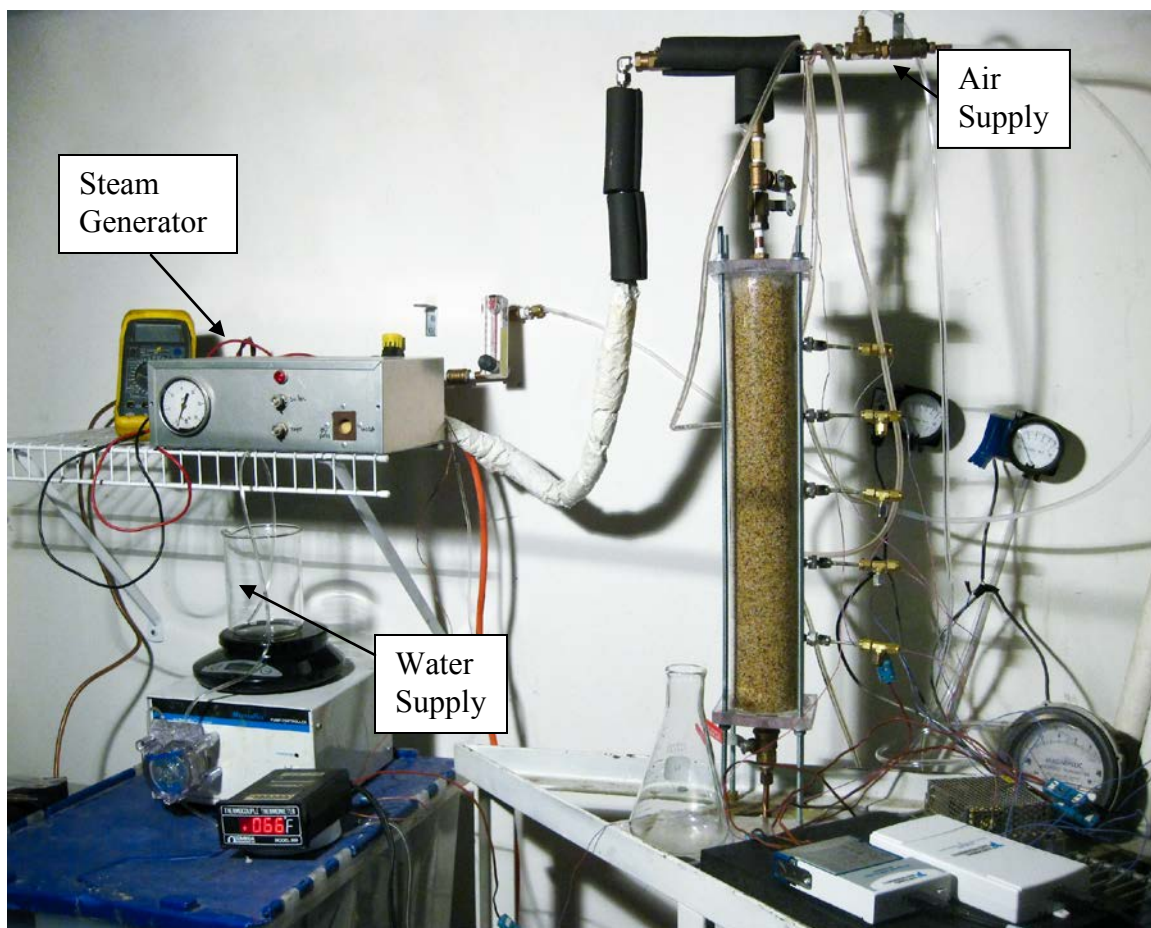
Figure E-1. Column Setup with Instrumentation

Overview of Mass Transfer Tests Performed

The sequence of procedures performed after the emplacement of the NAPL was as follows:

	Saturate the column with water (648 g) and rest for about 53 hours
Test 1.	Dissolution test with water flow at 3.514 g/min for 311 minutes
	Drain the column to residual saturation (507 g) and rest 15 hours
Test 2a.	Volatilization test with air flow at 0.66 Lpm for 12 minutes
Test 2b.	Volatilization test with air flow at 2.36 Lpm for 7 minutes
	Rest period (24 hours)
Test 3a.	Volatilization test with air flow at 0.94 Lpm mixed with steam flow at 0.73 g/min for 218 minutes
Test 3b.	Volatilization test with air flow at 0.94 Lpm mixed and no steam flow for 90 minutes
	Rest period (24 hours)
Test 4a.	Volatilization test with air flow at 0.94 Lpm for 4 minutes
Test 4b.	Volatilization test with air flow at 2.36 Lpm for 4 minutes
	Saturate the column with water (512 g)
	Rest period (48 hours)
Test 5.	Dissolution test with water flow at 3.40 g/min
	Drain the column to residual saturation (525 g)
Test 6a.	Volatilization test with air flow at 0.94 Lpm for 16 minutes
Test 6b.	Volatilization test with air flow at 2.36 Lpm for 120 minutes

The results of each test are discussed in the following sections.

Test 1: Initial Dissolution Test with Water Flow through the NAPL Zone

As described above, the 3-component NAPL was uniformly emplaced in a section of the column at a residual saturation of 10.1%. Given the high permeability of the sand pack, a portion of the NAPL was likely mobile and the final residual saturation lower. The column was saturated with 648 g of water from the bottom up and this process may have mobilized some of the NAPL yielding a non-uniform saturation in the column. The column was allowed to rest undisturbed for 53 hours before water injection was initiated. The Test 1 dissolution measurements were performed with a steady water injection rate of 3.514 g/min for 311 minutes corresponding to the injection of 1,093 g of water. An equivalent volume was recovered. The temperature of the column was held constant at 18.5 °C. The injection rate of water corresponds to a Darcy velocity of 0.092 cm/min and an interstitial velocity of 0.243 cm/min.

The concentration histories of TCE and o-xylene are provided in Figure E-2. Figure E-3 illustrates the calculated cumulative masses extracted. The large variability in concentrations is the likely result of a partially mobile NAPL and a non-uniform NAPL distribution. Average mass extraction rates for TCE and o-xylene were 0.733 and 0.313 mg/min, respectively, and mass fluxes were 0.0191 and 0.00817 mg/min/cm^2, respectively. Given the initial mole fraction (i.e., volume fraction) of each compound in the NAPL and its theoretical pure component solubility, the ideal maximum concentration of each compound at the start of the dissolution test was as follows:

Initial Ideal TCE Solubility Limit = (1,100 mg/L) * 0.057 = 63 mg/L
Initial Ideal o-Xylene Solubility Limit = (175 mg/L) * 0.141 = 25 mg/L

Based on the average mass extraction rates, the average effluent concentrations for TCE and o-xylene were 209 and 89 mg/L, respectively. Hence, the concentrations of both compounds were roughly 3 and a half times higher than the ideal solubility limit. TCE was 3.3 times higher and o-xylene was 3.6 times higher. At the end of this initial dissolution test, the TCE had been reduced by 206 mg and the o-xylene by 84 mg. The final mole fractions of the compounds, as estimated by the calculated masses removed, were 4.7% and 13.7% for TCE and o-xylene, respectively.

At the completion of Test 1, the column was drained to a residual liquid. The total water extracted was 507g containing estimated masses of 88 mg and 35 mg of TCE and o-xylene, respectively. The final residual water saturation was calculated to be 25%.
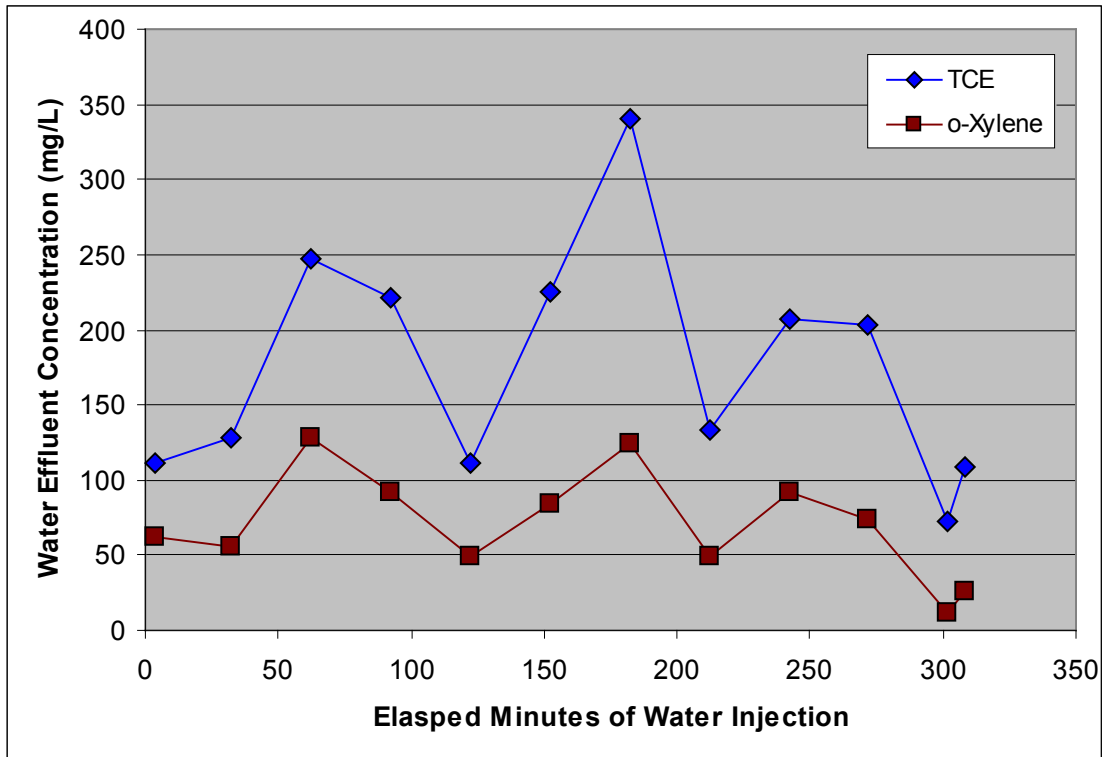
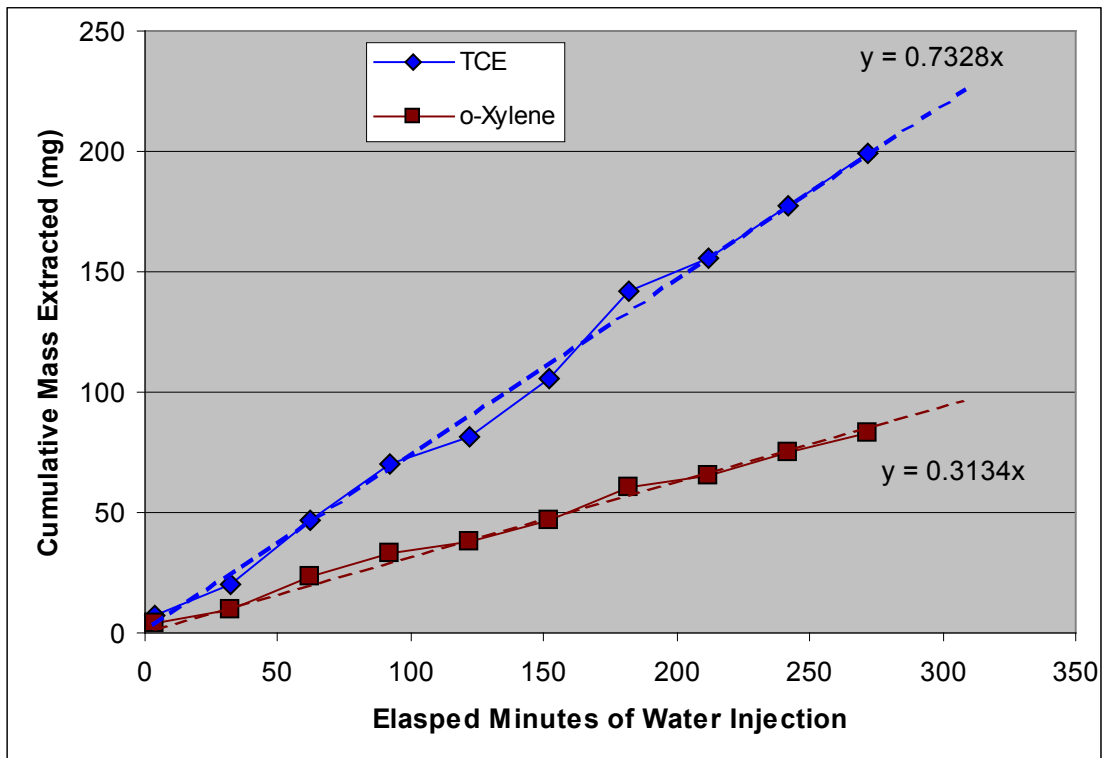**Figure E-2. Effluent Dissolved Concentrations Measured during Test 1**

Figure E-3. Cumulative Masses Extracted during Test 1

The ratio of the dissolved TCE concentration to the o-xylene concentration in the water effluent is plotted in Figure E-4 as a function of the water injection duration. The ratio of concentrations is shown to be commensurate with the ideal theoretical value of 2.5 for the initial mole fractions (i.e., 63 / 25).
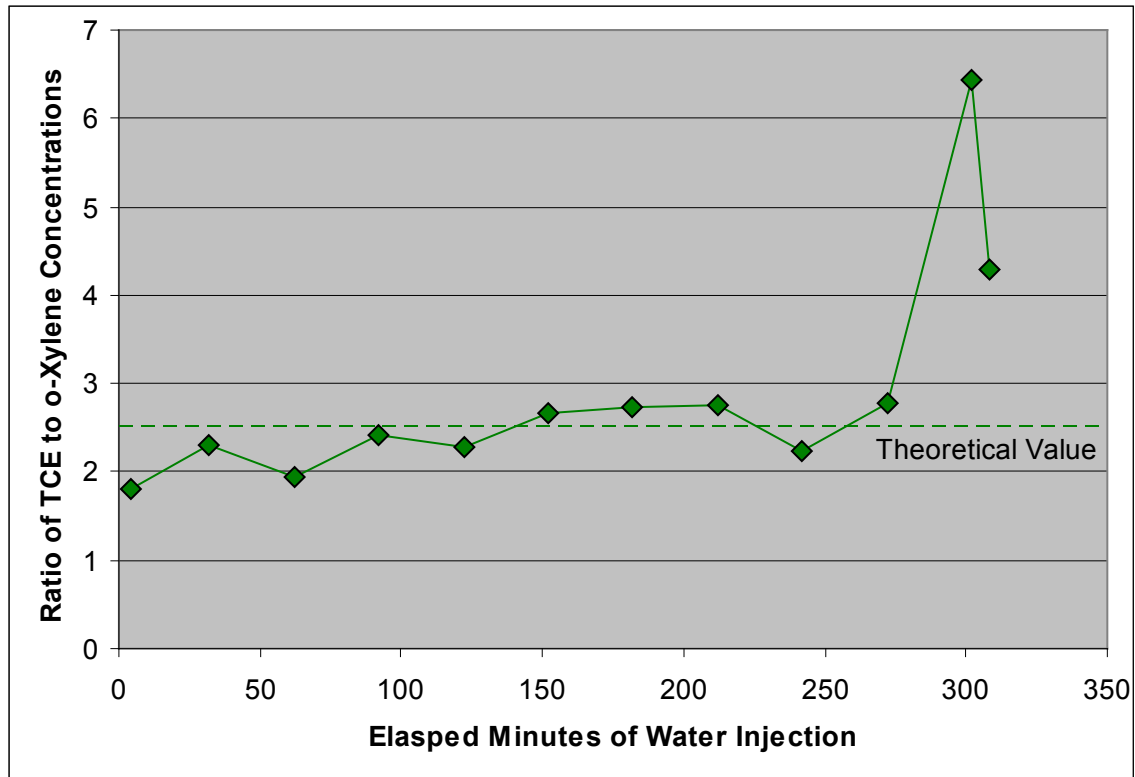

Figure E-4. Ratio of Dissolved Effluent Concentrations during Test 1

Test 2: Initial Volatilization Tests with Air Flow through the NAPL Zone

At the completion of the initial mass dissolution test, the column was drained as described previously yielding a residual water saturation of 25% and a theoretical immobile NAPL saturation of 10%. The column was allowed to rest for approximately 15 hours before vapor mass transfer testing was initiated. Tests were run at two air injection rates for brief periods. First, air was injected at 0.66 Lpm for 12 minutes with vapor samples collected in Tedlar bags every minute. The air flow rate was then increased to 2.36 Lpm for seven minutes and a vapor sample was collected every minute in a Tedlar bag. The air injection rate of 0.66 Lpm corresponds to a Darcy velocity of 17.2 cm/min and an interstitial velocity of 45.4 cm/min. The air injection rate of 2.36 Lpm corresponds to a Darcy velocity of 61.6 cm/min and an interstitial velocity of 162 cm/min. The temperature of the column was held constant at 18 °C. The vapor samples were analyzed with the calibrated GC.

The concentration histories of TCE and o-xylene during the initial volatilization testing are provided in Figure E-5. The calculated cumulative masses removed are illustrated in Figure E-6. The small variability in vapor concentrations during the initial volatilization test is the likely result of a non-mobile NAPL and a relatively uniform flow through the immobile NAPL zone. Average mass extraction rates for TCE and o-xylene were 14.9 and 3.4 mg/min, respectively, for a flow of 0.66 Lpm and 29 and 12.4 mg/min, respectively, for a flow of 2.36 Lpm. Hence, a flow increase of 358% yielded an increase in the mass extraction rate of TCE by only 195% while o-xylene increased by 365%. Hence, the TCE was mass transfer constrained at the higher flow rate while the o-xylene was not. The vapor mass fluxes for TCE and o-xylene at the higher vapor flow rate were 0.758 and 0.323 mg/min/cm^2, respectively.

Given the initial mole fraction (i.e., volume fraction) of each compound in the NAPL at the start of the initial volatilization test and its theoretical pure component vapor concentration, the ideal maximum concentration of each compound at the start of the volatilization test was:

> Ideal TCE Vapor Concentration Limit = (361 mg/L) * 0.047 = 17 mg/L
> Ideal o-Xylene Vapor Concentration Limit = (20 mg/L) * 0.137 = 2.74 mg/L

Based on the average mass extraction rates, the average effluent concentrations for TCE and o-xylene were 22.6 and 5.2 mg/L, respectively, during vapor injection at 0.66 Lpm. For a vapor injection rate of 2.39 Lpm, the average effluent concentrations for TCE and o-xylene were 12.3 and 5.25 mg/L, respectively. Hence, the TCE vapor concentration decreased by approximately 46% with an increase in flow of 362%. The TCE vapor extraction was mass transfer limited. Conversely, the o-xylene vapor concentration was unchanged by the increase in flow by 362% and the mass removal rate was not mass transfer limited. At the lower flowrate, the TCE vapor concentration was slightly higher than the ideal limit while the o-xylene vapor concentration was roughly double the ideal value for both flowrates.

At the end of this initial volatilization test, the TCE mass in the column had been reduced by 425 mg and the o-xylene by 140 mg. Hence, the final mole fractions of the compounds at the end of the initial volatilization test were 1.6% and 12.4% for TCE and o-xylene, respectively. These

mole fractions yield ideal vapor concentration limits of 5.8 mg/L and 2.48 mg/L for TCE and o-xylene, respectively.

The ratio of the volatilized TCE concentration to the o-xylene vapor concentration in the vapor effluent is plotted in Figure E-7 as a function of the air injection duration. The initial ratio of ideal vapor concentrations was 6.2 and the final value was 2.34. These limits are indicated on Figure E-7.

Finally, the pressures at the inlet (P inlet), a distance 15.2 cm from the inlet (P1), and 30.5 cm into the column (P2) were recorded during the air injection testing. These pressures are illustrated in Figure E-8. The spikes in pressure correspond to the connection of Tedlar bags at the outlet for sample collection. The decrease in pressure during the higher flow rate injection was the result of moisture re-distribution within the column.
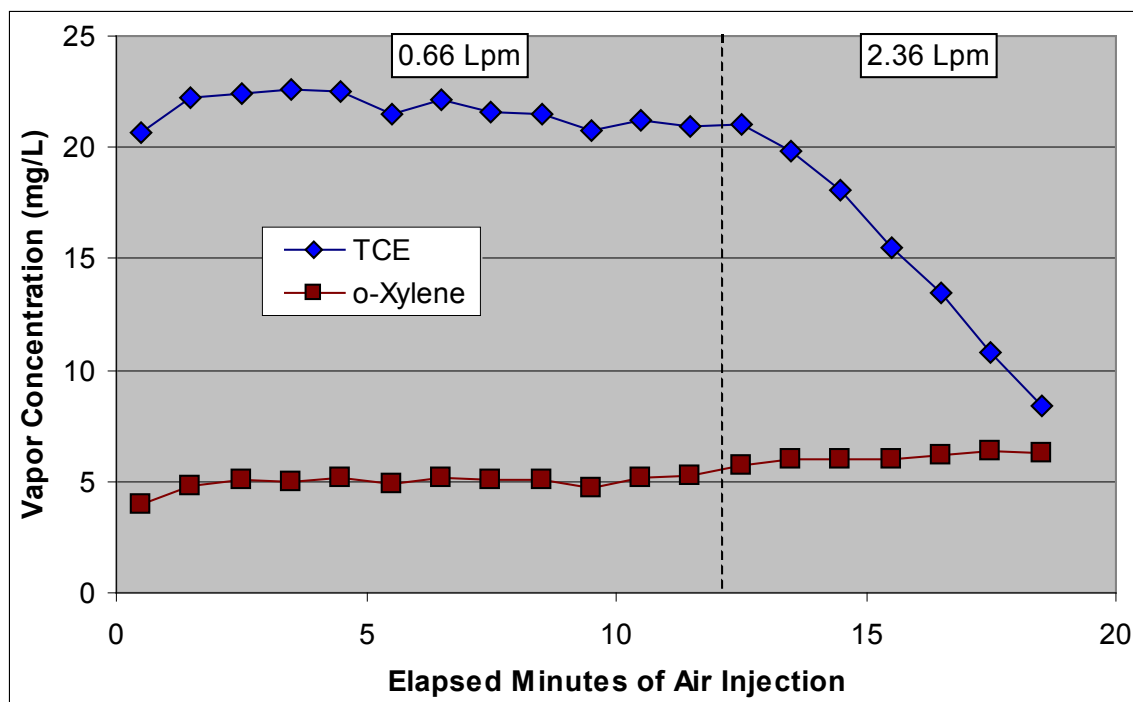

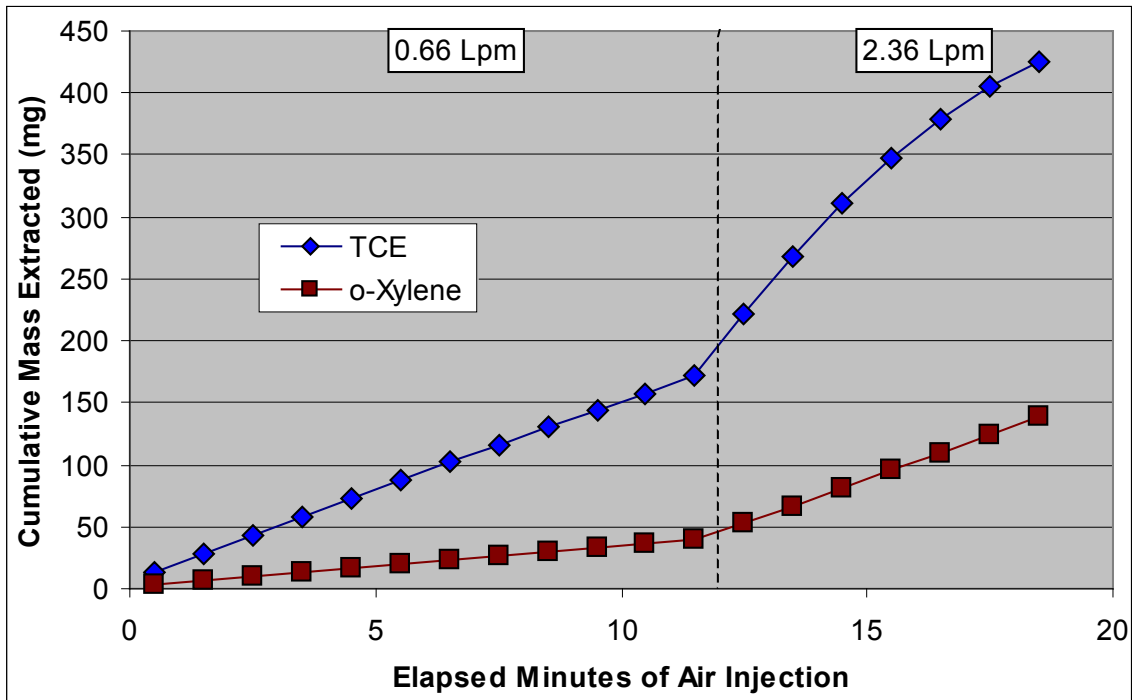**Figure E-5. Effluent Vapor Concentrations during Test 2**

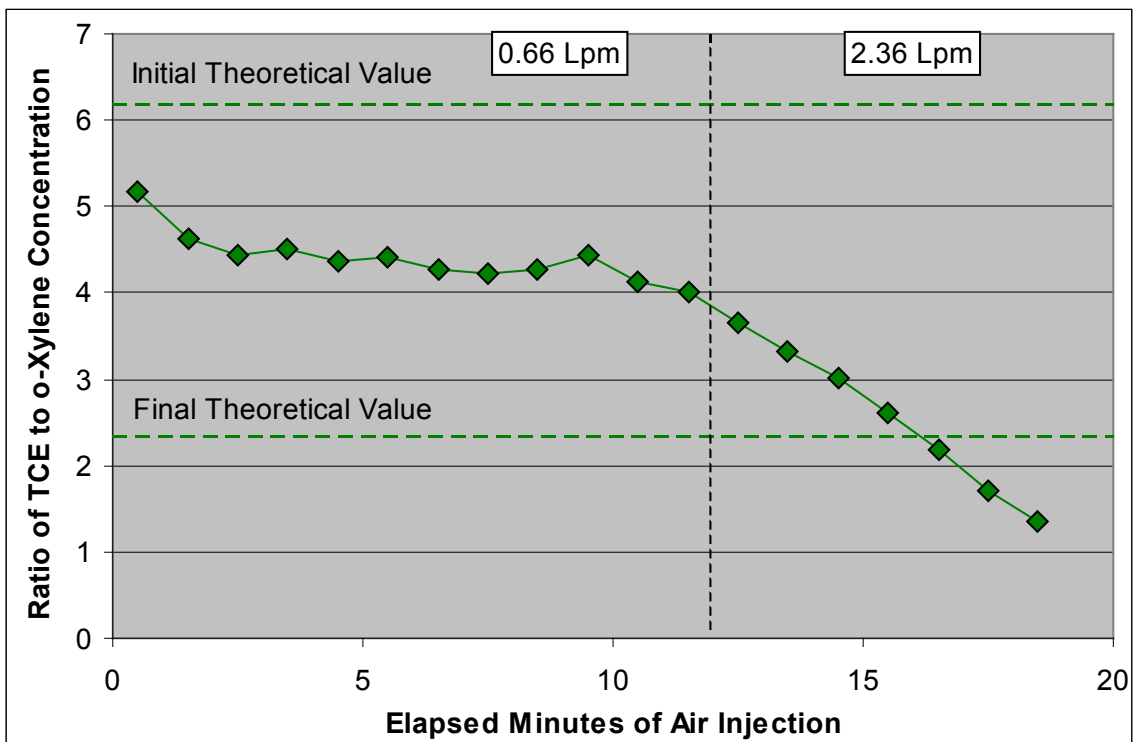**Figure E-6. Cumulative Masses Extracted during Test 2**

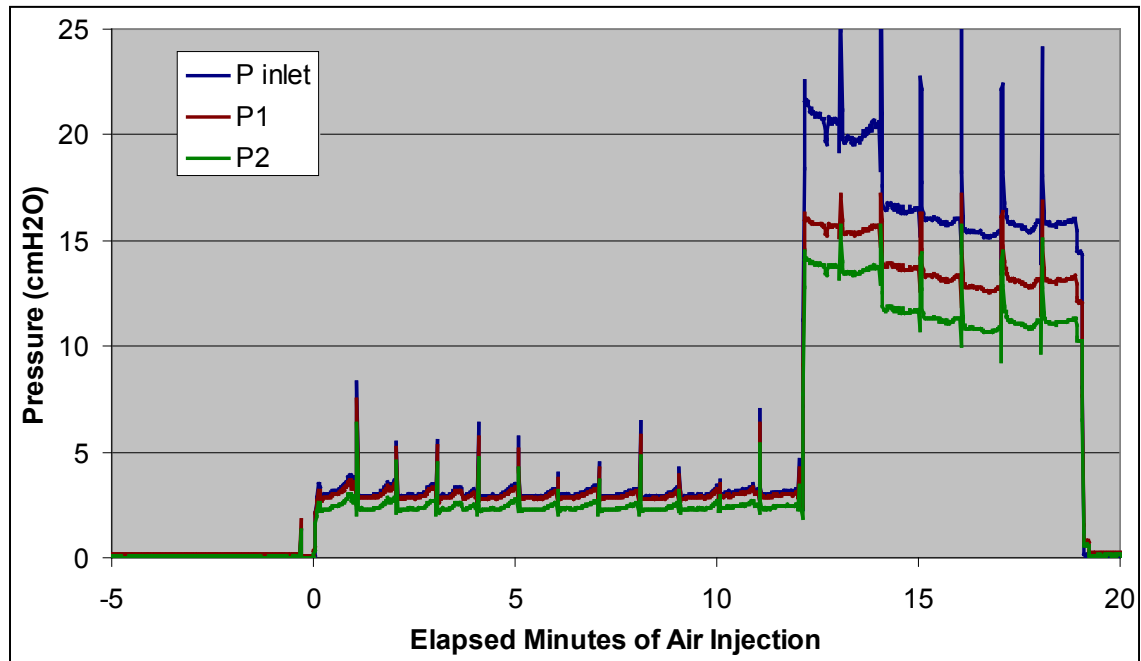**Figure E-7. Ratio of Volatilized Effluent Concentrations during Test 2**

Figure E-8. Vapor Pressures Recorded during Test 2

Test 3: Thermal Enhanced Volatilization Tests through the NAPL Zone

At the completion of the initial mass volatilization test, the column was allowed to sit closed and undisturbed for 24 hours. After this period, a test of thermal enhancement to mass transfer was undertaken. Air injection was introduced at 0.94 Lpm and after five minutes, slightly superheated steam was mixed into the injected air at a rate of 0.73 g/min. The air/steam mixture resulted in an injected vapor with a temperature of about 68 °C. This vapor mixture was injected at a constant rate for 218 minutes when the steam injection was terminated. The air injection was allowed to continue alone for another 90 minutes and resulted in evaporative cooling of the column. Samples of the vapor effluent were collected periodically and analyzed with the GC. The vapor samples were cooled to room temperature before collection.

The concentration histories of TCE and o-xylene during the thermal enhanced volatilization test are provided in Figure E-9. The calculated cumulative masses removed are plotted in Figure E-10. The TCE vapor concentration began decaying immediately while the o-xylene vapor concentration increased during the early injection period. The o-xylene vapor concentration leveled off around 6.3 mg/L and remained relatively steady as heating of the column progressed while the TCE concentration continued to decay by two orders of magnitude. After heat had impacted the entire column, the o-xylene concentration began to decay exponentially. After 218 minutes of steam injection, the steam was terminated and the o-xylene concentration decayed more slowly. The TCE vapor concentration leveled off above 0.01 mg/L during the end of steam injection and increased when the steam injection was terminated suggesting evaporative cooling increased the mass extraction rate of TCE. About 70% of the initial o-xylene mass emplaced in the column was removed during Test 3 as compared to the approximately 70% of the TCE removed in Tests 1 and 2. Only about 7.8% of the total TCE emplaced was removed during the thermal enhanced extraction but this also represented approximately 25% of the mass in place at the start of Test 3.

The ratio of the volatilized TCE concentration to the o-xylene concentration in the vapor effluent is plotted in Figure E-11 as a function of the vapor injection duration. The initial ratio of ideal vapor concentrations was 1.5 and rapidly decayed two orders of magnitude during the heating. The increase in TCE vapor concentration during the evaporative cooling is evident in the increase of the concentration ratio after steam was terminated.

The temperature histories recorded at various lengths along the column are plotted in Figure E-12 along with the vapor injection temperature. As compared to pure steam injection where a definitive steam condensation front is formed, the co-injection of air smears the condensation front over some length which increases with distance from the injection point. Temperature 1 was located 7.6 cm from the injection point and each subsequent thermocouple was place 7.6 cm beyond the previous thermocouple. Temperature 5 was located 38 cm from the injection point and only slight heating was observed at this distance at the end of steam injection. After steam injection was terminated, the temperatures decayed in sequence as the evaporative cooling front moved through the column.
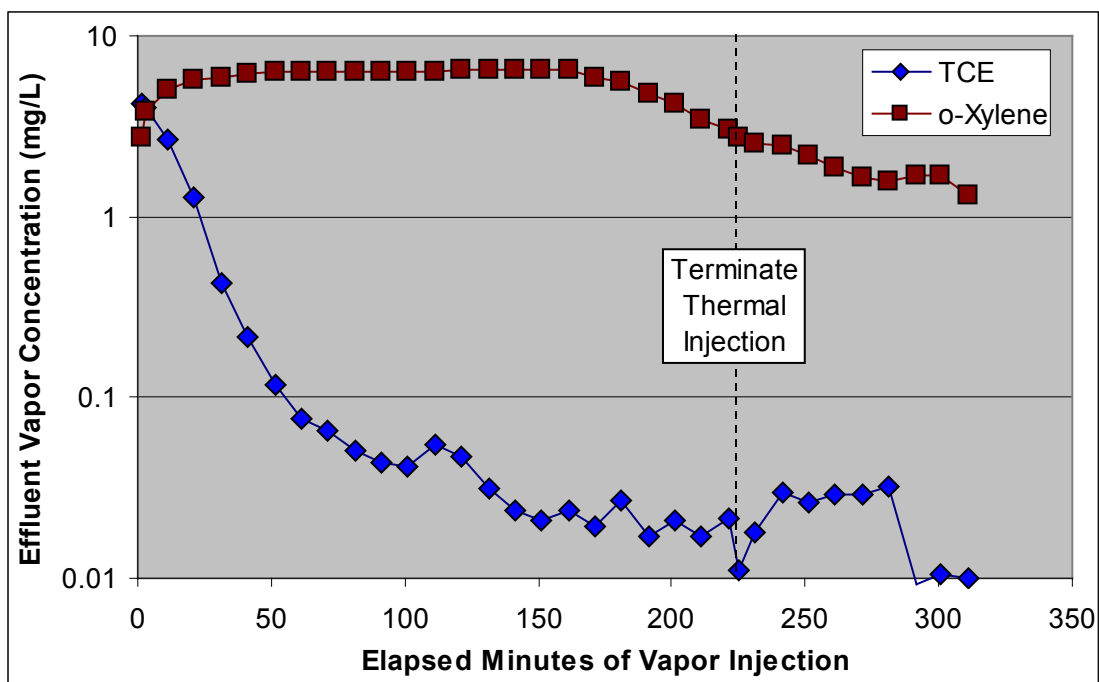
Figure E-9. Effluent Vapor Concentrations during Test 3
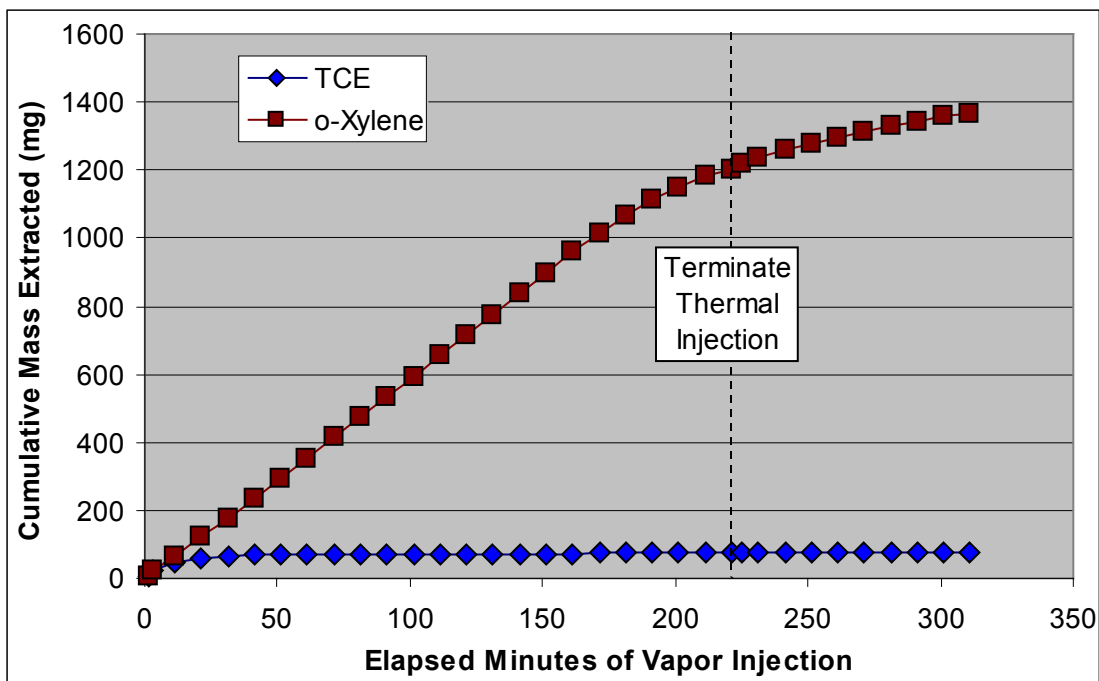

Figure E-10. Cumulative Masses Extracted during Test 3
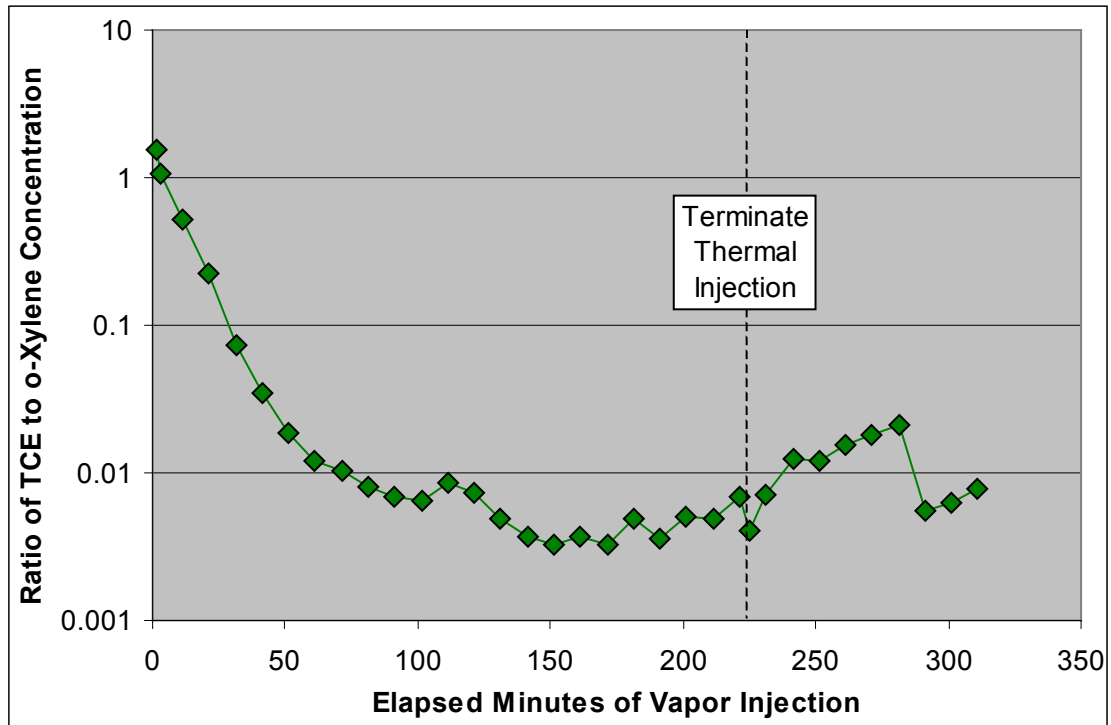
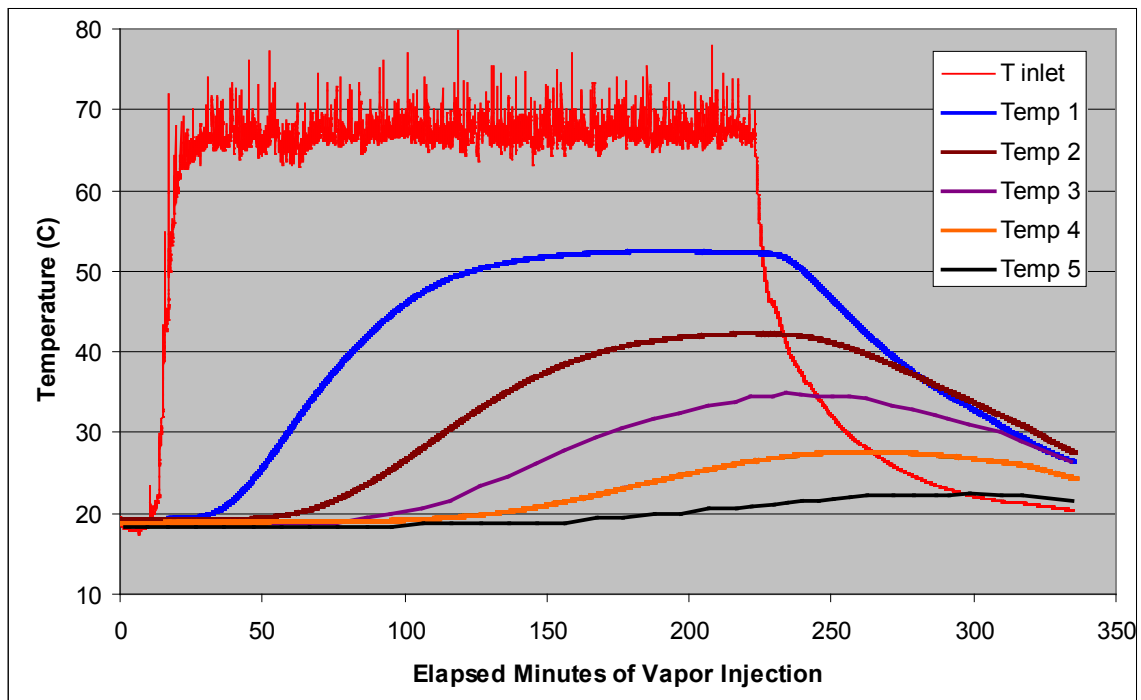**Figure E-11. Ratio of Volatilized Effluent Concentrations during Test 3**

Figure E-12. Temperatures Recorded during the Thermal Enhancement of Test 3

The temperature histories in the column are plotted co-incident with the effluent vapor concentrations in Figure E-13. The left hand y-axis is temperature and the right hand y-axis is vapor concentration on a log scale. This Figure E-shows the decay in o-xylene vapor concentration started as heat reached the last thermocouple (T5) and all of the emplaced NAPL had been heated.
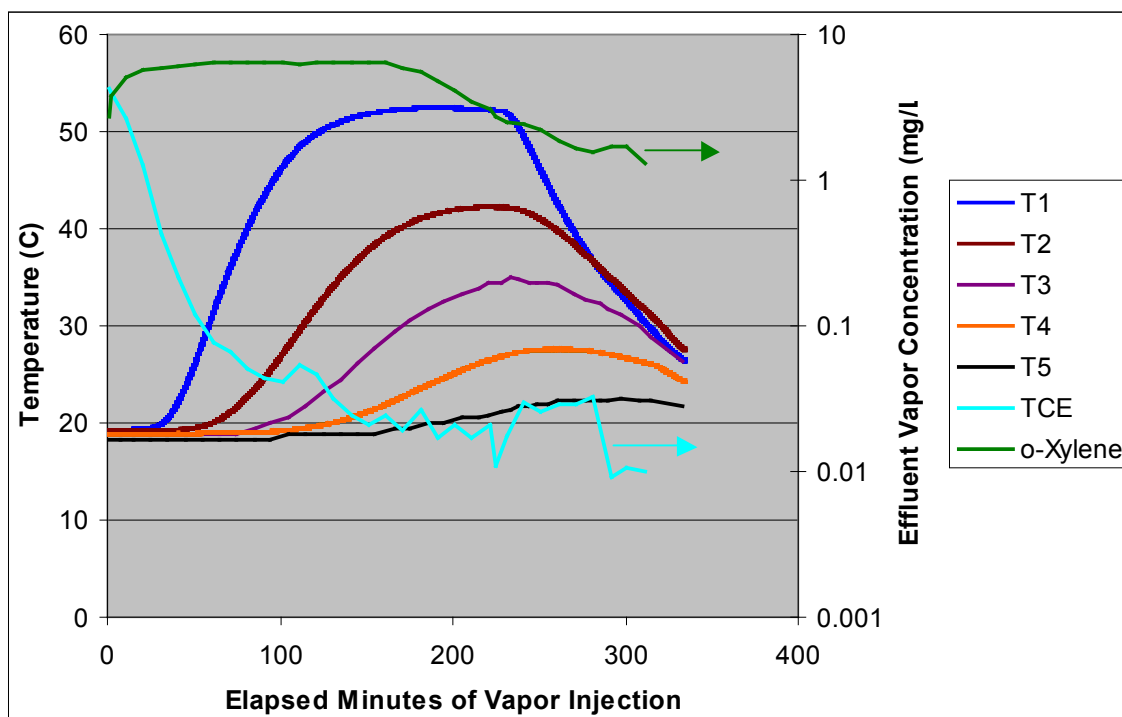
Figure E-13. Temperatures and Effluent Vapor Concentrations over Time in Test 3

Given the initial mole fraction (i.e., volume fraction) of each compound in the NAPL at the start of the initial volatilization test and its theoretical pure component vapor concentration at 52 °C, the ideal maximum concentration of each compound at the start of the thermal enhanced volatilization test was as follows:

Ideal TCE Vapor Concentration Limit = (1,464 mg/L) * 0.017 = 25 mg/L
Ideal o-Xylene Vapor Concentration Limit = (119.5 mg/L) * 0.13 = 16 mg/L

The vapor concentration of o-xylene peaked at 6.5 mg/L in the effluent, or about half of the theoretical maximum, while the TCE vapor concentration was much lower than theoretical maximum.

At the end of this thermal enhanced volatilization test, the TCE mass in the column had been reduced by 76 mg and the o-xylene by 1,367 mg. Hence, the final mole fractions of the

compounds at the end of the thermal volatilization test were 1.3% and 3.0% for TCE and o-xylene, respectively.

Finally, the pressures at the inlet (P inlet), a distance 15.2 cm from the inlet (P1), and 30.5 cm into the column (P2) were recorded during the thermal injection testing. These pressures are illustrated in Figure E-14. The short spikes in pressure correspond to the connection of Tedlar bags at the outlet for sample collection. The sustained increase in pressure observed after 100 minutes of injection corresponded to the appearance of condensate in the effluent tubing. The condensate provided a back pressure to flow through the column. The pressure decreased after steam injection was terminated and a crack appeared in the column inlet around 280 minutes. This crack leaked some of the injected air and was repaired as indicated by the increasing pressure at the end of the test when air injection was terminated.
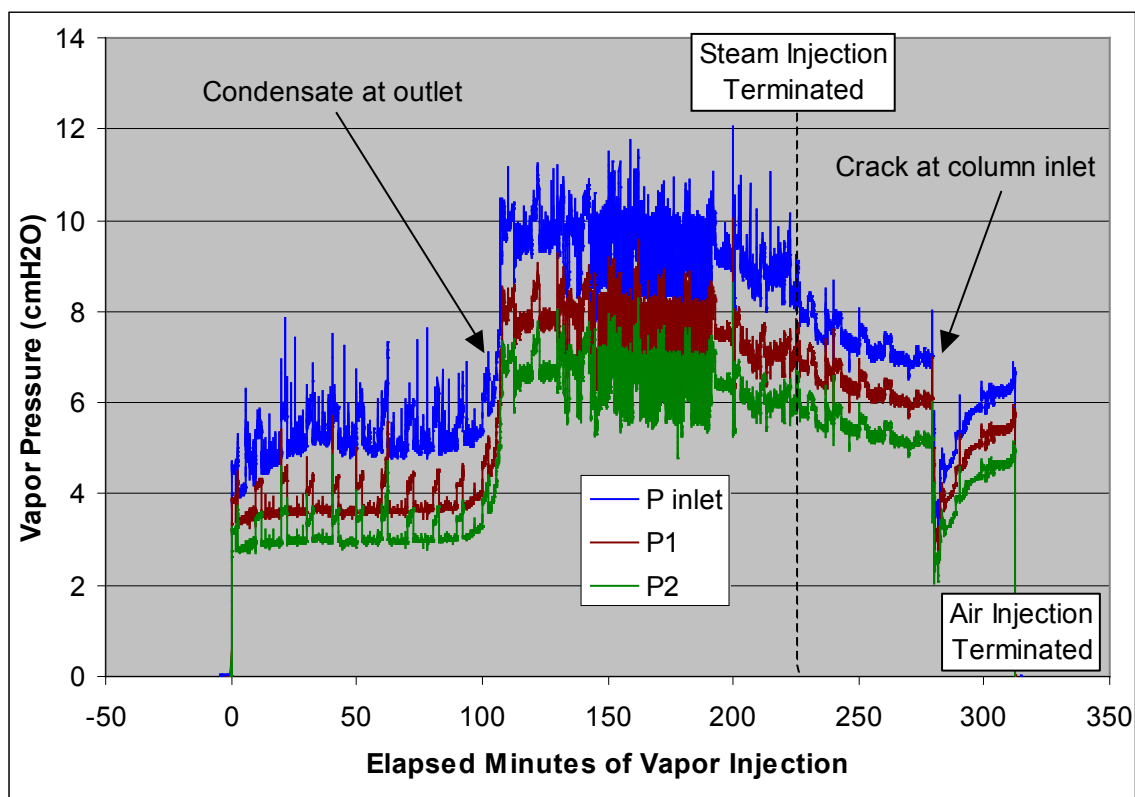
Figure E-14. Vapor Pressures Recorded during the Thermal Enhancement of Test 3

During Test 3, the mass of water injected as steam was 155 g while the mass of condensate collected at the outlet was 115 g. The estimated mass of water in the column at the start of Test 3 was 157 g, corresponding to an average water saturation of 23%. The net addition of 42 grams of water during the test yielded a final average water saturation of 29%. The condensate collected during Test 3 also contained an observable, but small and unmeasured, volume of emulsified mineral oil indicating the mineral oil was somewhat mobile under heated conditions.

Test 4: Post-TEE Volatilization Tests with Air Flow through the NAPL Zone

After the thermal extraction test, the column was allowed to sit undisturbed over night and cooled to ambient temperature (19 °C). A brief volatilization test was then undertaken to assess the ambient vapor concentrations. The estimated average water saturation was 29%. Tests were run at two air injection rates for brief periods. First, air was injected at 0.94 Lpm for 4 minutes with vapor samples collected in Tedlar bags every minute. The air flow rate was then increased to 2.36 Lpm for three minutes and a vapor sample was collected every minute in a Tedlar bag. The air injection rate of 0.94 Lpm corresponds to a Darcy velocity of 24.6 cm/min. The air injection rate of 2.36 Lpm corresponds to a Darcy velocity of 61.6 cm/min. The vapor samples were analyzed with the calibrated GC.

The concentration histories of TCE and o-xylene during the volatilization test are provided in Figure E-15. The first vapor sample corresponded to the first pore volume of vapor from the column and the first pore volume to pass through the column. The initial TCE concentration was 0.14 was mg/L while o-xylene was 1.49 mg/L. This TCE concentration is more than an order-of-magnitude higher than the average of the last three vapor samples analyzed from Test 3 (i.e., 0.010 mg/L); however, TCE decayed steadily throughout the test to a final value of 0.034 mg/L. The initial o-xylene concentration was commensurate with the average of the final three samples from Test 3 (i.e., 1.56 mg/L). The o-xylene vapor concentration was relatively constant throughout the test, even with the increased air injection rate, at an average of 1.7 mg/L.

The calculated cumulative masses removed are illustrated in Figure E-16. The total TCE mass removed was 0.0007 mg and the total o-xylene was 0.019 mg. The average mass extraction rates for TCE and o-xylene were 0.000084 and 0.0017 mg/min, respectively, for a flow of 0.94 Lpm and 0.000096 and 0.0041 mg/min, respectively, for a flow of 2.36 Lpm. Hence, a flow increase of 250% yielded an increase in the mass extraction rate of TCE by only 14% while o-xylene increased by 240%. Hence, the TCE was mass transfer constrained at the higher flow rate while the o-xylene was not.

Based on a mass balance, the estimated initial mole fraction (i.e., volume fraction) of each compound dissolved in the NAPL at the start of the volatilization test was 0.0139 for TCE and 0.030 for o-xylene. For these mole fractions and the theoretical pure component vapor concentrations, the ideal maximum concentration of each compound at the start of the volatilization test was:

Ideal TCE Vapor Concentration Limit = (361 mg/L) * 0.0139 = 5.0 mg/L
Ideal o-Xylene Vapor Concentration Limit = (20 mg/L) * 0.030 = 0.6 mg/L

As described above, the initial TCE vapor concentration measured during this volatilization test was 0.14 mg/L; more than 35 times less than the calculated ideal limit. For o-xylene, the vapor concentrations during the volatilization test were about 3 times higher than the ideal theoretical limit. A portion of this difference can be attributed to partitioning into the pore water.
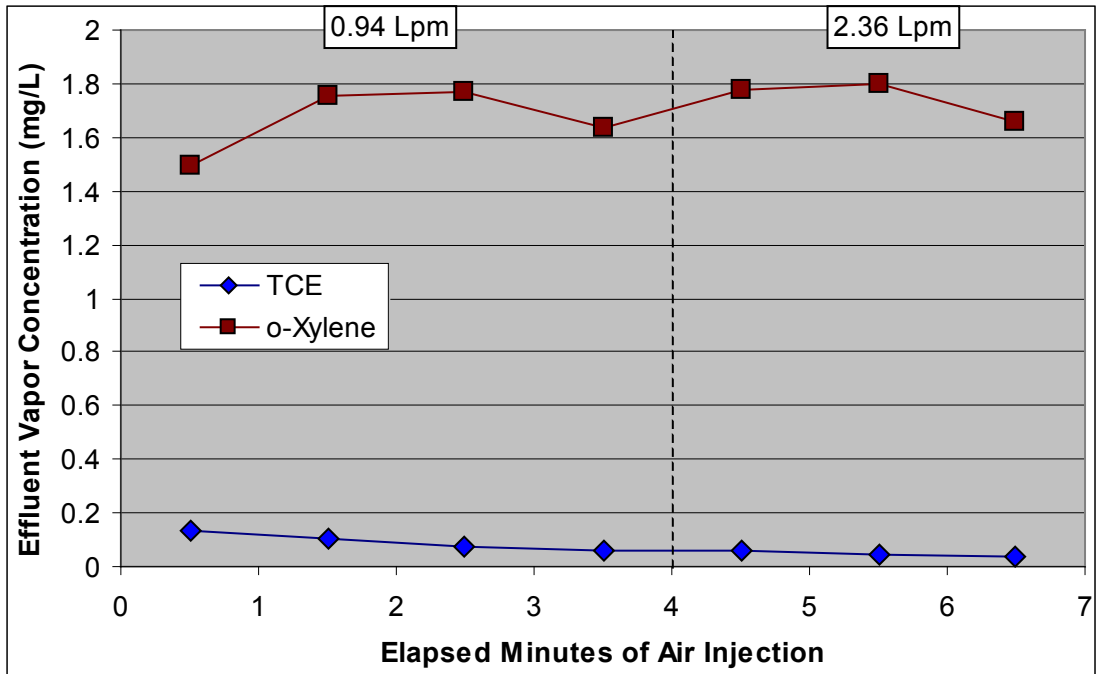
Figure E-15. Effluent Vapor Concentrations during Test 4
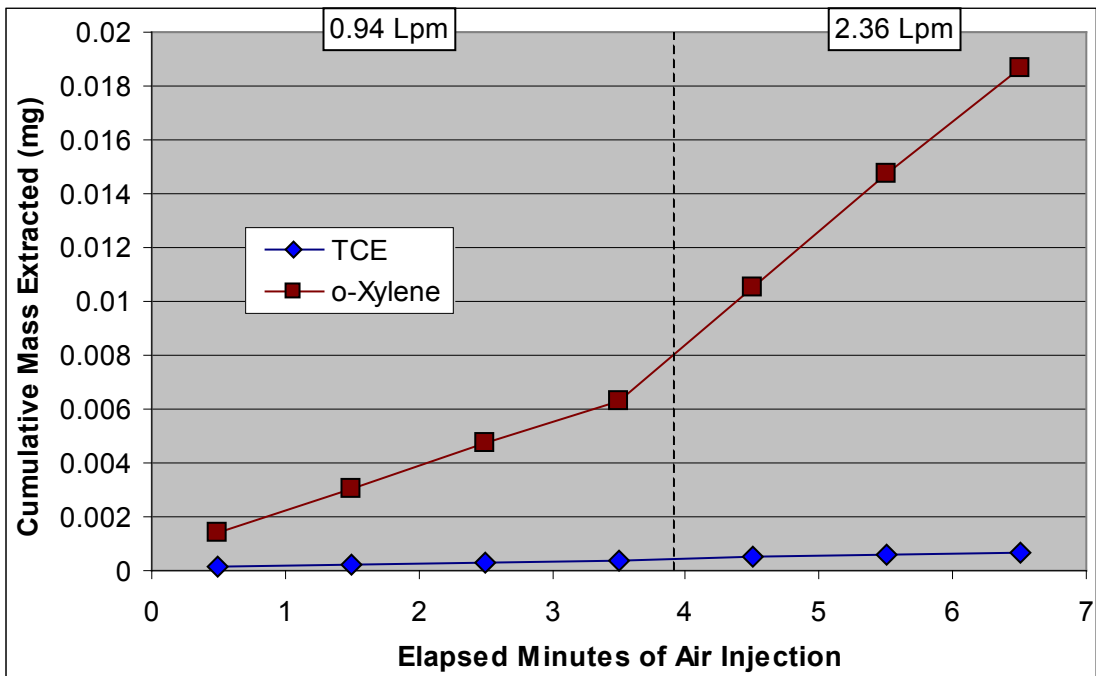
Figure E-16. Cumulative Masses Extracted during Test 4

At the end of this initial volatilization test, the TCE mass in the column had been reduced by 0.0007 mg and the o-xylene by 0.019 mg. Hence, the final mole fractions of the compounds at the end of the initial volatilization test were 1.39% and 2.82% for TCE and o-xylene, respectively. These mole fractions yield ideal vapor concentration limits of 5.0 mg/L and 0.56 mg/L for TCE and o-xylene, respectively.

The ratio of the volatilized TCE concentration to the o-xylene vapor concentration in the vapor effluent is plotted in Figure E-7 as a function of the air injection duration. The ratio of ideal vapor concentrations based on the mass balance was 8.9. As shown in Figure E-17, the measured ratio was about 100 times less and increased as the effluent TCE concentration decayed over time.
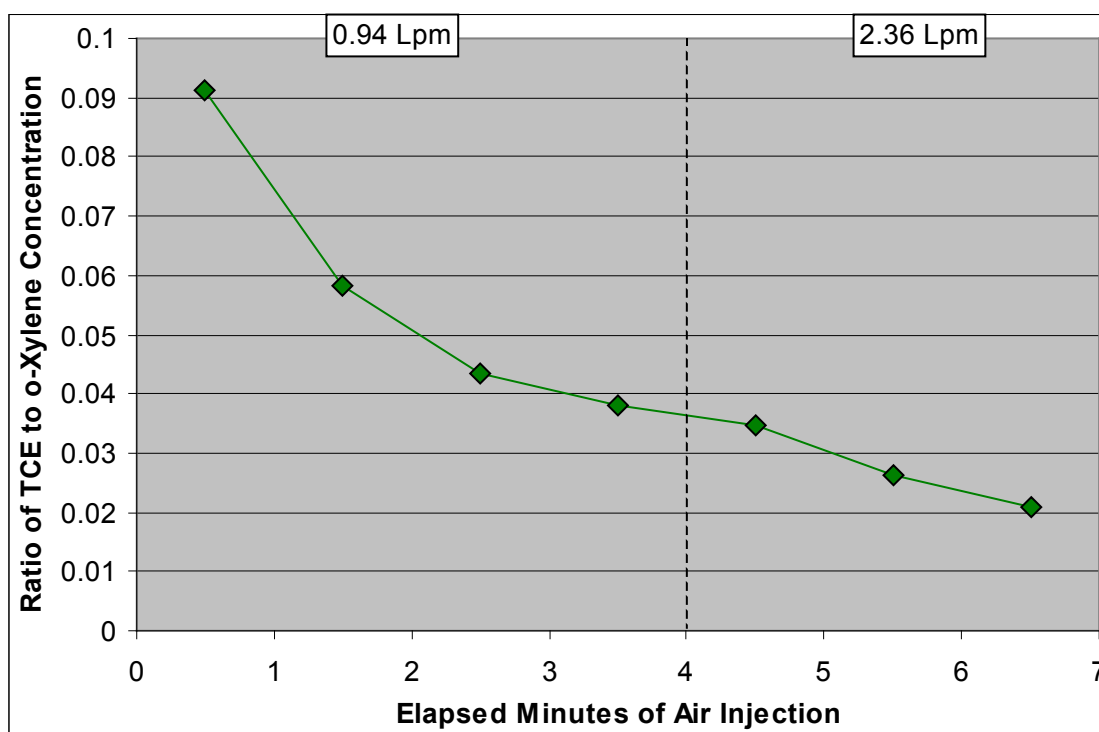
Figure E-17. Ratio of Volatilized Effluent Concentrations during Test 4

Finally, the pressures at the inlet (P inlet), a distance 15.2 cm from the inlet (P1), and 30.5 cm into the column (P2) were recorded during the air injection testing. These pressures are illustrated in Figure E-18. The spikes in pressure correspond to the connection of Tedlar bags at the outlet for sample collection.
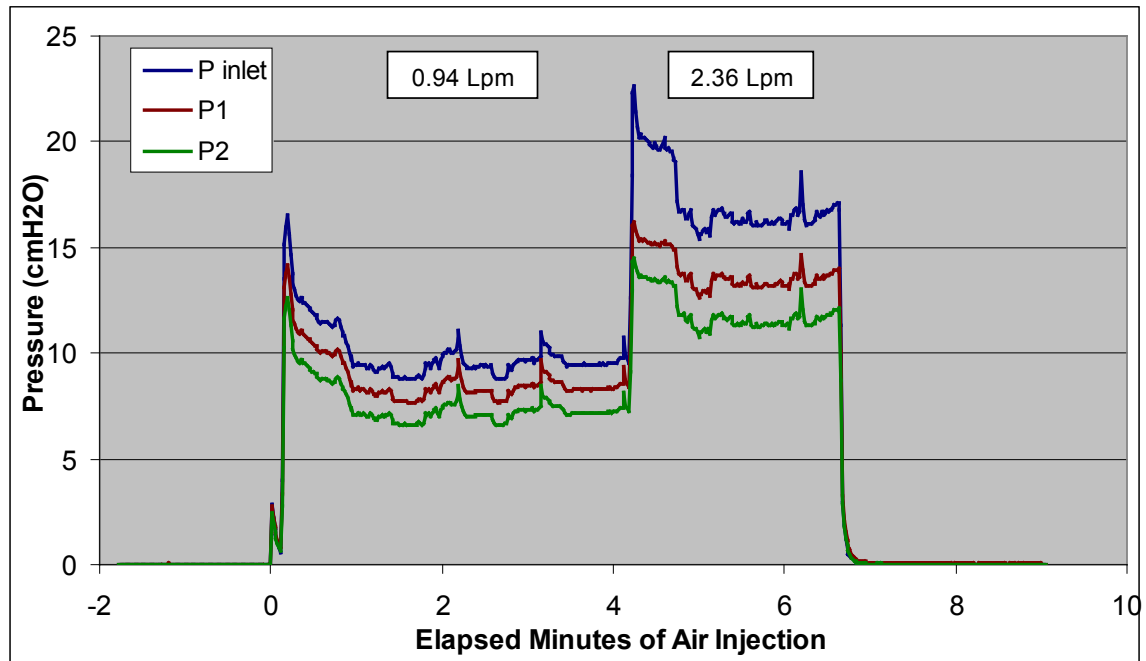
Figure E-18. Vapor Pressures Recorded during Test 4

Test 5: Final Dissolution Test with Water Flow through the NAPL Zone

The first dissolution test was repeated after the ambient and thermal enhanced volatilization testing. A very small volume of emulsified NAPL was observed in the condensate collected from the effluent of the thermal enhanced volatilization test such that the average NAPL saturation was effectively unchanged. The average water saturation in the column after the volatilization test was 26%. The column was re-saturated with 505 g of water. The column was allowed to rest undisturbed for 46 hours before water injection was initiated. Test 5 dissolution measurements were performed with a steady injection rate of 3.18 g/min for 1,595 minutes (26.5 hours) corresponding to the injection of 5,080 g of water. An equivalent volume was recovered. The temperature of the column was constant at 19 °C. The water injection rate corresponded to a Darcy velocity of 0.083 cm/min and an interstitial velocity of 0.22 cm/min.

The concentration histories of TCE and o-xylene are provided in Figure E-19. Both compounds exhibit a logarithmic decay and decreased by nearly an order of magnitude during the test. Figure E-20 illustrates the calculated cumulative masses extracted. Given the estimated mole fraction of each compound in the NAPL from the previous volatilization test and its theoretical pure component solubility, the ideal maximum concentration of each compound at the start of the dissolution test was as follows:

Initial Ideal TCE Solubility Limit = (1,100 mg/L) * 0.0139 = 15.3 mg/L
Initial Ideal o-Xylene Solubility Limit = (175 mg/L) * 0.0282 = 4.9 mg/L
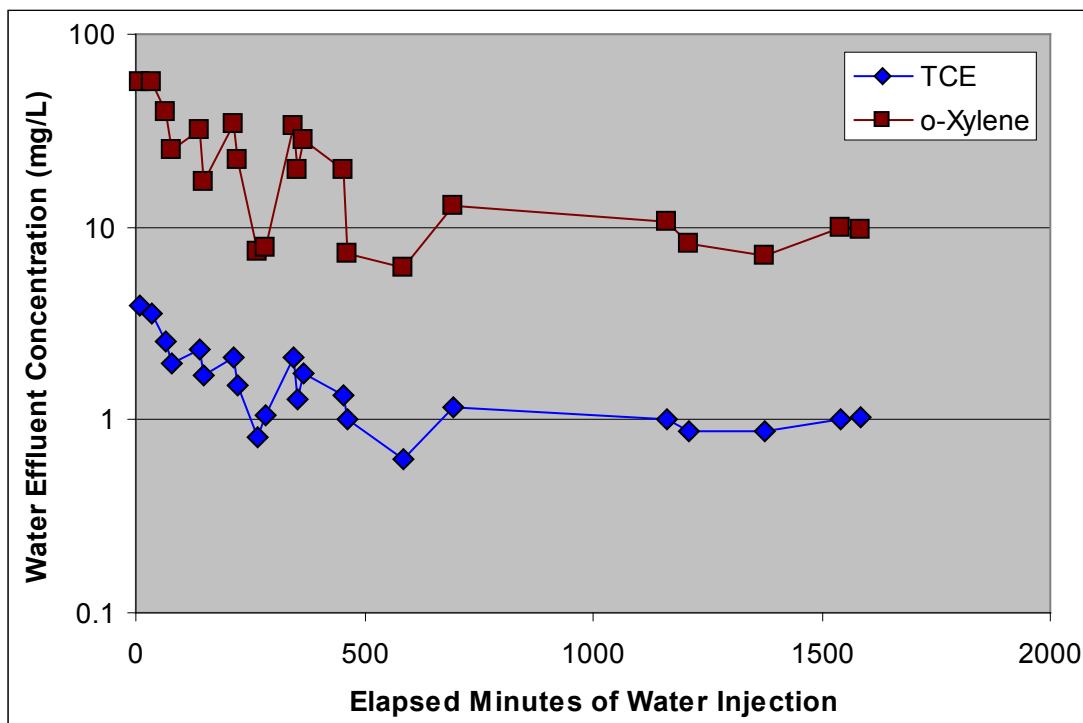
Figure E-19. Effluent Dissolved Concentrations Measured during Test 5
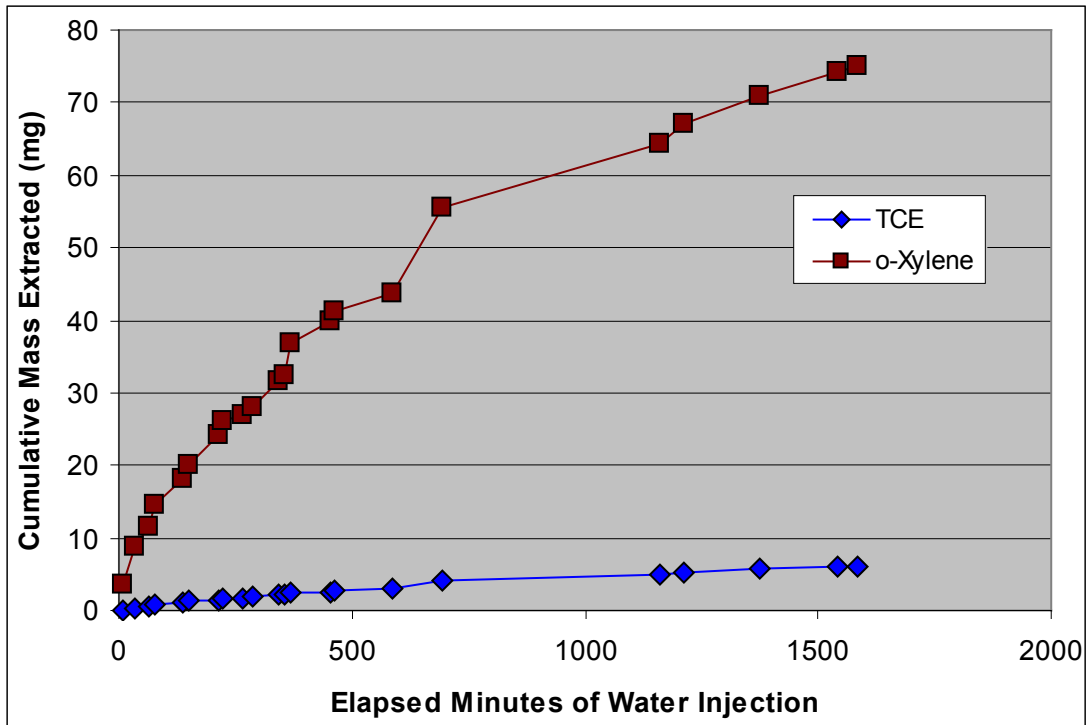
Figure E-20. Cumulative Masses Extracted during Test 5

The initial TCE and o-xylene concentrations in the effluent were 3.9 mg/L and 56 mg/L, respectively, and were expected to represent the near-solubility limit. The TCE concentration was a factor of four below the calculated limit. However, the o-xylene concentration was an order of magnitude higher than the mass-balanced based value of 4.9 mg/L suggesting enhanced solubilization of the o-xylene.

The ratio of the dissolved TCE concentration to the o-xylene concentration in the water effluent is plotted in Figure E-4 as a function of the water injection duration. The relatively high o-xylene concentration and the relatively low TCE concentration, as compared to the theoretical equilibrium limit, resulted in a ratio much less than the theoretical equilibrium value of three.
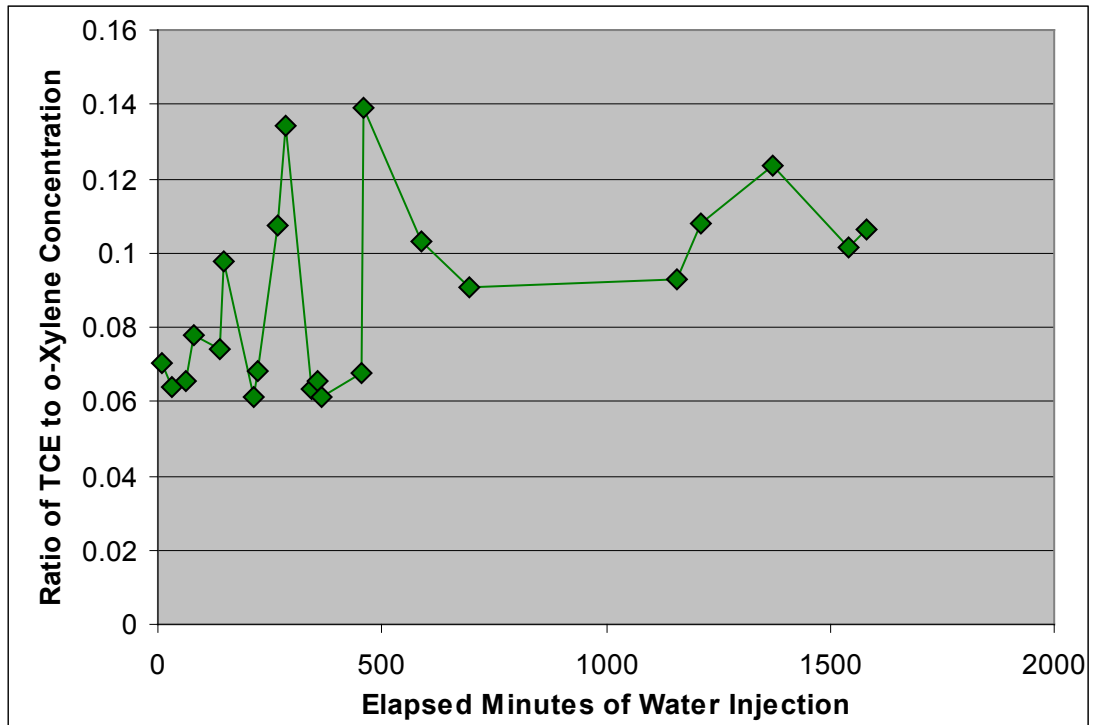
Figure E-21. Ratio of Dissolved Effluent Concentrations during Test 5

At the completion of Test 5, the column was drained to a residual liquid. The total water extracted was 500 g leaving 170 g and an average residual water saturation of 25%.

Test 6: Final Volatilization Tests with Air Flow through the NAPL Zone

After the final dissolution test and draining, the column was allowed to sit undisturbed for 26 hours. A longer duration volatilization test was then undertaken. The estimated average water saturation was 25%. The test was run at two air injection rates. First, air was injected at 0.94 Lpm for 16 minutes with five vapor samples collected in Tedlar bags. The air flow rate was then increased to 2.36 Lpm for 121 minutes and nine vapor sample were collected in Tedlar bags. The air injection rate of 0.94 Lpm corresponds to a Darcy velocity of 24.6 cm/min. The air injection rate of 2.36 Lpm corresponds to a Darcy velocity of 61.6 cm/min. The vapor samples were analyzed with the calibrated GC.

The concentration histories of TCE and o-xylene during the volatilization test are provided in Figure E-22. The first vapor sample corresponded to the first pore volume of vapor from the column and the first pore volume to pass through the column. The initial TCE concentration was 0.05 was mg/L while o-xylene was 1.0 mg/L. This TCE concentration was commensurate with the vapor concentrations measured in the previous volatilization test of Test 4. As in Test 4, the TCE concentration decayed steadily although the decay rate increased with the onset of the higher air injection rate. The initial o-xylene concentration was only slightly less than the average vapor concentration from Test 3 (i.e., 1.7 mg/L). However, the o-xylene vapor concentration decayed exponentially whereas in Test 4 the concentration was relatively constant throughout the test. Unlike TCE, the o-xylene vapor concentration decay rate did not appear to increase with the increased air injection rate.

The calculated cumulative masses removed are illustrated in Figure E-23. The total TCE mass removed was 0.0006 mg and the total o-xylene mass was 0.039 mg. Based on a mass balance, the estimated mole fraction (i.e., volume fraction) of each compound dissolved in the NAPL at the start of the volatilization test was 0.0135 for TCE and 0.0211 for o-xylene. For these mole fractions and the theoretical pure component vapor concentrations, the ideal maximum concentration of each compound at the start of the volatilization test was:

> Ideal TCE Vapor Concentration Limit = (361 mg/L) * 0.0135 = 4.9 mg/L
> Ideal o-Xylene Vapor Concentration Limit = (20 mg/L) * 0.0211 = 0.42 mg/L

As described above, the initial TCE vapor concentration measured during this volatilization test was 0.05 mg/L; 100 hundred times less than the calculated ideal limit. For o-xylene, the initial vapor concentration of 1.0 mg/L for the volatilization test was 2.5 times higher than the ideal theoretical limit for a vapor in contact with the NAPL.
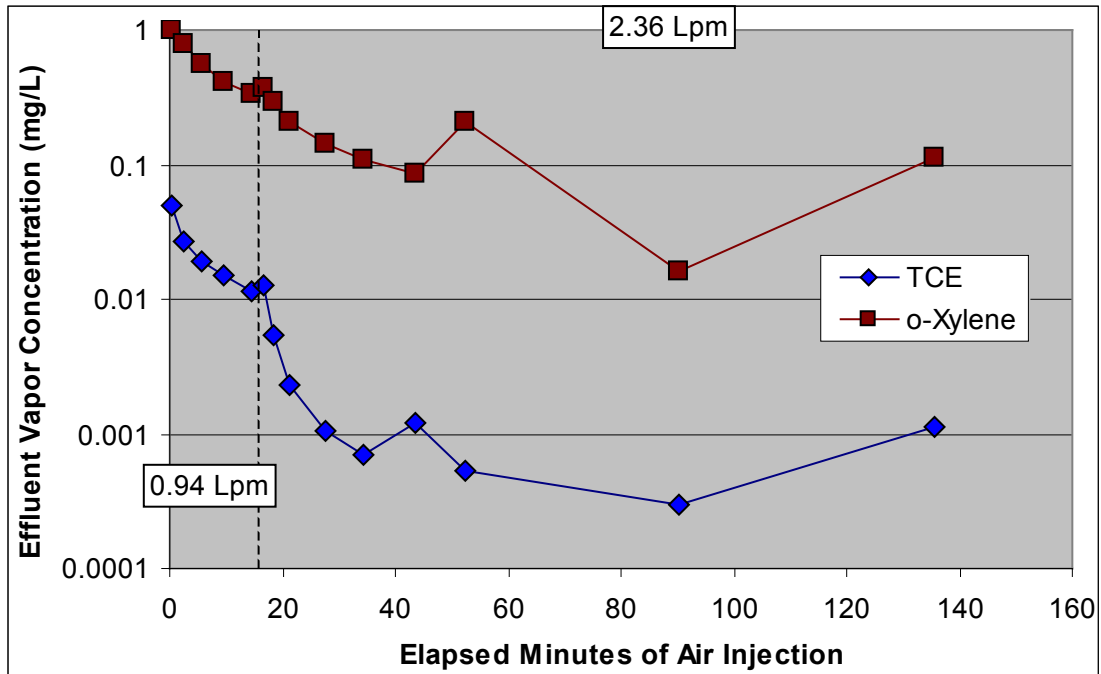
Figure E-22. Effluent Vapor Concentrations during Test 6
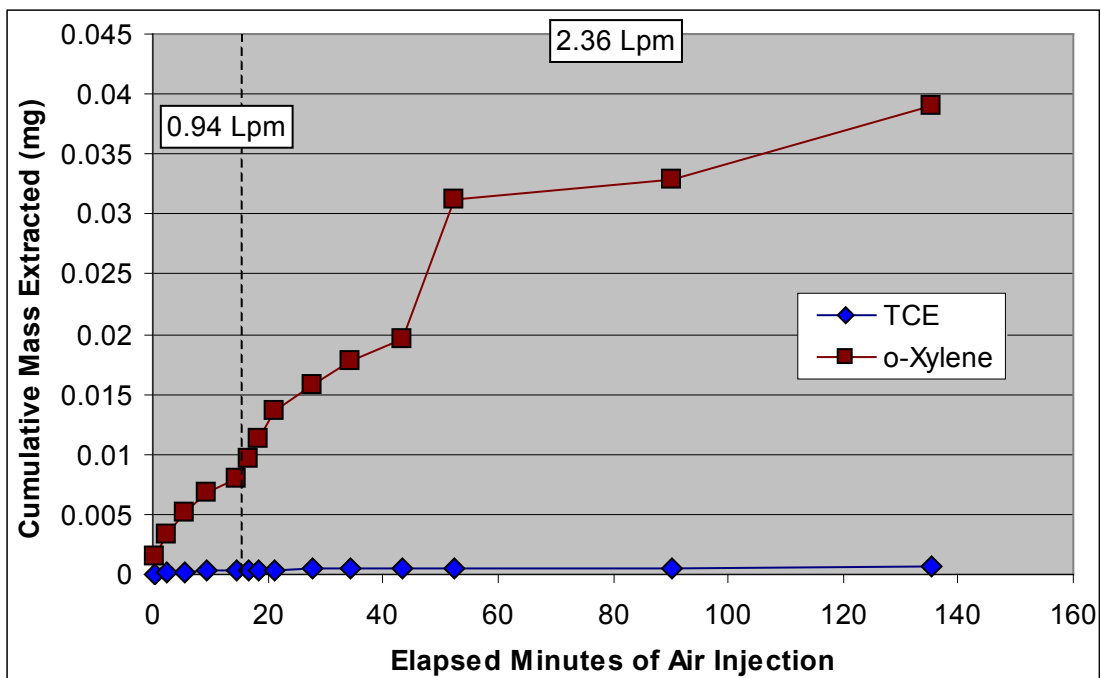
Figure E-23. Cumulative Masses Extracted during Test 6

At the end of this final volatilization test, the TCE mass in the column had been reduced by 0.0006 mg and the o-xylene by 0.039 mg. Hence, the estimated final mole fractions of the compounds at the end of the final volatilization test were 1.35% and 1.78% for TCE and o-xylene, respectively, yielding ideal equilibrium vapor concentrations of 4.9 mg/L and 0.36 mg/L, respectively.

The ratio of the volatilized TCE concentration to the o-xylene vapor concentration in the vapor effluent is plotted in Figure E-24 as a function of the air injection duration. The ratio of ideal vapor concentrations based on the mass balance was 14. As shown in Figure E-24, the measured ratio was orders of magnitude less and decreased with the higher extraction rate.
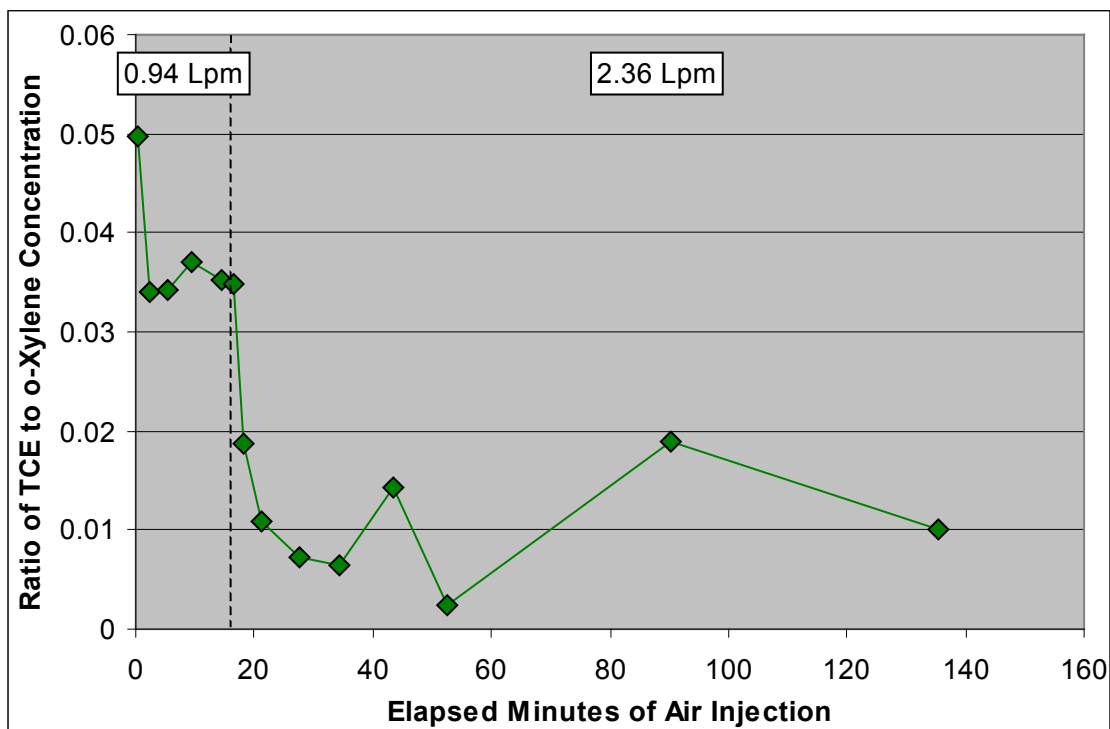
Figure E-24. Ratio of Volatilized Effluent Concentrations during Test 6

Finally, the pressures at the inlet (P inlet), a distance 15.2 cm from the inlet (P1), and 30.5 cm into the column (P2) were recorded during the air injection testing. These pressures are illustrated in Figure E-25. The spikes in pressure correspond to the connection of Tedlar bags at the outlet for sample collection. The vapor pressures decreased over time as the moisture was re-distributed and a small portion was evaporated.
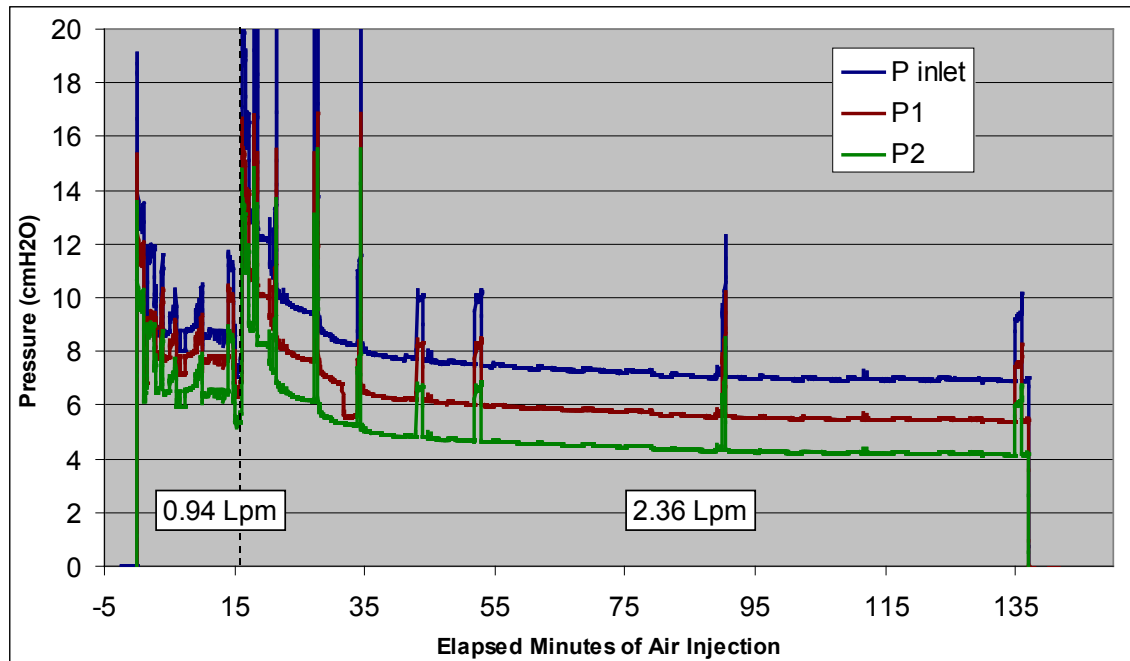
Figure E-25. Vapor Pressures Recorded during Test 6

Mass Balances

Mass balances for TCE and o-xylene based on the measured masses emplaced and extracted in each step are provided in Table E-1. The measured recovered mass of TCE was 0.803 grams representing 81% of the initial TCE mass while an estimated 5% was lost in liquid leaks. The mass lost in vapor leaks is assumed to represent the unaccounted balance. The measured recovered mass of o-xylene was 1.773 grams representing 90% of the initial o-xylene mass. Liquid leaks released another 1% while the remainder of the unaccounted balance was likely lost to vapor leaks from the column. The mass balance for o-xylene was expected to be better than for TCE as more of the TCE mass than o-xylene mass was lost to volatilization during handling of the experiment.

Table E-1. Mass Balances for TCE and o-Xylene

Step	TCE Mass (g)	o-Xylene Mass (g)
Emplaced NAPL in Column	0.998	1.976
Extract Masses		
Water Flow through Residual NAPL	0.206	0.084
Drain Column to Residual Saturation	0.088	0.035
Air Flow through Wet NAPL Column	0.425	0.139
TEE Flow through NAPL Column	0.076	1.367
Air Flow through Wet NAPL Column	0.001	0.019
Water Flow through Residual NAPL	0.006	0.075
Drain Column to Residual Saturation	0.001	0.011
Air Flow through Wet NAPL Column	0.001	0.039
Total Mass Extracted	0.803	1.769
Mass Lost to liquid Leaks	0.052	0.022
Percentage of Emplaced Mass Extracted (or Leaked)	86%	91%

The chemical mass balances suggest dissolution can be an effective method for removing a significant mass of a soluble compound such as TCE from NAPL. The addition of heat can provide a substantial extraction enhancement to a relatively low solubility, low volatility compound such as o-xylene.

The water mass balance from the testing is provided in Table E-2. The average water saturation in the column was calculated from the water mass balance, the measured pore volume of 670 g, and the measured porosity of 0.38.

Table E-2. Water Mass Balance

Step	Initial Water Mass (g)	Water Mass In (g)	Water Mass Out (g)	Final Water Mass (g)	Final Water Saturation (%)
Test 1: Initial Dissolution Test	670	1093	1093	670	1.00
Drain 1	670	0	507	163	0.24
Test 2: Volatilization Test	163	0	6	157	0.23
Test 3: Thermal Enhanced Test	157	155	115	196	0.29
Test 4: Volatilization Test	196	0	25	171	0.26
Re-Saturation	171	505	6	670	1.00
Test 5: Final Dissolution Test	670	5080	5080	670	1.00
Drain 2	670	0	500	170	0.25
Test 6: Volatilization	170	0	25	145	0.22

Mass Transfer Characteristics

The chemical properties of TCE and o-xylene relevant to mass transfer are listed in Table E-3.

Table E-3. Compound Mass Transfer Properties

Property	TCE	o-Xylene
Properties at 18 °C		
Aqueous Solubility (mg/L)	1,100	175
Saturated Vapor Concentration (mg/L)	352	19.4
Aqueous Diffusion Coefficient (cm^2/day)	0.372	0.563
Air Diffusion Coefficient (cm^2/day)	7,294	6,166
Henry's Constant (dimensionless)	0.381	0.219
Properties at 50 °C		
Aqueous Solubility (mg/L)	?	?
Saturated Vapor Concentration (mg/L)	1,361	109
Aqueous Diffusion Coefficient (cm^2/day)	1.67	1.31
Air Diffusion Coefficient (cm^2/day)	8,898	7,534
Henry's Constant (dimensionless)	0.344	0.197

During flow, the concentration of dissolved compounds increases as the water travels through a NAPL-bearing soil, limited by the compound's solubility in water. For a multi-component NAPL such as that used in this bench-scale study, the equilibrium solubility of component i is proportional to its mole fraction in the NAPL (y_i) and its pure component aqueous solubility (C_i^{sol}). After achieving transport equilibrium throughout the zone, the combined mass removal rate ($\dot{M}_i$) at the extraction point defines a bulk mass transfer coefficient (K_i) for the entire soil volume (V) flushed with clean water:

$$\dot{M}_i = K_i \, y_i \, C_i^{sol} V = Q C_{i,ext} \qquad\qquad \text{Equation (1)}$$

The bulk mass transfer coefficient is generally related to flow velocity (U), average soil grain size, soil porosity, NAPL saturation, and characteristic source length in the direction of flow (L) through a Sherwood number correlation (Mayer & Miller, 1996):

$$K_i = \left(\frac{D_{w,i}}{d_p^2} \right) \beta_0 \, (\text{Re})^{\beta_1} \, (\theta S_N)^{\beta_2} \qquad\qquad \text{Equation (2)}$$

where:

$\quad$ Re $\quad = \dfrac{U d_p}{\nu_w}$ = Reynolds Number

$\quad K_i \quad$ = lumped mass transfer coefficient between NAPL ganglion and water
$\quad S_N \quad$ = saturation of NAPL in the soil
$\quad D_{w,i} \quad$ = molecular diffusion coefficient of compound i in water
$\quad d_p \quad$ = mean soil particle diameter
$\quad \theta \quad$ = soil porosity
$\quad U \quad$ = groundwater velocity
$\quad \nu_w \quad$ = kinematic viscosity of water
$\quad \beta \quad$ = mass transfer correlation parameters

Given these relationships and considering a multi-component NAPL such as the one used in this study in which the majority of the NAPL was effectively inert, the ratio of concentrations of compounds measured in the effluent are given by:

$$\frac{C_{TCE}}{C_{o-xylene}} = \left(\frac{D_{w,TCE}}{D_{w,o-xylene}} \right) \left(\frac{y_{TCE} C_{TCE}^{sol}}{y_{o-xylene} C_{o-xylene}^{sol}} \right) \qquad\qquad \text{Equation (3)}$$

Substituting component properties provided in Table E-3 yields,

$$\frac{C_{TCE}}{C_{o-xylene}} = 4.15 \left(\frac{y_{TCE}}{y_{o-xylene}} \right) \qquad\qquad \text{Equation (4)}$$

This ratio assumes the physical parameters for the bulk mass transfer coefficient are identical for both compounds. At the start of the first dissolution test, the mole fractions for TCE and o-xylene were 0.057 and 0.141, respectively, yielding a theoretical ratio of 1.7. This ratio should hold even if the flowing water does not attain equilibrium with the NAPL assuming this bulk mass transfer coefficient is applicable. As measured in the first dissolution test (Test 1), the initial measured value was 1.8 and increased to 2.7 during the first three hours of water injection. The ratio was expected to decrease as the TCE mole fraction was decreasing more rapidly than o-xylene because of its higher solubility. Hence, the validity of this bulk mass transfer coefficient

E-29

for use in evaluating the bench scale testing is questionable. Additional research into mass dissolution from multi-component NAPL, such as that reported by Carroll and Brusseau (2009), is recommended. Mass transfer during vapor flow is more complicated than saturated water flow with the presence of pore water for partitioning of the compounds. This bench scale study provides data for further study of volatilization from a multi-component NAPL and includes the enhancement of increased temperature. Other data and a description of the complexities of the vapor mass transfer can be found in Carroll et al. (2009).

Measured values of the ratio of the TCE concentration to the o-xylene concentration are provided in Table 4 for the other tests performed in this bench scale study.

Table E-4. Measured Concentrations and Calculated Mass Balance Mole Fractions

Test	TCE Conc (mg/L)	TCE Mole Fraction	o-Xyl Conc (mg/L)	o-Xyl Mole Fraction	Conc Ratio (TCE / o-Xyl)
Test 1: Initial Dissolution Test	193	0.057	81	0.141	2.38
Test 2: Volatilization Test	21.8	0.017	5.0	0.136	4.36
Test 3: Thermal Enhanced Test	0.021	0.014	6.5	0.130	0.00323
Test 4: Volatilization Test	0.094	0.014	1.66	0.030	0.05663
Test 5: Final Dissolution Test	3.9	0.0135	56	0.028	0.06964
Test 6: Volatilization	0.05	0.0135	1.0	0.022	0.050

References

Carroll, K.C. and M.L. Brusseau. 2009. Dissolution, Cyclodextrin-Enhanced Solubilization, and Mass Removal of an Ideal Multicomponent Organic Liquid. J Contam Hydrol. 106(1-2): 62–72. doi:10.1016/j.jconhyd.2009.01.002.

Carroll, K.C., R. Taylor, E. Gray and M.L. Brusseau. 2009. The Impact of Composition on the Physical Properties and Evaporative Mass Transfer of a PCE-Diesel Immiscible Liquid. J Hazard Mater. 164(2-3): 1074–1081. doi:10.1016/j.jhazmat.2008.09.003.

Mayer, A.S., Miller, C.T. 1996. The influence of mass transfer characteristics and porous media heterogeneity on nonaqueous phase dissolution. Water Resources Research, 32(6), 1551-1567.

Appendix F

Description of Flow and Solute Transport Modeling

1 Groundwater Flow Model

1.1 Site Model for Groundwater Flow

A comprehensive numerical site model for groundwater flow at ST012 served as the foundation for a smaller-scale, local model for simulating mass transfer tests (MTTs) performed in the Lower Saturated Zone (LSZ), known as the B and C intervals. The USGS finite-difference flow modeling code MODFLOW was applied for the purpose of this study, and pre- and post-processing tasks were conducted using the Groundwater Modeling Software (GMS) software suite. The following sections describe the components and assumptions associated with the site-scale simulations.

1.1.1 Model Design

1.1.1.1 Model Domain and Grid

The site-scale model domain (Figure F-1) covers slightly more than 135 acres and spans nearly 28 vertical feet, the latter of which corresponds to the approximate vertical dimensions of the LSZ. The numerical grid contains 111 rows and 138 columns situated in a single model layer; therefore, flow in the LSZ was simulated as strictly two-dimensional. The model domain was oriented in an east-west direction parallel to the general direction of local groundwater flow. This approach implies confidence in the assumption of integrity with respect to the laterally-extensive low-permeability units known to be separating the LSZ and Upper Water Bearing Zone (UWBZ) and the LSZ from deeper water-bearing units. Representative cell dimensions within the constantly-spaced grid are roughly 6 meters in the x-direction by roughly 6 meters in the y-direction by 8.5 meters vertically.

1.1.1.2 Boundary Conditions

Boundary conditions on the up-gradient and down-gradient faces within the LSZ site-scale model were simulated as generalized head-dependent features using the MODFLOW General Head Boundary (GHB) package. Hydraulic head assignments and conductance parameters associated with these boundary condition types were determined using automated parameter estimation, which is described in a later section. Vertical recharge and seepage to/from the LSZ were assumed to represent negligible terms in the cumulative mass balance, thus fluxes from these processes were negated in this modeling study.
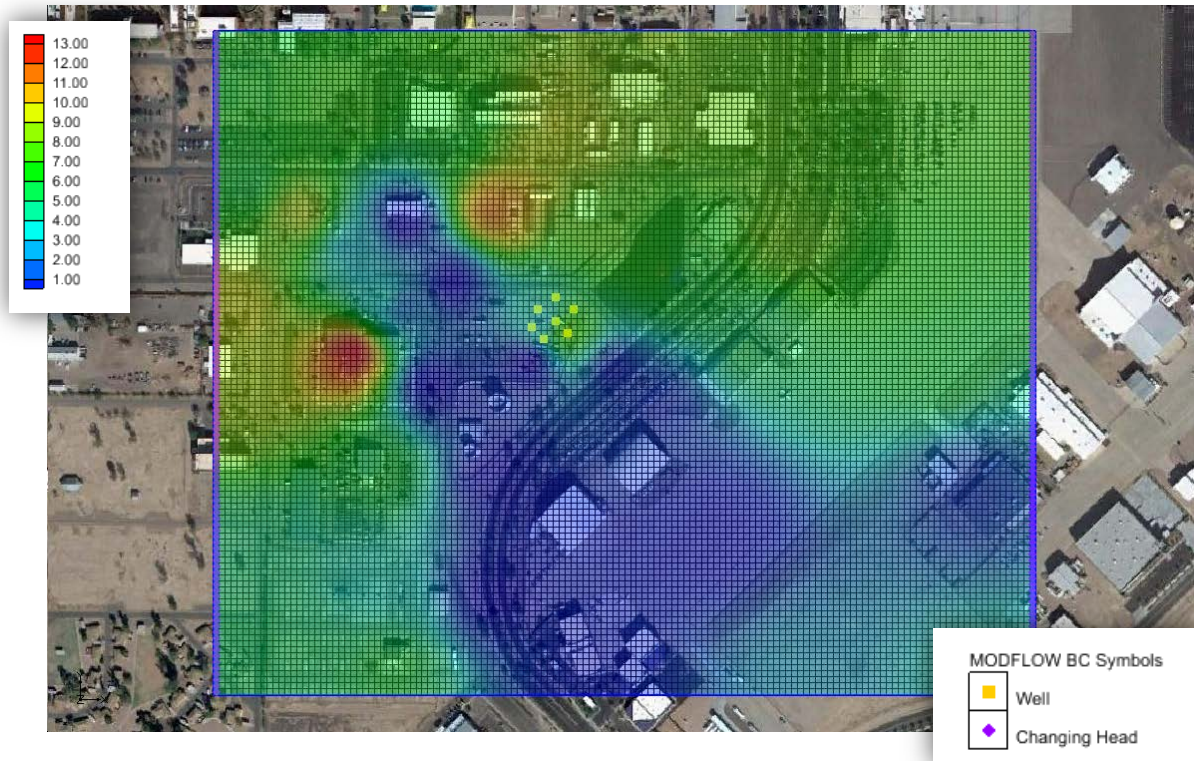
Figure F-1: Boundary conditions, sources and sinks and hydraulic conductivity field in site-scale model – legend indicating hydraulic conductivity in meters per day.

1.1.1.3 Temporal Discretization

Flow conditions were observed over a relatively extensive period of record in the vicinity of the ST0-12 site, and the resulting assumption of steady-state flow was derived from the behavior of the more recent hydraulic head data. Following the onset of confined conditions, measurements of head in the LSZ have indicated relatively normal behavior, both with respect to hydraulic gradient magnitude and direction. These observations served as justification for the simulation of steady state flow conditions in the LSZ.

1.1.2   Calibration Approach and Results

Final calibration of the site-scale LSZ flow model was performed using the automated parameter optimization tool PEST (*Parameter ESTimation Tool*) (Doherty, 2004). This tool compared the results of several flow model simulations to a dataset of compiled head observations (i.e., head "targets") in the vicinity of the ST0-12 site and extracted the optimal set of parameter inputs representing the best match between model results and observed conditions. Figure F-2 compares the observed and modeled head values at each target location. Figure F-3 depicts the ST012 site model calibrated to water levels observed in November 2004. This data set was selected as the best representative data set for model calibration in terms of matching the time trend in hydraulic gradient and spatial coverage.
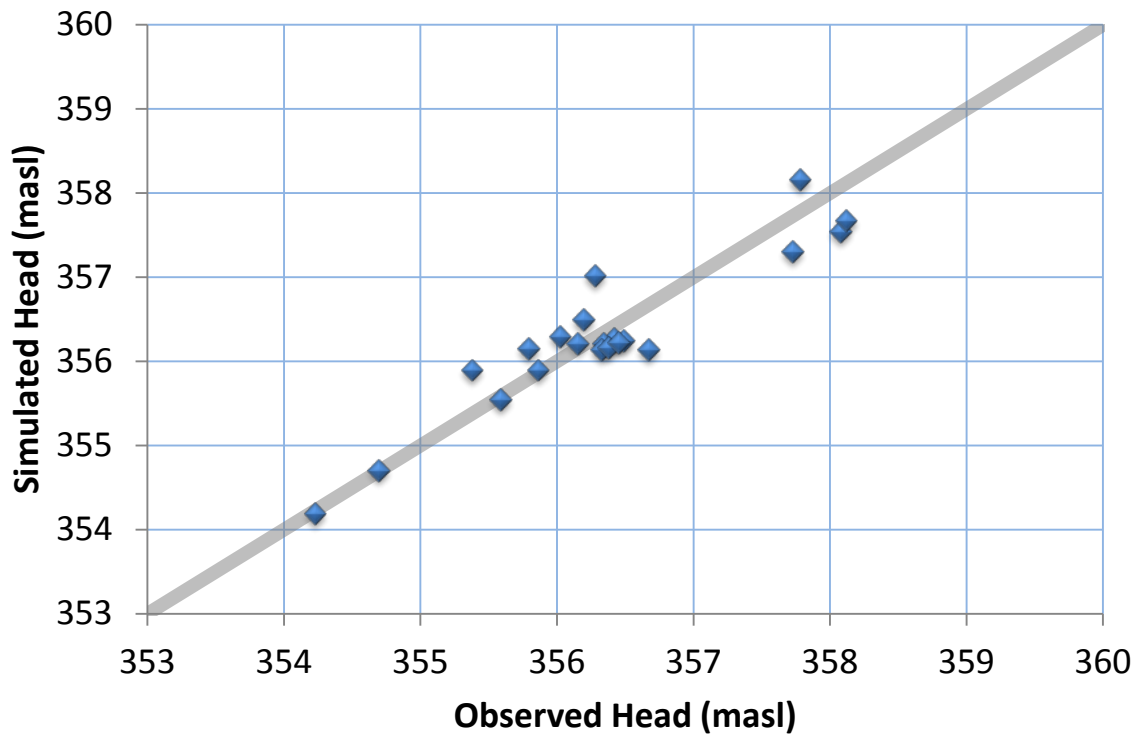
Figure F-2: Comparison of simulated and observed heads in the LSZ for steady-state, site-scale model.

Figure F-3: Simulated Hydraulic Head Distribution in the LSZ and Calibration Targets for the ST012 Site Model.

Model calibration was most sensitive variables to the assigned values of head and conductance at the up-gradient and down-gradient boundaries and the representative field of hydraulic conductivity within the flow model domain. Head assignments at the boundaries were constrained by recorded observations near the boundary locations, while conductance parameters were allowed to vary more significantly to account for uncertainty along the boundaries themselves. This approach protects flow in the interior of the model from being arbitrarily defined by inaccurate specifications.

The hydraulic conductivity field (shown in Figure F-1) was determined using a "pilot-points" approach which creates a variable field of values determined from an automated interpolation process. The points were set using values at locations where pumping tests were performed (fixed) supplemented with additional locations where values were initialized using reasonable estimates of hydraulic conductivity but remained flexible and accessible to the optimization process (variable). This approach was appropriate in this case because a single model layer was used to represent a highly-stratified and complex LSZ unit over which material properties are known to vary significantly.

1.2   *Local Model for Groundwater Flow*

The site-scale model was translated to a more focused, local model for the purpose of simulating the MTTs prior to and following the Thermal Enhanced Extraction (TEE) pilot test. Model

translation was necessary when considering the level of precision required to capture variability in tracer breakthrough times, Darcy velocities, aqueous phase NAPL constituent concentrations and NAPL constituent mass fluxes observed during the MTTs. Preliminary experiments with the site-scale model showed unsatisfactory results due to grid precision, thus an improved, fully three-dimensional (multi-layered), local-scale model was stressed according to the pumping and injection schedule coinciding with the pre- and post-TEE MTTs. Flow simulations differed in the steps that follow according to the purpose of the simulation – tracer breakthrough reproduction included a representation of transient flow behavior, while mass flux and aqueous phase concentration assessments were performed using a steady flow field derived from time-averaged pumping and injection rates and boundary condition specifications. Model assumptions associated with each step of the MTT flow simulations are described below.\

1.2.1   Model Domain and Grid Design

 Figure F-4 shows a comparison of the local-scale model to the site-scale model, highlighting the difference in the total active areas. The local model domain covers approximately 2.5 acres and incorporates the TEE cell and adjacent areas Boring logs taken from locations in the vicinity of the TEE cell were interpolated, and, where necessary, extrapolated to generate a three-dimensional representation of the hydrostratigraphic units comprising the LSZ. The materials derived from this analysis were translated to a variably-spaced, three-dimensional numerical grid and used to represent spatial variations in unit thicknesses and hydraulic properties. The resulting local model includes 395,352 cells over 19 model layers reflecting the permeable and semi-permeable units within the LSZ (Figure F-5). The variably-spaced model grid is divided into 130 rows and 150 columns with a maximum cell area of approximately 4 meters and a minimum cell area of 0.17 meters.
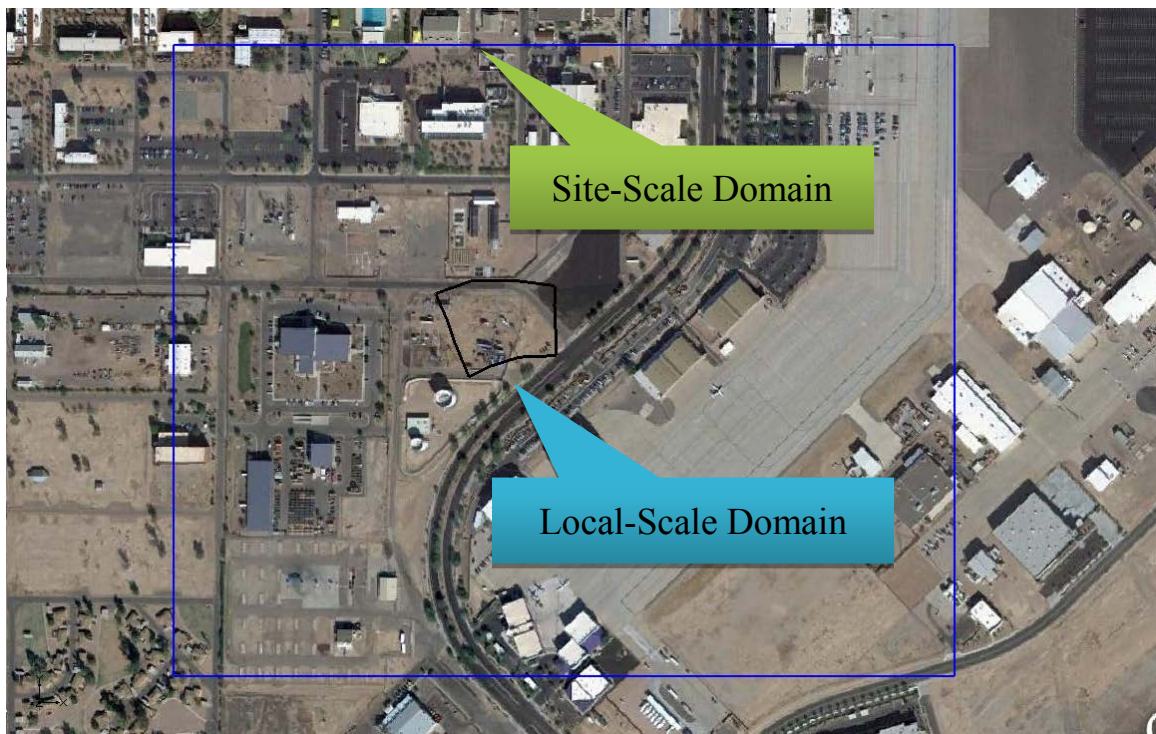
Figure F-4: Comparison of site-scale and local-scale model active domains.
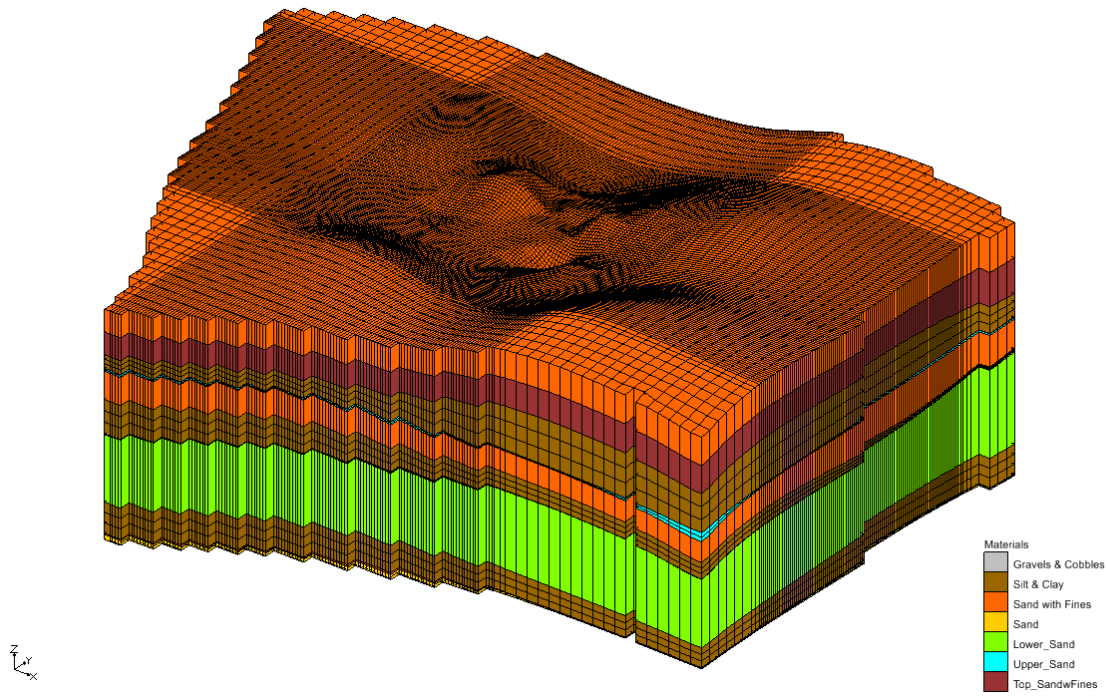
Figure F-5: Distribution of materials in tracer test model.

1.2.1 Sources and Sinks

The primary source and sink of/for water in the flow simulations was injection and pumping associated with the induced gradient within the TEE cell. Pumping and injection rates were distributed among the 19 model layers based on the local transmissivity (T_i) of each layer, which is the product of the hydraulic conductivity (K_i) and the vertical thickness (b_i) of layer i (i.e., $T_i = K_i b_i$). Calibration was executed as an iterative process allowing updates to hydraulic conductivity parameters to improve the match between observed and simulated data.

Two different approaches were used to represent the rates of injection and extraction within the TEE cell confines, each being controlled by the requirements of the specific simulation. The following sections describe how the approaches differ.

1.2.1.1 *Tracer Test Simulations*

Due to the relatively short period over which tracer breakthroughs were observed (with respect to the time of injection in each case), the observed daily pumping rates were exactly replicated as model input. This provided the highest level of precision while sacrificing some computational efficiency due to the relatively large number of stress periods.

1.2.1.2 Mass Flux Simulations

In the case of the mass flux simulations, calculation times were much more significant when compared to the tracer simulations. This factor, along with the results of several sensitivity analyses, led to the simplification of the pumping rates to time-averages over the specific model period in question.

1.2.2 Boundary Conditions

Boundary conditions used for the local scale model were derived from flow simulations conducted using the site-scale model. Figure F-6 shows the orientation of the specified-head cells used to translate site-scale boundary fluctuations to the local model grid.

In a similar manner to the allocation of model stresses, two different approaches were used to represent the maturation of heads along the boundaries; however, both approaches relied on results of the site-scale flow model being stressed using the observed injection/extraction rates at the LSZ injection/pumping well network. The boundary condition development process is described below with more specificity with respect to each alternative.
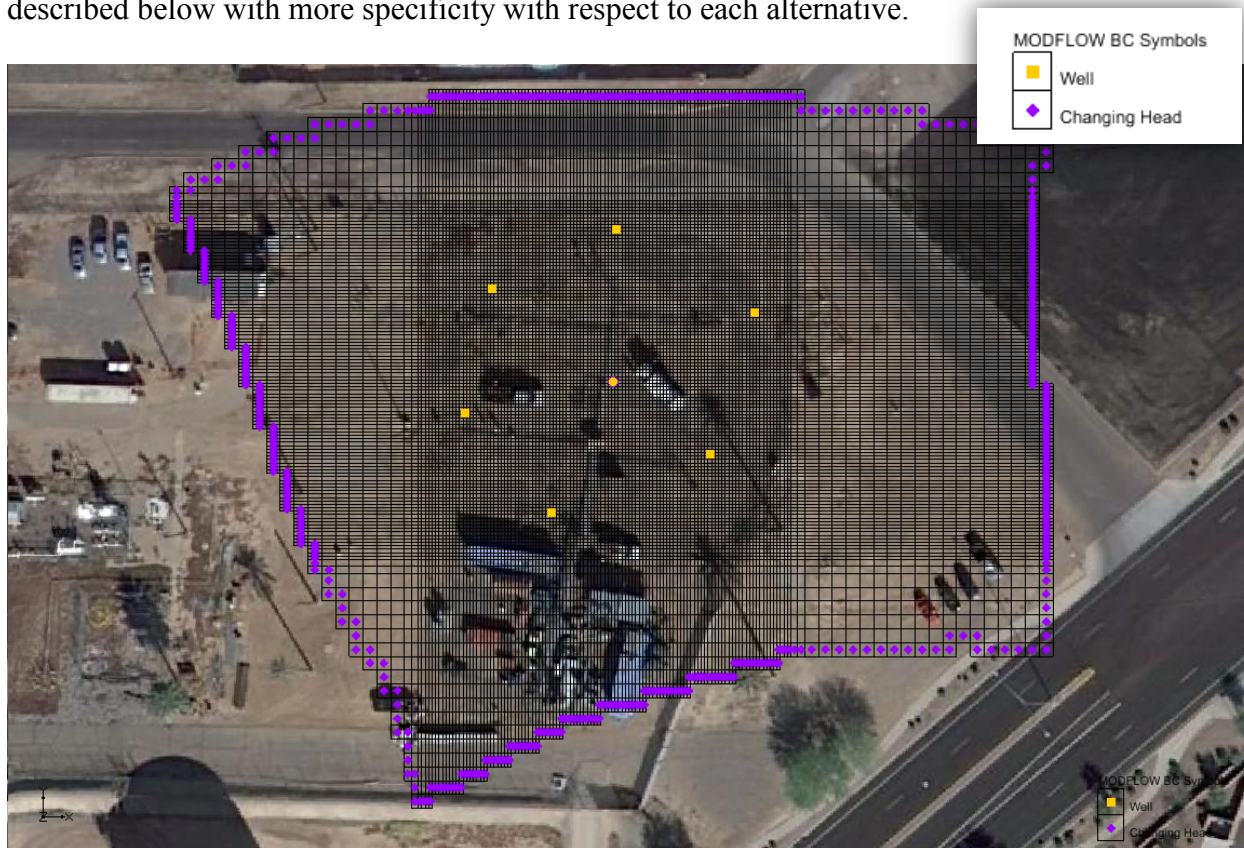
Figure F-6: Boundary conditions and sources and sinks in local-scale flow model.

1.2.2.1 Tracer Test Simulations

Boundary conditions for the tracer test simulations were generated using transient simulations during which the site-scale model was stressed using the daily average injection/pumping rate at each injection/pumping well screened in the LSZ. The observed transient behavior in heads at locations in the site-scale model corresponding to the boundary locations in the local-scale model were then used to generate specified-head boundaries in the local-scale model. The ability of the flow and transport models to operate within reasonable computational efficiency parameters allowed for the inclusion of this high level of transient detail in the tracer test simulation process. The key assumption associated with this approach is that vertical variations in heads across the individual units comprising the LSZ are relatively minor.

1.2.2.2 Mass Flux Simulations

The mass flux-dedicated flow and transport simulations required a more simplified approach to simulating boundary condition behavior due to the calculation times associated with periods of particularly high flow. Experiments performed with different alternative models indicated that time-averaged boundary conditions were an appropriate simplification; thus, the transient behavior of simulated hydraulic heads along boundary locations in the local-scale model was time-averaged over the period corresponding to two different periods of observed dissolved NAPL constituent behavior.

1.2.3   Modeling Approach

For the purpose of simulating the pre-TEE and post-TEE MTTs in the LSZ, the aforementioned local model was simplified by limiting the active area to the model layers corresponding to the upper region of the LSZ with focus on data collected from wells screened in the B-horizon (Figure F-7). Before and after the TEE pilot test, PFMs were deployed in the B-horizon and not in the deeper C-horizon.

Different periods were simulated for each MTT. The pre-TEE MTT included a transient period when the injection of clean water in the center well was initiated and the interior monitoring well concentrations of NAPL constituents were undisturbed. The two MTTs were both modeled assuming a pseudo-steady period during flushing of the permeable zones with clean water and the equilibration of mass transfer to this flow condition. The pre-TEE transient period modeled responses in hydraulic head and benzene concentrations at monitoring wells. Initial conditions for the pre-TEE simulation were based on observed water levels and BTEX concentrations at the start of water injection.

Flow simulations corresponding to the tracer test periods were used to identify and optimize the key hydraulic parameters in the more detailed representation of the LSZ. More specifically, the observed tracer breakthrough times were used as metrics by which the hydraulic conductivity of the individual materials, the porosity of the materials and the storage parameters associated with each unit could be calibrated. Post-TEE tracer data were preferentially used relative to pre-TEE data due to issues with the bromide sensor equipment.
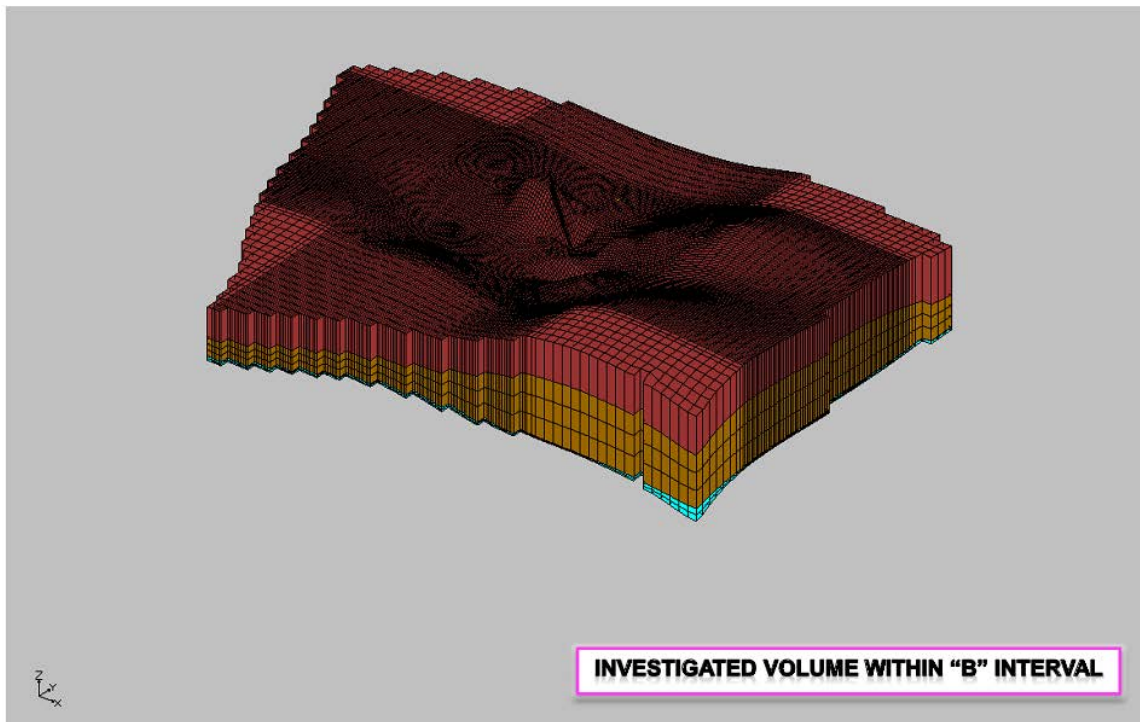
Figure F-7. Revised Local Model for Simulating the Pre- and Post-TEE MTTs in the B Horizon.

2   Solute Transport Model

Models dedicated to simulating the pre- and post-TEE MTTs were generated using two specific solute transport codes. The tracer test simulations were conducted using the MT3DMS code in a non-reactive format given that bromide behaved as a conservative tracer during both tests. Alternatively, the mass flux-dedicated simulations were conducted using the more robust modeling code SEAM3D, a model with the unique ability to simulate equilibrium-constrained mass transfer from a non-aqueous phase liquid (NAPL) to mobile, sub-equilibrium ground water. The application of SEAM3D, in this particular case, represents an appropriate and innovative method by which the rate of mass transfer could be directly evaluated by comparing observed and simulated site conditions.

2.1   *Local Model for Solute Transport – Tracer Test Simulations*

2.1.1   Boundary and Initial Conditions

Boundary and initial conditions were assigned in a relatively simple manner in the tracer test simulations due to the fact that each test was conducted following an extensive period of gradient establishment (prolonged injection at the central location combined with pumping at the extraction wells on the periphery of the TEE cell). Because of this condition, it was appropriate to initialize the model with a zero concentration for the bromide tracer compound, and since the

compound is known to be conservative in nature, it was also appropriate to neglect sorption and biodegradation within the examined area.

2.1.2 Transport Input Parameter Estimates

Transport parameters were limited in the case of the tracer test simulations, again, due to the simplifying assumptions associated with a conservative tracer compound. The longitudinal dispersivity values assigned to the grid were the primary parameters being evaluated, and the resulting breakthrough curves display evidence that an appropriate value was assigned.

2.2 Calibration Approach

The tracer test simulations were calibrated by evaluating the normalized time-to-observed tracer breakthrough at the monitoring well network locations. Accurate replication of the breakthrough times was ensured by replacing absolute concentration data with concentrations normalized to the maximum observed/simulated value. This approach removed the potential influence of deviations from the known injection concentration. Bromide breakthroughs at two monitoring well locations were evaluated in the B-interval (*MWN02B, MWN06B*), and four locations were evaluated in the C-interval (*MWN01C, MWN02C, MWN04C, MWN06C*). Pre- and post-TEE data were used to compare the simulated and observed breakthroughs; however, the post-TEE data were treated preferentially due to the previously-discussed sensor fouling issue.

2.3 Local Model for Solute Transport – Mass Transfer Simulations

2.3.1 Boundary and Initial Conditions

Within the closed flow cells created by the injection and pumping wells, NAPL constituent concentration inputs were limited to those derived from mass transfer from the NAPL source. Additionally, the water injected at the central well (*LSZ07*) was assumed to be free of contaminants; therefore, the simulated incoming flux of water produced a flushing effect as it radiated away from the injection point. This assumption was supported by the conditions observed during the MTTs. The effect of biodegradation on the NAPL compounds was also assumed to be negligible over the period corresponding to the MTTs; thus, incoming water fluxes were not assumed to replenish or reduce the existing electron accepting compound or biotic population concentrations.

The same assumptions mentioned above also apply to the initial conditions used when modeling mass transfer within the TEE cell. Specifically, the initial concentrations of the electron accepting compounds and biological populations were assumed to not influence the rate of mass transfer during the MTTs. However, the initial concentrations of the NAPL constituents were reflected in each of the modeling phases by interpolating the observed concentrations prior to each modeling step. More specifically, the constituents not grouped as part of the inert fraction were initialized prior to the start of a transport simulation by evaluating the observed concentrations at the monitoring well network (corresponding to each specific point in time), interpolating the resulting dataset, and finally, translating the interpolated dataset to the numerical grid.

2.3.2 Transport Input Parameter Estimates

As opposed to the simulations involving the conservative tracer compound, a unidirectional, linear isotherm was used to represent sorption of NAPL constituents to aquifer solids, and the constituent-specific sorption parameters were specified according to published values for each compound. Since some of the more-soluble components were grouped (e.g., toluene, ethyl benzene and the various xylenes were grouped together as "TEX"), the resulting sorption parameters were calculated as mass-fraction averages using the observed composition of the NAPL prior to aquifer steaming activities. Although the distribution of mass fractions within the NAPL is observed to change following the injection of steam, the sorption values are assumed to remain constant and thus do not change from model to model.

2.3.3 NAPL Input Parameter Estimates

The NAPL dissolution package (NPL) portion of SEAM3D requires several mixture-specific inputs which are used by the model code when calculating the equilibrium concentration expected for each constituent, the maximum rate of dissolution into the flowing, sub-equilibrium groundwater, and the total mass and mass depletion associated with the dissolving source. Tables 1 and 2 show the primary input parameters provided to the NPL package.

Table F-1: NPL input parameters, pre-TEE condition.

NAPL Constituent	Mass Fraction	Solubility (mg/L)	Molecular Weight (g/mol)
Benzene	0.0083	1780.0	78.1
TEX Group	0.0733	299.8	100.6
Semi-Volatiles Group	0.0197	58.3	122.2
Inert Fraction	0.8987	--	114.8

Table F-2: NPL input parameters, post-TEE condition.

NAPL Constituent	Mass Fraction	Solubility (mg/L)	Molecular Weight (g/mol)
Benzene	0.0010	1780.0	78.1
TEX Group	0.0179	264.9	102.0
Semi-Volatiles Group	0.0171	63.3	121.1
Inert Fraction	0.9641	--	114.8

The model parameter values included in Table E-1 and Table E-2 represent data collected from interpretations of NAPL material sampled prior to and following the TEE activities performed within the test cell, respectively. The most notable F-change is the reductions in the mass fractions of the more soluble and volatile compounds and constituent groups (e.g., benzene and the "TEX" group). This reduction in total benzene mass is reflected by the model as a reduction in the potential equilibrium concentration in the aqueous phase – a reduction which is captured in the model results.

Two additional key parameter inputs to the NPL package portion of SEAM3D are the source footprint (i.e., the volume of the aquifer contaminated with NAPL) and the residual saturation within the contaminated volume. Since equilibrium concentrations are only affected by the later input parameter in cases where transfer is mass-limited, the model results were found to be insensitive to this value. More specifically, the model periods are relatively short, and mass depletion is not significant during these intervals, although it may be significant from pre- to post-TEE conditions. Thus, mass transfer is observed as equilibrium controlled as opposed to mass-limited in both the pre- and post-TEE conditions. Sensitivity to the latter input parameter, or the volume of contaminated area, was also not significant; therefore, since the TEE cell region of the ST0-12 site is known to be relatively uniformly-contaminated, particularly with respect to the LSZ, source material was uniformly distributed within the interior of the modeled area. A sensitivity analysis to more and less densely specified source material showed little to no impact on mass transfer rates, which is a reasonable finding when dealing with sites that are experiencing equilibrium-controlled as opposed to mass-limited conditions.

2.4   Calibration Approach

Calibration of the mass transfer models was initially performed using a trial-and-error procedure that revisited the hydraulic parameter estimates derived from the tracer test model. During this process, simulated aqueous phase benzene and TEX group concentrations were compared to observed concentration data taken during the pre- and post-TEE MTTs. Concentrations were flux-averaged over multiple model layers to arrive at values representative of what would be observed from screen-specific observed concentrations. More specifically, the concentration data available for comparison to model results represented a laboratory analysis of water taken from wells screened over multiple layers. To appropriately compare model-derived concentrations to such values, predicted concentrations over multiple cells had to be weighted by the calculated flow through each cell.

Once a reasonable match between the simulated and observed data was achieved by finalizing the hydraulic parameter estimates, SEAM3D simulations were conducted using and externally-applied form of the PEST software capable of optimizing the key parameter in the simulation of NAPL dissolution: the mass transfer coefficient. Calibration was constrained by allowing PEST to only predict a uniform value over the entirety of the source area – a representative value for the pre- and post-TEE source zones (constrained to the TEE cell). The resulting estimates of the mass transfer coefficient represent optimized results corresponding to the TEE cell area under pre- and post-TEE conditions.

2.5   Summary of Calibration Results

Tables 3 and 4 provide a direct comparison of the observed and simulation concentrations for benzene and TEX during pre- and post-TEE MTTs.

Table F-3: Observed and simulation concentrations, pre-TEE Mass Transfer Test.

Location	Date	Observed Benzene (mg/L)	Observed TEX (mg/L)	Simulated Benzene (mg/L)	Simulated TEX (mg/L)
ST012-MWN06B	8/25/2008	17.22	20.54	16.72	20.15
ST012-MWN06B	8/27/2008	8.57	17.82	8.54	18.39
ST012-MWN06B	8/29/2008	0.86	1.32	2.51	10.07
ST012-MWN06B	9/2/2008	1.31	3.05	2.68	2.88
ST012-MWN06B	9/9/2008	3.92	6.33	2.67	3.10
ST012-MWN06B	9/16/2008	2.47	4.14	N/A	N/A

Table F-4: Observed and simulation concentrations, post-TEE Mass Transfer Test.

Location	Date	Observed Benzene (mg/L)	Observed TEX (mg/L)	Simulated Benzene (mg/L)	Simulated TEX (mg/L)
ST012-MWN06B	9/29/2009	1.85	6.91	1.87	7.11
ST012-MWN06B	10/9/2009	0.08	0.75	0.09	0.21
ST012-MWN06B	10/30/2009	1.18	3.30	0.09	0.22

Figure F-8 shows the benzene (upper plot) and TEX (lower plot) concentrations observed at monitoring well MWN-06B during the pre-TEE LSZ MTT and simulated using the local transport model. With the introduction of clean groundwater at the central injection well (LSZ07), concentrations declined as the cleaner water reached various monitoring wells. Steady-state benzene and TEX concentrations were reached within days. Evaluation of the transient behavior of concentrations was limited by the availability of data. Breakthrough of cleaner water mimicked the tracer breakthrough, and, as a result, equilibrium concentration was the primary target for comparison.

The gradual increase in the observed equilibrium concentrations reflected a decrease in the groundwater velocity when the pumping well LSZ01 was turned off on 9/2/2008 (Figure F-8). This variation in pumping was not included in the groundwater flow model, and as such, the rise in the equilibrium concentrations would not be simulated by the transport model. For both the benzene and TEX, the model accurately captured responses following injection including the equilibrium concentrations of the pre-TEE MTT. The model input variables that most directly

controlled the equilibrium concentrations were the NAPL mass transfer coefficient and the NAPL composition, specifically the benzene mass fraction.

For the post-TEE test, concentrations in the TEE cell showed much greater variability among the monitoring wells compared to the pre-TEE case. This variability was primarily the result of variable treatment within the cell that yielded non-uniform NAPL composition and distribution in the cell. The initial rise and drop in the simulated benzene concentrations (Figure F-9, upper plot) reflected an inconsistency between the initial condition and the initial equilibrium concentration determined using the NAPL Package. A similar response was observed in the simulated TEX concentrations (Figure F-9, lower plot). However, the local solute transport model provided a reasonable representation of the decrease in the concentration over time at MWN-06B. The simulated equilibrium benzene concentration (340 µg/L) was within an order of magnitude of the observed value (79 µg/L), whereas the match between the observed and simulated TEX equilibrium concentrations (750 µg/L and 690 µg/L, respectively) was much improved.

The sensitivity of the post-TEE equilibrium benzene and TEX concentrations at MWN-06B to the NAPL mass transfer coefficient and the NAPL mass fraction of benzene are also shown in Figure F-9. By reducing the NAPL mass transfer coefficient an order of magnitude relative to the pre-TEE test, an improved match with the benzene concentration was realized, but a poorer match with the TEX concentration was apparent (Figure F-8, upper and lower plots, respectively). The mass fraction of benzene in the post-TEE NAPL likely varied by an order-of-magnitude across the cell whereas the TEX content was likely more consistent. To assess sensitivity of the benzene mass fraction, simulations were performed in which the percent benzene in the NAPL was reduced and increased by a factor of 2. Using the lower NAPL mass transfer coefficient (0.05 d^{-1}), equilibrium benzene concentration varied from 130 to 6 µg/L and bracketed the baseline simulated and observed concentrations (80 µg/L and 79 µg/L, respectively).
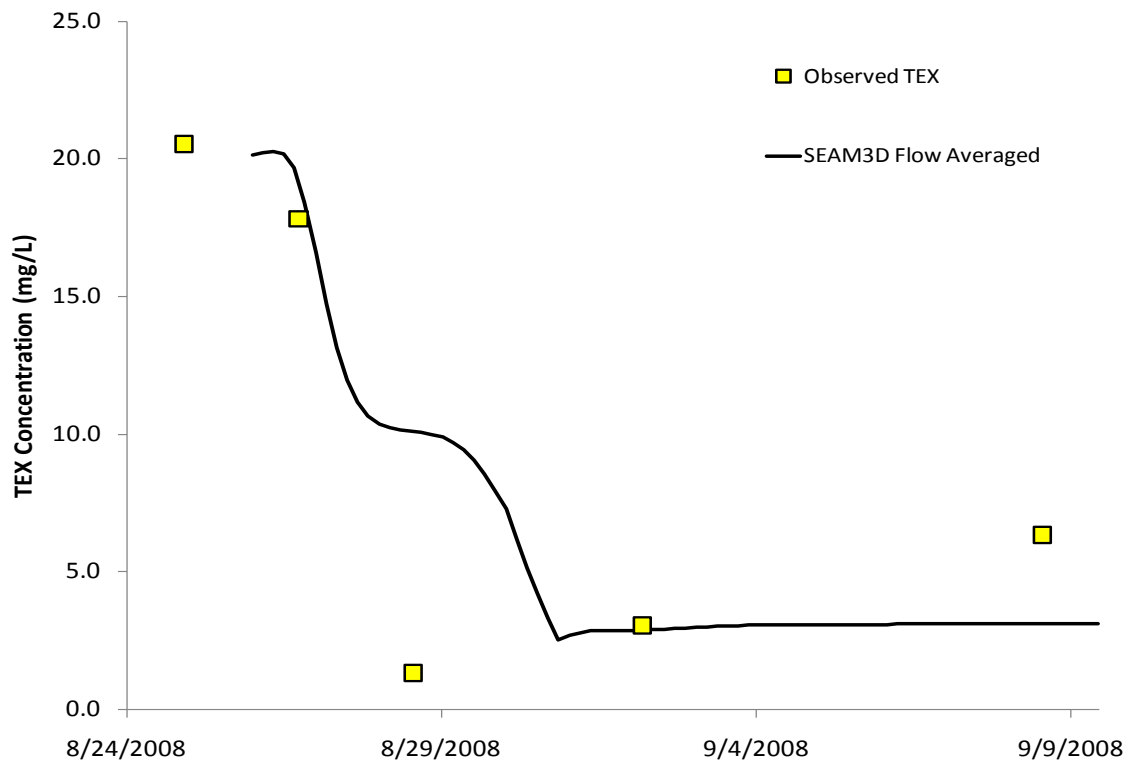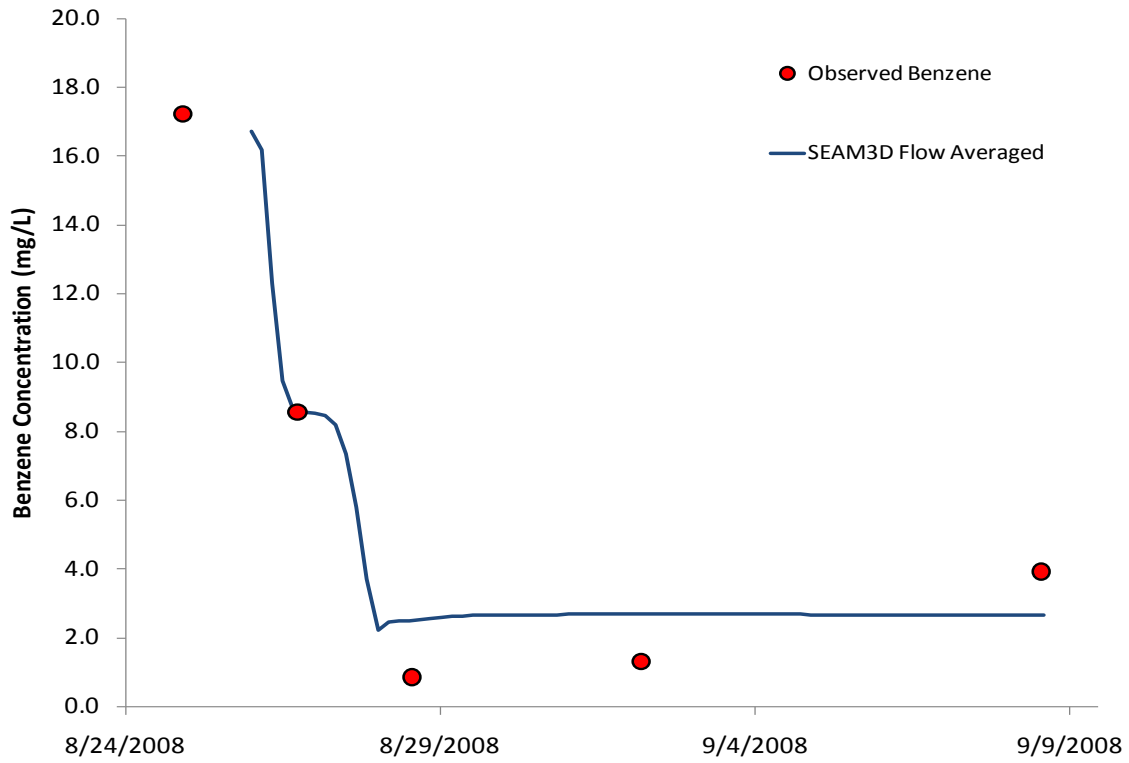
Figure F-8. Pre-TEE Mass Transfer Test Results Showing Observed and Simulated Flow-Weighted Benzene (upper) and TEX (lower) Concentrations at MWN-06B.
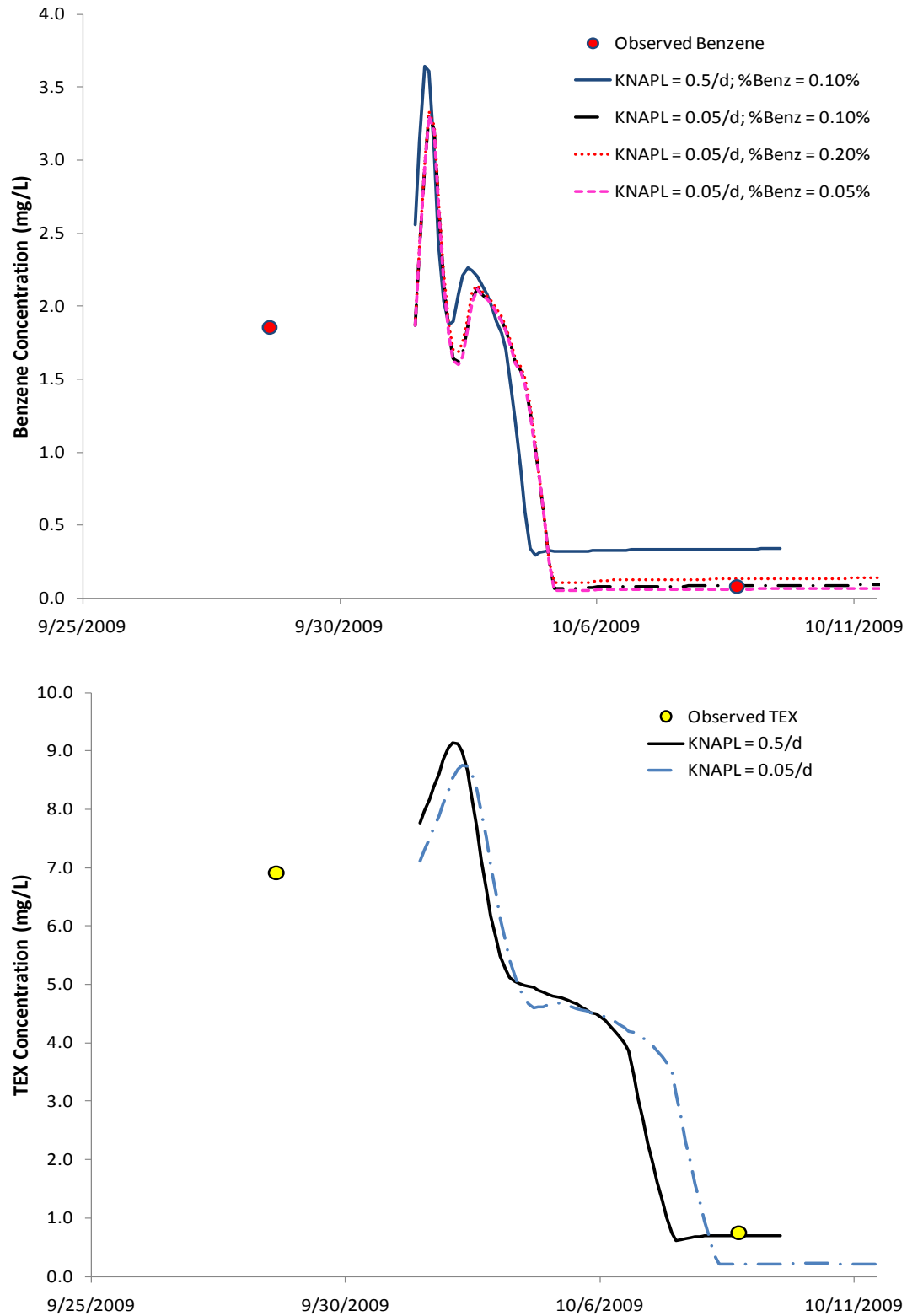
Figure F-9. Post-TEE Mass Transfer Test Results Showing Observed and Simulated Flow-Weighted Benzene (upper) and TEX (lower) Concentrations at MWN-06B. KNAPL refers to the NAPL mass transfer coefficient.

APPENDIX G: PRE- AND POST-REMEDIATION MASS FLUX MEASUREMENTS AT THE FORMER WILLIAMS AIR FORCE BASE, ARIZONA

Prepared by the University of Florida

PRE- AND POST-REMEDIATION MASS FLUX MEASUREMENTS AT THE FORMER WILLIAMS AIR FORCE BASE, ARIZONA

Prepared for
BEM

Prepared by
University of Florida

Gainesville, FL 32611

April 26, 2010

TABLE OF CONTENTS

LIST OF FIGURES

LIST OF TABLES

Executive Summary

Passive Flux Meters (PFMs) were used to measure the groundwater flux and contaminant mass flux during induced gradient conditions (injection and extraction wells were active) both before and after a pilot test of thermal enhanced extraction (TEE) remediation at the former liquid fuels storage site ST012, Williams Air Force Base, Arizona. Flux refers to the mass of water and or contaminants flowing per unit area at a measured depth in a well screen averaged over a given period of time. The expected contaminants at Williams were benzene and total petroleum hydrocarbon (TPH).

When comparing pre- and post-remediation flux profiles the most noticeable difference is an observed decrease in benzene and TPH flux in the A-Horizon of the Upper Water Bearing Zone (UWBZ) and an increase in the intermediate wells in the B-Horizon of the Lower Saturated Zone (LSZ). However, it should be noted that the intermediate wells were screened across a relatively low permeability section (B-Horizon) of the LSZ. Contaminant fluxes were not directly measured using PFM in the more permeable C-Horizon of the LSZ. But, contaminant concentrations measured in monitoring wells that were screened across the C-Horizon were observed to decrease which would also correspond to a decrease in mass flux.

The benzene flux profiles show a fairly significant reduction in mass flux for the wells that had the highest pre-remediation mass flux (MWN-02A and 05A) in the UWBZ. In contrast, benzene flux increases were observed in LSZ wells MWN-01B and 03B. The flux increases in the intermediate B wells is likely associated with the accumulation of free phase NAPL in wells that previously had no evidence of NAPL during pre-treatment, or possibly a lack of treatment by the TEE pilot system. It should be noted that based upon the TEE system design, flux reductions were expected to be highest in wells close to the thermal injection well while those near extraction wells were expected to show less change as the intensity of remediation varied with distance from the injection well.

Trends in the TPH flux profiles typically agree with the benzene data, while showing more significant increases in wells MWN-01B and -03B. Again, this supports the accumulation of free-phase NAPL in the B wells.

For standard applications (using fence row transects of wells), the mass discharge per unit width can be used to estimate the mass discharge (Kg/day) through a specified region of the aquifer. This provides a metric for comparing the change in total mass discharge between pre- and post-remedial conditions. However, for the flow conditions at the TEE Treatment Cell, this method may not be directly applicable due to radial flow conditions, fluctuations of the induced gradients over time, and relative proximity of monitoring wells with respect to injection/extraction wells. Bearing these issues in mind, an estimate for mass discharge was calculated for the TEE Treatment Cell using a cylinder having a radius equal to the average radius of the flux wells from the central injection. Each well was assumed to have equal representation over the 40 ft radius and treated as if they were on the circumference of the cylinder. Again, it is noted that this is not a direct representation of the physical system, but it allows for a general estimate of the total mass discharge from the site in order to provide a metric for comparison of pre- and post-remediation. Performing this calculation for the benzene flux resulted in estimated total mass

discharges of 5.6 and 1.2 Kg/day for pre- and post-remediation respectively in the UWBZ. The LSZ values were 1.1 and 1.8 Kg/day showing an overall increase as noted earlier. For TPH the UWBZ values were 61 to 9.0 Kg/day while the LSZ were 4.7 to 13 Kg/day again showing an increase. The estimated increase in mass flux in the LSZ is consistent with the observation that there was minimal or no free-phase NAPL in the LSZ wells pre-remediation, but there was free phase NAPL present in the wells post-remediation. The integrated values provide an overall summary of the remedial changes in mass discharge within the portions of the UWBZ and LSZ where flux measurements were taken during the applied water flood at the TEE Treatment Cell. But, as noted above, these estimates are only applicable to the measured intervals of the aquifers and do not include any changes that may have occurred in the more permeable C-Horizon and do not account for variable treatment across the test volume. In particular, MWN-03B was located near an extraction well and mobilized contaminants were drawn to this location.

The integrated observations comparing pre- and post-remediation flux measurements showed a decrease in the TEE Treatment Cell average benzene mass flux in the UWBZ of approximately 78%. The associated TPH flux reduction was approximately 85%. This was accompanied by an increase in mass flux of benzene in the less permeable B-Horizon of the LSZ of about 70% for benzene and 180% for TPH. As mentioned previously, this is likely due to the accumulation of NAPL in the LSZ wells as evidenced by TPH spikes in the bottom segment of multiple PFM deployed in some of the LSZ B-Horizon wells. Because, the majority of the directly measured mass flux was in Horizon-A of the UWBZ, the overall combined TEE Treatment Cell mass flux (for Horizon-A and Horizon-B) was reduced by about 54% for benzene and 66% for TPH. Based upon observed aqueous concentrations, the mass flux in the more permeable C-Horizon of the LSZ was also reduced but was not directly measured by PFM and is not included in the overall site reductions cited above.

In the UWBZ a correction was evaluated for the presence of NAPL in the wells using a pre-deployment swipe test in the wells. The magnitude of the measured mass flux was reduced by the correction; however, the pre- and post-remedial flux comparisons remained fairly constant at approximately 80% reduction in flux in the UWBZ.

Introduction

Passive Flux Meters (PFMs) were used to measure the ambient groundwater flux and contaminant mass flux at the former Williams Air Force Base, Arizona. For a description of the PFM fundamentals see Hatfield et al. 2004 and for field implementation see Annable et al. 2005. Flux refers to the mass of water and or contaminants flowing per unit area at a measured point in a well screen averaged over a given period of time. Based upon this general definition, the units associated with mass flux are determined as:

$$flux = \frac{mass}{area \cdot time} = \left[\frac{M}{L^2 T} \right]$$

where the terms M, L, and T represent the base units of mass, length, and time respectively. For consistency with common practice, the ambient groundwater flux will be discussed in terms of the specific discharge or Darcy velocity, which is the volumetric water flux (or flowrate) through a specified cross-sectional area. The resulting units are L/T and for this report the Darcy velocity will be represented with the units of cm/day. For this report the contaminant flux will be discussed in terms of mass flux ($M/(L^2 T)$) and represented with the units of ($mg/(m^2 day)$) or ($g /(m^2 day)$) depending on the magnitude of the observed flux values.

Based upon previous TEE Treatment Cell assessments, the expected contaminants at Williams were benzene and total petroleum hydrocarbon (TPH) (USAF, 2007).

The intent of this project was to observe and compare the relative flux values pre- and post-remediation. A site map including injection wells, extraction wells, monitoring and PFM well locations is shown in Figure 1, and a general TEE Treatment Cell cross-section plan is provided in Figure 2.

Methods and Procedures

Pre-remediation flux measurements
On September 18, 2008 eighteen (18) passive flux meters (PFMs) were deployed in the 6 UWBZ A wells. Three PFMs were deployed in each well and all PFMs were constructed in 5-foot lengths. In three wells (MWN-01A, MWN-03A, MWN-06A) the PFMs were deployed with 5-foot spacing between (i.e. there was one 5-foot PFM at the base of the well screen, 5-feet of open screen, another 5-foot PFM, 5-feet of open screen, and a final 5-foot PFM at the top of screen). In the three remaining wells (MWN-02A, MWN-04A, MWN-05A) three connected PFMs were deployed (for 15 feet of continuous PFM) at the base of the well screen.

On September 22, 2008 all 18 PFMs were successfully retrieved and sampled (corresponding to a deployment length of 4 days).

On September 23, 2008 (one day after retrieval of the UWBZ PFMs), a PFM was inserted and immediately retrieved and sampled in each of the UWBZ wells. These "swipe tests" were taken in order to provide a background comparison to consider the effect of passing the PFM through free product at the water table.

On October 23, 2008 eighteen (18) PFMs were deployed in the 6 LSZ B wells (three PFMs were deployed in each well). In all six wells, three connected PFMs were deployed (for 15 feet of continuous PFMs) covering the entire 15-foot length of well screen. These wells were screened from about 205 ft bgs to 220 ft bgs. PFMs were not deployed in deeper C-Horizon wells, generally screened from 230 to 245 ft bgs, that intersect more permeable strata of the LSZ.

On October 27, 2008 all 18 PFMs were successfully retrieved and sampled (corresponding to a deployment length of 4 days).

Post-remediation flux measurements
On November 12, 2009 twenty one (21) PFMs were deployed in seven of the wells at the TEE Treatment Cell. The next day the remaining PFMs (15) were deployed for a total of 36 PFMs in the UWBZ and LSZ wells. The location of each PFM in the wells followed the description provided in the pre-remedial deployment conducted in 2008.

On November 16, 2009 PFMs from six of the seven wells deployed four days earlier were successfully retrieved and sampled (corresponding to a deployment length of 4 days). Three PFMs, located in well 5B, were lodged in the well and could not be removed following application of several removal techniques. These PFM were abandoned in the well after unsuccessful attempts to retrieve using heavier equipment.

On November 17, 2009 the PFMs from the remaining 5 wells were successfully retrieved and sampled (corresponding to a deployment length of 4 days). The remaining swipe tests were conducted following removal of the PFMs.

Results

Pre-remediation flux
Both pre-remediation and post-remediation flux profiles are displayed in Figures 4-6. The profiles include the results from both the shallow and intermediate well deployments and are referenced to depth below ground surface. The average contaminant flux per well is shown in figures 7 & 8. It should be noted that figures 7 and 8 provide a method for comparison of average flux on a well-by-well basis, but does not take into account the vertical variability of the fluxes within each well. The corresponding data are summarized in Appendix A.

The pre-remedial Darcy velocities range from a high of 160 cm/day observed in the UWBZ well MWN-02A to a low of about 10 cm/day in several of the wells. The high value in MWN-02A is likely due to the close proximity to the injection wells (UWBZ07 and LSZ07 in Figure 3). Well MWN-06 also showed higher values of Darcy velocity up to 40 cm/day and is also located near the injection well (UWBZ07 and LSZ07 in Figure 3). During the pre-remedial measurements the average Darcy flux in the UWBZ (43 cm/day) was higher than the LSZ (13 cm/day). Based

upon relative permeability of the formation, it is likely that the majority of the flow in the LSZ traveled through the deeper C-Horizon of the LSZ from about 232 to 244 ft bgs (see Figure 2). PFMs were not deployed in this interval.

The average benzene flux during the pre-remediation deployment was highest in wells MWN-02A and 05A in the UWBZ (Figure 7). With the highest observed benzene flux being 68 g/m^2/day in well MWN-05A (Figure 4). The next highest flux was observed in well MWN-04A with one sample at 50 g/m^2/day. All other wells exhibited much lower benzene mass flux during the pre-remediation deployment.

TPH mass flux followed a similar trend to the benzene with wells MWN-02A, 05A and 04A having the highest average mass flux (Figure 8). In general, TPH showed similar trends to benzene in the flux profiles with the exception that TPH spikes were observed in the bottom segment for several of the UWBZ wells including MWN-01A, 02A, 04A and 05A. These wells likely had free-phase NAPL present in the well prior to PFM deployment and the bottom portion of the first PFM likely accumulated significant NAPL mass elevating the calculated TPH mass flux.

Post-remediation flux
The post-remedial Darcy velocities range from a high of 122 cm/day in the LSZ well MWN-02B and 115 cm/day the UWBZ well MWN-03A to a low of about 3 cm/day in the LSZ well MWN-03B. The high value in MWN-02 is likely due to the close proximity to the injection well (LSZ-07 in Figure 3). During the post-remedial measurements the average Darcy flux in the UWBZ (26 cm/day) was roughly equivalent to the LSZ (25 cm/day).

The benzene mass flux during the post-remediation test was highest in wells MWN-01B and 03B in the LSZ, with values of 23.5 g/m^2/day and 34.5 g/m^2/day respectively. These two wells also had higher average mass flux when compared to the other wells (Figure 7). The next highest average flux was observed in well MWN-5A in the UWBZ (Figure 7).

TPH mass flux followed a similar trend to the benzene with wells MWN-01B and 03B having the highest average mass flux (Figure 8). In general TPH showed similar trends to benzene in the flux profiles with the exception that TPH spikes were observed in the bottom segment for wells MWN-01B and 03B. These wells likely had free-phase NAPL present prior to PFM deployment.

Pre and Post-remediation comparisons
The flux profiles in Figures 4 through 6 provide a comparison between pre and post-remedial PFM deployments. Darcy velocity profiles show some fairly significant differences between the two deployments. Well MWN-02 shows a shift from high flow in the UWBZ to high flow in the LSZ while well MWN-03 shows an increase in the UWBZ. Well MWN-01 shows a general increase in flow throughout the profile. The shifts in Darcy velocities may be due to the operation of wells during the two deployments. The flow rates applied during the two tests were not identical and shifts in wells used and flow applied may explain some of the observed differences. Also, changes in aquifer and well permeability may contribute to the observed differences. Overall, a decrease was observed in the average Darcy velocity in the UWBZ (43 to

26 cm/day). The observed decrease is primarily due to decreases observed in Wells MWN-02A and 06A which appeared to be relatively uniform over the vertical segments (Figure 6). An overall increase in average Darcy velocity was observed in the LSZ (13 to 25 cm/day). The observed increase was primarily due to changes observed in Well MWN-02B (Figure 6). It should be noted that the UWBZ and LSZ each had independent injection wells. Also, as noted previously, based upon relative permeability of the formation, it is likely that the majority of the flow in the LSZ traveled through the deeper C-Horizon of the LSZ from about 232 to 244 ft bgs (see Figure 2). PFMs were not deployed in this interval.

The benzene flux profiles show a fairly significant reduction in mass flux for the wells that had the highest pre-remediation flux, MWN-02A and 05A. In contrast, benzene flux increases were observed in the LSZ wells MWN-01B and 03B. This can be seen in Figures 4 and 7. The increased flux in the intermediate B wells is likely associated with accumulation of NAPL in wells that previously had no evidence of NAPL present.

The TPH flux profiles typically agree with the benzene data showing even more significant increases in the intermediate wells MWN-01B and 03B (Figures 4 and 8). Again, this suggests the accumulation of free-phase NAPL in these wells.

Flux average contaminant concentrations. For comparison to other contaminant characterization efforts performed at the site, the measured fluxes and Darcy velocities can be used to estimate flux averaged contaminant concentrations, these values are summarized in Figures 9 and 10. The point estimates for flux averaged concentration can be compared to the average flux average contaminant concentration for each well (shown in the figures as a dashed vertical line), which allows for evaluation of the vertical variability of contaminant concentrations in each well. The well having the greatest variability for both Benzene and TPH was MWN 03B. This well also had the highest observed Benzene and TPH concentrations (Figure 9 and 10). The benzene and TPH concentrations were so much higher in well MWN 03B that the scale of the horizontal axes (concentration) used in the figures is three times greater than the 5 other wells. It is important to note that Well MWN 03 is located in close proximity to extraction well (LSZ03) and as such this well was anticipated to have higher observed contaminant fluxes (and flux averaged concentrations).

Normalized contaminant mass discharge. The contaminant mass flux values measured at the local scale (1.25 foot vertical intervals) can be represented in terms of mass discharge per unit width of aquifer (g/m/day) and are summarized in Table 1. The normalized contaminant mass discharge of each segment can be calculated by dividing each point estimate by the total mass discharge for the entire well screen. For this case, the normalized values are equivalent to the percent of contaminant mass discharge contributed by each interval to the total mass discharge through the well. These values are summarized in Figures 11 and 12 and the tabular data are provided in Appendix C. For Benzene there are only two instances in which a single vertical interval contributed more than 20% of the total mass discharge: MWN 03B (29%) and MWN 04A (33%). On the other hand, for TPH there are 8 cases in which a single interval contributes more than 20%. For three of these instances a single interval contributes 40% or more of the total mass discharge: MWN 01A (49%), MWN 03A (40%), and MWN 04A (42%). The interesting thing to note regarding these spikes in estimated mass discharge is that for the UWBZ (A) wells,

they occur pre-remediation, while for the LSZ (B) wells they typically occur post-remediation. These trends again correspond with the presence of free phase NAPL in some of the UWBZ wells pre-remediation, which was reduced post-remediation; and the accumulation of free phase NAPL in some of the LSZ wells post-remediation. The impact of these single intervals on the estimates for total mass discharge should be kept in mind when discussing pre- and post-remedial changes in the following section.

Estimated mass discharge. The summation of the product of flux and the cross-sectional flow area represents an integration of mass flux and can be used to estimate mass discharge for a transect of wells. Kübert and Finkel (2006) present a review of the methods and errors associated with mass flux integrations. The following equation is used.

$$ W_{cp} = \sum_{n=1}^{n_{well}} \left(\sum_{m}^{m_{ver}} F_{n,m} A_{n,m} \right) $$

For standard applications (using fence row transects of wells), the mass discharge per unit width can be used to estimate the mass discharge (Kg/day) through a specified region of the aquifer. This provides a metric for comparing the change in total mass discharge between pre- and post-remedial conditions. However, for the flow conditions at the TEE Treatment Cell, this method may not be directly applicable due to radial flow, fluctuations of the induced gradients over time, and differing proximity of monitoring wells to injection/extraction wells. Bearing these issues in mind, an estimate for mass discharge was calculated for the TEE Treatment Cell using a cylinder having a radius equal to the average radius of the flux wells from the central injection well (estimated at 40 ft). Each well was assumed to have equal representation over the 40 ft radius cylinder and treated as if they were on the circumference of the cylinder. Again, it is noted that this is not a direct representation of the physical system, but it allows for a general estimate of the total mass discharge from the site in order to provide a metric for comparison of pre- and post-remediation. Performing this calculation for the benzene flux resulted in estimated total mass discharges of 5.6 and 1.2 Kg/day for pre- and post-remediation respectively in the UWBZ. The LSZ values were 1.1 and 1.8 Kg/day showing an overall increase as noted earlier. For TPH the UWBZ values were 61 to 9.0 Kg/day while the LSZ were 4.7 to 13 Kg/day again showing an increase. The estimated increase in mass flux in the LSZ is consistent with the observation that there was minimal or no free-phase NAPL in the LSZ wells pre-remediation, but there was free phase NAPL present in the wells post-remediation. The integrated values provide an overall summary of the remedial changes in mass discharge within the portions of the UWBZ and LSZ where flux measurements were taken during the applied water flood at the TEE Treatment Cell.

NAPL impact on mass flux
During the pre-remediation deployment, NAPL was observed in some of the wells located in the UWBZ. The NAPL was removed from the wells the day before deployment but likely some NAPL remained. Based on this information the swipe tests described earlier were conducted in all six shallow wells of the UWBZ. The integrated mass per unit width for each well removed during the swipe test is reported in Table 3. Average mass flux values are provided in Table 4. It is evident from the results that the insertion and immediate removal of the PFMs in these wells recorded a substantial mass of benzene and TPH. These values were used as a correction to the

mass flux reported for each well assuming that the mass represents accumulation associated with installation of the PFM rather than mass flux through the well during the deployment. The swipe test corrected values are provided in Tables 3 and 4. Using the pre- and post-remediation swipe tests both corrected and uncorrected mass discharge per unit width are plotted in Figure 9.

The benzene results with and without the correction are similar. Wells MWN-02A and 05A had the largest mass discharge with about a 20% decrease due to the correction. Well MWN-03A showed the most significant change due the correction. Overall the general conclusion of a 78% flux reduction is unchanged by the correction. Thus the overall magnitude of mass discharge is changed by the correction but the observed relative changes before and after remediation is not affected.

The TPH results show a bit more significant change due to the swipe test correction. Wells MWN-02A and 04A showed significant overall mass discharge reduction due to the correction and thus the overall mass discharge is reduced by about 50% due to the correction. The observation that TPH is more significantly changed by the NAPL presence is reasonable given the strong correlation between NAPL and TPH. When comparing pre- and post-remedial changes in TPH mass discharge the uncorrected estimate was an 85% reduction and when applying the correction the value decreases to an 81% reduction, overall a fairly minor change.

Summary and Conclusions

The integrated observations comparing pre- and post-remediation flux measurements showed a decrease in the TEE Treatment Cell average benzene mass flux in the UWBZ of about 78%. The associated TPH reduction was about 85%. This was accompanied by an increase in mass flux of benzene in the LSZ of about 70% for benzene and 180% for TPH. As mentioned throughout this discussion, the increase of mass flux in the LSZ corresponds to the presence of free-phase NAPL in multiple LSZ wells that was not present during pre-remediation measurements. Also, it should be noted that based upon relative permeability of the formation, it is likely that a majority of the flow in the LSZ passed through the deeper C-Horizon of the LSZ (Figure 2). PFMs were not deployed in this interval. But, based upon observed aqueous concentrations, the mass flux in the more permeable C-Horizon of the LSZ was also reduced but was not directly measured by PFM and is not included in the overall site reductions cited above.

In the UWBZ a correction was evaluated for the presence of NAPL in the wells using a pre-deployment swipe test in the wells. The magnitude of the measured mass flux was reduced by the correction however the pre- and post-remedial flux comparisons remained consistent at approximately 80% reduction in flux in the UWBZ.
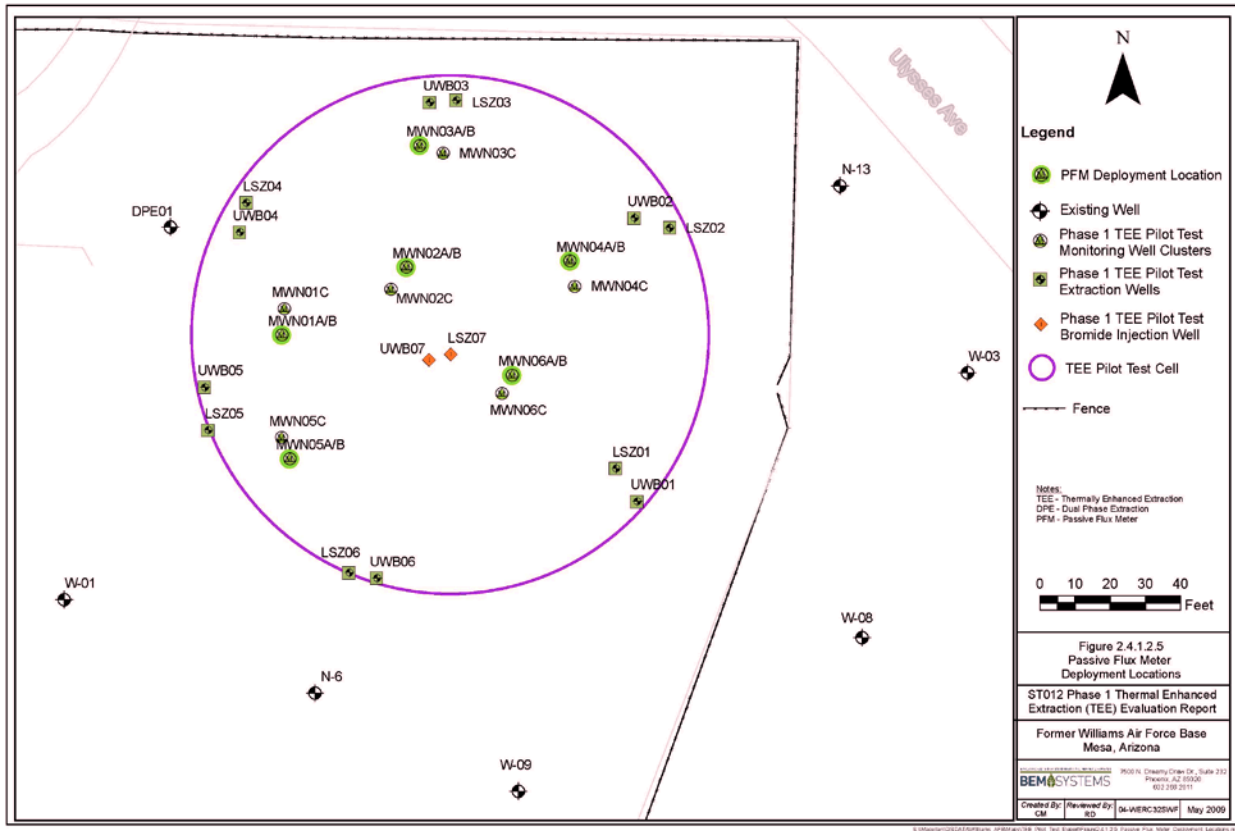
Figure 1. Site map showing monitoring well and flux well locations for former Williams Air Force Base.
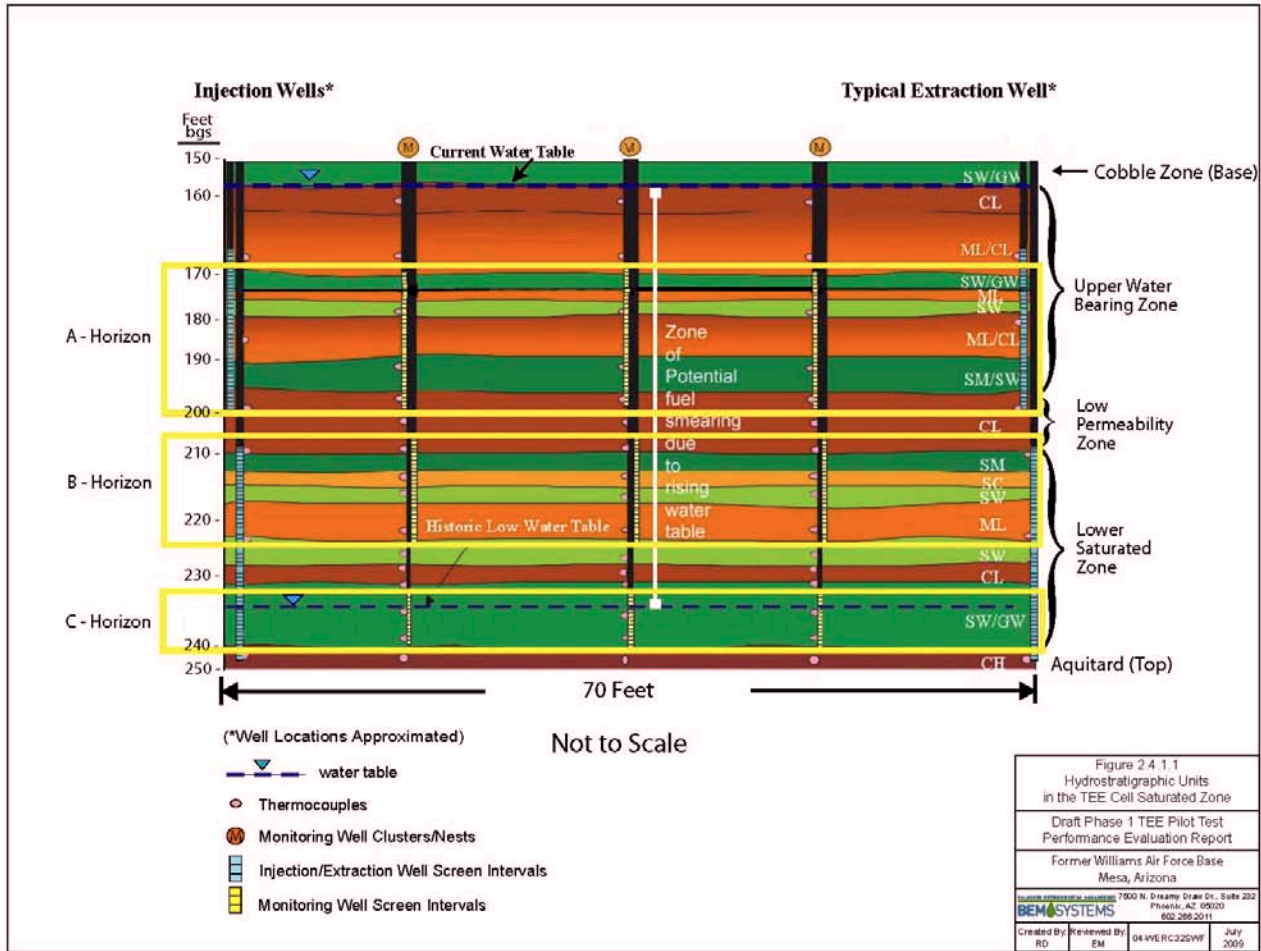
Figure 2. Cross-section of well field for mass flux study at former Williams Air Force Base.
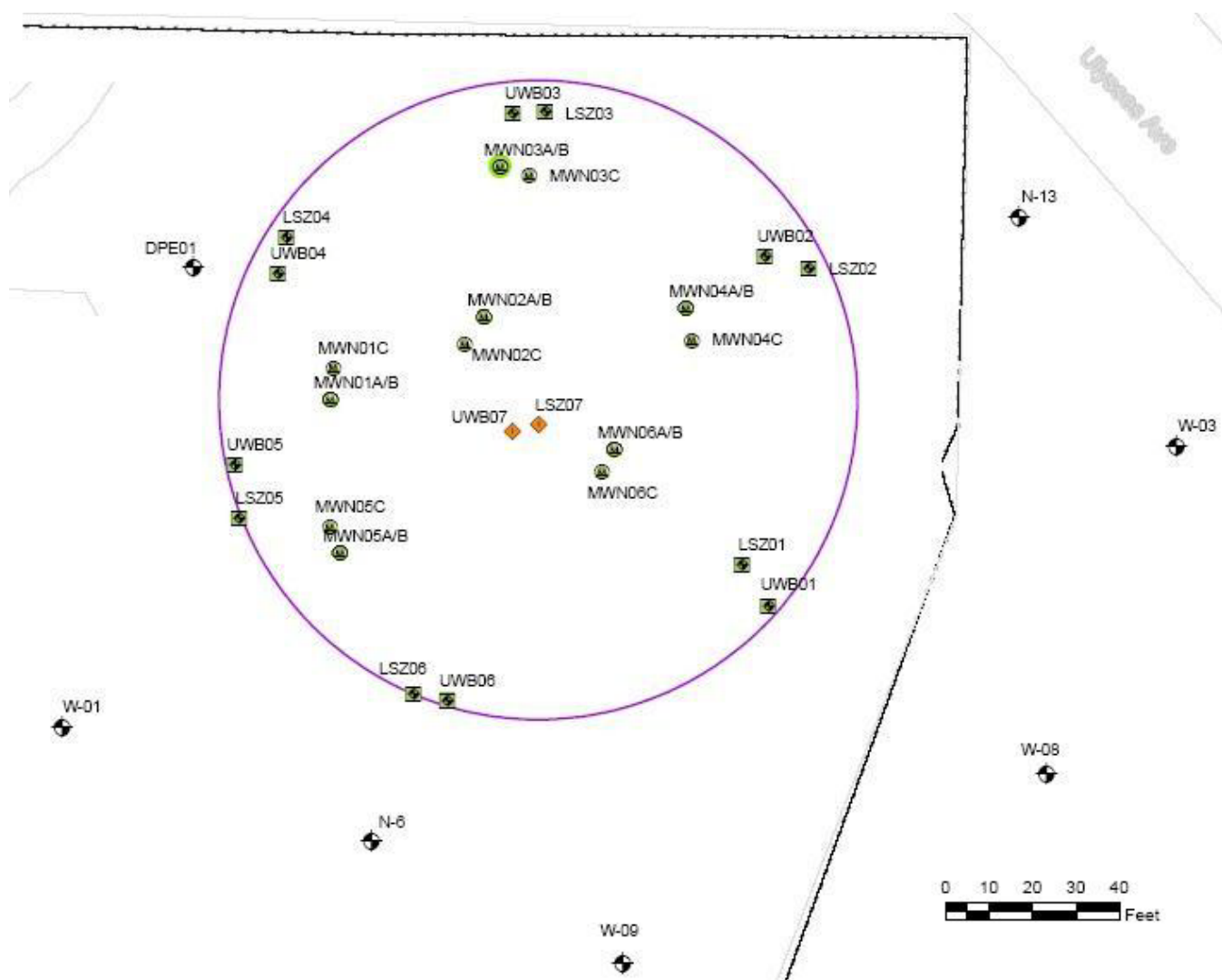
Figure 3. General Well TEE Treatment Cell layout plan Williams Air Force Base.
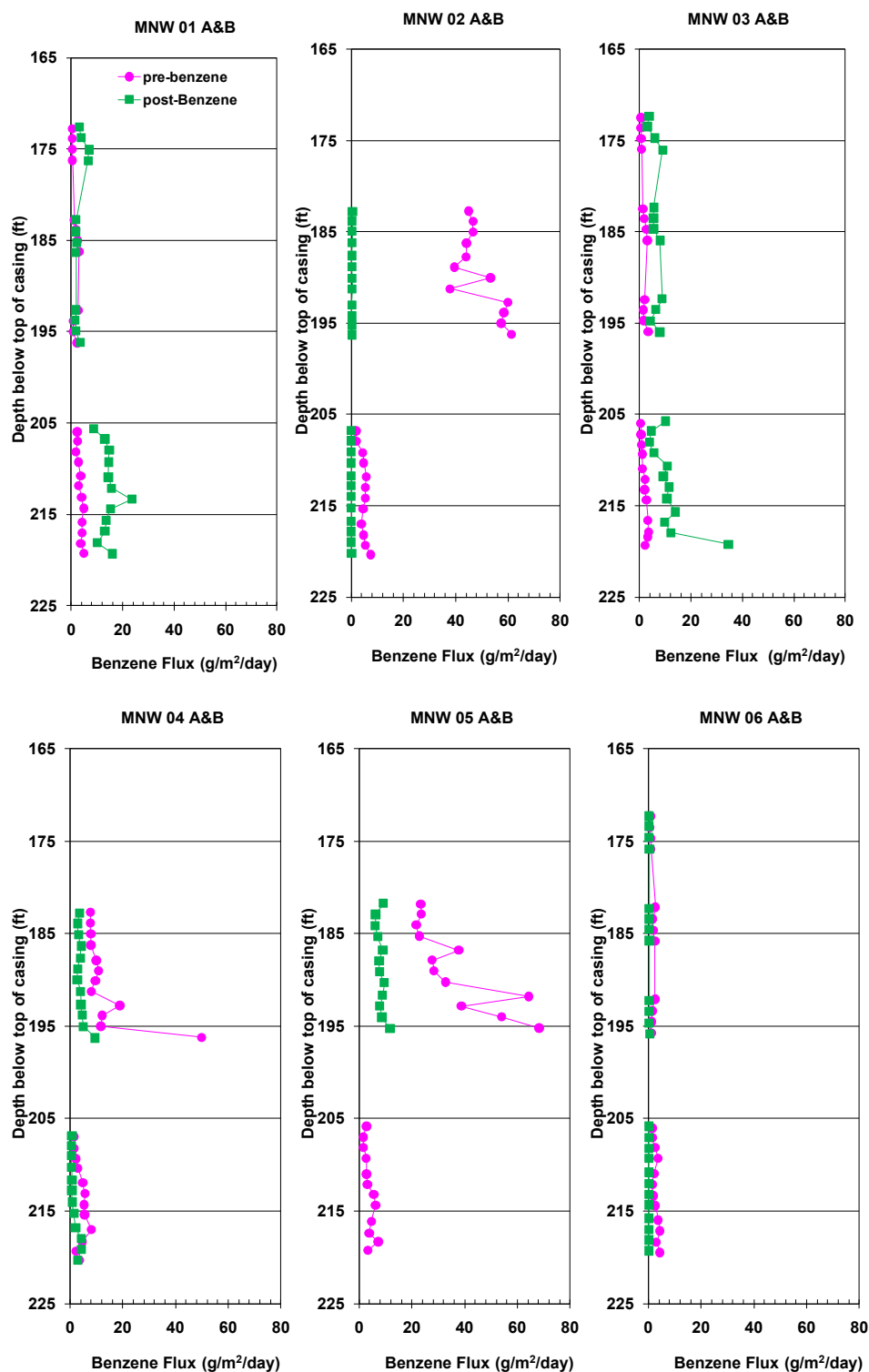
Figure 4. Pre- and Post-remediation flux profiles of benzene.
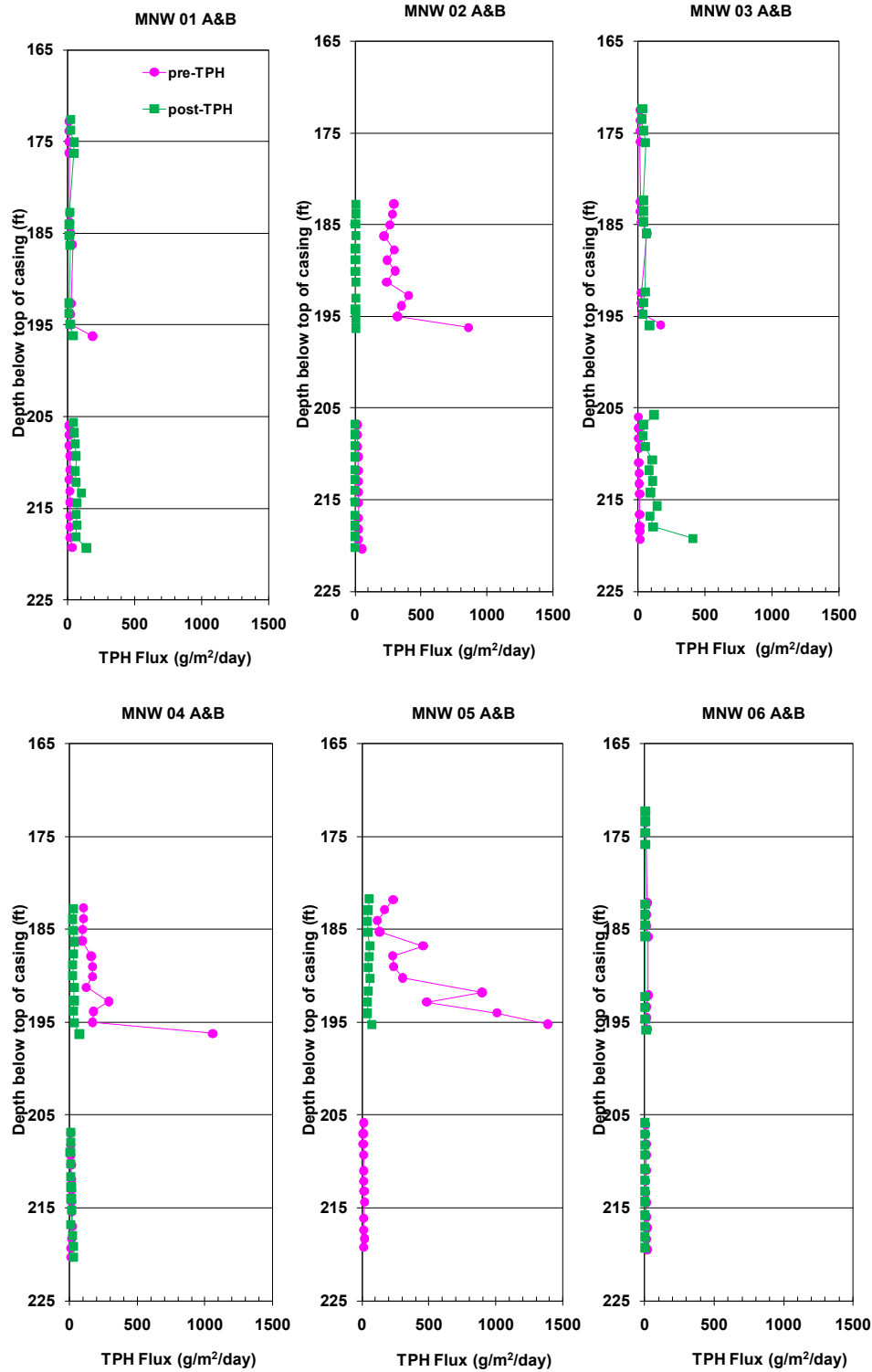
Figure 5. Pre- and Post-remediation flux profiles of TPH.
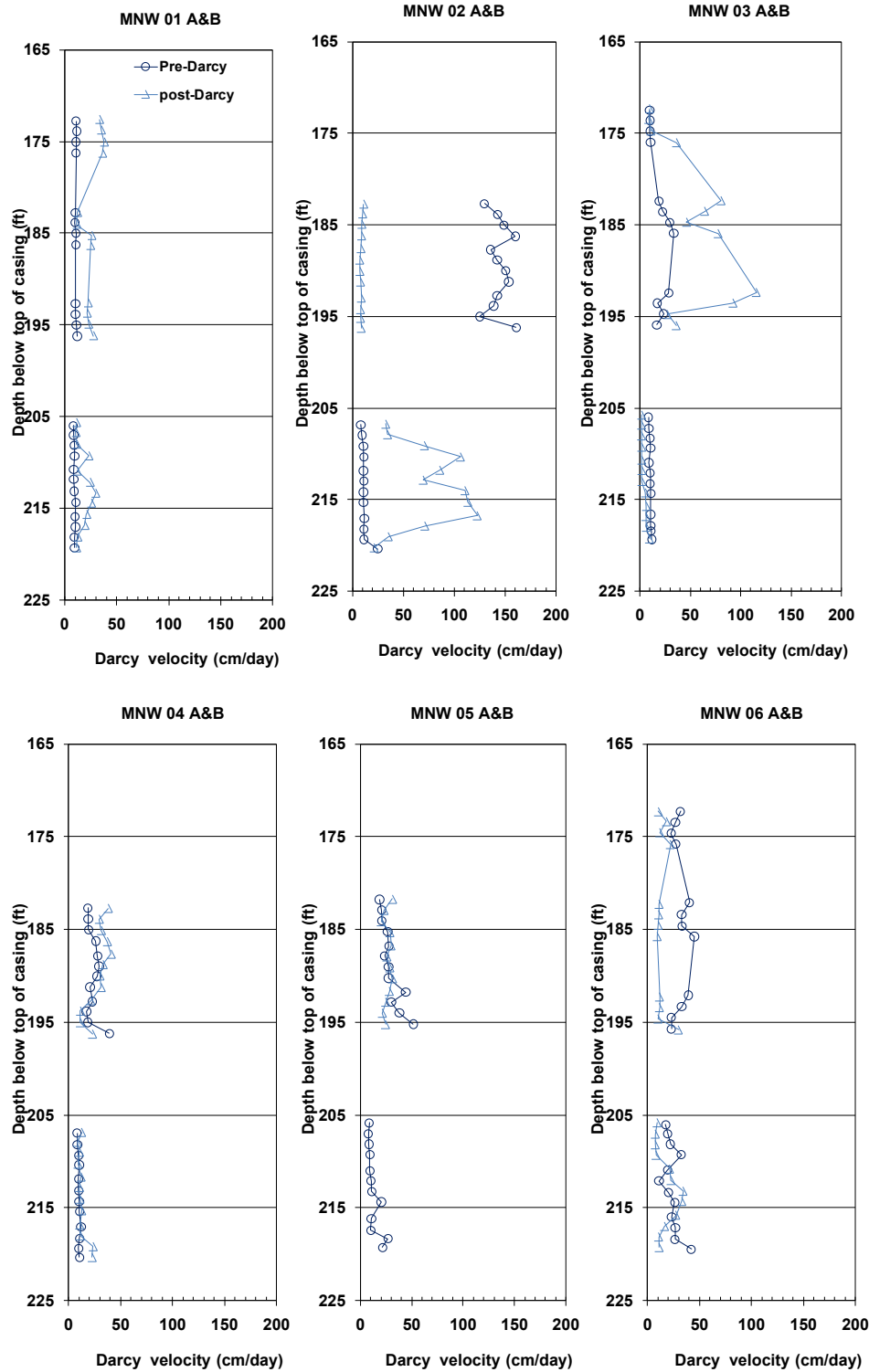
Figure 6. Pre and Post-remediation Darcy flux profiles.
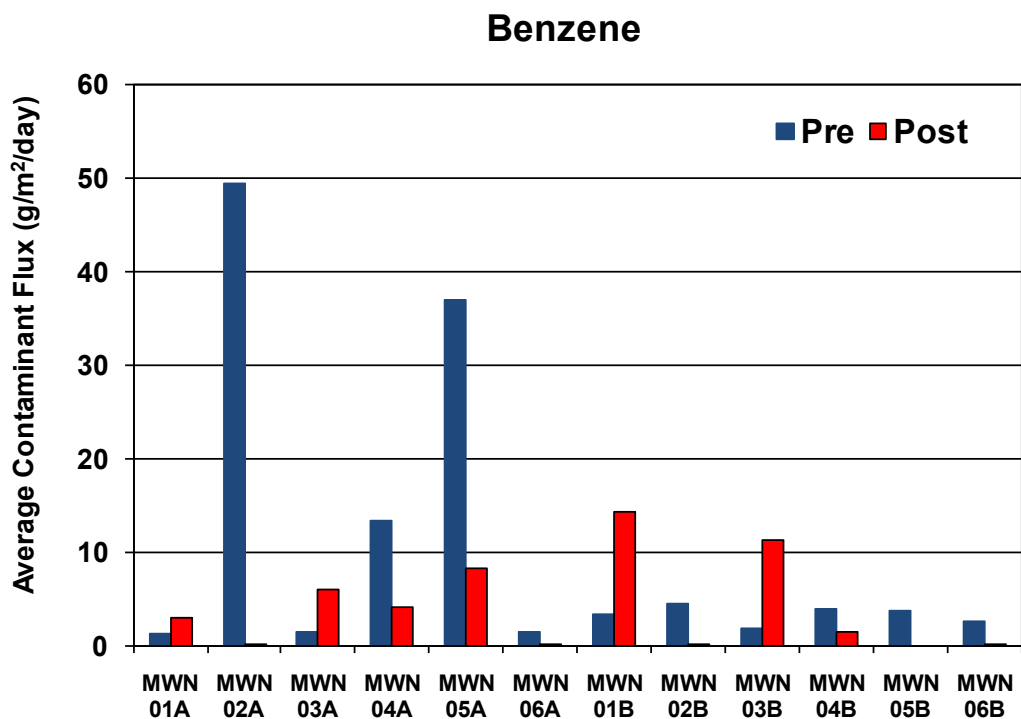
Benzene

Figure 7. Average mass flux of benzene at each well before and after remediation.

TPH as Benzene
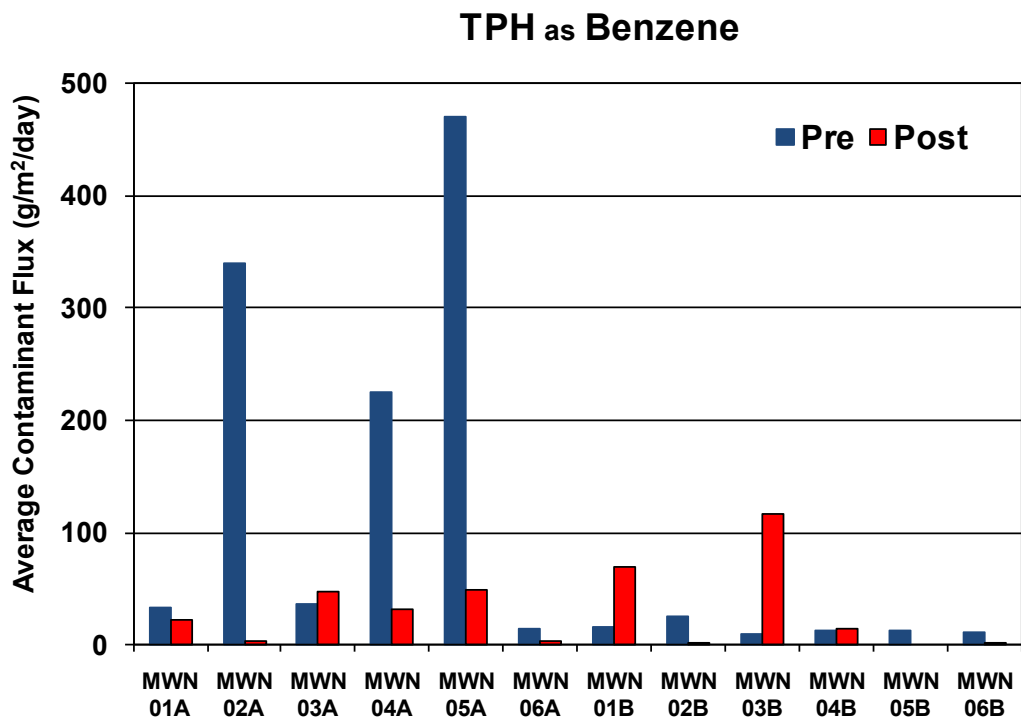
Figure 8. Average mass flux of TPH at each well before and after remediation.
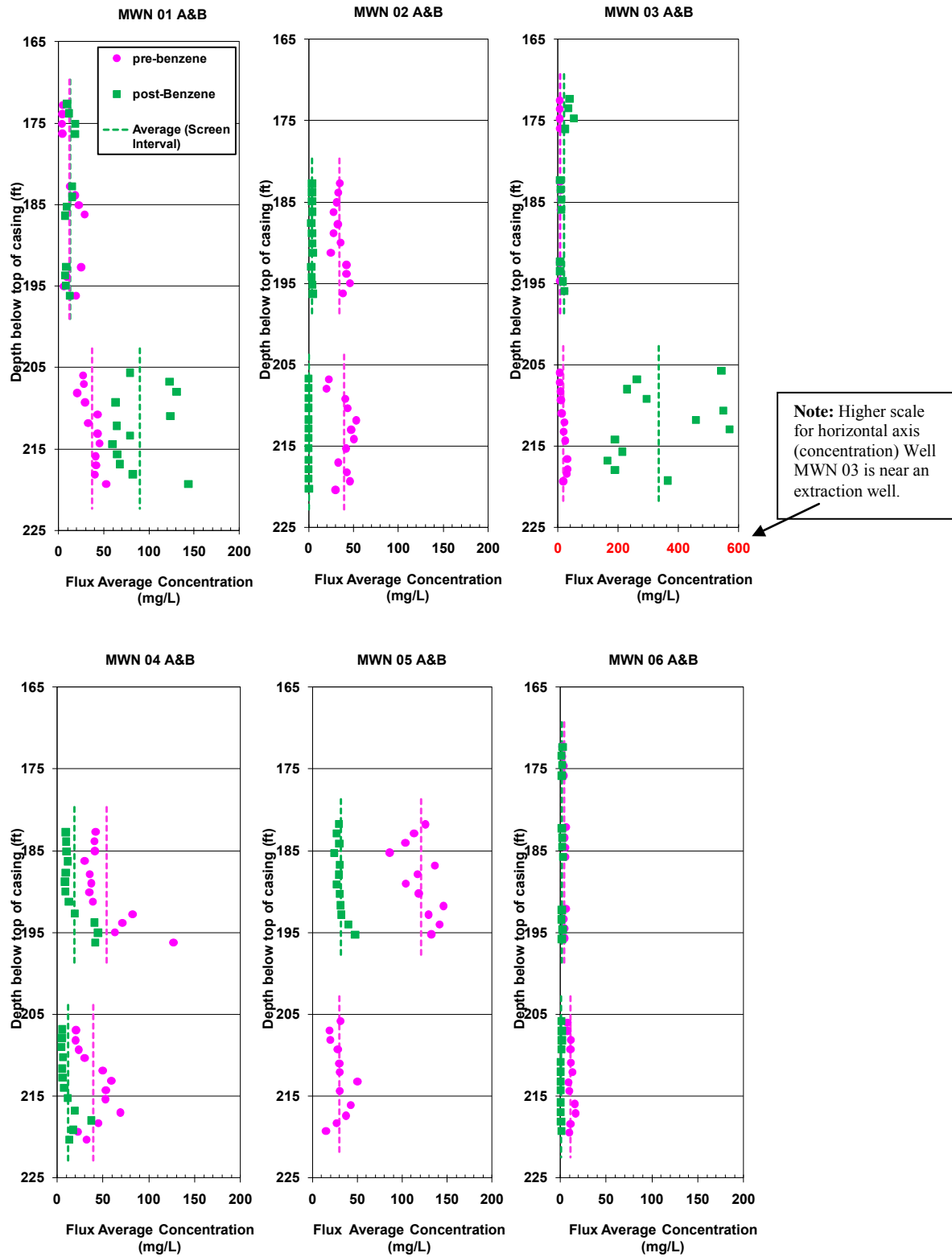
Figure 9. Benzene point estimates for flux average contaminant concentrations compared to average concentration for entire well.
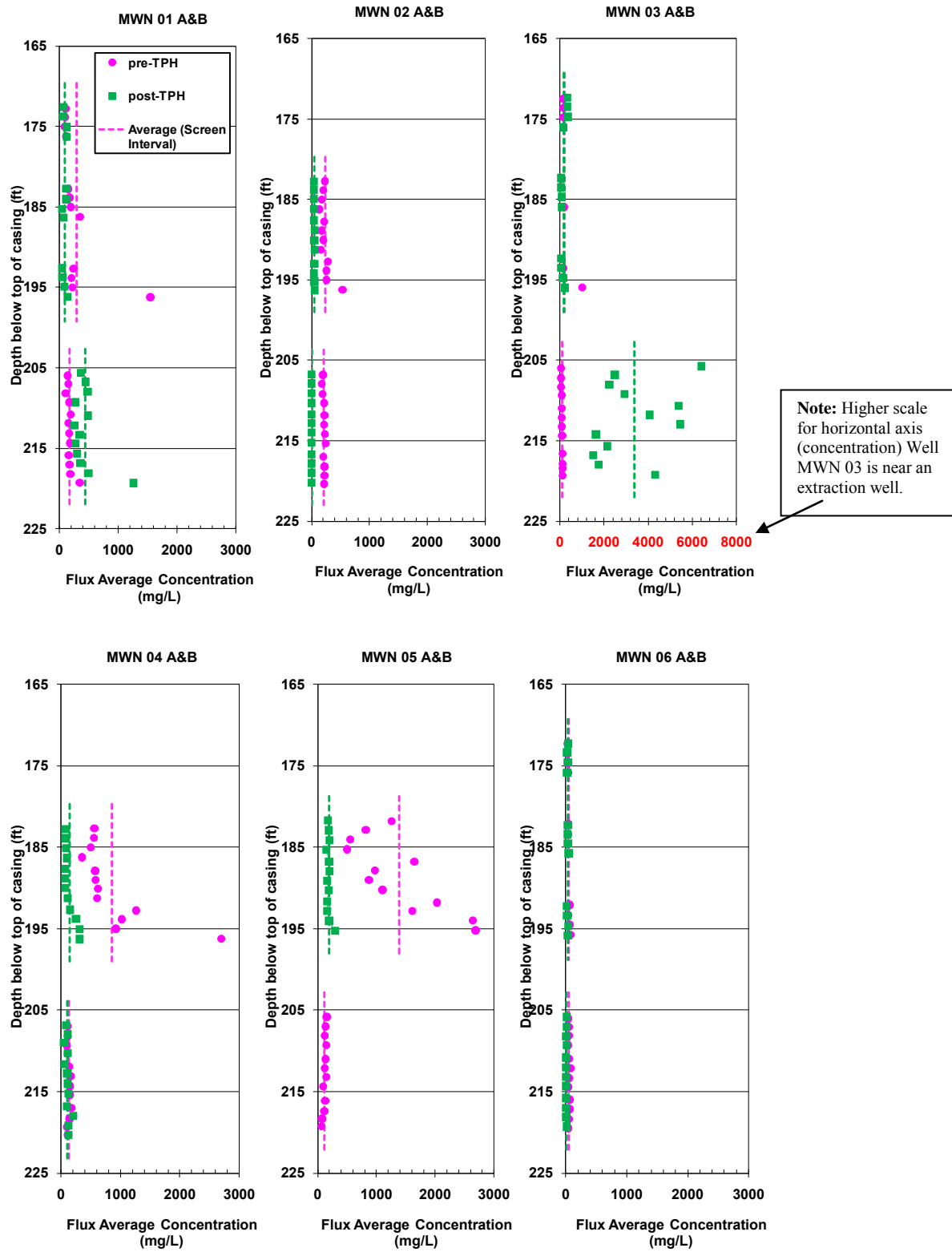
Figure 10. TPH point estimates for flux average contaminant concentrations compared to average concentration for entire well.
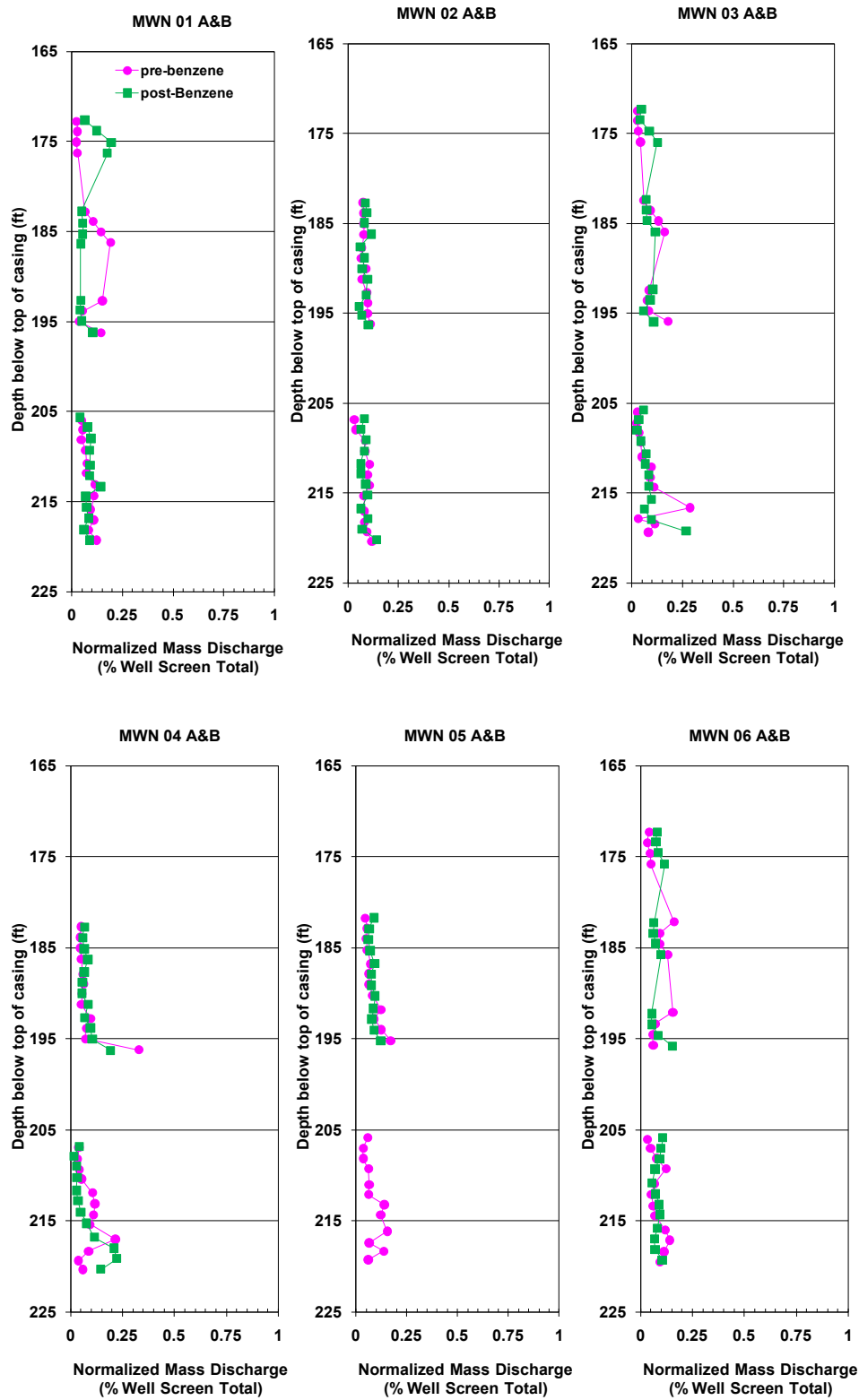
Figure 11. Benzene normalized mass discharge (as percent of total mass discharge for the well).
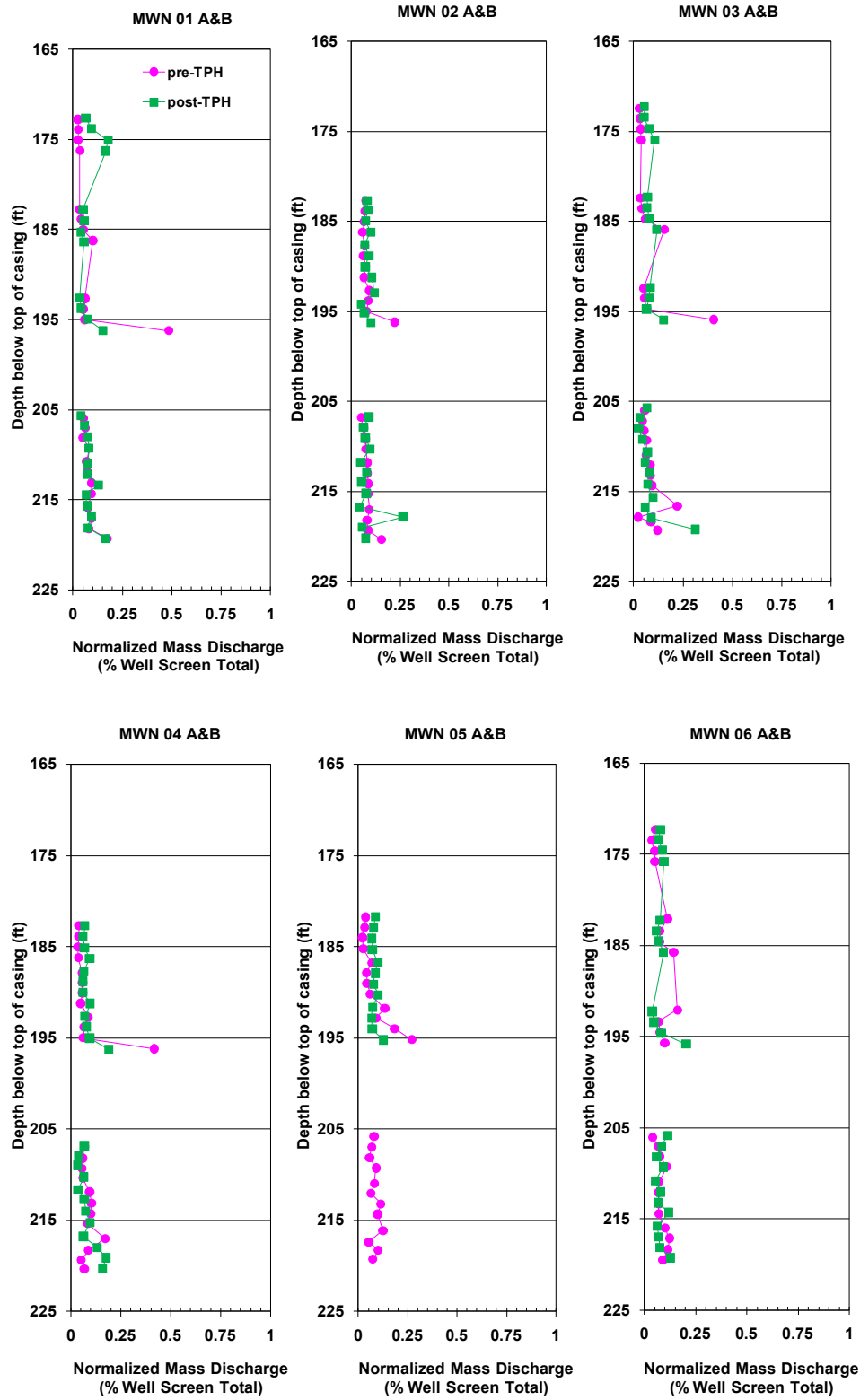
Figure 12. TPH normalized mass discharge (as percent of total mass discharge for the well).
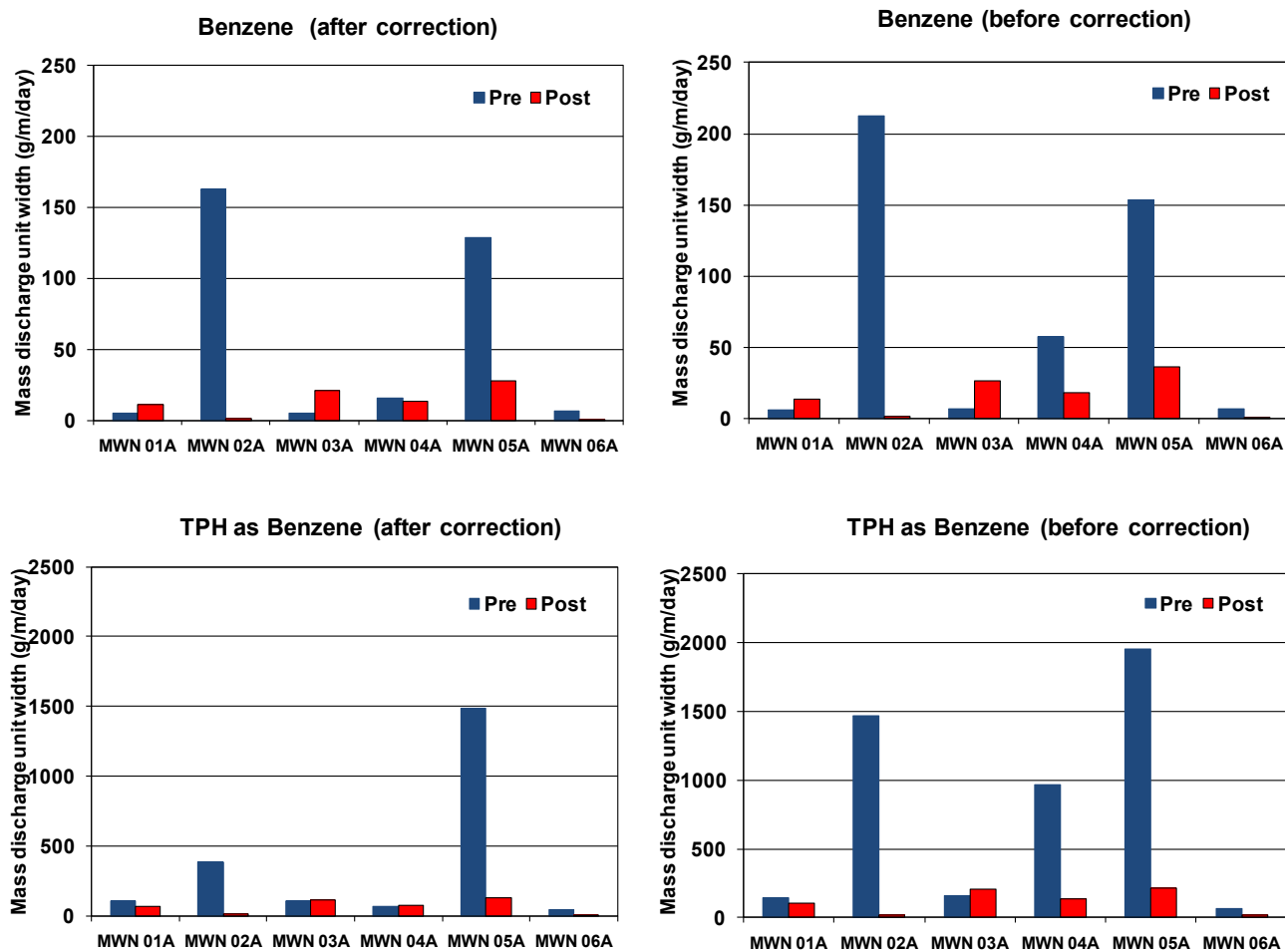
Figure 13. Comparison of mass discharge per unit width for UWBZ wells with and without correction for swipe tests.

Table 1.   Pre- and Post-remediation mass discharge per unit width of aquifer for each well.

Well	Darcy velocity (cm/day)		Benzene (g/m/day)		TPH as Benzene (g/m/day)		TPH as Williams NAPL (g/m/day)	
	Pre	Post	Pre	Post	Pre	Post	Pre	Post
MWN 01A	10.9	26.0	6.1	13.5	145.3	102.1	343.1	246.8
MWN 02A	144.0	8.7	212.2	1.5	1465.7	16.6	3460.1	40.1
MWN 03A	19.3	50.5	7.1	26.9	160.6	208.6	379.0	504.1
MWN 04A	23.8	28.1	57.7	18.3	967.2	139.7	2283.3	337.7
MWN 05A	29.7	26.5	153.2	36.2	1958.5	217.4	4623.6	525.4
MWN 06A	31.3	13.9	6.7	1.2	65.9	18.4	155.5	44.3
MWN 01B	9.4	17.6	14.5	62.4	69.3	298.2	163.7	720.7
MWN 02B	11.9	72.8	19.1	0.2	103.8	1.6	245.1	4.0
MWN 03B	10.2	3.9	7.6	49.6	38.8	507.6	91.6	1226.7
MWN 04B	9.8	12.8	17.3	6.9	55.1	61.6	130.1	148.8
MWN 05B	12.9	-	15.3	-	56.4	-	133.2	-
MWN 06B	23.8	17.4	10.9	0.5	47.7	3.8	112.5	9.12

Table 2. Pre- and Post-remediation average mass flux for each well.

Well	Darcy velocity (cm/day)		Benzene (g/m²/day)		TPH as Benzene (g/m²/day)		TPH as Williams NAPL (g/m²/day)	
	Pre	Post	Pre	Post	Pre	Post	Pre	Post
MWN 01A	10.9	26.0	1.4	3.1	32.9	23.3	77.8	56.2
MWN 02A	144.0	8.7	49.5	0.3	339.8	3.8	802.2	9.2
MWN 03A	19.3	50.5	1.7	6.1	36.6	47.3	86.4	114.3
MWN 04A	23.8	28.1	13.5	4.2	225.6	32.3	532.5	78.0
MWN 05A	29.7	26.5	37.0	8.3	471.0	49.8	1111.9	120.3
MWN 06A	31.3	13.9	1.5	0.3	14.7	4.3	34.6	10.4
MWN 01B	9.4	17.6	3.5	14.4	16.7	69.3	39.5	167.4
MWN 02B	11.9	72.8	4.6	0.1	25.3	0.4	59.8	0.9
MWN 03B	10.2	3.9	1.9	11.4	9.7	116.6	22.9	281.9
MWN 04B	9.8	12.8	4.0	1.6	13.0	14.3	30.6	34.6
MWN 05B	12.9	-	3.8	-	13.8	-	32.7	-
MWN 06B	23.8	17.4	2.7	0.1	11.9	0.9	28.0	2.1

Table 3. Mass discharge per unit width for UWBZ wells including correction for swipe tests.

Well	Benzene (g/m/day)		TPH as Benzene (g/m/day)		TPH as Williams NAPL (g/m/day)	
	Pre	Post	Pre	Post	Pre	Post
Before correction						
MWN 01A	6.1	13.5	145.3	102.1	343.1	246.8
MWN 02A	212.2	1.5	1465.7	16.6	3460.1	40.1
MWN 03A	7.1	26.9	160.6	208.6	379.0	504.1
MWN 04A	57.7	18.3	967.2	139.7	2283.3	337.7
MWN 05A	153.2	36.2	1958.5	217.4	4623.6	525.4
MWN 06A	6.7	1.2	65.9	18.4	155.5	44.3
MWN 01A-push & pull	0.9	2.6	37.7	29.9	88.9	72.1
MWN 02A-push & pull	49.8	0.5	1076.0	2.3	2540.3	5.6
MWN 03A-push & pull	2.2	5.9	53.5	88.8	126.3	214.7
MWN 04A-push & pull	42.2	4.9	897.3	59.1	2118.3	142.9
MWN 05A-push & pull	24.2	8.5	471.8	84.2	1113.7	203.4
MWN 06A-push & pull	0.1	0.7	16.8	10.0	39.6	24.2
After correction						
MWN 01A	5.2	10.9	107.7	72.3	254.2	174.7
MWN 02A	162.5	0.9	389.6	14.3	919.8	34.5
MWN 03A	4.9	20.9	107.1	119.8	252.8	289.4
MWN 04A	15.4	13.5	69.9	80.6	165.0	194.8
MWN 05A	129.0	27.7	1486.7	133.3	3509.8	322.0
MWN 06A	6.6	0.5	49.1	8.3	115.9	20.1

Table 4. Average mass flux for UWBZ wells including correction for swipe tests.

Well	Benzene (g/m²/day)		TPH as Benzene (g/m²/day)		TPH as Williams NAPL (g/m²/day)	
	Pre	Post	Pre	Post	Pre	Post
Before correction						
MWN 01A	1.4	3.1	32.9	23.3	77.8	56.2
MWN 02A	49.5	0.3	339.8	3.8	802.2	9.2
MWN 03A	1.7	6.1	36.6	47.3	86.4	114.3
MWN 04A	13.5	4.2	225.6	32.3	532.5	78.0
MWN 05A	37.0	8.3	471.0	49.8	1111.9	120.3
MWN 06A	1.5	0.3	14.7	4.3	34.6	10.4
MWN 01A-push & pull	0.20	0.61	8.76	6.94	20.68	16.78
MWN 02A-push & pull	11.57	0.12	250.24	0.54	590.77	1.31
MWN 03A-push & pull	0.52	1.38	12.44	20.66	29.37	49.93
MWN 04A-push & pull	9.82	1.14	208.67	13.75	492.63	33.23
MWN 05A-push & pull	5.63	1.98	109.71	19.57	259.01	47.30
MWN 06A-push & pull	0.01	0.15	3.90	2.33	9.20	5.63
After correction						
MWN 01A	1.2	2.5	24.2	16.3	57.1	39.4
MWN 02A	37.9	0.2	89.6	3.3	211.4	7.9
MWN 03A	1.1	4.7	24.1	26.7	57.0	64.4
MWN 04A	3.7	3.1	16.9	18.5	39.9	44.8
MWN 05A	31.3	6.3	361.3	30.2	852.9	73.0
MWN 06A	1.5	0.1	10.8	2.0	25.4	4.8

References

Annable, M.D., K. Hatfield, J. Cho, H. Klammler, B.L. Parker, J.A. Cherry, P.S.C. Rao, "Field-Scale Evaluation of the Passive Flux Meter for Simultaneous Measurement of Groundwater and Contaminant Fluxes". Environmental Science & Technology. Vol. 39, 2005, pp. 7194-7201.

Hatfield, K., M.D. Annable, J. Cho, P.S.C. Rao, H. Klammler. " A Direct Passive Method for Measuring Water and Contaminant Fluxes in Porous Media". Journal of Contaminant Hydrology Vol. 75, No. 3-4, 2004, pp. 155-181.

Kübert, M. and Finkel M., "Contaminant Mass Discharge Estimation in Groundwater Based on Multi-level Point Measurements: A Numerical Evaluation of Expected Errors". Journal of Contaminant Hydrology Vol. 84, No. 1-2, 2006, pp. 55-80.

United States Air Force (USAF), Final ST012 Phase 1 Thermal Enhanced Extraction (TEE) Pilot Test Work Plan, 2007

Appendix A: Pre- and Post-Remediation Flux Data

Flux values for MWN-01 through 03 A & B.

Well_ID	Approximate Depth below top of well casing (ft)		Darcy Velocity (cm/day)		Benzene flux (g/m^2/day)		TPH flux as benzene (g/m^2/day)		TPH flux as NAPL (g/m^2/day)	
	Pre	Post	Pre	Post	Pre	Post	Pre	Post	Pre	Post
MNW 01A	172.78	172.62	10.91	33.43	0.47	3.10	11.58	23.64	27.34	57.13
MNW 01A	173.89	173.77	11.46	35.19	0.49	3.98	11.22	22.60	26.49	54.61
MNW 01A	175.06	175.08	11.09	38.07	0.39	6.91	10.39	47.79	24.52	115.49
MNW 01A	176.26	176.30	11.05	36.39	0.46	6.60	13.22	47.10	31.20	113.83
MNW 01A	182.78	182.76	10.53	12.13	1.32	1.81	16.12	14.46	38.05	34.95
MNW 01A	183.86	184.04	9.76	11.47	1.80	1.74	16.98	13.66	40.09	33.01
MNW 01A	185.03	185.27	11.04	25.98	2.48	2.24	21.20	12.05	50.05	29.11
MNW 01A	186.24	186.35	10.81	24.77	3.09	1.83	38.33	17.37	90.50	41.97
MNW 01A	192.67	192.60	10.45	22.45	2.60	1.90	25.19	10.62	59.48	25.65
MNW 01A	193.84	193.72	10.30	21.52	0.94	1.54	21.00	11.74	49.57	28.37
MNW 01A	195.00	194.92	11.30	22.90	0.65	1.79	24.68	19.61	58.26	47.38
MNW 01A	196.21	196.18	12.00	27.63	2.32	3.48	185.39	38.47	437.67	92.97
MNW 01B	205.96	205.65	8.37	11.14	2.29	8.82	11.66	41.07	27.53	99.24
MNW 01B	207.01	206.73	8.82	10.65	2.47	13.09	13.61	47.88	32.12	115.72
MNW 01B	208.12	207.99	9.20	11.31	1.89	14.75	9.75	54.38	23.02	131.42
MNW 01B	209.29	209.27	9.53	23.11	2.79	14.58	16.03	63.85	37.85	154.31
MNW 01B	210.76	210.93	8.61	11.70	3.72	14.47	16.68	57.10	39.38	138.00
MNW 01B	211.85	212.14	8.75	24.41	2.87	15.72	13.39	61.44	31.61	148.47
MNW 01B	213.13	213.34	9.35	29.72	4.04	23.52	15.87	102.17	37.45	246.90
MNW 01B	214.34	214.42	10.74	25.58	4.87	15.25	19.39	69.77	45.78	168.61
MNW 01B	215.88	215.64	10.11	21.04	4.14	13.63	16.24	62.91	38.33	152.04
MNW 01B	217.03	216.85	10.27	19.27	4.25	13.04	17.72	69.57	41.83	168.12
MNW 01B	218.16	218.11	9.37	12.38	3.73	10.17	17.59	60.77	41.53	146.87
MNW 01B	219.28	219.29	9.50	11.16	4.99	16.04	33.02	140.11	77.95	338.60
MNW 02A	182.70	182.73	129.53	11.27	44.87	0.42	294.31	4.41	694.80	10.66
MNW 02A	183.86	183.79	142.42	10.18	46.59	0.38	284.31	4.00	671.20	9.67
MNW 02A	185.03	184.93	148.81	9.38	46.65	0.35	262.61	3.51	619.97	8.49
MNW 02A	186.24	186.19	159.75	9.12	44.12	0.39	219.95	3.82	519.27	9.22
MNW 02A	187.72	187.58	135.55	8.56	43.94	0.26	295.24	3.29	697.01	7.95
MNW 02A	188.85	188.83	142.18	7.28	39.43	0.28	244.59	3.50	577.44	8.47
MNW 02A	190.02	190.06	150.40	7.49	53.30	0.31	303.70	3.56	716.97	8.61
MNW 02A	191.22	191.23	153.36	8.09	37.88	0.37	240.69	4.61	568.23	11.15
MNW 02A	192.71	192.97	142.20	8.78	60.00	0.27	406.02	3.98	958.54	9.63
MNW 02A	193.84	194.24	138.48	8.03	58.38	0.28	349.20	2.96	824.39	7.16
MNW 02A	195.00	195.19	125.00	8.08	57.44	0.34	319.91	3.71	755.26	8.97
MNW 02A	196.21	196.27	160.88	8.71	61.43	0.40	857.07	4.54	2023.37	10.97
MNW 02B	206.81	206.73	8.35	32.80	1.87	0.05	16.23	0.40	38.32	0.97
MNW 02B	207.96	207.88	9.50	34.56	1.90	0.04	16.80	0.30	39.67	0.71
MNW 02B	209.19	209.07	10.93	70.71	4.47	0.05	20.79	0.29	49.09	0.71
MNW 02B	210.32	210.30	11.06	106.03	4.79	0.05	23.70	0.44	55.96	1.06
MNW 02B	211.83	211.75	10.90	85.78	5.81	0.04	24.02	0.23	56.72	0.56
MNW 02B	212.98	212.83	11.15	69.53	5.30	0.04	24.06	0.39	56.80	0.94
MNW 02B	214.16	213.98	10.78	110.44	5.45	0.05	24.32	0.22	57.41	0.54
MNW 02B	215.31	215.24	10.91	113.33	4.57	0.06	26.51	0.31	62.58	0.76
MNW 02B	217.03	216.72	11.86	122.43	3.92	0.05	23.60	0.22	55.72	0.53
MNW 02B	218.23	217.83	11.15	71.09	4.78	0.06	24.90	1.17	58.79	2.84
MNW 02B	219.33	219.00	11.56	35.26	5.35	0.05	25.54	0.27	60.30	0.64
MNW 02B	220.38	220.21	24.99	21.36	7.50	0.08	53.38	0.30	126.02	0.72
MNW 03A	172.48	172.29	9.68	9.60	0.61	3.71	14.54	32.95	34.33	79.62
MNW 03A	173.59	173.46	9.96	8.76	0.57	2.97	14.53	28.86	34.31	69.75
MNW 03A	174.76	174.72	9.96	10.97	0.62	5.84	15.87	41.10	37.46	99.32
MNW 03A	175.96	176.00	10.59	36.37	0.80	9.01	16.06	58.12	37.90	140.46
MNW 03A	182.44	182.33	18.84	80.54	1.31	5.56	16.38	42.01	38.68	101.53
MNW 03A	183.56	183.48	22.60	64.22	1.83	5.49	18.95	39.51	44.73	95.47
MNW 03A	184.73	184.68	29.72	46.39	2.66	5.45	26.09	43.98	61.59	106.28
MNW 03A	185.94	185.92	33.59	77.62	3.06	8.00	65.64	62.19	154.95	150.30
MNW 03A	192.43	192.34	28.67	115.41	1.93	8.77	25.76	54.62	60.82	132.00
MNW 03A	193.54	193.50	17.30	92.37	1.49	6.30	25.14	42.21	59.35	102.00
MNW 03A	194.70	194.75	23.71	27.27	1.67	4.27	29.71	36.70	70.13	88.69
MNW 03A	195.91	195.96	16.82	36.02	3.38	7.86	170.33	85.49	402.12	206.60
MNW 03B	205.99	205.72	8.48	1.87	0.51	10.13	5.11	119.96	12.07	289.90
MNW 03B	207.20	206.81	8.88	1.75	0.57	4.58	5.43	43.68	12.83	105.57
MNW 03B	208.29	207.99	9.90	1.68	0.81	3.86	6.13	37.54	14.46	90.73
MNW 03B	209.35	209.22	10.55	1.88	1.08	5.54	8.04	55.35	18.99	133.75
MNW 03B	210.96	210.63	8.90	1.99	1.10	10.90	7.09	106.98	16.73	258.53
MNW 03B	212.09	211.77	10.33	2.01	2.16	9.20	9.79	81.53	23.11	197.04
MNW 03B	213.24	212.96	10.30	2.01	1.92	11.46	9.14	109.61	21.58	264.88
MNW 03B	214.34	214.21	11.02	5.64	2.70	10.67	11.88	91.87	28.05	222.02
MNW 03B	216.62	215.69	10.50	6.55	3.20	13.96	12.54	141.49	29.60	341.93
MNW 03B	217.85	216.78	10.73	5.99	3.42	9.86	13.14	90.08	31.03	217.70
MNW 03B	218.41	217.96	11.25	6.41	3.21	12.13	12.60	112.98	29.74	273.03
MNW 03B	219.34	219.24	11.79	9.47	2.08	34.54	15.75	408.69	37.19	987.67

Flux values for MWN-04 through 06 A & B.

Well_ID	Approximate Depth below top of well casing (ft)		Darcy Velocity (cm/day)		Benzene flux (g/m^2/day)		TPH flux as benzene (g/m^2/day)		TPH flux as NAPL (g/m^2/day)	
	Pre	Post	Pre	Post	Pre	Post	Pre	Post	Pre	Post
MNW 04A	183.86	183.89	18.83	29.30	7.71	2.91	103.71	22.66	244.84	54.75
MNW 04A	185.03	185.11	19.05	31.31	7.88	3.26	95.14	24.92	224.62	60.22
MNW 04A	186.24	186.30	26.13	37.02	7.86	4.24	91.92	36.53	217.00	88.27
MNW 04A	187.87	187.66	27.82	40.67	9.96	3.86	159.03	28.96	375.43	69.98
MNW 04A	188.97	188.78	29.21	32.97	10.86	2.84	170.27	22.52	401.97	54.44
MNW 04A	190.06	190.00	27.27	29.92	9.64	2.71	169.04	22.15	399.07	53.54
MNW 04A	191.22	191.24	20.57	31.11	8.05	4.00	124.10	34.49	292.97	83.35
MNW 04A	192.77	192.66	22.87	21.12	18.87	4.12	289.11	31.95	682.53	77.22
MNW 04A	193.84	193.78	17.17	11.38	12.25	4.62	175.72	28.42	414.84	68.68
MNW 04A	195.00	195.03	18.43	11.25	11.68	5.04	169.68	34.62	400.59	83.67
MNW 04A	196.21	196.26	39.19	22.83	49.79	9.55	1056.10	71.59	2493.26	173.01
MNW 04B	206.94	206.84	8.10	12.38	1.67	0.73	9.15	10.45	21.61	25.25
MNW 04B	208.20	207.91	8.27	8.33	1.67	0.43	8.89	8.93	21.00	21.59
MNW 04B	209.34	208.98	9.62	10.43	2.26	0.52	9.51	5.25	22.45	12.68
MNW 04B	210.37	210.26	10.11	8.99	3.03	0.57	10.94	10.27	25.82	24.83
MNW 04B	211.91	211.65	9.62	11.95	4.79	0.66	13.52	7.15	31.92	17.27
MNW 04B	213.13	212.77	9.56	10.42	5.65	0.65	15.72	10.75	37.12	25.99
MNW 04B	214.31	214.03	10.13	10.89	5.39	0.85	15.34	11.68	36.21	28.24
MNW 04B	215.39	215.27	10.30	12.56	5.45	1.45	15.56	15.86	36.75	38.32
MNW 04B	217.03	216.80	11.79	10.64	8.14	2.09	20.45	10.01	48.27	24.18
MNW 04B	218.33	217.98	10.23	11.35	4.60	4.26	14.66	23.68	34.61	57.22
MNW 04B	219.36	219.15	9.59	23.47	2.19	4.19	9.42	29.48	22.25	71.24
MNW 04B	220.34	220.31	10.48	22.50	3.41	2.98	12.31	28.54	29.07	68.98
MNW 05A	181.78	181.71	18.57	31.37	23.40	9.21	233.62	54.17	551.53	130.90
MNW 05A	182.86	182.91	20.83	23.17	23.59	6.28	170.62	43.82	402.81	105.91
MNW 05A	184.03	184.12	20.98	20.46	21.70	6.11	115.57	41.82	272.84	101.07
MNW 05A	185.24	185.30	26.49	28.78	22.78	7.03	131.93	42.68	311.45	103.15
MNW 05A	186.79	186.73	27.67	29.78	37.80	9.00	455.33	58.38	1074.96	141.08
MNW 05A	187.85	187.93	23.59	25.88	27.68	7.62	229.32	51.92	541.38	125.48
MNW 05A	189.02	189.11	27.36	28.72	28.43	7.74	238.35	46.01	562.71	111.18
MNW 05A	190.22	190.29	27.57	31.32	32.67	9.50	304.28	60.21	718.34	145.50
MNW 05A	191.77	191.65	44.09	28.22	64.36	8.85	896.09	44.86	2115.51	108.41
MNW 05A	192.84	192.82	30.01	24.74	38.77	7.88	483.64	40.29	1141.78	97.37
MNW 05A	194.00	194.02	38.14	21.54	54.08	8.67	1006.33	41.64	2375.75	100.62
MNW 05A	195.21	195.25	51.62	24.52	68.27	11.67	1386.89	71.67	3274.18	173.20
MNW 05B	205.84		8.82		2.76		13.61		32.13	
MNW 05B	206.99		7.84		1.50		10.27		24.24	
MNW 05B	208.14		8.30		1.66		9.65		22.77	
MNW 05B	209.27		9.36		2.64		14.07		33.23	
MNW 05B	211.01		9.21		2.77		12.62		29.79	
MNW 05B	212.09		10.42		3.18		12.15		28.68	
MNW 05B	213.23		10.99		5.50		16.50		38.96	
MNW 05B	214.36		20.45		6.20		18.32		43.24	
MNW 05B	216.15		10.82		4.61		13.79		32.57	
MNW 05B	217.41		10.11		3.80		11.34		26.76	
MNW 05B	218.31		26.94		7.23		19.47		45.96	
MNW 05B	219.26		21.60		3.24		14.24		33.61	
MNW 06A	172.26	172.29	31.41	10.51	0.73	0.28	9.40	4.22	22.20	10.19
MNW 06A	173.47	173.35	26.55	18.22	0.61	0.29	6.56	4.13	15.48	9.98
MNW 06A	174.64	174.53	22.60	11.80	0.88	0.25	9.47	3.90	22.36	9.42
MNW 06A	175.81	175.81	27.12	21.96	0.94	0.37	9.51	4.70	22.46	11.35
MNW 06A	182.11	182.26	40.22	11.12	2.66	0.22	18.23	3.85	43.03	9.32
MNW 06A	183.40	183.39	32.76	10.73	1.65	0.22	13.03	3.28	30.76	7.93
MNW 06A	184.61	184.52	33.13	10.33	1.77	0.24	13.45	3.60	31.75	8.71
MNW 06A	185.78	185.74	44.91	9.30	2.47	0.31	26.41	4.52	62.35	10.92
MNW 06A	192.09	192.25	38.97	11.48	2.57	0.20	26.12	2.13	61.67	5.15
MNW 06A	193.34	193.40	32.77	11.46	1.34	0.18	12.79	2.36	30.20	5.71
MNW 06A	194.50	194.63	22.91	10.12	1.11	0.27	13.99	3.98	33.02	9.61
MNW 06A	195.71	195.81	22.74	29.70	1.07	0.54	17.10	10.97	40.37	26.51
MNW 06B	206.02	205.82	17.20	9.25	1.36	0.14	7.47	1.11	17.63	2.69
MNW 06B	207.02	207.04	19.36	7.48	1.51	0.14	8.92	0.87	21.07	2.10
MNW 06B	208.14	208.19	21.95	7.47	2.59	0.13	11.01	0.67	25.98	1.62
MNW 06B	209.29	209.32	32.44	8.15	3.62	0.10	13.80	1.00	32.59	2.40
MNW 06B	210.93	210.81	19.13	21.21	2.22	0.08	10.40	0.57	24.55	1.38
MNW 06B	212.11	212.04	11.04	22.63	1.49	0.09	8.47	0.76	20.00	1.84
MNW 06B	213.34	213.20	20.03	34.24	1.85	0.14	9.20	0.79	21.73	1.90
MNW 06B	214.41	214.30	26.03	33.08	2.61	0.13	11.60	1.27	27.39	3.06
MNW 06B	215.98	215.78	23.09	27.24	3.69	0.10	13.74	0.60	32.44	1.46
MNW 06B	217.13	217.00	26.48	16.42	4.40	0.10	16.56	0.74	39.11	1.78
MNW 06B	218.39	218.13	26.22	10.67	2.94	0.10	13.12	0.84	30.98	2.02
MNW 06B	219.48	219.28	42.12	11.21	4.32	0.14	18.04	1.33	42.60	3.22

Appendix B: Flux Average Contaminant Concentrations

Flux average concentrations for MWN-01 through 03 A & B.

Well_ID	Approximate Depth below top of well casing (ft)		Darcy Velocity (cm/day)		Benzene (mg/L)		TPH flux as benzene (mg/L)		TPH flux as NAPL (mg/L)	
	Pre	Post	Pre	Post	Pre	Post	Pre	Post	Pre	Post
MWN 01A	172.78	172.62	10.91	33.43	4.28	9.27	106.18	70.73	250.67	170.92
MWN 01A	173.89	173.77	11.46	35.19	4.27	11.30	97.89	64.21	231.10	155.17
MWN 01A	175.06	175.08	11.09	38.07	3.53	18.16	93.65	125.54	221.09	303.38
MWN 01A	176.26	176.30	11.05	36.39	4.18	18.12	119.59	129.44	282.33	312.80
MWN 01A	182.78	182.76	10.53	12.13	12.56	14.92	153.08	119.22	361.40	288.11
MWN 01A	183.86	184.04	9.76	11.47	18.49	15.16	174.03	119.07	410.85	287.74
MWN 01A	185.03	185.27	11.04	25.98	22.45	8.62	192.00	46.36	453.28	112.05
MWN 01A	186.24	186.35	10.81	24.77	28.55	7.41	354.71	70.12	837.40	169.46
MWN 01A	192.67	192.60	10.45	22.45	24.92	8.48	241.19	47.28	569.40	114.25
MWN 01A	193.84	193.72	10.30	21.52	9.12	7.17	203.92	54.54	481.41	131.80
MWN 01A	195.00	194.92	11.30	22.90	5.72	7.83	218.44	85.60	515.70	206.87
MWN 01A	196.21	196.18	12.00	27.63	19.34	12.61	1544.27	139.26	3645.73	336.55
				Average	13.12	11.59	291.58	89.28	688.36	215.76
MWN 01B	205.96	205.65	8.37	11.14	27.31	79.19	139.30	368.79	328.85	891.23
MWN 01B	207.01	206.73	8.82	10.65	28.00	122.87	154.31	449.57	364.31	1086.46
MWN 01B	208.12	207.99	9.20	11.31	20.51	130.49	105.99	481.00	250.22	1162.43
MWN 01B	209.29	209.27	9.53	23.11	29.24	63.09	168.28	276.33	397.29	667.80
MWN 01B	210.76	210.93	8.61	11.70	43.22	123.66	193.68	487.96	457.25	1179.24
MWN 01B	211.85	212.14	8.75	24.41	32.84	64.41	153.01	251.67	361.23	608.19
MWN 01B	213.13	213.34	9.35	29.72	43.16	79.15	169.66	343.74	400.54	830.70
MWN 01B	214.34	214.42	10.74	25.58	45.34	59.62	180.55	272.70	426.24	659.03
MWN 01B	215.88	215.64	10.11	21.04	40.98	64.81	160.60	299.07	379.14	722.75
MWN 01B	217.03	216.85	10.27	19.27	41.40	67.67	172.53	361.08	407.30	872.60
MWN 01B	218.16	218.11	9.37	12.38	39.79	82.17	187.78	490.99	443.32	1186.57
MWN 01B	219.28	219.29	9.50	11.16	52.53	143.65	347.58	1255.13	820.57	3033.24
				Average	37.03	90.06	177.77	444.84	419.69	1075.02
MWN 02A	182.70	182.73	129.53	11.27	34.64	3.70	227.20	39.14	536.38	94.59
MWN 02A	183.86	183.79	142.42	10.18	32.71	3.74	199.63	39.29	471.29	94.95
MWN 02A	185.03	184.93	148.81	9.38	31.35	3.69	176.47	37.44	416.62	90.48
MWN 02A	186.24	186.19	159.75	9.38	27.62	4.27	137.69	41.85	325.05	101.13
MWN 02A	187.72	187.58	135.55	9.38	32.42	3.07	217.81	38.43	514.21	92.87
MWN 02A	188.85	188.83	142.18	9.38	27.73	3.91	172.03	48.11	406.13	116.27
MWN 02A	190.02	190.06	150.40	9.38	35.44	4.14	201.93	47.56	476.71	114.93
MWN 02A	191.22	191.23	153.36	9.38	24.70	4.56	156.95	57.01	370.53	137.78
MWN 02A	192.71	192.97	142.20	9.38	42.20	3.06	285.54	45.36	674.09	109.63
MWN 02A	193.84	194.24	138.48	9.38	42.16	3.54	252.17	36.91	595.32	89.21
MWN 02A	195.00	195.19	125.00	9.38	45.95	4.22	255.93	45.90	604.21	110.91
MWN 02A	196.21	196.27	160.88	9.38	38.18	4.60	532.73	52.13	1257.68	125.97
				Average	34.59	3.87	234.67	44.09	554.02	106.56
MWN 02B	206.81	206.73	8.35	32.80	22.45	0.15	194.37	1.22	458.87	2.95
MWN 02B	207.96	207.88	9.50	34.56	20.00	0.12	176.93	0.86	417.69	2.07
MWN 02B	209.19	209.07	10.93	70.71	40.86	0.07	214.23	0.41	448.95	1.00
MWN 02B	210.32	210.30	11.06	106.03	43.26	0.05	214.23	0.41	505.77	1.00
MWN 02B	211.83	211.75	10.90	85.78	53.28	0.05	220.48	0.27	520.51	0.65
MWN 02B	212.98	212.83	11.15	69.53	47.51	0.06	215.75	0.56	509.34	1.35
MWN 02B	214.16	213.98	10.78	110.44	50.53	0.05	225.51	0.20	532.39	0.49
MWN 02B	215.31	215.24	10.91	113.33	41.93	0.05	243.04	0.28	573.77	0.67
MWN 02B	217.03	216.72	11.86	122.43	33.08	0.04	198.97	0.18	469.72	0.43
MWN 02B	218.23	217.83	11.15	71.09	42.83	0.08	223.29	1.65	527.16	3.99
MWN 02B	219.33	219.00	11.56	35.26	46.28	0.13	220.87	0.75	521.43	1.82
MWN 02B	220.38	220.21	24.99	21.36	30.02	0.38	213.61	1.40	504.30	3.39
				Average	39.34	0.10	211.43	0.68	499.16	1.65
MWN 03A	172.48	172.29	9.68	9.60	6.33	38.66	150.16	343.23	354.50	829.47
MWN 03A	173.59	173.46	9.96	8.76	5.70	33.94	145.91	329.60	344.46	796.54
MWN 03A	174.76	174.72	9.96	10.97	6.23	53.28	159.38	374.80	376.27	905.77
MWN 03A	175.96	176.00	10.59	36.37	7.58	24.77	151.58	159.81	357.85	386.20
MWN 03A	182.44	182.33	18.84	80.54	6.97	6.91	86.98	52.17	205.35	126.07
MWN 03A	183.56	183.48	22.60	64.22	8.09	8.54	83.83	61.52	197.91	148.67
MWN 03A	184.73	184.68	29.72	46.39	8.95	11.75	87.79	94.79	207.25	229.08
MWN 03A	185.94	185.92	33.59	77.62	9.10	10.31	195.39	80.13	461.28	193.64
MWN 03A	192.43	192.34	28.67	115.41	6.73	7.60	89.88	47.33	212.18	114.38
MWN 03A	193.54	193.50	17.30	92.37	8.61	6.82	145.29	45.69	343.00	110.43
MWN 03A	194.70	194.75	23.71	27.27	7.03	15.65	125.28	134.58	295.76	325.24
MWN 03A	195.91	195.96	16.82	36.02	20.08	21.82	1012.68	237.34	2390.75	573.57
				Average	8.45	20.00	202.85	163.42	478.88	394.92
MWN 03B	205.99	205.72	8.48	1.87	5.99	542.16	142.40	6419.21	142.30	15513.08
MWN 03B	207.20	206.81	8.88	1.75	6.43	261.36	61.22	2490.64	144.52	6019.04
MWN 03B	208.29	207.99	9.90	1.68	8.23	229.25	61.91	2232.24	146.15	5394.57
MWN 03B	209.35	209.22	10.55	1.88	10.21	294.00	76.28	2939.47	180.09	7103.72
MWN 03B	210.96	210.63	8.90	1.99	12.37	548.04	79.60	5379.73	187.91	13001.01
MWN 03B	212.09	211.77	10.33	2.01	20.91	457.74	94.78	4058.40	223.77	9807.79
MWN 03B	213.24	212.96	10.30	2.01	18.63	569.51	88.76	5447.35	209.55	13164.43
MWN 03B	214.34	214.21	11.02	5.64	24.52	189.23	107.87	1629.68	254.65	3938.40
MWN 03B	216.62	215.69	10.50	6.55	30.50	213.02	119.38	2158.62	281.83	5216.68
MWN 03B	217.85	216.78	10.73	5.99	31.91	164.62	122.55	1504.65	289.31	3636.23
MWN 03B	218.41	217.96	11.25	6.41	28.56	189.32	111.94	1762.82	264.26	4260.16
MWN 03B	219.34	219.24	11.79	9.47	17.62	364.82	133.56	4316.43	315.31	10431.38
				Average	17.99	335.26	93.18	3361.60	219.97	8123.88

Flux average concentrations for MWN-04 through 06 A & B.

Well_ID	Approximate Depth below top of well casing (ft)		Darcy Velocity (cm/day)		Benzene (mg/L)		TPH flux as benzene (mg/L)		TPH flux as NAPL (mg/L)	
	Pre	Post	Pre	Post	Pre	Post	Pre	Post	Pre	Post
MWN 04A	182.67	182.73	18.47	37.86	42.24	9.66	557.74	75.25	1316.73	181.84
MWN 04A	183.86	183.89	18.83	29.30	40.92	9.95	550.75	77.32	1300.22	186.85
MWN 04A	185.03	185.11	19.05	31.31	41.33	10.42	499.33	79.60	1178.83	192.37
MWN 04A	186.24	186.30	26.13	37.02	30.08	11.45	351.73	98.66	830.37	238.44
MWN 04A	187.87	187.66	27.82	40.67	35.80	9.50	571.55	71.20	1349.31	172.07
MWN 04A	188.97	188.78	29.21	32.97	37.18	8.62	582.99	68.31	1376.32	165.09
MWN 04A	190.06	190.00	27.27	29.92	35.36	9.06	619.79	74.05	1463.20	178.95
MWN 04A	191.22	191.24	20.57	31.11	39.15	12.86	603.31	110.88	1424.30	267.97
MWN 04A	192.77	192.66	22.87	21.12	82.49	19.50	1264.13	151.31	2984.38	365.65
MWN 04A	193.84	193.78	17.17	11.38	71.34	40.60	1023.49	249.62	2416.27	603.25
MWN 04A	195.00	195.03	18.43	11.25	63.39	44.78	920.87	307.83	2174.00	743.93
MWN 04A	196.21	196.26	39.19	22.83	127.03	41.84	2694.79	313.53	6361.88	757.70
				Average	53.86	19.02	853.37	139.80	2014.65	337.84
MWN 04B	206.94	206.84	8.10	12.38	20.59	5.93	113.04	84.36	266.86	203.87
MWN 04B	208.20	207.91	8.27	8.33	20.15	5.20	107.49	107.20	253.75	259.06
MWN 04B	209.34	208.98	9.62	10.43	23.54	4.96	98.87	50.30	233.41	121.55
MWN 04B	210.37	210.26	10.11	8.99	29.99	6.29	108.16	114.26	255.35	276.13
MWN 04B	211.91	211.65	9.62	11.95	49.78	5.54	140.53	59.81	331.78	144.54
MWN 04B	213.13	212.77	9.56	10.42	59.14	6.21	164.42	103.17	388.16	249.33
MWN 04B	214.31	214.03	10.13	10.89	53.24	7.85	151.46	107.27	357.57	259.23
MWN 04B	215.39	215.27	10.30	12.56	52.92	11.53	151.05	126.23	356.60	305.05
MWN 04B	217.03	216.80	11.79	10.64	69.06	19.64	173.48	94.08	409.56	227.36
MWN 04B	218.33	217.98	10.23	11.35	45.00	37.48	143.27	208.54	338.23	503.97
MWN 04B	219.36	219.15	9.59	23.47	22.84	17.86	98.30	125.60	232.06	303.55
MWN 04B	220.34	220.31	10.48	22.50	32.53	13.23	117.45	126.86	277.27	306.57
				Average	39.90	11.81	130.63	108.97	308.38	263.35
MWN 05A	181.78	181.71	18.57	31.37	126.02	29.37	1258.10	172.64	2970.13	417.23
MWN 05A	182.86	182.91	20.83	23.17	113.26	27.13	819.12	189.17	1933.79	457.15
MWN 05A	184.03	184.12	20.98	20.46	103.43	29.85	550.87	204.38	1300.51	493.92
MWN 05A	185.24	185.30	26.49	28.78	86.00	24.41	498.11	148.29	1175.94	358.37
MWN 05A	186.79	186.73	27.67	29.78	136.62	30.23	1645.79	196.02	3885.39	473.70
MWN 05A	187.85	187.93	23.59	25.88	117.34	29.42	972.07	200.61	2294.87	484.80
MWN 05A	189.02	189.11	27.36	28.72	103.91	26.94	871.06	160.20	2056.42	387.14
MWN 05A	190.22	190.29	27.57	31.32	118.50	30.32	1103.57	192.24	2605.31	464.57
MWN 05A	191.77	191.65	44.09	28.22	145.99	31.35	2032.46	158.98	4798.26	384.21
MWN 05A	192.84	192.82	30.01	24.74	129.19	31.86	1611.63	162.85	3804.77	393.55
MWN 05A	194.00	194.02	38.14	21.54	141.79	40.24	2638.53	193.29	6229.07	467.13
MWN 05A	195.21	195.25	51.62	24.52	132.25	47.58	2686.70	292.32	6342.79	706.44
				Average	121.19	31.56	1390.67	189.25	3283.10	457.35
MWN 05B	205.84		8.82		31.24		154.28		364.22	
MWN 05B	206.99		7.84		19.07		130.91		309.06	
MWN 05B	208.14		8.30		20.03		116.27		274.49	
MWN 05B	209.27		9.36		28.21		150.35		354.95	
MWN 05B	211.01		9.21		30.05		137.01		323.46	
MWN 05B	212.09		10.42		30.55		116.56		275.19	
MWN 05B	213.23		10.99		50.04		150.20		354.60	
MWN 05B	214.36		20.45		30.33		89.58		211.48	
MWN 05B	216.15		10.82		42.59		127.46		300.91	
MWN 05B	217.41		10.11		37.63		112.16		264.80	
MWN 05B	218.31		26.94		26.85		72.27		170.61	
MWN 05B	219.26		21.60		15.01		65.91		155.61	
				Average		30.13		118.58		279.95
MWN 06A	172.26	172.29	31.41	10.51	2.32	2.67	29.95	40.09	70.70	96.90
MWN 06A	173.47	173.35	26.55	18.22	2.29	1.57	24.70	22.68	58.32	54.80
MWN 06A	174.64	174.53	22.60	11.80	3.88	2.08	41.90	33.01	98.93	79.77
MWN 06A	175.81	175.81	27.12	21.96	3.45	1.70	35.08	21.39	82.82	51.68
MWN 06A	182.11	182.26	40.22	11.12	6.61	1.95	45.32	34.66	106.98	83.77
MWN 06A	183.40	183.39	32.76	10.73	5.03	2.08	39.78	30.58	93.92	73.89
MWN 06A	184.61	184.52	33.13	10.33	5.34	2.35	40.60	34.88	95.84	84.28
MWN 06A	185.78	185.74	44.91	9.30	5.50	3.35	58.80	48.55	138.83	117.34
MWN 06A	192.09	192.25	38.97	11.48	6.59	1.71	69.04	18.57	158.26	44.87
MWN 06A	193.34	193.40	32.77	11.46	4.10	1.55	39.05	20.60	92.18	49.77
MWN 06A	194.50	194.63	22.91	10.12	4.83	2.68	61.06	39.30	144.16	94.97
MWN 06A	195.71	195.81	22.74	29.70	4.71	1.83	75.21	36.93	177.56	89.24
				Average	4.55	2.13	46.54	31.77	109.87	76.77
MWN 06B	206.02	205.82	17.20	9.25	7.89	1.50	43.40	12.03	102.47	29.08
MWN 06B	207.02	207.04	19.36	7.48	7.81	1.83	46.10	11.63	108.83	28.11
MWN 06B	208.14	208.19	21.95	7.47	11.78	1.79	50.14	8.96	118.37	21.65
MWN 06B	209.29	209.32	32.44	8.15	11.15	1.22	42.56	12.22	100.47	29.53
MWN 06B	210.93	210.81	19.13	21.21	11.61	0.37	54.36	2.68	128.34	6.49
MWN 06B	212.11	212.04	11.04	22.63	13.51	0.41	76.76	3.37	181.23	8.15
MWN 06B	213.34	213.20	20.03	34.24	9.21	0.41	45.96	2.30	108.50	5.55
MWN 06B	214.41	214.30	26.03	33.08	10.04	0.39	44.58	3.83	105.26	9.26
MWN 06B	215.98	215.78	23.09	27.24	15.97	0.38	59.51	2.22	140.50	5.35
MWN 06B	217.13	217.00	26.48	16.42	16.61	0.59	62.56	4.48	147.70	10.82
MWN 06B	218.39	218.13	26.22	10.67	11.22	0.97	50.04	7.84	118.18	18.95
MWN 06B	219.48	219.28	42.12	11.21	10.24	1.29	42.84	11.88	101.13	28.70
				Average	11.42	0.93	51.57	6.95	121.74	16.80

Appendix C: Normalized Mass Discharge per Unit Width

Normalized mass discharge for MWN-01 through 03 A & B.

Well_ID	Approximate Depth below top of well casing (ft)		Darcy Velocity (cm/day)		Benzene (Percent)		TPH flux as benzene (Percent)		TPH flux as NAPL (Percent)	
	Pre	Post	Pre	Post	Pre	Post	Pre	Post	Pre	Post
MWN 01A	172.78	172.62	10.91	33.43	0.02	0.06	0.03	0.06	0.03	0.06
MWN 01A	173.89	173.77	11.46	35.19	0.03	0.12	0.03	0.09	0.03	0.09
MWN 01A	175.06	175.08	11.09	38.07	0.02	0.19	0.03	0.18	0.03	0.18
MWN 01A	176.26	176.30	11.05	36.39	0.03	0.18	0.03	0.17	0.03	0.17
MWN 01A	182.78	182.76	10.53	12.13	0.07	0.05	0.03	0.05	0.03	0.05
MWN 01A	183.86	184.04	9.76	11.47	0.10	0.05	0.04	0.06	0.04	0.06
MWN 01A	185.03	185.27	11.04	25.98	0.14	0.05	0.05	0.04	0.05	0.04
MWN 01A	186.24	186.35	10.81	24.77	0.19	0.04	0.10	0.06	0.10	0.06
MWN 01A	192.67	192.60	10.45	22.45	0.15	0.05	0.06	0.03	0.06	0.03
MWN 01A	193.84	193.72	10.30	21.52	0.05	0.04	0.05	0.04	0.05	0.04
MWN 01A	195.00	194.92	11.30	22.90	0.04	0.05	0.06	0.07	0.06	0.07
MWN 01A	196.21	196.18	12.00	27.63	0.14	0.10	0.49	0.15	0.49	0.15
				Total	1.00	1.00	1.00	1.00	1.00	1.00
MWN 01B	205.96	205.65	8.37	11.14	0.05	0.04	0.05	0.04	0.05	0.04
MWN 01B	207.01	206.73	8.82	10.65	0.05	0.08	0.06	0.06	0.06	0.06
MWN 01B	208.12	207.99	9.20	11.31	0.05	0.09	0.05	0.07	0.05	0.07
MWN 01B	209.29	209.27	9.53	23.11	0.07	0.09	0.08	0.08	0.08	0.08
MWN 01B	210.76	210.93	8.61	11.70	0.07	0.09	0.07	0.07	0.07	0.07
MWN 01B	211.85	212.14	8.75	24.41	0.07	0.09	0.07	0.07	0.07	0.07
MWN 01B	213.13	213.34	9.35	29.72	0.11	0.14	0.09	0.13	0.09	0.13
MWN 01B	214.34	214.42	10.74	25.58	0.11	0.07	0.09	0.07	0.09	0.07
MWN 01B	215.88	215.64	10.11	21.04	0.09	0.07	0.08	0.07	0.08	0.07
MWN 01B	217.03	216.85	10.27	19.27	0.11	0.08	0.09	0.09	0.09	0.09
MWN 01B	218.16	218.11	9.37	12.38	0.08	0.06	0.08	0.08	0.08	0.08
MWN 01B	219.28	219.29	9.50	11.16	0.12	0.09	0.17	0.16	0.17	0.16
				Total	1.00	1.00	1.00	1.00	1.00	1.00
MWN 02A	182.70	182.73	129.53	11.27	0.08	0.09	0.07	0.08	0.07	0.08
MWN 02A	183.86	183.79	142.42	10.18	0.08	0.09	0.07	0.08	0.07	0.08
MWN 02A	185.03	184.93	148.81	9.38	0.08	0.08	0.06	0.07	0.06	0.07
MWN 02A	186.24	186.19	159.75	9.12	0.08	0.12	0.06	0.10	0.06	0.10
MWN 02A	187.72	187.58	135.55	8.56	0.07	0.06	0.07	0.07	0.07	0.07
MWN 02A	188.85	188.83	142.18	7.28	0.07	0.08	0.06	0.09	0.06	0.09
MWN 02A	190.02	190.06	150.40	7.49	0.09	0.07	0.07	0.07	0.07	0.07
MWN 02A	191.22	191.23	153.36	8.09	0.07	0.10	0.06	0.11	0.06	0.11
MWN 02A	192.71	192.97	142.20	8.78	0.09	0.09	0.09	0.12	0.09	0.12
MWN 02A	193.84	194.24	138.48	8.03	0.10	0.06	0.08	0.05	0.08	0.05
MWN 02A	195.00	195.19	125.00	8.08	0.10	0.07	0.08	0.07	0.08	0.07
MWN 02A	196.21	196.27	160.88	8.71	0.11	0.10	0.22	0.10	0.22	0.10
				Total	1.00	1.00	1.00	1.00	1.00	1.00
MWN 02B	206.81	206.73	8.35	32.80	0.03	0.08	0.05	0.09	0.05	0.09
MWN 02B	207.96	207.88	9.50	34.56	0.04	0.06	0.06	0.06	0.06	0.06
MWN 02B	209.19	209.07	10.93	70.71	0.08	0.09	0.07	0.07	0.07	0.07
MWN 02B	210.32	210.30	11.06	106.03	0.08	0.08	0.08	0.10	0.08	0.10
MWN 02B	211.83	211.75	10.90	85.78	0.11	0.06	0.08	0.05	0.08	0.05
MWN 02B	212.98	212.83	11.15	69.53	0.10	0.06	0.08	0.08	0.08	0.08
MWN 02B	214.16	213.98	10.78	110.44	0.11	0.09	0.09	0.05	0.09	0.05
MWN 02B	215.31	215.24	10.91	113.33	0.08	0.10	0.08	0.07	0.08	0.07
MWN 02B	217.03	216.72	11.86	122.43	0.08	0.06	0.09	0.04	0.09	0.04
MWN 02B	218.23	217.83	11.15	71.09	0.08	0.10	0.08	0.26	0.08	0.26
MWN 02B	219.33	219.00	11.56	35.26	0.10	0.07	0.08	0.06	0.08	0.06
MWN 02B	220.38	220.21	24.99	21.36	0.12	0.14	0.15	0.07	0.15	0.07
				Total	1.00	1.00	1.00	1.00	1.00	1.00
MWN 03A	172.48	172.29	9.68	9.60	0.03	0.05	0.03	0.05	0.03	0.05
MWN 03A	173.59	173.46	9.96	8.76	0.03	0.04	0.03	0.05	0.03	0.05
MWN 03A	174.76	174.72	9.96	10.97	0.03	0.09	0.04	0.08	0.04	0.08
MWN 03A	175.96	176.00	10.59	36.37	0.04	0.13	0.04	0.11	0.04	0.11
MWN 03A	182.44	182.33	18.84	80.54	0.06	0.07	0.03	0.07	0.03	0.07
MWN 03A	183.56	183.48	22.60	64.22	0.09	0.07	0.04	0.07	0.04	0.07
MWN 03A	184.73	184.68	29.72	46.39	0.13	0.08	0.06	0.08	0.06	0.08
MWN 03A	185.94	185.92	33.59	77.62	0.16	0.12	0.16	0.12	0.16	0.12
MWN 03A	192.43	192.34	28.67	115.41	0.09	0.10	0.05	0.08	0.05	0.08
MWN 03A	193.54	193.50	17.30	92.37	0.07	0.09	0.06	0.08	0.06	0.08
MWN 03A	194.70	194.75	23.71	27.27	0.08	0.06	0.07	0.07	0.07	0.07
MWN 03A	195.91	195.96	16.82	36.02	0.18	0.11	0.40	0.15	0.40	0.15
				Total	1.00	1.00	1.00	1.00	1.00	1.00
MWN 03B	205.99	205.72	8.48	1.87	0.03	0.06	0.06	0.07	0.06	0.07
MWN 03B	207.20	206.81	8.88	1.75	0.02	0.04	0.04	0.03	0.04	0.03
MWN 03B	208.29	207.99	9.90	1.68	0.04	0.03	0.05	0.03	0.05	0.03
MWN 03B	209.35	209.22	10.55	1.88	0.04	0.05	0.06	0.04	0.06	0.04
MWN 03B	210.96	210.63	8.90	1.99	0.05	0.07	0.06	0.07	0.06	0.07
MWN 03B	212.09	211.77	10.33	2.01	0.10	0.07	0.09	0.06	0.09	0.06
MWN 03B	213.24	212.96	10.30	2.01	0.09	0.09	0.08	0.08	0.08	0.08
MWN 03B	214.34	214.21	11.02	5.64	0.11	0.08	0.09	0.07	0.09	0.07
MWN 03B	216.62	215.69	10.50	6.55	0.29	0.10	0.22	0.10	0.22	0.10
MWN 03B	217.85	216.78	10.73	5.99	0.03	0.06	0.02	0.06	0.02	0.06
MWN 03B	218.41	217.96	11.25	6.41	0.11	0.10	0.09	0.09	0.09	0.09
MWN 03B	219.34	219.24	11.79	9.47	0.08	0.27	0.12	0.31	0.12	0.31
				Total	1.00	1.00	1.00	1.00	1.00	1.00

Normalized mass discharge for MWN-04 through 06 A & B.

Well_ID	Approximate Depth below top of well casing (ft)		Darcy Velocity (cm/day)		Benzene (Percent)		TPH flux as benzene (Percent)		TPH flux as NAPL (Percent)	
	Pre	Post	Pre	Post	Pre	Post	Pre	Post	Pre	Post
MWN 04A	182.67	182.73	18.47	37.86	0.05	0.07	0.04	0.07	0.04	0.07
MWN 04A	183.86	183.89	18.83	29.30	0.05	0.06	0.04	0.06	0.04	0.06
MWN 04A	185.03	185.11	19.05	31.31	0.05	0.07	0.03	0.07	0.03	0.07
MWN 04A	186.24	186.30	26.13	37.02	0.05	0.08	0.04	0.09	0.04	0.09
MWN 04A	187.87	187.66	27.82	40.67	0.06	0.07	0.06	0.07	0.06	0.07
MWN 04A	188.97	188.78	29.21	32.97	0.06	0.06	0.06	0.06	0.06	0.06
MWN 04A	190.06	190.00	27.27	29.92	0.06	0.05	0.06	0.06	0.06	0.06
MWN 04A	191.22	191.24	20.57	31.11	0.05	0.09	0.05	0.10	0.05	0.10
MWN 04A	192.77	192.66	22.87	21.12	0.10	0.07	0.09	0.07	0.09	0.07
MWN 04A	193.84	193.78	17.17	11.38	0.08	0.10	0.06	0.08	0.06	0.08
MWN 04A	195.00	195.03	18.43	11.25	0.07	0.10	0.06	0.09	0.06	0.09
MWN 04A	196.21	196.26	39.19	22.83	0.33	0.19	0.42	0.19	0.42	0.19
				Total	1.00	1.00	1.00	1.00	1.00	1.00
MWN 04B	206.94	206.84	8.10	12.38	0.04	0.04	0.07	0.07	0.07	0.07
MWN 04B	208.20	207.91	8.27	8.33	0.03	0.02	0.06	0.04	0.06	0.04
MWN 04B	209.34	208.98	9.62	10.43	0.04	0.03	0.06	0.03	0.06	0.03
MWN 04B	210.37	210.26	10.11	8.99	0.05	0.03	0.06	0.07	0.06	0.07
MWN 04B	211.91	211.65	9.62	11.95	0.11	0.03	0.09	0.03	0.09	0.03
MWN 04B	213.13	212.77	9.56	10.42	0.12	0.04	0.10	0.07	0.10	0.07
MWN 04B	214.31	214.03	10.13	10.89	0.11	0.05	0.10	0.07	0.10	0.07
MWN 04B	215.39	215.27	10.30	12.56	0.09	0.08	0.08	0.10	0.08	0.10
MWN 04B	217.03	216.80	11.79	10.64	0.22	0.11	0.17	0.06	0.17	0.06
MWN 04B	218.33	217.98	10.23	11.35	0.09	0.21	0.09	0.13	0.09	0.13
MWN 04B	219.36	219.15	9.59	23.47	0.04	0.22	0.05	0.18	0.05	0.18
MWN 04B	220.34	220.31	10.48	22.50	0.06	0.15	0.07	0.16	0.07	0.16
				Total	1.00	1.00	1.00	1.00	1.00	1.00
MWN 05A	181.78	181.71	18.57	31.37	0.05	0.09	0.04	0.09	0.04	0.09
MWN 05A	182.86	182.91	20.83	23.17	0.05	0.07	0.03	0.08	0.03	0.08
MWN 05A	184.03	184.12	20.98	20.46	0.05	0.06	0.02	0.07	0.02	0.07
MWN 05A	185.24	185.30	26.49	28.78	0.06	0.07	0.03	0.07	0.03	0.07
MWN 05A	186.79	186.73	27.67	29.78	0.07	0.09	0.07	0.10	0.07	0.10
MWN 05A	187.85	187.93	23.59	25.88	0.06	0.08	0.04	0.09	0.04	0.09
MWN 05A	189.02	189.11	27.36	28.72	0.07	0.08	0.04	0.08	0.04	0.08
MWN 05A	190.22	190.29	27.57	31.32	0.08	0.09	0.06	0.10	0.06	0.10
MWN 05A	191.77	191.65	44.09	28.22	0.12	0.09	0.13	0.07	0.13	0.07
MWN 05A	192.84	192.82	30.01	24.74	0.09	0.08	0.09	0.07	0.09	0.07
MWN 05A	194.00	194.02	38.14	21.54	0.13	0.09	0.18	0.07	0.18	0.07
MWN 05A	195.21	195.25	51.62	24.52	0.17	0.12	0.27	0.13	0.27	0.13
				Total	1.00	1.00	1.00	1.00	1.00	1.00
MWN 05B	205.84		8.82		0.06		0.08		0.08	
MWN 05B	206.99		7.84		0.04		0.07		0.07	
MWN 05B	208.14		8.30		0.04		0.06		0.06	
MWN 05B	209.27		9.36		0.06		0.09		0.09	
MWN 05B	211.01		9.21		0.07		0.08		0.08	
MWN 05B	212.09		10.42		0.06		0.06		0.06	
MWN 05B	213.23		10.99		0.14		0.11		0.11	
MWN 05B	214.36		20.45		0.12		0.10		0.10	
MWN 05B	216.15		10.82		0.15		0.12		0.12	
MWN 05B	217.41		10.11		0.06		0.05		0.05	
MWN 05B	218.31		26.94		0.14		0.10		0.10	
MWN 05B	219.26		21.60		0.06		0.07		0.07	
				Total	1.00		1.00		1.00	
MWN 06A	172.26	172.29	31.41	10.51	0.04	0.08	0.05	0.08	0.05	0.08
MWN 06A	173.47	173.35	26.55	18.22	0.03	0.07	0.04	0.07	0.04	0.07
MWN 06A	174.64	174.53	22.60	11.80	0.05	0.08	0.05	0.09	0.05	0.09
MWN 06A	175.81	175.81	27.12	21.96	0.05	0.12	0.05	0.09	0.05	0.09
MWN 06A	182.11	182.26	40.22	11.12	0.16	0.06	0.11	0.08	0.11	0.08
MWN 06A	183.40	183.39	32.76	10.73	0.09	0.06	0.08	0.06	0.08	0.06
MWN 06A	184.61	184.52	33.13	10.33	0.09	0.07	0.07	0.07	0.07	0.07
MWN 06A	185.78	185.74	44.91	9.30	0.13	0.10	0.14	0.09	0.14	0.09
MWN 06A	192.09	192.25	38.97	11.48	0.16	0.05	0.16	0.04	0.16	0.04
MWN 06A	193.34	193.40	32.77	11.46	0.07	0.05	0.07	0.05	0.07	0.05
MWN 06A	194.50	194.63	22.91	10.12	0.06	0.09	0.08	0.08	0.08	0.08
MWN 06A	195.71	195.81	22.74	29.70	0.06	0.15	0.10	0.20	0.10	0.20
				Total	1.00	1.00	1.00	1.00	1.00	1.00
MWN 06B	206.02	205.82	17.20	9.25	0.03	0.11	0.04	0.11	0.04	0.11
MWN 06B	207.02	207.04	19.36	7.48	0.05	0.10	0.07	0.08	0.07	0.08
MWN 06B	208.14	208.19	21.95	7.47	0.08	0.09	0.08	0.06	0.08	0.06
MWN 06B	209.29	209.32	32.44	8.15	0.12	0.07	0.11	0.09	0.11	0.09
MWN 06B	210.93	210.81	19.13	21.21	0.07	0.06	0.07	0.05	0.07	0.05
MWN 06B	212.11	212.04	11.04	22.63	0.05	0.07	0.07	0.08	0.07	0.08
MWN 06B	213.34	213.20	20.03	34.24	0.06	0.09	0.07	0.07	0.07	0.07
MWN 06B	214.41	214.30	26.03	33.08	0.07	0.09	0.07	0.12	0.07	0.12
MWN 06B	215.98	215.78	23.09	27.24	0.12	0.08	0.10	0.06	0.10	0.06
MWN 06B	217.13	217.00	26.48	16.42	0.14	0.07	0.12	0.07	0.12	0.07
MWN 06B	218.39	218.13	26.22	10.67	0.11	0.07	0.12	0.08	0.12	0.08
MWN 06B	219.48	219.28	42.12	11.21	0.09	0.10	0.09	0.13	0.09	0.13
				Total	1.00	1.00	1.00	1.00	1.00	1.00

Appendix H

Interpretation of Mass Transfer Tests with Analytical Models

This appendix describes the results of applying simple analytical-numerical models to the flow, flux, and concentration data collected during the mass transfer testing. The models assume uniform radial flow from a central injection well to a continuous extraction ring. A closed solution is derived for quasi-steady mass dissolution from residual NAPL. The field data suggest only a small fraction of the NAPL was mobilized and recovered during the thermal enhanced extraction test. However, significant fractions of the soluble compounds (e.g., benzene) were recovered resulting in substantial changes in the composition of the NAPL. The models assume the NAPL is immobile.

1. SOURCE TERM

1.1. NAPL AND COMPONENT PROPERTIES

Properties of benzene, toluene, ethylbenzene and xylenes (BTEX) relevant to mass dissolution estimates for fuel NAPL are provided in Table H-1.

Table H-1. Physical and Chemical Properties of Soluble Components.

Property	Unit	Benzene	Toluene	Ethyl-benzene	m-Xylene	o-Xylene
Molecular Weight	g/mol	78.114	92.141	106.168	160.168	106.168
Density at 20 C	g/mL	0.885	0.867	0.867	0.864	0.880
Solubility at 20 C	mg/L	1780	515	152	162	175
Diffusion Coefficient in Water	cm^2/day	0.772	0674	0.593	0.591	0.600
Octanol-Water Coeff. (K_{ow})	mL/g	135	447	1350	1350	890
MCL	mg/L	0.005	1.0	0.7	10.0	10.0

A model for the components of the NAPL at Site ST012 was provided in Section 5. That section also discussed the effective solubility of each NAPL component based on its mole fraction in the NAPL. Separate models were derived for the NAPL makeup before the TEE pilot test (Pre TEE) and after the TEE pilot test (Post TEE). These models were used in this appendix to determine the degree of disequilibrium introduced by water injection during the integral pumping test and, hence, the mass transfer coefficient.

1.2. MASS TRANSFER MODEL

A model for mass transfer from a block of soil with a uniform distribution of NAPL ganglia is based on data fits to column studies of mass dissolution. The general relationship for the mass release rate of a single component from a multi-component NAPL mixture into the surrounding groundwater is as follows:

[Mass Release Rate of Component i from NAPL ganglia]
      = [Bulk Mass Transfer Coefficient for Component i] / [Soil Porosity]
         * [Equilibrium Solubility of Component i – Groundwater Concentration of i]
         * [Volume of NAPL-contaminated Soil]

$$\dot{m}_i(t) = K_i(t)\left(C_i^{eq} - C_i^0\right)V_{NAPL} \qquad (1)$$

where:

$\dot{m}_i$ = mass release rate of component i from ganglia-contaminated soil volume
K_i = bulk mass transfer coefficient for component i between NAPL and groundwater
V_{NAPL} = volume of the NAPL-contaminated soil
C_i^{eq} = equilibrium aqueous solubility of component i in water
C_i^0 = concentration of component i in groundwater entering the source zone

The bulk mass transfer coefficient, K, must be determined experimentally and is a fluid mechanical property of the system. Mass transfer coefficients have been studied extensively and correlated for a vast array of flow configurations, shapes, areas and soils. The correlations assume steady flow over and through the source zone with unchanging geometry and outer area. However, the dimensions of NAPL ganglion will change with time. This temporal effect will reduce the mass release rate from the initial rate assuming a steady flow. In this work, existing correlations for the bulk mass transfer coefficient during advective dissolution in a porous medium are employed to estimate the mass release rate and the NAPL saturation is assumed to remain constant with the vast majority of the NAPL considered insoluble for the timescales considered.

Mass transfer coefficients describing the dissolution of contaminants into soil from immobile sources were reviewed by (Mayer & Miller, 1996). The following general correlation is applicable to the bulk mass transfer coefficient of component i from an NAPL ganglion composed of multiple, uniformly mixed compounds:

$$K_i = \left(\frac{D_{w,i}}{d_p^2}\right)\beta_0 \left(Re\right)^{\beta_1} \left(\phi S_N\right)^{\beta_2} \qquad (2)$$

$$Re = \frac{U d_p}{\nu_w} = \text{Reynolds Number} \qquad (3)$$

where:

K_i = lumped mass transfer coefficient between NAPL ganglion and soil
S_N = saturation of NAPL in the soil
$D_{w,i}$ = molecular diffusion coefficient of compound i in water
d_p = mean soil particle diameter
U = groundwater velocity
ϕ = soil porosity

$$\nu_w \quad = \quad \text{kinematic viscosity of water}$$

$$\beta \quad = \quad \text{mass transfer correlation parameters}$$

Equation (2) can be used to predict the mass transfer coefficient for individual source terms. The source term per unit volume is defined as the mass release rate divided by the contaminated volume:

$$g_i(t) = K_i(t) \left[C_i^{eq} - C_i^0(t) \right] \text{ in the volume } \left(X_2 - X_1 \right)\left(Y_2 - Y_1 \right)\left(Z_2 - Z_1 \right) \tag{4}$$

For a given correlation of the bulk mass transfer coefficient, Equation (4) is used directly in transport equations as a volumetric generation term within the defined source volume. Further development of Equation (4) is explored later

2.   DERIVATION OF THE SOURCE ZONE RADIAL TRANSPORT MODEL

The mass transfer tests were performed with central injection of clean water. The tracer studies reported elsewhere in this report revealed preferential flowpaths that varied in thickness and direction from the injection well. Modeling to account for this variability was performed with SEAM3D and is reported in a separate appendix and in Section 6. For the analytical modeling, the flow was assumed to be purely radial, uniform and axisymmetric. The two-dimensional, transient transport of a dissolved chemical in radial groundwater flow through a uniform, anisotropic aquifer with a uniform residual NAPL saturation is governed by [Bear, 1972; p. 621, Eqn (10.5.26)]:

ASSUMPTION: NAPL saturation is steady and uniform throughout the space and time considered.

$$\frac{U}{\phi(1-S_N)} \left\{ \frac{\partial}{\partial r}\left[\left(\alpha_r + \phi(1-S_N)\frac{D_i^* T}{U} \right)\frac{\partial C_i}{\partial r} \right] + \frac{\partial}{\partial z}\left[\left(\alpha_z + \phi(1-S_N)\frac{D_i^* T}{U} \right)\frac{\partial C_i}{\partial z} \right] - \frac{\partial C_i}{\partial r} \right\}$$
$$= R_i \frac{\partial C_i}{\partial t} - g_i(r,z,t) \tag{5}$$

where the immobile NAPL saturation is accounted for in the pore space according to Imhoff et al., 1993 [Eqn (1)]

ASSUMPTION: Molecular diffusion in the flowing domain is negligible

$$\frac{U}{\phi(1-S_N)}\left(\alpha_r \frac{\partial^2 C_i}{\partial r^2} + \alpha_z \frac{\partial^2 C_i}{\partial z^2} - \frac{\partial C_i}{\partial r} \right) = R_i \frac{\partial C_i}{\partial t} - g_i(r,z,t) \tag{6}$$

with the definitions:

$$C_i \quad = \quad \text{groundwater concentration of component i}$$

$$R_i \quad = \quad \text{retardation coefficient in groundwater } (= 1 + \Box_b K_{d,i}/\phi)$$

U	=	Darcy velocity of ground water
α_r	=	longitudinal dispersivity
α_z	=	vertical dispersivity
D_i^*	=	aqueous diffusion coefficient for component i
T	=	tortuosity (~0.667)
g_i	=	mass generation term
φ	=	soil porosity
r	=	radial coordinate in the direction of groundwater flow
z	=	vertical coordinate
t	=	time

The model assumes the dispersivities are proportional to the local velocity and a uniform aquifer thickness of H. The sources of contaminants are specified volumes of soil containing residual saturations of NAPL that are assumed to have a negligible effect on the flow of groundwater.

From equation (4), the mass generation per unit volume created by mass transfer in a source zone is (Mayer and Miller, 1996):

$$g_i(r,z,t) = K_i(r,z,t)\left[C_i^{eq}(t) - C_i(r,z,t)\right] \tag{7}$$

The equilibrium concentration changes over time as the mole fraction of individual NAPL components changes over time. The mole fraction change is determined from a mass balance on the residual NAPL components. Substituting in equation (6) the generation term specified by equation (7) yields:

$$\frac{U}{\phi(1-S_N)}\left(\alpha_r \frac{\partial^2 C_i}{\partial r^2} + \alpha_z \frac{\partial^2 C_i}{\partial z^2} - \frac{\partial C_i}{\partial r}\right) = R_i \frac{\partial C_i}{\partial t} - K_i(r,z,t)\left[C_i^{eq}(t) - C_i(r,z,t)\right] \tag{8}$$

For steady injection of clean water and steady extraction assuming a circular ring, appropriate boundary conditions in the radial direction to solve (8) are:

$$C_i = 0 \qquad\qquad \text{at } r = r_{inj} \tag{9c}$$

$$\frac{\partial C_i}{\partial r} = 0 \qquad\qquad \text{at } r = r_{ext} \tag{9d}$$

ASSUMPTION: Top and bottom of aquifer are impermeable and residual NAPL saturation is uniform with depth.

$$\frac{U}{\phi(1-S_N)}\left(\alpha_r \frac{\partial^2 C_i}{\partial r^2} - \frac{\partial C_i}{\partial r}\right) = R_i \frac{\partial C_i}{\partial t} - K_i(r,t)\left[C_i^{eq}(t) - C_i(r,t)\right] \tag{10}$$

The groundwater Darcy velocity is defined by the water injection rate and is related to the aquifer thickness and radial distance from the injection well by:

$$U = \frac{Q}{2\pi H r} \tag{11}$$

where:

Q   =   volumetric water injection rate
H   =   aquifer thickness

Recall, the mass transfer coefficient includes the water velocity that is a function of the radius from the injection well. Hence, the mass transfer coefficient is also dependent on the radius within the Reynolds Number. This dependence can be separated out of the mass transfer correlation as:

$$K_i U^{-\beta_1} = \left(\frac{D_{w,i}}{d_p^2}\right) \beta_0 \left(\frac{d_p}{\nu_w}\right)^{\beta_1} (\phi S_N)^{\beta_2} \tag{12}$$

Substituting equation (12) into (10) yields:

$$
\begin{aligned}
\alpha_r \frac{\partial^2 C_i}{\partial r^2} - \frac{\partial C_i}{\partial r} = {}& r \frac{2\pi H R_i \phi(1-S_N)}{Q} \frac{\partial C_i}{\partial t} \\
& - r^{1-\beta_1} \left(K_i U^{-\beta_1}\right) \left(\frac{Q}{2\pi H}\right)^{\beta_1 - 1} \phi(1-S_N) \left[C_i^{eq}(t) - C_i(r,t)\right]
\end{aligned}
\tag{13}
$$

An exact solution to this governing equation does not exist; however, the equation can be readily solved to an acceptable accuracy with a simple finite difference method. Note the generation term is very weakly dependent on the position in the domain as the parameter β_1 is generally close to one. In the absence of matrix heterogeneity, the mass transfer is governed primarily by the injection rate, the longitudinal dispersivity, representative particle size, and NAPL saturation assuming the NAPL is uniformly distributed in the matrix.

3. SOLUTIONS TO THE SOURCE ZONE RADIAL TRANSPORT MODEL

The dimensionless form of equation (13) for steady, purely radial flow can be written as:

$$\alpha' \frac{\partial^2 X_i}{\partial \eta^2} - \frac{\partial X_i}{\partial \eta} - \eta^{1-\beta_1} \sigma X_i = \eta \frac{\partial X_i}{\partial \tau} - \eta^{1-\beta_1} \sigma \left(1 - \frac{C_i^{eq}(t)}{C_{i,0}^{eq}}\right) \tag{14}$$

where:

$$X_i = \frac{C_{i,0}^{eq} - C_i}{C_{i,0}^{eq}}$$

$$\eta = \frac{r}{r_{inj}}$$

$$\tau = \frac{Qt}{2\pi H R_i \phi (1 - S_N) r_{inj}^2}$$

$$\alpha' = \frac{\alpha_r}{r_{inj}}$$

$$\sigma = r_{inj}^{2-\beta_1} \left(\frac{Q}{2\pi H} \right)^{\beta_1 - 1} \phi (1 - S_N)(U^{-\beta_1} K_i)$$

Equation (14) is a relatively simple nonlinear partial differential equation that can be solved with readily available finite difference methods given boundary and initial conditions and a mass balance on the NAPL. Typically, the fitting parameter, β_1, has a value from ~ 0.598 to 0.75 such that the nonlinearity is not strong. However, for data fitting, other applicable simplifying assumptions allow closed form solutions.

3.1.   SOLUTION FOR PSEUDO-STEADY MASS DISSOLUTION AND NEGLIGABLE DISPERSION

For conditions of steady flow and a slowly dissolving NAPL component such that its mole fraction does not change substantially over a few pore volumes of water flow through the system, the equilibrium concentration can be considered a constant. If the following conditions are met, the mass dissolution is steady and the pseudo-steady assumption is applicable.

$$\tau >> \frac{\eta}{\sigma} \text{ and } \tau >> \eta^2$$

ASSUMPTION: Pseudo-steady-state conditions for mass dissolution and a slowly changing NAPL composition:

$$\alpha' \frac{\partial^2 X_i}{\partial \eta^2} - \frac{\partial X_i}{\partial \eta} - \eta^{1-\beta_1} \sigma X_i = 0 \tag{15}$$

Further, the dispersion term is relatively small and can be neglected if the following conditions are met:

$$\alpha' << \eta^{3-\beta_1} \sigma \text{ and } \alpha' << \eta$$

These conditions can only be checked after the mass transfer parameter has been determined.

ASSUMPTION: Dispersion is negligible compared to advection and mass transfer:

$$\frac{dX_i}{d\eta} + \eta^{1-\beta_1} \, \sigma \, X_i = 0 \tag{16}$$

This equation can be directly integrated to yield:

$$\ln(X_i) = -\sigma \int \eta^{1-\beta_1} \, d\eta + A = -\frac{\sigma \, \eta^{2-\beta_1}}{2-\beta_1} + A \tag{17}$$

At the injection well ($\eta_{inj} = 1$), the concentration is zero in the water ($X_i = 1$) and the integration constant is:

$$\ln(1) = -\frac{\sigma \, \eta_{inj}^{2-\beta_1}}{2-\beta_1} + A \qquad \text{or} \qquad A = \frac{\sigma}{2-\beta_1}$$

Substituting the integration constant into the integrated equation (17) yields a closed form solution subject to the assumptions delineated previously:

$$X_i(\eta) = 1 - \frac{C_i(\eta)}{C_{i,0}^{eq}} = \exp\left[-\frac{\sigma}{2-\beta_1}\left(\eta^{2-\beta_1} - 1\right)\right] \tag{18}$$

For the assumption of a small dispersion coefficient, only two parameters appear in this solution: β_1 and σ. Estimates for β_1 are available in the literature and therefore the data can be fit with the single mass transfer parameter σ to evaluate the mass dissolution in the source zone during the mass transfer testing. A typical value for β_1 is 0.75 (Miller et al., 1990). For this value of β_1, curves of varying σ values for mass dissolution as a function of radial distance are illustrated in Figure H-1. For high mass transfer rates, the water rapidly comes to equilibrium with the NAPL and for decreasing rates, the distance to reach equilibrium increases.
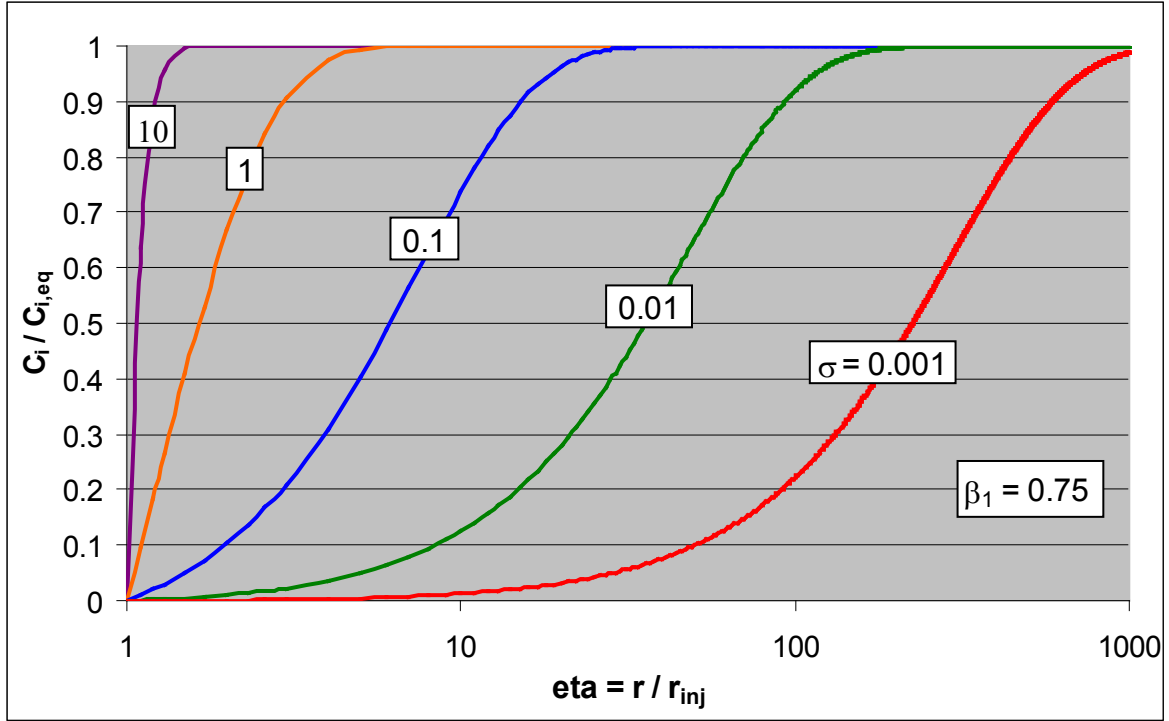
Figure H-1. Type Curves for Various Values of the Mass Transfer Parameter.

3.2. SOLUTION FOR PSEUDO-STEADY MASS DISSOLUTION AND SPECIAL CASE $\beta_1 = 1$

For the special case of β_1 equal to one and a pseudo-steady state condition is achieved, the governing equation (14) reduces to:

$$\alpha' \frac{\partial^2 X_i}{\partial \eta^2} - \frac{\partial X_i}{\partial \eta} - \sigma X_i = 0 \qquad (19)$$

and is subject to the boundary conditions:

$$X_i = 1 \qquad \text{at } \eta = 1$$

$$\frac{dX_i}{d\eta} = 0 \qquad \text{at } \eta = \eta_{\,ext}$$

If the mass transfer correlation parameter is on the order of one, the mass transfer rate is governed almost linearly by the NAPL saturation and inversely with the longitudinal dispersivity and the representative particle dimension. It is also evident the transport is strongly effected by the curvature near the injection well where the dispersivity is on the order of the distance from the injection well.

For the special case of β_1 equal to one and quasi-steady state conditions, the exact solution to (19) is:

$$X_i = A_i e^{\omega^+ \eta} + B_i e^{\omega^- \eta} \qquad ; \left(\omega^{\pm}\right) = \frac{1 \pm \sqrt{1 + 4\sigma\alpha'}}{2\alpha'} \qquad (20)$$

and the conditions:

$$1 = A_i e^{\omega^+} + B_i e^{\omega^-}$$

$$0 = \omega^+ A_i e^{\omega^+ \eta_{ext}} + \omega^- B_i e^{\omega^- \eta_{ext}}$$

Solving for the integration constants yields the solution:

$$X_i(\eta) = \frac{\omega^- e^{-\omega^+ (\eta_{ext} - \eta)} - \omega^+ e^{-\omega^- (\eta_{ext} - \eta)}}{\omega^- e^{-\omega^+ (\eta_{ext} - 1)} - \omega^+ e^{-\omega^- (\eta_{ext} - 1)}} \qquad (21)$$

For the special case of $\beta_1 = 1$, two parameters appear in this solution: α' and σ. Estimates for α' are available from the tracer tests and therefore the data could be fit with the single mass transfer parameter σ to evaluate the mass dissolution in the source zone during the mass transfer testing. Values for α' from the tracer testing are on the order of 1 with variation from 0.2 to 9 (see Section 5.7). Curves of varying α' values for a mass dissolution parameter of 0.1 and $\beta_1 = 1$ are illustrated in
Figure H-2. This figure illustrates that dispersion can be neglected with a relatively small error in the data fitting as long as the scaled dispersion coefficient is on the order of one. This condition was found in the ST012 mass transfer testing such that equation (18) can be used to evaluate the data from ST012.
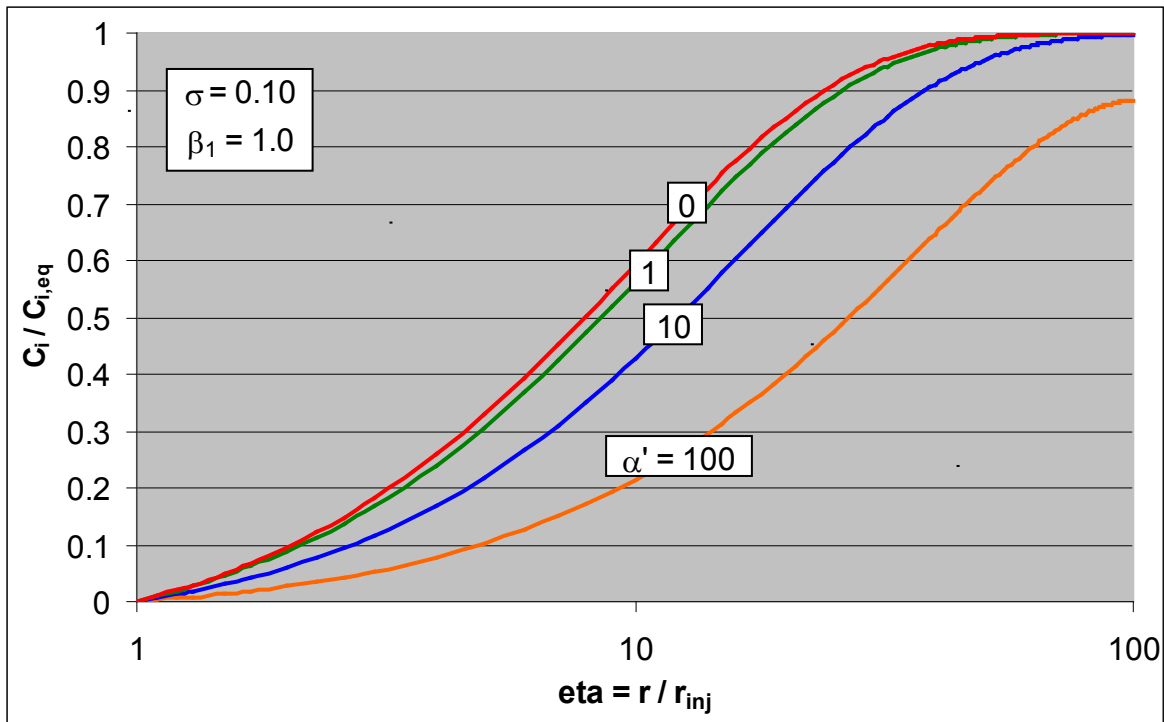
Figure H-2. Type Curves for Various Values of the Dispersion Coefficient.

4.   APPLICATION OF THE MODEL TO THE ST012 MASS TRANSFER TESTS

The benzene concentrations from the mass transfer testing described in Section 5 of the main report were non-dimensionalized with the injection well radius for distance and the local equilibrium concentrations measured before the Pre-TEE mass transfer testing and after the site had re-equilibrated (sampling performed two to three months after the termination of all testing and pumping). These data are presented in Table H-2. The table also includes the minimum error, best-fit value for the dimensionless mass transfer parameter, σ, for each soil horizon from both the Pre-TEE and Post-TEE mass transfer testing. Theoretically, if NAPL was not removed and was not re-distributed in the subsurface, the mass transfer parameter should not have changed between the Pre-TEE and Post-TEE testing as long as the flow configuration was also changed. As described in Section 5, the flow regime was approximately the same at the monitoring wells in both test periods. However, the data fitting indicates the B-horizon mass transfer was reduced by 66% and the C-horizon by 83%. The results also indicate the Pre-TEE mass transfer in the B-horizon was more than double the mass transfer rate in the C-horizon. Similarly, in the Post-TEE testing, the B-horizon mass transfer was five times greater than in the C-horizon. These results are consistent with other test results indicating the majority of the NAPL in the LSZ resides in the finer-grained B-horizon.

Table H-2. Pseudo-Steady-State Benzene Concentrations from the Pre-TEE and Post-TEE Mass Transfer Testing.

Well	Radius (feet)	η	Scaled Concentrations	
			Pre-TEE / Initial	Post-TEE / Final
MWN01B	48.3	96.7	1.00	1.00
MWN02B	27.7	55.4	0.80	0.50
MWN03B	59.8	119.6	0.89	0.37
MWN04B	42.9	85.7	0.59	0.38
MWN05B	54.0	108.1	0.92	-
MWN06B	18.2	36.4	0.16	0.25
B-Horizon Fit for σ =			0.0073	0.0025
MWN01C	49.0	98.0	0.62	0.19
MWN02C	25.1	50.3	0.65	0.01
MWN03C	57.4	114.8	0.30	0.18
MWN04C	40.2	80.4	0.09	0.16
MWN05C	53.6	107.2	0.68	0.01
MWN06C	18.2	36.4	0.57	0.00
C-Horizon Fit for σ =			0.0030	0.00052

Fits to the mass transfer benzene data in the B-horizon of the LSZ are illustrated in Figure H-3 for the Pre-TEE and Post-TEE tests. Fits to the mass transfer data in the C-horizon of the LSZ are illustrated in Figure H-4 for the Pre-TEE and Post-TEE tests. As indicated by the curves in Figure H-2, excluding dispersion likely leads to a slight overprediction of the mass transfer parameter, σ. However, given the scatter in the data, this error is negligible. As discussed above, the mass transfer parameter was reduced by the application of TEE although only a small percentage of the NAPL estimated to reside in the subsurface was removed. For a uniform distribution of residual NAPL, the change in mass transfer was expected to be small if the NAPL architecture and flow configuration did not change. The reduction in mass transfer is indicative of heterogeneity in the subsurface, i.e., NAPL residing in more permeable flow zones was more effectively treated than that in fine-grained units. Further, the reduction in mass transfer resulting from a reduction of contaminant diffusion between permeable and fine-grained units was not explicitly included in the model.

The fitted mass transfer parameters were of similar magnitude except for the value from the Post-TEE C-horizon that was almost an order-of-magnitude less. As described in Section 5, the C-horizon contained a lesser saturation of residual NAPL than the B-horizon and it is probable that a significant portion of that was flushed out during the TEE Pilot Test resulting in the observed reduction in mass transfer.
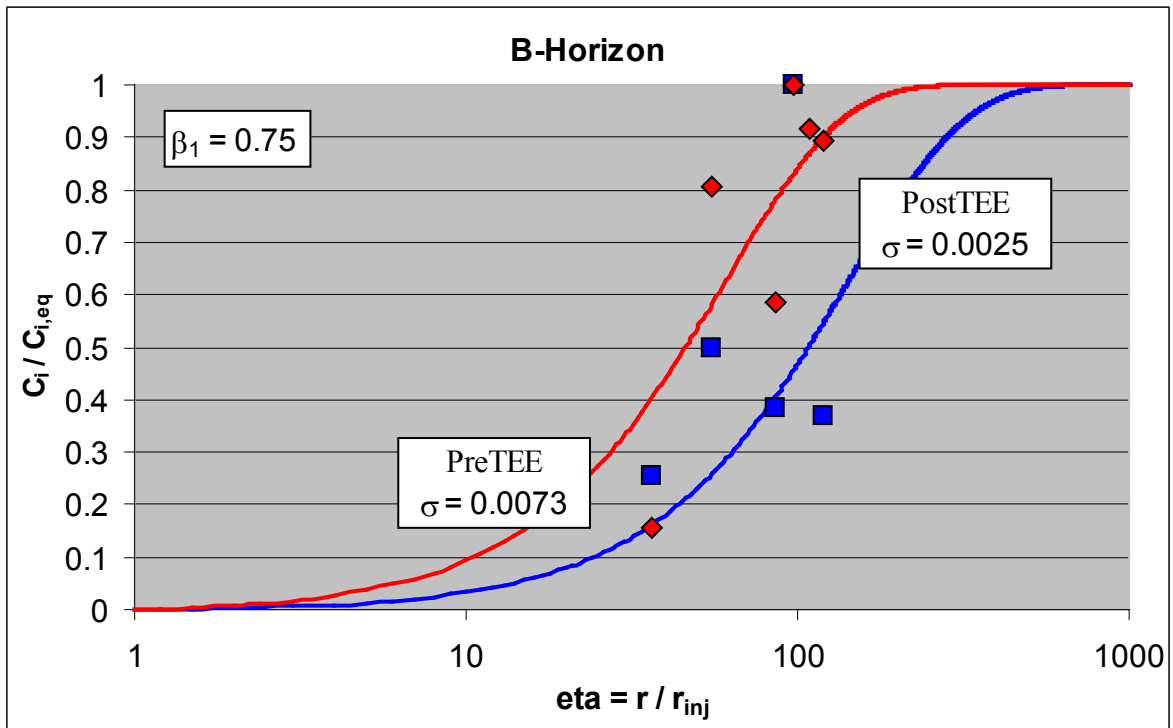
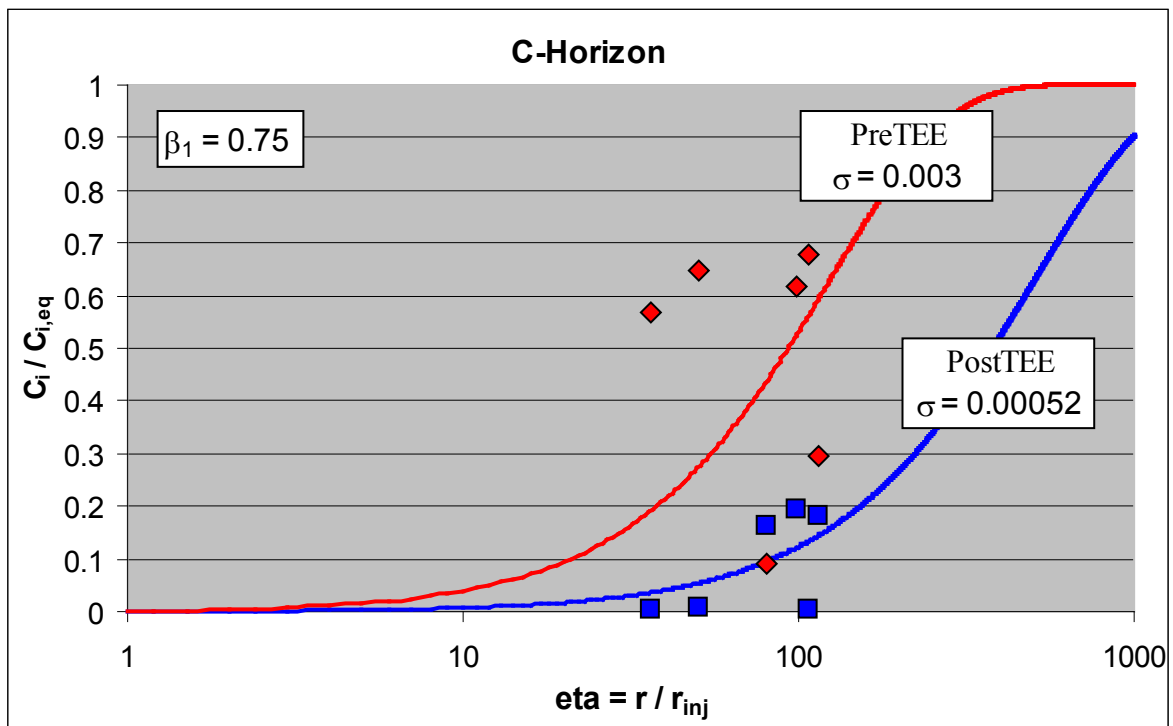**Figure H-3. Model Mass Transfer Fits to Concentrations in the B-Horizon.**

Figure H-4. Model Mass Transfer Fits to Concentrations in the C-Horizon.

Finally, these fitted mass transfer parameters can be compared to literature correlations developed from column studies for flow through zones of residual NAPL. Recall equation (2):

$$K_i = \left(\frac{D_{w,i}}{d_p^2}\right)\beta_0\left(\frac{Ud_p}{\nu_w}\right)^{\beta_1}(\phi S_N)^{\beta_2} \tag{2}$$

The mass transfer coefficient has a radial dependence through the velocity that can be eliminated by rearranging (2):

$$\left(U^{-\beta_1}K_i\right)_{correlation} = \left(\frac{D_{w,i}}{d_p^2}\right)\beta_0\left(\frac{d_p}{\nu_w}\right)^{\beta_1}(\phi S_N)^{\beta_2} \tag{22}$$

The definition of the dimensionless mass transfer parameter from equation (14) is:

$$\sigma = r_{inj}^{2-\beta_1}\left(\frac{Q}{2\pi H}\right)^{\beta_1-1}\phi(1-S_N)\left(U^{-\beta_1}K_i\right)$$

and with rearrangement yields:

$$\left(U^{-\beta_1}K_i\right)_{data\ fit} = \frac{\sigma}{\phi(1-S_N)r_{inj}^{2-\beta_1}}\left(\frac{Q}{2\pi H}\right)^{1-\beta_1} \tag{23}$$

The parameters required to quantify the benzene mass transfer during the tests are provided in Table H-3. These parameters were taken from the data presented in Section 5 and the TEE Pilot Test Evaluation Report (BEM Systems, 2010).

Table H-3. Site Parameters for Calculating Benzene Mass Transfer Characteristics.

Parameter	B-Horizon	C-Horizon
$D_{w,i}$ (cm^2/day)	0.661	0.661
ν_w (cm^2/day)	872.64	872.64
d_p (mm)	0.05	0.1
S_{NAPL}	0.047	0.039
Porosity, ϕ	0.33	0.32
β_0	12	12
β_1	0.75	0.75
β_2	0.60	0.60
r_{inj} (m)	0.15	0.15
r_{ext} (m)	21.3	21.3
H (m)	12.2	12.2
Q (m^3/day)	196.2	196.2

The mass transfer parameters calculated with equations (22) and (23) and the parameters from Table H-3 are provided in Table H-4. The mass transfer parameters shown have the radial dependence of the flow removed to allow a direct comparison. The fits to field data are roughly three orders of magnitude less than the values calculated from correlations based on flow through a uniformly distributed residual NAPL. This large difference was not unexpected as the heterogeneities in a real subsurface tend to discourage contact between flowing water and residual NAPL whereas the flow is forced through the residual NAPL in laboratory column studies.

Table H-4. Comparison of Mass Transfer Correlation Results with Data Fits.

Test	σ	$\left(U^{-\beta_1}K_i\right)_{\text{data fit}}$	$\left(U^{-\beta_1}K_i\right)_{\text{correlation}}$	Correlation / Data Fit
Pre-TEE B-Horizon	0.0073	0.315	96.5	307
Post-TEE B-Horizon	0.0025	0.108	96.5	896
Pre-TEE C-Horizon	0.0030	0.132	35.6	269
Post-TEE C-Horizon	0.00052	0.023	35.6	1,550

To provide a more intuitive comparison between the data fit parameter, σ, and mass transfer correlations in the literature, the mass transfer correlations from the literature were averaged over the radius of testing as follows:

$$\left(\overline{K}_i\right)_{\text{correlation}} = \left(\frac{D_{w,i}}{d_p^2}\right)\beta_0\left(\frac{Qd_p}{2\pi H\nu_w}\right)^{\beta_1}\left(\phi S_N\right)^{\beta_2}\left(\frac{1}{r_{\text{ext}}-r_{\text{inj}}}\right)^2\left(\frac{2}{2-\beta_1}\right)\left(r_{\text{ext}}^{2-\beta_1}-r_{\text{inj}}^{2-\beta_1}\right) \qquad (24)$$

Similarly, the average mass transfer coefficient was also be calculated from the data fit by integrating over the radius from injection to extraction:

$$\left(\overline{K}_i\right)_{\text{data fit}} = \frac{2\sigma}{\phi(1-S_N)r_{\text{inj}}^{2-\beta_1}}\left(\frac{Q}{2\pi H}\right)\left(\frac{1}{r_{\text{ext}}-r_{\text{inj}}}\right)^2\left(\frac{r_{\text{ext}}^{2-\beta_1}-r_{\text{inj}}^{2-\beta_1}}{2-\beta_1}\right) \qquad (25)$$

The volume-averaged bulk mass transfer coefficients calculated with equations (24) and (25) and the parameters from Table H-3 are provided in Table H-5. The radial dependence of the bulk mass transfer coefficients was averaged out. The bulk mass transfer coefficients determined from the field data are roughly three orders of magnitude less than the values calculated from literature correlations based on flow through a uniformly distributed residual NAPL. As before, this large difference was not unexpected because of subsurface heterogeneities. However, the average bulk mass transfer coefficients determined from the field data provide a defensible measure of this parameter for use in modeling. The average bulk mass transfer coefficients range from 0.0076 to 0.104 1/day. The values employed in the numerical modeling reported in Section 6 of this report ranged from 0.05 to 0.5 1/day and therefore may have modestly overpredicted the mass dissolution rate in the source zone.

Table H-5. Comparison of Average Bulk Mass Transfer Coefficients.

Test	σ	$(\overline{K}_i)_{\text{data fit}}$ (1/day)	$(\overline{K}_i)_{\text{correlation}}$ (1/day)
Pre-TEE B-Horizon	0.0073	0.104	31.9
Post-TEE B-Horizon	0.0025	0.036	31.9
Pre-TEE C-Horizon	0.0030	0.044	11.8
Post-TEE C-Horizon	0.00052	0.0076	11.8

In conclusion, and most importantly, the mass transfer parameter values presented in Table H-4 from equation (23) also allow mass transfer under ambient conditions to be estimated. The redefined dimensionless mass transfer parameter, σ, is independent of velocity. <u>The ambient groundwater velocity at the site can be substituted into equation (23) to calculate estimates of the bulk mass transfer coefficients in the two horizons under ambient conditions and, hence, the mass dissolution rate from the source area over time</u> and the time to remediation for natural attenuation at the site.

5. REFERENCES

Bear, J. 1972. Dynamics of Fluids in Porous Media. Dover Publications Inc. New York. 764 pp.

BEM Systems, Inc. 2010. Draft Final Phase I Thermal Enhanced Extraction (TEE) Pilot Test Performance Evaluation Report. Former Williams Air Force Base, Mesa, Arizona. United States Air Force. November 2010.

Imhoff, P.T., Jaffe, P.R., and G.F. Pinder 1993. An experimental study of complete dissolution of a nonaqueous phase liquid in saturated porous media. Water Resources Research, 30(2), 307-320.

Mayer, A.S., Miller, C.T. 1996. The influence of mass transfer characteristics and porous media heterogeneity on nonaqueous phase dissolution. Water Resources Research, 32(6), 1551-1567.

Miller, C.T., Poirier-McNeill, M.M., Mayer, A.S., 1990. Dissolution of trapped nonaqueous phase liquids: Mass transfer characteristics. Water Resources Research, 26(11), 2783-2796.